

**Development of Quality Assurance and Quality Control
System for Post Tensioned Segmental Bridges in Florida:
Case of Ringling Bridge – Phase II**

**FDOT Contract No. BDV29-977-34
FINAL REPORT**

Submitted by:

Atorod Azizinamini, Ph.D., P.E., Florida International University

Submitted to:

FDOT Research Center
605 Suwannee Street
Tallahassee, FL 32399

Project manager:

Ivan Lasa
Florida Department of Transportation, State Materials Office
5007 NE 39th Avenue
Gainesville, FL 32069

Florida International University
10555 W. Flagler Street,
Miami, FL 33174

December, 2018

DISCLAIMER

The opinions, findings, and conclusions expressed in this publication are those of the authors and not necessarily those of the State of Florida Department of Transportation.

Report Prepared by

Sheharyar e Rehmat

Kingsley Lau, Ph.D.

Atorod Azizinamini, Ph.D., PE

CONVERSION TABLES

Approximate conversion to SI Units

Symbol	When you know	Multiply by	To find	Symbol
Length				
in	inches	25.4	millimeters	mm
ft	feet	0.305	meters	m
yd	yards	0.914	meters	m
mi	miles	1.61	kilometers	km
Area				
in ²	square inches	645.2	square millimeters	mm ²
ft ²	square feet	0.093	square meters	m ²
yd ²	square yard	0.836	square meters	m ²
ac	acres	0.405	hectares	ha
mi ²	square miles	2.59	square kilometers	km ²
Volume				
fl oz	fluid ounces	29.57	milliliters	mL
gal	gallons	3.785	liters	L
ft ³	cubic feet	0.028	cubic meters	m ³
yd ³	cubic yards	0.765	cubic meters	m ³
Mass				
oz	ounces	28.35	grams	g
lb	pounds	0.454	kilograms	kg
T	short tons (2000 lb)	0.907	megagrams (or "metric ton")	Mg (or "t")
Temperature				
°F	Fahrenheit	5 (F-32)/9 or (F-32)/1.8	Celsius	°C
Illumination				
fc	foot-candles	10.76	lux	lx
fl	foot-Lamberts	3.426	candela/m ²	cd/m ²
Force and Pressure or Stress				
lbf	pound force	4.45	newtons	N
lbf/in ²	pound force per square inch	6.89	kilopascals	kPa

Approximate conversion to U.S. Customary Units

Symbol	When you know	Multiply by	To find	Symbol
Length				
mm	millimeters	0.039	inches	in
m	meters	3.28	feet	ft
m	meters	1.09	yards	yd
km	kilometers	0.621	miles	mi
Area				
mm ²	square millimeters	0.0016	square inches	in ²
m ²	square meters	10.764	square feet	ft ²
m ²	square meters	1.195	square yards	yd ²
ha	hectares	2.47	acres	ac
km ²	square kilometers	0.386	square miles	mi ²
Volume				
mL	milliliters	0.034	fluid ounces	fl oz
L	liters	0.264	gallons	gal
m ³	cubic meters	35.314	cubic feet	ft ³
m ³	cubic meters	1.307	cubic yards	yd ³
Mass				
g	grams	0.035	ounces	oz
kg	kilograms	2.202	pounds	lb
Mg (or "t")	megagrams (or "metric ton")	1.103	short tons (2000 lb)	T
Temperature				
°C	Celsius	1.8C+32	Fahrenheit	°F
Illumination				
lx	lux	0.0929	foot-candles	fc
cd/m ²	candela/m ²	0.2919	foot-Lamberts	fl
Force and Pressure or Stress				
N	newtons	0.225	pound force	lbf
kPa	kilopascals	0.145	pound force per square inch	lbf/in ²

TECHNICAL REPORT DOCUMENTATION

1. Report No.	2. Government Accession No.	3. Recipient's Catalog No.	
4. Title and Subtitle Development of Quality Assurance and Quality Control System for Post Tensioned Segmental Bridges in Florida: Case of Ringling Bridge – Phase II		5. Report Date December 2018	
		6. Performing Organization Code	
7. Author(s) Sheharyar e Rehmat, Kingsley Lau, Atorod Azizinamini		8. Performing Organization Report No.	
9. Performing Organization Name and Address Florida International University, Miami University Park, Room P.C. 539 Miami, FL 33199-0000 breslint@servax.fiu.edu		10. Work Unit No. (TRAIS)	
		11. Contract or Grant No. Final Report BDV29-977-34	
12. Sponsoring Agency Name and Address Florida Department of Transportation 605 Suwannee Street Tallahassee, FL 32399-0450 U.S.		13. Type of Report and Period Covered Draft final April 2017 - December 2018	
		14. Sponsoring Agency Code	
15. Supplementary Notes			
16. Abstract The failure of two external post-tensioned (PT) tendons in the Ringling bridge was caused by corrosion of strands in deficient grout conditions. This prompted a thorough inspection of the tendons, as a result of which, fifteen other PT tendons were replaced in 2011-2012. Despite extensive repair work, practical limitations and technical constrains did not allow a thorough assessment of corrosion activity. An alternative assessment using nondestructive testing was desired to validate the corrosion activity and deficient grout. As part of Phase I of the project, NDT Corporation and Tokyo Rope Inc. successfully demonstrated their capabilities on blind mockup specimens using ultrasonic/sonic testing (UST) and magnetic main flux method (MMFM), respectively. During Phase II, these two testing companies were selected to carry out testing on Ringling bridge. Florida International University (FIU) provided support for on-site testing and independently evaluated the efficiency and effectiveness of these technologies. The UST company (USTC) carried out testing on the tendons located in the center cell of Ringling bridge using ultrasonic/sonic method to detect grout anomalies. The full length of tendon, including low horizontal, inclined, and high points, were tested for all spans. The MMFM testing company (MTC) carried out testing on inclined and high points of all tendons in the center cell (including additional tendons in Span 8 and Span 9) using the MMFM to detect steel strand loss. A total of nine sites were selected for tendon condition and nondestructive evaluation results verification which was carried out by Concorr FL. Of the four test sites recommended by MTC, site 1 and site 4 showed strong positive correlation with severe strand corrosion in the former and large embedded steel debris in the latter. MTC testing at sites 2 and 5a gave indication of cross-section loss, but tendon openings revealed clean strands in predominantly normal hardened grout. The verification of four locations recommended by USTC for grout anomaly did not indicate the anomalous grout conditions (voids, soft grout, and segregation). However, UST did give differentiation in through duct and circumferential resonant frequencies, indicating grout anomalies such as circumferential cracking. USTC requires more refinement of the data to characterize anomalous grout.			
17. Key Word Nondestructive testing, Magnetic Main Flux Method, Magnetic flux leakage, Ultrasonic/sonic Testing, Post Tensioned systems		18. Distribution Statement	
19. Security Classif. (of this report)	20. Security Classif. (of this page)	21. No. of Pages 439	22. Price

ACKNOWLEDGEMENTS

The authors would like to thank the Florida Department of Transportation (FDOT) and project manager Ivan Lasa.

EXECUTIVE SUMMARY

Failures of two longitudinal external post-tensioned (PT) tendons in the Ringling causeway bridge in 2011 after almost 8 years of service were related to severe corrosion of steel strands embedded in deficient grout. Subsequent tendon inspections, repairs, and replacement were made where 15 other PT tendons in the bridge were deemed to have severe steel corrosion. At the time of inspection in 2011-2012, some instances of strand in this deficient grout did not exhibit severe corrosion, but corrosion activity assessment could not be easily validated in the field due to practical and technical constraints. Alternative assessment of strand corrosion within the tendons was highly desirable to verify the condition of the repaired tendons as well as the other tendons with possible grout separation or with more than five years since their previous assessment.

In Phase I of the project, several commercially available nondestructive testing technologies and the practitioners offering testing services were evaluated by means of blind mockup tests. An ultrasonic/sonic testing company (USTC) demonstrated their capabilities to use ultrasonic/sonic (impact echo) testing technology to identify grout anomalies within a duct. A magnetic main flux method testing company (MTC) successfully demonstrated their capabilities to detect steel strand metal loss with their modified magnetic main flux method (MMFM). The intent of the Phase II project was to document activities of the two companies selected for field testing of the Ringling bridge and provide them with support for on-site testing of external PT tendons of the Ringling bridge.

A compilation of submittals by USTC is presented in Section 2. This includes the scope of work, financial proposal, field testing, and technical memos from Florida International University (FIU) that reviewed the testing and submitted documentation. The submittals are included as Appendices A and B. The nondestructive testing of external PT tendons at Ringling bridge was carried out from Nov. 8 to Nov. 15, 2017 by USTC to identify tendon material deficiencies. In total, 44 tendons with an approximate length of 12,000 linear ft. were tested. USTC recommended four locations to be opened for verification.

Section 3 compiles the list of submittals by MTCs, including scope of work, proposal, field testing, and technical memos from FIU that reviewed the testing and submitted documentation. The submittals are included as Appendices C to E. The testing on external PT tendons was carried out using permanent magnet type MMFM. The field testing on the bridge was conducted from Feb. 5 to Feb. 21, 2018. Testing was conducted on all tendons (44 tendons) in the center aisle of the precast segments at all high free span and deviated portions of the tendons along with additional tendons. MTC proposed a list of recommended locations to be opened for verification.

A total of nine test sites were selected, based on the recommendations from USTC and MTC; one of the sites was an extra exploratory site (Site S) to assess a tendon duct deformation. A summary of opening of tendons for verification is given in Section 4. The tendon verification was carried out from July 9 to July 12, 2018. The results of the nondestructive technologies to assess the condition of the tendon were documented to provide a history of the condition of the tendon (in terms of cross-section loss by MMFM and general tendon material condition by ultrasonic/sonic testing). These baseline

results, presented in Section 5, may be useful if future monitoring by these nondestructive technologies is employed. The summary of results is provided in Section 6. After completion of validation testing, USTC and MTC assessed their results and provided their comments, which is provided in Section 7.

MMFM was able to detect severe strand corrosion at tendon location 403R-7 that was previously inspected in 2012. Also, MMFM accurately detected the presence and position of steel debris in tendon 303L-5. The lack of strong indicators of grout anomalies by ultrasonic/sonic testing would reflect the generally good condition of the grout in the previously inspected and repaired tendons. Ultrasonic/sonic testing did give differentiation in through-duct and circumferential resonant frequencies, and there were indicators that physical grout anomalies such as circumferential cracking can be sensed. However, better characterization of that defect modality should be made. Further refinement in data interpretation to identify grout cracking would provide useful assessment of tendon durability such as cracking induced by strand corrosion or strand breaks.

TABLE OF CONTENTS

Disclaimer	ii
Conversion Tables	iii
Technical Report Documentation	v
Acknowledgements	vi
Executive Summary	vii
List of Figures.....	xi
List of Tables.....	xii
List of Abbreviations and Acronyms	xiii
1 Introduction	1
1.1 Background Statement	1
1.2 Benefit to the State	1
1.3 Project Objectives	2
1.4 Organization of Report.....	3
2 Ultrasonic/sonic Testing	4
2.1 Introduction	4
2.2 Field Testing	4
2.3 USTC Proposal, Field Testing, and Tendon for Verification.....	5
3 Magnetic Main Flux Method Testing	7
3.1 Introduction	7
3.2 Field Testing	7
3.3 MTC Proposal, Field Testing, and Tendon for Verification.....	11
4 Tendon Validation Testing.....	12
4.1 Introduction	12
4.2 Summary of Field Testing.....	12
4.3 Field Testing Schedule and Summary of Important Findings.....	16
4.4 Detailed Field Notes by Concorr FL	21
4.5 Photo Documentation of Tendon Condition	26
4.6 Details of Photo Documentation of Tendon Condition	35
4.7 Test Validation	37
4.8 On-site Duct Openings and Test Validation Procedures	40
5 Bridge Tendon Base Condition	44
6 Summary.....	61
7 Comments of USTC and MTC after Validation Testing.....	65
7.1 USTC Comments on Validation Testing	65

7.2	MTC Comments on Validation Testing	68
	References	69
Appendix A	USTC Proposal (NDT Corp.).....	70
Appendix B	USTC Field Testing and Tendon Validation (NDT Corp.).....	77
Appendix C	MTC Proposal (Tokyo Rope Inc.).....	196
Appendix D	MTC Field Testing (Tokyo Rope Inc.).....	199
Appendix E	MTC Tendons for Verification (Tokyo Rope Inc.)	398
Appendix F	MTC Comments on Validation Testing (Tokyo Rope Inc.)	406

LIST OF FIGURES

Figure 2-1: Measurements on tendon (left) and high elevation tendon spans (right).	4
Figure 2-2: Testing on high elevation tendon and data processing unit.	5
Figure 3-1: Installation of search coil and magnetizer on PT tendon.	7
Figure 3-2: Installation of magnetizer at high elevations.	8
Figure 3-3: Offset of magnetizer from face of walls and deviators.	8
Figure 3-4: Scanning of tendons using MMFM.	10
Figure 4-1: Ultrasonic/sonic testing on external PT tendons.	13
Figure 4-2: MMFM testing on external PT tendons.	13
Figure 4-3: Tendon verification at site 1	16
Figure 4-4: Tendon verification at site 2	17
Figure 4-5: Tendon verification at site 4	17
Figure 4-6: Tendon verification at site 6	18
Figure 4-7: Tendon verification at site 3	18
Figure 4-8: Tendon verification at site 5	19
Figure 4-9: Tendon verification at site 7	19
Figure 4-10: Tendon verification at site 8	20
Figure 4-11: Tendon verification at site s	21
Figure 4-12 Circumferential and longitudinal cuts for tendon opening	40
Figure 4-13: Removal of HDPE pipe	40
Figure 4-14: Sampling of grout material	41
Figure 4-15: Documentation of corrosion activity	41
Figure 4-16: Half-cell potentials of steel strands	42
Figure 4-17: Temporary repair work on tendon	42
Figure 4-18: Permanent repair work on tendon	43
Figure 5-1: MTC tendon measurement procedures.	44
Figure 5-2: USTC tendon measurement procedures.	44

LIST OF TABLES

Table 1. Tendon site location.	15
Table 2. Reported test results and outcome of field tendon openings.....	39
Table 3. Tendon base condition.	45
Table 4. A summary table of field application of MMFM and ultrasonic/sonic testing....	61
Table 5. Field observations of tendon openings.....	62

LIST OF ABBREVIATIONS AND ACRONYMS

Acronym	Definition
FIU	Florida International University
MFL	Magnetic Flux Leakage
MMFM	Magnetic Main Flux Method
PT	Post-Tensioned
FDOT	Florida Department of Transportation
HDPE	High Density Polyethylene
LMA	Loss of Metal Area
UST	Ultrasonic/sonic Testing
USTC	Ultrasonic/sonic Testing Company
MTC	Magnetic Main Flux Method Testing Company

1 INTRODUCTION

1.1 BACKGROUND STATEMENT

Failures of two longitudinal external post-tensioned (PT) tendons in the Ringling causeway bridge in 2011 after approximately eight years of service were related to severe corrosion of steel strands embedded in deficient grout. The deficient grout was characterized as a segregated material with high moisture content and enhanced sulfate content. Subsequent tendon inspections, repairs, and replacement were made where 15 other PT tendons in the bridge were deemed to have severe steel corrosion. The tendon inspections required destructive opening of the high-density polyethylene (HDPE) duct to observe the grout and steel strand condition. As the external tendons were highly congested with 22, seven-wire strands placed within a four-inch diameter duct, only the outer surfaces of the strand bundle could be readily assessed by visual inspection after duct removal. The corrosion initiation sites can be highly localized supported by extended macrocell coupling, and unobserved steel loss within the strand bundle cannot be ruled out. The extent of grout segregations varied in magnitude. The most extensive corrosion occurred in soft deficient grout with moisture content sometimes as high as 80%; however, there was a larger amount of hardened segregated grout with moisture content greater than 20% which also contained enhanced pore water concentrations of aggressive ionic species thought to contribute to corrosion development. At the time of inspection in 2011-2012, some instances of strand in this deficient grout did not exhibit severe corrosion, but corrosion activity assessment could not be easily validated in the field due to practical and technical constraints. Also, there was a possibility that some of grout that facilitated corrosion initiation could not be fully removed, especially within strand interstitial sites, during repairs. In the repair cases where new grout was introduced with pre-existing grout, corrosion at local anodic regions may have been enhanced due to differences in grout chemical and electrical conditions.

Alternative assessment of strand corrosion within the tendons is highly desirable to verify the condition of the repaired tendons as well as the other tendons with various amount and degree of grout segregation after nearly five years since initial assessment. In Phase I of the project, several commercially available nondestructive testing technologies and the practitioners offering testing services were evaluated by means of blind mockup tests. NDT Corp. successfully demonstrated their capabilities to use ultrasonic/sonic (UST) or direct wave impact echo testing technology to identify grout anomalies within a duct. Tokyo Rope Inc. successfully demonstrated their capabilities to detect steel strand metal loss with their modified magnetic main flux (MMFM) method. Both companies expressed interest to provide services for on-site testing of external tendons in the Ringling bridge, and both companies provided cost proposals.

1.2 BENEFIT TO THE STATE

Testing by both companies allowed nondestructive evaluation (NDE) of the Ringling bridge with two different technologies to provide the State with important information of both identification of anomalous PT grout conditions and metal loss of the steel strand. This information is important for the State to determine further remediation and base

conditions for future assessments. Also, the testing will allow for useful case studies for two nondestructive technologies that may be considered for other bridge assessments.

1.3 PROJECT OBJECTIVES

The intent of the project was to document activities of the two companies selected for field testing of the Ringling bridge and provide them with support for on-site testing of external PT tendons of the Ringling bridge. The scope of this project differed from that specified in project BDV29-977-18 as follows:

- Documentation of the field tests to be conducted by consultants
- Staff from the Florida International University (FIU) will be present at the job site, during critical phases of the work to document the consultant's activities and provide the Florida Department of Transportation (FDOT) with better picture of time and efforts required to utilize the services and technologies offered by the two consultants.

Specific objectives and approach is proposed:

- **Vendors to conduct field testing and reporting.** The vendors will finalize their scope of work and then conduct field testing in the Ringling bridge.
- **Documenting Vendors Activities.** FIU staff will independently document the entire activities of ultrasonic/sonic testing company (USTC) and magnetic main flux method testing company (MTC).
- **Validate vendor assessment.** Each vendor at conclusion of their activities will submit a report to FIU that will provide their entire activities as well as their results and conclusions. The vendor reports will be evaluated by FIU staff. Select locations (at minimum two locations with testing identification of some deficiencies if detected and two locations with testing identification of no deficiency) will be physically tested by opening the ducts by FDOT to validate findings. This operation will be carried out by staffs identified by FDOT. The physical testing may include some sampling to be provided to FDOT but otherwise minimally invasive. Repairs will be made by FDOT.
- **Provide supporting evidence of nondestructive testing efficacy.** Each vendor will be asked to submit a complete report, at the conclusion of their testing. These reports together with validation tests, as described above, will be assessed by the FIU staff, to determine the effectiveness and efficiency of the nondestructive technologies used by each vendor. The efficiency of each technology and their field applications will be assessed based on the metrics developed in the volume II final report of project BDK80 977-13. Please see the reference section for complete citation of these final reports.
- **Identify tendon base conditions for future bridge assessments.** Based on the findings, results of the testing will be compiled to provide the FDOT with a report on the base condition of the tendons that can be consulted for future bridge assessments. The base condition should include both positive and negative findings as well as location and magnitude of deficiency if present.

1.4 ORGANIZATION OF REPORT

The report is organized into seven sections. Section 2 and 3 summarizes the activities of USTC and MTC, respectively. These sections include technical memo from FIU which reviews the testing and submitted documentation. The submittals of both vendors which includes proposal, field activities, and recommendation for tendon validation are provided from Appendix A to Appendix E. Section 4 presents the field activities during tendon validation testing and a summary of findings by FIU. The section also contains detailed notes by the Concorr FL, who was responsible for tendon opening and repair works. Section 5 provides a baseline condition of the tendons based on the results of the nondestructive technologies. The summary of results are provided in Section 6. After the tendon validation, both vendors submitted their comments which are provided in Section 7.

2 ULTRASONIC/SONIC TESTING

2.1 INTRODUCTION

The USTC carried out ultrasonic/sonic testing on external PT ducts with the aim of evaluating material deficiencies. This section contains the proposals and documentation of field activities by UTSC. An assessment of the field testing is presented by FIU in Section 2.2. The testing was carried on all tendons in central cell of all spans of the Ringling bridge. The testing commenced after mobilization, assemblage of scaffolding and safety protocols had been undertaken. The proposal is attached as Appendix A.

2.2 FIELD TESTING

The nondestructive testing of external PT tendons at Ringling bridge was started from Nov. 8, 2017, by USTC to identify duct filler deficiencies. Representatives of FIU were present throughout the testing and representatives of FDOT bridge office were present on Nov. 8, 14, and 15, 2017. A debriefing meeting between representative of FIU and USTC was made on Nov. 15, 2017. The access to the bridge was provided by District and ICA via a hatch on the west end. USTC used scaffolding to access the testing points along the profile of the tendons. Testing was conducted each day approximately from 8 am to 4 pm except for a break on Sunday Nov. 12, 2017. The detailed technical report is attached as 0.

A total number of 44 tendons with an approximate length of 12,000 linear ft. were tested. The central cell of the girder accommodates four tendons (401L, 401R, 402L, 402R) in all spans and two additional tendons (303R, 303L) in span 5 and 7. The testing was performed on all the tendons in the central cell. Some of the tested tendons were replacement tendons from earlier repairs in 2012.



Figure 2-1: Measurements on tendon (left) and high elevation tendon spans (right).

The full length of each tendon (including sections along the floor of the precast segments, along the free span with vertical deviation, and high elevation tendon spans) were tested as shown in Figure 2-1. Before commencing of testing, the tendons were marked at every one feet. The marking procedure was standardized to allow easy

retracing of possible defect locations. The length of tendon in intermediate spans was measured between the faces of pier/abutment diaphragm. At each measurement point, transducer and contact sensor were orthogonally positioned on circumference of tendon.

- Measurements were typically made at 2-ft intervals for tendons along the precast segment floor and along the deviated free span. Shorter intervals were sometimes made especially when measurements indicated some form of tendon anomaly.
- Measurements were always made at 1-ft intervals for high elevation tendon spans.
- Measurements typically were made in alternating sensor positions at 1-7 o'clock and 11-5 o'clock positions at the intervals described above for the deviated and high elevation tension spans. 3-9 o'clock sensor positions were used for the floor tendon spans due to low clearance.

A data acquisition system was used for processing data (Figure 2-2). There were early indications of tendon grout anomalies in tendon 401-7L. Three other locations in spans 1-6 showed results that may be indicative of voids. The testing was completed by Nov. 15, 2017 and it was believed that field testing requirements have been met by USTC.

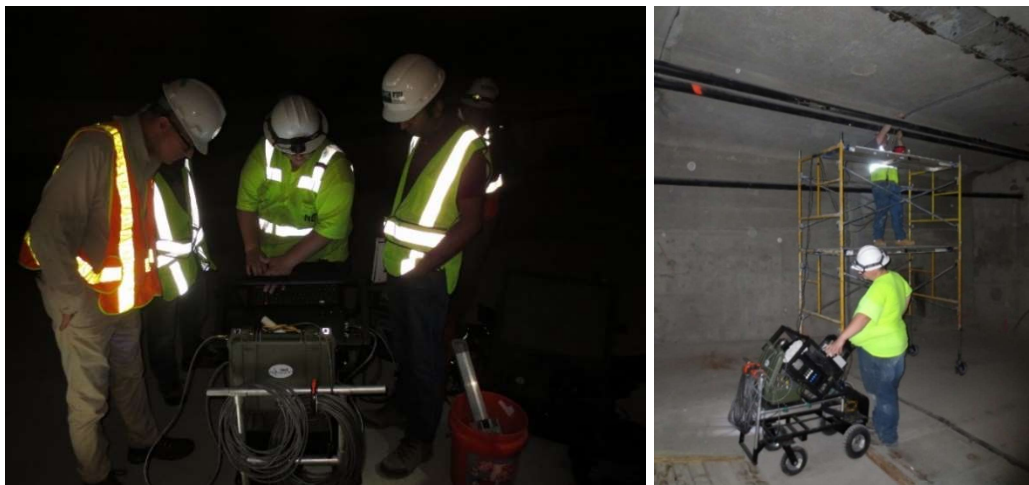


Figure 2-2: Testing on high elevation tendon and data processing unit.

2.3 USTC PROPOSAL, FIELD TESTING, AND TENDON FOR VERIFICATION

The proposal submitted by USTC is attached as Appendix A. The proposal contains the work plan and brief description of the testing procedure. Based on the work plan, USTC anticipated that 25% to 33% of the tendons can be tested in six days. For the scope of work, a breakdown of cost was provided. The total cost of testing by USTC was \$70,305. A detailed field testing report (Appendix B) was submitted by USTC after the conclusion of testing.

The report summarizes the calibration procedures, test protocols, results and recommendations for tendon verification. The calibration study was carried on salvaged

tendon segments at FDOT materials department, Gainesville, FL. The salvaged tendon segments were extracted during earlier repairs at Ringling bridge. USTC provided their interpretation of data obtained from the tendons in terms of resonant frequencies. The detailed results, present in Appendix B, are shown graphically (Page 111-195) and summarized in tabular form (Page 91-100) for each tendon segment. Based on the data analysis, USTC recommended four test sites having anomalous grout conditions, to be opened for verification purpose.

3 MAGNETIC MAIN FLUX METHOD TESTING

3.1 INTRODUCTION

MTC carried out testing on external PT tendons using MMFM with the aim of evaluating steel section loss. The testing was carried on upper horizontal and sloped regions of center cell and some additional tendons in right and left cell. An assessment of the field testing by FIU is presented in Section 3.2. The section provides overview of submittals of MTC which are referenced from Appendix C to Appendix E.

3.2 FIELD TESTING

MTC has demonstrated field applicability of permanent magnet type MMFM. The equipment consists of a magnetizer, a controller and data acquisition system. This MMFM technology does not require external power sources making it a feasible choice when testing sites with no power access. The magnetizer assembly consisting of search coil and permanent magnet was wound over the external PT as shown in Figure 3-1. The installation of the magnetizer on the tendon was accomplished in a short period of time.

Testing was only carried on high horizontal and inclined tendons. The low horizontal tendons were not tested due to low clearance. After the MMFM assembly was installed on the tendon, the magnetization of the tendon was carried multiple times before a reading was taken. The installation at high elevations required use of ladders, and a pulley assembly was used to move the magnetizer along the length of tendon (Figure 3-2).



Figure 3-1: Installation of search coil and magnetizer on PT tendon.

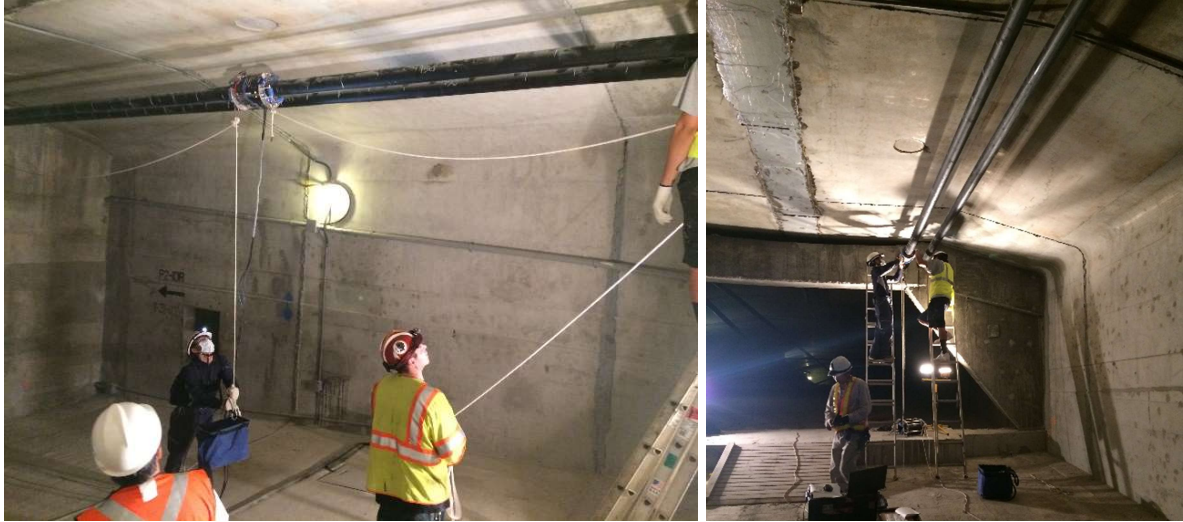


Figure 3-2: Installation of magnetizer at high elevations.

The lengths of the segments were measured between the walls and diaphragm. However, the starting point for magnetizer assembly was away from the face of the walls due to increased thicknesses of the HDPE sheathing at these locations as shown in Figure 3-3. Few locations on the tendon spans had spiral deformation which caused irregular movement and bumping of magnetizer. The joint in the HDPE was typically located between the scanned segments causing an abrupt change in signal. The location of this joint was recorded so that it may not be confused with a defect signal. Typically for each tendon, multiple readings were taken. Based on preliminary data, additional readings were taken or if an anomalous signal was encountered.



Figure 3-3: Offset of magnetizer from face of walls and deviators.

The MTC was efficient and robust method for scanning the tendon segments. The logistics from one span to the next was relatively easy due to portability of the equipment. MTC typically used two magnetizer units in parallel. While one team of crew magnetized the tendon, the other crew took readings for the next tendon segment. A

typical tendon segment consisted of 16 tendon sections (8 horizontal and 8 inclined). MTC were initially able to scan about 12 sections per day which improved to about 24 sections at later stages of testing. The testing at inclined tendon sections was more robust than high horizontal sections. One of the main advantages of MMFM technology was identification of anomalous signal during testing. The data was processed in real-time using data acquisition system and a laptop. This identification at the location allowed the MTC to take multiple verification readings on test site.

The nondestructive testing on external PT tendons of Ringling bridge by MTC was carried by MTC to identify steel strand corrosion. A pre-test meeting was made on Feb. 04, 2018 with FIU representatives and a contingent from MTC. The field testing on the bridge was conducted from Feb. 05 to Feb. 21, 2018. A debriefing meeting between representatives of FIU, MTC, and FDOT bridge office was made on Feb. 21, 2018. Bridge access from the west access hatch was provided by District and ICA. The field testing, conducted approximately 8am to 5pm each day, typically consisted of 5 crew members including two specialists from MTC and three assistants. Representatives from FIU, including the principal investigator, were present on Feb. 5-9, 13-16, 21 to monitor the testing and FDOT bridge office representatives were present for several days throughout the course of the field testing. The detailed technical report is attached as Appendix D.

In the time and budget allocated for the testing and demonstration, MTC was able to test additional tendon sites beyond the original agreed-upon scope, demonstrating field practicality. In total, MTC conducted testing on following tendons:

- All tendons (44 tendons) in the center aisle of the precast segments at all high free span and deviated portions of the tendons (401L, 401R, 402R, 402L)
- Additional tendons in center aisle in Span 5 and 7 (303R and 303L)
- Additional tendons in Span 8 and 9 on the left and right segment aisles

Only the high free span and deviated portions of each tendon were tested. Tendon locations with low clearance inhibited the movement of the sensor and were not tested. Scaffolding was not needed as the sensor head could be placed at lower tendon elevations using extension ladders as shown in Figure 3-4. Measurements were typically made continuously along the length of the tendons in the high free span and deviated portions of the tendons via installment of a temporary pulley system or manual carriage. Some tendon locations directly adjacent to concrete deviators that had excess repair wrap material prohibiting placement of the sensor (up to 2 feet) were not tested. Tendons that had deformation of the HDPE duct were tested without major disruption to test procedures.



Figure 3-4: Scanning of tendons using MMFM.

there were early indications of strand metal loss approximately 2-3% at three locations on two tendons (P9-406L and P9-401L). Several tendon locations throughout the tendons had indication of loss of metal area (LMA) less than 1%. MTC has provided tentative recommendations for tendon openings:

- P9-406L-I1
 - near 4 m and 16 m
 - around 4 m: approximately 3% LMA
 - around 16 m: approximately 3% LMA
 - around 9 m: very small LMA
 - around 13 m: could be the joint
- P9-406L-H1
 - near 4–6 m
 - around 3–6 m: approx.2% LMA
- P9-401L-H2
 - near 5m
 - around 5–6 m: approx. 1% LMA
 - around 10–15 m: approx. 1% LMA

Also several locations showed an increase in flux that may be indicative of increased metal section. This was thought to be due possible metal debris contamination; opening

at some of these locations may be of interest. All testing was completed by Feb. 21, 2018 and it was believed that field testing requirements have been met by MTC.

3.3 MTC PROPOSAL, FIELD TESTING, AND TENDON FOR VERIFICATION

MTC submitted the quotation and proposal which is attached as Appendix C. The proposal includes the work plan and an index for reporting of steel section loss. The quotation includes detailed breakdown of cost. The total cost of testing by MTC was \$178,531.

The field testing report, attached as Appendix D, was submitted at the conclusion of field testing. The report summarizes the system calibration, test protocols, results, and recommendations for tendon verification. Before commencement of testing at the bridge site, a calibration of the MMFM system was carried out at the FDOT Manatee Operations Center. This calibration was carried on salvaged tendon extracted during Ringling bridge repairs. These salvaged tendons were unstressed segments of limited length and allowed a pretest calibration of testing equipment. Test results were provided for the salvaged tendon segments for different calibration scenarios.

The field testing results are tabulated from Page 235 to 244 of Appendix D. These tables summarize the location, orientation, and estimation of cross-section loss. The results from different sensors are graphically shown for all tested locations from Page 267 to 397. Based on the results, MTC recommended locations of sectional loss for verification purposes which is attached as Appendix E. Among the proposed locations, one site showed an increase of magnetic flux. All proposed tendon verification sites demonstrated a cross-section loss of less than 5%.

4 TENDON VALIDATION TESTING

4.1 INTRODUCTION

At the conclusion of field testing, both vendors submitted their detailed reports to FIU. The reports provided detailed results and recommendations for tendon openings. FIU summarized the testing of USTC and MTC in Section 4.2 and provided a list of select locations identified by these vendors. For the physical opening of the tendons, FDOT identified Concorr FL as a specialized vendor to carry out the tendon opening and repair. The field validation testing was carried out by Concorr FL between July 09-12, 2018 which was also attended by representatives of FIU, USTC and MTC. The summary of field activities during tendon validation is summarized by FIU in Section 4.3. Concorr FL followed FDOT guidelines for opening and repair of tendons and documented their field activities independently which is provided in Section 4.4 to 4.6. At the conclusion of tendon validation, FIU assessed the findings in light of the recommendations of both vendors and provided a summary of results in Section 4.7.

4.2 SUMMARY OF FIELD TESTING

Nondestructive testing including UST and MMFM was conducted on portions of the external PT tendons in the Ringling bridge by USTC and MTC, respectively. The testing was conducted in part to identify capabilities of the technology in the assessment of external tendons (including grout deficiencies and corrosion of steel strand) as well as to provide condition assessment of external tendons in the Ringling bridge after previous inspection and repairs made in 2012 (after identification of severe corrosion due to the presence of deficient grout).

Ultrasonic/sonic testing conducted on Nov. 8-15, 2017 by USTC was made to identify tendon material deficiencies. USTC conducted ultrasonic/sonic testing on all tendons (44 tendons) in the center aisle of the precast segments at all locations (tendons 402L, 401L, 402R, 401R and additional tendons in spans 5 and 7). Some of the tested tendons were replacement tendons from earlier repairs in 2012.

The full length of each tendon (including sections along the floor of the precast segments, along the free span with vertical deviation, and high elevation tendon spans) were tested. Measurements were typically made at 2-ft intervals for tendons along the precast segment floor and along the deviated free span. Shorter intervals were sometimes made especially when measurements indicated some form of tendon anomaly. Measurements were always made at 1-ft intervals for the high elevation tendon spans. Measurements typically were made in alternating sensor positions at 1-7 o'clock and 11-5 o'clock positions at the intervals described above for the deviated and high elevation tendon spans. 3-9 o'clock sensor positions were used for the floor tendon spans.



Figure 4-1: Ultrasonic/sonic testing on external PT tendons.

Although it was understood that data interpretation requires processing and analysis, there were early indications of tendon grout anomalies in tendon 401-7L. Three other locations in spans 1-6 showed results that may be indicative of voids. After receipt and review of report of test results provided by USTC, a revised list of recommended locations to be opened for verification included:

- Span 1 Duct 401L-1W Station 167 [Test Site 7]
- Span 2 Duct 402L-1E Station 114 [Test Site 3]
- Span 4 Duct 401L-3E Station 139 [Test Site 6]
- Span 1 Duct 401R-1W Station 44 [Test Site 8]

Test sites 7, 3, and 6 did not show impact echo resonant frequencies associated with through-duct resonance (20 or 25 kHz) or circumferential resonance (15 kHz). Test site 8 showed no through duct resonance but maintained circumferential resonance. Verification site candidates are shown in Table 1.

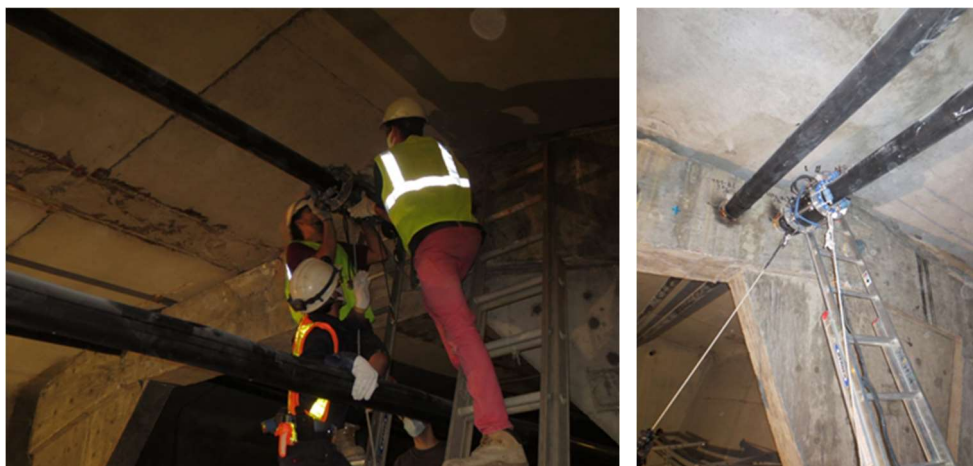


Figure 4-2: MMFM testing on external PT tendons.

MMFM testing on the external tendons on Feb. 5-22, 2018 by MTC was conducted to identify steel strand corrosion. In the time and budget allocated for the testing and demonstration, MTC was able to test additional tendon sites beyond the original agreed-upon scope, demonstrating field practicality. In total, MTC conducted MMFM testing on all tendons (44 tendons) in the center aisle of the precast segments at all high free span and deviated portions of tendons (tendons 402L, 401L, 401R, 402R and additional tendons 303R and 303L in spans 5 and 7) as well as additional tendons in span 8 and 9 on the left and right segment aisles.

Only the high free span and deviated portions of each tendon were tested. Tendon locations with low clearance inhibited the movement of the sensor and were not tested. Measurements were typically made continuously along the length of the tendons in the high free span and deviated portions of the tendons via installment of a temporary pulley system or manual carriage. Some tendon locations directly adjacent to concrete deviators that had excess repair wrap material prohibiting placement of the sensor (up to 2 feet) were not tested. Tendons that had deformation of the HDPE duct were tested without major disruption to test procedures.

Although it's understood that data interpretation requires processing and analysis, there were early indications of strand metal loss about 2%–3% at three locations on two tendons (P9-406L and P9-401L). Several tendon locations throughout the tendons had indication of metal loss less than 1%. After preliminary analysis, MTC provided tentative recommendations for tendon openings including P9-406L-I1, P9-406L-H1, and P9-401L-H2. Also several locations showed an increase in flux that may be indicative of increased metal section. This was thought to be due to possible metal debris contamination. After receipt and review of report on field results received from MTC in March and updated final report in May 2018, a revised list of recommended locations to be opened for verification included:

- P9-406L-I1 [Test Site 2]
- P8-403R-H1 [Test Site 1]
- P5-402L-H1 [Test Site 5]
- P9-405L-I2 [Location not selected]
- P5-303L-I4 [Test Site 4]

From the recommendation list, test sites 2, 1, and 5 were made candidates to identify steel cross-section loss and test site 4 was made candidate to identify mass increase. It is noted that at the request of MTC on site of test verification, test site 5 was replaced with an alternative location P2-402L-I1 [Test Site 5a] to be opened. Verification site candidates are shown in Table 1. The onsite duct openings and test validation procedures are explained in Section 4.8.

Table 1. Tendon site location.

Site	Label	Span	Cell	Tendon	Place	Height	Location	Length	(o'clock)	Defect*
1‡	P8-403R-H1	8	Right (South)	403R-7	Hi Hor.	~14'	9'10" from Pier 8	2.6' (2' 7.2")	10-12	1.5% CS
2‡	P9-406L-I1	9	Left (North)	406L-8	Slope	~8'	12.8' (12' 9.6") from high deviator	3.6' (3' 7.2")	2-4	1.4% CS
3	S2-402L-1E S114	2	Center	402L-1	Low Hor.	Low	Station 114 (~14' from low deviator)	~10' (S107-117)		No 15 kHz, No 20-25 kHz
4	P5-303L-I4	5	Center	303L-5	Slope	~11'	19' from high deviator	0.7' (7.9")	4-7	(-)2.2% CS
5	P5-402L-H1	5	Center	402L-4	Hi Hor.	~14'	24.6' (24' 7.3") from Pier 5	4.6' (4' 7")	8-11	1.3% CS
5a†	P2-402L-I1	2	Center	402L-1	Slope	<10'	26.9' from high deviator	~6'	6-8	2.4% CS
6	S4-401L-3E S139	4	Center	401L-3	Low Hor.	Low	Station 139 (Near anchor)	~4' (S138-142)		No 15 kHz, No 20-25 kHz
7	S1-401L-1W S167	1	Center	401L-1	Hi Hor.	~14'	Station 167 (Near Pier 2)	~5' (S164-169)		No 15 kHz, No 20-25 kHz
8	S1-401R-1W	1	Center	401R-1	Slope	~3'	Station 44 (~44' from anchor, Near low deviator)			15 kHz, No 20-25 kHz
S†	402R Span 8	8	Center	402R-7	Slope	<5'	489" from low deviator	Periodic on tendon	12	Visual Duct Deformation

† Alternative or Additional Test Site

‡ Additional Test Site for USTC.

* CS- Cross-Section (negative value indicated mass increase)

4.3 FIELD TESTING SCHEDULE AND SUMMARY OF IMPORTANT FINDINGS

Repair of ducts was multi-step requiring more than 1 day. Repair procedures were made on the third and fourth day and are not elaborated in the schedule below.

Day 1 - 07/09/18

- Briefing at Ringling bridge hatch at west abutment with representatives from FIU, Concorr FL, USTC, and MTC. Bridge access was provided by DBi.
- Receive scaffolding.

TEST SITE 1 (403R-7)

- Tendon opening recentered to 9'10" off of Pier 8 wall per recommendation by MTC.
- Opening of 1' tendon segment revealed deficient grout and severe steel corrosion. Pits up to 1.77 mm depth.
- Open circuit potentials -150 to -260 mV_{CSE}. Deficient grout pH 9-11. Hardened grout pH 13.

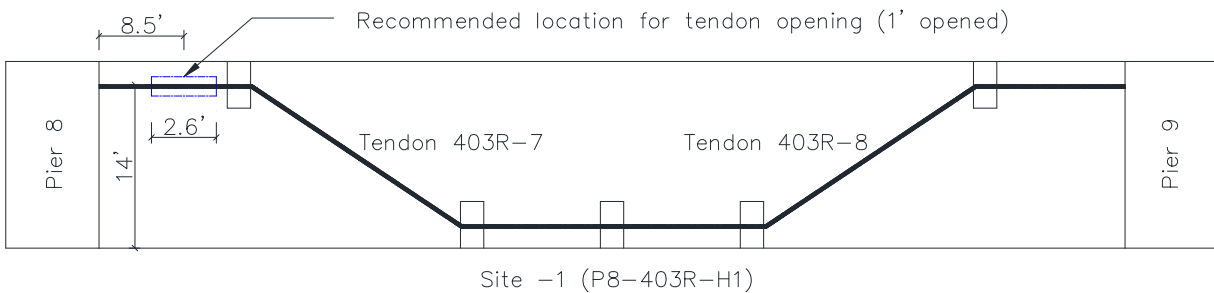


Figure 4-3: Tendon verification at site 1

TEST SITE 2 (406L-8)

- Opening of 16" tendon segment revealed grout bleed trail (about 7 mm depth) at 12 o'clock position with accumulated carbon black/silica fume.
- Grout bleed trail pH 9-11. Freshly fractured hardened grout pH 11.
- Open circuit potential -111 to -211 mV_{CSE}.



Figure 4-4: Tendon verification at site 2

Day 2 - 07/10/18

TEST SITE 4 (303L-5)

- Opening of 1' tendon segment revealed grout bleed trail at 12 o'clock position with grout pH 9 but no indication of steel corrosion.
- Steel debris embedded within tendon grout revealed around 7 o'clock position. Ball-headed smooth hollow cylindrical steel pin (about 8.5 cm length) embedded parallel lengthwise to the tendon.

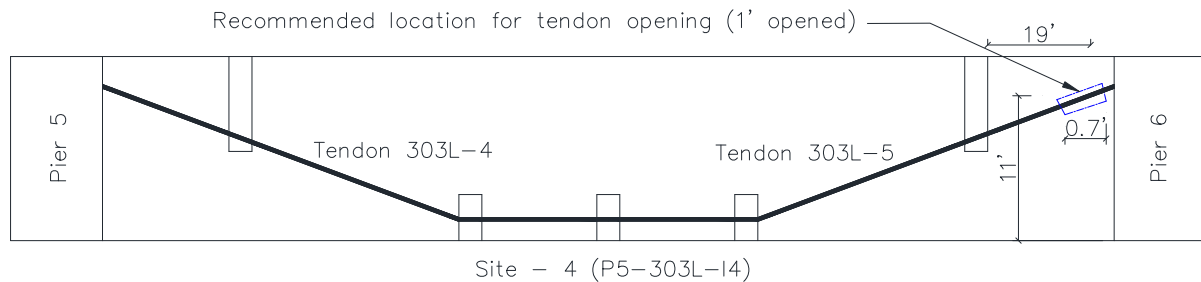


Figure 4-5: Tendon verification at site 4

RETURN TO TEST SITE 2 (406L-8)

- Additional grout removed from test site 2. No indication of strand corrosion. Normal hardened grout observed outside of 12 o'clock bleed trail.
- Observation of strand bundle clustering at approx. 9 o'clock position. Grout cover depth at 9 o'clock (0 mm). Grout cover depth at 3 o'clock position (18 mm).

TEST SITE 6 (401L-3)

- Opening of 1' tendon segment revealed minor bleed trail at 12 o'clock but normal hardened grout elsewhere throughout.

- Observation of strand bundle clustering towards bottom tendon cross-section. Grout cover depth at 12 o'clock (20 mm).

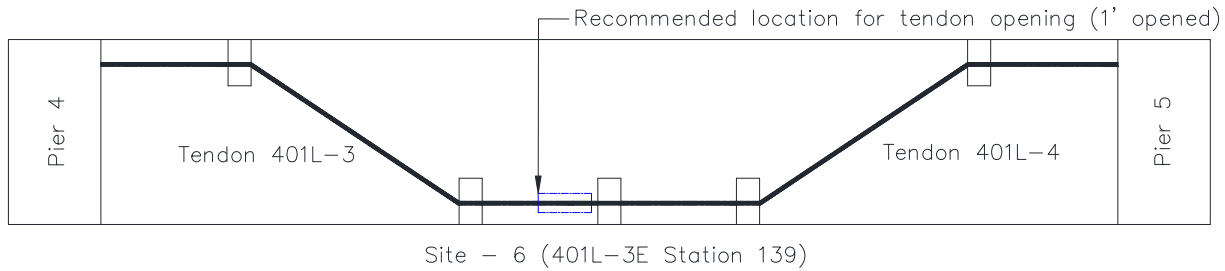


Figure 4-6: Tendon verification at site 6

TEST SITE 3 (402L-1)

- Opening of 1' tendon segment revealed minor bleed trail at 12 o'clock position with friable dark grey grout particles. Strand at bleed trail retained bright finish.
- Grout from tendon interior showed no deficiency and no indication of corrosion activity.

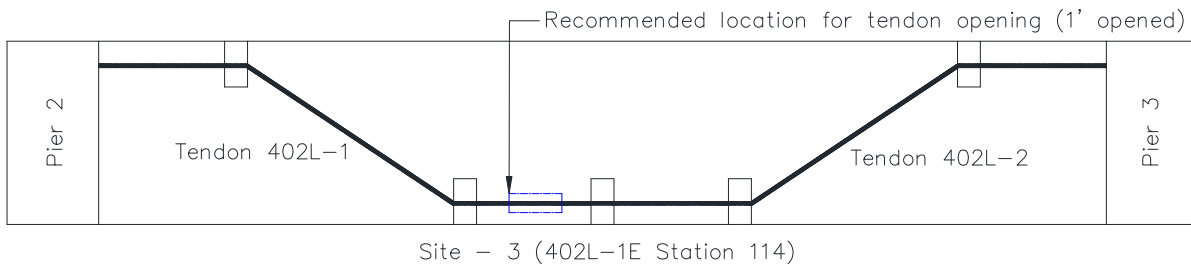


Figure 4-7: Tendon verification at site 3

RETURN TO TEST SITE 2 (406L-8)

- Small window opened about 80" east of initial opening site. Removal of grout indicated similar strand bundling as in the initial opening site. Grout cover depth at 3 o'clock position (11 mm).

Day 3 - 07/11/18

ALTERNATIVE TEST SITE 5 (402L-1)

- Per request by MTC, an alternative site on tendon 402L-1 (around 8.2 m from the high deviator) was tested instead of Site 5.
- Opening of 1' tendon segment revealed abnormal grout at bleed channel at 12 o'clock position but normal hardened grout elsewhere with no indication of

strand corrosion. pH 9 on surface at bleed trail and pH 13 on surface of hardened grout.

- Observation of well-distributed strand within the cross-section of the tendon duct.
- Open circuit potential was -108 to -194 mV_{CSE}.
- Per request by MTC, a second 1' opening was made 1 m west of the initial opening (approximately 23.6' from the high deviator). The HDPE duct at this position had a deformed squashed cross-section. Opening revealed small bleed channel at 12 o'clock and normal hardened grout elsewhere.

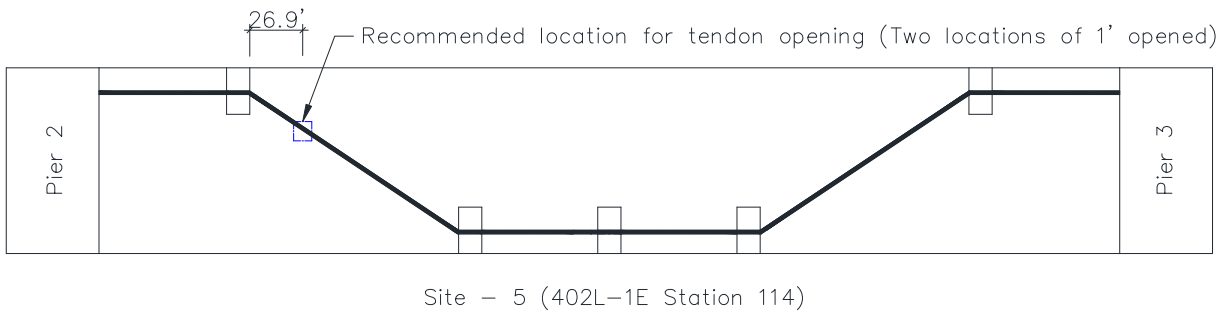


Figure 4-8: Tendon verification at site 5

TEST SITE 7 (401L-1)

- Opening of 1' tendon segment revealed small bleed trail at 12 o'clock position with friable grout showing impressions of air bubbles.
- Duct delamination could not be discerned.
- Observation of deep fine transverse cracking up to 4 mils in width.

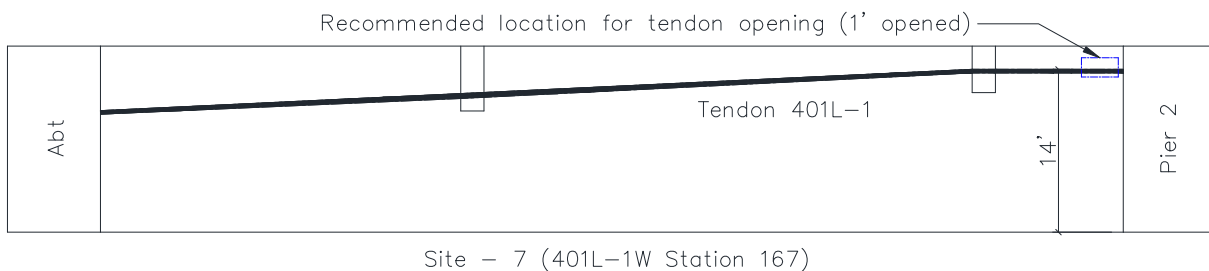


Figure 4-9: Tendon verification at site 7

RETURN TO TEST SITE 3 (402L-1)

- Fine transverse cracks observed.

RETURN TO ALTERATIVE TEST SITE 5 (402L-1)

- Fine transverse cracks observed.

RETURN TO TEST SITE 6 (401L-3)

- Several circumferential hairline cracks.

RETURN TO TEST SITE 4 (303L-5)

- Several circumferential hairline cracks

TEST SITE 8 (401R-1)

- Opening of 1' tendon segment revealed bleed train at 12 o'clock position with friable grout.
- Numerous circumferential hairline cracks.

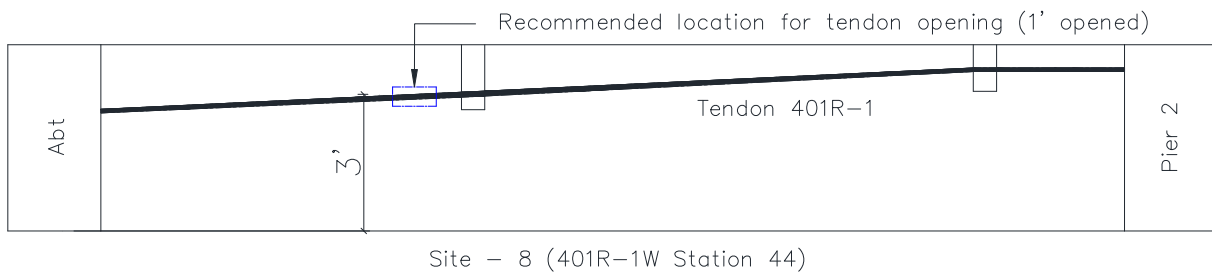


Figure 4-10: Tendon verification at site 8

Day 4. 07/12/18

ADDITIONAL TEST SITE "S" (402R span 8)

- Replacement tendon showed periodic spiraling deformation on the HDPE duct.
- 6" opening made at 489" west of the low deviator on a hump portion of the deformed HDPE.
- Opening revealed loose or broken strand following the contour of the spiral deformation. Movement of wires can be made by placement of a screwdriver between wires.
- No steel corrosion observed.
- No deficient grout observed.
- No cracking or physical damage of grout observed.

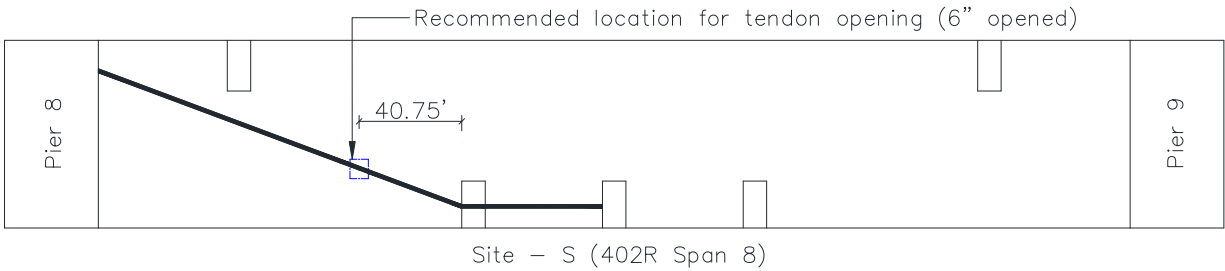


Figure 4-11: Tendon verification at site s

- Cleanup and scaffolding return.

4.4 DETAILED FIELD NOTES BY CONCORR FL

The following field notes were taken by Concorr FL during tendon validation. Concorr FL was identified as a specialized vendor to carry out tendon opening and repair.

Post-tensioned strands and grout were investigated at select external tendons in the Ringling bridge from July 9 to 12, 2018. The investigations were conducted by representatives from Florida International University and Concorr FL. Representatives from NDT Corp. (USTC) and Tokyo Rope (MTC) were also present during all of the investigative work.

The investigations were conducted after removing small sections of polyethylene duct at a total of eight pre-selected locations on various tendons. Field notes collected by Bill Scannell (representative of Concorr FL) at each of the locations that were investigated are summarized below. All of the clock positions referred to below are referenced when looking up-station. The pH measurements referred to below were obtained using a liquid indicator provided by Kingsley Lau (representative of FIU). The color scale provided on the pH indicator bottle included a pHs of 5, 7, 9, 11, and 13. 'Stations' in the field notes refer to one foot increments along tendons that had been previously marked on the ducts by NDT Corp. (USTC).

After the investigation was completed at each location, the exposed strands and grout were temporarily protected by tightly wrapping the area with Saran wrap. Permanent repairs were made after all of the investigation work was completed. Masterflow 1205 grout and Canusa wraps were used to make the permanent repairs. All of the material samples that were collected during the investigation were given to a representative of FIU.

Location P8-403R-H1 [Test Site 1]

A 12"-long section of duct was removed, and the center of the opening was 9'-10" east of the pier wall. There was a mix of white, gray, and black crumbling grout centered at 12 o'clock. The abnormal grout was concentrated in an area

about 3 $\frac{1}{2}$ " wide by $\frac{1}{2}$ " deep. All of the remaining grout was of normal color, consistency, and hardness. There were three corroded strands in the abnormal grout at 11, 12, and 1 o'clock. The corrosion products consisted mostly of red rust, but there were a few small areas with black corrosion products. The corroded strands exhibited severe corrosion and extensive pitting after being cleaned using a wire brush. The depth of the pitting was measured on individual wires using a gauge provided by Kingsley Lau (representative of FIU) and measurements at two locations that represented worst-case conditions were 1.44 mm and 1.77 mm. There was a $\frac{1}{2}$ " deep void at 12 o'clock, and the void extended along the entire length of the opening. The width of the void could not be estimated due to the location of the corroded strands. Samples of the abnormal and normal grouts were collected (total of two samples). The pH of the normal grout was 13. As a result of extracting a sample of the normal grout, two strands with no corrosion were exposed at 3 and 4 o'clock.

Location P9-406L-I1 [Test Site 2]

The length of the duct opening was changed from 12" to 16" at the request of Tokyo Rope. The center of the opening was 12'-10" from the high deviator. There was a mix of white and black crumbling grout centered at 12 o'clock. The abnormal grout was concentrated in an area about $\frac{11}{16}$ " wide by $\frac{9}{32}$ " deep. All of the remaining grout was of normal color, consistency, and hardness. There was a $< \frac{1}{8}$ " deep void at 12 o'clock, and the void extended along the entire length of the opening (the void may have been an indent in the grout as opposed to an actual void). Samples of the abnormal and normal grouts were collected (total of two samples). The pH at 12 o'clock after the sample of abnormal grout was collected was 9. The pH of the normal grout was 11. As a result of extracting the grout samples, two strands with no significant corrosion were exposed at 12 and 10 o'clock (i.e. in abnormal and normal grout respectively).

Based on subsequent findings at different tendons, this location was revisited twice in order to conduct additional investigations. The purpose of the additional investigations was twofold; 1) to confirm whether or not there was any loss in the steel mass at this location and 2) to assess the position of the strands in the grout (i.e. to determine if the strands were concentrated to one side of the duct). The grout was removed in about a 4" wide strip located in the center of the original opening lengthwise and around the entire circumference of the tendon. No section loss or other abnormalities were observed on any of the strands that were exposed after the grout was removed. In addition, a second and smaller duct opening (3 $\frac{1}{2}$ " wide by 3" high) was made on the south side of the duct about 79 $\frac{1}{2}$ " up station from the original opening. No wires were exposed upon removing the duct. Grout was then removed to expose strands and Kingsley Lau (representative of FIU) took measurements in the original opening and in the second opening to assess if there was any difference in the position of the strands.

Location S2-402L-1E S114 [Test Site 3]

A 12"-long section of duct was removed and the center of the opening was at Station 114. Only the top half of the duct was removed due to the limited space between the bottom of the duct and the concrete floor at this location. There was a mix of dark gray and black soft grout centered at 12 o'clock. The abnormal grout was concentrated in an area about 1" wide by $< \frac{1}{8}$ " deep. No corrosion was observed on portions of wires that were exposed in the abnormal grout. No void was found and all of the remaining grout was of normal color, consistency, and hardness. The grout was removed in about a 2" wide strip located in the center of the opening lengthwise and around the entire circumference of the tendon. A sample of the grout was collected during this process. The sample consisted of normal and abnormal grout, but most of the sample was comprised of normal grout. No corrosion was observed on any of the strands that were exposed after the grout was removed, including portions of the strand that had been encased in abnormal grout, and no other grout deficiencies were found.

Based on subsequent findings at a different tendon, this location was revisited to determine if there was any cracking in the grout. Circumferential cracks with a maximum width of 4 mils were found in the grout on the south side of the opening.

Location P5-303L-14 [Test Site 4]

A 12"-long section of duct was removed and the center of the opening was 19' from the high deviator. There was a mix of white, gray, and black crumbling grout centered at 12 o'clock. The abnormal grout was concentrated in an area about $1\frac{1}{2}$ " wide by $\frac{1}{8}$ " deep. No void was found and all of the remaining grout was of normal color, consistency, and hardness. There was a portion of a strand exposed in the abnormal grout and no significant corrosion was observed. There was also a piece of miscellaneous steel (the type of metal was solely determined using a magnet) exposed at 7 o'clock. This piece of steel was removed by chipping away grout. The miscellaneous steel looked like some type of pin that consisted of a solid ball of steel attached to a hollow steel tube. The total length of the steel element was $3\frac{7}{16}$ " and the outside and inside diameters of the steel tube were $\frac{3}{4}$ " and $\frac{5}{8}$ " respectively. No corrosion was observed on the miscellaneous steel element. Samples of the abnormal and normal grouts were collected (total of two samples). The sample of the normal grout was extracted immediately adjacent to the miscellaneous steel. The pH at 12 o'clock after the sample of abnormal grout was collected was 9. As a result of extracting the grout samples, more of the strand that was in the abnormal grout was exposed and four strands were exposed in normal grout. No corrosion was observed on any of the strands.

Location S4-401L-3E S139 [Test Site 6]

A 12"-long section of duct was removed and the center of the opening was at Station 139. Only the top half of the duct was removed due to the limited space between the bottom of the duct and the concrete floor at this location. All of the

grout was of normal color, consistency, and hardness and no voids were found. The grout was removed in about a 2" wide strip located in the center of the opening lengthwise and around the entire circumference of the tendon. A sample of the grout was collected during this process. No corrosion was observed on any of the strands that were exposed after the grout was removed and no grout deficiencies were found.

Based on subsequent findings at a different tendon, this location was revisited to determine if there was any cracking in the grout. Circumferential cracks with a maximum width of 4 mils were found in the grout.

Location S1-401L-1W S167 [Test Site 7]

A 12"-long section of duct was removed and the center of the opening was at Station 167. There was a mix of dark gray and black abnormal grout centered at 12 o'clock. The abnormal grout was concentrated in an area about $\frac{7}{8}$ " wide by $\frac{1}{16}$ " deep. No portion of any wire was directly exposed anywhere in the duct removal area. No void was found and all of the remaining grout was of normal color, consistency, and hardness. However, there were several circumferential cracks in the grout that were a maximum of 4 mils wide. The grout was removed in about a 1 $\frac{1}{2}$ " wide strip located in the center of the opening lengthwise and around the top half of the circumference of the tendon. A sample of the grout was collected during this process. The sample consisted of normal and abnormal grout, but most of the sample was comprised of normal grout. No corrosion was observed on any of the strands that were exposed after the grout was removed, including a strand at 12 o'clock, and no other grout deficiencies were found.

Location S1-401R-1W S44 [Test Site 8]

A 12"-long section of duct was removed and the center of the opening was at Station 44. The duct was removed after cracks were found in the grout at other tendon locations. To assess whether the duct removal process could be causing cracks in the grout, the duct at this location was removed without using a hammer or pry bar. Upon removing the duct, circumferential cracks with a maximum width of 4 mils were found in the grout. There was a mix of dark gray and black abnormal grout centered at 12 o'clock. The abnormal grout was concentrated in an area about $\frac{7}{8}$ " wide by $\frac{1}{16}$ " deep. Portions of wires were exposed at 11, 3, and 9 o'clock. The grout around the perimeter of the wires at 11 o'clock was black. The grout around the perimeter of the wires at 3 and 9 o'clock was white. No corrosion was observed on any of the exposed wires. All of the remaining grout was of normal color, consistency, and hardness and no voids were found. The grout was removed in about a 1 $\frac{1}{2}$ " wide strip located in the center of the opening lengthwise and around the top half of the circumference of the tendon. A sample of the grout was collected during this process. The sample consisted of normal and abnormal grout, but most of the sample was comprised of normal grout. No corrosion was observed on any of the strands that were exposed after the grout was removed, including the strand at 11 o'clock and a strand at 12 o'clock, and no other grout deficiencies were found.

Location P2-402L-I1 (originally P5-402L-H1 but changed at the request of Tokyo Rope [MTC]) [Test Site 5a]

A 12"-long section of duct was removed and the center of the opening was 26.9' from the high deviator. There was a mix of dark gray and black abnormal grout centered at 12 o'clock. The abnormal grout was concentrated in an area about 1½" wide by ⅛" deep. Portions of wires were exposed at 2, 4, and 9 o'clock. The wires at 2 o'clock were covered with black abnormal grout. The grout around the perimeter of the wires at 4 and 9 o'clock was white and the exposed portions of the wires exhibited no corrosion. All of the remaining grout was of normal color, consistency, and hardness and no voids were found. The grout was removed in about a 2" wide strip located in the center of the opening lengthwise and around the entire circumference of the tendon. A sample of the grout was collected during this process. The sample consisted of normal and abnormal grout, but most of the sample was comprised of normal grout. The pH at 12 o'clock after the grout sample was collected was 13. No corrosion was observed on any of the strands that were exposed after the grout was removed, including portions of strands that had been encased in abnormal grout, and no other grout deficiencies were found.

At the request of Kingsley Lau (representative of FIU), a second 12"-long section of duct was removed 42" up station from the original opening. The duct at this location was deformed and was more of an oval shape than a circular shape. The only noteworthy finding was a strand at 9 o'clock that appeared to be positioned at an angle.

Based on subsequent findings at a different tendon, both of the openings at this location were re-examined to determine if there was any cracking in the grout. Circumferential cracks with a maximum width of 4 mils were found in the grout at both of the openings.

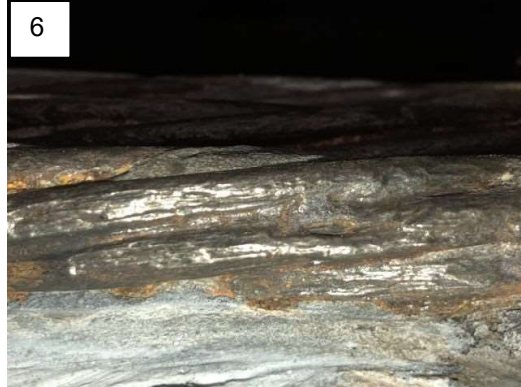
Preliminary Investigation of a Tendon with a Spiraled Duct [Test Site S]

While work was being performed at the bridge, it was observed that the duct on Tendon 402R in Span 8 was deformed and had a spiraled shape. This tendon is a new tendon that was installed some time ago to replace a defective tendon. At the direction of FDOT personnel, a preliminary investigation was conducted to determine the cause of the misshaped duct. A 6"-long section of the duct was removed, and the center of the opening was located 489" down-station from the low deviator. The opening was positioned at a hump in the duct, and only the top half of the duct was removed. Upon removing the duct, one loose strand was found. The grout was of normal color, consistency, and hardness. Other observations made along the length of the duct led to a preliminary conclusion that the loose strand had failed somewhere along its length as opposed to having pulled out from its wedge at the anchor.

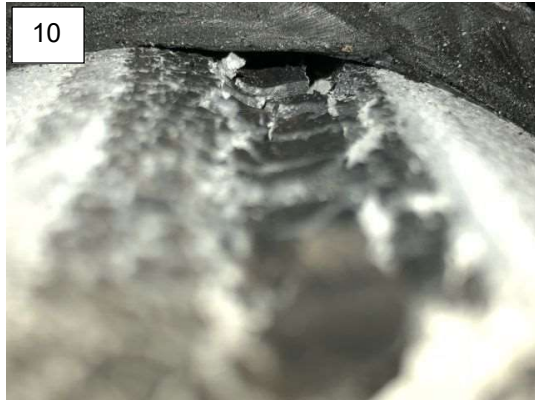
4.5 PHOTO DOCUMENTATION OF TENDON CONDITION

The image details can be found in Section 4.6.

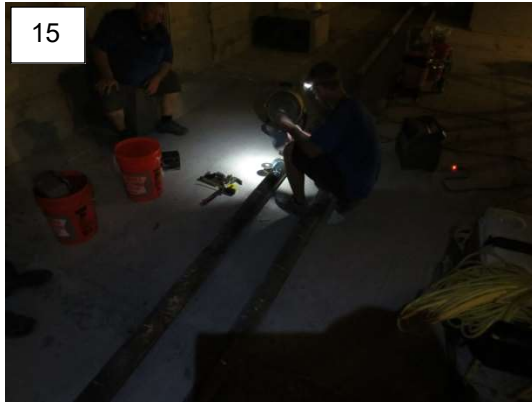
TEST SITE 1 (403R-7)



TEST SITE 2 (406L-8)



TEST SITE 3 (402L-1)



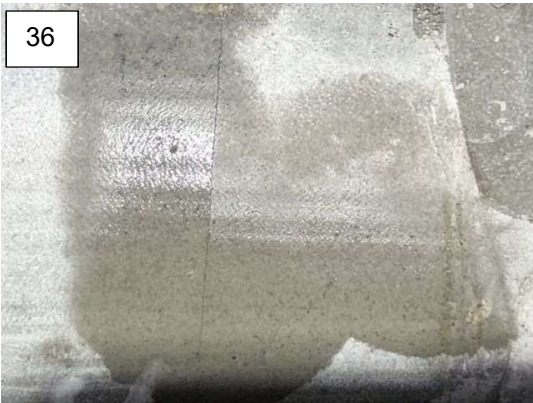
TEST SITE 4 (303L-5)



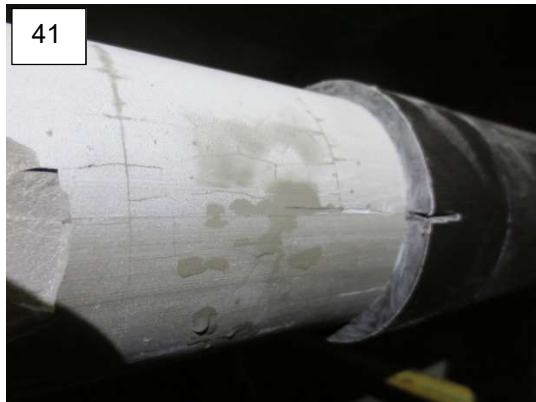
TEST SITE 5a (402L-1)



TEST SITE 6 (401L-3)



TEST SITE 7 (401L-1)



TEST SITE 8 (401R-1)



TEST SITE S (402R-7)



4.6 DETAILS OF PHOTO DOCUMENTATION OF TENDON CONDITION

The detail of images in Section 4.5 are given below. The numbering below refers to the labels placed on images at left top corner.

1. Test Site 1. 403R-7. Tendon wide shot.
2. Test Site 1. 403R-7. Top of tendon. Deficient grout and strand corrosion.
3. Test Site 1. 403R-7. Top of tendon. Close-up of deficient grout and strand corrosion.
4. Test Site 1. 403R-7. Top of tendon. Longitudinal view. Minor void at 12 o'clock bleed channel.
5. Test Site 1. 403R-7. Top of tendon. Close-up of strand corrosion.
6. Test Site 1. 403R-7. Top of tendon. Close-up of strand cross-section loss (grout removed).
7. Test Site 1. 403R-7. Bottom of tendon. Hardened grout.
8. Test Site 1. 403R-7. Bottom of tendon. Close-up of strand with bright luster after removal of hardened grout.
9. Test Site 2. 406L-8. Tendon wide shot.
10. Test Site 2. 406L-8. Top of tendon. Longitudinal view. Minor void at 12 o'clock bleed channel.
11. Test Site 2. 406L-8. Top of tendon. Accumulation of carbon black/silica fume at 12 o'clock bleed channel.
12. Test Site 2. 406L-8. Close-up of strand after removal of grout.
13. Test Site 2. 406L-8. Side of tendon. Second duct opening revealing hardened grout.
14. Test Site 2. 406L-8. Side of tendon. Clean strand after removal of hardened grout.
15. Test Site 3. 402L-1. Tendon wide shot.
16. Test Site 3. 402L-1. Top of tendon. Bleed channel at 12 o'clock position.
17. Test Site 3. 402L-1. Side of tendon. Clean strand after removal of hardened grout.
18. Test Site 3. 402L-1. Hairline circumferential crack.
19. Test Site 4. 303L-5. Tendon wide shot.
20. Test Site 4. 303L-5. Top of tendon. Longitudinal view. Bleed trail at 12 o'clock position.
21. Test Site 4. 303L-5. Top of tendon. Bleed trail at 12 o'clock position.
22. Test Site 4. 303L-5. Bottom angled view. Impression of steel debris in grout and clean strand after removal of grout.
23. Test Site 4. 303L-5. Bottom angled view. Steel debris embedded in tendon.
24. Test Site 4. 303L-5. Steel debris removed from tendon.
25. Test Site 4. 303L-5. Hairline circumferential cracking.
26. Test Site 5a. 402L-1. Tendon wide shot.
27. Test Site 5a. 402L-1. Top of tendon. Longitudinal view. Bleed trail at 12 o'clock position. Negligible void.
28. Test Site 5a. 402L-1. Side of tendon. Clean strand after grout removal.
29. Test Site 5a. 402L-1. Top of tendon. Bleed trail at 12 o'clock position.
30. Test Site 5a. 402L-1. Side of tendon. Hairline circumferential cracking.
31. Test Site 5a. 402L-1. Second opening. Showing bleed trail at 12 o'clock and hardened grout. Angled strand positioning.
32. Test Site 5a. 402L-1. Second opening. Side of tendon. Hairline circumferential cracking.

33. Test Site 6. 401L-3. Tendon wideshot
34. Test Site 6. 401L-3. Top of tendon. Deficient grout at 12 o'clock position.
35. Test Site 6. 401L-3. Top of tendon. Strand with bright luster after removal of grout.
36. Test Site 6. 401L-3. Hairline circumferential cracking.
37. Test Site 7. 401L-1. Tendon wideshot.
38. Test Site 7. 401L-1. Top of tendon. Longitudinal view. Negligible void. Bleed trail at 12 o'clock position.
39. Test Site 7. 401L-1. Top angled view. Bleed trail at 12 o'clock position.
40. Test Site 7. 401L-1. Top of tendon. Clean strand after grout removal. Deep flat faceted grout fracture plane.
41. Test Site 7. 401L-1. Side of tendon. Hairline circumferential cracking. Map cracking.
42. Test Site 8. 401R-1. Hardened grout with bleed trail at 12 o'clock position.
43. Test Site 8. 401R-1. Clean strand after grout removal.
44. Test Site S. 402R-7. Tendon wideshot showing duct deformation.
45. Test Site S. 402R-7. Side of tendon showing duct deformation.
46. Test Site S. 402R-7. Top of tendon showing hardened grout and buckled clean strand. No grout distress except for small air bubble void.
47. Test Site S. 402R-7. Loose strand exposed after removal of grout.
48. Test Site S. 402R-7. Loose strand exposed after removal of grout.
49. Test Site S. 402R-7. Loose strand exposed after removal of grout.

4.7 TEST VALIDATION

The nine test sites listed in Table 1 were selected based on the recommendations from MTC and USTC; one of the sites was an extra exploratory site (Site S) to assess a tendon duct deformation. Four test sites were opened to verify the defects detected by MMFM, and four additional sites were opened to verify the grout defects suggested by USTC. In addition to these primary defect modes, the results from the earlier field testing by MTC and USTC were reviewed for additional verification of findings for each of the test sites, when possible. Comparisons of the primary and additional test results to observations made during tendon openings are shown in Table 2.

For the primary defect verification, MMFM testing by MTC indicated cross-section loss (at sites 1, 2, and 5a) and mass increase (at site 4). Of those test sites, site 1 and site 4 showed strong positive correlation with severe strand corrosion in the former and with large embedded steel debris in the latter. MMFM testing at sites 2 and 5a gave indication of 1.4% and 2.4% cross-section loss, respectively; but tendon openings revealed clean strands in predominantly normal hardened grout. Half-cell potential measurements generally revealed passive conditions. From the visual observations of the strand outer bundle surface and good grout physical conditions, it was likely that any possible cross-section loss was not due to corrosion. Although absolute validation of cross-section condition within the strand bundle was not possible, it was unlikely that any cross-section loss existed there.

As additional consideration of MMFM at the other five test sites (3, 6-8, S), sites 3 and 6 could not be assessed as MMFM at tendons with low horizontal spans on the box girder floor could not be tested. MMFM at site 7 indicated mass increase at the 12-2 o'clock position but no indication of steel debris was evident in the limited grout excavation made at that site. MMFM at site 8 indicated mass loss centered at about 38 ft from the pier wall and having length of approximately 5.5 ft. Unfortunately, primary testing at site 8 was made at 44 ft with a one-foot window, just outside of the region of detection. If that mass loss was due to corrosion, that tendon deficiency did not extend the additional 3 feet to the test site. The opening there revealed clean strands in mostly hardened grout and half-cell potentials indicative of passive corrosion conditions. At test site S, MMFM did not detect any steel cross-section loss, and tendon opening revealed clean strands, albeit with one broken/loose strand.

For primary grout defect verification, ultrasonic/sonic testing by USTC, indicated some grout anomaly at sites 3, 6-8. At sites 3, 6, and 7, no through-duct or circumferential resonant frequencies were detected. These sites also contained a bleed trail at the 12 o'clock position, minor void space at the bleed trail, and hairline circumferential cracks that can be deep. It was posited that the circumferential cracks may influence attenuation of the ultrasonic/sonic (impact echo) and, thus, the lack of through-duct resonant frequencies. The lack of circumferential resonant frequency may be affected by duct delamination (not detectable by available resources during the openings) and the bleed trail and void at the 12 o'clock position. Test site 8, which also showed no through-duct resonant frequencies, also had the hairline circumferential cracking. The test location did show circumferential resonant frequencies, but the openings revealed similar bleed trail and a minor void at the 12 o'clock position.

As additional verification of ultrasonic/sonic testing applications for external PT tendons, testing at sites 4 and 5a showed no grout defects (i.e. presence of both through-duct and circumferential resonant frequencies). However, both sites showed bleed trail and minor voids and hairline circumferential cracking. Ultrasonic/sonic testing at sites 1 and 2 were not part of the original test scope. At test site S, testing indicated no grout defects (presence of both through-duct and circumferential resonant frequencies) and opening revealed hardened grout with no grout distress.

Table 2. Reported test results and outcome of field tendon openings.

Site	Tendon	Place	Cross-Section Loss*		Ultrasonic/Sonic		Field Observations**		
			Defect	Length	Resonant Freq.	Length	CS Verification	Grout Verification	
1‡	403R-7	Hi Hor.	1.5% CS	2.6'	tbd‡	tbd‡	Severe strand corrosion , Deficient grout. Bleed trail at 12 o'clock. Minor void.	✓	tbd‡
2‡	406L-8	Slope	1.4% CS	3.6'	tbd‡	tbd‡	<i>No corrosion on visible outer strand bundle. Bleed trail at 12 o'clock. Minor void. Hardened grout elsewhere.</i>	☒	tbd‡
3	402L-1	Low Hor.	NA	NA	No 15 kHz, No 20-25 kHz	~10' (S107-117)	No corrosion on visible outer strand bundle. Bleed trail at 12 o'clock. Minor void. Hardened grout elsewhere. Hairline circumferential cracking.	NA	-
4	303L-5	Slope	(-)2.2% CS	0.7'	No defect	No defect	Large steel debris. No corrosion on visible outer strand bundle. <i>Bleed trail at 12 o'clock. Minor void.</i> Hardened grout elsewhere. <i>Hairline circumferential cracking.</i>	✓	☒
5a	402L-1	Slope	2.4% CS	~6'	No defect@~S58	No defect	<i>No corrosion on visible outer strand bundle. Bleed trail at 12 o'clock. Minor void.</i> Hardened grout elsewhere. <i>Hairline circumferential cracking.</i>	☒	☒
6	401L-3	Low Hor.	NA	NA	No 15 kHz, No 20-25 kHz	~4' (S138-142)	No corrosion on visible outer strand bundle. Bleed trail at 12 o'clock. Minor void. Hardened grout elsewhere. Hairline circumferential cracking.	NA	-
7	401L-1	Hi Hor.	(P1-401L-H3) ~S166 7.8m, (-)2.4% 12-2o'clock	0.3	No 15 kHz, No 20-25 kHz	~5' (S164-169)	No corrosion on visible outer strand bundle. Bleed trail at 12 o'clock. Minor void. Hardened grout elsewhere. Hairline circumferential cracking. <i>(No indication of steel debris in limited grout removal).</i>	☒	-
8	401R-1	Slope	(P1-401R-H1) ~S38 11.7m, 1.5% CS, 1.7m L	5.6'	15 kHz, No 20-25 kHz	S44	<i>No corrosion on visible outer strand bundle. Bleed trail at 12 o'clock. Minor void.</i> Hardened grout elsewhere. Hairline circumferential cracking.	☒	-
S†	402R-7	Slope	(P8-402R-I1) No defect	no defect	No defect	No defect	No corrosion on visible outer strand bundle. Hardened grout elsewhere. No grout distress. Broken/loose strand.	-	-

Grey field represents primary defect mode to be verified. Other reported data also compared for additional consideration.

† Deformed HDPE Duct with Broken/Loose Strand ‡ Additional Test Site for USTC.

* CS- Cross-Section (negative value indicated mass increase)

** **Bold** represent supporting characteristics to suggested defects by testing. *Italics* represent inconsistent characteristics to suggested defects by testing.

4.8 ON-SITE DUCT OPENINGS AND TEST VALIDATION PROCEDURES

The tendon verification was carried out by Concorr FL. The section describes the sequence and procedures undertaken for tendon opening and repair.

- Photo-documentation with a picture at 12, 3, 6, and 9 o'clock (when possible) taken before and after each step.

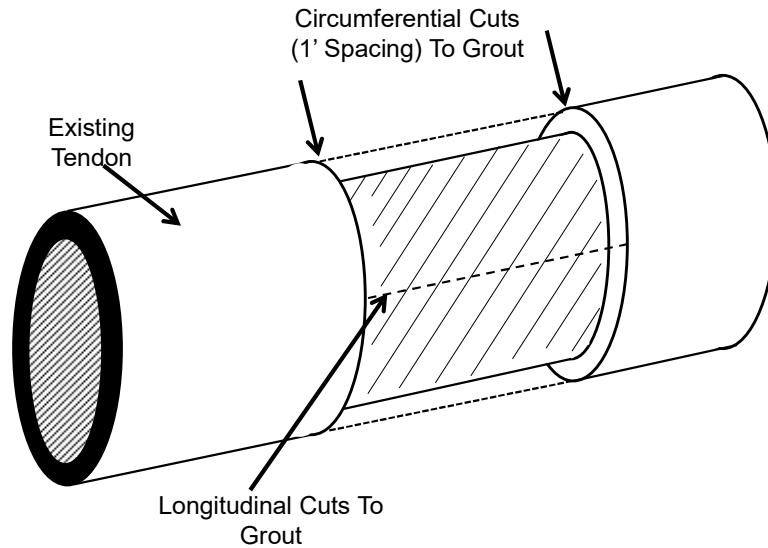


Figure 4-12 Circumferential and longitudinal cuts for tendon opening

- Cuts tentatively made to avoid hitting steel strand (Figure 4-12).
- After two circumferential cuts and two parallel longitudinal cuts at 3 and 9 o'clock, the top half pipe carefully removed to reveal underlying grout.
- Bottom half pipe carefully removed to avoid disturbance, breakage and loss of grout material.
- Only the top half pipe was cut and removed for strand with low ground clearance (Figure 4-13).

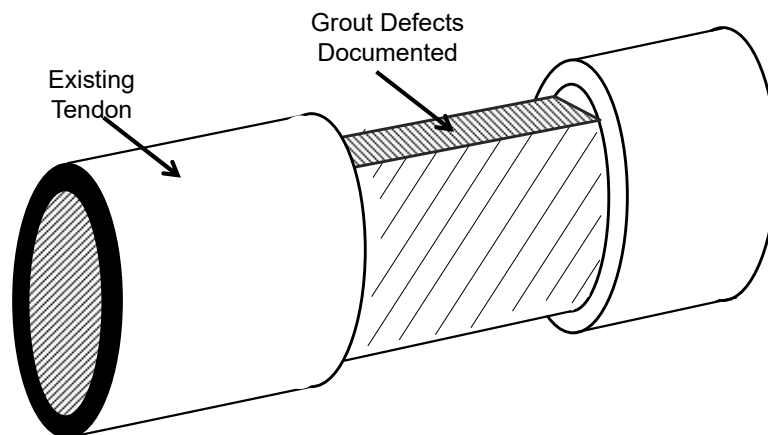


Figure 4-13: Removal of HDPE pipe

- Geometry of voids was documented.
- Depth, length, and coverage of deficient grout was documented.

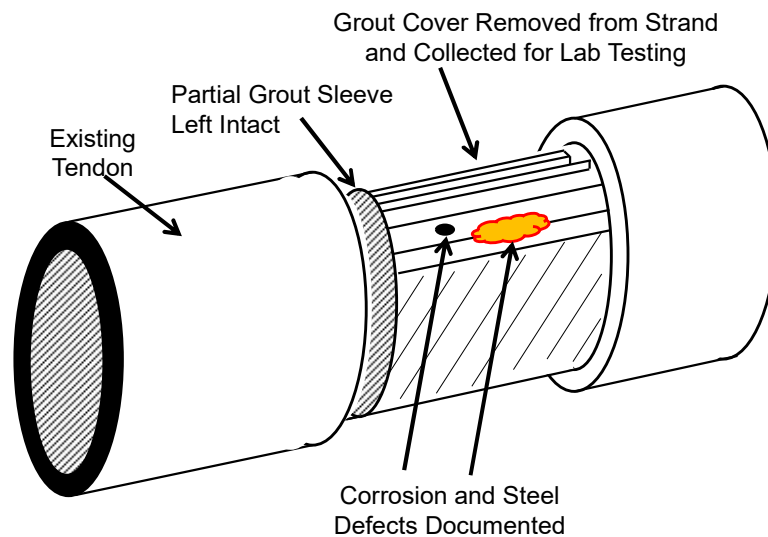


Figure 4-14: Sampling of grout material

- Grout carefully removed by hammer and scoop to reveal underlying steel (Figure 4-14).
- A partial grout sleeve was left intact at one or both cut window edges.
- All grout materials are sealed in labeled plastic bags for later testing.
- Grout was separated into groups if variability in grout deficiencies exist.
- Any visual rust staining and rust accumulation was documented.

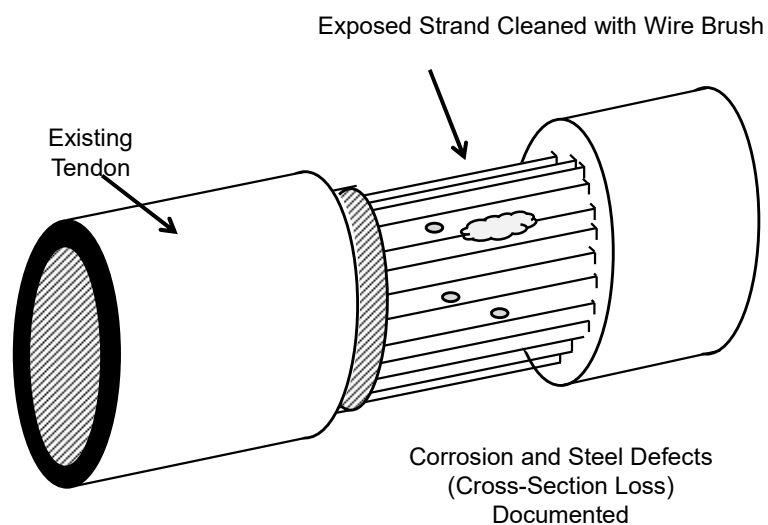


Figure 4-15: Documentation of corrosion activity

- After removal of grout around the circumference of the steel bundle, the exposed steel was hand cleaned with a wire brush to remove (as much as attainable by hand) loose grout and rust particles.
- Steel defects and cross-section loss was documented (Figure 4-15). A pit-depth gage was used if localized corrosion observed.

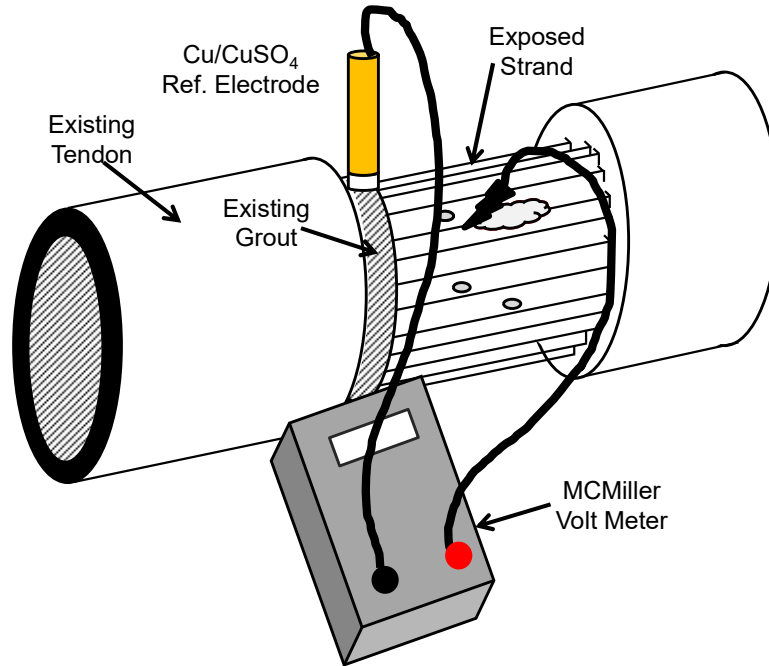


Figure 4-16: Half-cell potentials of steel strands

- Half-cell potentials was made by placing a slender Cu/CuSO₄ electrode on the existing grout sleeve. The tip of the reference electrode may be covered with a wet sponge. The working electrode contact was placed on each exposed steel strand regardless of electrical continuity (Figure 4-16).
- Each measurement was recorded with notes on ref electrode placement, circumferential location of each strand, and observation of rust.

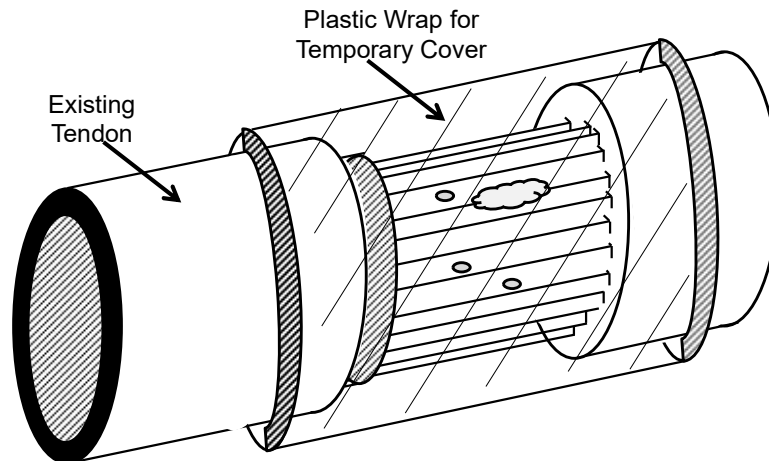


Figure 4-17: Temporary repair work on tendon

- If a permanent repair was delayed, a temporary cover using plastic wrap and duct tape may be used for up to 2 days (Figure 4-17).

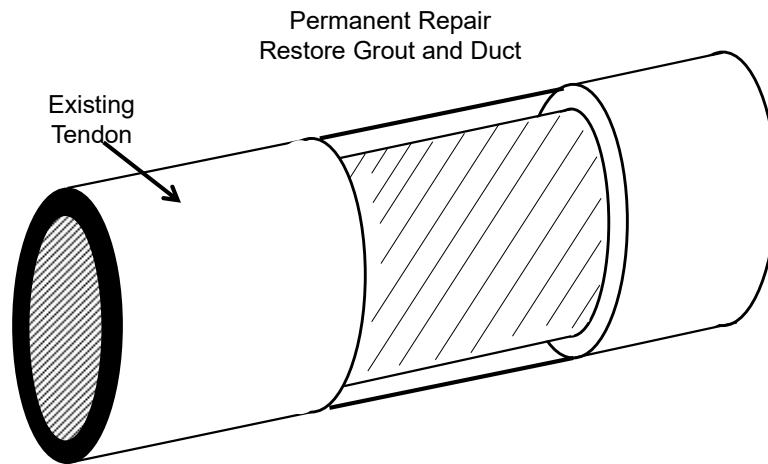


Figure 4-18: Permanent repair work on tendon

- Permanent repairs conforming to FDOT requirements was made (Figure 4-18).
- Quality Control of the permanent repair was made after 1 day.

5 BRIDGE TENDON BASE CONDITION

To assess the condition of the tendon, the results of the nondestructive technologies were documented to provide a history of the condition of the tendon in terms of cross-section loss by MMFM and general tendon material condition by ultrasonic/sonic testing. These baseline results may be useful if future monitoring by these nondestructive technologies is employed.

The baseline conditions presented here are based only on the results of nondestructive testing carried out by USTC and MTC. No additional analysis or laboratory evaluations were performed on grout extracted during tendon openings. The detailed results for each location provided by USTC and MTC are attached as Appendix B and Appendix D, respectively. Although a number of factors can affect the repeatability of the nondestructive testing, a baseline measurement can provide generic data trends.

In the submittals, both vendors used different nomenclature to identify the tendon segments. In order to refer back to the locations, the data of both vendors have been combined for similar tendon segments to provide a uniform report for future reference. There was a difference in measuring spans between the segments. MTC measured tendon segments lengths between deviators and pier walls as shown in Figure 5-1. USTC took linear measurements along the length of the tendon, thus eliminating effect of any slope or variation in deviator thicknesses (Figure 5-2).

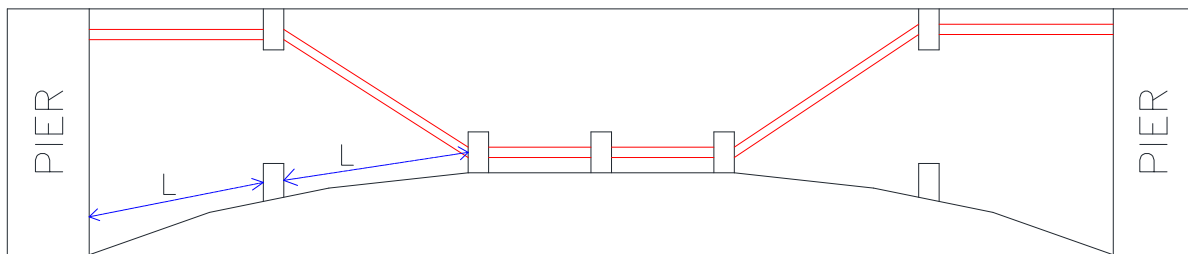


Figure 5-1: MTC tendon measurement procedures.

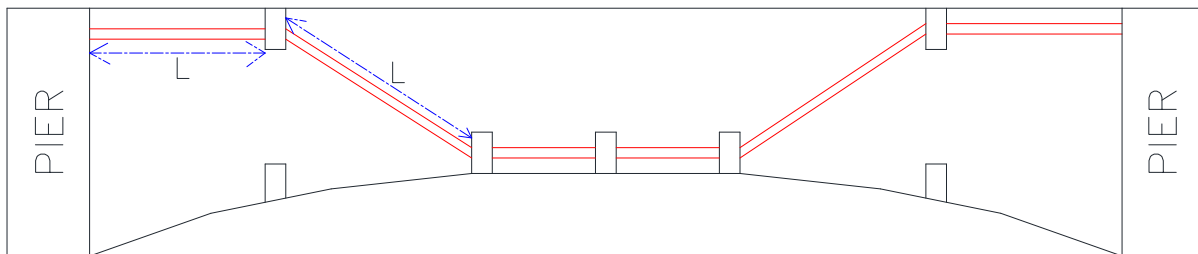


Figure 5-2: USTC tendon measurement procedures.

Table 3. Tendon base condition.

Tendon No.	Cell	Location	Section Label	MMFM testing			Ultrasonic/sonic testing		
				Center of damage (m)	Length of damage (m)	Estimated section loss (%)	Tendon ID	Location (ft)	No thru frequencies
Span 1									
401R	Center	Low inclined	P1-401R-H1	11.7	1.7	1.5	401R-1W	26-30, 36-46	20 kHz and 25 kHz
		High inclined	P1-401R-H2	-	-	-			
		High horizontal	P1-401R-H3	-	-	-			
402R	Center	Low inclined	P1-402R-I1	18.12	0.2	-4.11	402R-1W	1-3, 5-8, 24-30, 139-140	20 kHz and 25 kHz
		High inclined	P1-402R-I2	-	-	-			
		High horizontal	P1-402R-H1	-	-	-			
401L	Center	Low inclined	P1-401L-H1	-	-	-	401L-1W	150-153, 158-161, 164-169	20 kHz and 25 kHz
		High inclined	P1-401L-H2	-	-	-			
		High horizontal	P1-401L-H3	7.8	0.1	-2.4			
402L	Center	Low inclined	P1-402L-I1	10.3	2.8	2.7	402L-1W	32-35, 48-51, 65-70, 92-107, 109-118	20 kHz and 25 kHz
		High inclined	P1-402L-I2	13.8	1.2	1.5			
		High horizontal	P1-402L-H1	-	-	-			

Table 3 (continued).

Tendon No.	Cell	Location	Section Label	MMFM testing			Ultrasonic/sonic testing		
				Center of damage (m)	Length of damage (m)	Estimated section loss (%)	Tendon ID	Location (ft)	No thru frequencies
Span 2									
401R	Center	High horizontal 1	P2-401R-H1	-	-	-	401R-1E	46-50, 83-86, 109-112, 127-131	20 kHz and 25 kHz
		Inclined 1	P2-401R-I1	15.4	0.2	-3.8			
		Low horizontal 1							
402R	Center	High horizontal 1	P2-402R-H1	-	-	-	402R-1E	29-38, 40-43, 46-50	20 kHz and 25 kHz
		Inclined 1	P2-402R-I1	-	-	-			
		Low horizontal 1							
401L	Center	High horizontal 1	P2-401L-H1	8.2	0.2	-5	401L-1E	69-72	20 kHz and 25 kHz
		Inclined 1	P2-401L-I1	-	-	-			
		Low horizontal 1							
402L	Center	High horizontal 1	P2-402L-H1	-	-	-	402L-1E	107-117	20 kHz and 25 kHz
		Inclined 1	P2-402L-I1	8.2	1.8	2.4			
		Low horizontal 1							
401R	Center	Low horizontal 2					401R-2W	-	
		Inclined 2	P2-401R-I2	-	-	-			
		High horizontal 2	P2-401R-H2	-	-	-			
402R	Center	Low horizontal 2				402R-2W	18-38, 66-69, 78-81, 114-120	20 kHz and 25 kHz	
		Inclined 2	P2-402R-I2	6.9	0.1				-2.3
		High horizontal 2	P2-402R-H2	3.8	1.1				1.7
401L	Center	Low horizontal 2				401L-2W	-		
		Inclined 2	P2-401L-I2	-	-				-
		High horizontal 2	P2-401L-H2	-	-				-
402L	Center	Low horizontal 2				402L-2W	142-142.5	20 kHz and 25 kHz	
		Inclined 2	P2-402L-I2	-	-				-
		High horizontal 2	P2-402L-H2	-	-				-

Table 3 (continued).

Tendon No.	Cell	Location	Section Label	MMFM testing			Ultrasonic/sonic testing		
				Center of damage (m)	Length of damage (m)	Estimated section loss (%)	Tendon ID	Location (ft)	No thru frequencies
Span 3									
401R	Center	High horizontal 1	P3-401R-H1	-	-	-	401R-2E	-	
		Inclined 1	P3-401R-I1	-	-	-			
		Low horizontal 1							
402R	Center	High horizontal 1	P3-402R-H1	-	-	-	402R-2E	17-21, 91-98	20 kHz and 25 kHz
		Inclined 1	P3-402R-I1	-	-	-			
		Low horizontal 1							
401L	Center	High horizontal 1	P3-401L-H1	-	-	-	401L-2E	1-6, 88-93, 111-117	20 kHz and 25 kHz
		Inclined 1	P3-401L-I1	-	-	-			
		Low horizontal 1							
402L	Center	High horizontal 1	P3-402L-H1	4.5	0.3	-1.5	402L-2E	1-5, 9-12, 21-24, 52-60	20 kHz and 25 kHz
		Inclined 1	P3-402L-I1	-	-	-			
		Low horizontal 1							
401R	Center	Low horizontal 2					401R-3W	44-47, 118-121	20 kHz and 25 kHz
		Inclined 2	P3-401R-I2	-	-	-			
		High horizontal 2	P3-401R-H2	-	-	-			
402R	Center	Low horizontal 2					402R-3W	69-75	20 kHz and 25 kHz
		Inclined 2	P3-402R-I2	-	-	-			
		High horizontal 2	P3-402R-H2	-	-	-			
401L	Center	Low horizontal 2					401L-3W	-	
		Inclined 2	P3-401L-I2	-	-	-			
		High horizontal 2	P3-401L-H2	-	-	-			
402L	Center	Low horizontal 2					402L-3W	-	
		Inclined 2	P3-402L-I2	-	-	-			
		High horizontal 2	P3-402L-H2	-	-	-			

Table 3 (continued).

Tendon No.	Cell	Location	Section Label	MMFM testing			Ultrasonic/sonic testing		
				Center of damage (m)	Length of damage (m)	Estimated section loss (%)	Tendon ID	Location (ft)	No thru frequencies
Span 4									
401R	Center	High horizontal 1	P4-401R-H1	-	-	-	401R-3E	-	
		Inclined 1	P4-401R-I1	17.6	0.7	1.2			
		Low horizontal 1							
402R	Center	High horizontal 1	P4-402R-H1	3.5	0.7	1.7	402R-3E	-	
		Inclined 1	P4-402R-I1	-	-	-			
		Low horizontal 1							
401L	Center	High horizontal 1	P4-401L-H1	-	-	-	401L-3E	-	
		Inclined 1	P4-401L-I1	-	-	-			
		Low horizontal 1							
402L	Center	High horizontal 1	P4-402L-H1	5.9	0.9	1	402L-3E	29-33, 97-101, 108-128, 138-142	20 kHz and 25 kHz
		Inclined 1	P4-402L-I1	-	-	-			
		Low horizontal 1							
401R	Center	Low horizontal 2					401R-4W	-	
		Inclined 2	P4-401R-I2	19.8	0.1	-1.8			
		High horizontal 2	P4-401R-H2	-	-	-			
402R	Center	Low horizontal 2					402R-4W	43-81	20 kHz and 25 kHz
		Inclined 2	P4-402R-I2	-	-	-			
		High horizontal 2	P4-402R-H2	-	-	-			
401L	Center	Low horizontal 2					401L-4W	-	
		Inclined 2	P4-401L-I2	9.1	0.2	-2.2			
		High horizontal 2	P4-401L-H2	-	-	-			
402L	Center	Low horizontal 2					402L-4W	-	
		Inclined 2	P4-402L-I2	-	-	-			
		High horizontal 2	P4-401L-H2	3.3	0.8	1			

Table 3 (continued).

Tendon No.	Cell	Location	Section Label	MMFM testing			Ultrasonic/sonic testing		
				Center of damage (m)	Length of damage (m)	Estimated Section Loss (%)	Tendon ID	Location (ft)	No thru frequencies
Span 5									
401R	Center	High horizontal 1	P5-401R-H1	-	-	-	401R-4E	24-26	20 kHz and 25 kHz
		Inclined 1	P5-401R-I1	2.3	0.6	1.4			
		Low horizontal 1							
402R	Center	High horizontal 1	P5-402R-H1	-	-	-	402R-4E	-	
		Inclined 1	P5-402R-I1	2.4	0.1	-2.8			
				18.8	0.6	1.2			
Low horizontal 1									
401L	Center	High horizontal 1	P5-401L-H1	-	-	-	401L-4E	77-83	20 kHz and 25 kHz
		Inclined 1	P5-401L-I1	9.6	0.1	-1.7			
		Low horizontal 1							
402L	Center	High horizontal 1	P5-402L-H1	7.5	1.4	1.3	402L-4E	49-53, 77-85	20 kHz and 25 kHz
		Inclined 1	P5-402L-I1	4	0.2	-3			
				12.2	0.4	-3.1			
Low horizontal 1									
303R	Center	Inclined 1	P5-303R-I1	-	-	-	303R-4E	85-89, 93-97, 123-131, 141-149	20 kHz and 25 kHz
			P5-303R-I2	-	-	-			
		Inclined 2	P5-303R-I2-1	-	-	-			
			P5-303R-I2-2	-	-	-			
		Inclined 3	P5-303R-I3	-	-	-			
		Inclined 4	P5-303R-I4	-	-	-			
		Low horizontal 1							
		Low horizontal 2							

Table 3 (continued).

Tendon No.	Cell	Location	Section Label	MMFM testing			Ultrasonic/sonic testing		
				Center of damage (m)	Length of damage (m)	Estimated Section Loss (%)	Tendon ID	Location (ft)	No thru frequencies
Span 5 (continued)									
303L	Center	Inclined 1	P5-303L-I1	-	-	-	303L-4E	-	
		Inclined 2	P5-303L-I2	-	-	-			
		Inclined 3	P5-303L-I3	-	-	-			
		Inclined 4	P5-303L-I4	5.8	0.2	-2.2			
		Low horizontal 1							
		Low horizontal 2							
401R	Center	Low horizontal 2					401R-5W	43-49	20 kHz and 25 kHz
		Inclined 2	P5-401R-I2	-	-	-			
		High horizontal 2	P5-401R-H2	-	-	-			
402R	Center	Low horizontal 2					402R-5W	61-71, 136-139	20 kHz and 25 kHz
		Inclined 2	P5-402R-I2	-	-	-			
		High horizontal 2	P5-402R-H2	-	-	-			
401L	Center	Low horizontal 2					401L-5W	-	
		Inclined 2	P5-401L-I2	-	-	-			
		High horizontal 2	P5-401L-H2	-	-	-			
402L	Center	Low horizontal 2					402L-5W	61-71, 136-139	20 kHz and 25 kHz
		Inclined 2	P5-402L-I2	-	-	-			
		High horizontal 2	P5-402L-H2	-	-	-			

Table 3 (continued).

Tendon No.	Cell	Location	Section Label	MMFM testing			Ultrasonic/sonic testing		
				Center of damage (m)	Length of damage (m)	Estimated section loss (%)	Tendon ID	Location (ft)	No thru frequencies
Span 6									
401R	Center	High horizontal 1	P6-401R-H1	-	-	-	401R-5E	-	
		Inclined 1	P6-401R-I1	-	-	-			
		Low horizontal 1							
402R	Center	High horizontal 1	P6-402R-H1	-	-	-	402R-5E	-	
		Inclined 1	P6-402R-I1	-	-	-			
		Low horizontal 1							
401L	Center	High horizontal 1	P6-401L-H1	-	-	-	401L-5E	-	
		Inclined 1	P6-401L-I1	-	-	-			
		Low horizontal 1							
402L	Center	High horizontal 1	P6-402L-H1	-	-	-	402L-5E	-	
		Inclined 1	P6-402L-I1	-	-	-			
		Low horizontal 1							
401R	Center	Low horizontal 2					401R-6W	-	
		Inclined 2	P6-401R-I2	-	-	-			
402R	Center	Low horizontal 2					402R-6W	-	
		Inclined 2	P6-402R-I2	-	-	-			
		High horizontal 2	P6-402R-H2	3.7	1.4	1.4			
401L	Center	Low horizontal 2					401L-6W	-	
		Inclined 2	P6-401L-I2	-	-	-			
402L	Center	Low horizontal 2					402L-6W	-	
		Inclined 2	P6-402L-I2	-	-	-			

Table 3 (continued).

Tendon No.	Cell	Location	Section Label	MMFM testing			Ultrasonic/sonic testing		
				Center of damage (m)	Length of damage (m)	Estimated Section Loss (%)	Tendon ID	Location (ft)	No thru frequencies
Span 7									
401R	Center	High horizontal 1	P7-401R-H1	-	-	-	401R-6E	-	
		Inclined 1	P7-401R-I1	-	-	-			
		Low horizontal 1							
402R	Center	High horizontal 1	P7-402R-H1	-	-	-	402R-6E	-	
		Inclined 1	P7-402R-I1	-	-	-			
		Low horizontal 1							
401L	Center	High horizontal 1	P7-401L-H1	-	-	-	401L-6E	-	
		Inclined 1	P7-401L-I1	-	-	-			
		Low horizontal 1							
402L	Center	High horizontal 1	P7-402L-H1	-	-	-	402L-6E	-	
		Inclined 1	P7-402L-I1	-	-	-			
		Low horizontal 1							
401R	Center	Low horizontal 2					401R-7W	-	
		Inclined 2	P7-401R-I2	-	-	-			
		High horizontal 2	P7-401R-H2	-	-	-			
402R	Center	Low horizontal 2					402R-7W	-	
		Inclined 2	P7-402R-I2	-	-	-			
401L	Center	Low horizontal 2					401L-7W	41-45	20 kHz and 25 kHz
		Inclined 2	P7-401L-I2	11.8	0.2	-2.6			
		High horizontal 2	P7-401L-H2	-	-	-			
402L	Center	Low horizontal 2					402L-7W	-	
		Inclined 2	P7-402L-I2	15.9	0.2	-2.5			
		High horizontal 2	P7-402L-H2	-	-	-			

Table 3 (continued).

Tendon No.	Cell	Location	Section Label	MMFM testing			Ultrasonic/sonic testing		
				Center of damage (m)	Length of damage (m)	Estimated Section Loss (%)	Tendon ID	Location (ft)	No thru frequencies
Span 7 (continued)									
303R	Center	Inclined 1	P7-303R-I1	-	-	-	303R-6E	-	
		Inclined 2	P7-303R-I2	-	-	-			
		Inclined 3	P7-303R-I3	-	-	-			
		Inclined 4	P7-303R-I4	-	-	-			
		Low horizontal 1							
		Low horizontal 2							
303L	Center	Inclined 1	P7-303L-I1	-	-	-	303L-6E	-	
		Inclined 2	P7-303L-I2	-	-	-			
		Inclined 3	P7-303L-I3	-	-	-			
		Inclined 4	P7-303L-I4	-	-	-			
		Low horizontal 1							
		Low horizontal 2							

Table 3 (continued).

Tendon No.	Cell	Location	Section Label	MMFM testing			Ultrasonic/sonic testing		
				Center of damage (m)	Length of damage (m)	Estimated section loss (%)	Tendon ID	Location (ft)	No thru frequencies
Span 8									
401R	Center	High horizontal 1	P8-401R-H1	-	-	-	401R-7E	-	
		Inclined 1	P8-401R-I1	-	-	-			
		Low horizontal 1							
402R	Center	Inclined 1	P8-402R-I1	-	-	-	402R-7E	-	
		Inclined 1							
401L	Center	High horizontal 1	P8-401L-H1	-	-	-	401L-7E	-	
		Inclined 1	P8-401L-I1	-	-	-			
		Low horizontal 1							
402L	Center	High horizontal 1	P8-402L-H1	-	-	-	402L-7E	-	
		Inclined 1	P8-402L-I1	-	-	-			
		Low horizontal 1							
401R	Center	Low horizontal 2					401R-8W	-	
		Inclined 2	P8-401R-I2	-	-	-			
		High horizontal 2	P8-401R-H2	-	-	-			
402R	Center	Low horizontal 2					402R-8W	-	
		Inclined 2	P8-402R-I2	-	-	-			
		High horizontal 2	P8-402R-H1	-	-	-			
401L	Center	Low horizontal 2					401L-8W	-	
		Inclined 2	P8-401L-I2	-	-	-			
		High horizontal 2	P8-401L-H2	-	-	-			
402L	Center	Low horizontal 2					402L-8W	-	
		Inclined 2	P8-402L-I2	-	-	-			
		High horizontal 2	P8-402L-H2	-	-	-			

Table 3 (continued).

Tendon No.	Cell	Location	Section Label	MMFM testing			Ultrasonic/sonic testing		
				Center of damage (m)	Length of damage (m)	Estimated section loss (%)	Tendon ID	Location (ft)	No thru frequencies
Span 9									
401R	Center	High horizontal 1	P9-401R-H1	-	-	-	401R-8E	-	
		Inclined 1	P9-401R-I1	9.4	0.3	-0.9			
		Low horizontal 1							
402R	Center	High horizontal 1	P9-402R-H1	-	-	-	402R-8E	-	
		Inclined 1	P9-402R-I1	-	-	-			
		Low horizontal 1							
401L	Center	High horizontal 1	P9-401L-H1	-	-	-	401L-8E	-	
		Inclined 1	P9-401L-I1	-	-	-			
		Low horizontal 1							
402L	Center	High horizontal 1	P9-402L-H1	-	-	-	402L-8E	-	
		Inclined 1	P9-402L-I1	12.3	3.2	1.6			
		Low horizontal 1							
401R	Center	Low horizontal 2					401R-9W		
		Inclined 2	P9-401R-I2	-	-	-			
402R	Center	Low horizontal 2					402R-9W		
		Inclined 2	P9-402R-I2	10.3	2.6	1.5			
		High horizontal 2	P9-402R-H2	-	-	-			
401L	Center	Low horizontal 2					401L-9W	85-89	20 kHz and 25 kHz
		Inclined 2	P9-401L-I2	-	-	-			
		High horizontal 2	P9-401L-H2	3.2	0.1	0.5			
402L	Center	Low horizontal 2					402L-9W		
		Inclined 2	P9-402L-I2	-	-	-			

Table 3 (continued).

Tendon No.	Cell	Location	Section Label	MMFM testing			Ultrasonic/sonic testing		
				Center of damage (m)	Length of damage (m)	Estimated section loss (%)	Tendon ID	Location (ft)	No thru frequencies
Span 10									
401R	Center	Inclined 1	P10-401R-I1	-	-	-	401R-9E	-	
		Low horizontal 1							
402R	Center	High horizontal 1	P10-402R-H1	-	-	-	402R-9E	-	
		Inclined 1	P10-402R-I1	-	-	-			
		Low horizontal 1							
401L	Center	High horizontal 1	P10-401L-H1	-	-	-	401L-9E	-	
		Inclined 1	P10-401L-I1	6.3	0.2	-3			
		Low horizontal 1							
402L	Center	Inclined 1	P10-402L-I1	-	-	-	402L-9E	-	
		Low horizontal 1							
401R	Center	Low horizontal 2					401R-10W	-	
		Inclined 2	P10-401R-I2	-	-	-			
		High horizontal 2	P10-401R-H1	-	-	-			
402R	Center	Low horizontal 2					402R-10W	-	
		Inclined 2	P10-402R-I2	-	-	-			
		High horizontal 2	P10-402R-H2	-	-	-			
401L	Center	Low horizontal 2					Page 112 of USTC	-	
		Inclined 2	P10-401L-I2	-	-	-			
		High horizontal 2	P10-401L-H2	-	-	-			
402L	Center	Low horizontal 2					Page 111 of USTC	-	
		Inclined 2	P10-402L-I2	2.1	0.2	-3.4			
				9.2	0.2	-3			
		High horizontal 2	P10-402L-H1	-	-	-			

Table 3 (continued).

Tendon No.	Cell	Location	Section Label	MMFM testing			Ultrasonic/sonic testing		
				Center of damage (m)	Length of damage (m)	Estimated section loss (%)	Tendon ID	Location (ft)	No thru frequencies
Span 11									
401R	Center	High horizontal	P11-401R-H1	-	-	-	401R-10E	-	
		High inclined	P11-401R-I1	-	-	-			
		Low inclined	P11-401R-I2	-	-	-			
402R	Center	High horizontal	P11-402R-H1	-	-	-	402R-10E	-	
		Low inclined	P11-402R-I1	-	-	-			
		Low inclined	P11-402R-I2	15	2.5	1.5			
401L	Center	High horizontal	P11-401L-H1	-	-	-	401L-10E	-	
		High inclined	P11-401L-I1	-	-	-			
		Low inclined	P11-401L-I2	-	-	-			
402L	Center	High horizontal	P11-402L-H1	-	-	-	402L-10E	-	
		Low inclined	P11-402L-I1	-	-	-			
		Low inclined	P11-402L-I2	7	1.6	1.3			
				12.4	2.1	1.8			

Table 3 (continued).

Tendon No.	Cell	Location	MMFM testing				Ultrasonic/sonic testing		
			Section Label	Center of damage (m)	Length of damage (m)	Estimated Section Loss (%)	Tendon ID	Location (ft)	No thru frequencies
Additional span tested (Span 9)									
403L	Left	High horizontal 1	P9-403L-H1	-	-	-	-	-	
		Inclined 1	P9-403L-I1	-	-	-	-	-	
404L	Left	High horizontal 1	P9-404L-H1	-	-	-	-	-	
		Inclined 1	P9-404L-I1	-	-	-	-	-	
405L	Left	High horizontal 1	P9-405L-H1	-	-	-	-	-	
		Inclined 1	P9-405L-I1	-	-	-	-	-	
406L	Left	High horizontal 1	P9-406L-H1	3.7	1	0.8	-	-	
		Inclined 1	P9-406L-I1	3.9	1.1	1.4	-	-	
				16.5	0.7	1.2	-	-	
403L	Left	Inclined 2	P9-403L-I2(new)	-	-	-	-	-	
404L	Left	Inclined 2	P9-404L-I2	-	-	-	-	-	
		High horizontal 2	P9-404L-H2	-	-	-	-	-	
405L	Left	Inclined 2	P9-405L-I2(new)	-	-	-	-	-	
406L	Left	Inclined 2	P9-406L-I2	-	-	-	-	-	
		High horizontal 2	P9-406L-H2	-	-	-	-	-	
406R	Right	High horizontal 1	P9-406R-H1	-	-	-	-	-	
		Inclined 1	P9-406R-I1	11.6	3.3	1.1	-	-	
405R	Right	High horizontal 1	P9-405R-H1	-	-	-	-	-	
		Inclined 1	P9-405R-I1	-	-	-	-	-	
403R	Right	High horizontal 1	P9-403R-H1	-	-	-	-	-	
		Inclined 1	P9-403R-I1	-	-	-	-	-	
404R	Right	High horizontal 1	P9-404R-H1	-	-	-	-	-	
		Inclined 1	P9-404R-I1	-	-	-	-	-	

Table 3 (continued).

Tendon No.	Cell	Location	Section Label	MMFM testing			Ultrasonic/sonic testing		
				Center of damage (m)	Length of damage (m)	Estimated Section Loss (%)	Tendon ID	Location (ft)	No thru frequencies
Additional span tested									
Span 9 (continued)									
406R	Right	Inclined 2	P9-406R-I2	-	-	-	-	-	
		High horizontal 2	P9-406R-H2	-	-	-	-	-	
405R	Right	Inclined 2	P9-405R-I2	18.4	1.3	1.5	-	-	
		High horizontal 2	P9-405R-H2	-	-	-	-	-	
403R	Right	Inclined 2	P9-403R-I2	7.2	0.2	-2.4	-	-	
				12.5	0.4	-3.9	-	-	
		High horizontal 2	P9-403R-H2	5.2	0.6	0.8	-	-	
404R	Right	Inclined 2	P9-404R-I2	-	-	-	-	-	
		High horizontal 2	P9-404R-H2	-	-	-	-	-	

Table 3 (continued).

Tendon No.	Cell	Location	Section Label	MMFM testing			Ultrasonic/sonic testing		
				Center of damage (m)	Length of damage (m)	Estimated section loss (%)	Tendon ID	Location (ft)	No thru frequencies
Additional span tested (Span 8)									
406R	Right	High horizontal 1	P8-406R-H1	-	-	-	-	-	
		Inclined 1	P8-406R-I1	16.8	1	1	-	-	
405R	Right	High horizontal 1	P8-405R-H1	-	-	-	-	-	
		Inclined 1	P8-405R-I1	14.9	1.7	1.3	-	-	
404R	Right	Inclined 1	P8-404?R-I1 (new)	-	-	-	-	-	
403R	Right	High horizontal 1	P8-403R-H1	2.6	0.8	1.5	-	-	
		Inclined 1	P8-403R-I1	-	-	-	-	-	
403R	Right	Inclined 2	P8-403R-I2	-	-	-	-	-	
		High horizontal 2	P8-403R-H2	-	-	-	-	-	
404R	Right	Inclined 2	P8-404R-I2	-	-	-	-	-	
		High horizontal 2	P8-404R-H1	-	-	-	-	-	
405R	Right	Inclined 2	P8-405R-I2	3.3	0.3	-3.1	-	-	
		High horizontal 2	P8-405R-H2	-	-	-	-	-	
406R	Right	Inclined 2	P8-406R-I2	-	-	-	-	-	
		High horizontal 2	P8-406R-H2	-	-	-	-	-	
							-	-	
403L	Left	High horizontal 1	P8-403L-H1	-	-	-	-	-	
404L	Left	High horizontal 1	P8-404L-H1	2.6	0.6	0.7	-	-	
405L	Left	High horizontal 1	P8-405L-H1	-	-	-	-	-	
406L	Left	High horizontal 1	P8-406L-H1	-	-	-	-	-	

6 SUMMARY

The failure of the external tendons in the Ringling bridge was attributed to the development of severe strand corrosion caused by deficient grout material. It has been advocated that assessment of steel cross-section loss alone would not adequately address the corrosion associated with deficient grout. It was observed in earlier research that the extent of grout segregation can vary in magnitude, and corrosion rates may vary as well. Remnant deficient grouts may provide conditions for incipient anodes. The discovery of a tendon with severe corrosion as detailed earlier even after the intensive field inspections in 2012 was indicative of the difficulties of fully identifying tendon deficiencies. Despite extensive repair works, practical constraints and limitations did not allow a thorough assessment of corrosion activity. An alternative assessment was highly desired to verify condition of these repaired tendons.

In Phase I of the project, different commercially available nondestructive technologies were carried out to evaluate the capabilities in detecting defects in tendons. MMFM and UST provided strong indicators to detect metal section loss and anomalous grout/filler conditions, respectively.

In Phase II, practitioners offering testing services were selected to carry out in situ testing on external PT tendons. NDT Corp. was selected to carry out ultrasonic/sonic (impact echo) testing and Tokyo Rope for MMFM testing. Both vendors carried out field testing on all spans of the Ringling bridge, mainly in the center cell.

One of the merits for selection of technologies was their field applicability. A few of the commonly available technologies that are efficient in laboratory or mockup specimen may have limitations in field applications. Some of the field limitations include portability, access, power source, safety, end user expertise, etc. which may undermine the benefits of these technologies. The identified technologies were effective and robust in their application. Although both USTC and MTC used different technologies to look for steel section loss and grout/filler anomalies, a matrix was developed in Table 4 to summarize the efficacy of these technologies for field testing conditions.

Table 4. A summary table of field application of MMFM and ultrasonic/sonic testing.

Vendor	Cost (\$)	Crew size (No.)	Time	Percent Tendon Tested (%)	Geometric limitations	End user expertise	Portability
USTC	70,305	4 min	Nov. 8-15	33% <	Scaffolding required	Expert	Portable compact
MTC	178,531	5	Feb. 5-22	33%	Ladders	Expert	Portable compact

Table 5. Field observations of tendon openings.

Tendon	Location Cell	Tested by	Prediction	Observations	Conclusion
Test Site 1					
403R-7	Span 8	MTC	1.5% cross-section loss	Corrosion observed in strand - Bleed trail – minor void	Difficult to determine magnitude of cross-section loss
	Right	USTC	-		
Test Site 2					
406L-8	Span 9	MTC	1.4% cross-section loss	No section loss observed - Bleed trail – Minor void	Cross-section loss not observed in outside bundle
	Left	USTC	-		
Test Site 3					
402L-1	Span 2	MTC	Not tested by MTC due to low clearance		
	Center	USTC	Anomalous grout (Missing freq's 15, 20 and 25)	No corrosion- Circumferential cracking - Bleed Trail - Minor void - Hardened grout elsewhere	May be circ cracking and bleed trail does not correlate with existing corrosion and section loss
Test Site 4					
303L-5	Span 5	MTC	2.2% additional mass	Steel debris found. No corrosion in outside bundle Circumferential cracking - Bleed Trail - Minor void - Hardened grout elsewhere	MMFM was able to predict additional mass
	Center	USTC	-	-	Debris should have changed freq's and alerted an anomaly. USTC tested every 1-ft. so they may have missed the location
Test Site 5a					
402L-1	Span 2	MTC	2.40% cross-section loss	Corrosion not observed - Bleed trail – Minor void - Circumferential cracking – Hardened grout elsewhere	Cross-section loss not observed in outside bundle
	Center	USTC	-	-	
Test Site 6					
401L-3	Span 4	MTC	Not tested by MTC due to low clearance		
	Center	USTC	Anomalous grout (Missing freq's 15, 20 and 25)	Not corrosion - Bleed trail- Small air bubble/void - Hardened grout elsewhere	Except hair line cracking, grout anomaly not found

Table 5 (continued).

Tendon	Location Cell	Tested by	Prediction	Observations	Conclusion
Test Site 7					
401L-1	Span 1	MTC	2.4% additional mass	No corrosion observed	Cross-section loss or additional mass not observed in outside bundle
	Center	USTC	Anomalous grout (Missing freq's 15, 20 and 25)	Minor void – Circumferential cracking – Hardened grout elsewhere	Ultra sonic method was too sensitive to any cracking and not able to relate the frequency to type of defect
Test Site 8					
401R-1	Span 1	MTC	1.5% cross-section loss	No corrosion observed on surface	Cross-section loss not observed in outside bundle
	Center	USTC	Anomalous grout (Missing freq's 15, 20 and 25)	Circumferential crack - Hardened grout elsewhere – Minor void	Except hair line cracking, grout anomaly not found
Test Site S					
402R-7	Span 8	MTC	-	No corrosion observed on surface	Broken loose strand
	Center	USTC	-	No grout distress – Hardened grout elsewhere	-

After the field testing, the testing companies assessed their data and submitted detailed reports. A total of nine test sites were selected out of which four were recommended by USTC, an additional four by MTC and an extra exploratory site. Tendon validation was carried on these test sites by opening the tendons. Table 5 presents the summary of results obtained by opening several locations along the tendons in the Ringling bridge for assessing the capabilities of the two nondestructive technologies. The table also presents the conclusions from these test results.

The outcome of the field validations indicated promising capabilities of MMFM for steel section loss in external PT tendons. MMFM was able to detect severe strand corrosion at tendon location (403R-7) that was previously inspected in 2012. Also, MMFM accurately detected the presence and position of steel debris in tendon 303L-5. The MTC was able to successfully identify their two recommended locations. An assessment of the other two recommended locations was difficult because the section loss could not be verified for strands located in the middle of the 22-strand bundle.

The results of ultrasonic/sonic (impact echo) testing showed a lack of strong indicators of grout anomalies. This reflects the generally good condition of the grout in the previously inspected and repaired tendons. Ultrasonic/sonic testing did give differentiation in through-duct and circumferential resonant frequencies and there were indicators that physical grout anomalies such as circumferential cracking can be sensed. Since tendon 403R-7 with observation of deficient grout and steel corrosion was not part of the scope of work for NDT Corp., it is recommended that the supplemental testing or additional testing on that tendon be made to clarify field-ready capability of the technology to identify grout segregation. This will enable a better characterization of that defect modality to be made. Further refinement in data interpretation to identify grout cracking would provide useful assessment of tendon durability such as cracking induced by strand corrosion or strand breaks. At the conclusion of field validation, the vendors took necessary data to reassess their original recommendations and submitted their comments on the results.

In summary, MTC suggested four locations for tendon validation. USTC also recommended four additional locations to be opened for validation. In addition, an extra exploratory site was included to assess duct deformation. The recommended locations for opening did not coincide for both vendors. During the earlier repair works, many tendons were re-grouted and not all corroding tendons were replaced. Therefore, there is a possibility of having section loss in good grout and no section loss in locations with voids/bad grout.

The major challenge in fully assessing the accuracy of the MTC technology is the ability to assess the health of steel wires inside the bundle. To this end x-ray could be used to assess the condition of wires not visible from surface. This step is to verify the accuracy of predictions made by MTC and not a recommendation for normal inspection process. Based on the outcomes of the study, following conclusions can be drawn:

- If the department utilizes MMFM for inspection of tendons, perform an initial calibration of verification using x-rays at the beginning of the work.
- MMFM is a promising method to assess the section loss in external tendons.
- Development of MMFM method that can also inspect tendons with low clearance, for inspection of tendons located near floor is recommended.

While ultrasonic/sonic method was able to differentiate the through duct and circumferential frequencies, however, it was unable to characterize the type of grout defect. In general, additional data is needed to make judgment about ultrasonic/sonic (impact echo) method.

7 COMMENTS OF USTC AND MTC AFTER VALIDATION TESTING

The tendon validation testing was attended by representatives of FIU, Concorr FL, USTC and MTC. The validation sites recommended by USTC and MTC were opened at the locations given in Table 2. The vendors documented the validation testing and took necessary data to reassess their recommendations. In view of the results of tendon verification openings, the vendors submitted their comments.

7.1 USTC COMMENTS ON VALIDATION TESTING

The following documentation was part of correspondence between representative of FIU and USTC after field validation was completed.

Other discussion points:

In summary Tokyo Rope (MTC) identified four locations as a problem area to be opened for verification. NDT (USTC) also identified four locations as a problem area. In general, the locations did not coincide.

In general, additional data is needed to make judgment about ultrasonic/sonic method. Ultrasonic/sonic method could be effective when soft grout exists. While ultrasonic/sonic testing is able to identify anomaly inside the tendon, however it is not able to distinguish types of defect in grout. Therefore, the data obtained from ultrasonic/sonic may not be very useful.

NDT (USTC) comments on Other discussion points:

The sequence of events of when and where testing was conducted has to be understood when correlating NDT (USTC) and Tokyo ropes (MTC) verification locations. Site 1 and 2 were in areas not tested by NDT (USTC) prior to validation. Sonic/ultrasonic test data acquired at site 1 (which had strand corrosion and section loss) by NDT (USTC) during the validation program before the duct was opened) had anomalous sonic/ultrasonic data. These results are not included in our report as it was submitted prior to the validation program. It should be noted that at the 2 Tokyo Rope problem locations selected for validation in the center cell; locations that were sonic/ultrasonic tested, hard uncracked grout and no indications of voiding were detected. Validating sonic/ultrasonic results of "good" grout conditions.

The results of the sonic/ultrasonic impact echo testing of the external tendons at the Ringling bridge determined that approximately 2% of the length of the duct tested have anomalous data. The data quality was good and the results in general did not indicate significant grout issues. Because there was going to be a follow up validation of results, 4 locations with anomalous impact echo readings were selected for validation. Validation at four locations of these anomalies detected circumferential/transverse cracking in the duct grout at all 4 locations.

Cracking in the grout explains and is the cause of the anomalies readings. The significance of these cracks can be debated but they could provide a conduit for moisture to penetrate to the tensioning strands and imitate corrosion.

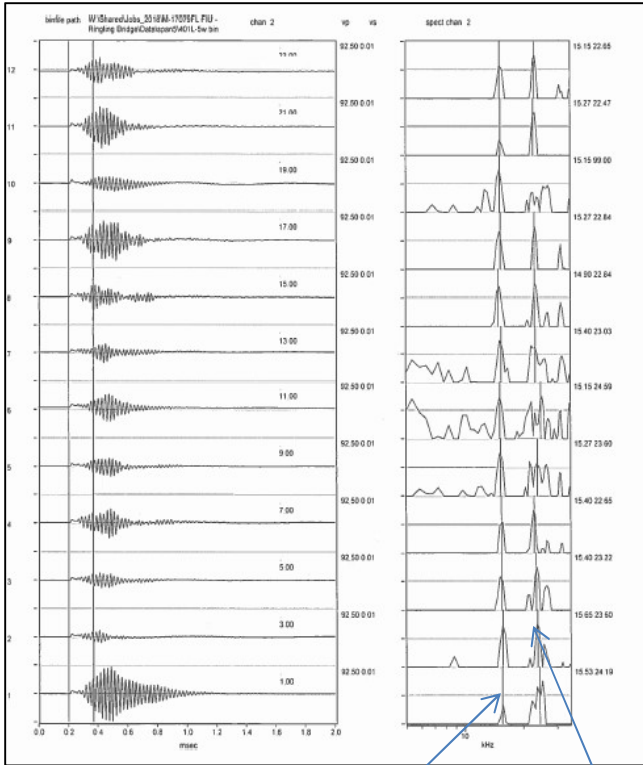
Additional data and test with validation of results would be helpful to refine the data interpretation and this is true of all testing methods. The Impact echo data interpretation could be improved with the addition of pulse velocity measurements. This can be easily accomplished by adding a sensor 1 or 2 feet laterally from the energy source used for impact echo testing. Pulse velocity data would provide an average compressional and shear wave velocity of the internal grout material. These velocity values could be used to make an evaluation of the internal grout similar to below:

- Compressional wave 12,000 to 14,000 ft/sec and shear wave velocity of 6,500 to 7,500 ft/sec for duct filled with hard grout
- Compressional wave 10,000 to 12,000 ft/sec and shear wave velocity less than 4,500 to 6,500 ft/sec for grout with minor cracking
- Compressional wave less than 10,000 ft/sec and no or very poor shear wave arrival for voided, soft grout or severely fractured grout.

The sonic/ultrasonic data is very useful to identify voids or soft grout which are associated with tendon corrosion but does not and cannot measure tendon strand loss of section. The sonic/ultrasonic results were useful in the case of the Ringling bridge, 12, 175 feet of external PT duct was tested approximately 232 feet had anomalous impact echo data. These results eliminated 11,943-ft of duct to be concerned about and focused the validation of results to specific locations. Validation of sonic/ultrasonic results detected circumferential cracking of the duct grout at all the locations selected.

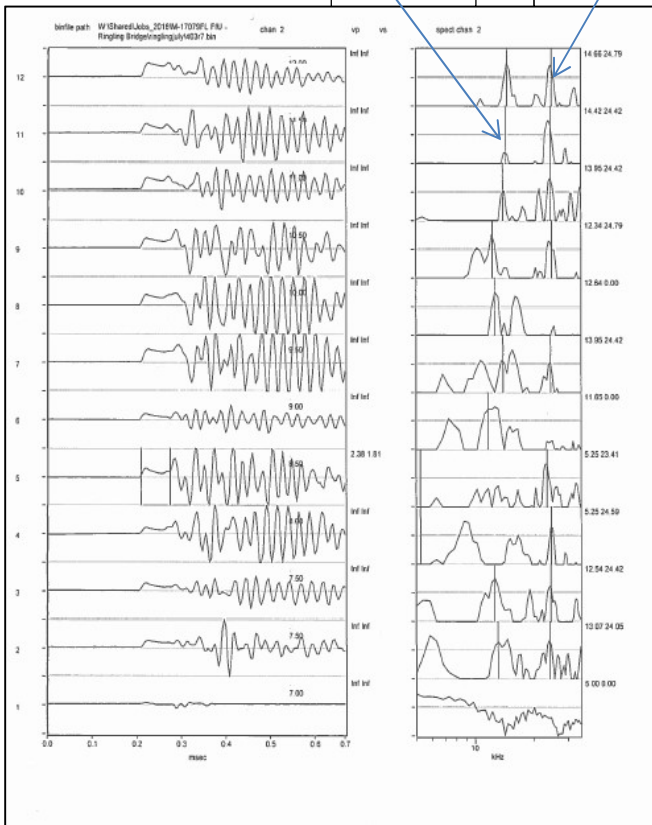
We appreciate the opportunity to work with and share information with FIU on this project and look forward to other opportunities to collaborate with FIU.

Paul Fisk
NDT Corporation
153 Clinton Road
Sterling, MA 01564
978-563-1327 Phone
978-563-1340Fax
paul.fisk@ndtcorporation.com
<http://www.ndtcorporation.com/>



Center Cell Span 5 duct 401L-5W
 "Good" strong 15 and 25 KHZ signal
 Duct filled with hard grout
 Station 1 to 23

15 KHZ 25 KHZ



Sonic/ultrasonic data collected
 During Validation after Report submittal
 Right South Cell span 8 duct 403R
 Stations 7 to 12
 Note low amplitude missing 15 and 25 KHZ
 Anomalous sonic/ultrasonic data

7.2 MTC COMMENTS ON VALIDATION TESTING

After the completion of field validation testing, the MTC analyzed their original data in view of the tendon validation results. The analysis was performed for all the sites recommended by MTC and based on this analysis, conclusions and suggestions for further investigation is provided. The comments are attached as Appendix F.

REFERENCES

Azizinamini, A., & Gull, J. (2012b). *Improved Inspection Techniques for Steel Prestressing/Post-Tensioning Strand (FDOT Research Project BDK80-977-13)*. Miami, FL: Florida International University.

Azizinamini, A., & Gull, J. (2012a). *FDOT Protocol for Condition Assessment of Steel Strands in Post-tensioned Segmental Concrete Bridges: Volume II (FDOT Research Project BDK80-977-13)*. Miami: Florida International University.

Rehmat, S. e, Sadeghnejad, A., Valikhani, A., Chunn, B., Lau, K., & Azizinamini, A. (2017). Magnetic Flux Leakage Method for Detecting Corrosion in Post Tensioned Segmental Concrete Bridges in Presence of Secondary Reinforcement. In Transportation Research Board 96th Annual Meeting (Vol. 221, pp. 1–15).

Permeh, S., Vigneshwaran, K. K., & Lau, K. (2016). *Corrosion of Post-Tensioned Tendons with Deficient Grout (FDOT Research Project BDV29-977-04)*. Miami, FL: Florida International University.

APPENDIX A USTC PROPOSAL (NDT CORP.)



153 Clinton Road • Sterling, MA 01564

Tel: 978-563-1327

Fax: 978-563-1340

March 23, 2016

Atorod Azizinamini, Ph.D., P.E.
Professor and Chairperson
Civil and Environmental Engineering Department
Florida International University
10555 W. Flag
Miami, Florida

Subject: Proposal for Nondestructive Testing of External PT Ducts, Ringling Bridge Sarasota, FL

Dear Dr. Azizinamini:

NDT Corporation is pleased to submit this proposal to conduct nondestructive testing to evaluate external post tensioning (PT) duct grout conditions. The testing proposed is similar to measures made on sample PT duct sections during a demonstration at FIU in the spring of 2015. This draft proposal is submitted for your review and comment.

Work Plan:

The plan is to have two -2 man crews working simultaneously. One crew will be moving and assembling scaffolding and mark stationing on the outside of each of the tendon ducts. The other crew will be conducting the sonic/ultrasonic testing. NDT's on site project coordinator will be evaluating data as it is acquired. It is believed with this set up 2 cells of the bridge can be tested a day and the 11 spans and 33 cells can be tested in approximately 18 days (3 weeks). Additional time will have to be allotted for verification of results.

The RFP indicates an assessment of results is to be made when 25% of the tendons have been tested. A suggestion would be to test the center cell in all 11 spans, 33% of the entire bridge and then do the assessment. This plan would have data from each span and the best access/efficiency for moving and assembling scaffolding. It is anticipated that 6 days (1 week) of testing will be required to evaluate the center 11 cells. Prior to starting work it will have to be agreed upon as to which cells and spans will be tested for the 25% or 33% complete before the program evaluation is conducted.

Scaffold rental is relatively inexpensive, \$94/month per scaffold. It is planned that 4 sets of scaffolding will be rented. By having 4 sets of scaffolding, 2 sets can be set up at the PT duct high points at each end of the span and 2 sets being relocated to the next span.

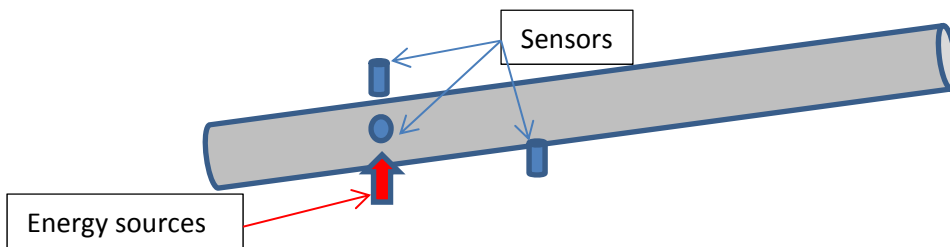
Access into the bridge will be from a ladder on the walking bike path at the west end of the bridge. The access area will be coned off. The ladder will be lifted into the bridge while the crew is working so that no unauthorized entrances can be made. The bridge is a non-permit confined space. NDT will have a sign in and sign out sheet to account for all workers in the bridge, each crew will have air monitors but there will not be a topside/bottom side safety watch.

The first day of work will be mobilizing and setting up scaffolding into the western most spans and stationing the 4 PT ducts in these spans. Ideal stationing will be marked at 1 foot interval with 10 foot marks labeled. These station marks will expedite data acquisition and insure that anomaly locations can be precisely determined for verification of results after the testing is complete. Each succeeding day sonic/ultrasonic testing will be done at one foot

intervals along each of the PT ducts in a cell by one crew while the other crew is moving and assembling scaffolding and stationing PT ducts.

Sonic/ultrasonic Testing:

The sonic/ultrasonic testing will use a high frequency, “clicker”, or projectile impact energy source and a four sensor array to acquire multiple data sets simultaneously. The energy source is to be positioned close to the bottom of the duct (or as close as it can be with a 1 inch clearance in some locations) where it is assumed that in most cases there will be grout in the bottom of the duct. Receiver sensors will be positioned 180, 90 and 240 degrees from the energy source on the circumferences of the PT duct. These sensors will measure direct through waves and impact echo data. A fourth sensor will be positioned 1 foot from the energy sources at the same position on the duct. This sensor will be used to measure refracted wave signals from the grout inside the duct. This data acquisition set up is displayed below:



It is anticipated that if the duct is filled with hard grout: all the circumferential sensors will have high amplitude, high velocity wave arrivals and impact echo resonate frequencies and the refracted wave velocities will be high. If the duct is partially voided or soft grout: the signal quality for the sensors the circumferential sensors will be poor and the refracted wave signals low velocity. If the duct is voided or filled with soft grout; there will be no or poor arrivals at all sensors.

Testing at deflectors and diaphragms will be done by positioning sensor circumferentially around the PT duct on one side of the deflector or diagram and generating energy on the opposite side. This procedure probably cannot be done for diagrams on the exterior cells because of the distances wires will have to be run to test both sides of the diagrams.

As part of the mobilization plan, NDT plans to examine and sonic/ultrasonic test several of the samples the Florida DOT has in Gainesville. This will serve as a calibration and perhaps adjustments in our testing program that will provide better results.

Results Verification:

When the testing is within a few days of the 25% threshold a meeting should be scheduled with FIU, and Florida DOT personnel to review the results and plan locations for verifications to verify results and retrieve grout samples.

Costing:

Costing is separated into 2 scenarios:

Scenario 1: Testing of 25% to 33% of the ducts and verification of results:

It is anticipated that 6 days of testing will be required for the sonic/ultrasonic testing.

Mobilization/Demobilization	\$18,805	
*6 days of sonic/ultrasonic testing	\$41,200	
Final Report	\$10,300	
Total Cost		\$70,305

Scenario 2: Testing of 100% of the ducts and verification of results:

It is anticipated that 18 days of testing will be required for the sonic/ultrasonic testing.

Mobilization/Demobilization	\$20,300	
*18 days of sonic/ultrasonic testing	\$125,100	
Final Report	\$17,500	
Total cost		\$162,900

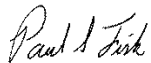
*this cost includes in field data analysis.

All work will be conducted in accordance with the attached General Terms and Conditions.

We look forward to working with you on this project.

Sincerely

NDT Corporation



Paul Fisk

GENERAL TERMS AND CONDITIONS

All services provided by NDT Corporation (CONSULTANT) are subject to these Terms and Conditions. The parties intend that in the event of a conflict between the Master Service Agreement and these Terms and Conditions, these Terms and Conditions shall prevail.

PARTIES:

“CONSULTANT” shall mean NDT CORPORATION and “CLIENT” shall mean the insert name of Company/Person

STANDARD OF CARE:

The Standard of Care applicable to the CONSULTANT’S services will be the degree of skill and diligence normally employed by professional consultants performing the same or similar services.

ACCESS:

The CLIENT shall furnish all access to property and rights-of-way for the performance of the CONSULTANT’S services.

RATES AND PAYMENT:

The quoted rates are exclusive of sales, use, excise, business and occupation, and similar taxes as well as import fees. Such taxes or fees, if applicable, shall be for the CLIENT’S account. Tax exemption identification and documentation must be provided when applicable.

Unless otherwise agreed and documented, invoices are due and payable upon receipt. The CLIENT shall also pay the CONSULTANT a late payment charge for any payments not made within (60) days of the date of applicable invoices at the rate provided by law or 1-1/2% per month, whichever is greater.

These rates will be in effect through December 31, 2016. If work on this project begins or extends beyond the effective date, our rates will be updated.

TIME OF PERFORMANCE:

The CONSULTANT shall commence work upon receipt of written notice to proceed from the CLIENT, and shall complete the work within the time period set forth in the Agreement, subject to any delays caused by the CLIENT, other agencies involved in review of the work or any other parties or factors not directly under the control of the CONSULTANT.

MODIFICATIONS:

In the event the CLIENT requires modifications and/or changes after services have been performed, which modifications and/or changes are through no fault of the CONSULTANT; or in the event the CLIENT desires additional work not covered by the agreement, the CONSULTANT shall perform such work as authorized by the CLIENT in writing and shall be paid for such work as agreed between the CLIENT and the CONSULTANT. The CONSULTANT shall not be obligated to commence the extra work until the additional fee is agreed to by the parties.

SUSPENSION OR TERMINATION:

In the event the work is terminated or suspended by the CLIENT prior to the completion of the Agreement, the CONSULTANT shall be paid an equitable amount proportional to the services rendered to the date of termination or suspension.

LEGAL:

The CLIENT shall furnish the CONSULTANT all legal services and opinions necessary in the performance of the services to be rendered by the CONSULTANT. CLIENT is responsible for the accuracy of information provided to CONSULTANT. CONSULTANT shall rely on the accuracy of information provided by CLIENT without independent verification.

INTELLECTUAL PROPERTY RIGHTS:

Upon payment in full, CLIENT shall have the right to use the results of CONSULTANT's analysis (work product) solely for purposes defined in the Agreement. CONSULTANT retains all rights, title and interest in and to any technology, methods, analysis tools, know-how and any inventions used by CONSULTANT to perform the services. No license, express or implied, by estoppel or otherwise, is granted by CONSULTANT to any intellectual property rights owned by or licensed to CONSULTANT or any of its Affiliates. CLIENT shall make no attempt to reverse engineer or otherwise circumvent CONSULTANT's method and tools.

In the event of a breach of its Intellectual Property Rights, CONSULTANT shall be entitled, in addition to any and all other remedies, to injunctive relief and other equitable damages without proof of monetary damages.

In addition, CLIENT agrees to refrain from soliciting or hiring any employees of CONSULTANT for a period of one year following termination of the work relationship with CONSULTANT.

DEFENSE OF CLAIMS:

In the event of a public hearing, arbitration hearing or proceeding relating in anyway to the Project, the CLIENT agrees to compensate the CONSULTANT consultant for the time devoted to preparing for hearings/litigation, responding to requests for production of documents by any party, appearance at depositions or trial, or any other matters involving such hearing or legal proceedings. Compensation shall be based upon hourly rates mutually agreed to by the parties prior to Consultant commencing such services. This provision does not apply to legal action in which Consultant is a named plaintiff or defendant in which event Consultant shall appear on its own behalf. Consultants legal cost cannot exceed the contract value.

INSURANCE:

The CONSULTANT during the performance of this Agreement, will at its own expense carry Worker's Compensation Insurance/Employer's Liability Insurance within limits required by law; Comprehensive General Liability Insurance with limits of not less that \$1,000,000/\$1,000,000 for bodily injury and \$1,000,000/\$1,000,000 for property damage; Comprehensive Automobile Liability Insurance with limits of not less the \$1,000,0000 combined single limit for bodily injury and property damage and Professional Liability Insurance with limits of \$1,000,000.

INDEMNIFICATION:

CLIENT agrees to indemnify and defend CONSULTANT from any claims resulting from inaccurate information or negligence of CLIENT. CONSULTANT agrees to indemnify CLIENT from damages directly resulting from CONSULTANT'S gross negligence in the performance of professional services under this Agreement.

LIMIT OF LIABILITY:

Under no circumstances shall the CONSULTANT be liable to the CLIENT for any consequential damages, including but not limited to loss of profit or costs.

COMPLIANCE WITH LAW:

The CONSULTANT shall comply with all applicable provisions of the Unemployment compensation, sickness and disability and Social Security laws, the Fair Labor Standards Act and all other Federal, State and Local laws or regulations relating to employment.

SEVERABILITY:

If any one or more of the provisions contained in this Agreement, for any reason, are held to be invalid, illegal or unenforceable in any respect, such invalidity, illegality or unenforceability shall not effect any other provision hereof and this Agreement shall be construed as if such invalid, illegal or unenforceable provision had never been herein.

DISPUTE RESOLUTION:

In the event of a dispute, the parties agree to use mediation to resolve it. If mediation is unsuccessful, the parties agree to binding arbitration to be conducted in the Worcester, MA area which will be determined under the laws of the Commonwealth of Massachusetts without regard to its conflicts of laws provisions.

**APPENDIX B USTC FIELD TESTING AND TENDON
VALIDATION (NDT CORP.)**

DRAFT
NDT SONIC/ULTRASONIC INSPECTION
OF EXTERNAL POST TENSIONING GROUT
RINGLING BRIDGE
OVER SARASOTA BAY
SARASOTA, FLORIDA



PREPARED FOR
FLORIDA INTERNATIONAL UNIVERSITY
JANUARY, 2018





153 Clinton Road • Sterling, MA 01564

Tel: 978-563-1327

Fax: 978-563-1340

January 24, 2018

Dr. Kingsley Lau, Ph.D.
Florida International University
Department of Civil & Environmental Engineering
10555 W. Flagler St.
Miami, FL 33174

Subject: NDT grout condition assessment of external post tensioning ducts,
Ringling Bridge, Sarasota, Florida.

Dear Dr. Lau:

In accordance with our contract agreement, NDT Corporation conducted nondestructive sonic ultrasonic measurements on 44 external tendon ducts in the center cell of spans 1 to 11 of the Ringling Bridge in Sarasota, Florida. The nondestructive sonic/ultrasonic testing was conducted from November 8th through November 15th, 2017. The objective of this investigation was to evaluate internal duct grout conditions and identify areas of soft, voided or segregated grout.

If you have any questions or comments, please contact the undersigned.

Sincerely,
NDT Corporation

Paul S. Fisk

Table of Contents

1.0	Summary	Page 1
2.0	Introduction & Purpose	Page 1
3.0	Investigation Method	Page 2
4.0	Discussion of Results	Page 5
5.0	Results	Page 9
6.0	Recommendations	Page 10

Table -1 Impact Echo Results

Appendix-1 Sonic/ultrasonic Nondestructive Testing

Appendix-2 Data Plots

1.0 Summary

The objective of this investigation was to evaluate grout condition of 44 external tendon ducts in the center cell of the 11 span Ringling Bridge and identify with impact echo data locations indicative of areas of soft grout or voids. Approximately 12,000 linear feet of sonic impact echo data was collected during this investigation.

Calibration sonic/ultrasonic testing was conducted at Florida DOT's Materials Department in Gainesville on duct segments 25b, 33b and 36 (FDOT designations) removed from the Ringling Bridge during repairs. This calibration determined that there is a full grout through thickness impact echo 20 kHz frequency indicative of "good" grout and when the 20 kHz was not present the ducts have weak segregated grout.

Most of the data acquired on the exterior PT ducts at the Ringling Bridge have the 20 +/- kHz full duct thickness resonant frequency, a 25 +/- kHz associated with the 3.5 inches of competent (high velocity) grout inside the PVC duct as well as a 15 +/- kHz associated with the compressional wave traveling around the circumference of the competent grout. The 20 and 25 kHz through duct frequency data are considered to be representative of internal duct conditions and used to evaluate grout conditions.

The PT ducts in Spans 1 through 5 have significantly more anomalies associated with weakened grout conditions (voids, soft grout or segregation) than spans 6 through 11. The anomalies considered to be most significant are:

- Span 1 duct 401L-1W Stations 164 to 169 (high point at diaphragm)
- Span 2 duct 4402L-1E Stations 107 to 117 (flat horizontal area of duct)
- duct 402R-2W Stations 19 to 38 (flat horizontal area of duct)
- Span 4 duct 402R-4W station 43 to 81 (flat horizontal area of duct)
- duct 401L-3E stations 138 to 142 (next to anchorage)
- duct 402L-3E stations 138 to 142 (next to anchorage)

Four locations have been suggested for opening of the PVC duct to examine internal grout conditions.

2.0 Introduction and Purpose

A nondestructive sonic/ultrasonic resonant frequency/pulse echo (sonic) investigation was conducted to evaluate the 44 external tendon ducts in the center cell of spans 1 to 11 of the Ringling Bridge in Sarasota, Florida (Figure 1, below). NDT Corporation conducted the nondestructive sonic testing investigation from November 8th through November 15th, 2017. On November 7th of 2017 NDT visited Florida Department of Transportation to test sections of removed external ducts for calibration.

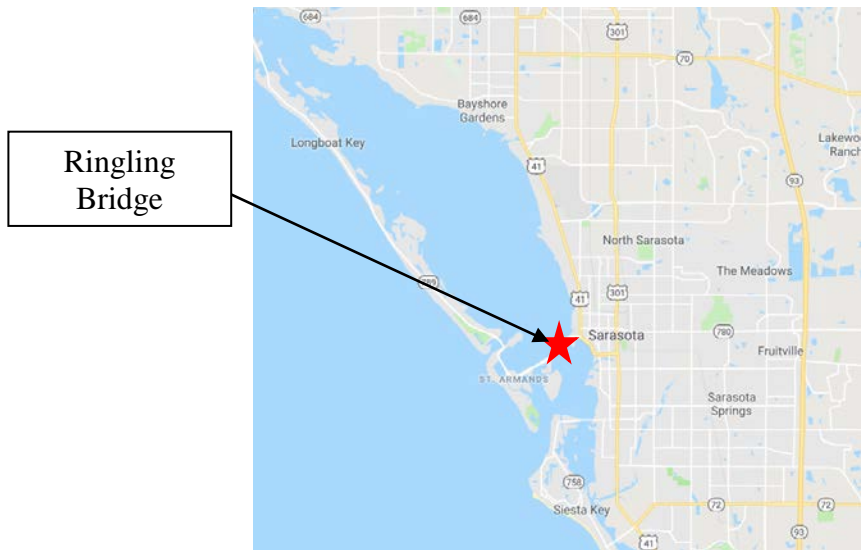


Figure 1: Bridge Location

3.0 Investigation Methods

For the sonic testing, energy input with a piezo-ceramic “clicker” energy source was at the 11:00 o’clock duct position and a sensor at the 5:00 o’clock duct position. The energy source creates a compressional wave that propagates through the PVC duct and into the grout filling the PVC duct and reflects from the back surface of the PT duct. This energy is trapped between the two surfaces and resonates at a frequency that is a function of the compressional wave velocity and the duct or grout thickness. When the thickness and the compressional wave velocity remain constant, which is the normal condition for duct filled with competent grout, the resonant frequency is expected to be approximately 20 kHz for the 4 inch thick external PT Duct. If the compressional wave is trapped within the 3.75 inch thick grout inside the PVC PT duct the resonant frequency is expected to be approximately 25 kHz. When the 20 and 25 kHz thickness resonant frequencies are missing, then anomalies such as voids, soft grout or grout delaminated from the PVC duct are suspected.

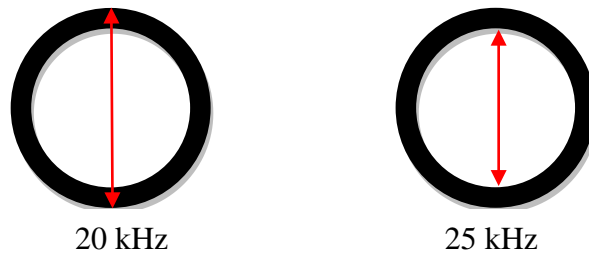


Figure 2: Sonic Wave paths for fully grouted external PT Ducts

The principal criterion for evaluating the tendon ducts is the resonant frequency value of the element. The resonant frequency of a free-free faced element (wall face to wall face) in its simplest form is given by:

$$f = \frac{nV}{2T}$$

Where f is the resonant frequency, n the mode 1, 2, 3 -- of a free-free element, V is the velocity of the sonic/ultrasonic wave in concrete (typically about 13,500+ ft. /sec). T is the thickness of the PT duct which in this case is 4 inches.

The resonant frequency for a fully-grouted duct should represent the thickness of the duct. If the duct grout is voided or has soft grout or grout delamination's exist, the normally established reflected wave may not be developed or the wave reflections may destructively interfere with the normally reflected wave preventing development of the normal thickness resonant frequency

3.1 Nondestructive Testing Measurements

Sonic/ultrasonic and impact echo/resonant (multiple reflections) frequency measurements were obtained using a piezo electric "clicker" energy source, a hand-held sensor and a portable computer to archive and provide a quality control field display of data (Photograph 1). Sonic/ultrasonic data were obtained for each tendon by positioning the energy source on one side of the PT duct and a sensor on the opposite side and incrementing the readings at 1 or 2 foot intervals. Sonic/ultrasonic impact echo measurements were made at 1 foot intervals at tendon high points and 2 foot intervals in transition and low areas. Measurements were made by positioning the "clicker" energy source at 11:00 o'clock and the sensor at 5:00 o'clock or 1:00 and 7:00 o'clock positions depending on access, activating the energy sources and recording the resulting signal for 4 milliseconds. A discussion of the sonic/ultrasonic survey method is included in Appendix 1.



Photograph 1-Data acquisition

3.2 Survey Control

Each duct was identified using the FDOT designations marked on anchorage, abutment, and diaphragms (see Photograph 2 below). PT ducts were stationed at 1 foot intervals from west to east using tape and measurements referenced to duct starting point at abutment and anchorage blocks and from the west face of diaphragm walls at piers. Spans 2 through 10 have anchoring blocks mid-span where the ducts are anchored (pictured below).



Photograph 2- Anchorage blocks at center of spans

One foot station marks with station labeling at 5 foot intervals was marked on the ducts with chalk (Photograph 3 below).



Photograph 3- Location station marks on duct

In span 1 and 11 the ducts were anchored to the abutments. See sketch Figure 2 below

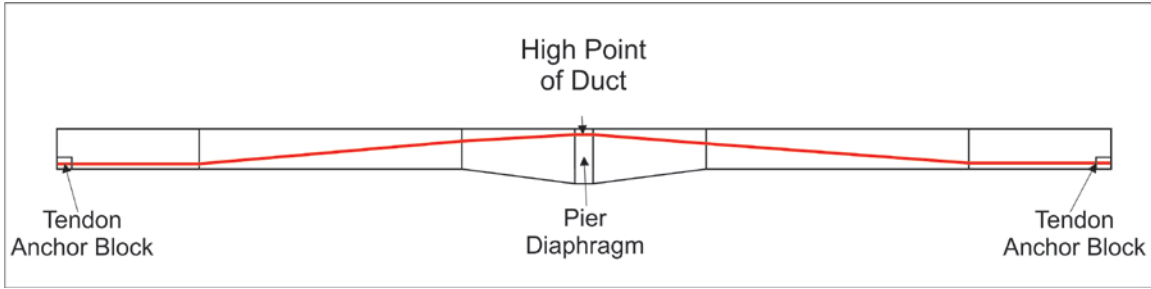


Figure 2- Sketch plan of the typical layout of a tendon duct.

4.0 DISCUSSION OF RESULTS

4.1 Calibration

Prior to initiating testing at the Ringling Bridge, sonic/ultrasonic testing was conducted at the Florida DOT's materials department in Gainesville on duct segments 25b, 33b and 36 (Photograph 4 below) removed from the Ringling Bridge during repairs.



Photograph 4- Duct segments 25b, 33b and 36

The objective of the testing was to determine the difference in signal characteristics associated with ducts filled with hard “good” grout versus those with anomalous grout conditions (voided, soft or segregated, etc. grout). Sonic/ultrasonic impact echo and direct wave measurements were made at 6 inch intervals the length of all 3 sample duct sections. Measurements were made by positioning the “clicker” energy source at 9:00 o’clock and the sensor at 3:00 o’clock on the duct section (Photograph 5 next page) and recording the resulting signal for 4 milliseconds.



Photograph 5- Sonic/ultrasonic impact echo testing

Measurements were repeated at the same location with the “clicker at 6:00 o’clock and sensor at 12:00 o’clock. The results were evaluated as data were acquired and duct segments 25b and 33b have a full through thickness impact echo 20 kHz frequency indicative of “good” grout and duct segment 36 did not have the 20 kHz and was suspect of having anomalous grout conditions. Data recordings of these signal characteristics are shown on Figure 3 and 4.

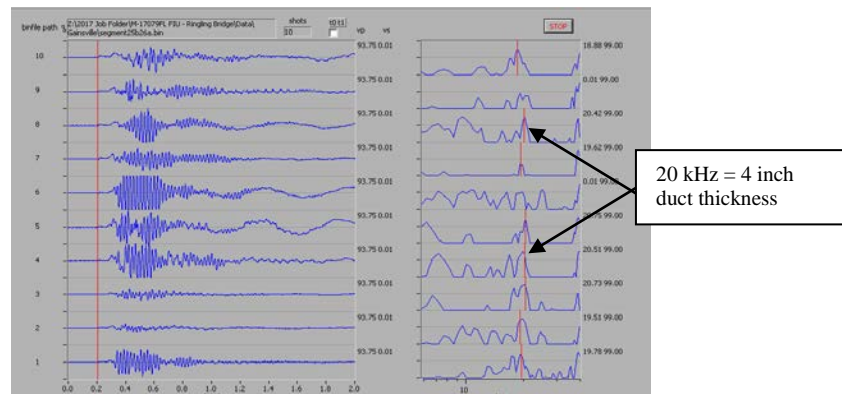


Figure 3-Duct 25b sonic/ultrasonic data – “good grout (note 20 kHz 4 inch duct thickness resonances)

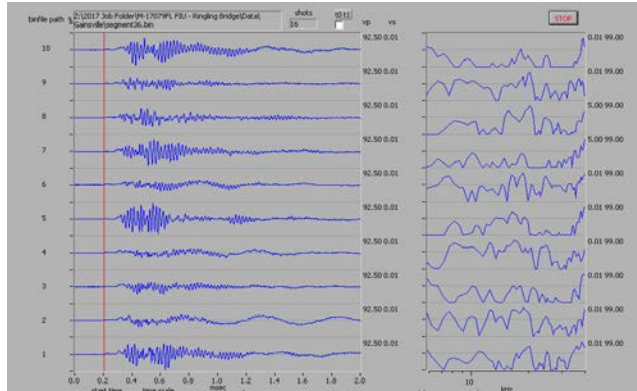


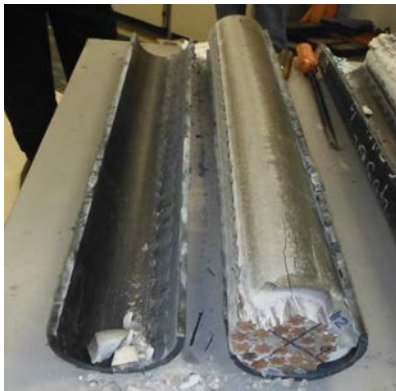
Figure 4 -Duct 36 sonic/ultrasonic data
Anomalous data/no 20 +/- kHz thickness resonance

The PVC jackets were cut open and grout conditions evaluated. Duct 36 (Photograph 6 below) has approximately 1 inch of fly ash segregated from grout.



Photograph 6- Duct 36 with PVC Jacket Removed

Duct 25b (Photograph 7 below) has hard “good” grout.



Photograph 7- Duct 25b with PVC Jacket Removed

4.2 Ringling External PT Ducts

The impact echo data from the external tendons at the Ringling Bridge had considerable more information than the calibration data. Most of the data acquired on the exterior PT ducts at the Ringling Bridge have the 20 +/- kHz full duct thickness resonant frequency but also have a 25 +/- kHz associated with the 3.5 inches of competent (high velocity) grout inside the PVC duct as well as a 15 +/- kHz associated with the compressional wave traveling around the circumference of the competent grout (Figure 5).

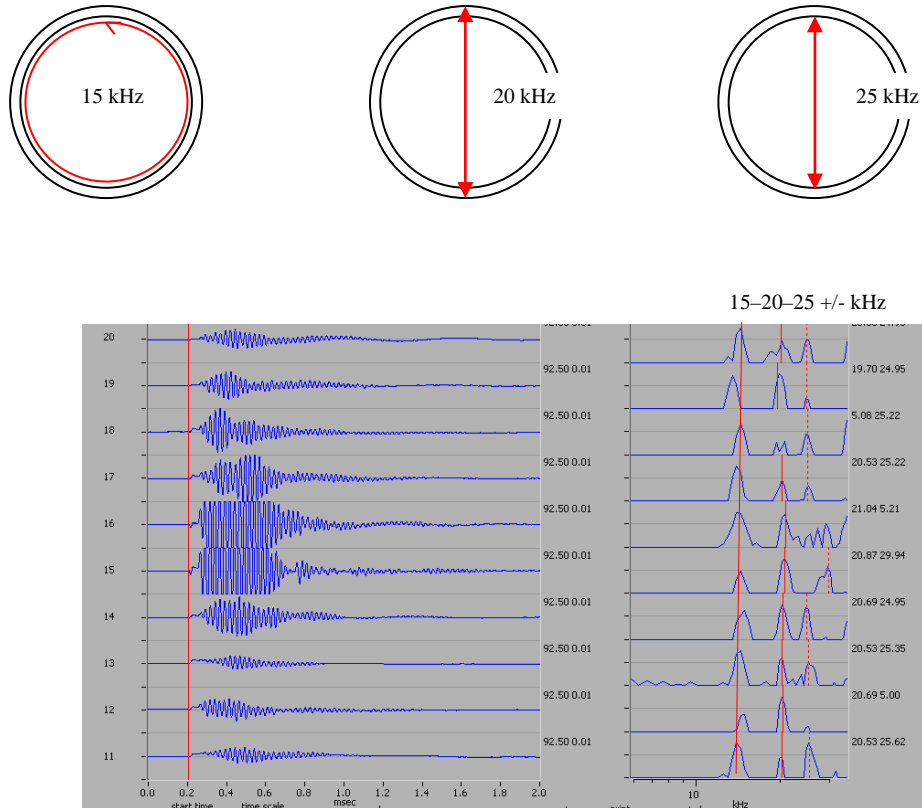


Figure 5-Sonic/ultrasonic data Ringling Bridge Span 1Tendon 401R-1W

The presences of the 20 or 25 kHz resonant frequency is an indication that the PT duct is filled with a competent grout. Locations with no 20 or 25 kHz resonant frequencies are an indication of voided or weak grout or grout delaminated from the PVC duct. Locations with 15 kHz and no 20 or 25 kHz are possible locations with voiding in the center of the duct.

Calibration results determined the 20 +/- kHz resonant frequency is indicative of a PT duct filled with a competent grout. The presence of the 15+/- and 25+/- kHz resonant frequency was not anticipated but is also an indicator of PT ducts filled with competent grout. At many locations, it was difficult to distinguish the 20 kHz from the 25 kHz because the readings would vary from 20 to 25 kHz. The 20 kHz signal would become higher frequency converge with the 25 kHz readings and vice versus the 25 kHz would

vary converging with the 20 kHz resulting in one frequency in the 20 to 25 kHz range. Both the 20 +/- and 25+/- kHz are indicative of PT ducts filled with competent grout, as result if one or both of the frequency are present the duct is considered to be filled with competent grout. If the 20+/- and 25+/- kHz thickness resonant frequencies are not present, anomalous internal PT Duct conditions are suspected. To filter out poor readings (loss of thickness frequencies) due to poor sensor coupling due to dirt or inadequate coupling compound, locations with no 20 kHz and 25 kHz had to be present for 3 feet or more to be considered anomalous.

The 15 +/- kHz was not anticipated and mathematically appears to be a signal traveling around the perimeter of competent duct grout. The presence the 15 kHz is an indication of competent grout but when this frequency is not present, or the 15 kHz is present, and the 20-25 kHz is missing, it is not certain what this signifies. The presences of the 15 kHz with the 20-25 kHz missing may indicate honey combed weakened grout at the center of the duct but this is speculative and should be confirmed. There does not appear to be any pattern to locations where the 15 kHz is missing. At least one location where the 15 kHz is present but the 20 and 25 kHz is not present, should be opened to evaluate internal grout conditions.

5.0 Results

The sonic/ultrasonic impact echo testing data are shown graphically in Appendix 2, and summarized in Table 1. Figures A-1 through A-84 in Appendix 2 are a graphical presentation of the impact echo data for each duct test by span. These Figures have a line plot of the through duct (average of 20 kHz and 25 kHz) and the circumferential (15 kHz) impact echo resonant frequency data with an elevation view of the duct with locations of the most significant anomalies. Table 1 list the length of the duct, location and percentage of anomalous through duct impact echo data.

The PT ducts in Spans 1 through 5 have significantly more anomalies associated with weakened grout conditions (voids, soft grout or segregation) then spans 6 through 11. A comparison of results for the east and west side of the ducts (same duct opposite side of the diaphragm between spans) indicated PT ducts 401L-1, 402L-1, 401R-1 and 402R-1 between spans 1 and 2 and 402R-2 between spans 2 and 3 have anomalous conditions on both sides of the diaphragm.

The anomalies considered to be the most significant are:

Span 1	duct 401L-1W Stations 164 to 169 (high point at diaphragm)
Span 2	duct 4402L-1E Stations 107 to 117 (flat horizontal area of duct)
	duct 402R-2W Stations 19 to 38 (flat horizontal area of duct)
Span 4	duct 402R-4W station 43 to 81 (flat horizontal area of duct)
	duct 401L-3E stations 138 to 142 (next to anchorage)
	duct 402L-3E stations 138 to 142 (next to anchorage)

Other anomalous areas are listed in Table 1.

The longest anomalous impact echo data were observed in span 2 duct 402R-2W (19 feet long), 402L-1E (10 feet long) and span 4 duct 402R-4W (38 feet long). All three of these anomalies are at the low flat/horizontal area of the duct and have similar frequency domain data appearance as the calibration data acquired at FDOT lab on duct 36 (discussed above in 4.1 Calibration section) with fly ash segregated from the grout. Anomalies were also detected close to anchorages (low end of duct) in span 4 duct 401L-3E and 402L-3E. These anomalies are 4 feet long. A 5 foot long anomaly was detected on PT Duct 401L-1W in span 1 at the high point near the diaphragm between spans 1 and 2.

6.0 Recommendations

If verification of the NDT results are to be done listed below are the priority and locations suggested for openings:

- 1) Span 1 duct 401L-1W Station 167
- 2) Span 2 duct 4402L-1E Stations 29
- 3) Span 4 duct 401L-3E stations 139
- 4) Span 1 duct 401R-1w Station 40 (location with circumferential 15 kHz and no through frequency – possible weak or voided grout near center of duct)

Table 1
Impact Echo Results

Table-1 - Impact Echo Results (missing frequencies possible grout anomalies)

Span #	Tendon ID	Station		No Through	%	Comments
		start	end	Frquency	Anomalous	
1	401L-1W	1	169	150-153		
				158-161		
				164-169	6.5	Tendon high point
402L-1w	1	169	32-35			
			48-51			
			65-70			
			92-107			
			109-118			
				20.7		
401R-1W	1	171	26-30			
			36-46			
				8.2		
402R-1W	1	171	1-3			
			5-8			
			24-30			
			139-140			
				7		
2	401L-1E	1	142.5			tendon high point
			69-72			
				2.1		
401L-2W	1	142.5				
				0		
401R-1E	1	142.5	46-50			
			83-86			
			109-112			
			127-131			
				9.8		

Span #	Tendon ID	Station		No Through	%	Comments
		start	end	Frquency	Anomalous	
2	401R-2W	1	143.5			
					0	
	402L-1E	1	142.5	107-117		
					7	
	402L-2W	1	142.5			
				142-142.5		HIGH POINT
					0.7	
	402R-1E	1	142.5	29-38 40-43 46-50		
					12.6	
	402R-2W	1	143	18-38 66-69 78-81 114-120		
					22.4	
3	401L-2E	1	141	1-6		
				88-93 111-117		
					11.3	
	401L-3W	1	141			
					0	

Span #	Tendon ID	Station		No Through	%	Comments
		start	end	Frquency	Anomalous	
3	401R-2E	1	141			
					0	
	401R-3W	1	142			
				44-47		
				118-121	4.2	
	402L-2E	1	142	1-5		
				9-12		
				21-24		
				52-60		
					12.7	
	402L-3W	1	142			
					0	
	402R-2E	1	141	17-21		
				91-98		
					7.8	
	402R-3W	1	142	69-75		
					4.2	
4	401L-3E	1	142			
					0	
	401L-4W	1	142			
					0	
	401R-3E	1	142			
					0	
	401R-4W	1	142			
					0	

Span #	Tendon ID	Station		No Through	%	Comments
		start	end	Frquency	Anomalous	
	402L-3E	1	142	29-33		
				97-101		
				108-128		
				138-142		
					14.8	
4	402L-4W	1	142			
					0	
	402-3E	1	142			
					0	
	402R-4W	1	142	43-81		
					26.1	
5	303L-4E	1	288			
					0	
	303R-4E	1	292			
				85-89 93-97		
				123-131		
				141-149		
					8.2	
	401L-4E	1	141			
				77-83		
					4.3	
	401L-5W	1	140			
					0	
5	401R-4E	1	141			
				24-26		
					1.4	

Span #	Tendon ID	Station		No Through	%	Comments
		start	end	Frquency	Anomalous	
	401R-5W	1	142	43-49		
					4.2	
5	402L-4E	1	141			
				49-53		
				77-85		
					8.5	
	402L-5W	1	140	61-71		
				136-139		
					9.3	
	402R-4E	1	139			
					0	
	402R-5W	1	140			
				61-71		
				136-139		
					9.3	
6	401L-5E	1	143			
					0	
	401L-6W	1	143			
					0	
	401R-5E	1	143			
					0	
	401R-6W	1	143			
					0	
	402L-5E	1	143			
					0	

Span #	Tendon ID	Station		No Through	%	Comments
		start	end	Frquency	Anomalous	
	402L-6W	1	143			
					0	
	402R-5E	1	143			
					0	
	402R-6W	1	143			
					0	
7	303L-6E	1	289			
					0	
	303R-6E	1	292			
					0	
	401L-6E	1	143			
					0	
	401L-7W	1	142			
				41-45		
					2.8	
	401R-6E	1	141			
	401R-7W	1	142			
					0	
	402L-6E	1	143			
					0	
	402L-7W	1	142			
					0	

Span #	Tendon ID	Station		No Through	%	Comments
		start	end	Frquency	Anomalous	
	402R-6E	1	143			
					0	
	402R-7W	1	141			
					0	
8	401L-7E	1	143			
					0	
	401L-8W	1	142			
					0	
8	401R-7E	1	143			
					0	
	401R-8W	1	141			
					0	
	402L-7E	1	143			
					0	
	402L-8W	1	142			
					0	
	402R-7E	1	143			
					0	
	402R-8W	1	143			
					0	
9	401L-8E	1	143			
					0	

Span #	Tendon ID	Station		No Through	%	Comments
		start	end	Frquency	Anomalous	
	401L-9W	1	142			
				85-89		
					2.8	
	401R-8E	1	143			
					0	
	401R-9W	1	143			
					0	
	402L-8E	1	143			
					0	
	402L-9W	1	143			
					0	
	402R-8E	1	143			
					0	
	402R-9W					
					0	
10	401L-9E	1	143			
					0	
	401L-10W	1	143			
					0	
	401R-9E	1	143			
					0	
	401R-10W	1	143			
					0	

Span #	Tendon ID	Station		No Through	%	Comments
		start	end	Frquency	Anomalous	
	402L-9E	1	143			
					0	
	402R-9E	1	143			
					0	
	402R-10W	1	143			
					0	
11	401L-10E	1	199			
					0	
	401R-10E	1	199			
					0	
	402L-10E	1	197			
					0	
	402R-10E	1	197			
					0	

APPENDIX 1

**SONIC/ULTRASONIC
METHOD OF INVESTIGATION**

APPENDIX SONIC/ULTRASONIC NONDESTRUCTIVE TESTING OF CONCRETE

The sonic/ultrasonic measurements made to determine the characteristics of concrete (or rock) are generated by a relatively low energy source as a single discrete wide band impulse with a pulsed transducer, projectile, mechanical hammer, etc. Practical problems and the condition of the concrete surface largely determine the source(s) to be used. A rough concrete surface that has deposits of organic materials or mineral deposits generally requires a more powerful energy source whereas a relatively new or wet concrete may be inspected by the use of a pulsed transducer or other higher frequency source. In general high frequency sources that may work well in the laboratory may be unusable for field conditions. High frequency sources have the advantage of high resolution but the disadvantage of low penetration. While metals can be tested in the megahertz range, such signals in concrete will not have measurable signals for more than an inch in thickness. The energy source should be sufficient to maximize the resolution, have sufficient penetration to examine the concrete being tested and enough energy to excite the fundamental frequencies being sought.

The transmitted energy is in the form of three principal wave types: compressional (contraction/expansion, spring-like particle motion), shear (traction-sliding motion), and surface waves (combination of motions). Each boundary that has density and or velocity contrast will reflect and/or refract these waves. Compressional and shear wave velocity values are determined by the Young's, shear and bulk moduli values as well as the density and Poisson's Ratio. In turn the velocity can be used to determine the moduli values and Poisson's Ratio given that the density is known or can be assumed. The moduli values measured are the dynamic moduli values at low strain. In general, the difference between the dynamic values and the static values is almost entirely controlled by the crack densities of the concrete. Using the modulus values, a reasonable estimate of the unconfined compressive strength can be determined. The strength is largely dependent on the crack density of the concrete and for static tests, the orientation of the cracks. For static testing, cracks perpendicular to the axis of the core and perpendicular to the directed stress will produce a strength (static) that is not greatly different from uncracked concrete. The applied stress closes or compresses the cracks. Cracks that are near 45° to the direction of stress will result in lowest static strength. The approximate orientation of the cracks can be determined with dynamic measurements of the velocity values in different directions.

NDT Corporation makes several determinations from one energy impact. The velocity is measured directly from the energy point of impact to a linear array(s) of sensors on the surface. The array length is usually in excess of the thickness of the concrete being tested. In addition to the velocity measurements, reflections are measured individually or determined from a frequency analysis of the time domain recordings. Each reflecting surface (change of density and/or velocity) produces a multi-path reflection in the layer it bounds. A generated wave will travel to a delamination surface and reflect back to the surface of the concrete where it is reflected back to the delamination, resulting in multi-reflections that are apparent in the frequency domain. These reverberations (echoes) are particularly diagnostic of delaminations and thickness of the concrete. They will readily distinguish the presence of local delaminations, cracked or decomposed inclusions by the particular frequency band generated at the mechanical discontinuity. If a delamination is

severe or large in area, the reflected signals are strong resulting in a low frequency, high amplitude, and long duration “ringing” signal or a drum head effect that is usually quite distinguishable. This is the basis of the ‘chain drag’ using the human ear as the sensor to recognize frequency differences. The ear however is limited in its perception and will only distinguish within the hearing range.

DIRECT AND REFRACTED ENERGY

One of the advantages of the sonic/ultrasonic method is its ability to “look through” overlying materials coatings, particularly decomposed “softer layers” when the array(s) is configured properly. This is done using refracted waves associated with the different layer velocities or by careful examination of the resonant frequencies associated with such layering.

The diagram below shows the wave path for refracted energy generated for a softer (1) lower velocity layer over a harder (2) higher velocity layer. For example asphalt (1) over good concrete (2). The wave is bent (similar to the appearance of a stick in water) and travels along the boundary between the lower velocity layer and the higher velocity layer and radiates back to the surface. The higher velocity of the good concrete allows the refracted wave to overtake the direct wave in layer 1 at some distance designated as $D_{1|2}$. To the left of this point the lower velocity of layer 1 will be measured and beyond it the velocity of the deeper layer 2 is measured.

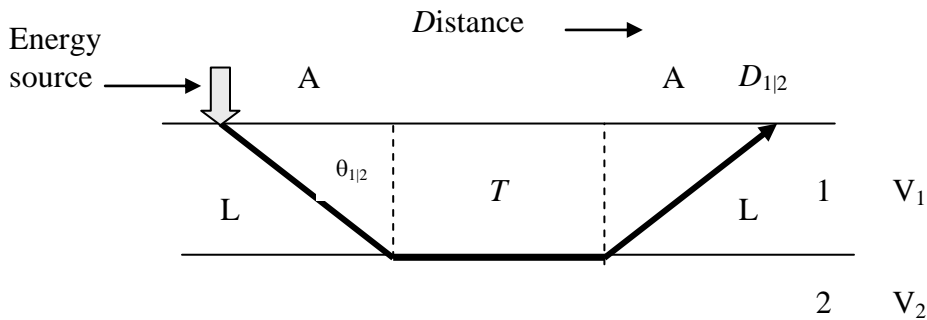


Figure A1

The time for the direct path is D/V_1 , the refracted path time is $2L/V_1 + (D_{1|2} - 2A)/V_2$. The array of sensors is placed in the distance direction and the time elapsed (travel time) from the time of energy impact to the sensor distance is measured. The velocity is determined from this time-distance measurement(s). The angle θ is the angle between the perpendicular to the layer and the incident wave that is critically refracted. The sine of this angle is the velocity of the first layer divided by that of the second layer (Snell's Law). The distance shown $D_{1|2}$ is the point on the surface where the refracted time arrival equals that of the direct wave (the refracted wave travels at a higher velocity than the direct wave).

$$\frac{D}{T} = \frac{D - 2 \tan \Theta}{V_2} + \frac{2T}{V_1 \cos \Theta}$$

The thickness is expressed as:

$$T = \frac{D_{1/2}}{2} \sqrt{\frac{V_2 - V_1}{V_2 + V_1}}$$

D is the distance and T is the thickness. Since the times as well as the distances are measured, then V_1 and V_2 are determined. If a plot of distance versus time is made then the resulting graph will look like Figure A2.

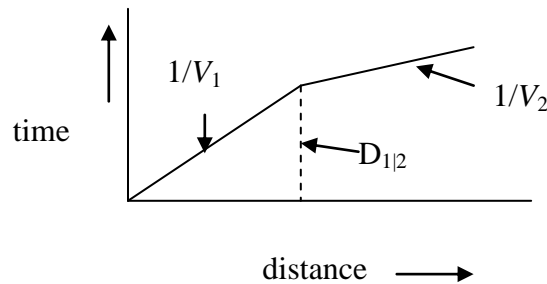


Figure A2

If the concrete has no overlay then the concrete velocity is simply D/T .

The resonant frequencies are determined by the thickness and velocity of the material. Since the velocity is measured as above, then the thickness can be determined directly.

The resonance of a simple beam is given by:

$$f = \frac{nV}{2L} \quad (\text{fixed - fixed, free - free}) \quad \text{where } n = 1, 2, 3, \dots$$

$$f = \frac{nV}{4L} \quad (\text{open - fixed}), \quad \text{where } n = 1, 3, 5, 7, \dots$$

Since the frequency and velocity are measured, the thickness is determined. This thickness can be the thickness of the concrete floor, deck slabs, or column being measured or it can be the thickness of concrete overlying a delamination.

While the refracted wave is dependent only on a contrast in velocity, a reflection can take place where there is a change in velocity or density or both. The impedance (RF reflection coefficient) which causes a wave to be reflected is given by:

$$RF = \frac{\rho_2 V_2 - \rho_1 V_1}{\rho_2 V_2 + \rho_1 V_1}$$

Where ρ is the density and V is the velocity of the material. The impedance determines the strength of the reflection. The contrast between an air filled void at the back of or within the concrete is significant; the velocity in air is 1,000ft/sec. and the velocity of good concrete is 13,000ft/sec. The density differences are of course very large between the concrete and air. A similar difference exists for a water filled void where the velocity in water is 5,000ft/sec. and concrete is nearly a factor of 2.5 denser. Voiding behind a liner or under a slab is usually well distinguished by a distinct “ringing” resonant frequency, referred to above as a drum head effect..

MODULI VALUES AND STRENGTH

The moduli values as stated above are determined from the velocity values using an assumed or measured density. The density is usually the best known or best estimated value for the concrete, its variance generally does not affect the calculations significantly.

The relationships for Young’s modulus versus the compressional velocity are shown in Figure A4; shear modulus versus the shear velocity Figure A5; Poisson’s Ratio versus the compressional and shear wave velocities Figure A6; and finally a relationship between the velocity values (compressional and shear) and the unconfined compressive strength of concrete, Figure A7.

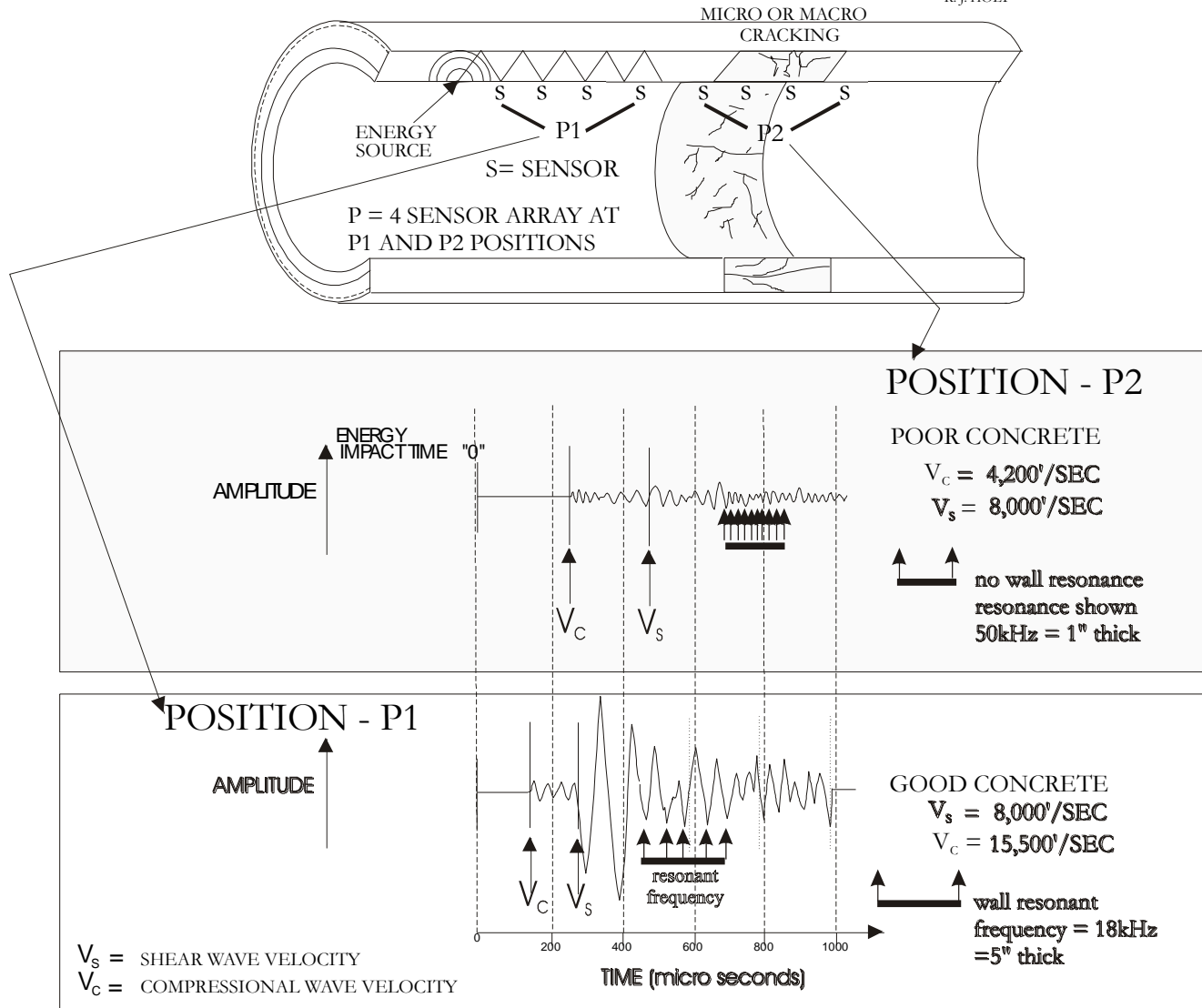
Figure A3 is illustrative of a tunnel liner or pipe investigation where there has been circumferential damage, perhaps at a construction joint or an outside zone of weakness (rock shear or fault, soil washout etc.) that has affected the integrity of the liner. The damage need not be visible; there can be a 20% reduction in the strength of the concrete from micro-cracking that is not visible to the naked eye. The process of deterioration of most concrete starts at the micro level and with continued stress the micro cracks coalesce into macro cracks and finally to spalling. The ability to measure at the micro level well in advance of future needed repairs provides a management tool for establishing priorities for repair, projected budgets, and asset valuation

SONIC/ULTRASONIC TUNNEL & PIPE LINE TESTING

Circumferential (face to back) Cracking

NDT ENGINEERING, INC.

R.J. HOLT



SONIC/ULTRASONIC TIME AMPLITUDE RECORDS
 FOR FOURTH SENSOR - POOR AND GOOD CONCRETE

FIGURE A3

YOUNG'S MODULUS - SHEAR VELOCITY- POISSON'S RATIO

NDT ENGINEERING, INC.
R. J. HOLT

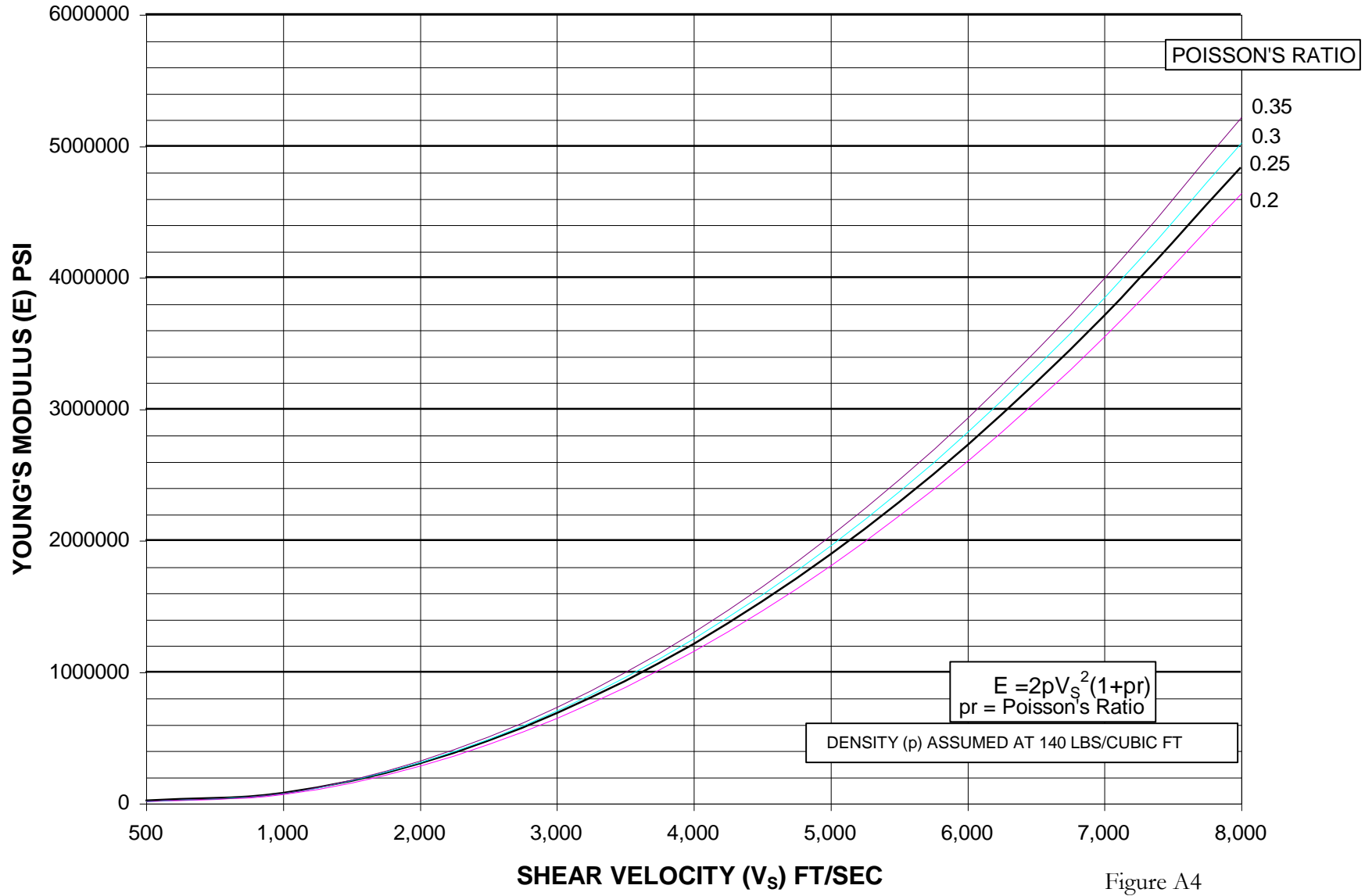


Figure A4

SHEAR MODULUS - SHEAR VELOCITY

NDT ENGINEERING, INC.
R.J.HOLT

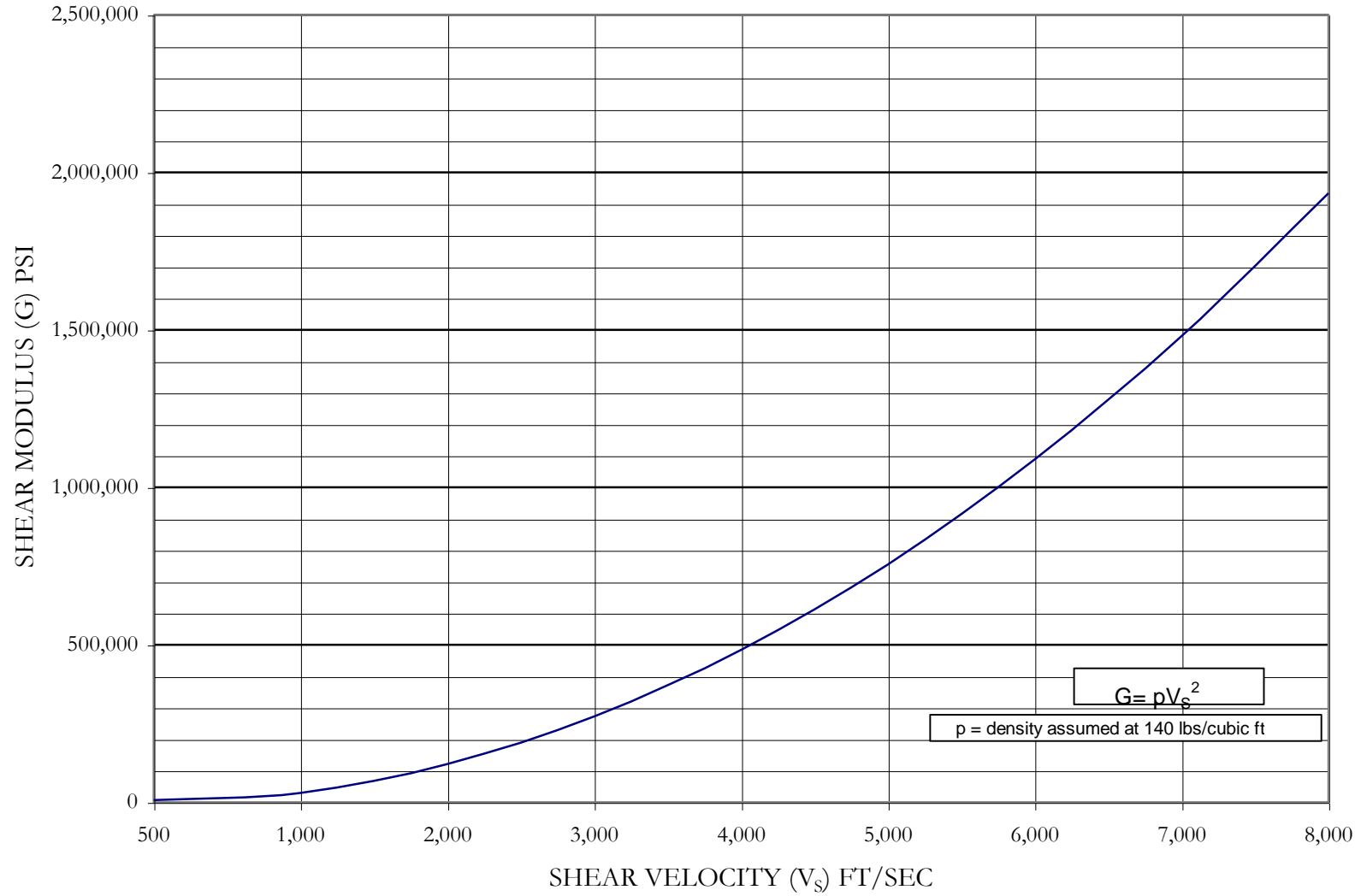


Figure A5

COMPRESSSIONAL VELOCITY - SHEAR VELOCITY - POISSON'S RATIO

NDT ENGINEERING, INC.
R J HOLT

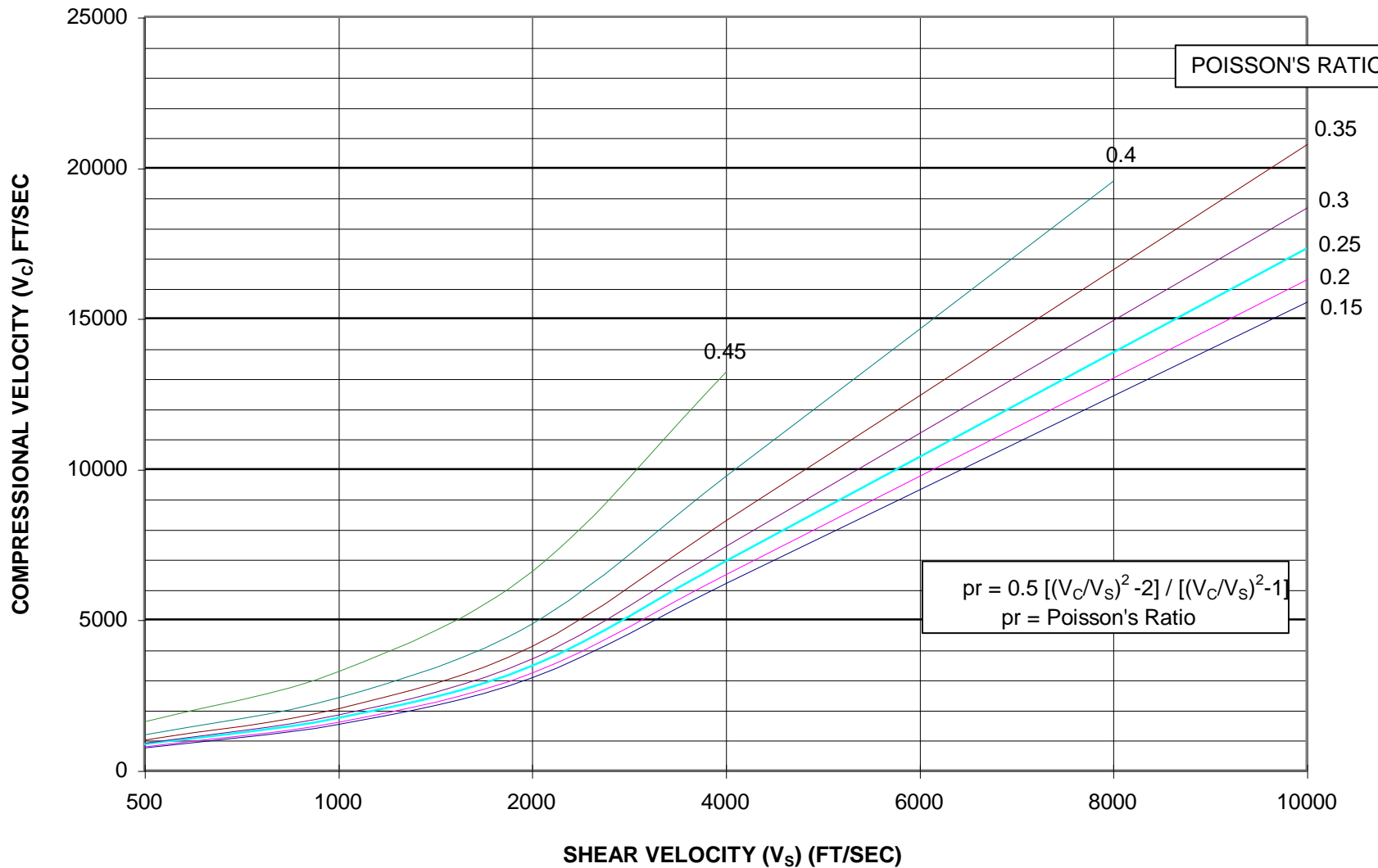
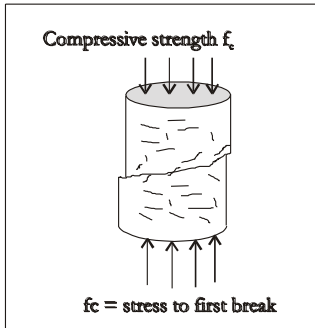
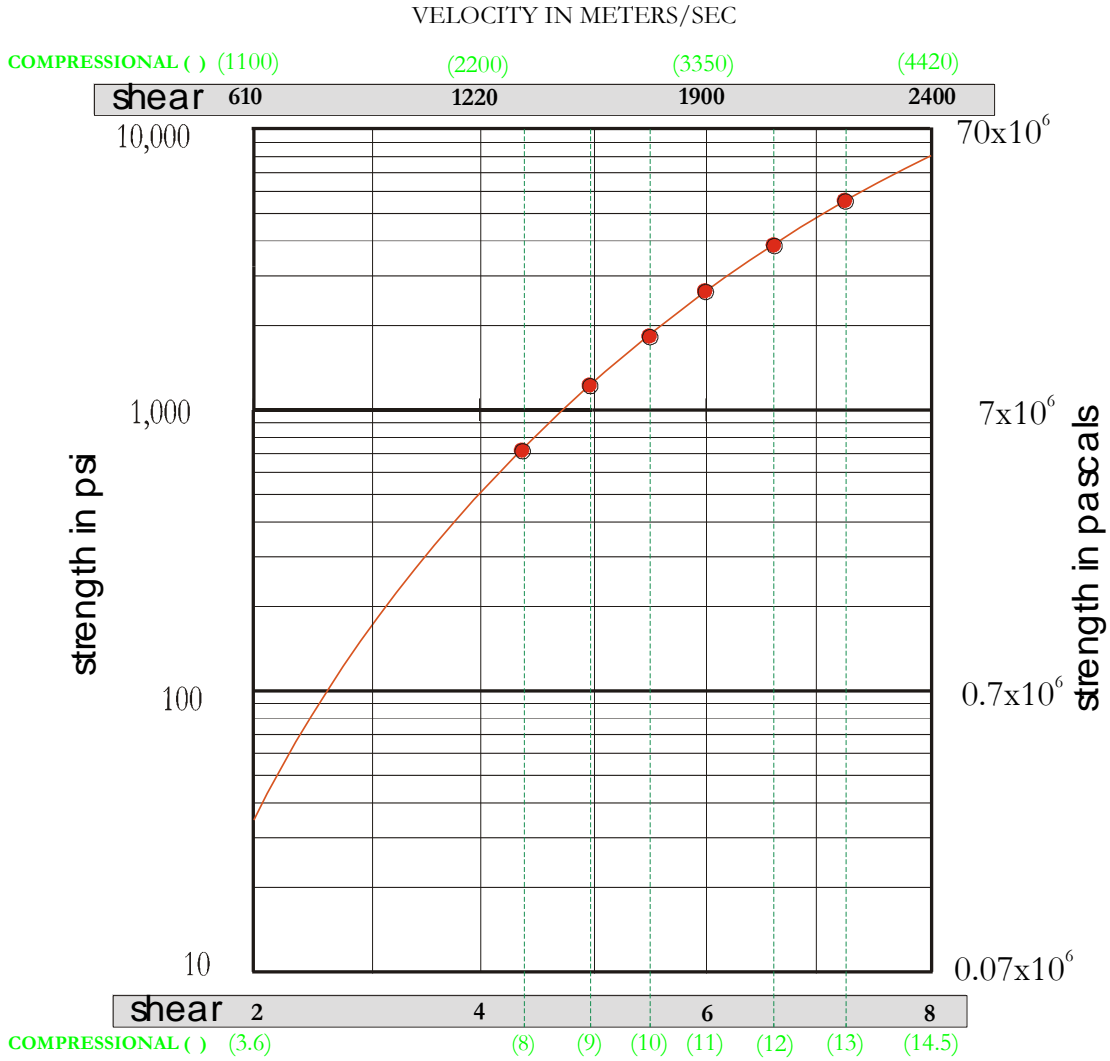


Figure A6

strength of concrete versus velocity

r. j. holt



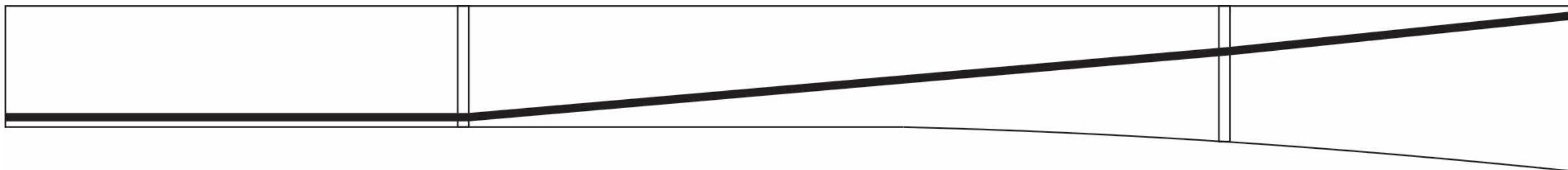
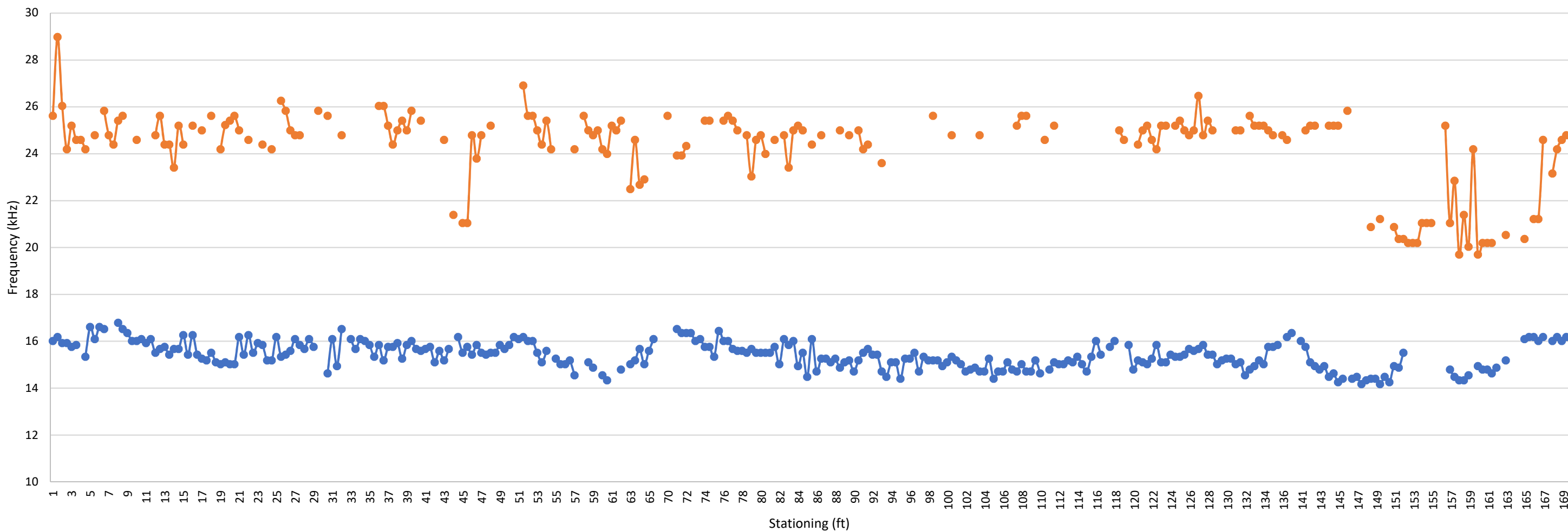
VELOCITY IN FEET/SEC (X 1,000)

CURVE FOR RATIO: $V_{SHEAR} / V_{COMPRESSIONAL} = 0.55$
 EQUALS POISSON'S RATIO OF 0.28

FIGURE A7
 NDTENGINEERING, INC.

Appendix 2 Data
Plots for
Ultrasonic Testing

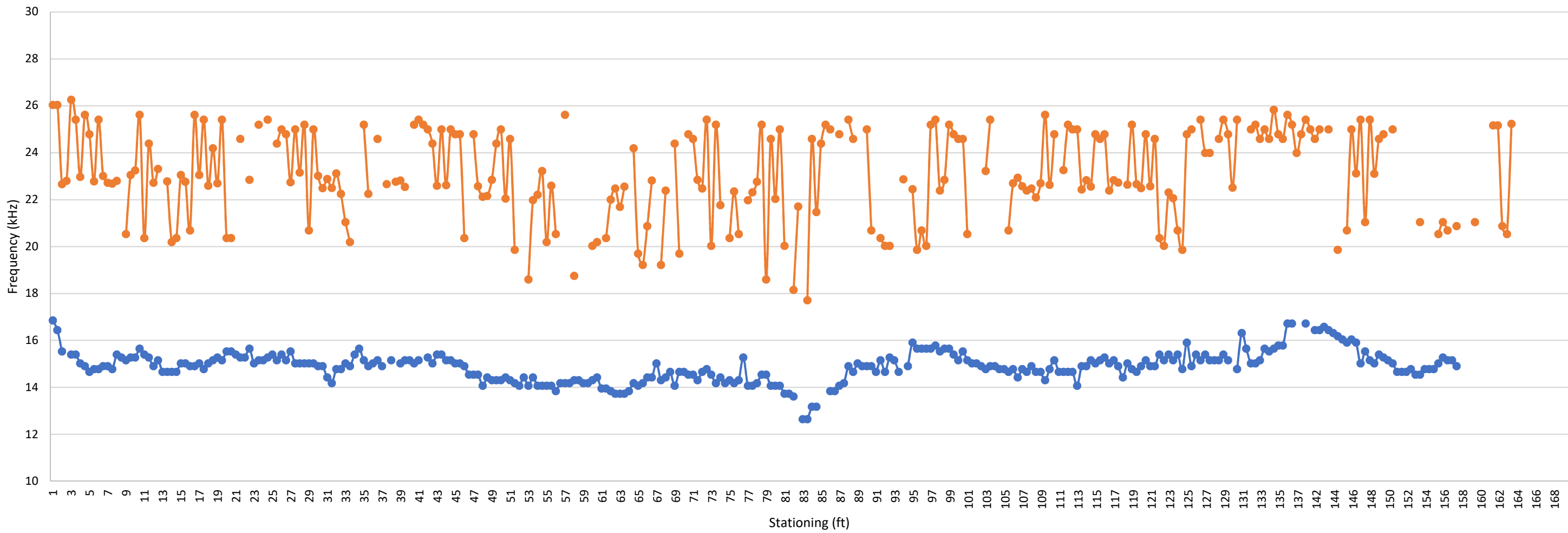
402L-1W



—●— Circumferential Frequency
 —●— Average Through Frequency
 ■ Anomalous Grout Condition

Nondestructive Testing External Tendon Ducts John Ringling Causeway Bridge Over Sarasota Bay Sarasota, Florida Prepared for Florida International University by NDT Corporation		Span 1 Tendon 402L-1W Graph Results	
January. 2018		Figure A1	

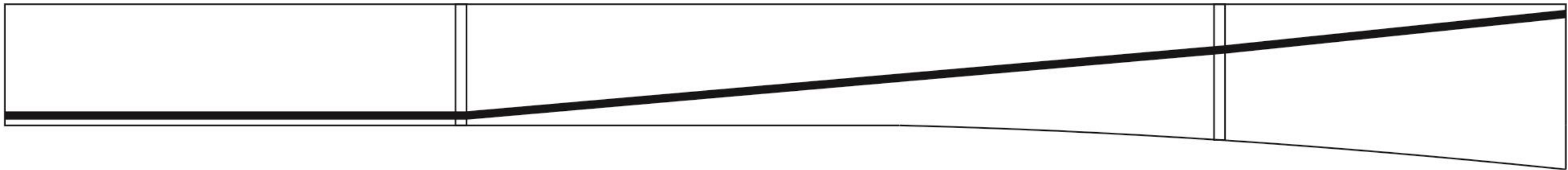
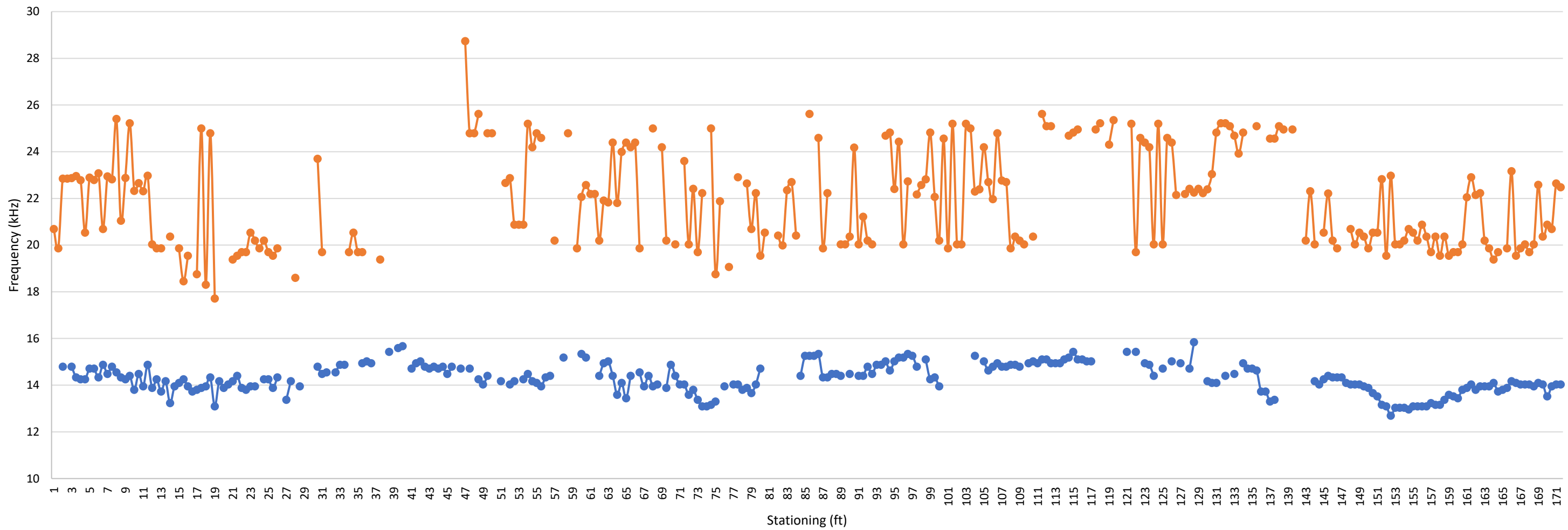
401L-1W



—●— Circumferential Frequency —●— Average Through Frequency ■ Anomalous Grout Condition

Nondestructive Testing External Tendon Ducts John Ringling Causeway Bridge Over Sarasota Bay Sarasota, Florida Prepared for Florida International University by NDT Corporation		Span 1 Tendon 401L-1W Graph Results	
		January. 2018	Figure A2

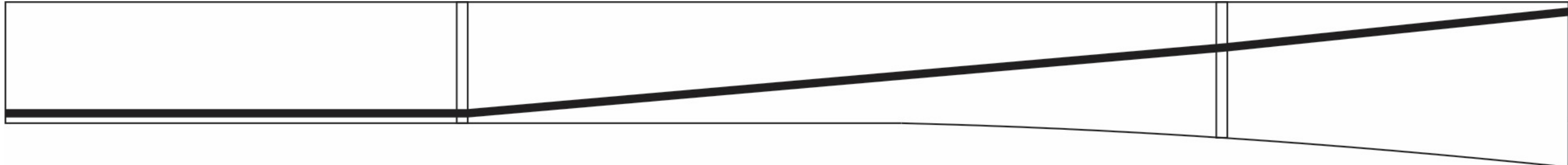
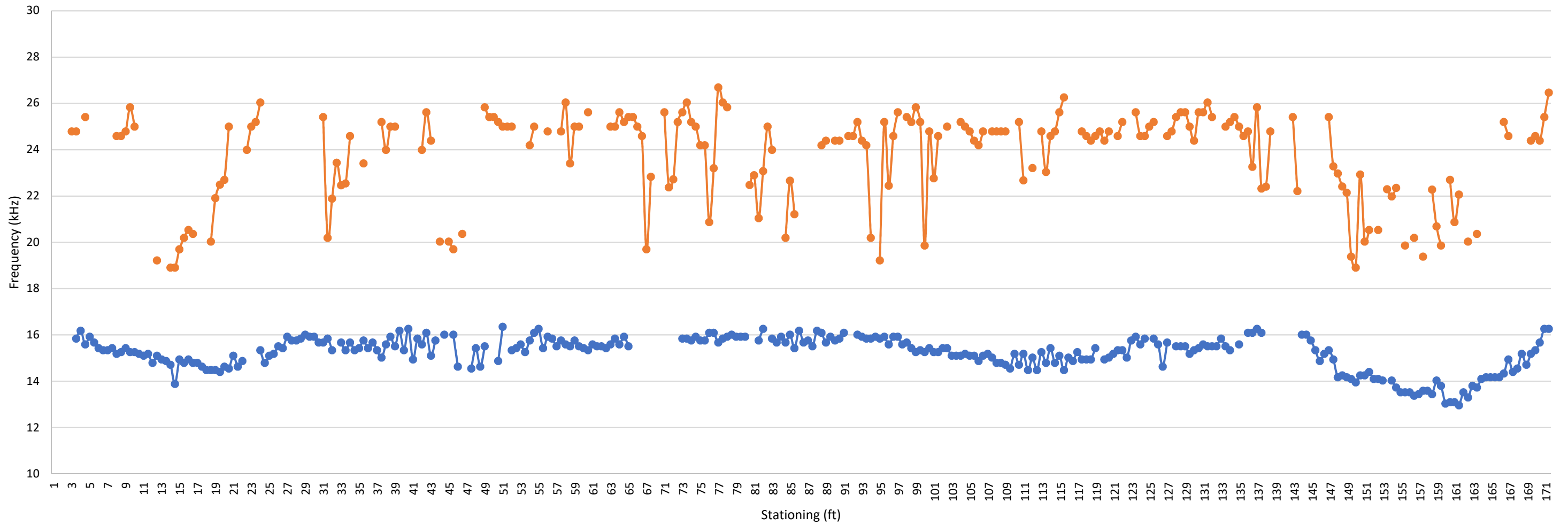
401R-1W



● Circumferential Frequency
 ● Average Through Frequency
 ■ Anomalous Grout Condition

Nondestructive Testing External Tendon Ducts John Ringling Causeway Bridge Over Sarasota Bay Sarasota, Florida Prepared for Florida International University by NDT Corporation		Span 1 Tendon 401R-1W Graph Results	
January. 2018		Figure A3	

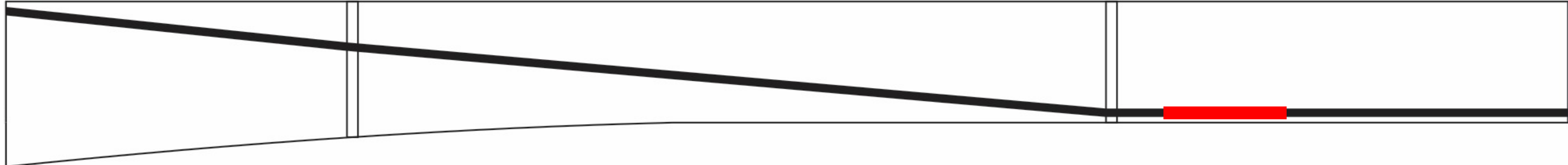
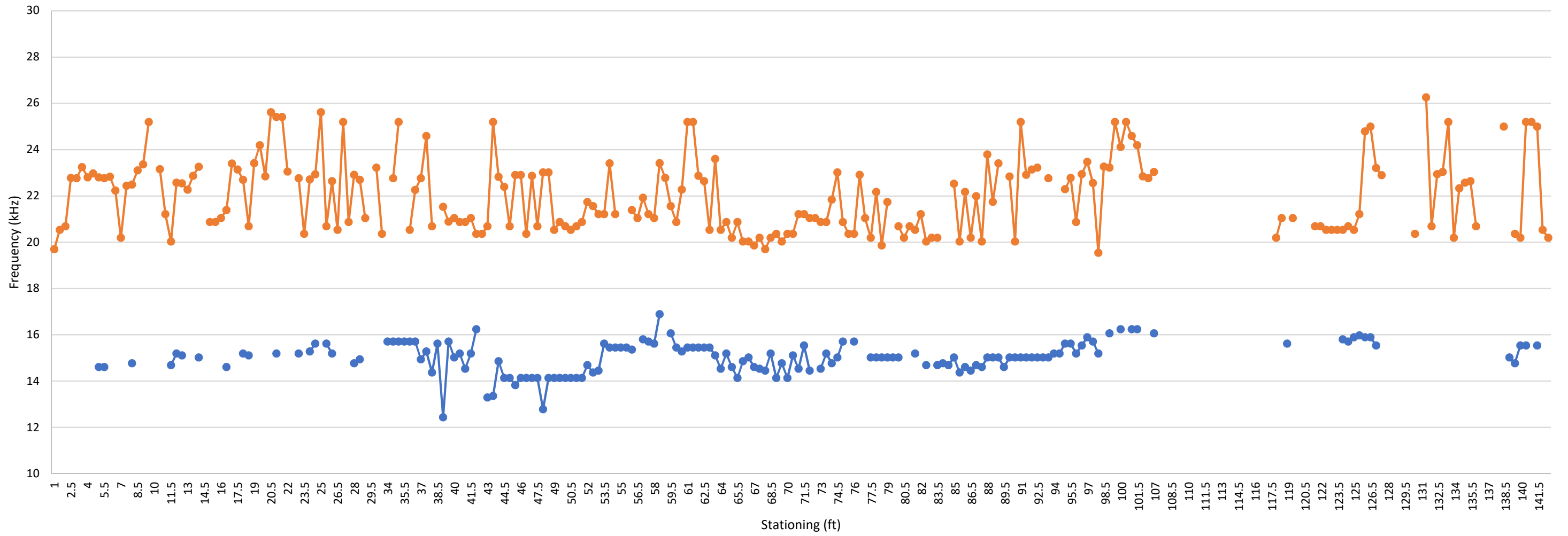
402R-1W



—●— Circumferential Frequency
 —●— Average Through Frequency
 ■ Anomalous Grout Condition

Nondestructive Testing External Tendon Ducts John Ringling Causeway Bridge Over Sarasota Bay Sarasota, Florida Prepared for Florida International University by NDT Corporation		Span 1 Tendon 402R-1W Graph Results	
January. 2018		Figure A4	

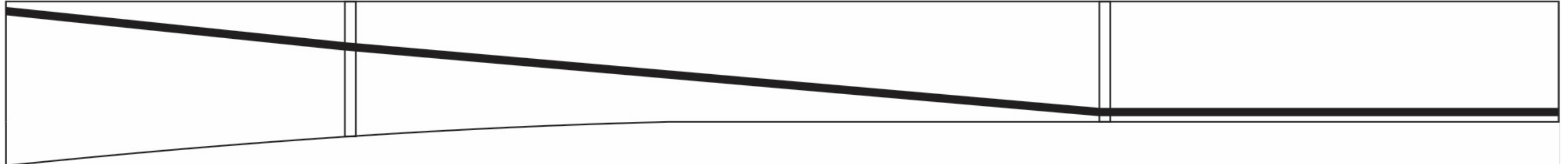
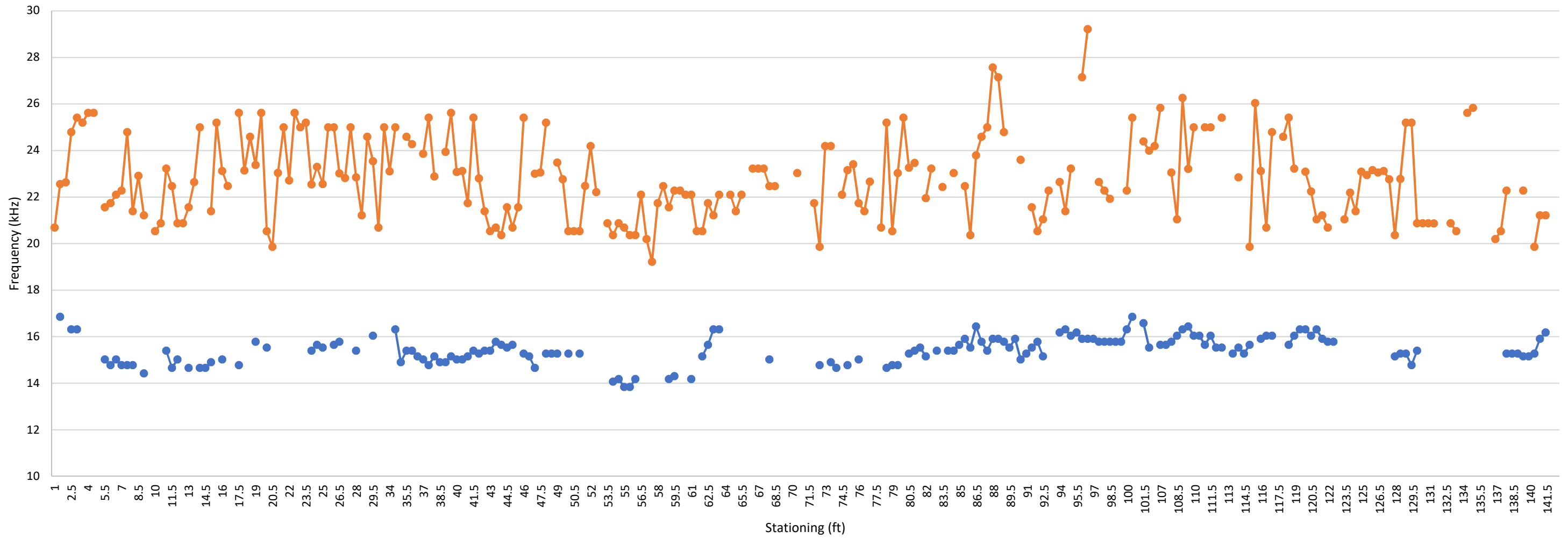
402L-1E



—●— Circumferential Frequency
 —●— Average Through Frequency
 ■ Anomalous Grout Condition

Nondestructive Testing External Tendon Ducts John Ringling Causeway Bridge Over Sarasota Bay Sarasota, Florida Prepared for Florida International University by NDT Corporation		Span 2 Tendon 402L-1E Graph Results	
January. 2018		Figure A5	

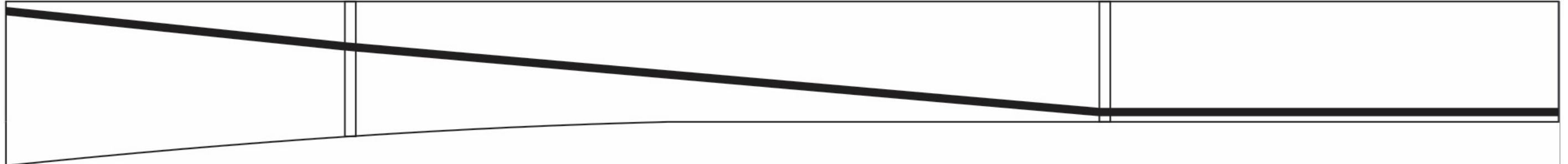
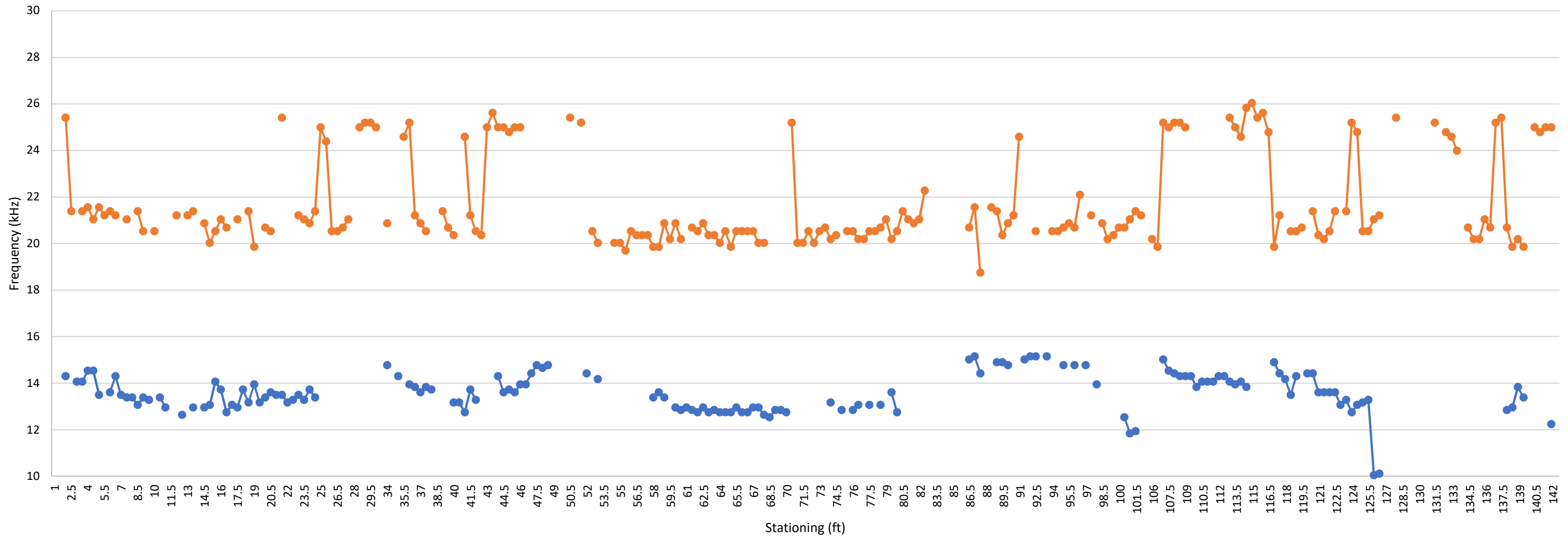
401L-1E



—●— Circumferential Frequency
 —●— Average Through Frequency
 ■ Anomalous Grout Condition

Nondestructive Testing External Tendon Ducts John Ringling Causeway Bridge Over Sarasota Bay Sarasota, Florida Prepared for Florida International University by NDT Corporation		Span 2 Tendon 401L-1E Graph Results	
January. 2018		Figure A6	

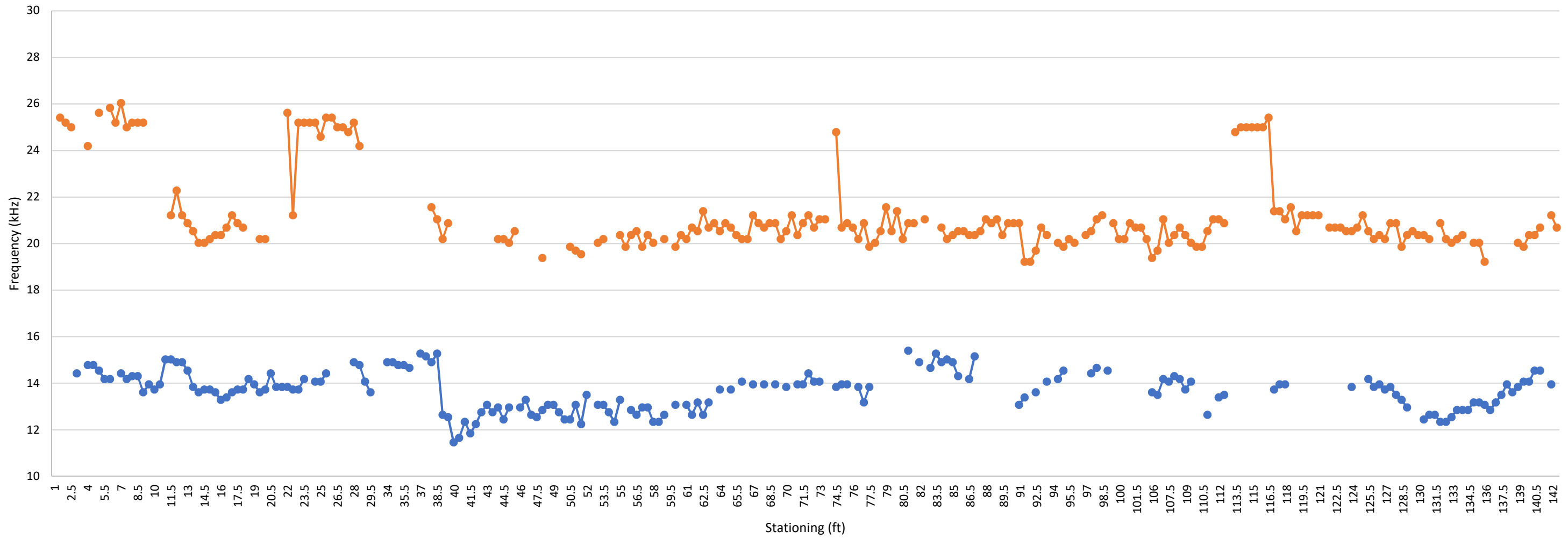
401R-1E



—●— Circumferential Frequency —●— Average Through Frequency ■ Anomalous Grout Condition

Nondestructive Testing External Tendon Ducts John Ringling Causeway Bridge Over Sarasota Bay Sarasota, Florida Prepared for Florida International University by NDT Corporation		Span 2 Tendon 401R-1E Graph Results	
		January. 2018	Figure A7

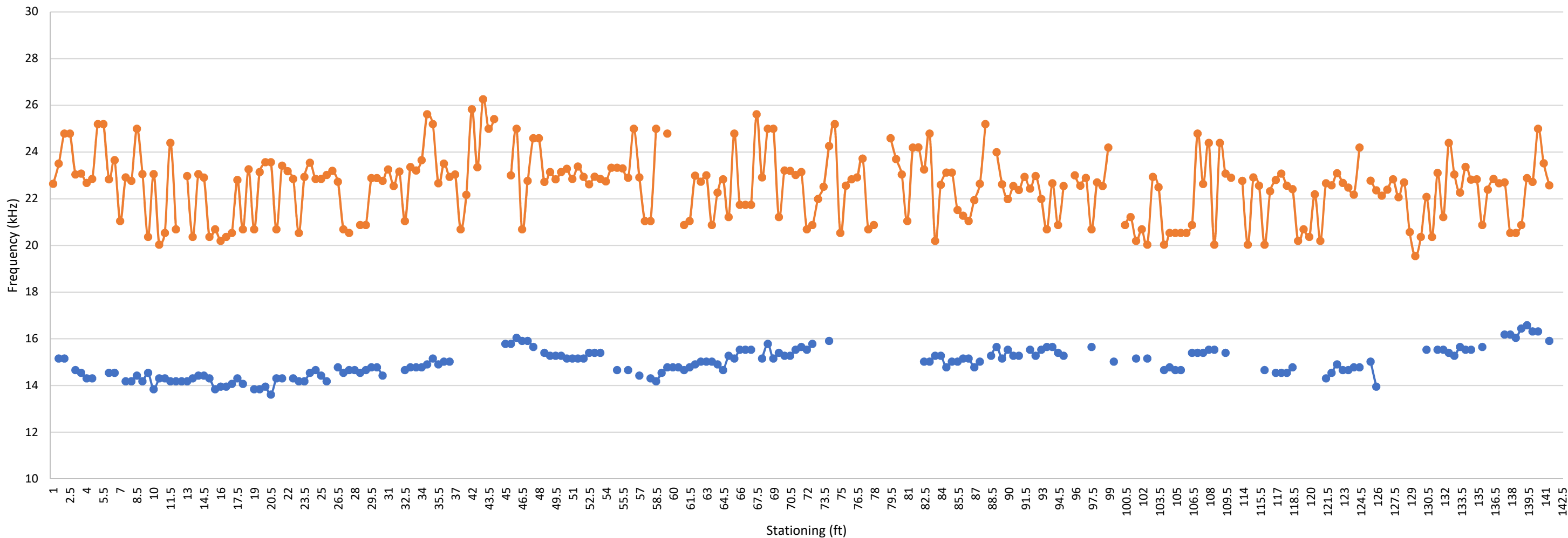
402R-1E



—●— Circumferential Frequency
 —●— Average Through Frequency
 ■ Anomalous Grout Condition

Nondestructive Testing External Tendon Ducts John Ringling Causeway Bridge Over Sarasota Bay Sarasota, Florida Prepared for Florida International University by NDT Corporation		Span 2 Tendon 402R-1E Graph Results	
January. 2018		Figure A8	

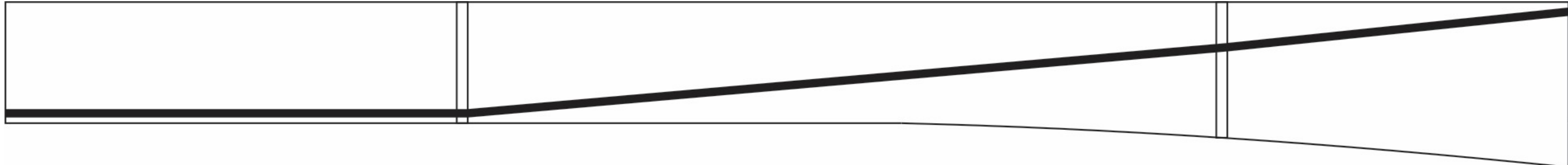
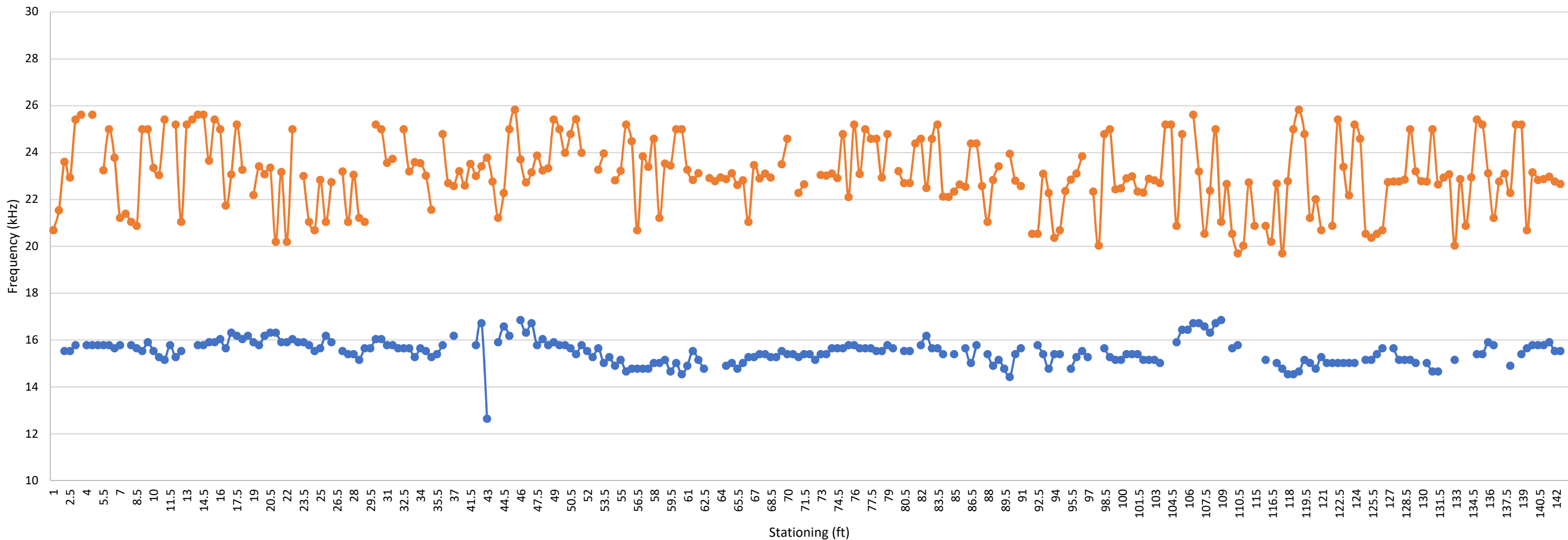
402L-2W



—●— Circumferential Frequency —●— Average Through Frequency ■ Anomalous Grout Condition

Nondestructive Testing External Tendon Ducts John Ringling Causeway Bridge Over Sarasota Bay Sarasota, Florida Prepared for Florida International University by NDT Corporation		Span 2 Tendon 402L-2W Graph Results	
		January. 2018	Figure A9

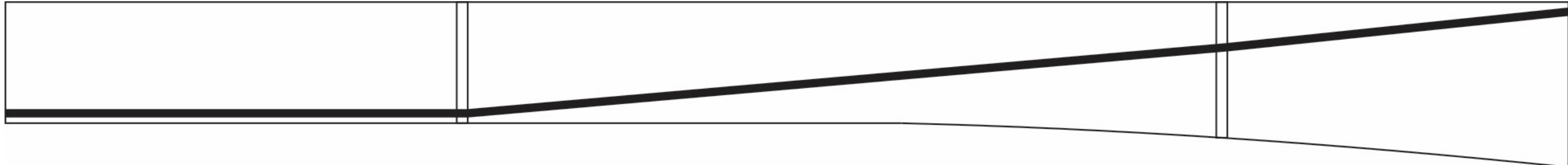
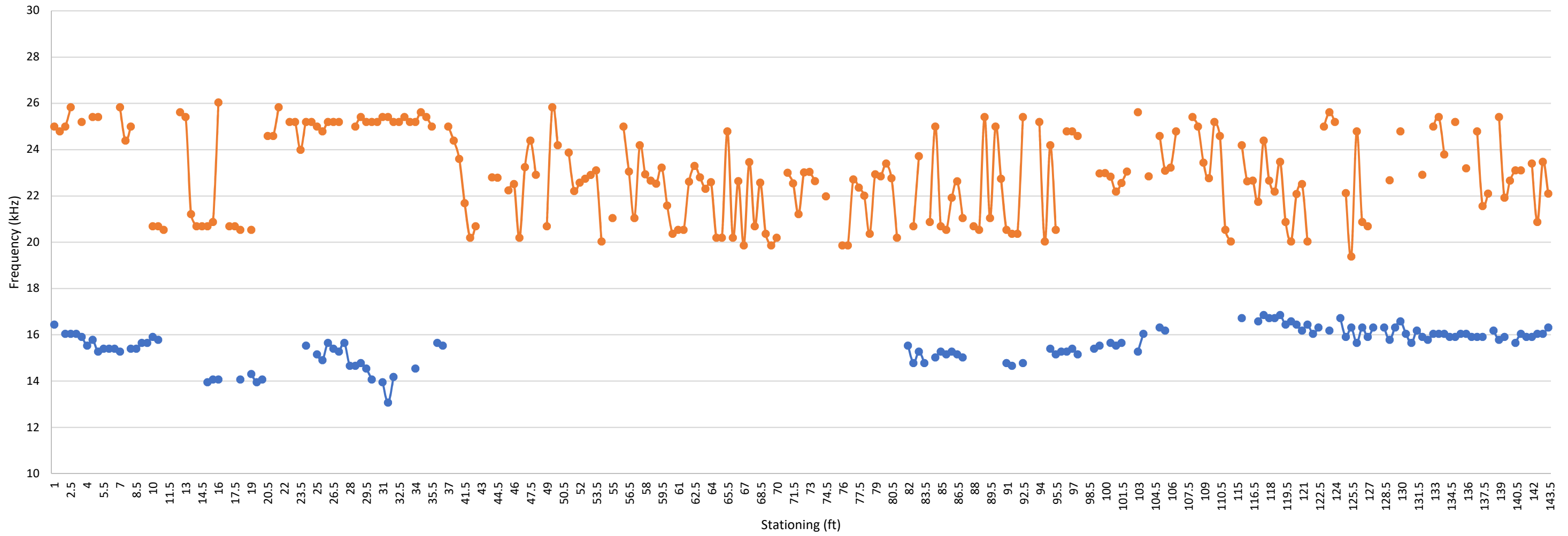
401L-2W



—●— Circumferential Frequency
 —●— Average Through Frequency
 ■ Anomalous Grout Condition

Nondestructive Testing External Tendon Ducts John Ringling Causeway Bridge Over Sarasota Bay Sarasota, Florida Prepared for Florida International University by NDT Corporation		Span 2 Tendon 401L-2W Graph Results	
January. 2018		Figure A10	

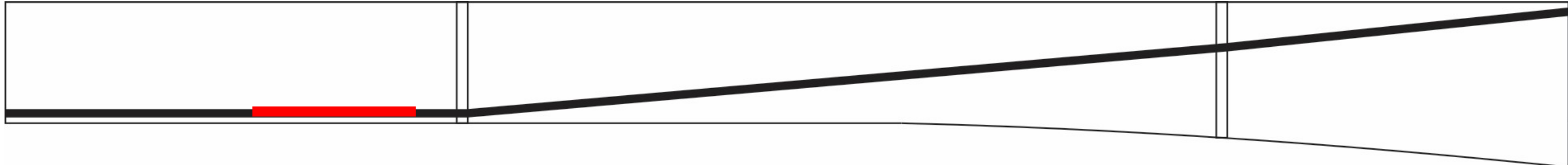
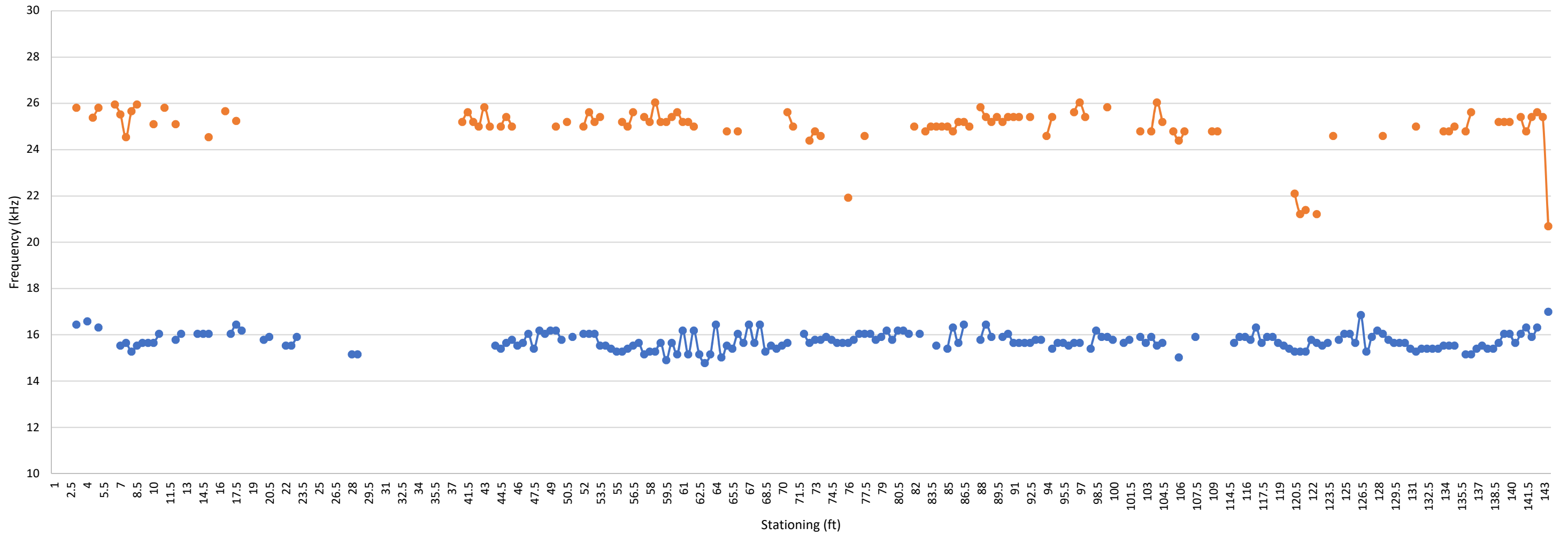
401R-2W



—●— Circumferential Frequency
 —●— Average Through Frequency
 ■ Anomalous Grout Condition

Nondestructive Testing External Tendon Ducts John Ringling Causeway Bridge Over Sarasota Bay Sarasota, Florida Prepared for Florida International University by NDT Corporation		Span 2 Tendon 401R-2W Graph Results	
January. 2018		Figure A11	

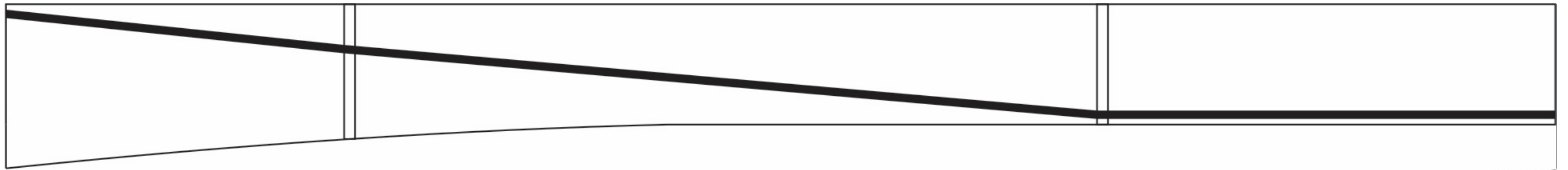
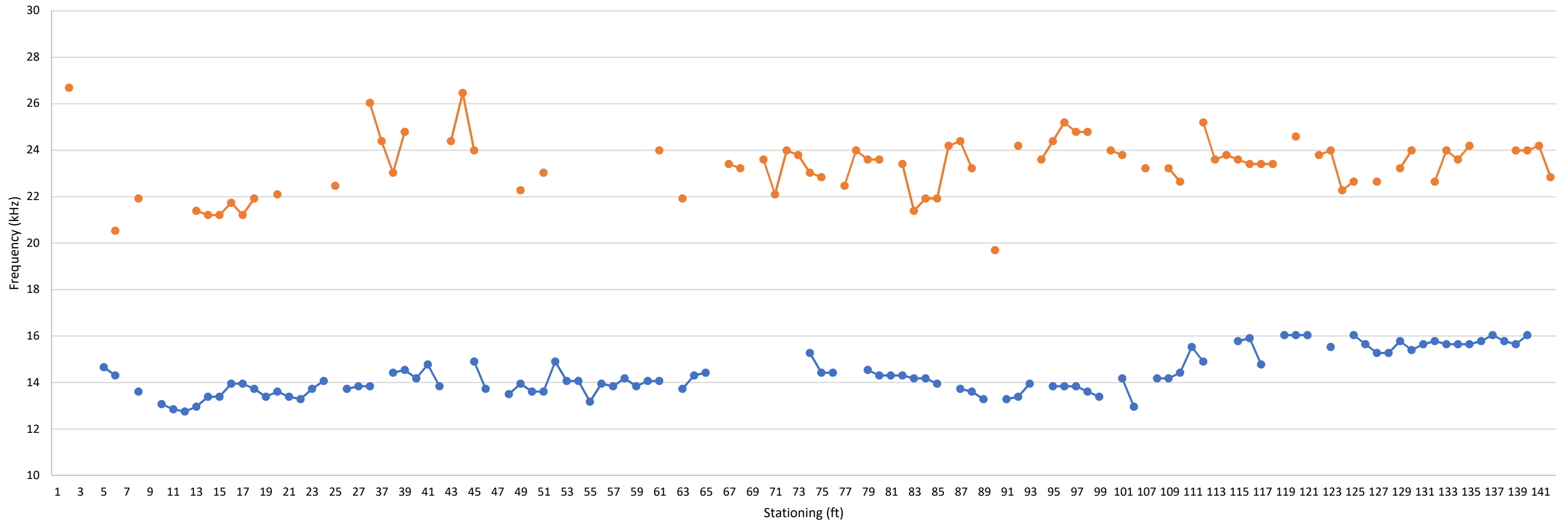
402R-2W



—●— Circumferential Frequency —●— Average Through Frequency ■ Anomalous Grout Condition

Nondestructive Testing External Tendon Ducts John Ringling Causeway Bridge Over Sarasota Bay Sarasota, Florida Prepared for Florida International University by NDT Corporation		Span 2 Tendon 402R-2W Graph Results	
		January. 2018	Figure A12

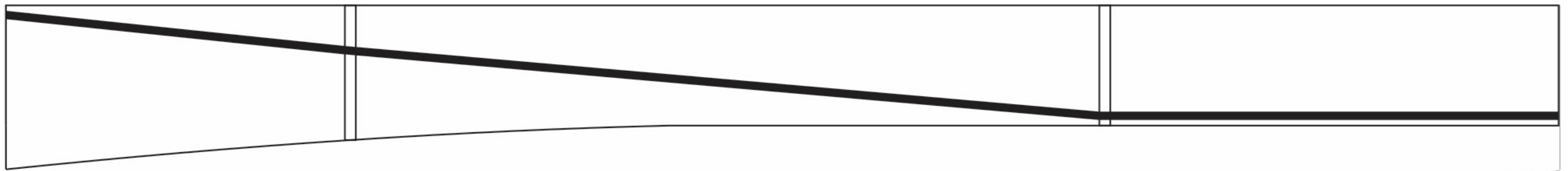
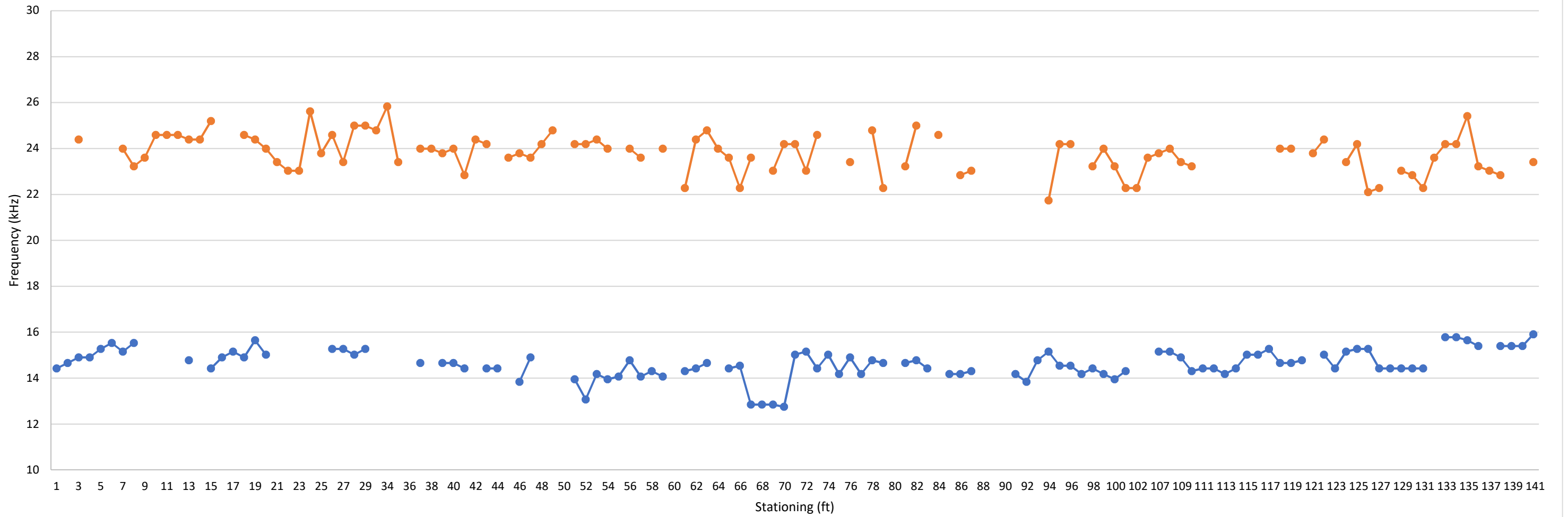
402L-2E



—●— Circumferential Frequency
 —●— Average Through Frequency
 ■ Anomalous Grout Condition

Nondestructive Testing External Tendon Ducts John Ringling Causeway Bridge Over Sarasota Bay Sarasota, Florida Prepared for Florida International University by NDT Corporation		Span 3 Tendon 402L-2E Graph Results	
		January. 2018	Figure A13

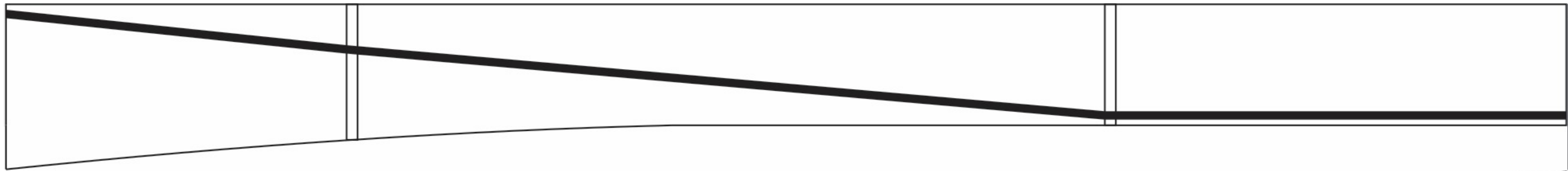
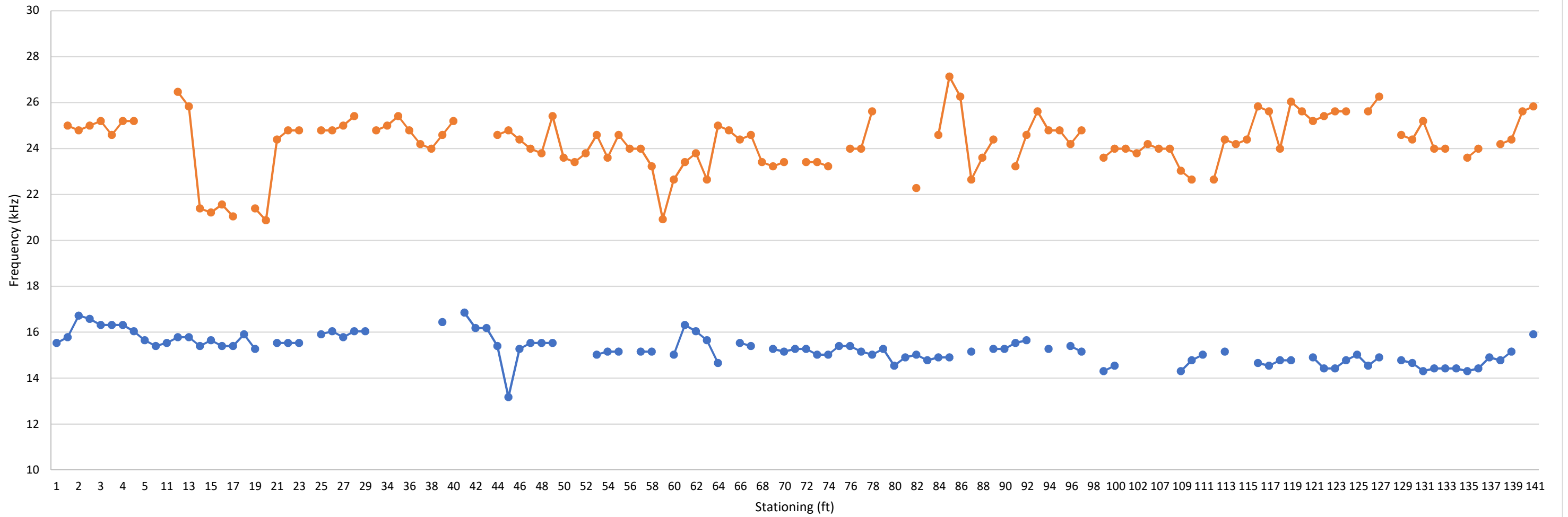
401L-2E



—●— Circumferential Frequency
 —●— Average Through Frequency
 ■ Anomalous Grout Condition

Nondestructive Testing External Tendon Ducts John Ringling Causeway Bridge Over Sarasota Bay Sarasota, Florida Prepared for Florida International University by NDT Corporation		Span 3 Tendon 401L-2E Graph Results	
		January. 2018	Figure A14

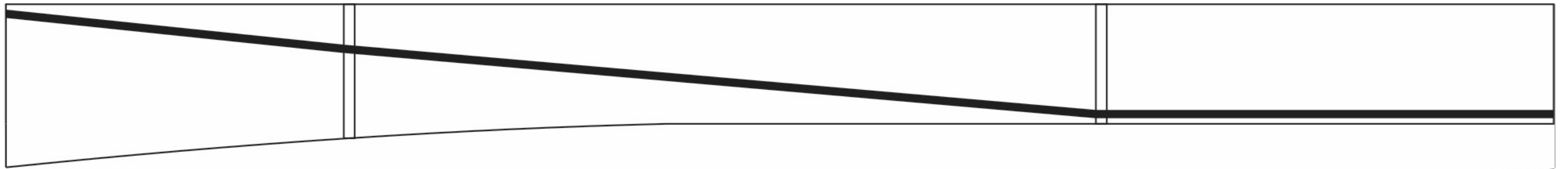
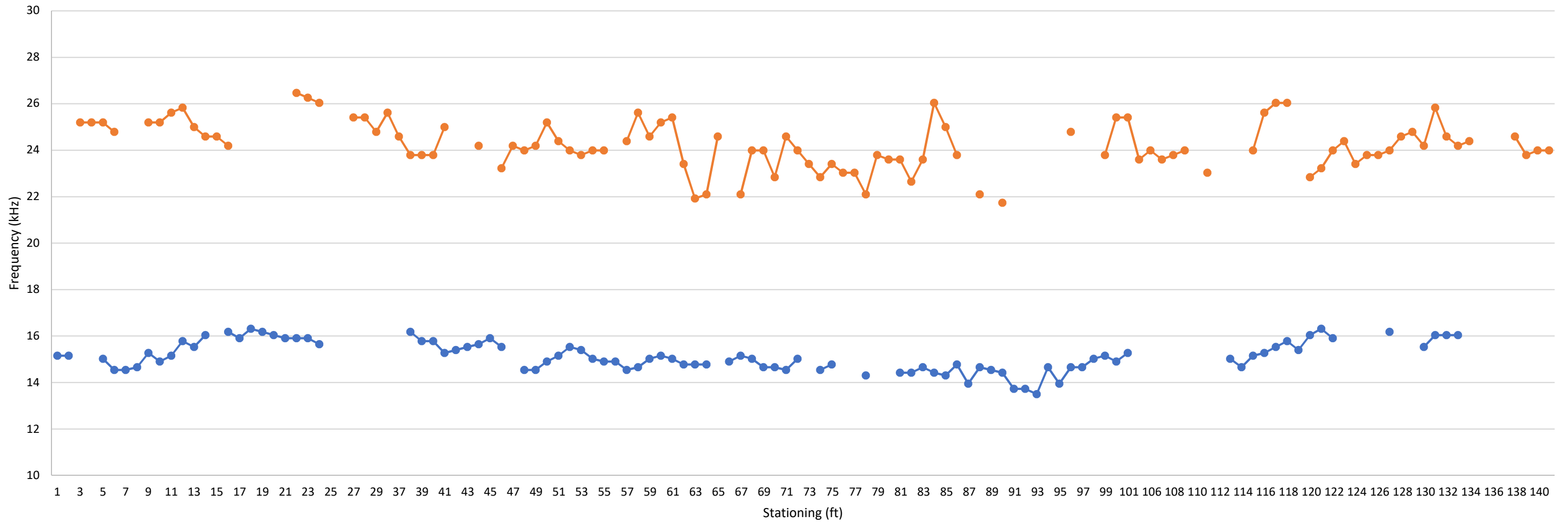
401R-2E



—●— Circumferential Frequency
 —●— Average Through Frequency
 ■ Anomalous Grout Condition

Nondestructive Testing External Tendon Ducts John Ringling Causeway Bridge Over Sarasota Bay Sarasota, Florida Prepared for Florida International University by NDT Corporation		Span 3 Tendon 401R-2E Graph Results	
January. 2018		Figure A15	

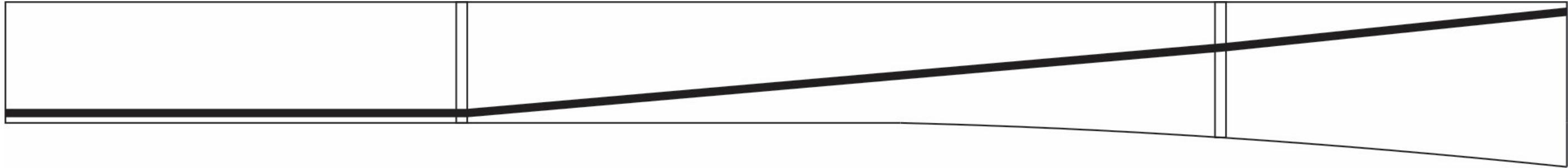
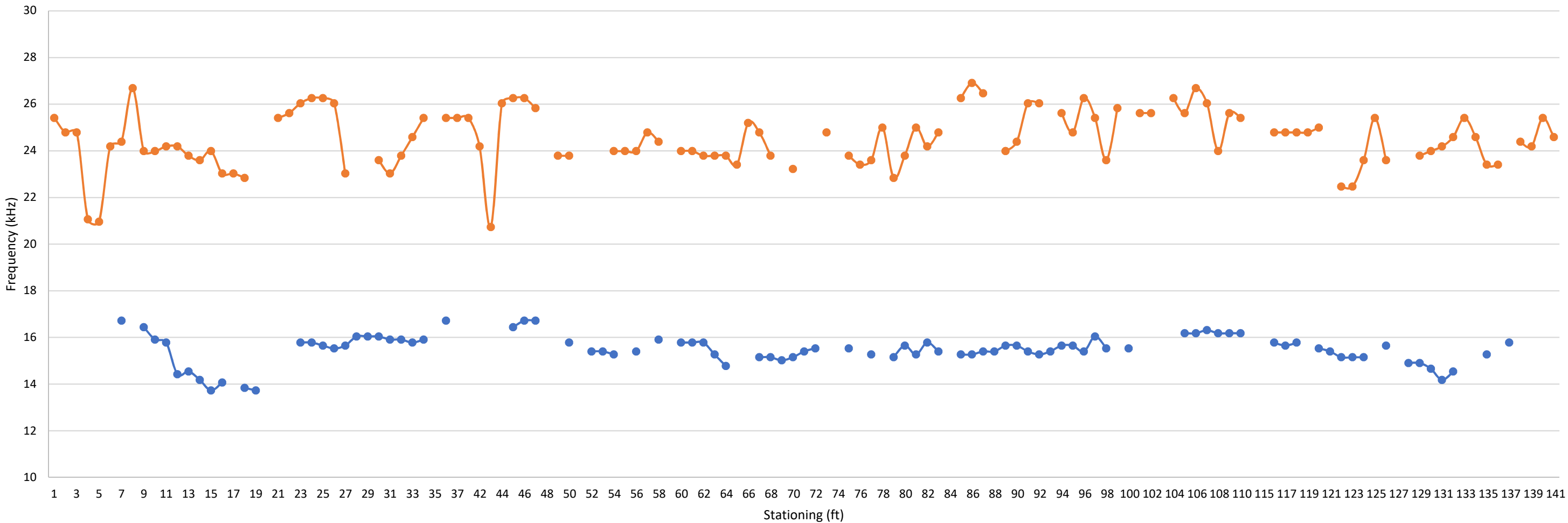
402R-2E



—●— Circumferential Frequency —●— Average Through Frequency ■ Anomalous Grout Condition

Nondestructive Testing External Tendon Ducts John Ringling Causeway Bridge Over Sarasota Bay Sarasota, Florida Prepared for Florida International University by NDT Corporation		Span 3 Tendon 402R-2E Graph Results	
		January. 2018	Figure A16

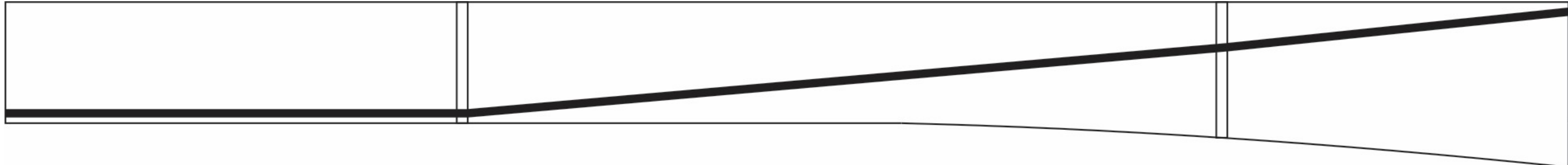
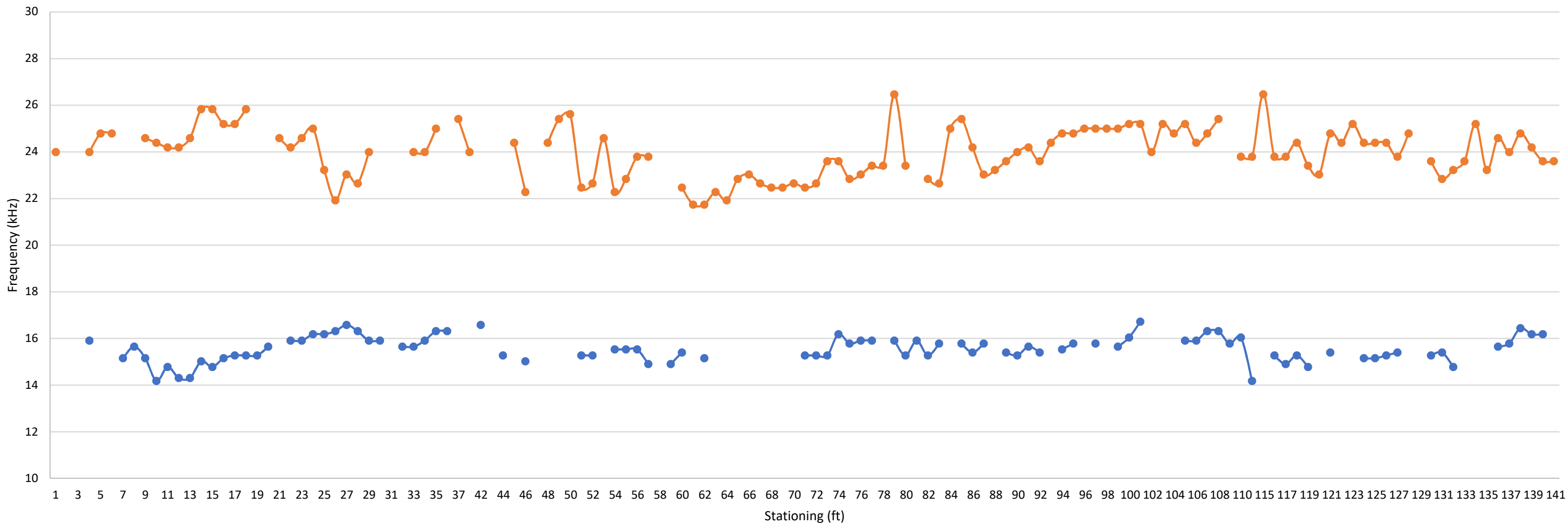
402L-3W



—●— Circumferential Frequency —●— Average Through Frequency ■ Anomalous Grout Condition

Nondestructive Testing External Tendon Ducts John Ringling Causeway Bridge Over Sarasota Bay Sarasota, Florida Prepared for Florida International University by NDT Corporation		Span 3 Tendon 402L-3W Graph Results	
		January. 2018	Figure A17

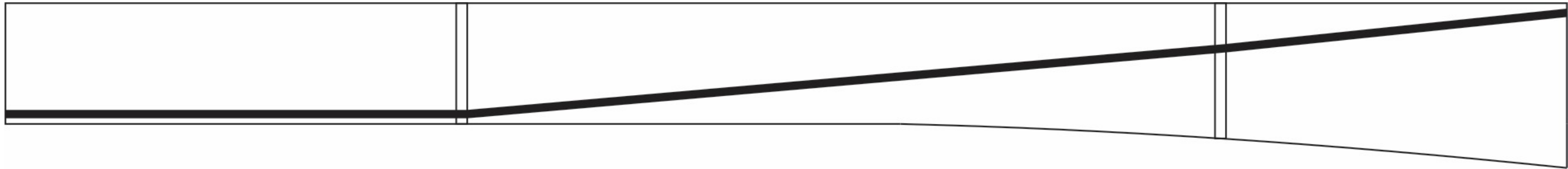
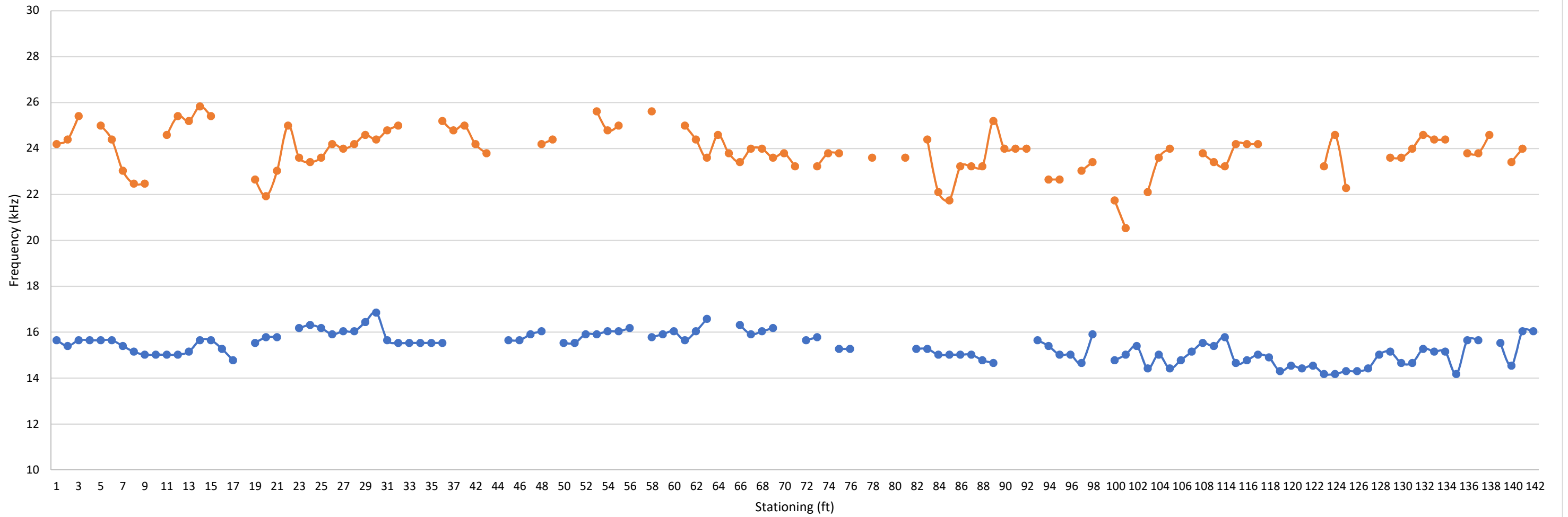
401L-3W



—●— Circumferential Frequency
 —●— Average Through Frequency
 ■ Anomalous Grout Condition

Nondestructive Testing External Tendon Ducts John Ringling Causeway Bridge Over Sarasota Bay Sarasota, Florida Prepared for Florida International University by NDT Corporation		Span 3 Tendon 401L-3W Graph Results	
January. 2018		Figure A18	

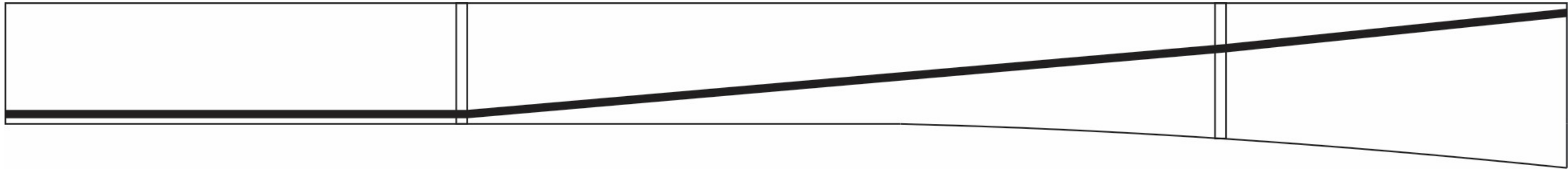
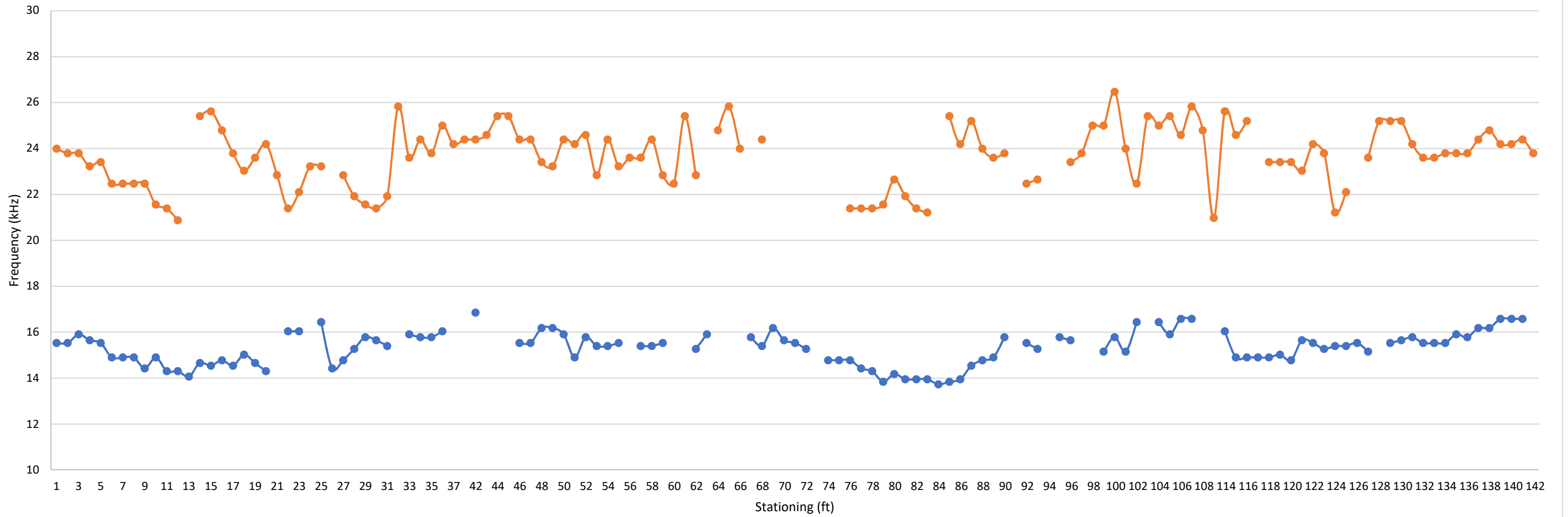
401R-3W



—●— Circumferential Frequency —●— Average Through Frequency ■ Anomalous Grout Condition

Nondestructive Testing External Tendon Ducts John Ringling Causeway Bridge Over Sarasota Bay Sarasota, Florida Prepared for Florida International University by NDT Corporation		Span 3 Tendon 401R-3W Graph Results	
		January. 2018	Figure A19

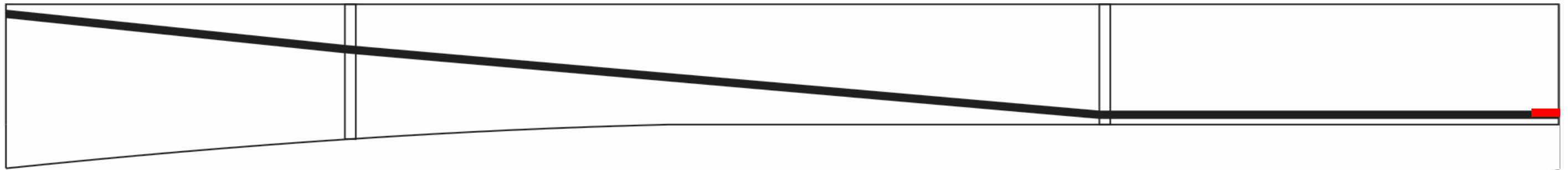
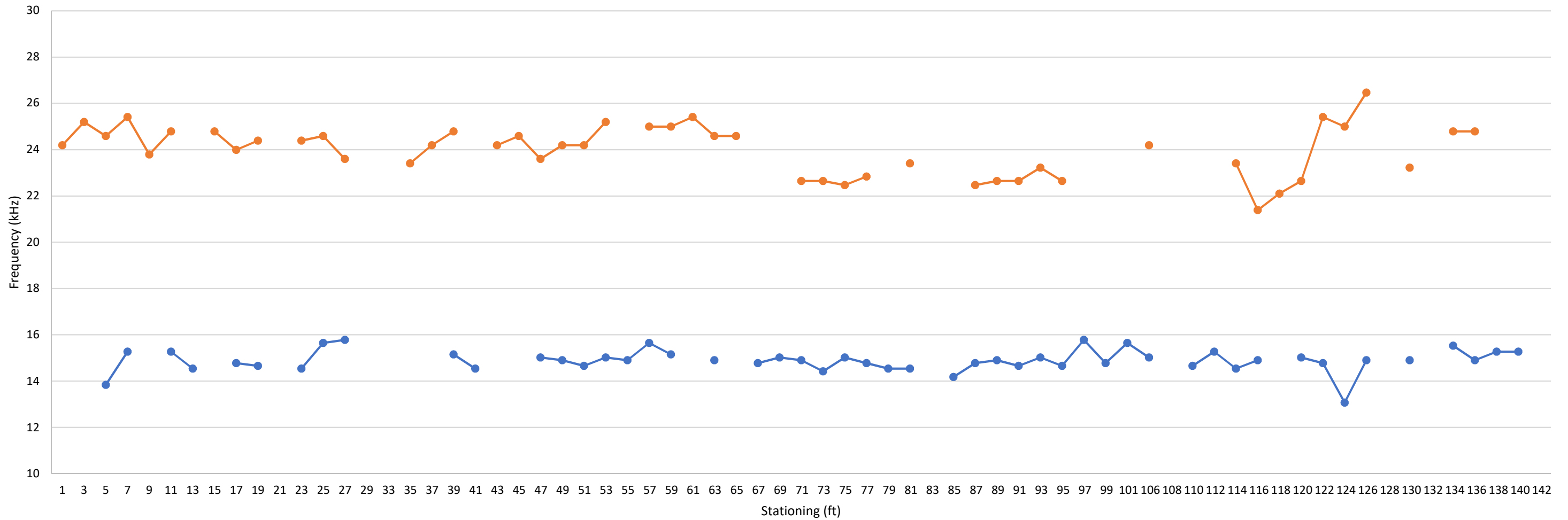
402R-3W



—●— Circumferential Frequency —●— Average Through Frequency ■ Anomalous Grout Condition

Nondestructive Testing External Tendon Ducts John Ringling Causeway Bridge Over Sarasota Bay Sarasota, Florida Prepared for Florida International University by NDT Corporation		Span 3 Tendon 402R-3W Graph Results	
		January. 2018	Figure A20

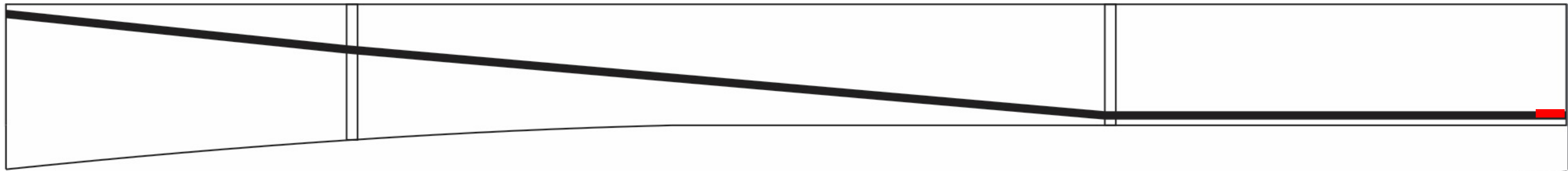
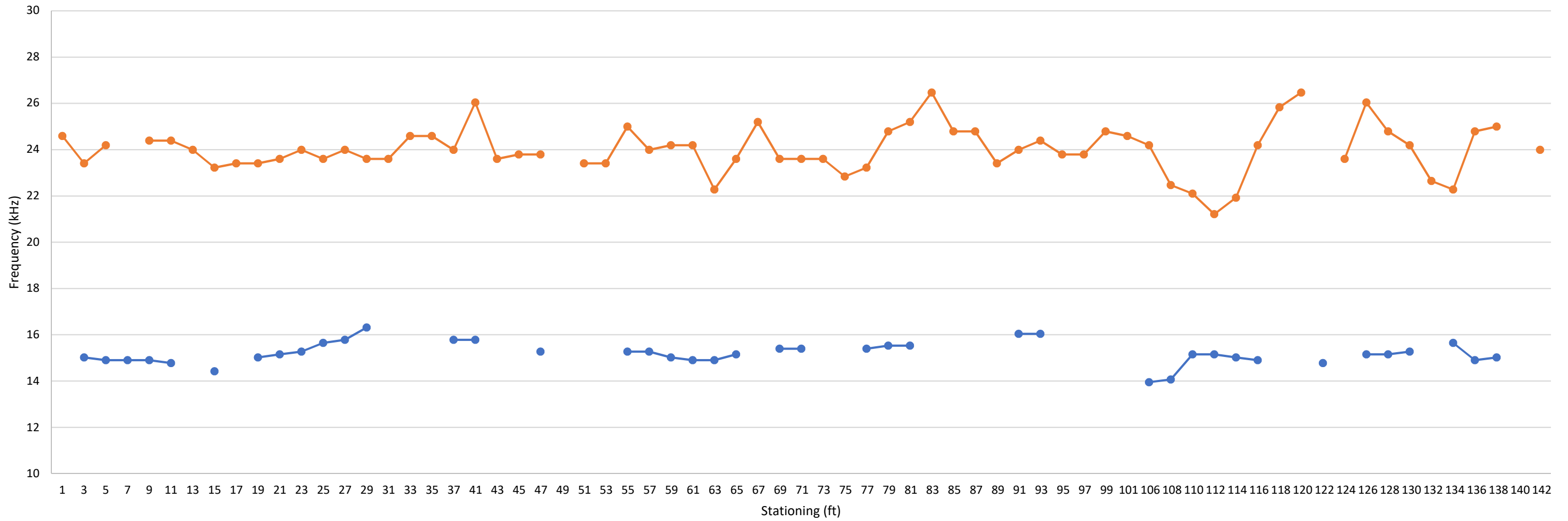
402L-3E



—●— Circumferential Frequency —●— Average Through Frequency ■ Anomalous Grout Condition

Nondestructive Testing External Tendon Ducts John Ringling Causeway Bridge Over Sarasota Bay Sarasota, Florida Prepared for Florida International University by NDT Corporation		Span 4 Tendon 402L-3E Graph Results	
		January. 2018	Figure A21

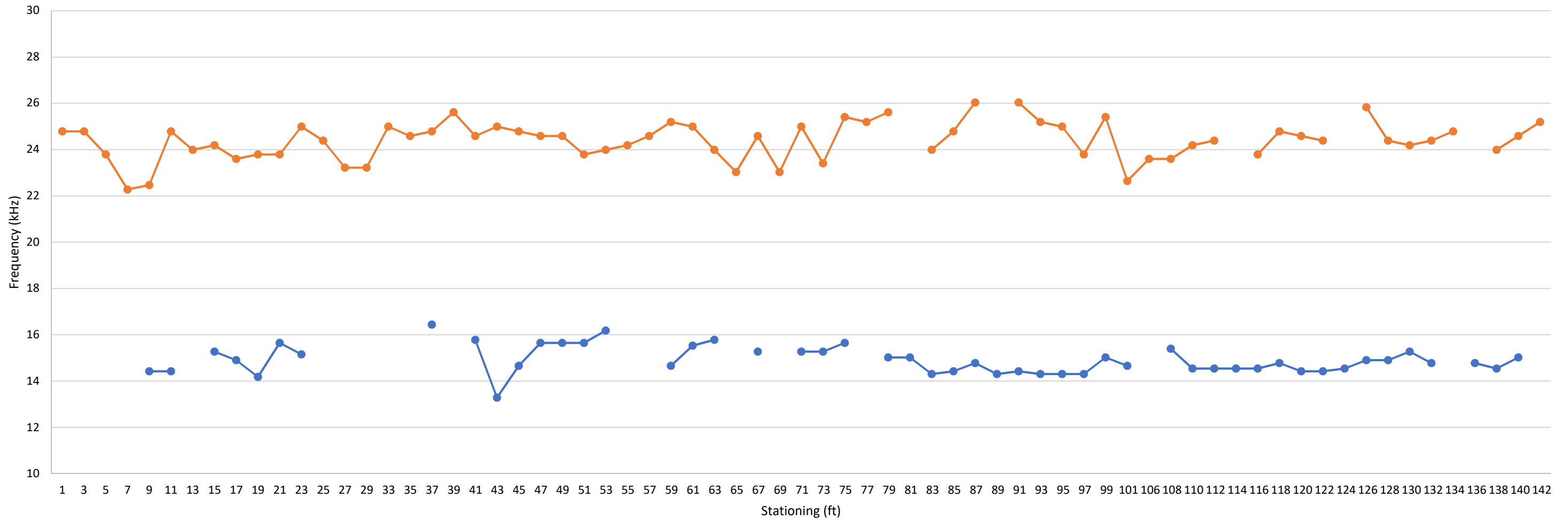
401L-3E



—●— Circumferential Frequency
 —●— Average Through Frequency
 ■ Anomalous Grout Condition

Nondestructive Testing External Tendon Ducts John Ringling Causeway Bridge Over Sarasota Bay Sarasota, Florida Prepared for Florida International University by NDT Corporation		Span 4 Tendon 401L-3E Graph Results	
		January. 2018	Figure A22

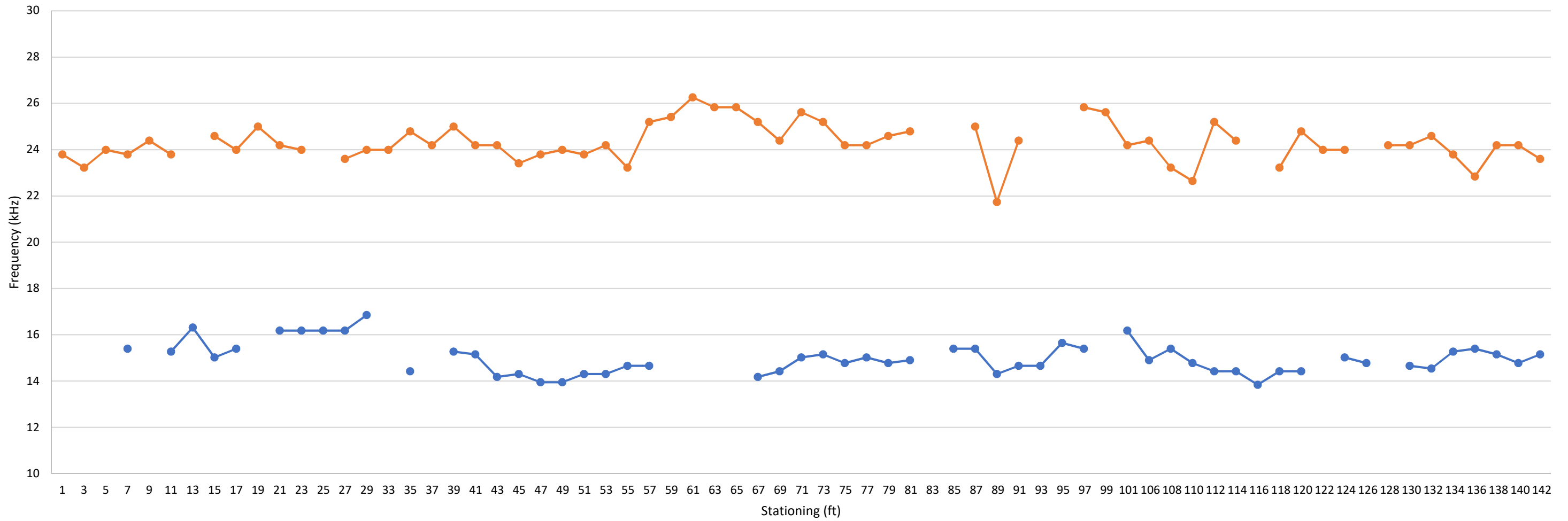
401R-3E



—●— Circumferential Frequency
 —●— Average Through Frequency
 ■ Anomalous Grout Condition

Nondestructive Testing External Tendon Ducts John Ringling Causeway Bridge Over Sarasota Bay Sarasota, Florida Prepared for Florida International University by NDT Corporation		Span 4 Tendon 401R-3E Graph Results	
		January. 2018	Figure A23

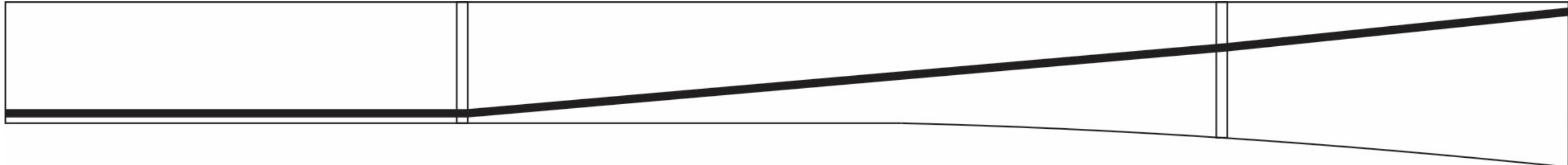
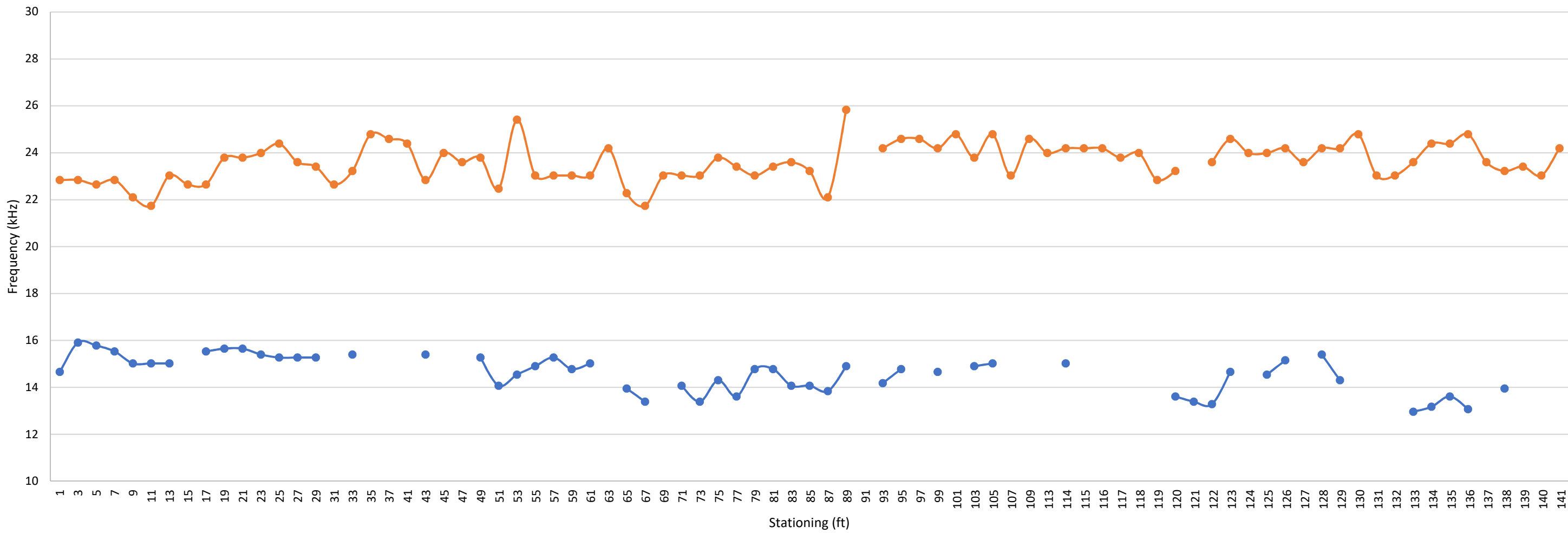
402R-3E



—●— Circumferential Frequency
 —●— Average Through Frequency
 ■ Anomalous Grout Condition

Nondestructive Testing External Tendon Ducts John Ringling Causeway Bridge Over Sarasota Bay Sarasota, Florida Prepared for Florida International University by NDT Corporation		Span 4 Tendon 402R-3E Graph Results	
		January. 2018	Figure A24

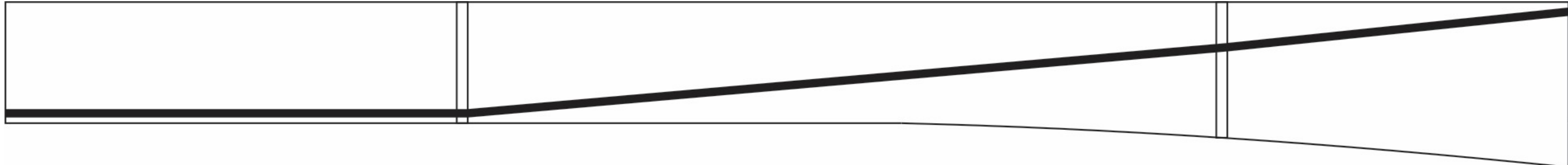
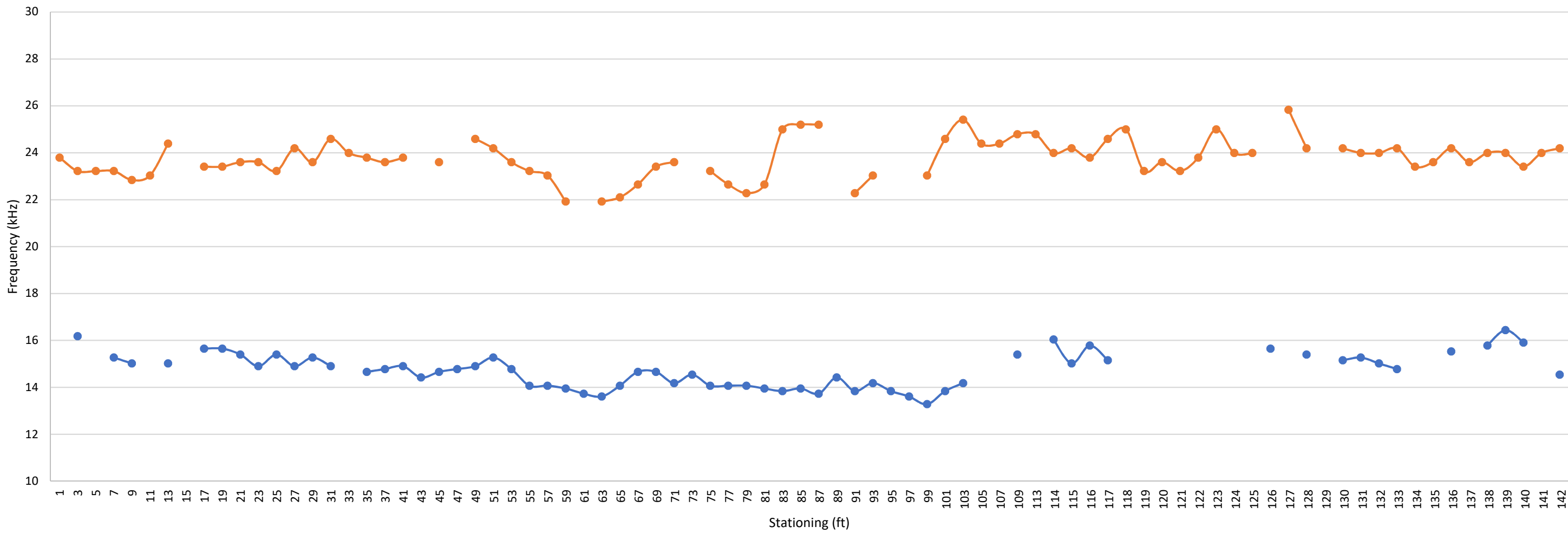
402L-4W



—●— Circumferential Frequency
 —●— Average Through Frequency
 ■ Anomalous Grout Condition

Nondestructive Testing External Tendon Ducts John Ringling Causeway Bridge Over Sarasota Bay Sarasota, Florida Prepared for Florida International University by NDT Corporation		Span 4 Tendon 402L-4W Graph Results	
January. 2018		Figure A25	

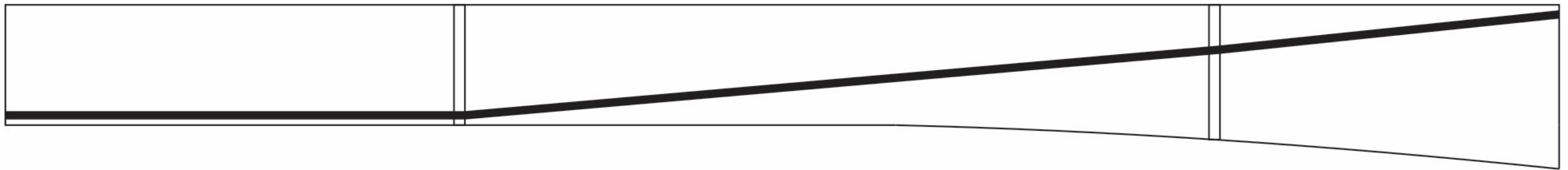
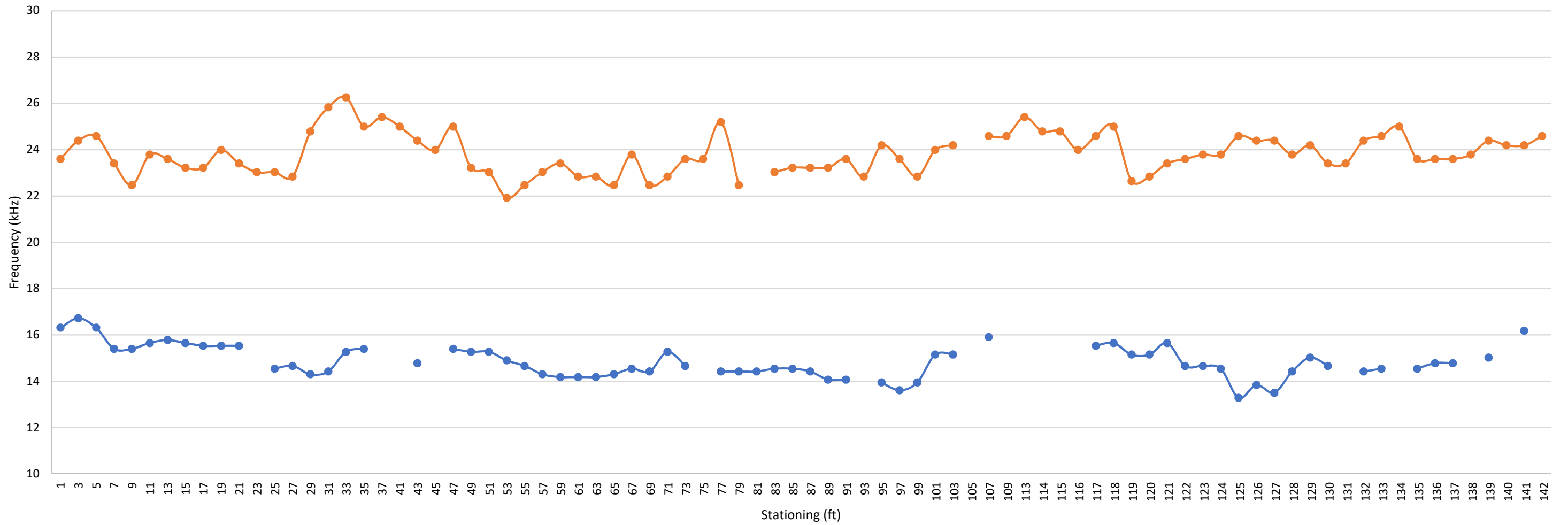
401L-4W



—●— Circumferential Frequency
 —●— Average Through Frequency
 ■ Anomalous Grout Condition

Nondestructive Testing External Tendon Ducts John Ringling Causeway Bridge Over Sarasota Bay Sarasota, Florida Prepared for Florida International University by NDT Corporation		Span 4 Tendon 401L-4W Graph Results	
January. 2018		Figure A26	

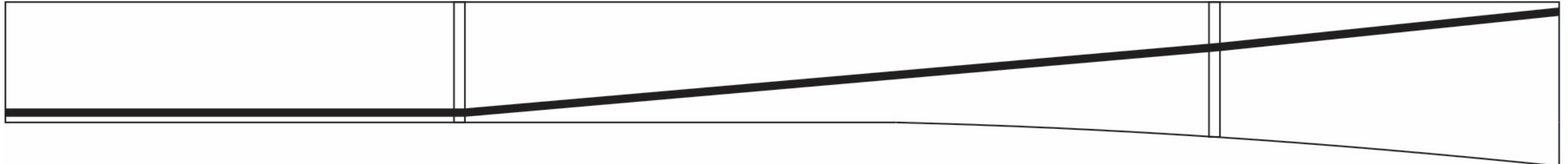
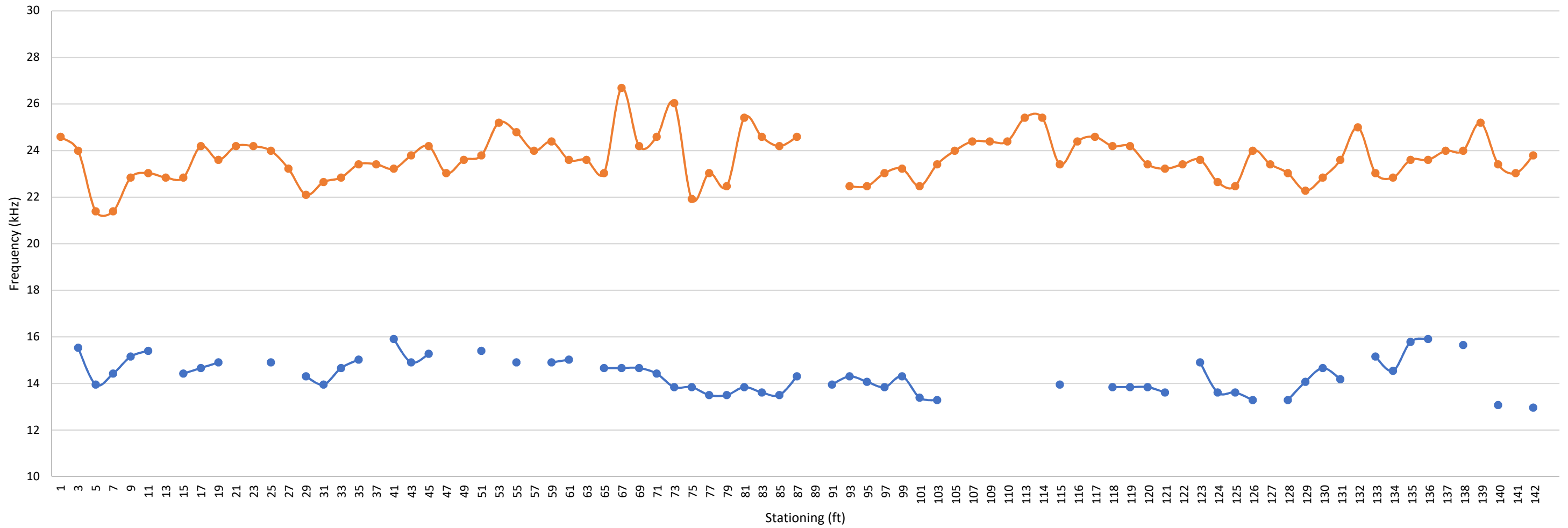
401R-4W



—●— Circumferential Frequency
 —●— Average Through Frequency
 ■ Anomalous Grout Condition

Nondestructive Testing External Tendon Ducts John Ringling Causeway Bridge Over Sarasota Bay Sarasota, Florida Prepared for Florida International University by NDT Corporation		Span 4 Tendon 401R-4W Graph Results	
January. 2018		Figure A27	

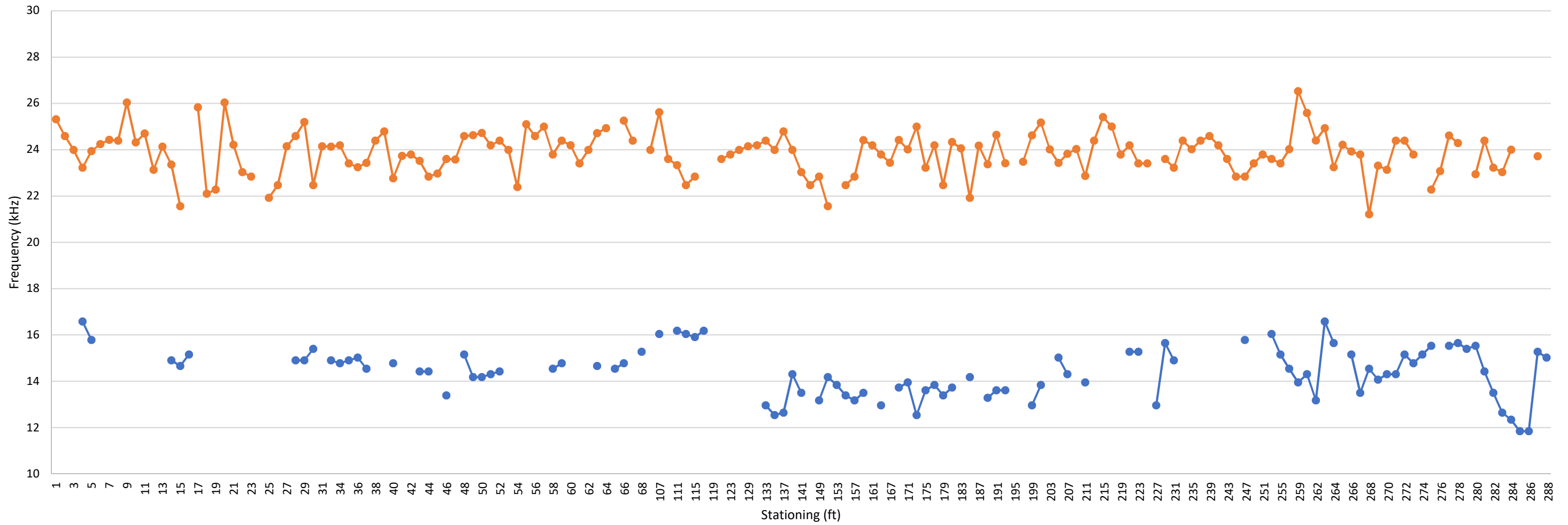
402R-4W



—●— Circumferential Frequency —●— Average Through Frequency ■ Anomalous Grout Condition

Nondestructive Testing External Tendon Ducts John Ringling Causeway Bridge Over Sarasota Bay Sarasota, Florida Prepared for Florida International University by NDT Corporation		Span 4 Tendon 402R-4W Graph Results	
		January. 2018	Figure A28

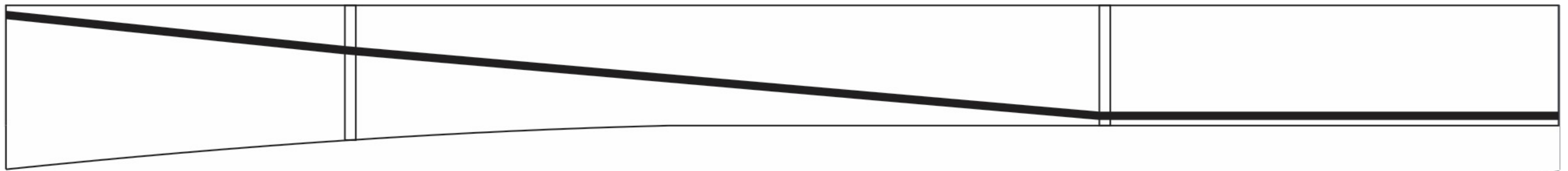
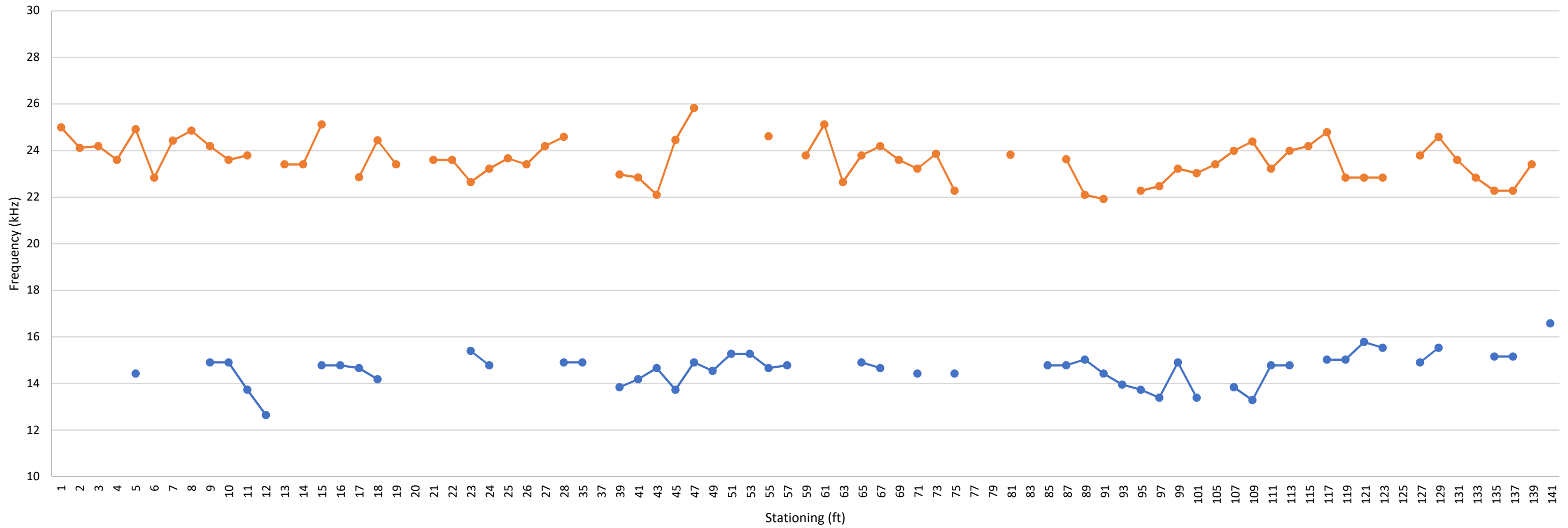
303L-4E



—●— Circumferential Frequency
 —●— Average Through Frequency
 ■ Anomalous Grout Condition

Nondestructive Testing External Tendon Ducts John Ringling Causeway Bridge Over Sarasota Bay Sarasota, Florida Prepared for Florida International University by NDT Corporation		Span 5 Tendon 303L-4E Graph Results	
January. 2018		Figure A29	

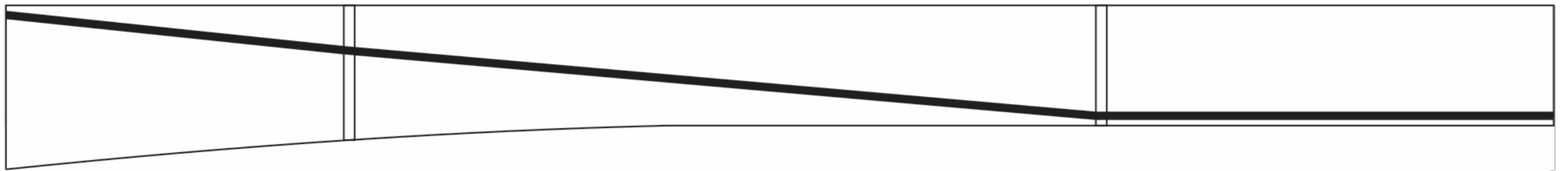
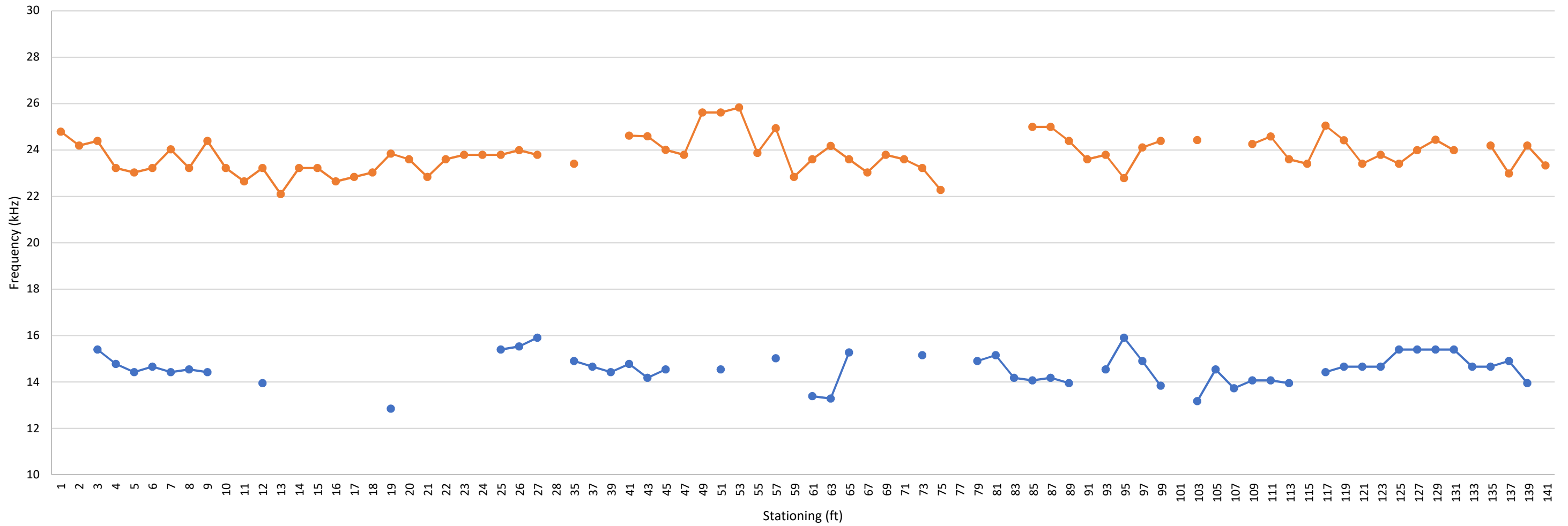
402L-4E



—●— Circumferential Frequency
 —●— Average Through Frequency
 ■ Anomalous Grout Condition

Nondestructive Testing External Tendon Ducts John Ringling Causeway Bridge Over Sarasota Bay Sarasota, Florida Prepared for Florida International University by NDT Corporation		Span 5 Tendon 402L-4E Graph Results	
January. 2018		Figure A30	

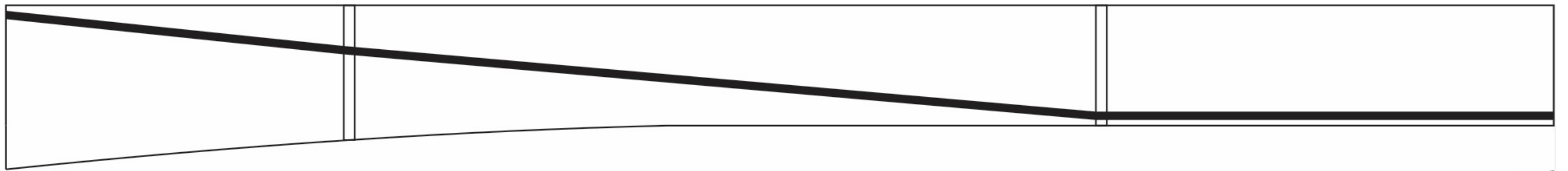
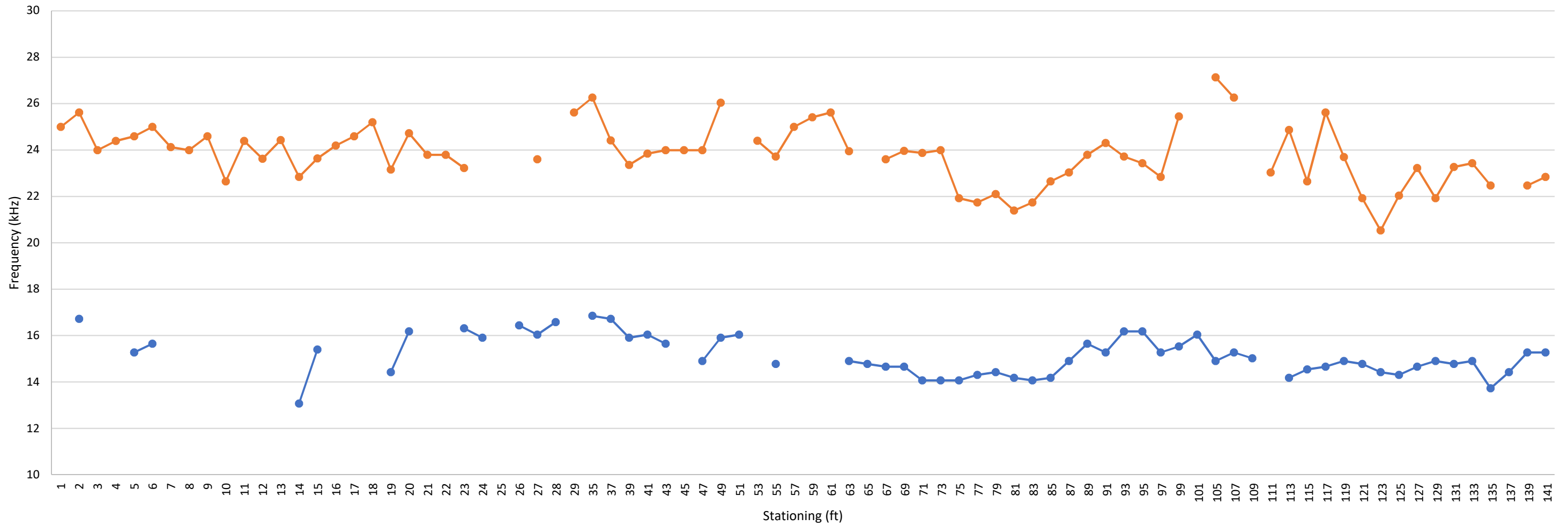
401L-4E



● Circumferential Frequency
 ● Average Through Frequency
 ■ Anomalous Grout Condition

Nondestructive Testing External Tendon Ducts John Ringling Causeway Bridge Over Sarasota Bay Sarasota, Florida Prepared for Florida International University by NDT Corporation		Span 5 Tendon 401L-4E Graph Results	
January. 2018		Figure A31	

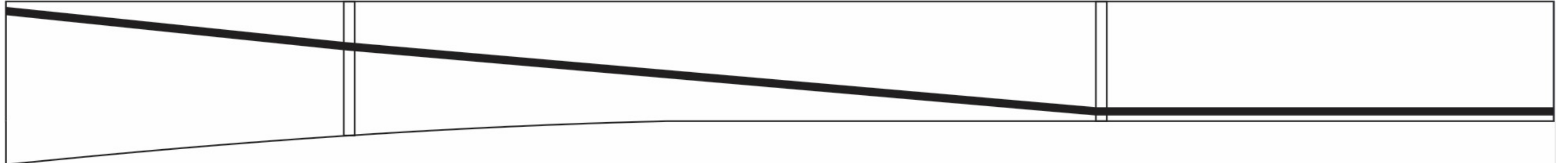
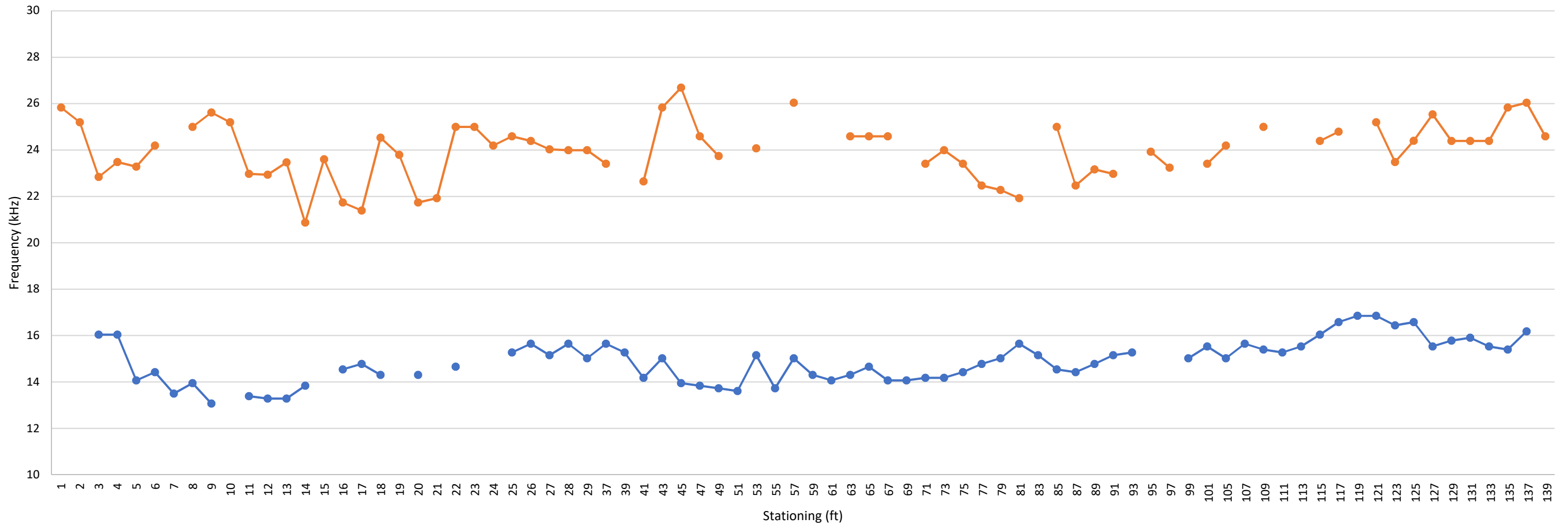
401R-4E



—●— Circumferential Frequency —●— Average Through Frequency ■ Anomalous Grout Condition

Nondestructive Testing External Tendon Ducts John Ringling Causeway Bridge Over Sarasota Bay Sarasota, Florida Prepared for Florida International University by NDT Corporation		Span 5 Tendon 401R-4E Graph Results	
		January. 2018	Figure A32

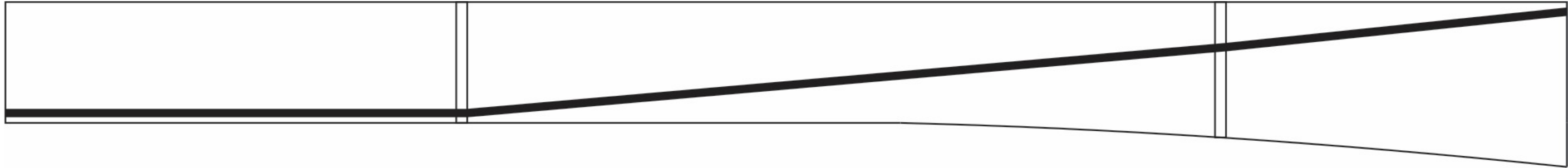
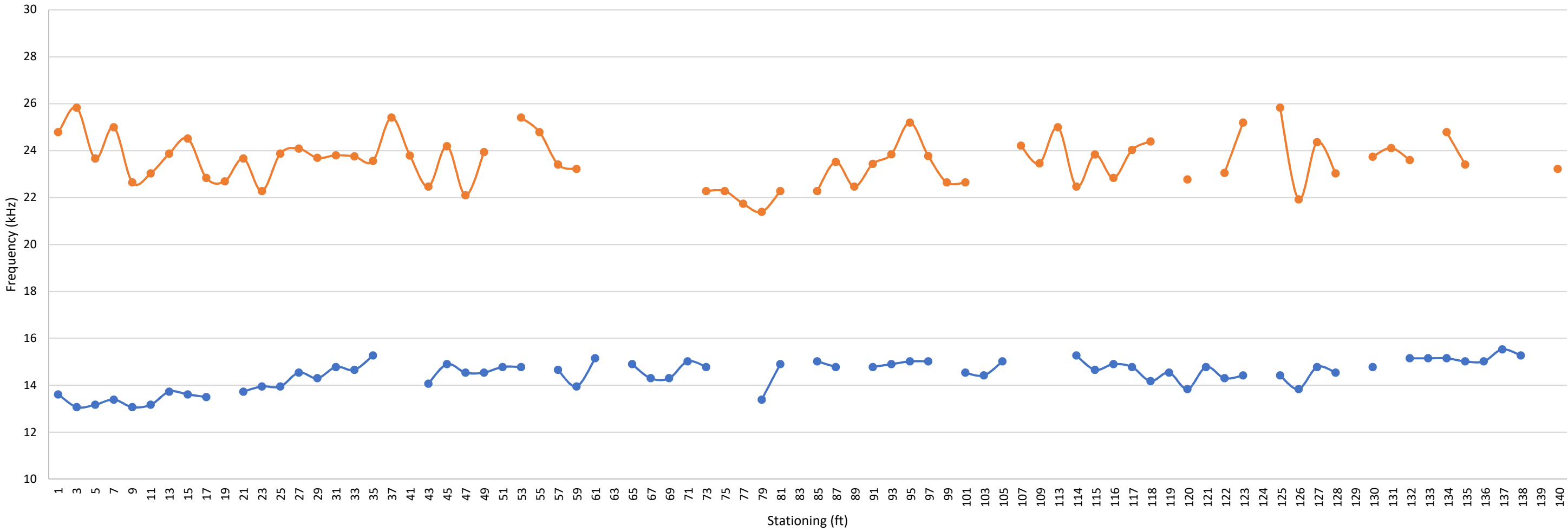
402R-4E



—●— Circumferential Frequency
 —●— Average Through Frequency
 ■ Anomalous Grout Condition

Nondestructive Testing External Tendon Ducts John Ringling Causeway Bridge Over Sarasota Bay Sarasota, Florida Prepared for Florida International University by NDT Corporation		Span 5 Tendon 402R-4E Graph Results	
January. 2018		Figure A33	

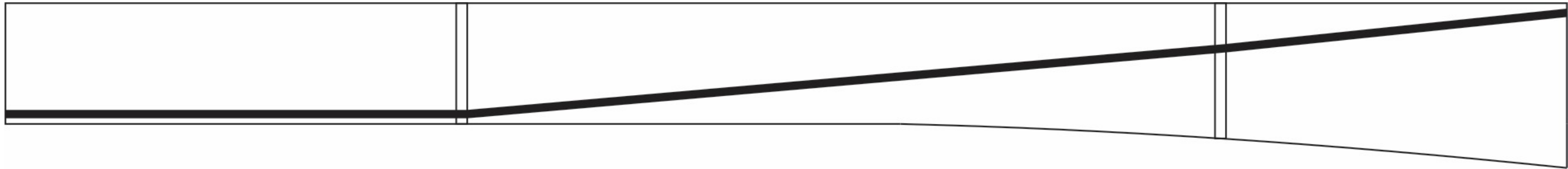
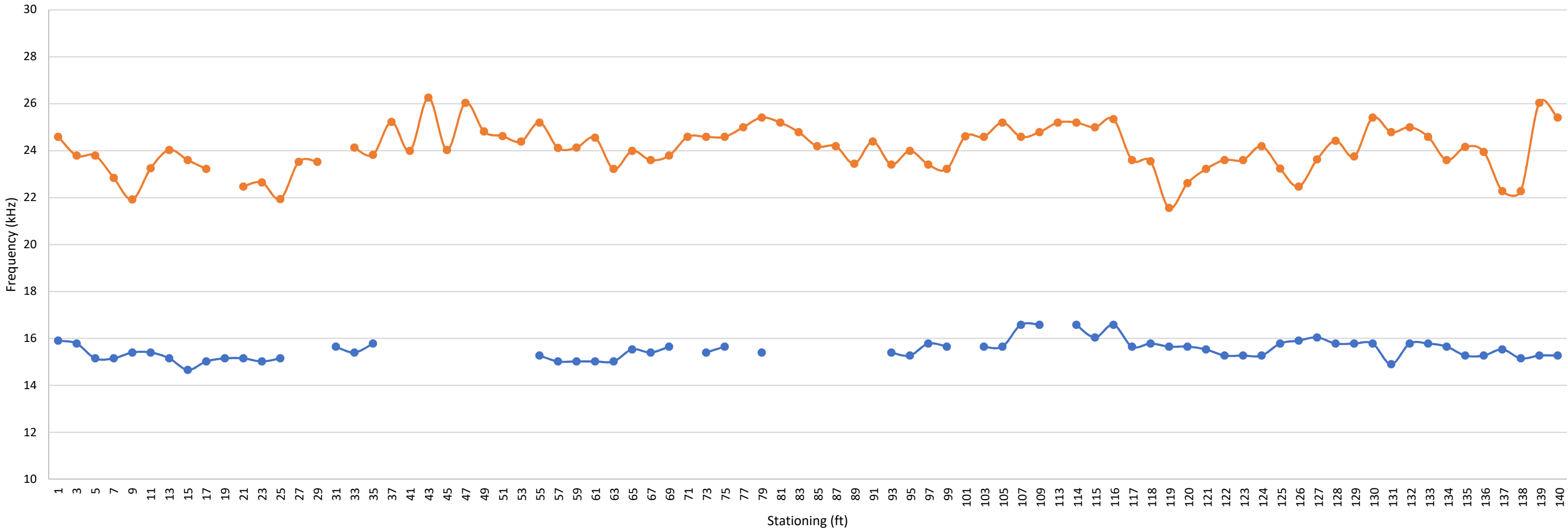
402L-5W



—●— Circumferential Frequency —●— Average Through Frequency ■ Anomalous Grout Condition

Nondestructive Testing External Tendon Ducts John Ringling Causeway Bridge Over Sarasota Bay Sarasota, Florida Prepared for Florida International University by NDT Corporation		Span 5 Tendon 402L-5W Graph Results	
		January. 2018	Figure A34

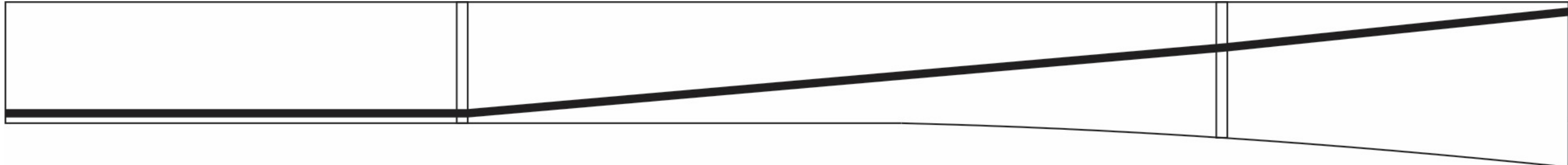
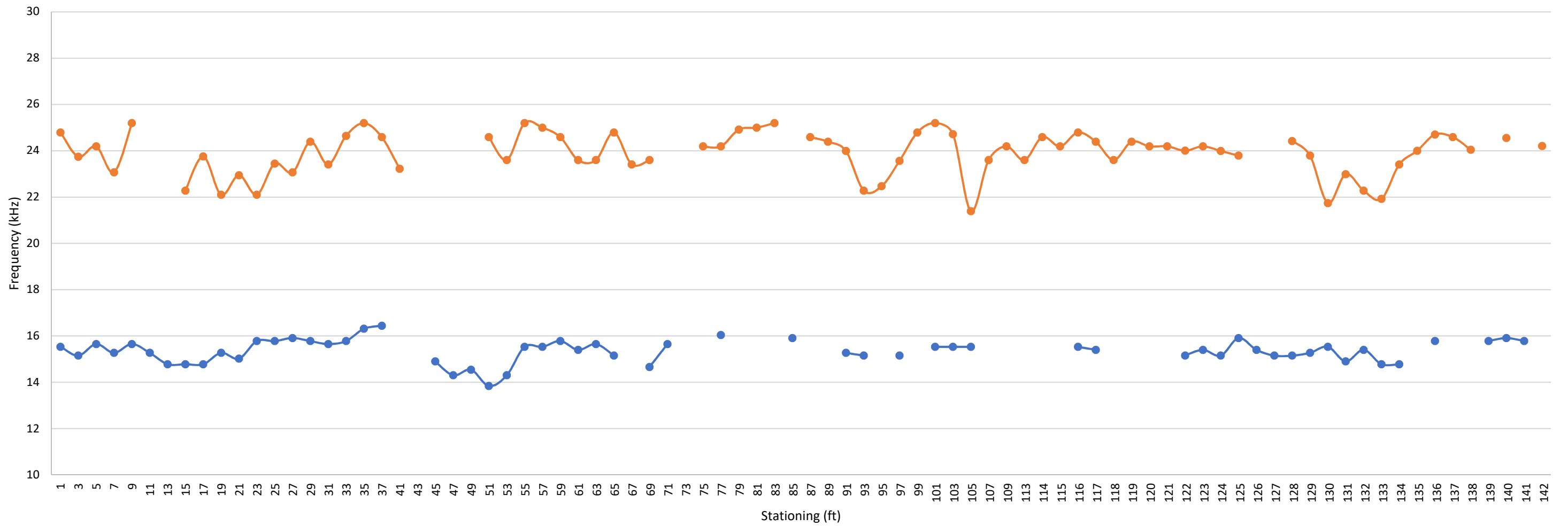
401L-5W



—●— Circumferential Frequency
 —●— Average Through Frequency
 ■ Anomalous Grout Condition

Nondestructive Testing External Tendon Ducts John Ringling Causeway Bridge Over Sarasota Bay Sarasota, Florida Prepared for Florida International University by NDT Corporation		Span 5 Tendon 401L-5W Graph Results	
January. 2018		Figure A35	

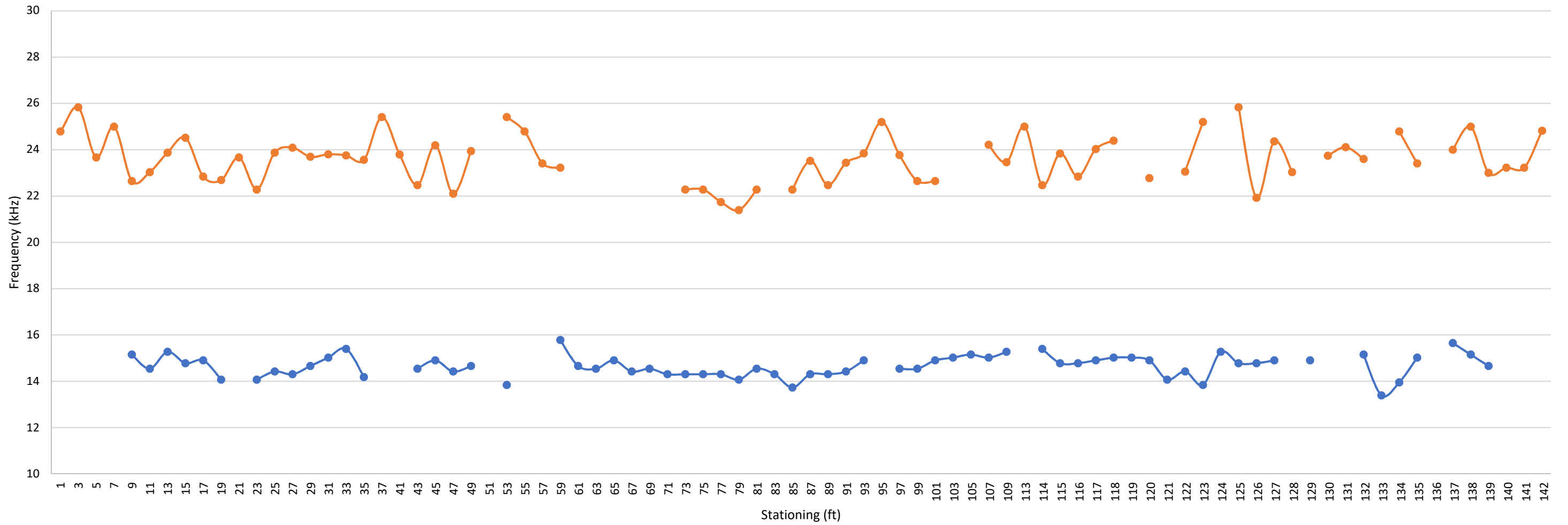
401R-5W



—●— Circumferential Frequency
 —●— Average Through Frequency
 ■ Anomalous Grout Condition

Nondestructive Testing External Tendon Ducts John Ringling Causeway Bridge Over Sarasota Bay Sarasota, Florida Prepared for Florida International University by NDT Corporation		Span 5 Tendon 401R-5W Graph Results	
January. 2018		Figure A36	

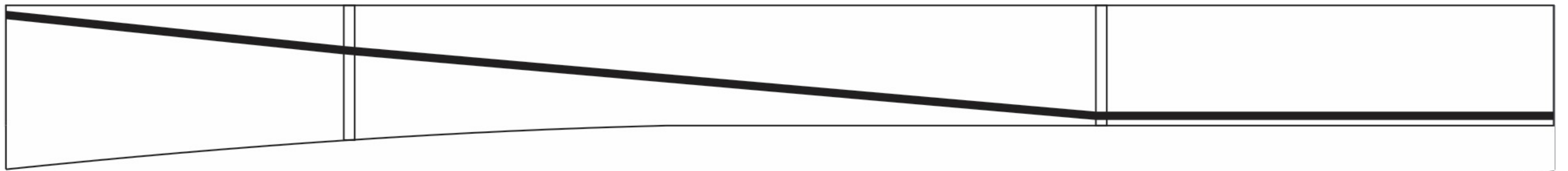
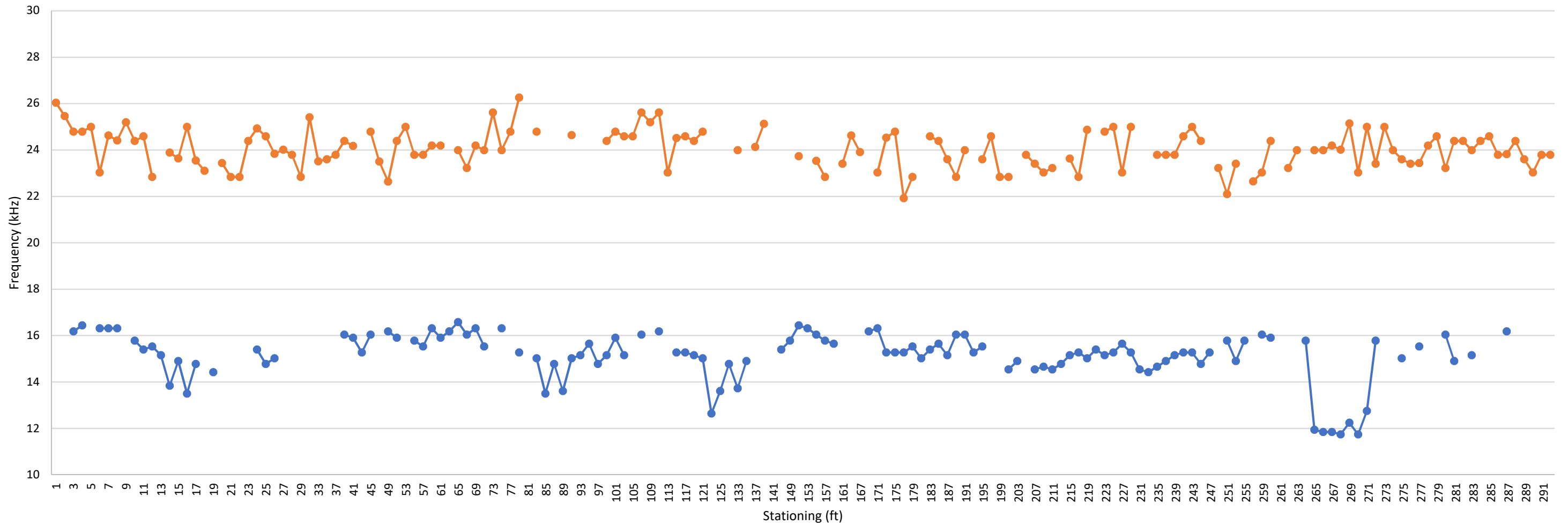
402R-5W



—●— Circumferential Frequency
 —●— Average Through Frequency
 ■ Anomalous Grout Condition

Nondestructive Testing External Tendon Ducts John Ringling Causeway Bridge Over Sarasota Bay Sarasota, Florida Prepared for Florida International University by NDT Corporation		Span 5 Tendon 402R-5W Graph Results	
January. 2018		Figure A37	

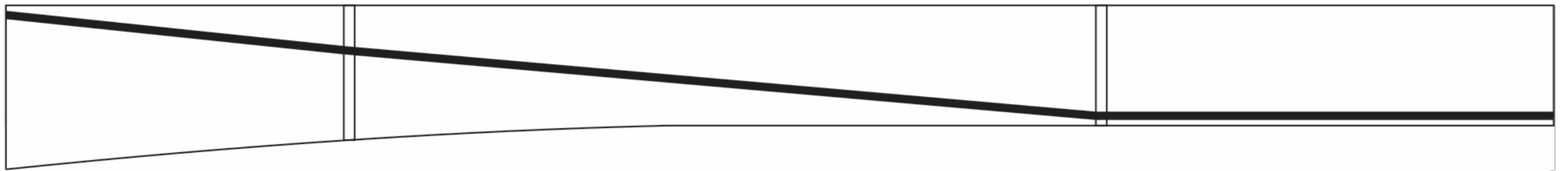
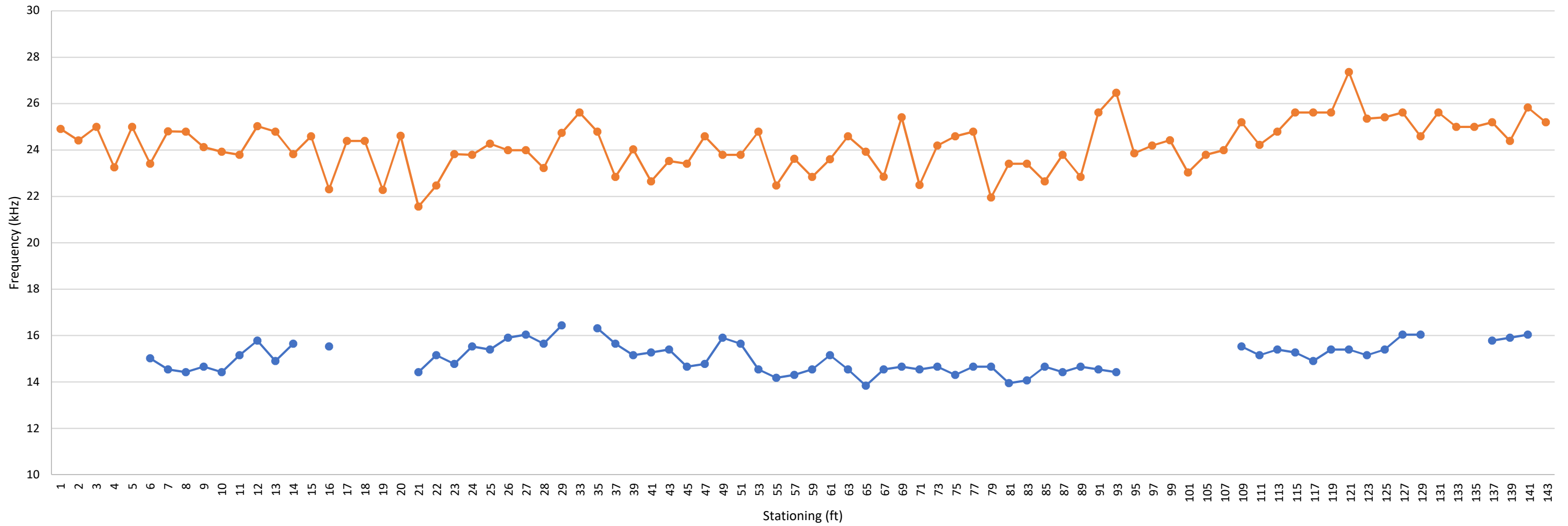
303R-4E



—●— Circumferential Frequency
 —●— Average Through Frequency
 ■ Anomalous Grout Condition

Nondestructive Testing External Tendon Ducts John Ringling Causeway Bridge Over Sarasota Bay Sarasota, Florida Prepared for Florida International University by NDT Corporation		Span 5 Tendon 303R-4E Graph Results	
		January. 2018	Figure A38

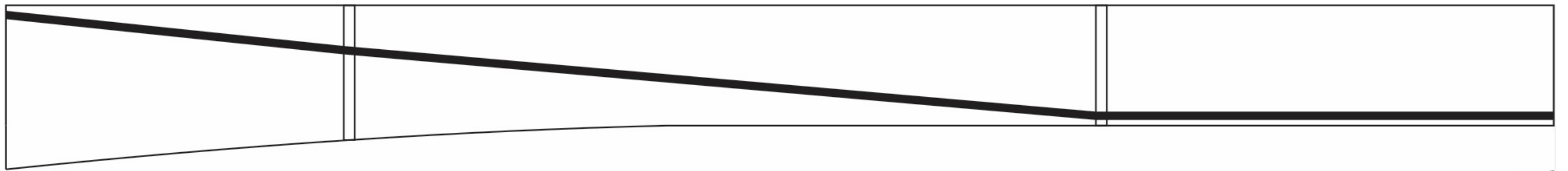
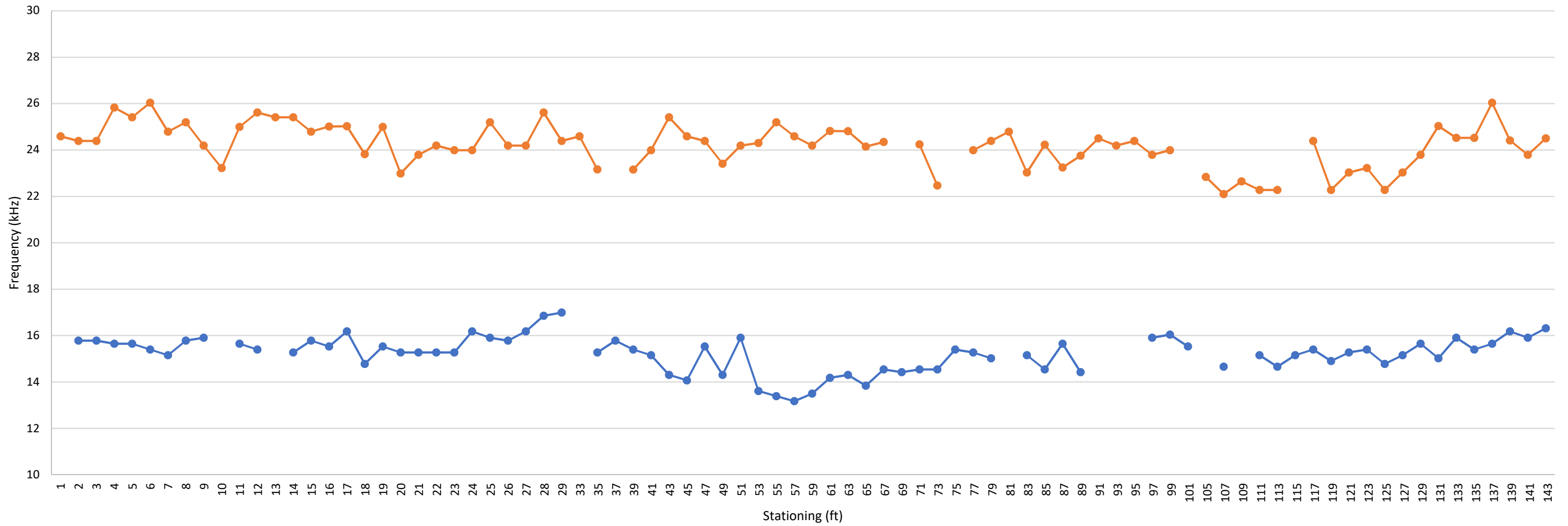
402L-5E



● Circumferential Frequency
 ● Average Through Frequency
 ■ Anomalous Grout Condition

Nondestructive Testing External Tendon Ducts John Ringling Causeway Bridge Over Sarasota Bay Sarasota, Florida Prepared for Florida International University by NDT Corporation		Span 6 Tendon 402L-5E Graph Results	
January. 2018		Figure A39	

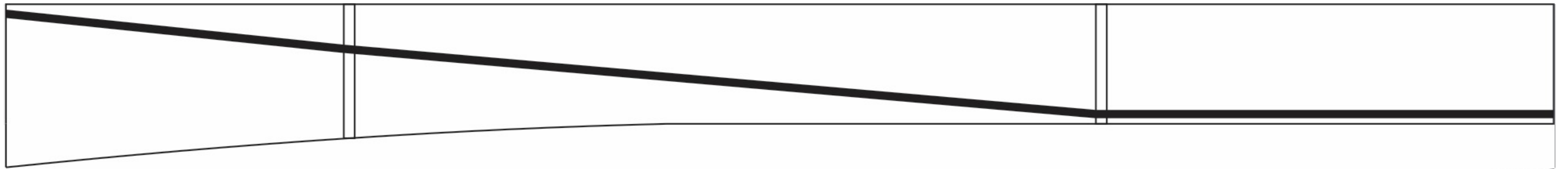
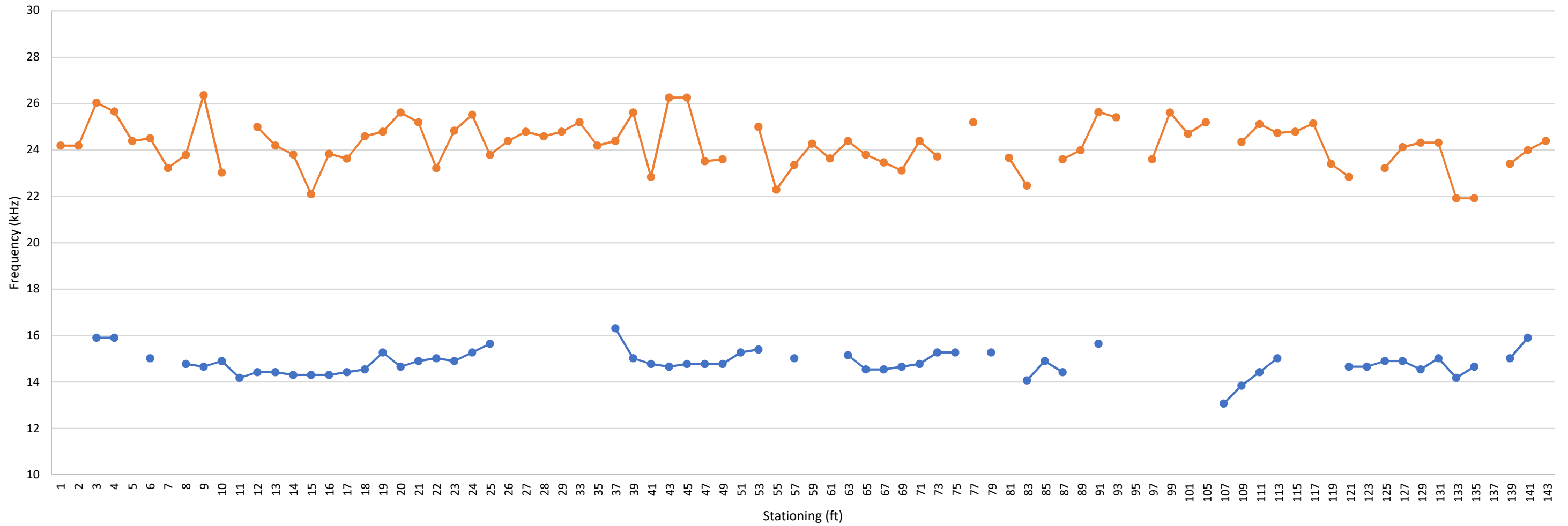
401L-5E



—●— Circumferential Frequency
 —●— Average Through Frequency
 ■ Anomalous Grout Condition

Nondestructive Testing External Tendon Ducts John Ringling Causeway Bridge Over Sarasota Bay Sarasota, Florida Prepared for Florida International University by NDT Corporation		Span 6 Tendon 401L-5E Graph Results	
January. 2018		Figure A40	

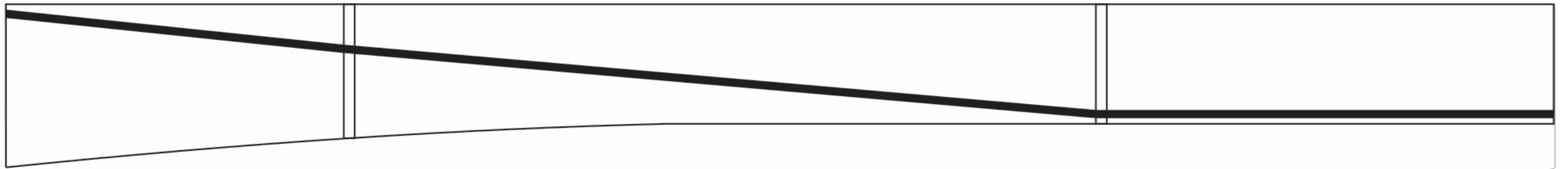
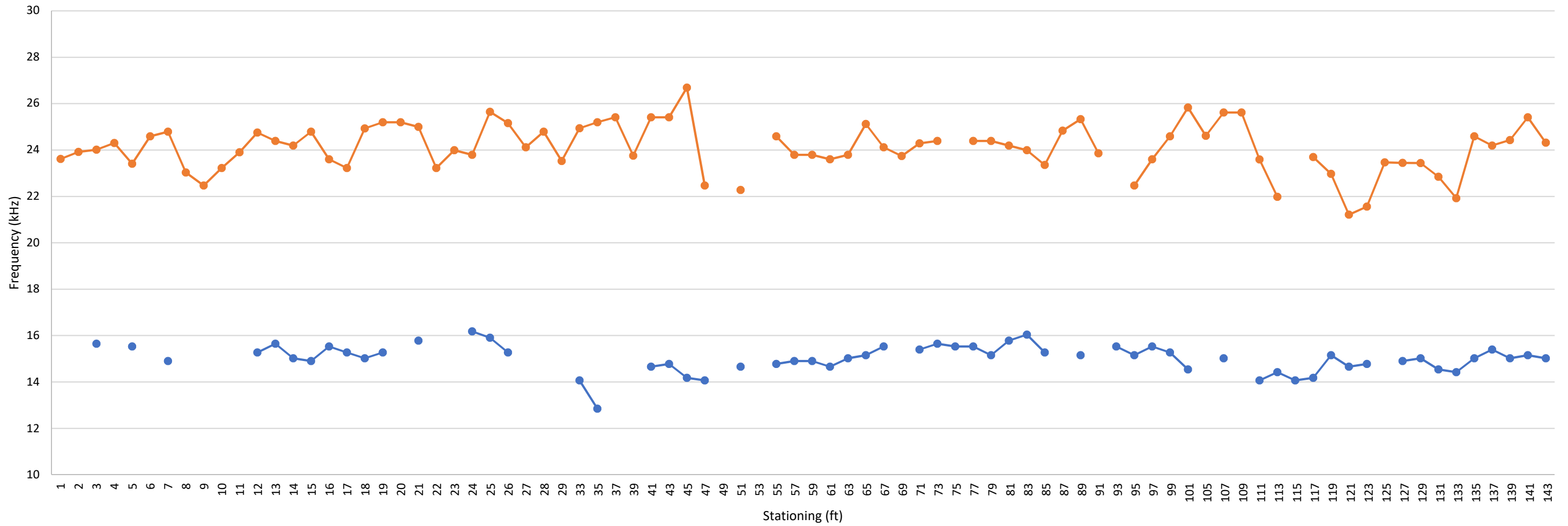
401R-5E



—●— Circumferential Frequency
 —●— Average Through Frequency
 ■ Anomalous Grout Condition

Nondestructive Testing External Tendon Ducts John Ringling Causeway Bridge Over Sarasota Bay Sarasota, Florida Prepared for Florida International University by NDT Corporation		Span 6 Tendon 401R-5E Graph Results	
January. 2018		Figure A41	

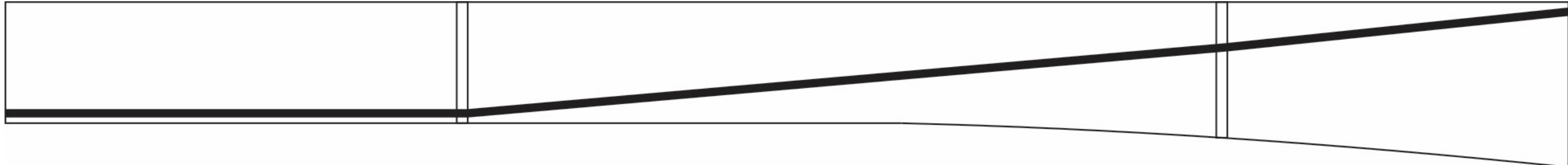
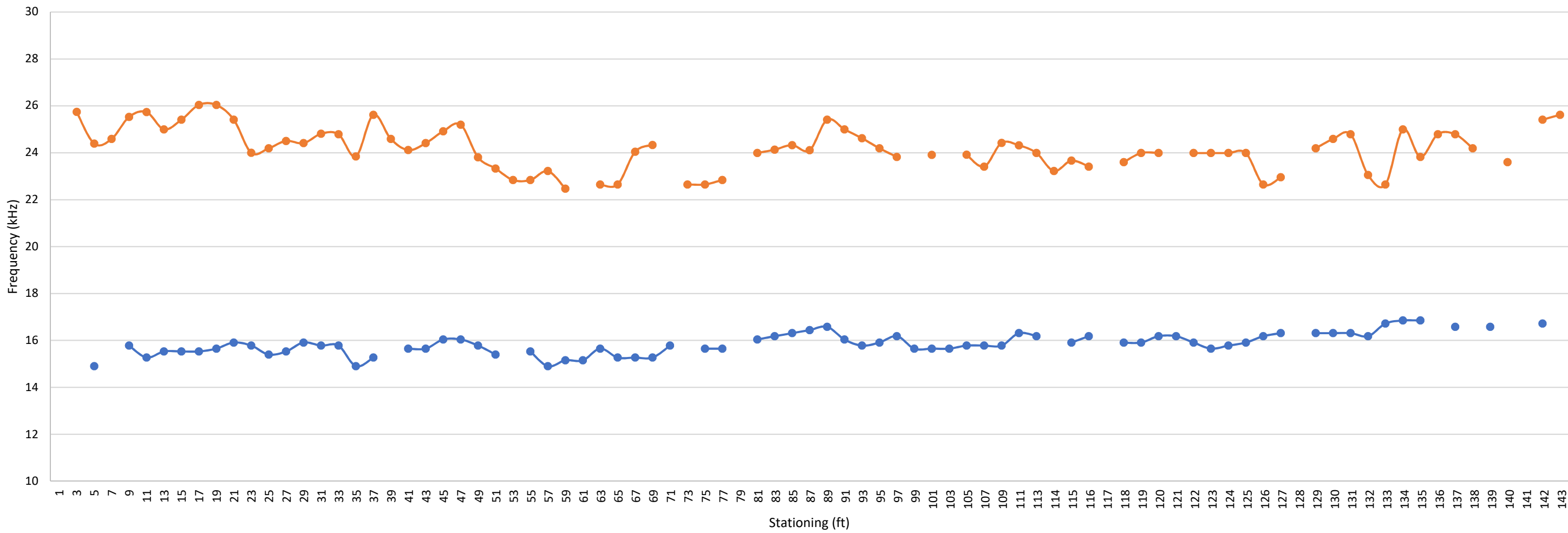
402R-5E



—●— Circumferential Frequency
 —●— Average Through Frequency
 ■ Anomalous Grout Condition

Nondestructive Testing External Tendon Ducts John Ringling Causeway Bridge Over Sarasota Bay Sarasota, Florida Prepared for Florida International University by NDT Corporation		Span 6 Tendon 402R-5E Graph Results	
January. 2018		Figure A42	

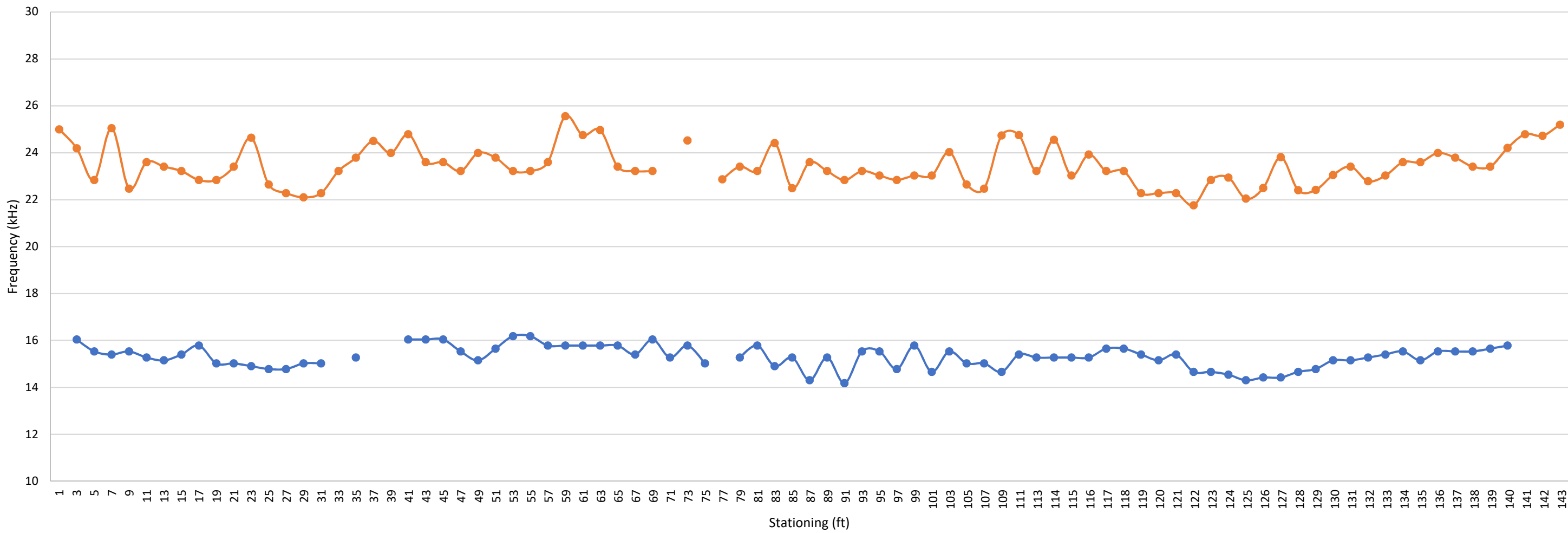
402L-6W



—●— Circumferential Frequency
 —●— Average Through Frequency
 ■ Anomalous Grout Condition

Nondestructive Testing External Tendon Ducts John Ringling Causeway Bridge Over Sarasota Bay Sarasota, Florida Prepared for Florida International University by NDT Corporation		Span 6 Tendon 402L-6W Graph Results	
January. 2018		Figure A43	

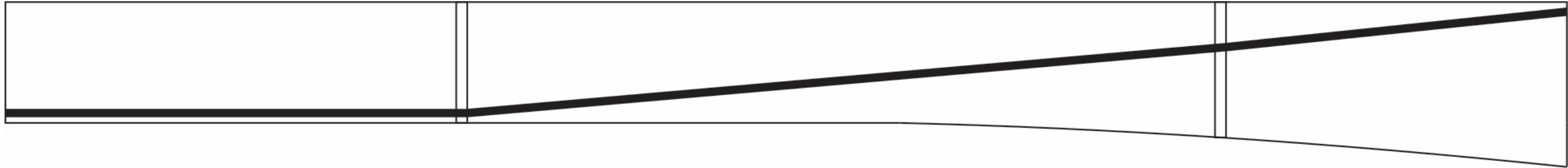
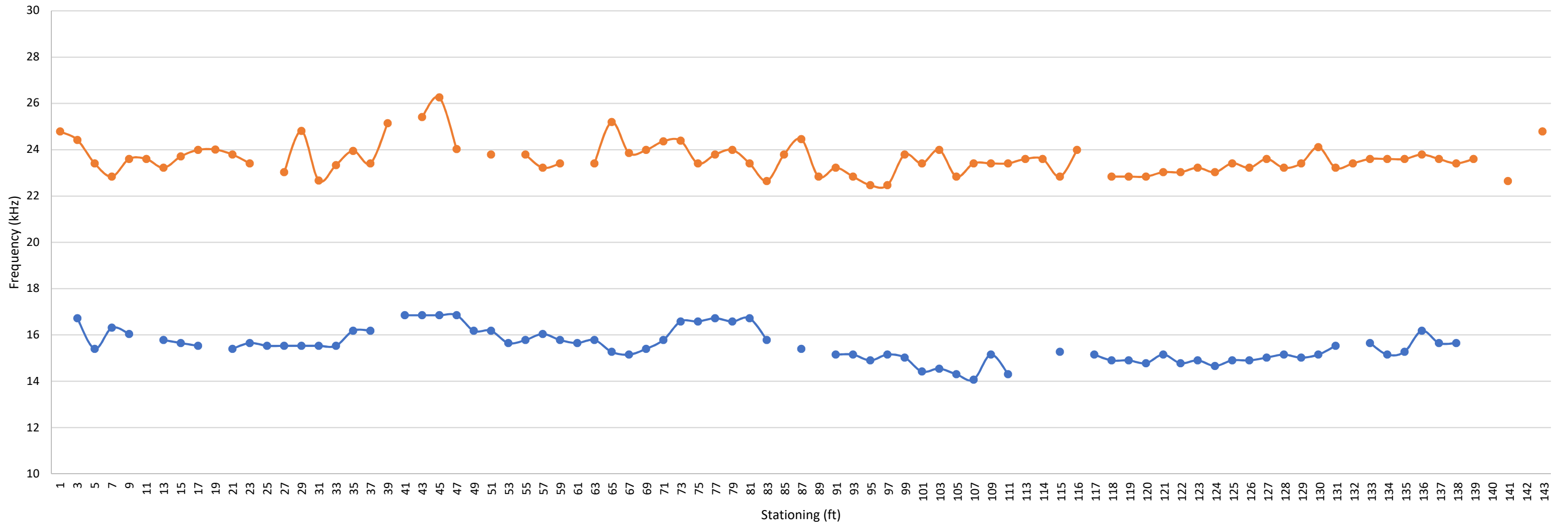
401L-6W



—●— Circumferential Frequency
 —●— Average Through Frequency
 ■ Anomalous Grout Condition

Nondestructive Testing External Tendon Ducts John Ringling Causeway Bridge Over Sarasota Bay Sarasota, Florida Prepared for Florida International University by NDT Corporation		Span 6 Tendon 401L-6W Graph Results	
January. 2018		Figure A44	

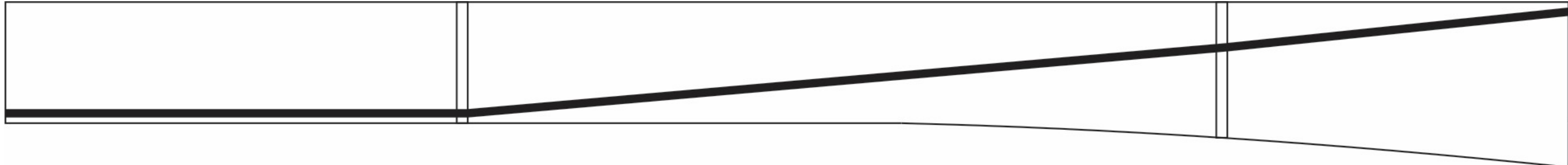
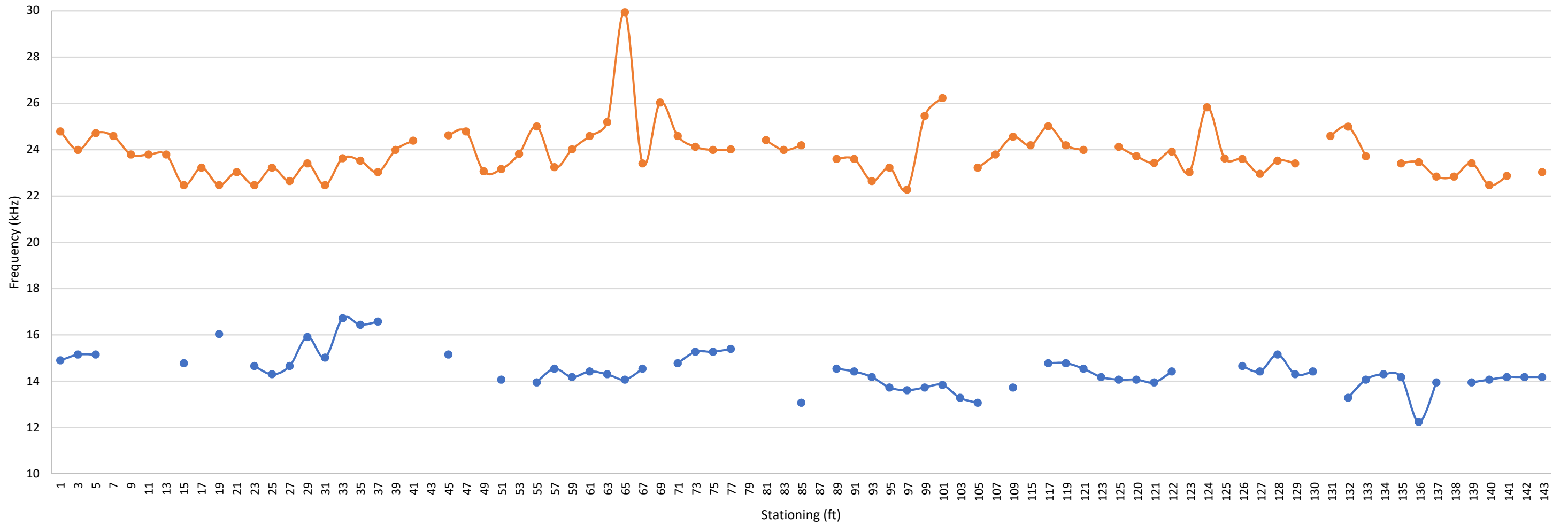
401R-6W



—●— Circumferential Frequency —●— Average Through Frequency ■ Anomalous Grout Condition

Nondestructive Testing External Tendon Ducts John Ringling Causeway Bridge Over Sarasota Bay Sarasota, Florida Prepared for Florida International University by NDT Corporation		Span 6 Tendon 401R-6W Graph Results	
		January. 2018	Figure A45

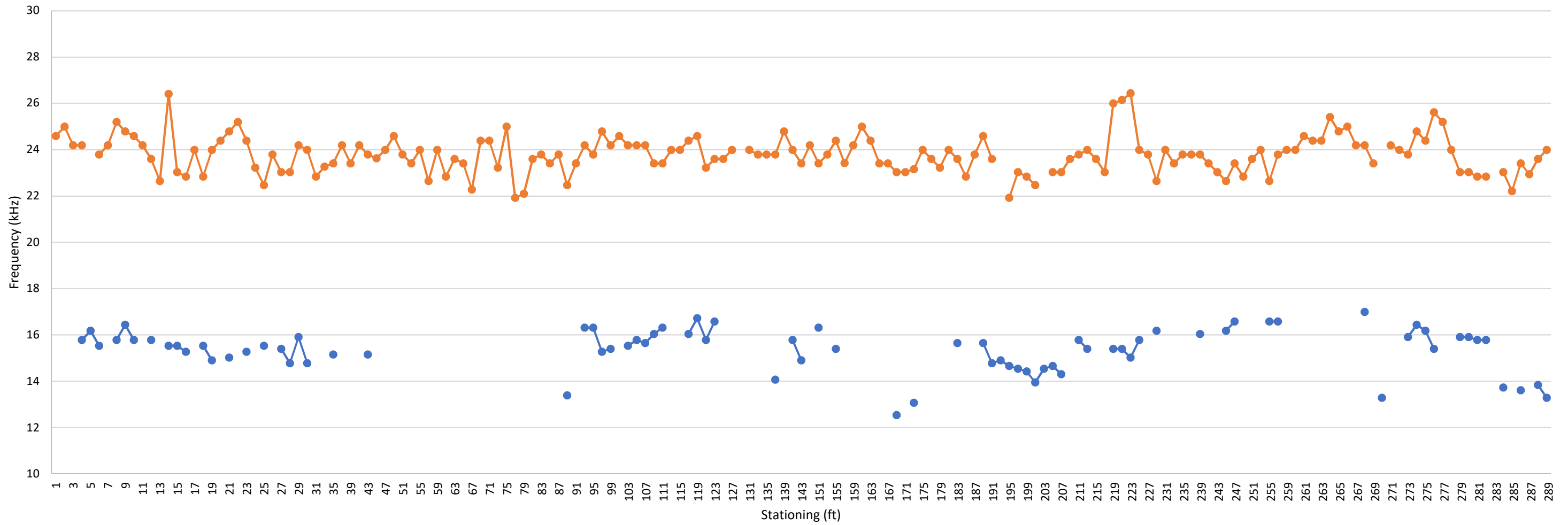
402R-6W



—●— Circumferential Frequency
 —●— Average Through Frequency
 ■ Anomalous Grout Condition

Nondestructive Testing External Tendon Ducts John Ringling Causeway Bridge Over Sarasota Bay Sarasota, Florida Prepared for Florida International University by NDT Corporation		Span 6 Tendon 402R-6W Graph Results	
January. 2018		Figure A46	

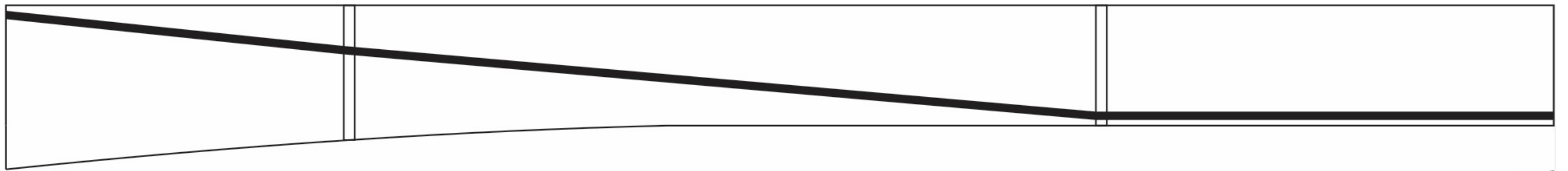
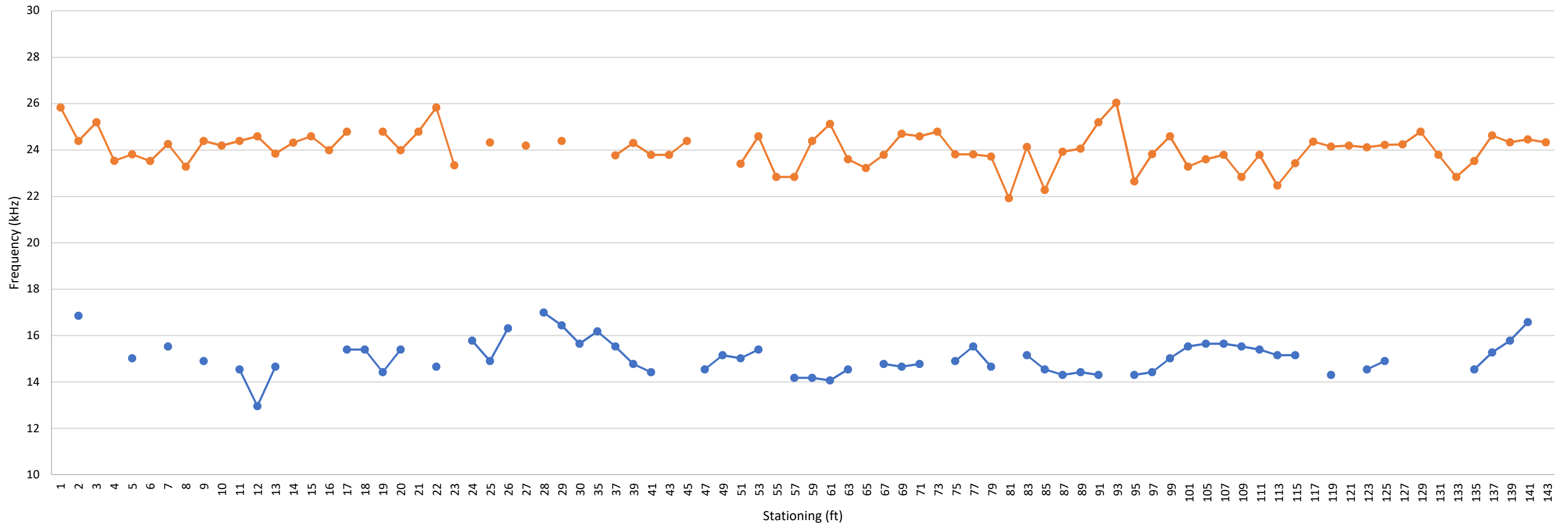
303L-6E



—●— Circumferential Frequency
 —●— Average Through Frequency
 ■ Anomalous Grout Condition

Nondestructive Testing External Tendon Ducts John Ringling Causeway Bridge Over Sarasota Bay Sarasota, Florida Prepared for Florida International University by NDT Corporation		Span 7 Tendon 303L-6E Graph Results	
January. 2018		Figure A47	

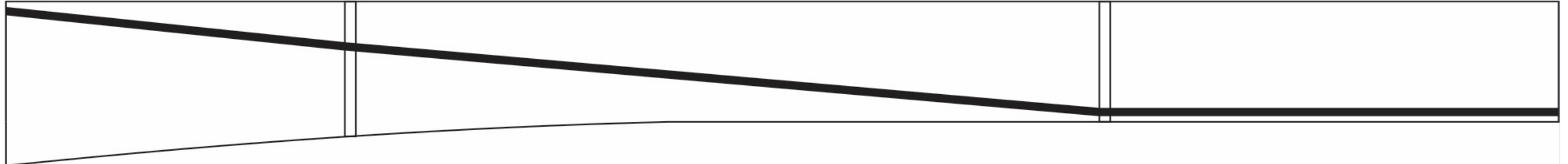
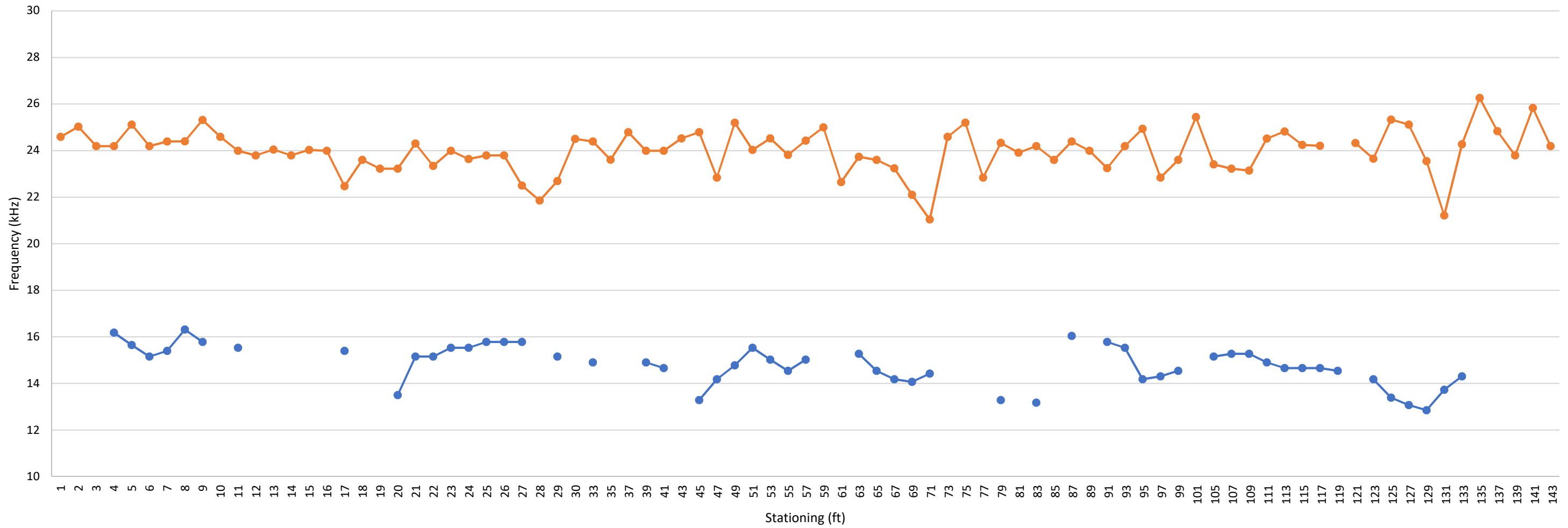
402L-6E



—●— Circumferential Frequency
 —●— Average Through Frequency
 ■ Anomalous Grout Condition

Nondestructive Testing External Tendon Ducts John Ringling Causeway Bridge Over Sarasota Bay Sarasota, Florida Prepared for Florida International University by NDT Corporation		Span 7 Tendon 402L-6E Graph Results	
January. 2018		Figure A48	

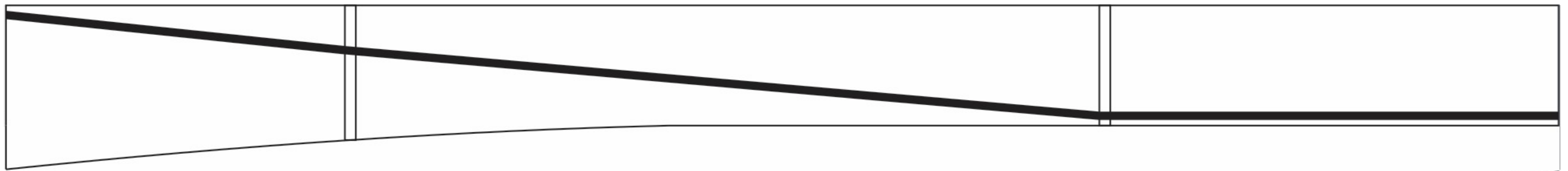
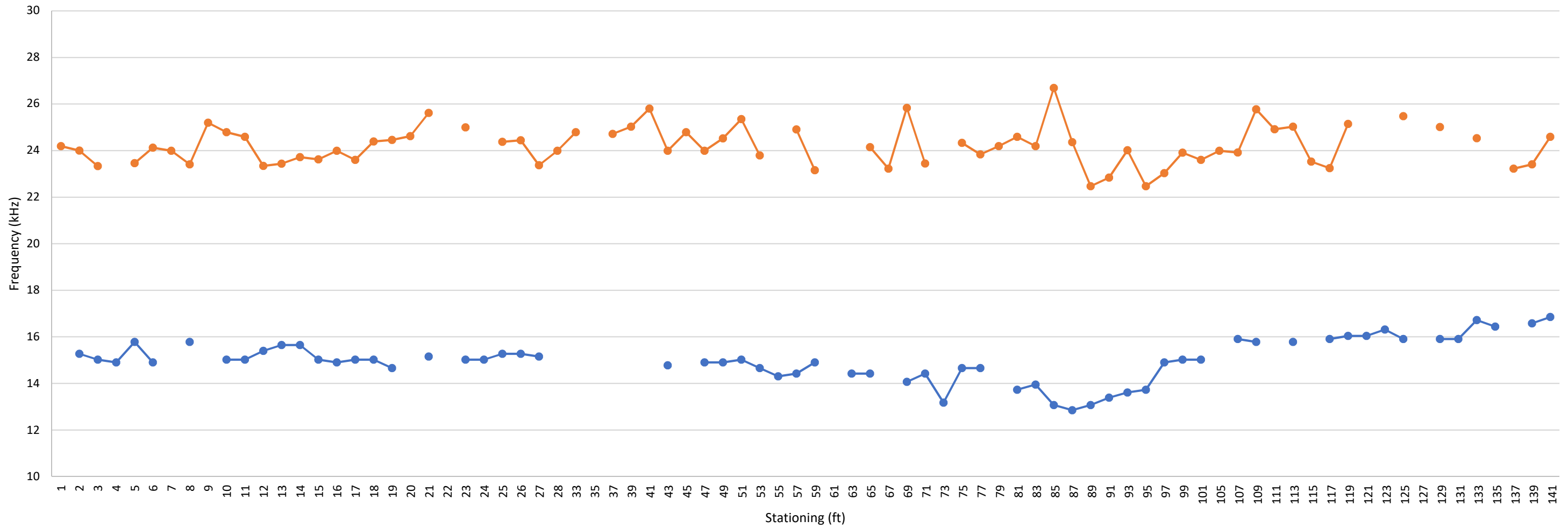
401L-6E



—●— Circumferential Frequency
 —●— Average Through Frequency
 ■ Anomalous Grout Condition

Nondestructive Testing External Tendon Ducts John Ringling Causeway Bridge Over Sarasota Bay Sarasota, Florida Prepared for Florida International University by NDT Corporation		Span 7 Tendon 401L-6E Graph Results	
January. 2018		Figure A49	

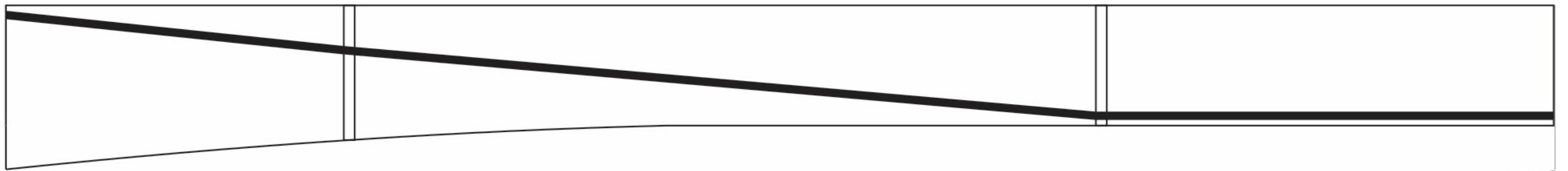
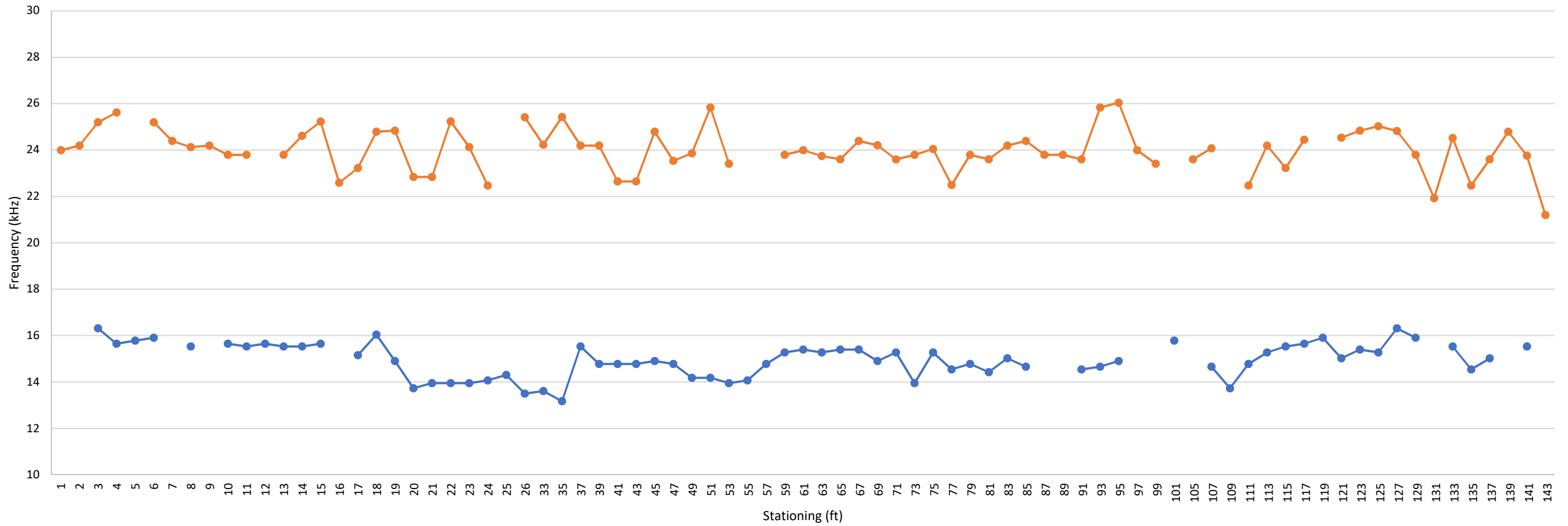
401R-6E



—●— Circumferential Frequency
 —●— Average Through Frequency
 ■ Anomalous Grout Condition

Nondestructive Testing External Tendon Ducts John Ringling Causeway Bridge Over Sarasota Bay Sarasota, Florida Prepared for Florida International University by NDT Corporation		Span 7 Tendon 401R-6E Graph Results	
January. 2018		Figure A50	

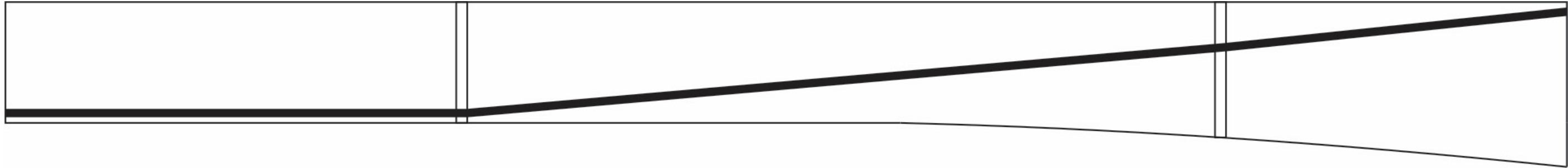
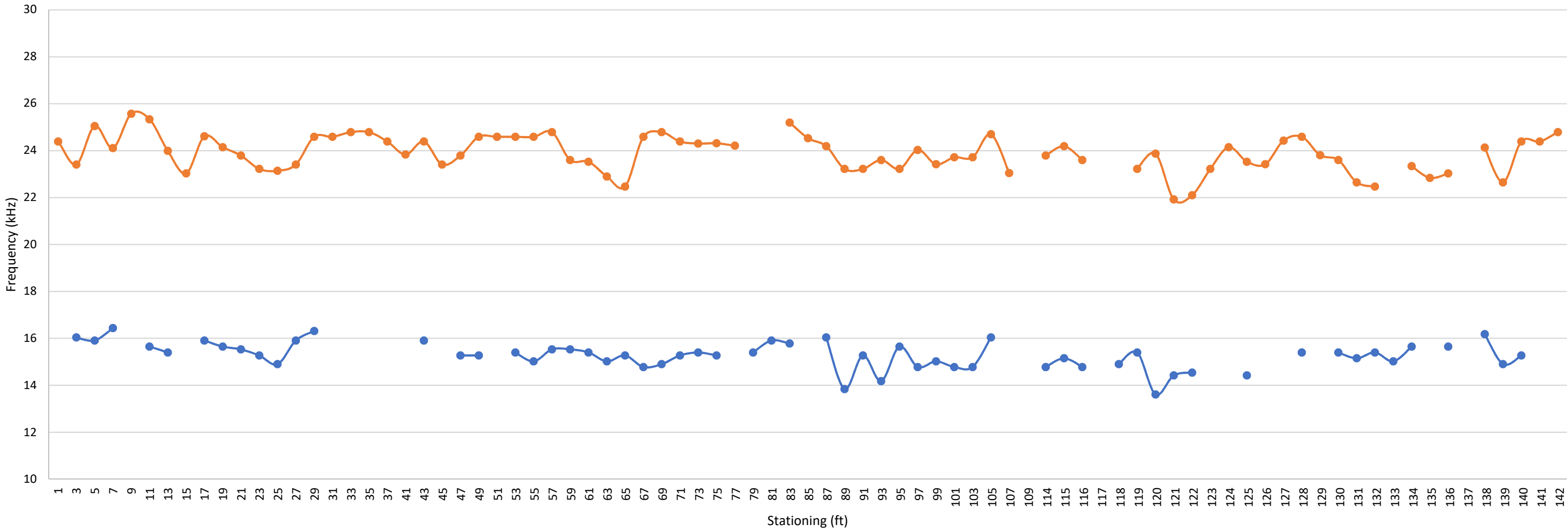
402R-6E



● Circumferential Frequency
 ● Average Through Frequency
 ■ Anomalous Grout Condition

Nondestructive Testing External Tendon Ducts John Ringling Causeway Bridge Over Sarasota Bay Sarasota, Florida Prepared for Florida International University by NDT Corporation		Span 7 Tendon 402R-6E Graph Results	
January. 2018		Figure A51	

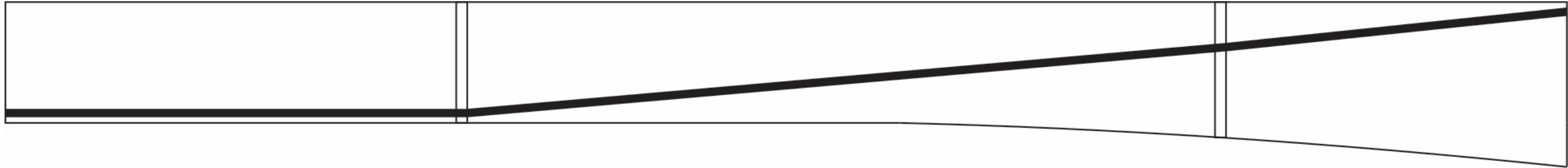
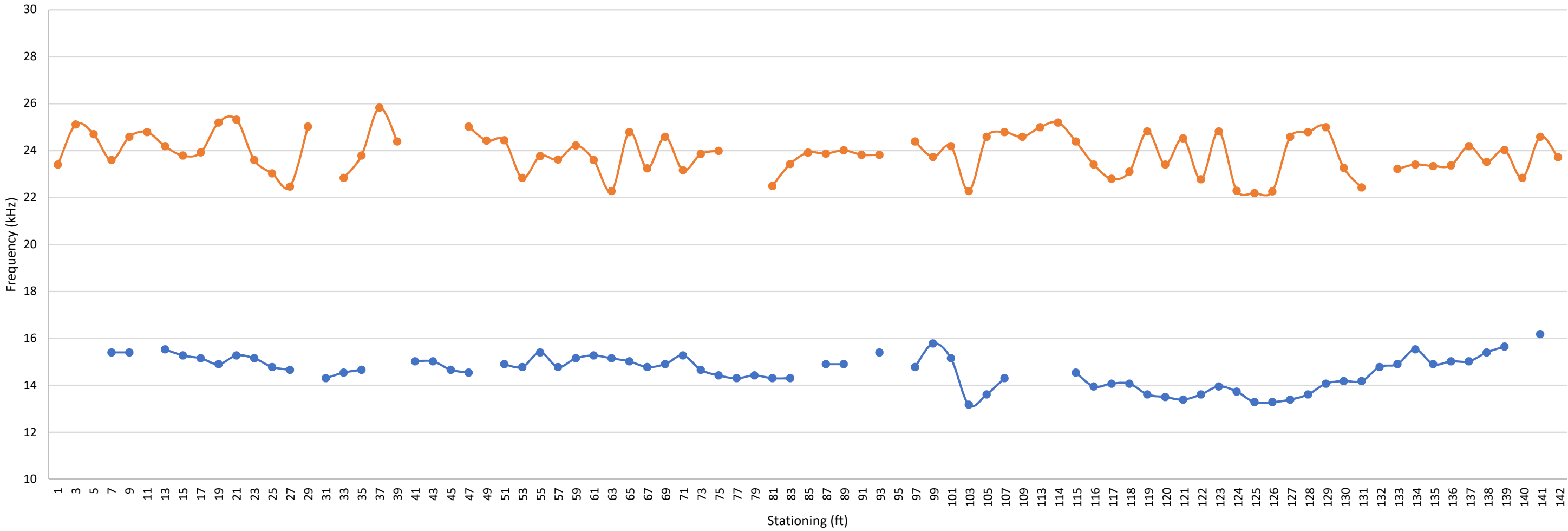
402L-7W



—●— Circumferential Frequency
 —●— Average Through Frequency
 ■ Anomalous Grout Condition

Nondestructive Testing External Tendon Ducts John Ringling Causeway Bridge Over Sarasota Bay Sarasota, Florida Prepared for Florida International University by NDT Corporation		Span 7 Tendon 402L-7W Graph Results	
January. 2018		Figure A52	

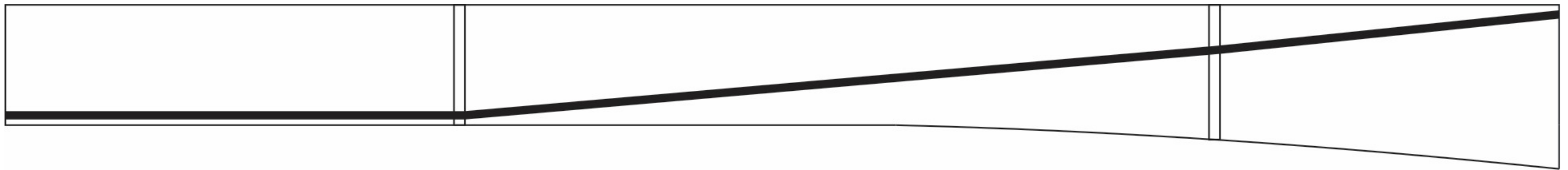
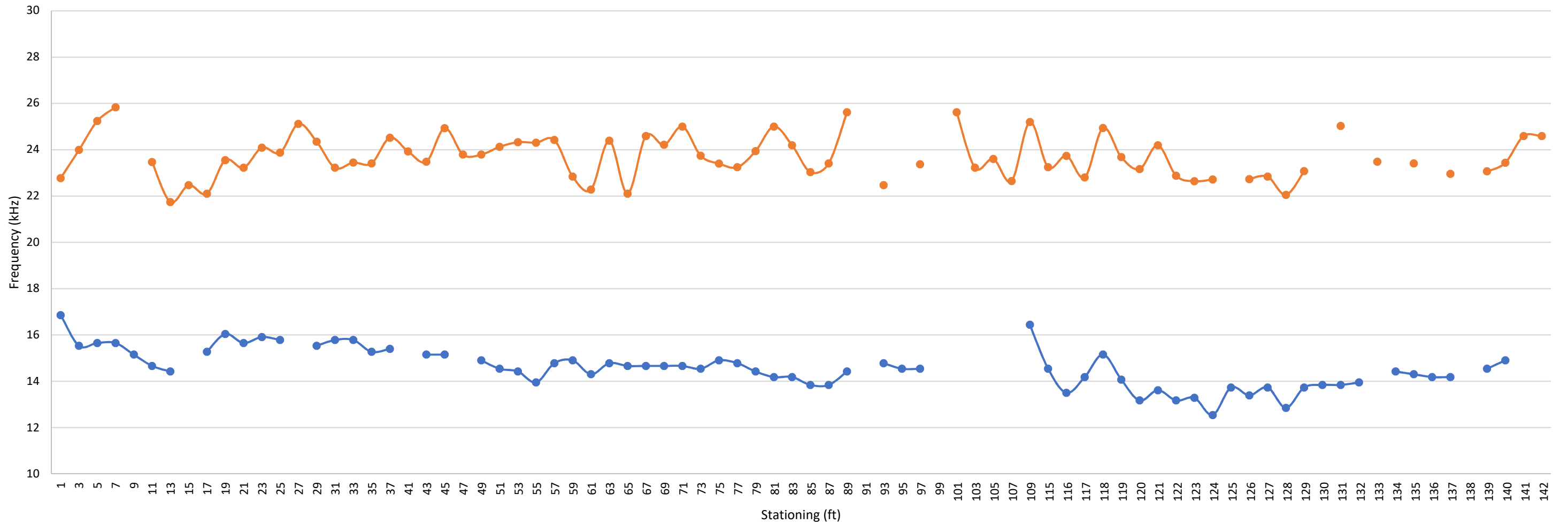
401L-7W



—●— Circumferential Frequency
 —●— Average Through Frequency
 ■ Anomalous Grout Condition

Nondestructive Testing External Tendon Ducts John Ringling Causeway Bridge Over Sarasota Bay Sarasota, Florida Prepared for Florida International University by NDT Corporation		Span 7 Tendon 401L-7W Graph Results	
January. 2018		Figure A53	

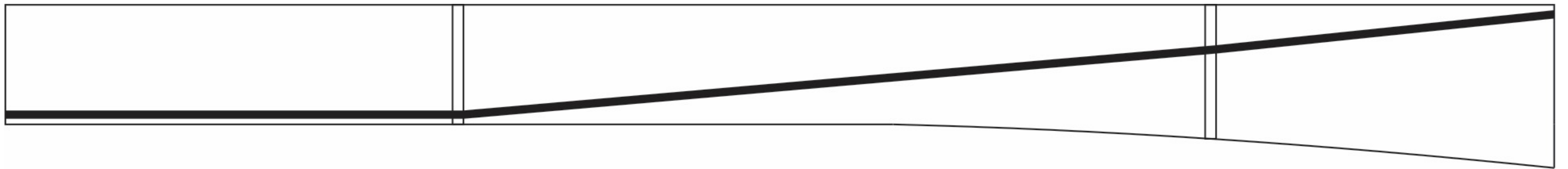
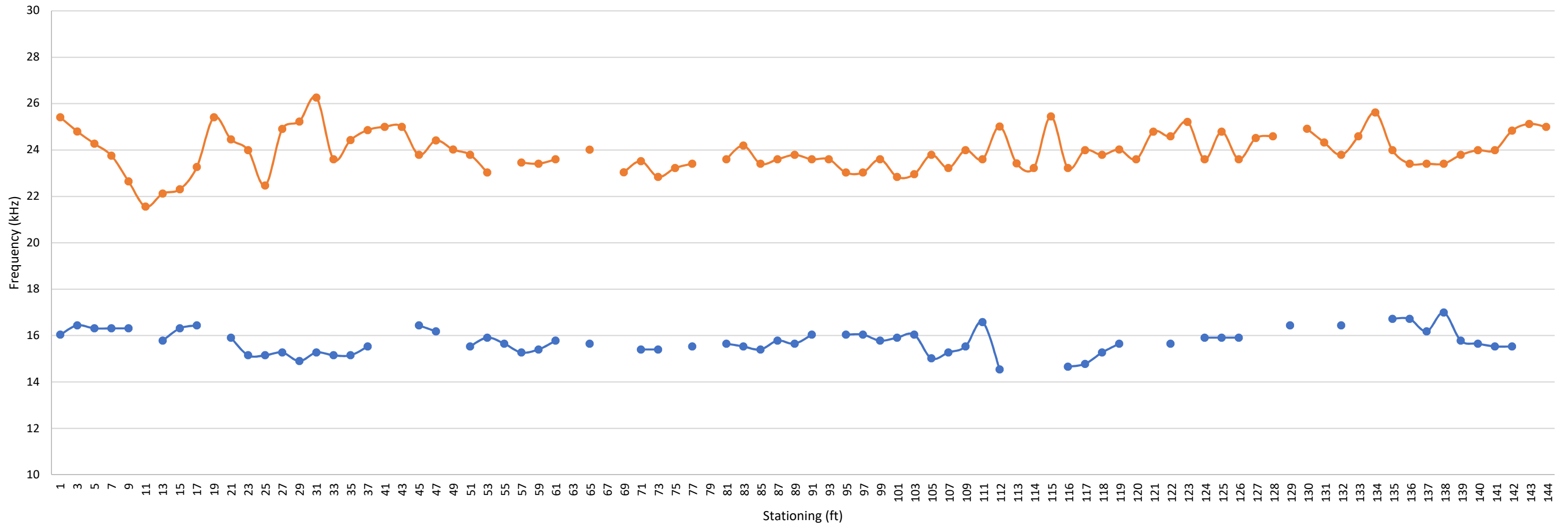
401R-7W



—●— Circumferential Frequency —●— Average Through Frequency ■ Anomalous Grout Condition

Nondestructive Testing External Tendon Ducts John Ringling Causeway Bridge Over Sarasota Bay Sarasota, Florida Prepared for Florida International University by NDT Corporation		Span 7 Tendon 401R-7W Graph Results	
		January. 2018	Figure A54

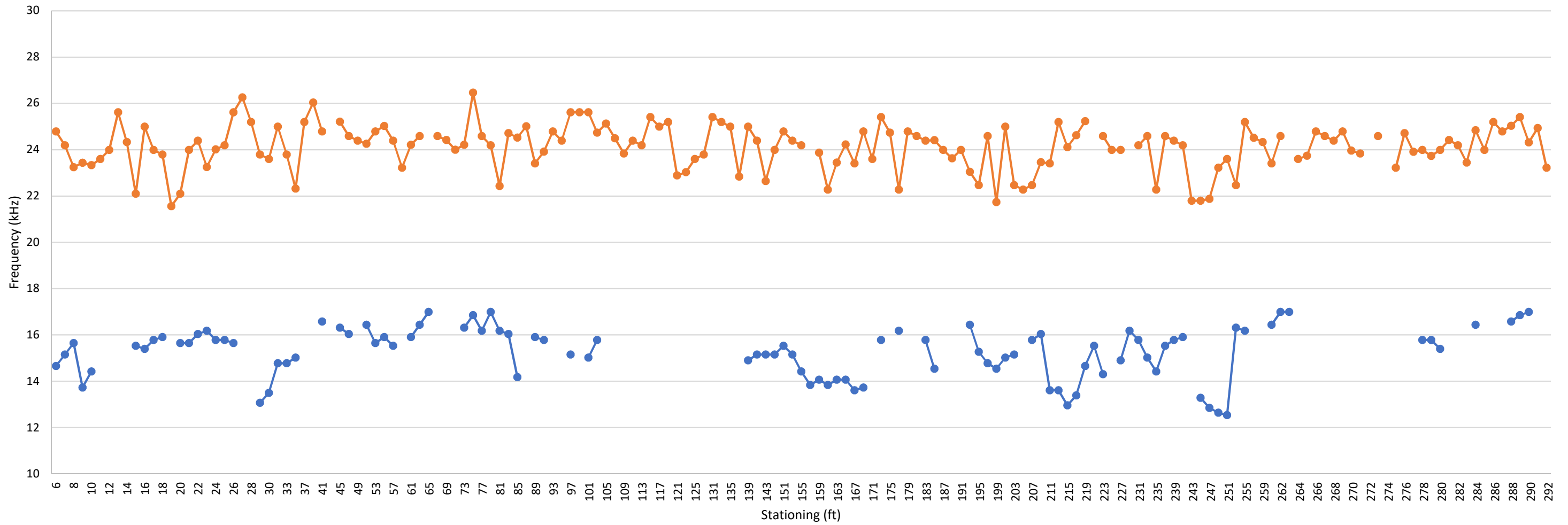
402R-7W



—●— Circumferential Frequency —●— Average Through Frequency ■ Anomalous Grout Condition

Nondestructive Testing External Tendon Ducts John Ringling Causeway Bridge Over Sarasota Bay Sarasota, Florida Prepared for Florida International University by NDT Corporation		Span 7 Tendon 402R-7W Graph Results	
		January. 2018	Figure A55

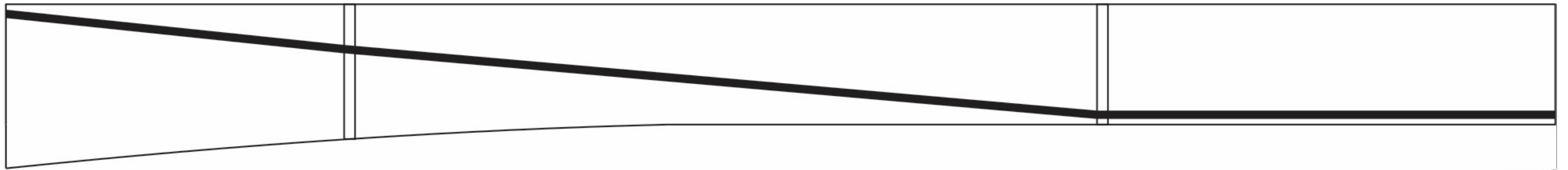
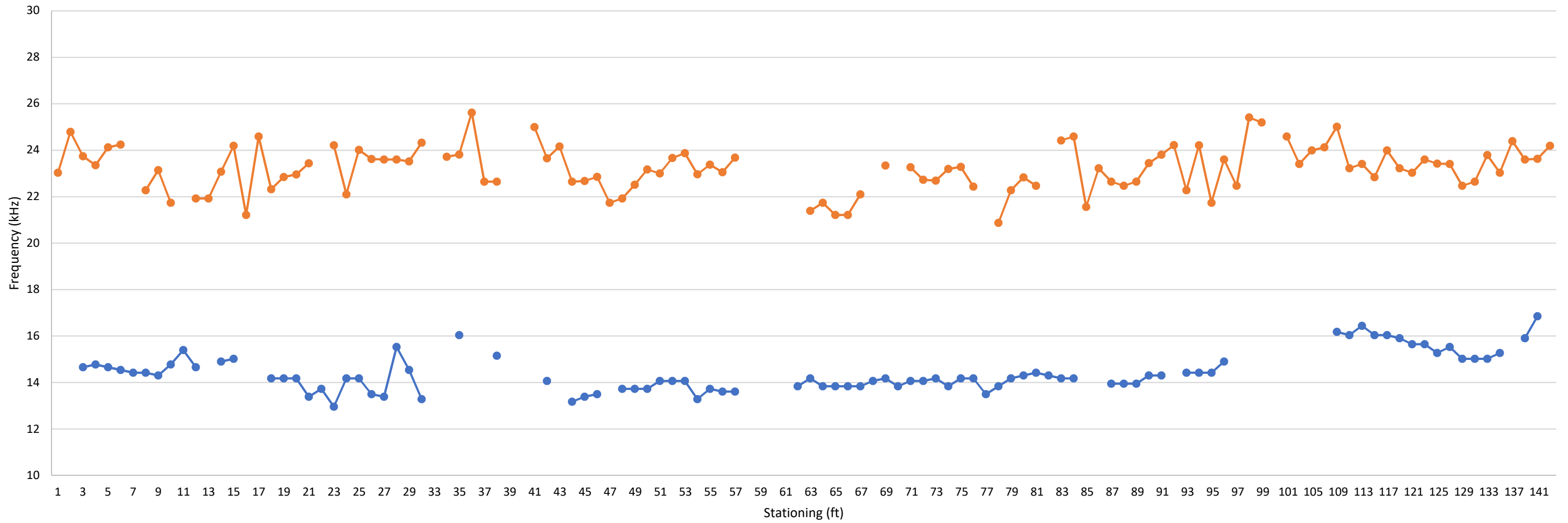
303R-6E



—●— Circumferential Frequency
 —●— Average Through Frequency
 ■ Anomalous Grout Condition

Nondestructive Testing External Tendon Ducts John Ringling Causeway Bridge Over Sarasota Bay Sarasota, Florida Prepared for Florida International University by NDT Corporation		Span 7 Tendon 303R-6E Graph Results	
January. 2018		Figure A56	

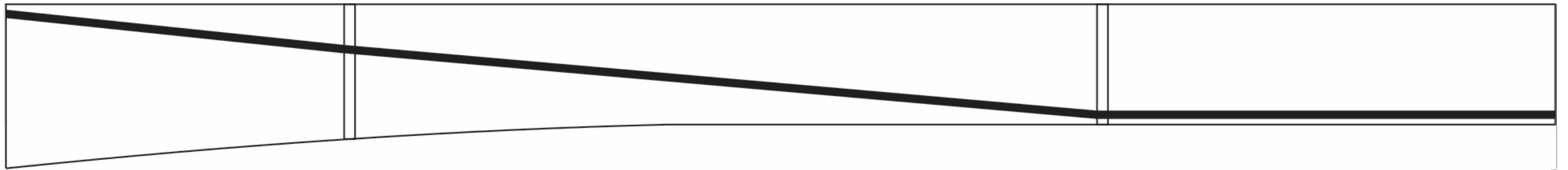
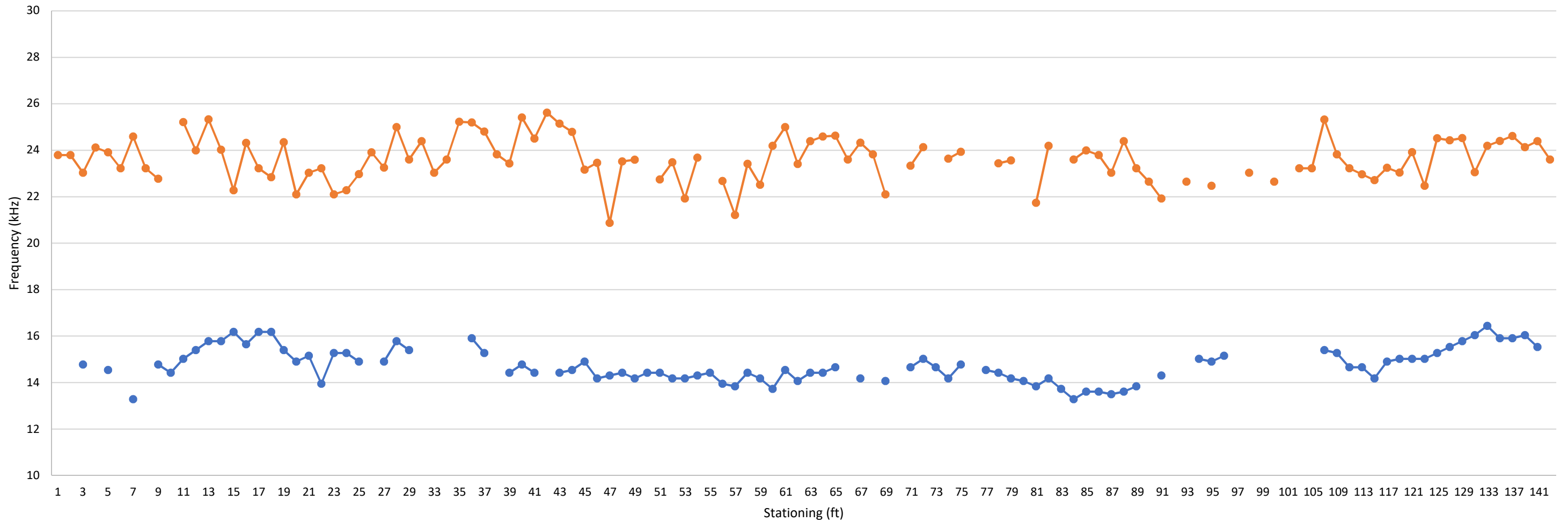
402L-7E



—●— Circumferential Frequency
 —●— Average Through Frequency
 ■ Anomalous Grout Condition

Nondestructive Testing External Tendon Ducts John Ringling Causeway Bridge Over Sarasota Bay Sarasota, Florida Prepared for Florida International University by NDT Corporation		Span 8 Tendon 402L-7E Graph Results	
		January. 2018	Figure A57

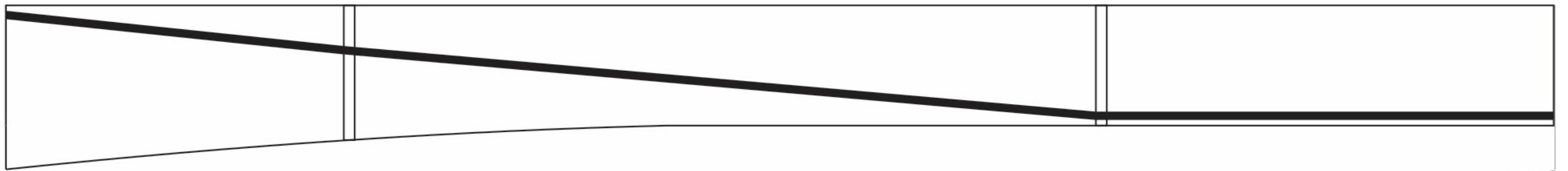
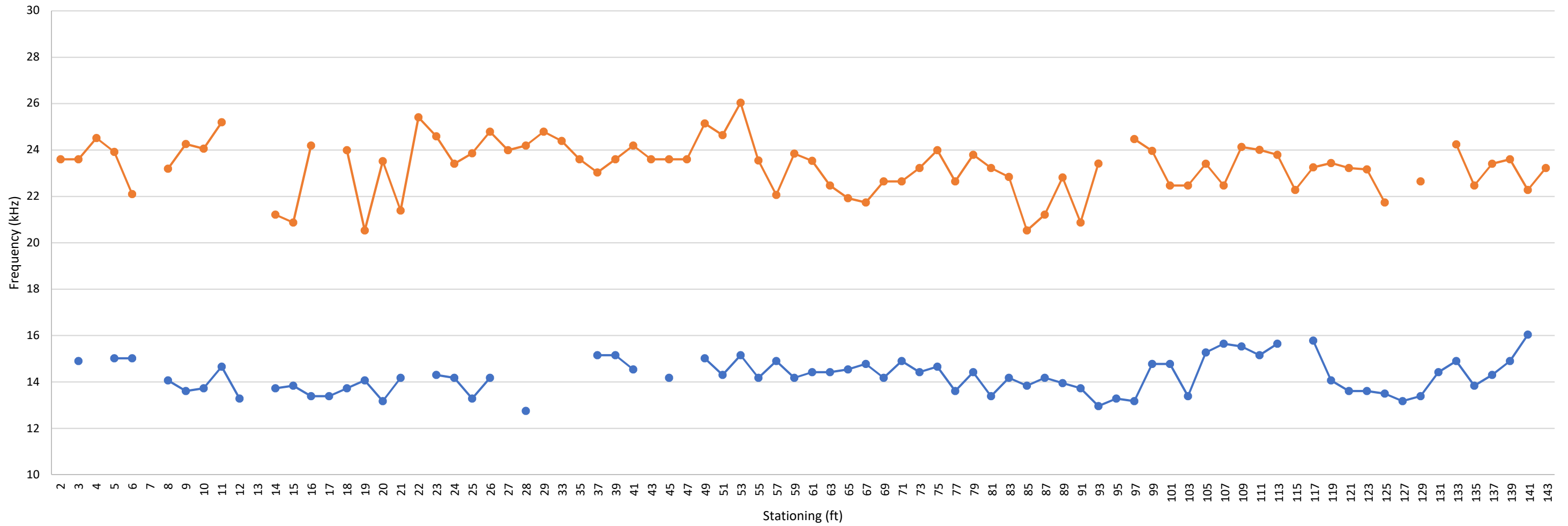
401L-7E



—●— Circumferential Frequency
 —●— Average Through Frequency
 ■ Anomalous Grout Condition

Nondestructive Testing External Tendon Ducts John Ringling Causeway Bridge Over Sarasota Bay Sarasota, Florida Prepared for Florida International University by NDT Corporation		Span 8 Tendon 401L-7E Graph Results	
January. 2018		Figure A58	

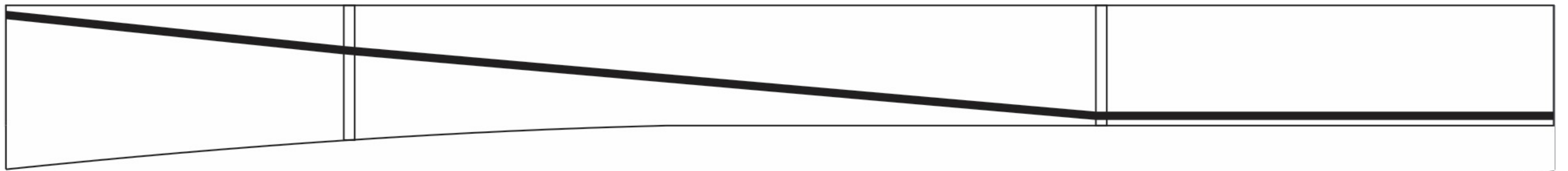
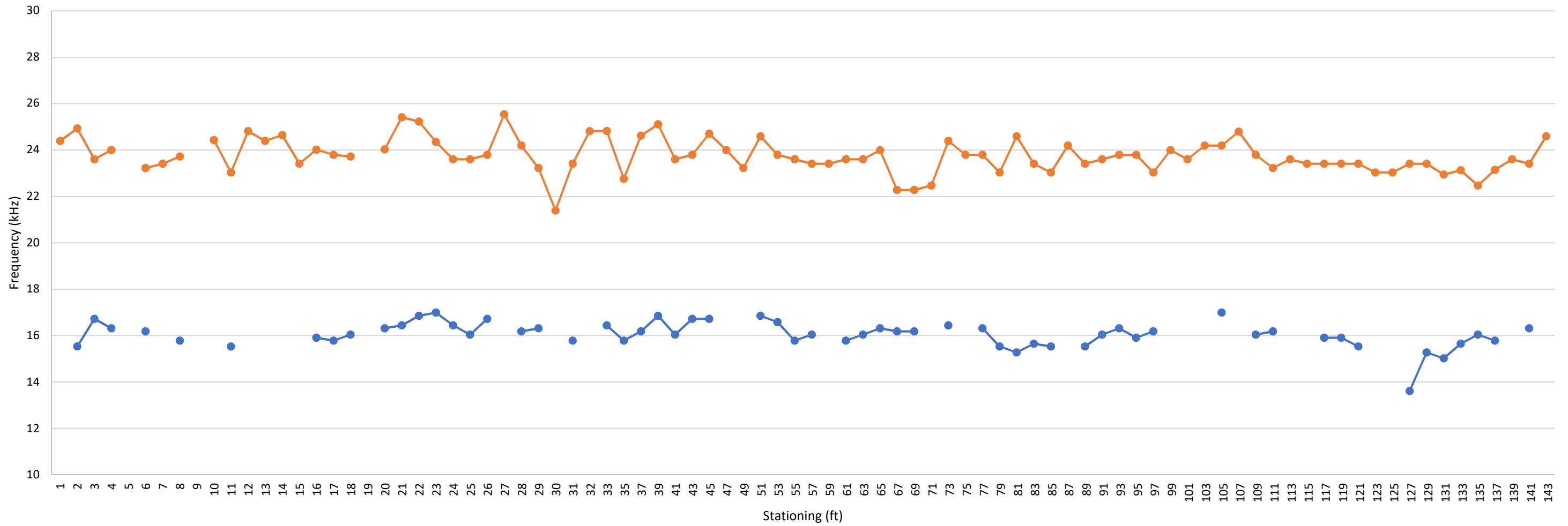
401R-7E



● Circumferential Frequency
 ● Average Through Frequency
 ■ Anomalous Grout Condition

Nondestructive Testing External Tendon Ducts John Ringling Causeway Bridge Over Sarasota Bay Sarasota, Florida Prepared for Florida International University by NDT Corporation		Span 8 Tendon 401R-7E Graph Results	
January. 2018		Figure A59	

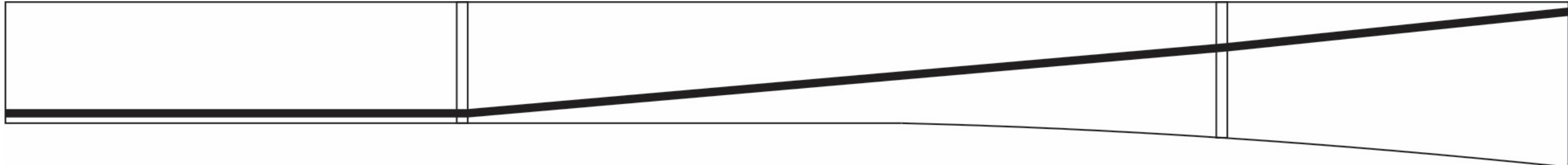
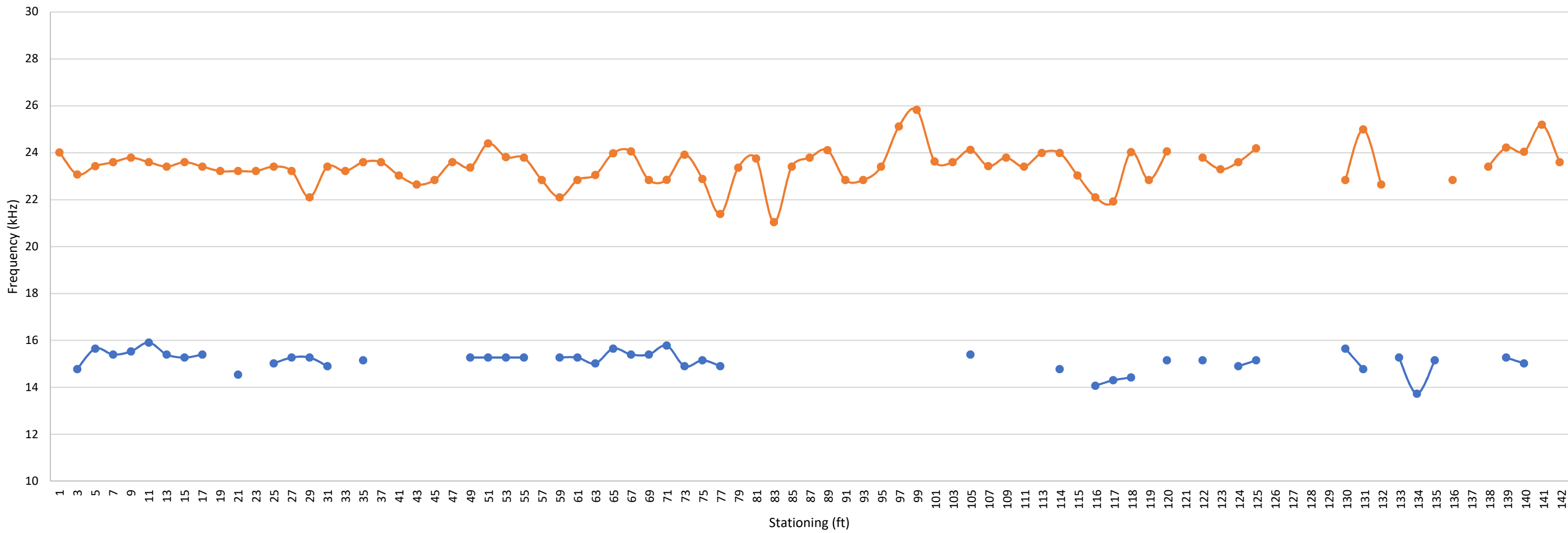
402R-7E



—●— Circumferential Frequency
 —●— Average Through Frequency
 ■ Anomalous Grout Condition

Nondestructive Testing External Tendon Ducts John Ringling Causeway Bridge Over Sarasota Bay Sarasota, Florida Prepared for Florida International University by NDT Corporation		Span 8 Tendon 402R-7E Graph Results	
		January. 2018	Figure A60

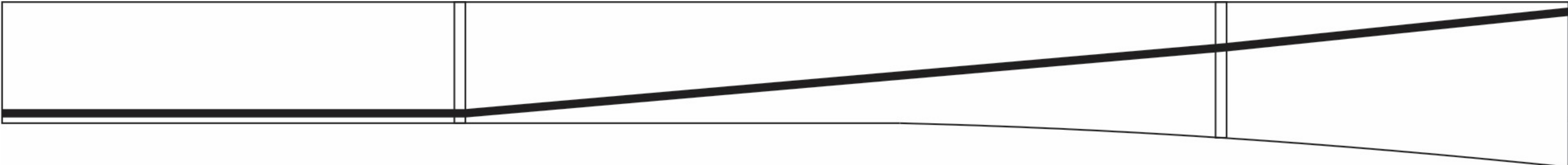
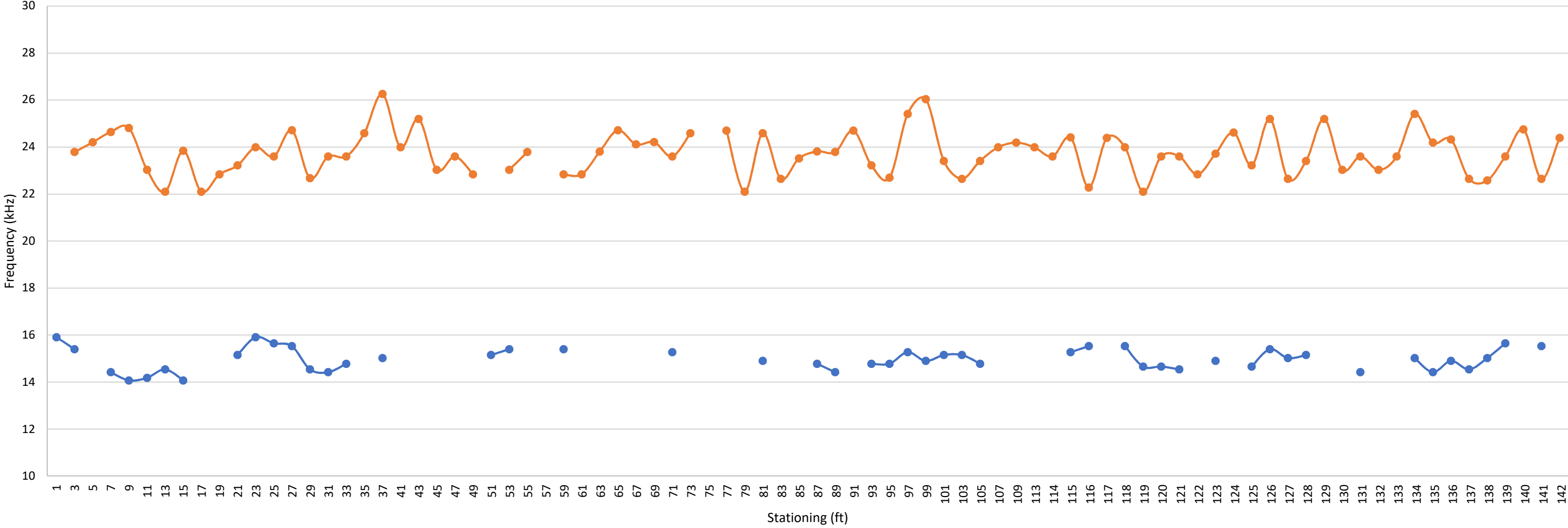
402L-8W



—●— Circumferential Frequency
 —●— Average Through Frequency
 ■ Anomalous Grout Condition

Nondestructive Testing External Tendon Ducts John Ringling Causeway Bridge Over Sarasota Bay Sarasota, Florida Prepared for Florida International University by NDT Corporation		Span 8 Tendon 402L-8W Graph Results	
January. 2018		Figure A61	

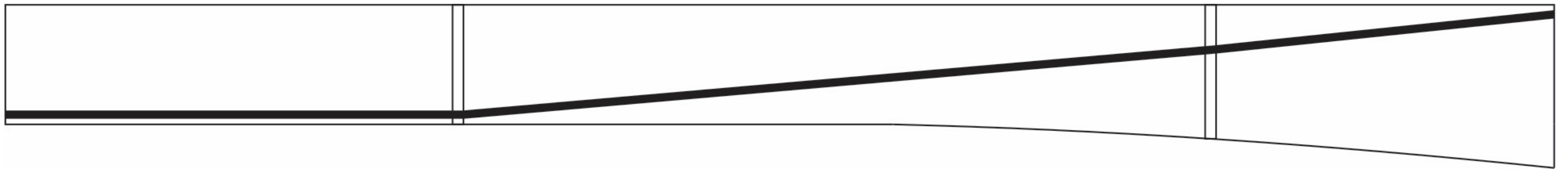
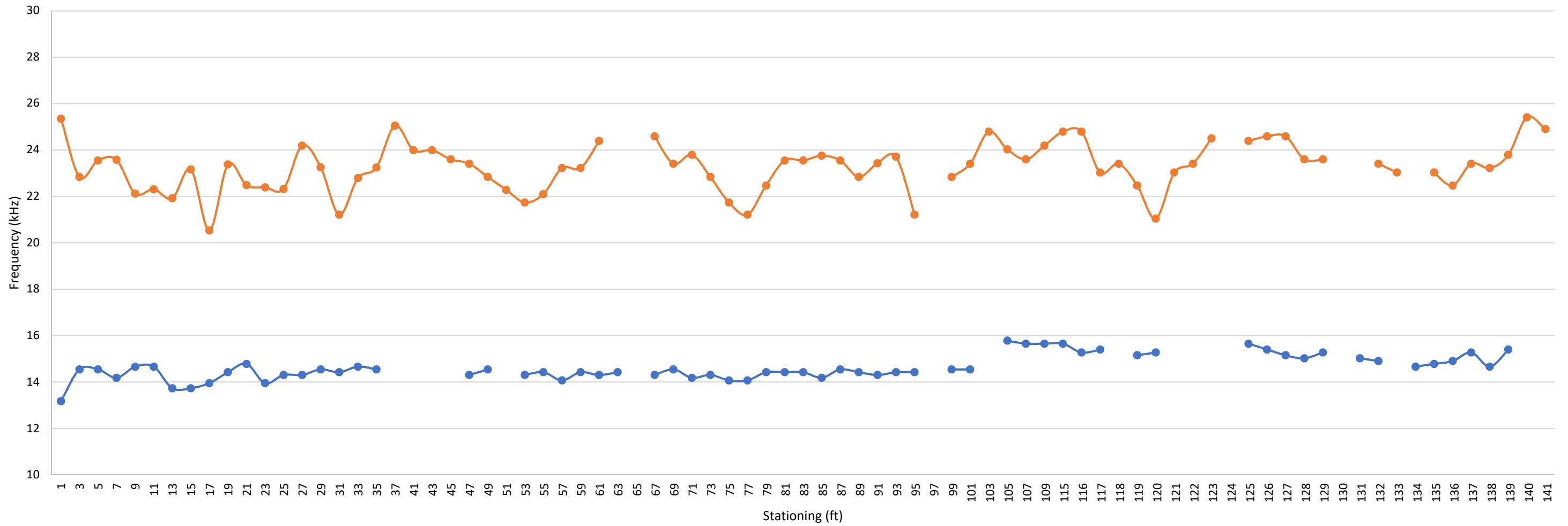
401L-8W



—●— Circumferential Frequency
 —●— Average Through Frequency
 ■ Anomalous Grout Condition

Nondestructive Testing External Tendon Ducts John Ringling Causeway Bridge Over Sarasota Bay Sarasota, Florida Prepared for Florida International University by NDT Corporation		Span 8 Tendon 401L-8W Graph Results	
January. 2018		Figure A62	

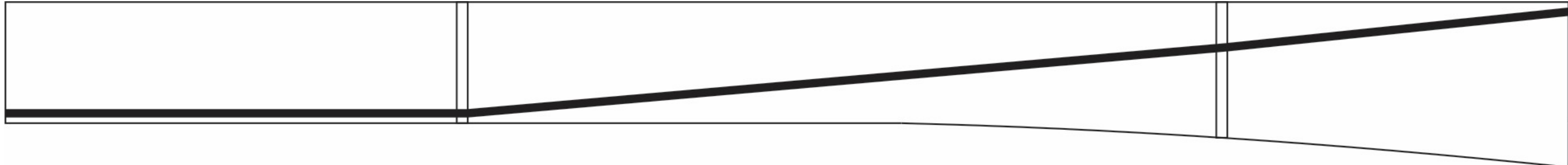
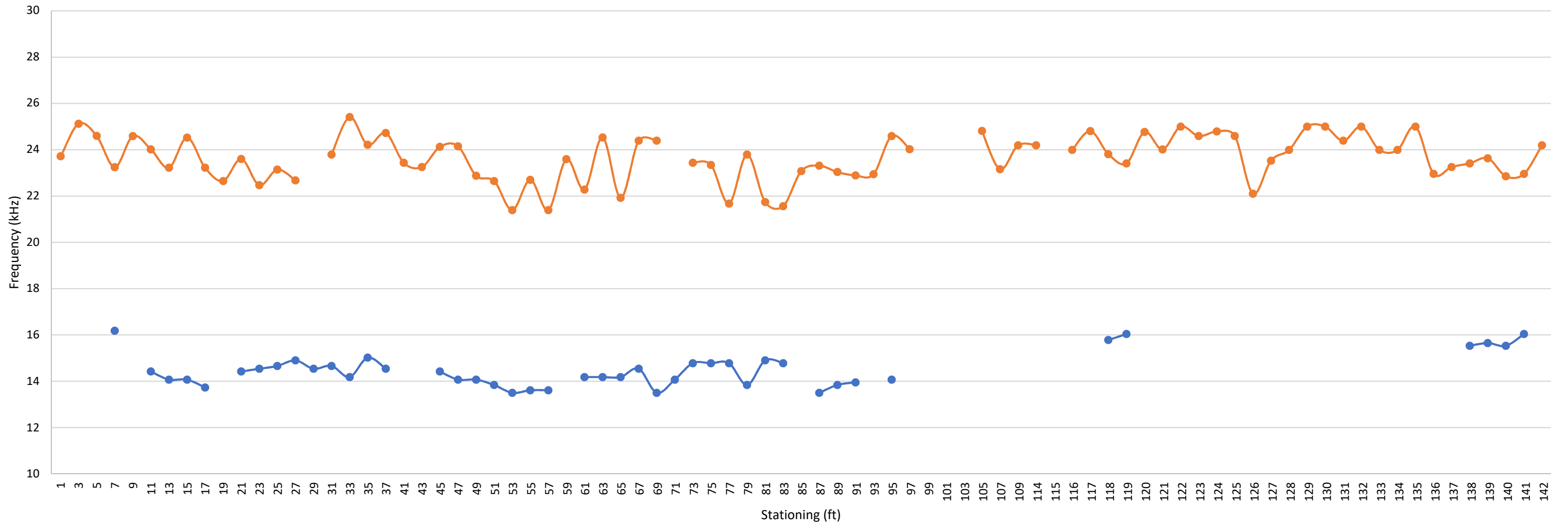
401R-8W



—●— Circumferential Frequency —●— Average Through Frequency ■ Anomalous Grout Condition

Nondestructive Testing External Tendon Ducts John Ringling Causeway Bridge Over Sarasota Bay Sarasota, Florida Prepared for Florida International University by NDT Corporation		Span 8 Tendon 401R-8W Graph Results	
		January. 2018	Figure A63

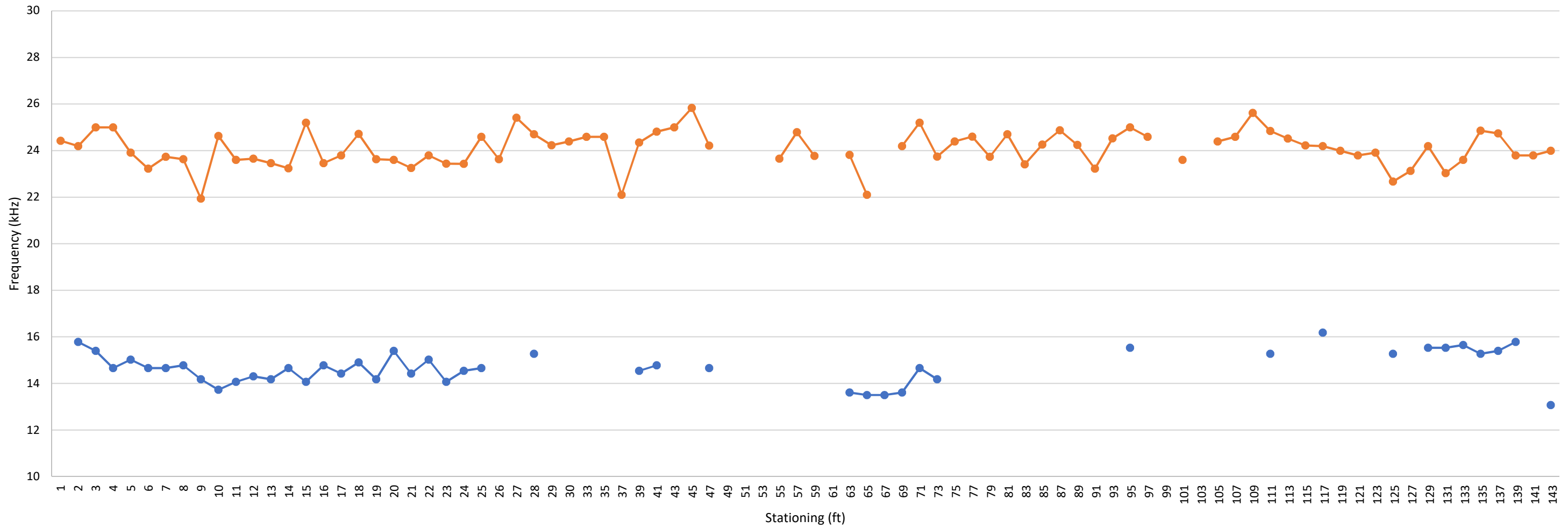
402R-8W



—●— Circumferential Frequency
 —●— Average Through Frequency
 ■ Anomalous Grout Condition

Nondestructive Testing External Tendon Ducts John Ringling Causeway Bridge Over Sarasota Bay Sarasota, Florida Prepared for Florida International University by NDT Corporation		Span 8 Tendon 402R-8W Graph Results	
January. 2018		Figure A64	

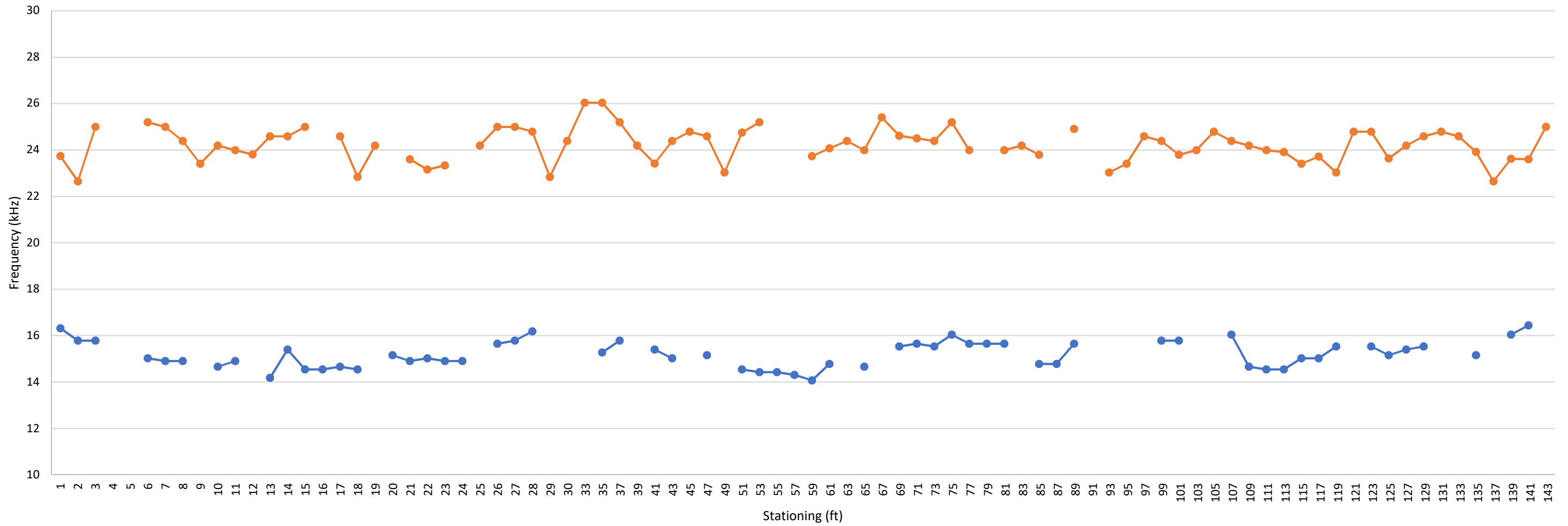
402L-8E



—●— Circumferential Frequency
 —●— Average Through Frequency
 ■ Anomalous Grout Condition

Nondestructive Testing External Tendon Ducts John Ringling Causeway Bridge Over Sarasota Bay Sarasota, Florida Prepared for Florida International University by NDT Corporation		Span 9 Tendon 402L-8E Graph Results	
January. 2018		Figure A65	

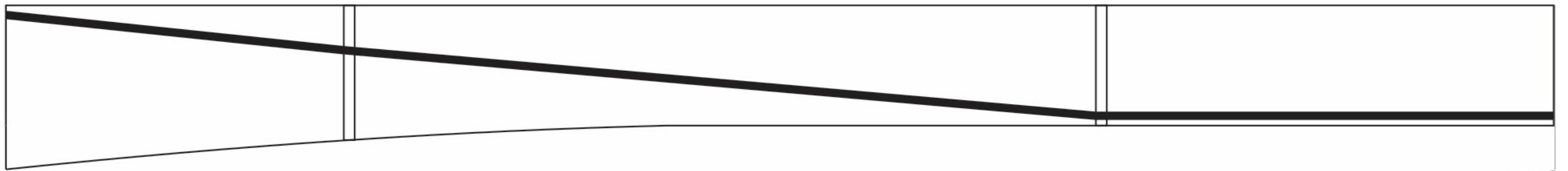
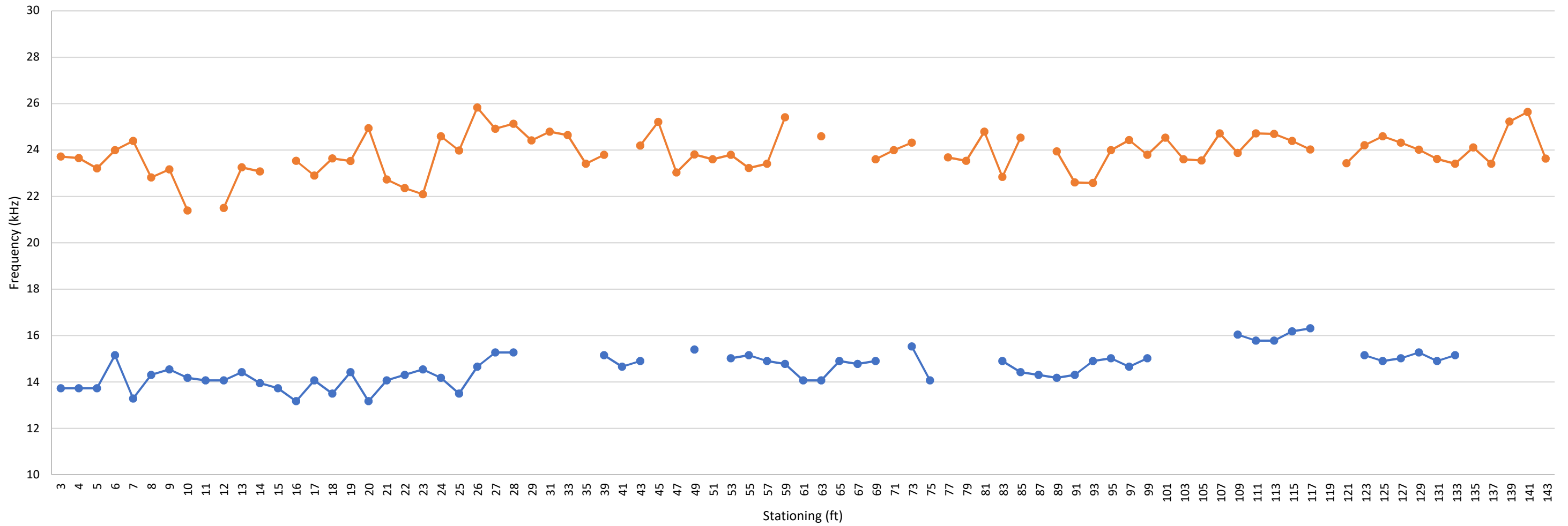
401L-8E



—●— Circumferential Frequency
 —●— Average Through Frequency
 ■ Anomalous Grout Condition

Nondestructive Testing External Tendon Ducts John Ringling Causeway Bridge Over Sarasota Bay Sarasota, Florida Prepared for Florida International University by NDT Corporation		Span 9 Tendon 401L-8E Graph Results	
January. 2018		Figure A66	

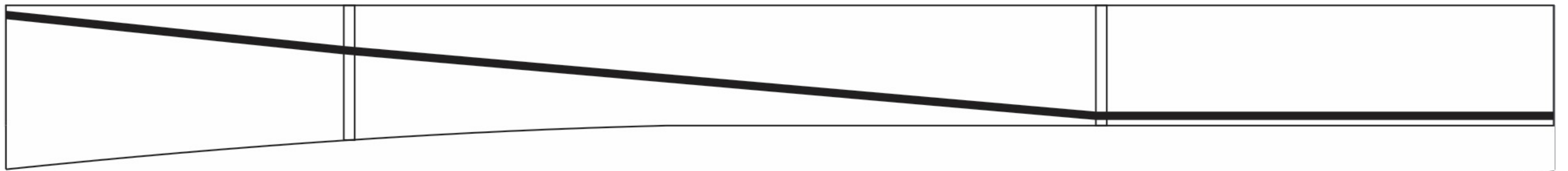
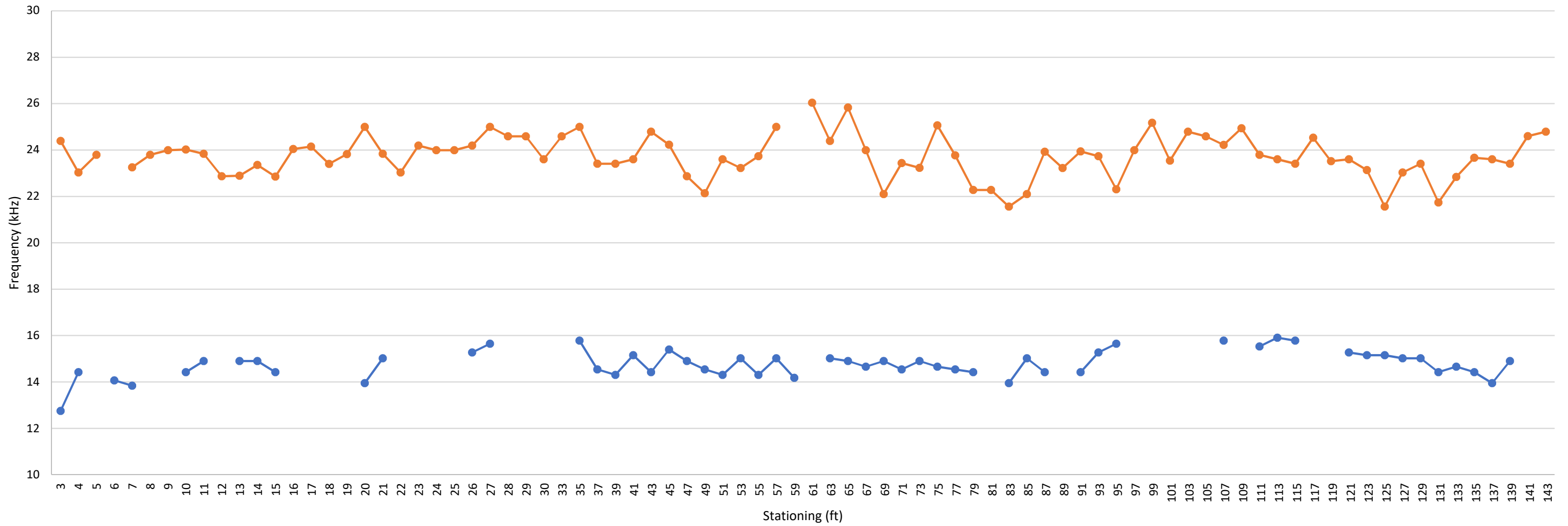
401R-8E



—●— Circumferential Frequency
 —●— Average Through Frequency
 ■ Anomalous Grout Condition

Nondestructive Testing External Tendon Ducts John Ringling Causeway Bridge Over Sarasota Bay Sarasota, Florida Prepared for Florida International University by NDT Corporation		Span 9 Tendon 401R-8E Graph Results	
January. 2018		Figure A67	

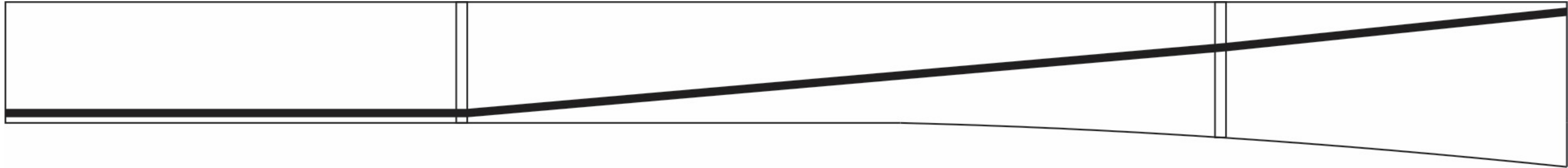
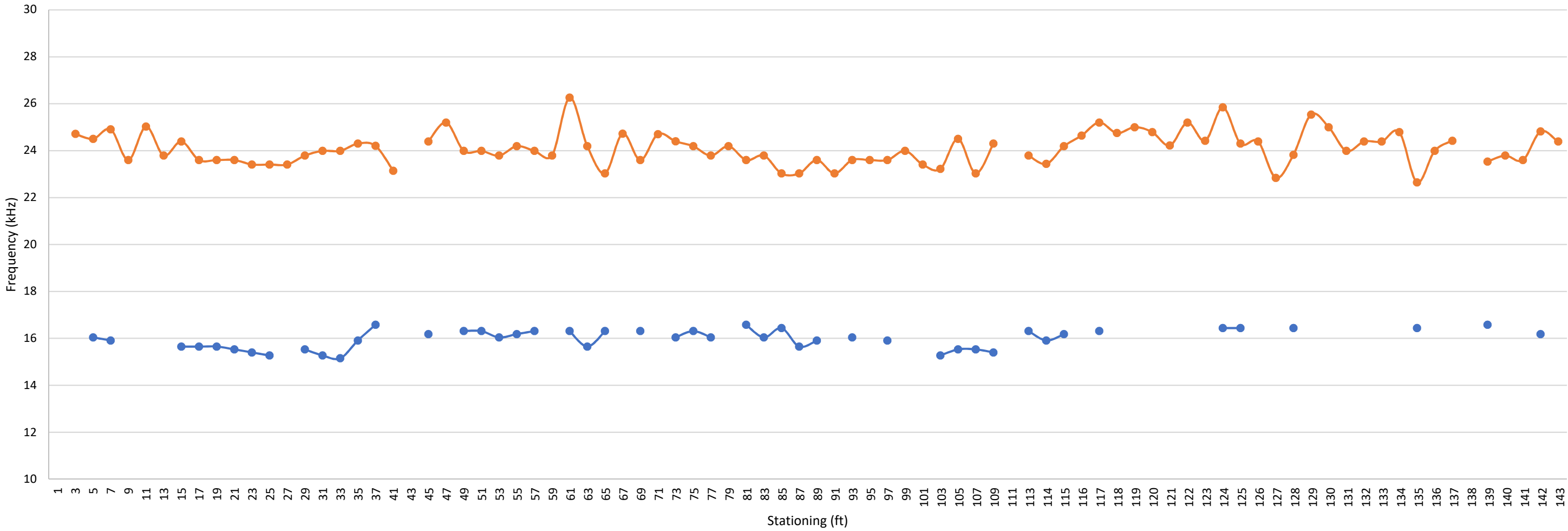
402R-8E



—●— Circumferential Frequency
 —●— Average Through Frequency
 ■ Anomalous Grout Condition

Nondestructive Testing External Tendon Ducts John Ringling Causeway Bridge Over Sarasota Bay Sarasota, Florida Prepared for Florida International University by NDT Corporation		Span 9 Tendon 402R-8E Graph Results	
January. 2018		Figure A68	

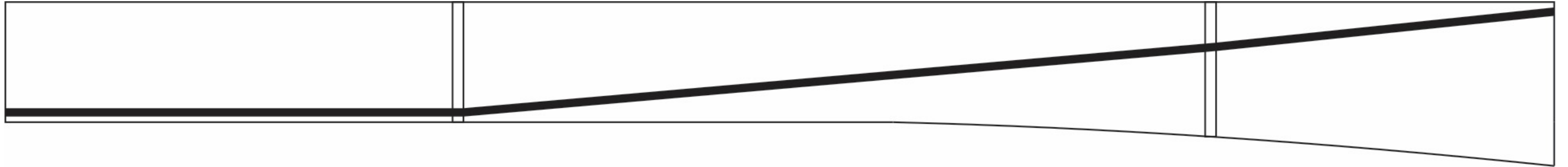
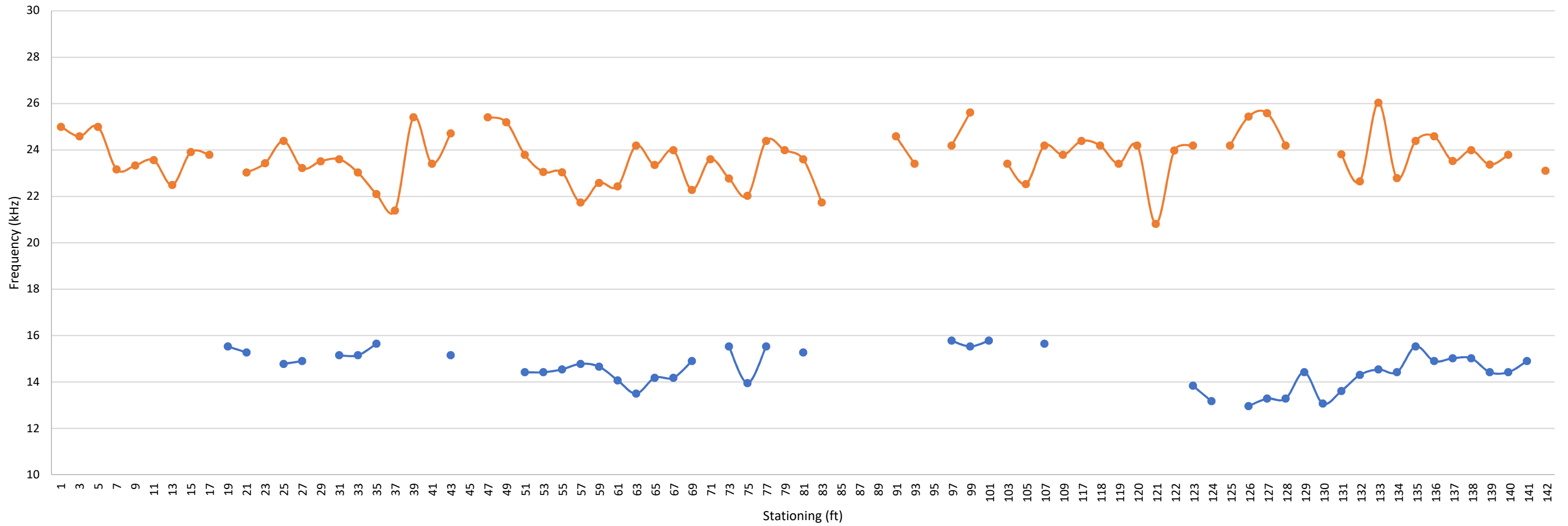
402L-9W



—●— Circumferential Frequency
 —●— Average Through Frequency
 ■ Anomalous Grout Condition

Nondestructive Testing External Tendon Ducts John Ringling Causeway Bridge Over Sarasota Bay Sarasota, Florida Prepared for Florida International University by NDT Corporation		Span 9 Tendon 402L-9W Graph Results	
January. 2018		Figure A69	

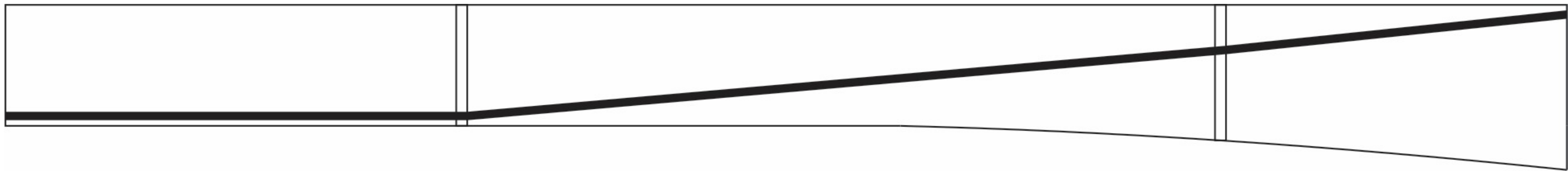
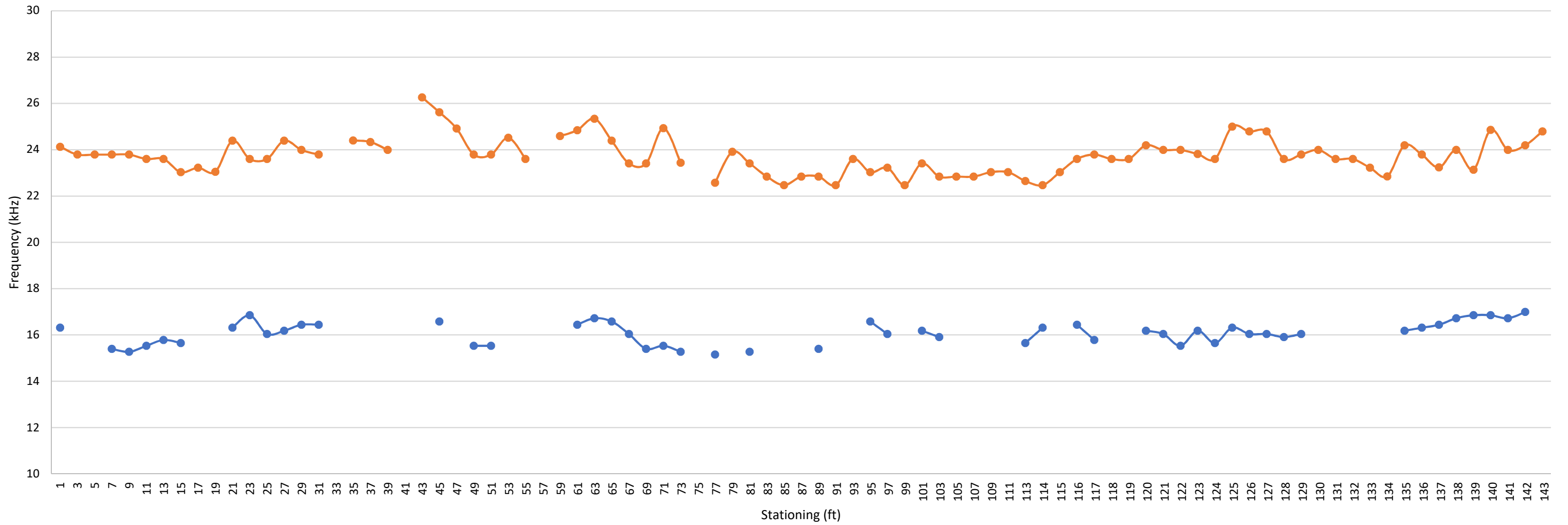
401L-9W



—●— Circumferential Frequency
 —●— Average Through Frequency
 ■ Anomalous Grout Condition

Nondestructive Testing External Tendon Ducts John Ringling Causeway Bridge Over Sarasota Bay Sarasota, Florida Prepared for Florida International University by NDT Corporation		Span 9 Tendon 401L-9W Graph Results	
January. 2018		Figure A70	

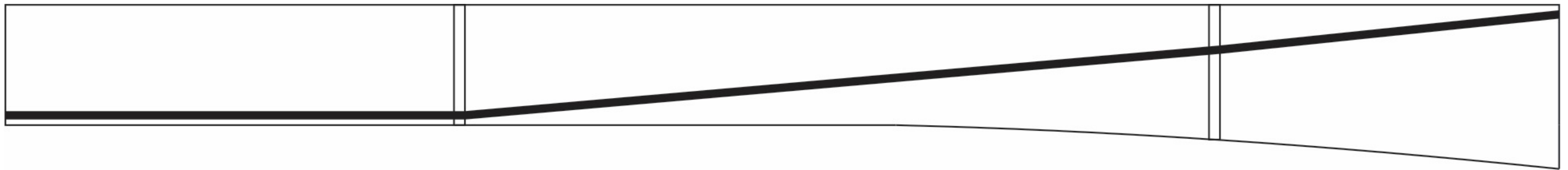
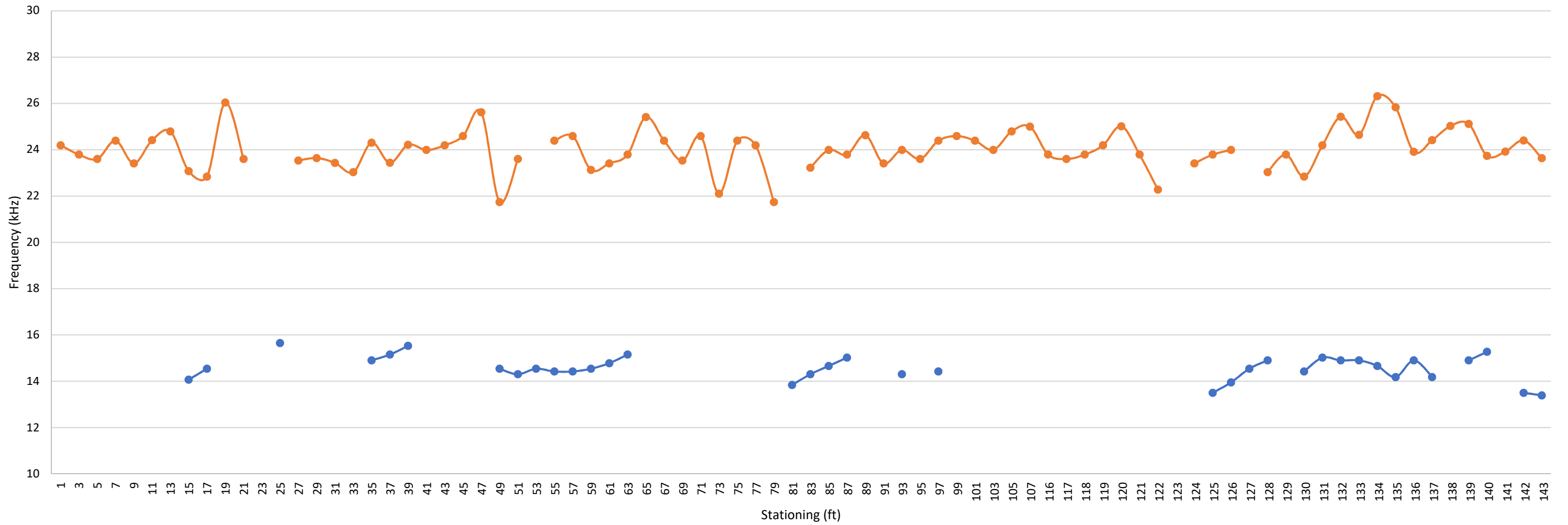
401R-9W



—●— Circumferential Frequency
 —●— Average Through Frequency
 ■ Anomalous Grout Condition

Nondestructive Testing External Tendon Ducts John Ringling Causeway Bridge Over Sarasota Bay Sarasota, Florida Prepared for Florida International University by NDT Corporation		Span 9 Tendon 401R-9W Graph Results	
January. 2018		Figure A71	

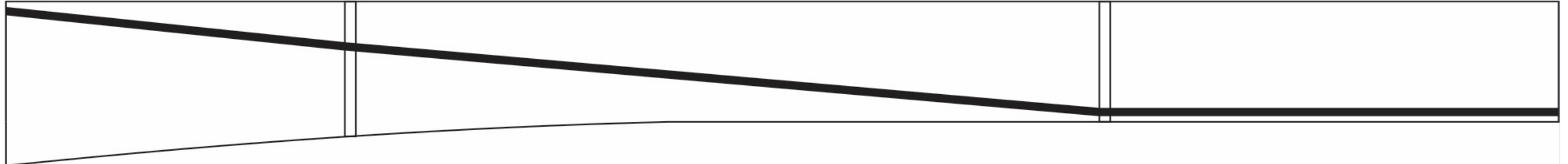
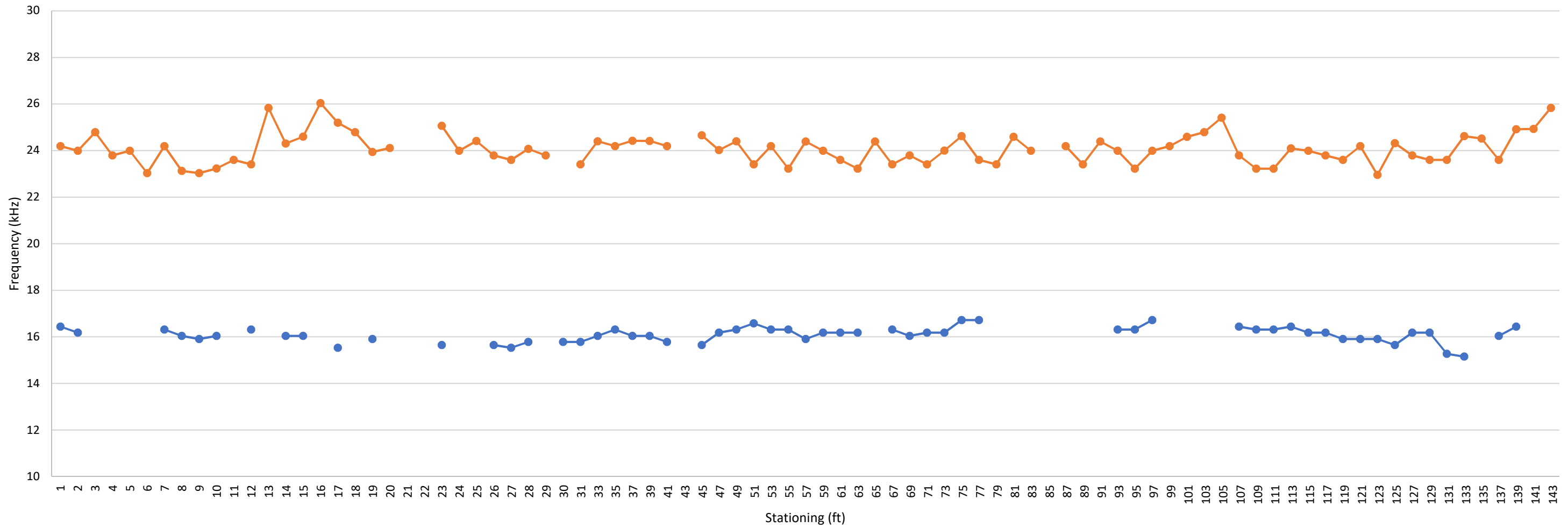
402R-9W



—●— Circumferential Frequency
 —●— Average Through Frequency
 ■ Anomalous Grout Condition

Nondestructive Testing External Tendon Ducts John Ringling Causeway Bridge Over Sarasota Bay Sarasota, Florida Prepared for Florida International University by NDT Corporation		Span 9 Tendon 402R-9W Graph Results	
January. 2018		Figure A72	

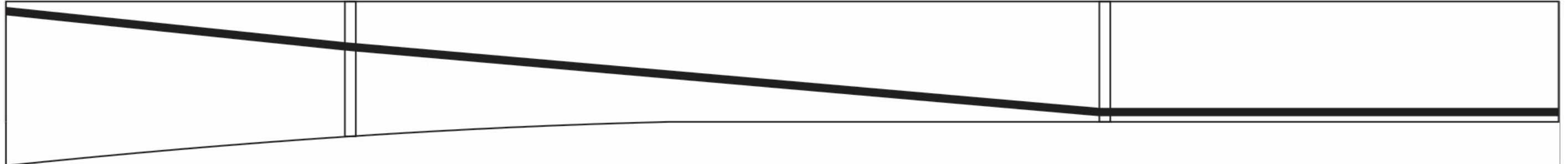
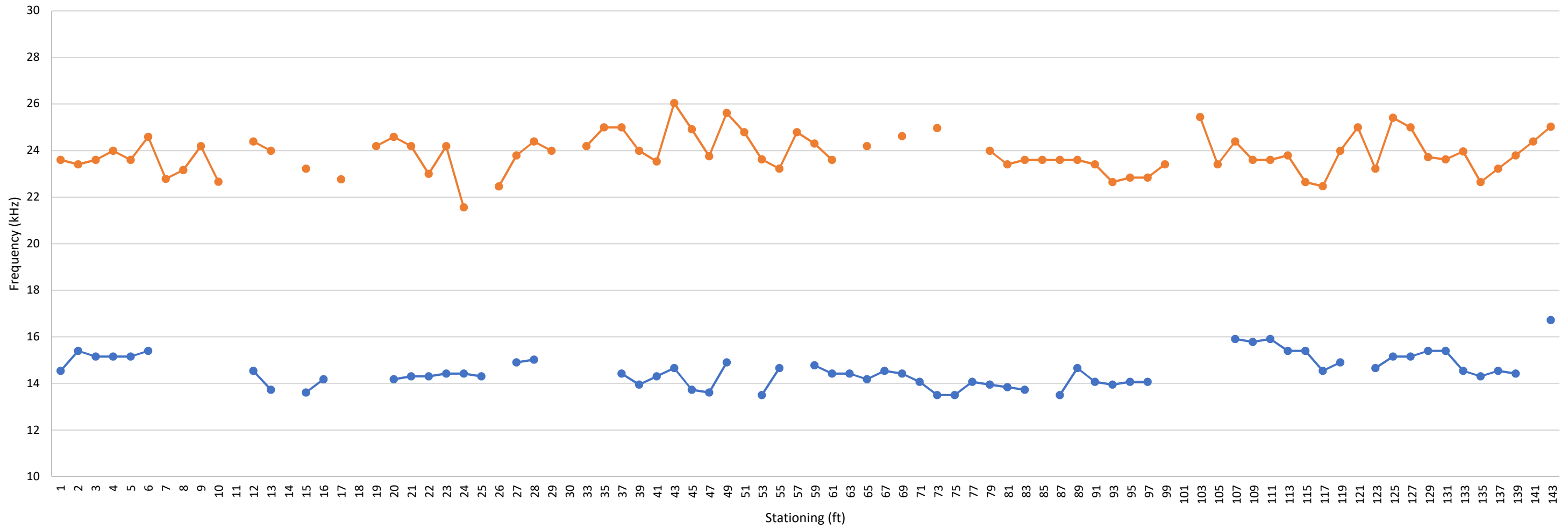
402L-9E



● Circumferential Frequency
 ● Average Through Frequency
 ■ Anomalous Grout Condition

Nondestructive Testing External Tendon Ducts John Ringling Causeway Bridge Over Sarasota Bay Sarasota, Florida Prepared for Florida International University by NDT Corporation		Span 10 Tendon 402L-9E Graph Results	
January. 2018		Figure A73	

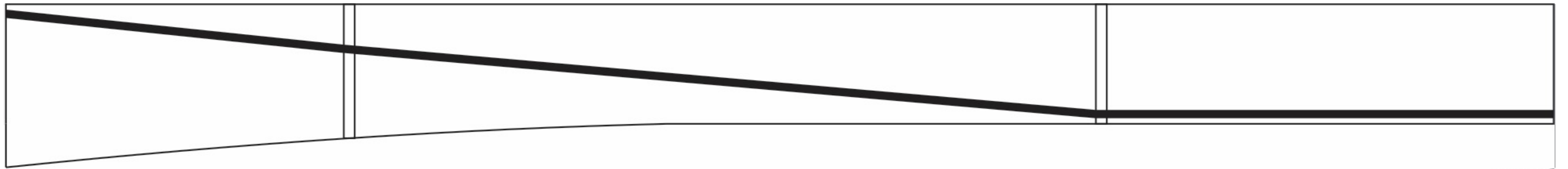
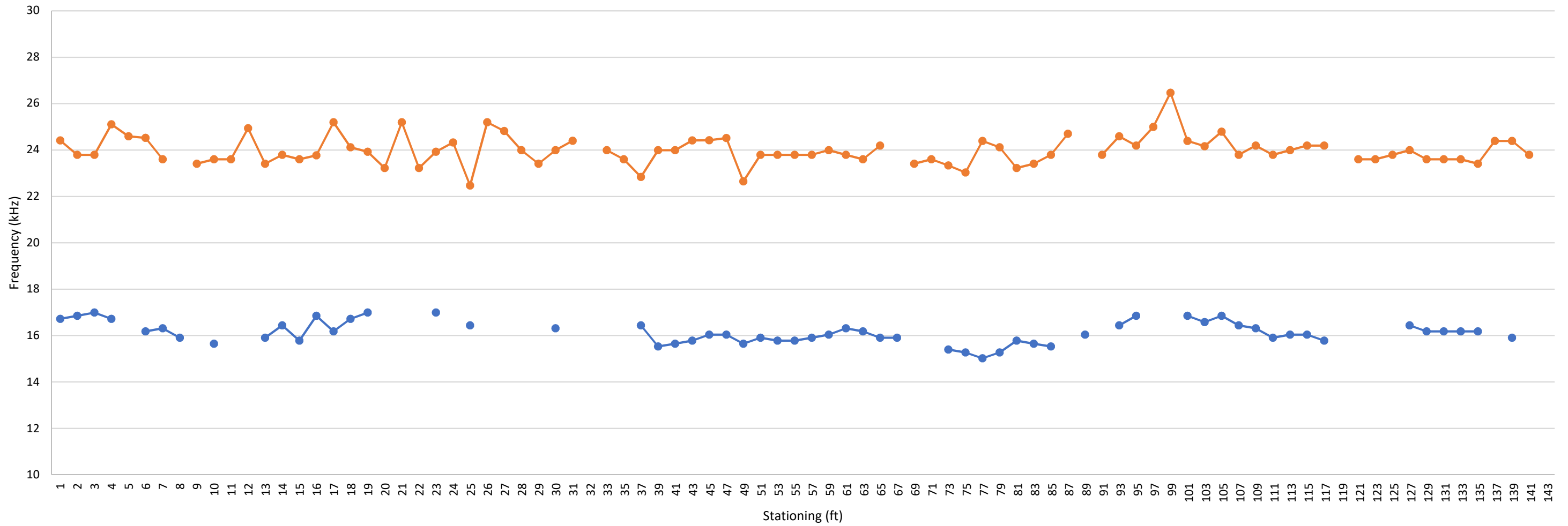
401L-9E



—●— Circumferential Frequency
 —●— Average Through Frequency
 ■ Anomalous Grout Condition

Nondestructive Testing External Tendon Ducts John Ringling Causeway Bridge Over Sarasota Bay Sarasota, Florida Prepared for Florida International University by NDT Corporation		Span 10 Tendon 401L-9E Graph Results	
January. 2018		Figure A74	

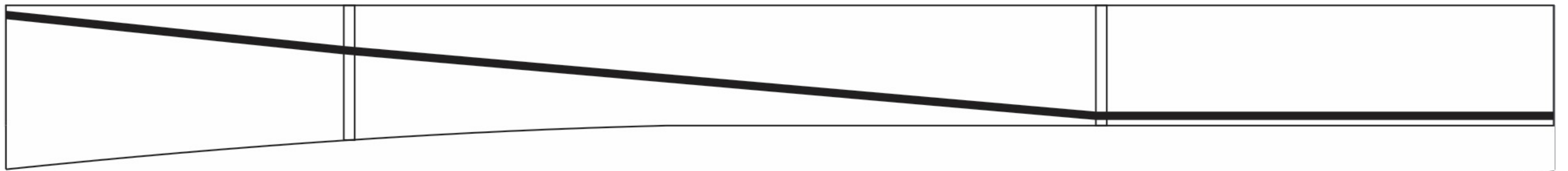
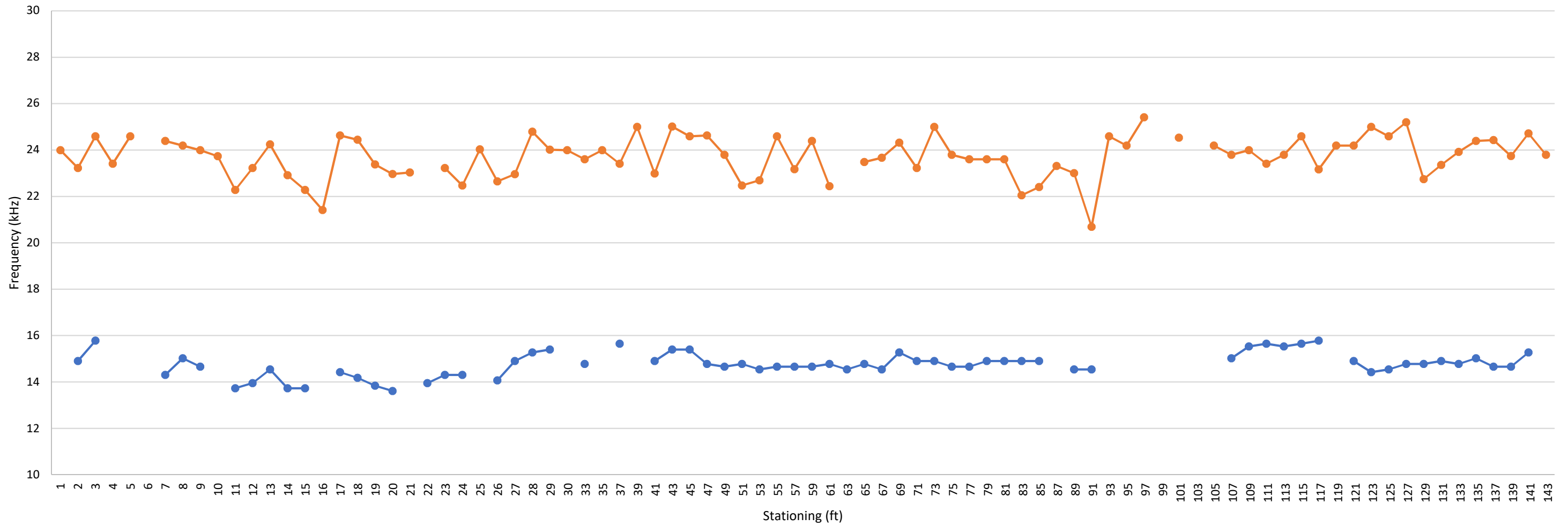
401R-9E



—●— Circumferential Frequency
 —●— Average Through Frequency
 ■ Anomalous Grout Condition

Nondestructive Testing External Tendon Ducts John Ringling Causeway Bridge Over Sarasota Bay Sarasota, Florida Prepared for Florida International University by NDT Corporation		Span 10 Tendon 401R-9E Graph Results	
		January. 2018	Figure A75

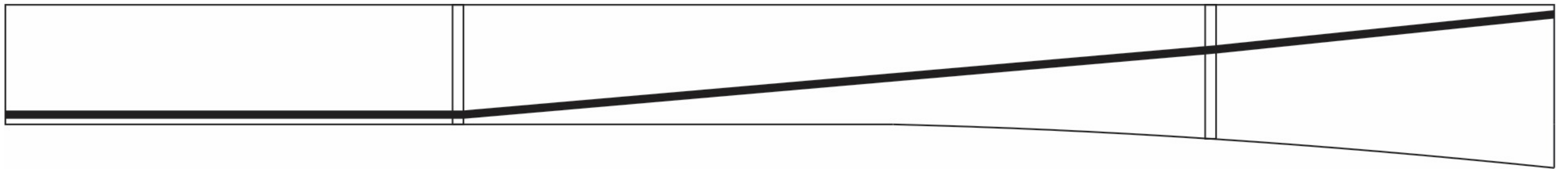
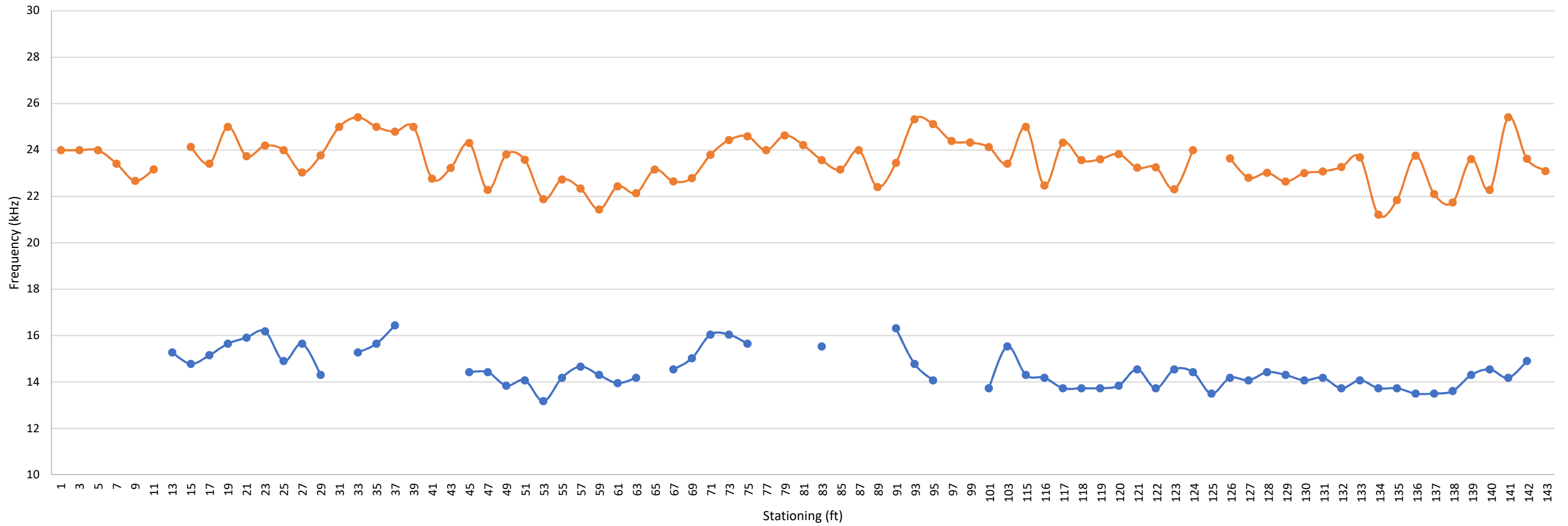
402R-9E



● Circumferential Frequency
 ● Average Through Frequency
 ■ Anomalous Grout Condition

Nondestructive Testing External Tendon Ducts John Ringling Causeway Bridge Over Sarasota Bay Sarasota, Florida Prepared for Florida International University by NDT Corporation		Span 10 Tendon 402R-9E Graph Results	
January. 2018		Figure A76	

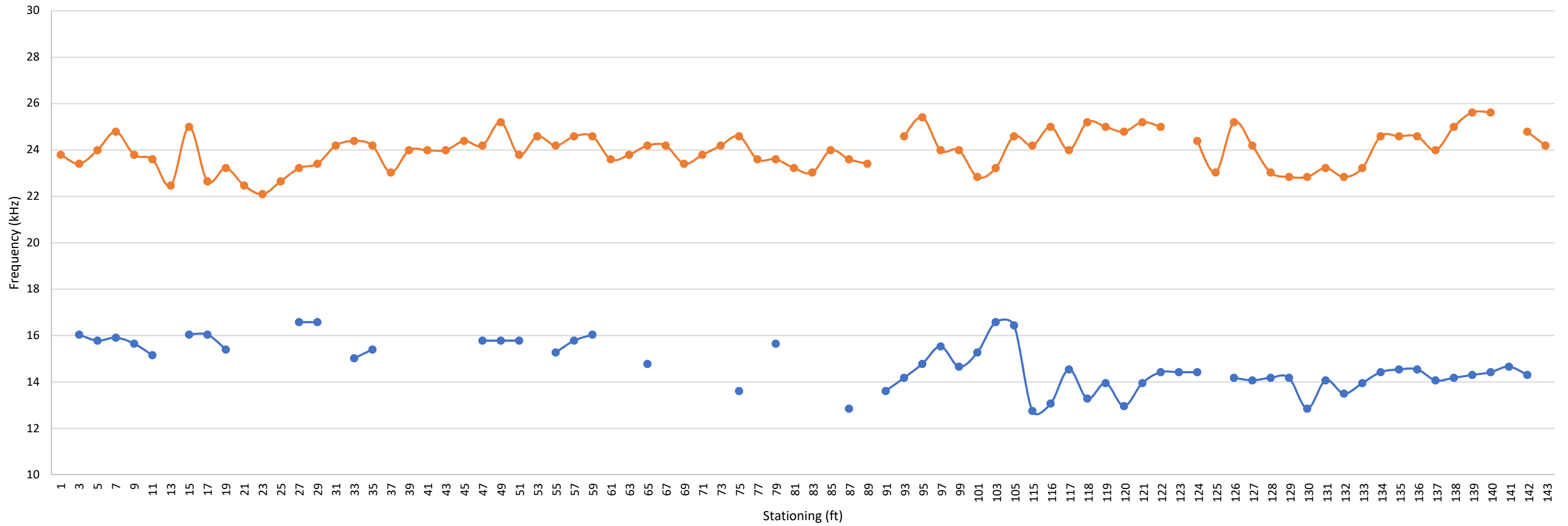
402L-10W



—●— Circumferential Frequency
 —●— Average Through Frequency
 ■ Anomalous Grout Condition

Nondestructive Testing External Tendon Ducts John Ringling Causeway Bridge Over Sarasota Bay Sarasota, Florida Prepared for Florida International University by NDT Corporation		Span 10 Tendon 402L-10W Graph Results	
January. 2018		Figure A77	

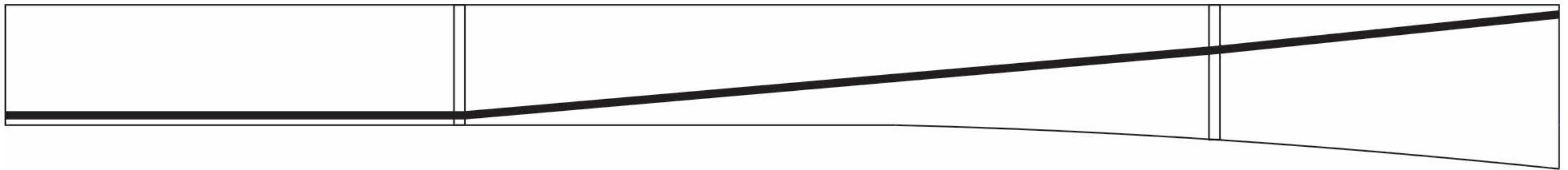
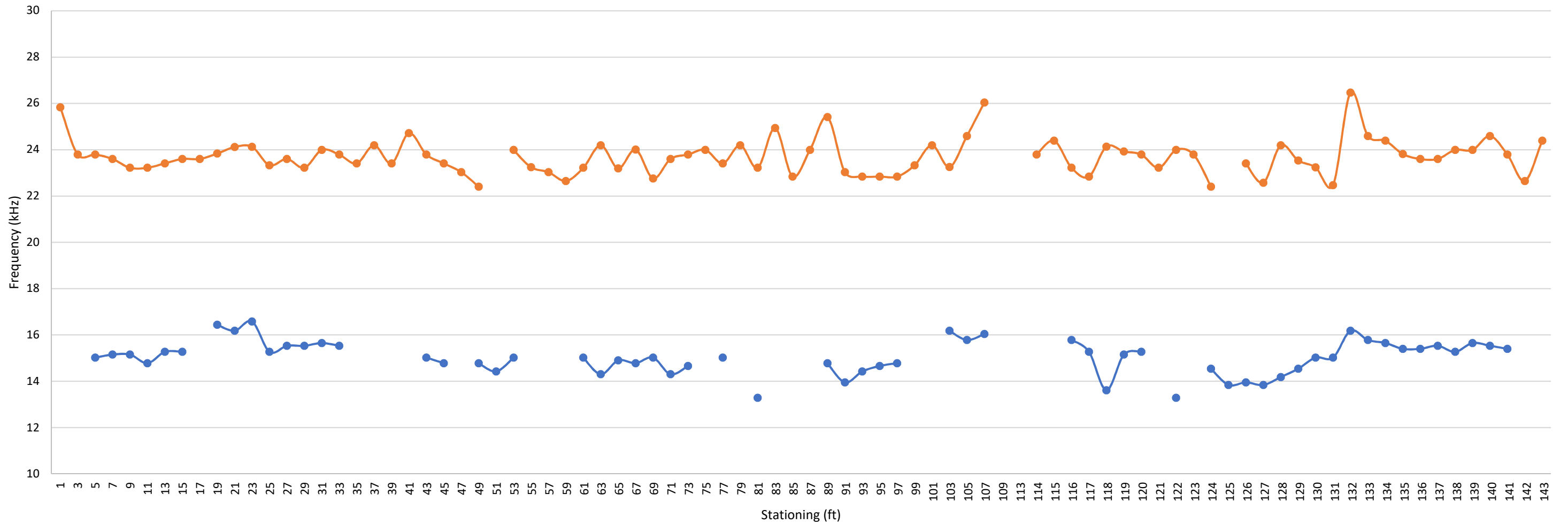
401L-10W



—●— Circumferential Frequency —●— Average Through Frequency ■ Anomalous Grout Condition

Nondestructive Testing External Tendon Ducts John Ringling Causeway Bridge Over Sarasota Bay Sarasota, Florida Prepared for Florida International University by NDT Corporation		Span 10 Tendon 401L-10W Graph Results	
		January. 2018	Figure A78

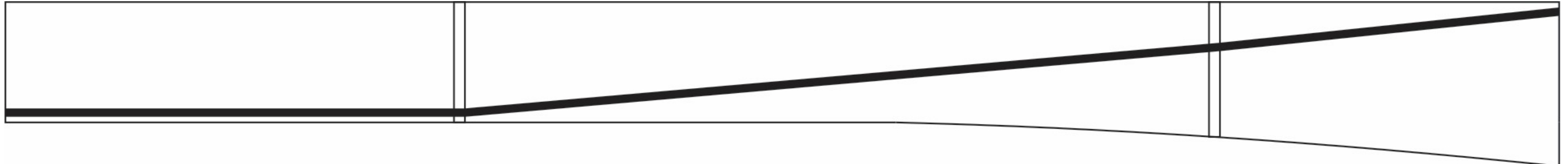
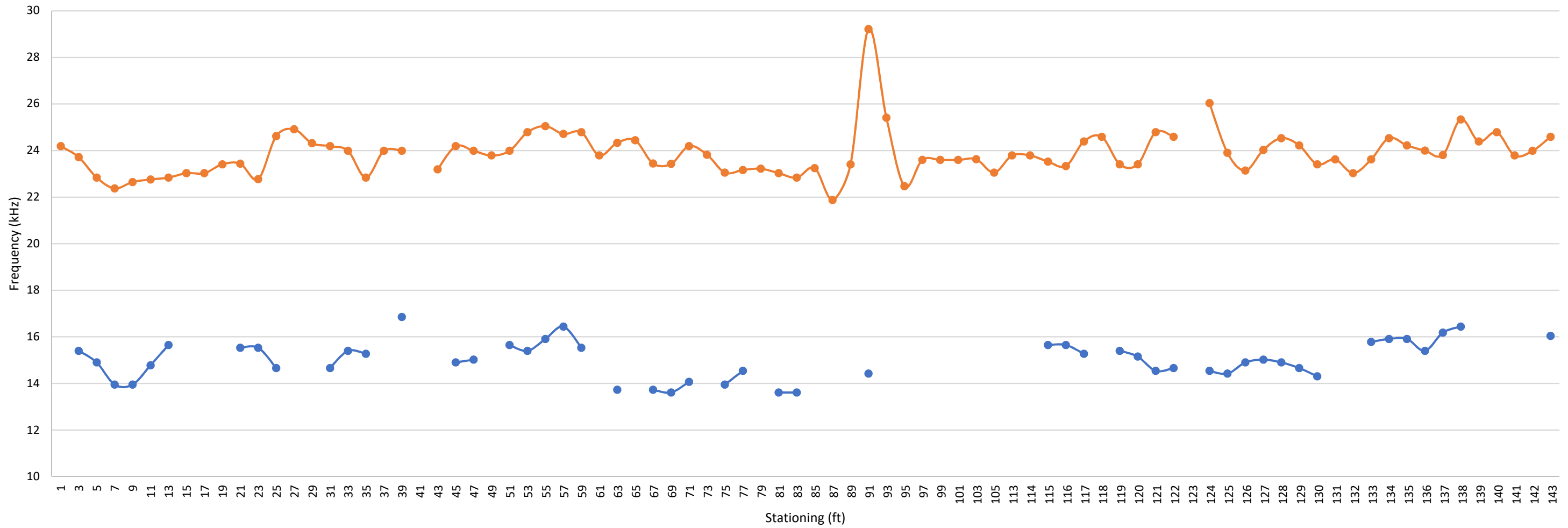
401R-10W



—●— Circumferential Frequency —●— Average Through Frequency ■ Anomalous Grout Condition

Nondestructive Testing External Tendon Ducts John Ringling Causeway Bridge Over Sarasota Bay Sarasota, Florida Prepared for Florida International University by NDT Corporation		Span 10 Tendon 401R-10W Graph Results	
		January. 2018	Figure A79

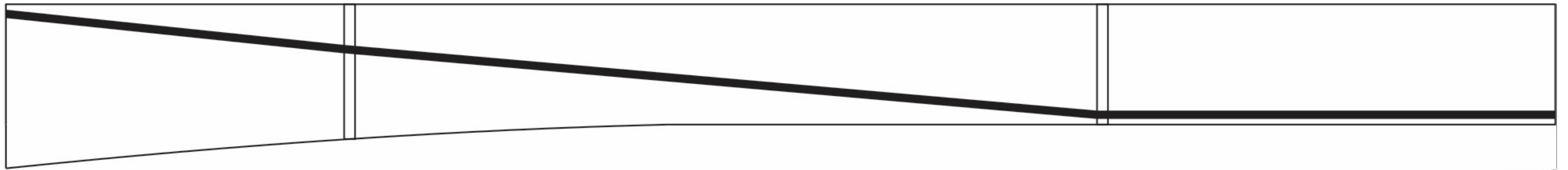
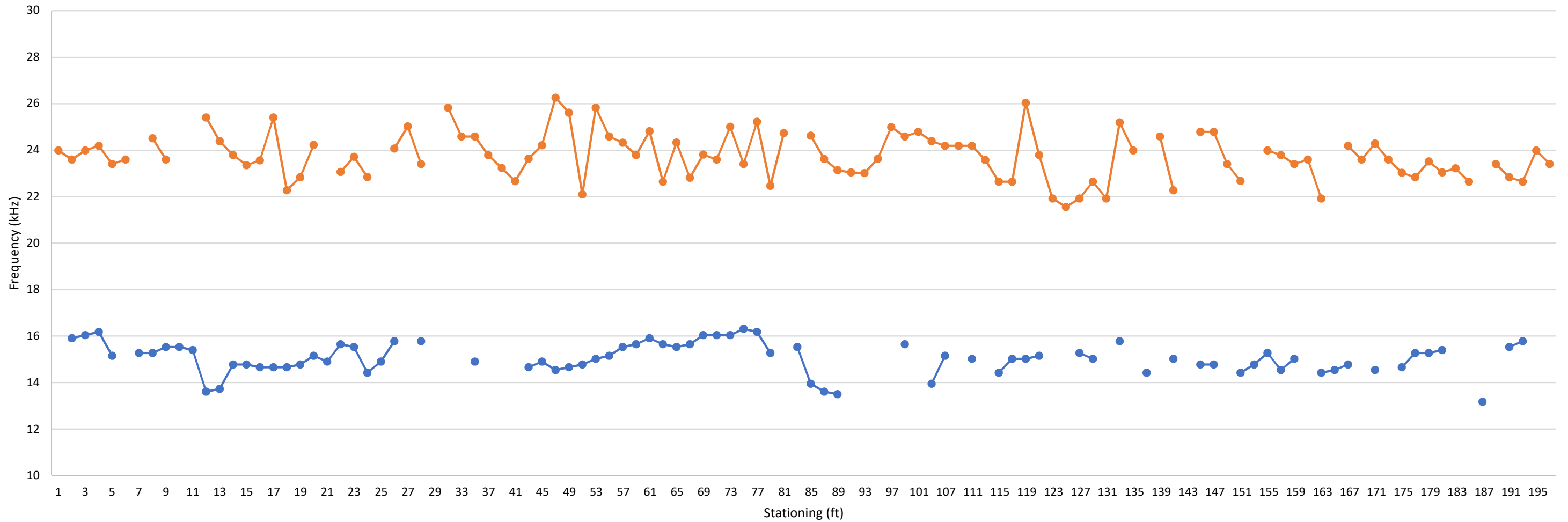
402R-10W



—●— Circumferential Frequency
 —●— Average Through Frequency
 ■ Anomalous Grout Condition

Nondestructive Testing External Tendon Ducts John Ringling Causeway Bridge Over Sarasota Bay Sarasota, Florida Prepared for Florida International University by NDT Corporation		Span 10 Tendon 402R-10W Graph Results	
January. 2018		Figure A80	

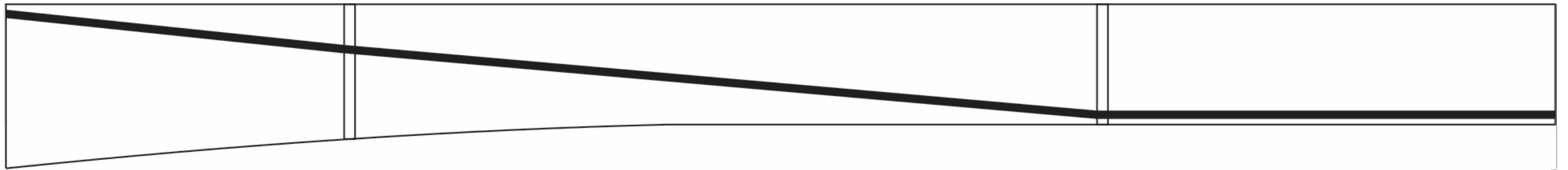
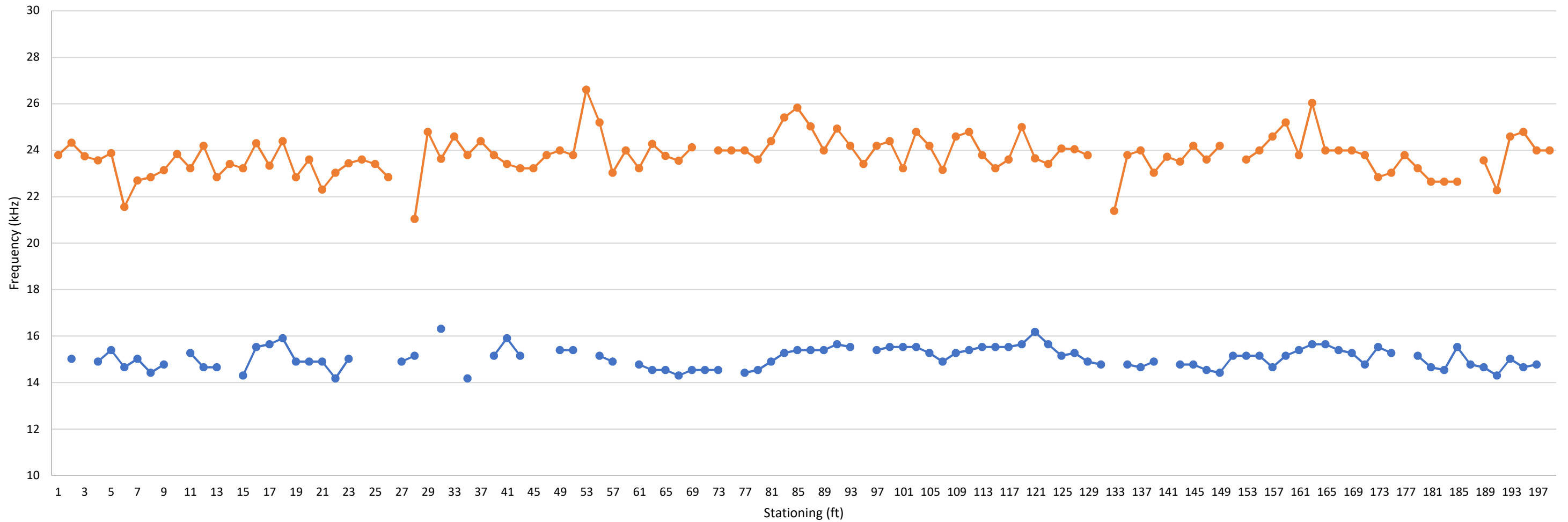
402L-10E



—●— Circumferential Frequency
 —●— Average Through Frequency
 ■ Anomalous Grout Condition

Nondestructive Testing External Tendon Ducts John Ringling Causeway Bridge Over Sarasota Bay Sarasota, Florida Prepared for Florida International University by NDT Corporation		Span 11 Tendon 402L-10E Graph Results	
		January. 2018	Figure A81

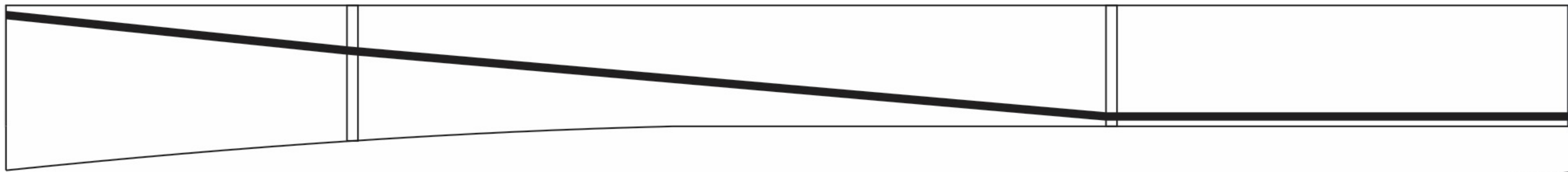
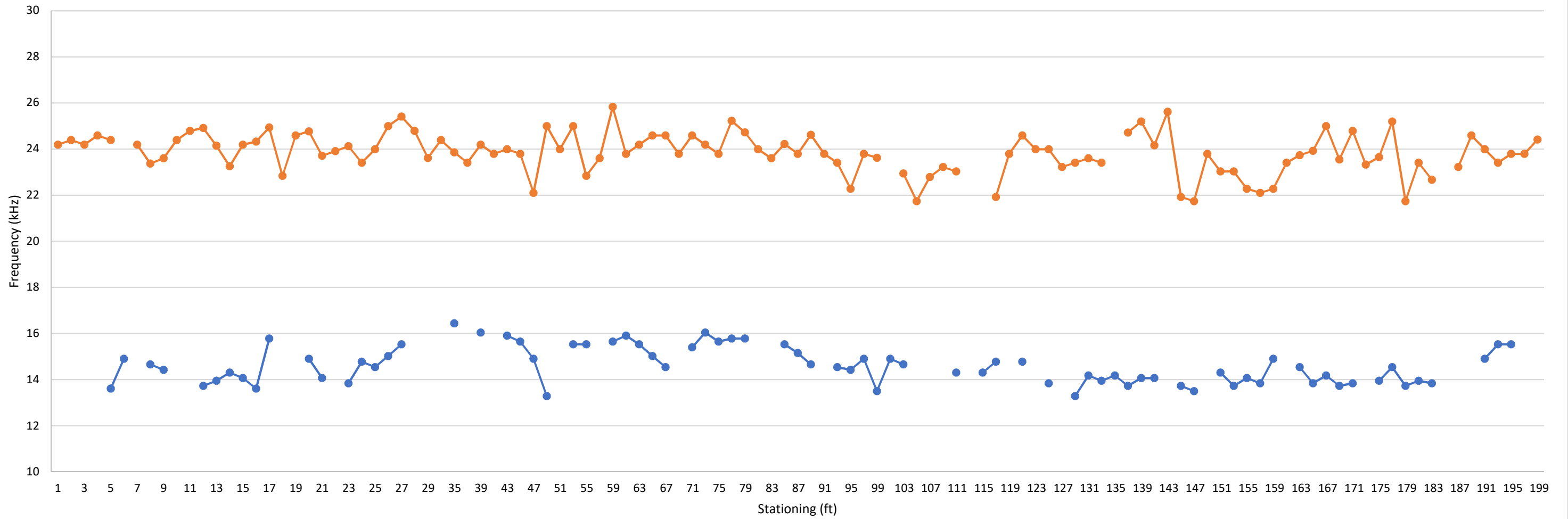
401L-10E



—●— Circumferential Frequency —●— Average Through Frequency ■ Anomalous Grout Condition

Nondestructive Testing External Tendon Ducts John Ringling Causeway Bridge Over Sarasota Bay Sarasota, Florida Prepared for Florida International University by NDT Corporation		Span 11 Tendon 401L-10E Graph Results	
		January. 2018	Figure A82

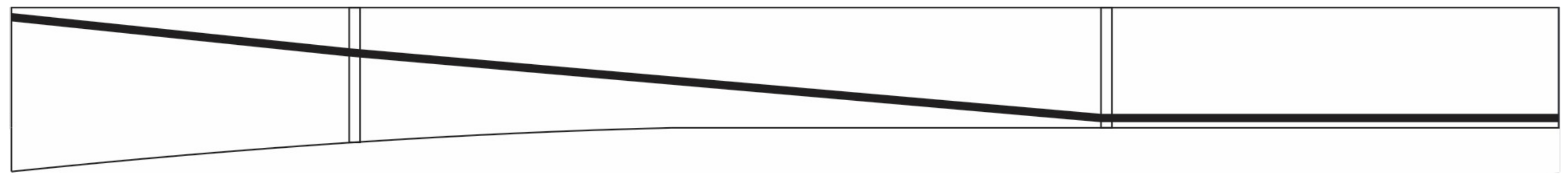
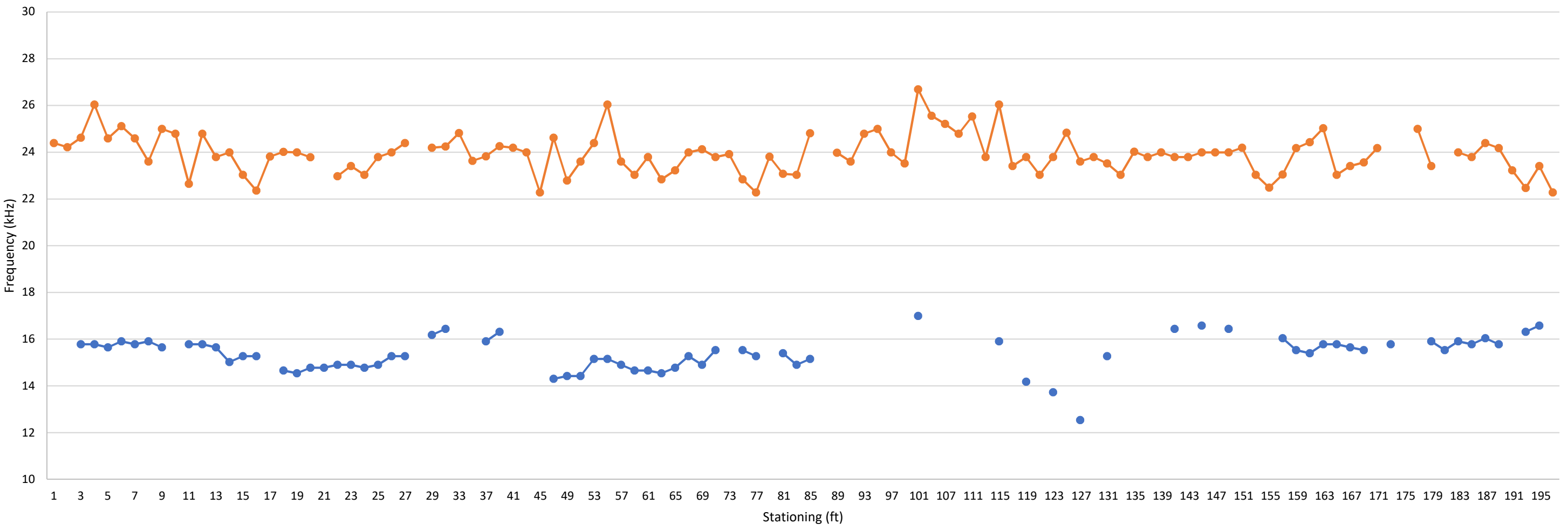
401R-10E



—●— Circumferential Frequency
 —●— Average Through Frequency
 ■ Anomalous Grout Condition

Nondestructive Testing External Tendon Ducts John Ringling Causeway Bridge Over Sarasota Bay Sarasota, Florida Prepared for Florida International University by NDT Corporation		Span 11 Tendon 401R-10E Graph Results	
January. 2018		Figure A83	

402R-10E



—●— Circumferential Frequency
 —●— Average Through Frequency
 ■ Anomalous Grout Condition

Nondestructive Testing External Tendon Ducts John Ringling Causeway Bridge Over Sarasota Bay Sarasota, Florida Prepared for Florida International University by NDT Corporation		Span 11 Tendon 402R-10E Graph Results	
January. 2018		Figure A84	

APPENDIX C MTC PROPOSAL (TOKYO ROPE INC.)



Tokyo Rope USA, Inc.
8301 Ronda Drive, Canton, MI 48187
Phone: 734-335-6037 Fax: 734-335-6576

February 2, 2018

Dr. Atorod Azizinamini
Florida International University
Department of Civil & Environmental Engineering
10555 West Flagler Street EC3607

Re: BDV29 977-34 Phase 2 Tokyo Rope Scope of Work for Ringling Bridge

Dear Dr. Azizinamini,

Tokyo Rope USA, Inc. (TRU), together with its parent company Tokyo Rope Mfg. Co., Ltd (TRM), is pleased to exercise the NDE testing of external post-tensioned (PT) tendons in Ringling Causeway Bridge using the Permanent Magnet Type MMFM.

As stated in our Statement of Work dated July 17, 2017, we will examine 25% of the external post-tensioned (PT) tendons in Ringling Causeway Bridge starting Monday, February 5, 2018. Our MMFM testing will be completed by Thursday, February 22, 2018 to examine at least 132 spans of upper horizontal and sloped region free spans. We will not examine the lower horizontal free span, pier section, upper and lower deviators, and anchors.

After the testing, we will analyze the data and submit our test report to you by Friday, May 4, 2018. The test report will explain our findings in 3 levels as follows:

1. 0 to 5% of section loss
2. 5 to 10% of section loss
3. over 10% of section loss

The cost of our work will be kept within US\$178,531.00, the amount which we have initially quoted as per the attached quotation.

Both TRM and TRU believe that our testing at the Ringling Causeway Bridge will prove MMFM technology to be the practical and effective NDE method to detect the location of corrosion in external PT tendons, and at the same time, will be beneficial for Florida DOT to cross check the condition of the Ringling Causeway Bridge tendons.

We thank you again for the opportunity, and look forward to working on the Project.

Sincerely yours,

Shotaro Nakahama
Vice President
Tokyo Rope USA, Inc.



Tokyo Rope USA, Inc.
A Tokyo Rope Company

8301 Ronda Drive, Canton, MI 48187

Tel: 734-335-6037 Fax: 734-335-6576

QUOTATION

Project:	RINGLING BRIDGE MMFM INSPECTION	Date:	TBD	
Location:	Sarasota, Florida	Code:	MMFM-FIU-25	
Client:	Florida Department of Transportation			
25% of all cables(33/132)		TSK group		Local
Task Description	Supervisor Hours	Administration Hours	Engineer Hours	Technician Hours
Staff	1	1	2	1
Labor Costs	---	---	---	---
1. Equipment preparation (8hr * 1days)	---	---	8.0	---
2. Moving day(8hr * 1days)	8.0	16.0	16.0	8.0
3. Machine parts and measurement preparations(8hr * 1days)	8.0	8.0	16.0	8.0
4. Measurement day(8hr * 13days)	104.0	---	208.0	104.0
5. Moving day(8hr * 1days)	8.0	16.0	16.0	8.0
6. Cleaning / Equipment check(8hr * 1days)	---	---	8.0	---
7. Report Preparation (8hr *15 days)	20.0	---	100.0	---
Total Hours	148.0	40.0	372.0	128.0
8. Overtime work (More than 40 hours) × 0.5	16.0	0.0	32.0	16.0
Labor Rates (per hour)	\$ 187.00	\$ 150.00	\$ 150.00	\$ 72.00
Labor	\$ 29,172	\$ 6,000	\$ 58,200	\$ 9,792
	\$ -		\$ -	\$ -
	\$ -		\$ -	\$ -
Labor Subtotal	\$ 29,172	\$ 6,000	\$ 58,200	\$ 9,792
Labor Cost				\$ 103,164

Travel Expenses	Unit	Quantity	Unit Cost	Total Cost
Per Diem (18days*3persons)(2days*1persons)	day	56	\$ 42	\$ 2,352
Hotel (16days*3persons)(2days*1persons)	night	50	\$ 125	\$ 6,250
Mileage	miles	170	\$ 0.558	\$ 95
Airfare 2,290(NRT) × 3+1,000(DTW)*2= \$8,870	trip		\$ 8,870	\$ 8,870
Rental Car	day	15	\$ 100	\$ 1,500
Gas	gallon	86	\$ 2.20	\$ 189
Travel Expenses Total				\$ 19,256

Inspection Fee	Measured points	Unit Cost	Total Cost
Location of Tendons	each 132	\$ 250	\$ 33,000
	each	\$ -	\$ -
	each	\$ -	\$ -
	each	\$ -	\$ -
Inspection Fee Total			\$ 33,000

Field Supplies	Unit	Quantity	Unit Cost	Total Cost
Equipment	each	1	\$ 5,700	\$ 5,700
Miscellaneous	each	1	\$ 850	\$ 850
Apparatus postage	each	2	\$ 2,000	\$ 4,000
Field Supplies Total				\$ 10,550

Expenses & Fees Total \$ 62,806

Labor Cost	\$ 103,164
Expenses & Fees Total	\$ 62,806
Overhead 20%	\$ 12,561

Total Cost \$ 178,531

Tokyo Rope USA, Inc.

**APPENDIX D MTC FIELD TESTING (TOKYO ROPE
INC.)**



Tokyo Rope USA, Inc.

8301 Ronda Drive, Canton, MI 48187
Phone: 734-335-6037 Fax: 734-335-6576

Final Report

**Non-destructive Evaluation of Selective External Grouted PT Tendons on Ringling
Causeway Bridge Using Permanent Magnet Type Magnetic Main Flux Method**

Prepared by

Tokyo Rope USA, Inc.

For

Florida International University

and

Florida Department of Transportation

May 3, 2018



Tokyo Rope USA, Inc.

TABLE OF CONTENTS

BACKGROUND	3
INTRODUCTION TO PERMANENT MAGNET TYPE MMFM SYSTEM	4
OBJECTIVES	9
FIELD INVESTIGATION PROCEDURE	10
Off-site Testing on Two Field Tendon Samples	10
Field Testing	12
Preparation of Duplicate MMFM Systems	12
Selection of Test Tendons	13
MMFM Testing Protocol	20
TEST RESULTS AND DISCUSSION	24
Understanding MMFM Data	24
Calibration Results from Tendon Sample #1	25
MMFM Data and Autopsy of Tendon Sample #2	32
Scan Results of Field Tendon Sections	35
CONCLUSIONS	51
REFERENCES	51
APPENDIX 1. Schematic Diagrams of Scanned Test Sections	52
APPENDIX 2. Collection of MMFM Data Containing Damage	68
APPENDIX 3. Collection of MMFM Data Containing No Damage	110



Tokyo Rope USA, Inc.

Non-destructive Evaluation of Selective External Grouted PT Tendons on Ringling Causeway Bridge Using Permanent Magnet Type Magnetic Main Flux Method

BACKGROUND

For over five decades in the United States, modern bridge structures used high strength wires as economic and efficient structural components. Typical bridge types constructed with high strength wires and 7-wire strands include suspension bridges, cable-stayed bridges, and prestressed concrete bridges including post-tensioned (PT) precast segmental bridges. Since 1999, some PT tendons and stay cables in the U.S. have experienced corrosion problems.

In 2007, the Federal Highway Administration (FHWA), partnering with the American Association of State Highway and Transportation Officials (AASHTO) and preservation industry, organized a national workshop to identify bridge preservation and corrosion mitigation research needs. This preservation workshop produced a comprehensive report entitled “Transportation System Preservation (TSP) Research, Development, and Implementation Roadmap.”⁽¹⁾ The workshop participants chose “improved inspection techniques for steel prestressing strands, cables, and ropes” as the most urgent and important issue for bridge preservation. It can be well justified because assessing the condition of highly stressed strands and wires embedded either in concrete (pre-tensioned girders and beams) or in ducts and anchorage trumpets (post-tensioned tendons and stay cables) is expensive, time-consuming, and even impossible, in some cases. The structural integrity of these bridges relies on a much smaller cross-sectional area compared to the ordinary reinforcing steel such that the loss of the former is more critical than the equivalent loss of the latter. Fracture of highly stressed wires and strands embedded in either concrete or enclosures such as ducts and anchorages can be unforeseen and catastrophic.

For prestressed concrete bridges, current inspection practices still depend primarily on visual inspections and NDE techniques such as the magnetic flux leakage (MFL) and impact echo (IE) were tried in some limited cases. In an earlier FHWA study, several NDE technologies were evaluated in the laboratory. These included Magnetic Flux Leakage (MFL), Magnetostrictive Sensor (MsS), Microwave Thermoreflectometry, Ultrasonic, Sonic Echo/Impulse Response (SE/IR), and solenoid type Magnetic Main Flux Method (MMFM). Among them, solenoid type MMFM of Tokyo Rope Manufacturing Co. Ltd. (TRM) was determined to be the most accurate and effective for evaluating external tendons and stay cables. MMFM is a unique non-destructive evaluation method in that it can detect the change of this magnetic flow and calculate the cross-sectional loss.

Despite its highest accuracy, utilization of the solenoid type MMFM in the field was time consuming due to requiring 3-phase 240-volt AC power, tedious wire wrapping process, etc. Therefore, TRM developed a permanent magnet type MMFM which is less precise, but can quickly identify external PT tendons that suffer from relatively large section loss.



INTRODUCTION TO PERMANENT MAGNET TYPE MMFM SYSTEM

Structural metal members of bridges such as steel tendon and cable are ferromagnetic. The MMFM relies on a fundamental principle that when a metal object is magnetized, magnetic flux flows in the longitudinal direction through the cross-sectional area of the metal. When there is a loss of cross-sectional area due to corrosion or wire breaks in the metal, magnetic flux leaks outside through the reduced cross-sectional area and thus the portion flowing inside of the metal decreases. Figure 1 depicts these conditions.

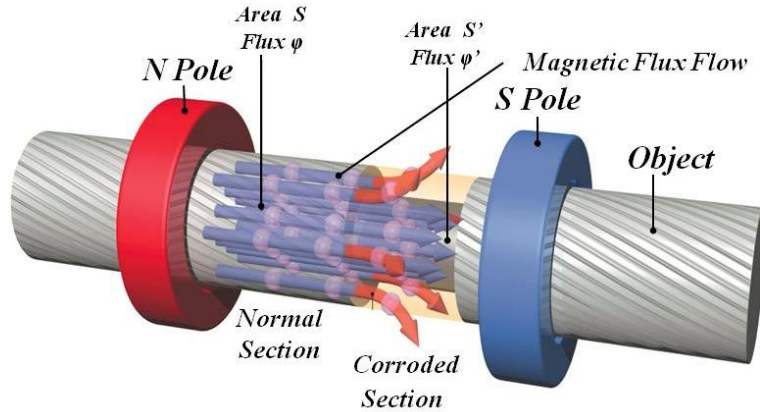


Figure 1. Flow of magnetic flux in a metal object.⁽²⁾

When magnetic flux (ϕ) flows inside the object as illustrated in Figure 2, a search coil reads the induced voltage which is proportional to the rate at which the magnetic flux changes. The total change in magnetic flux ($\Delta\phi$) is calculated by integrating the induced voltage over time, according to the equation embedded in Figure 2.

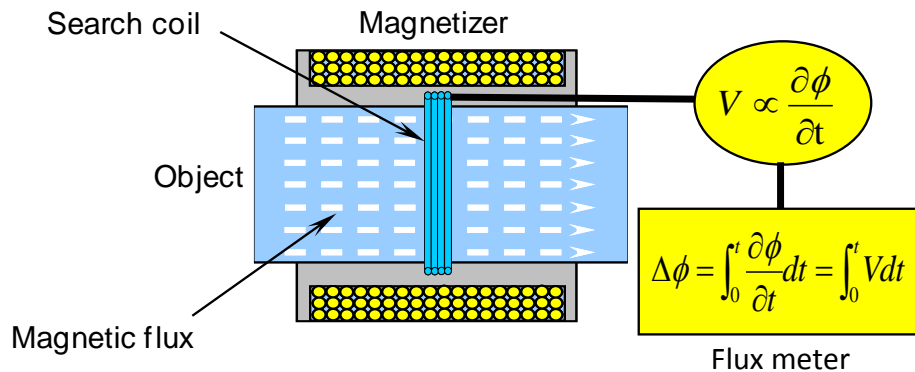


Figure 2. Schematic of magnetic flux measurement.⁽²⁾

As mentioned earlier, the permanent magnet type MMFM system was introduced to simplify MMFM systems for field applications by eliminating an AC power source and wire wrapping work around the bobbin of the solenoid type magnetizer. The permanent magnet type MMFM system consists of a no-electricity-required magnetizer, a controller, and data acquisition/analysis



software on a laptop computer. Figure 3 illustrates the magnetic flux flow in the permanent magnet type magnetizer which has four pairs of the permanent magnet, a search coil, radial Hall effect sensors, and axial Hall effect sensors. This particular example also shows how the flow of magnetic flux is affected by the presence of a defect in the metal object.

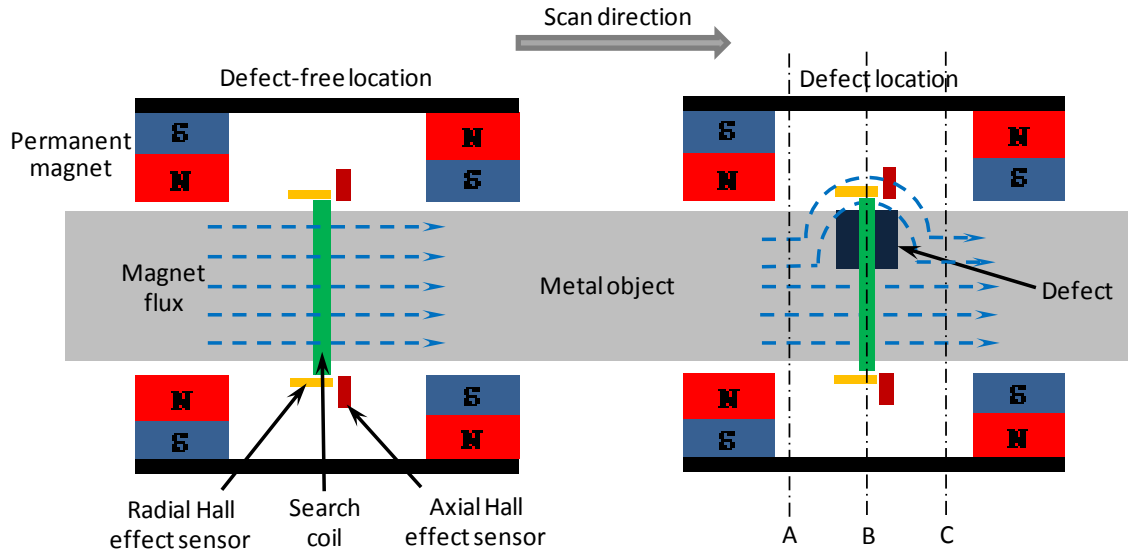


Figure 3. Schematic of the magnetic flux flow in the permanent magnet type magnetizer.

Figure 4 shows an interior view of the magnetizer when the half-split outer steel shell is opened. A cylindrical shape plastic sensor holder and two permanent magnets can be seen. Two more magnets are hidden under the sensor holder. The steel shell has eight rollers attached to the front and rear faces of the magnetizer. The magnetizer is also equipped with a rotary encoder type distance meter as shown in Figure 5. This device allows synchronizing magnetizer scan distance with the magnetic flux data. The weight of the magnetizer is approximately 56 lb.

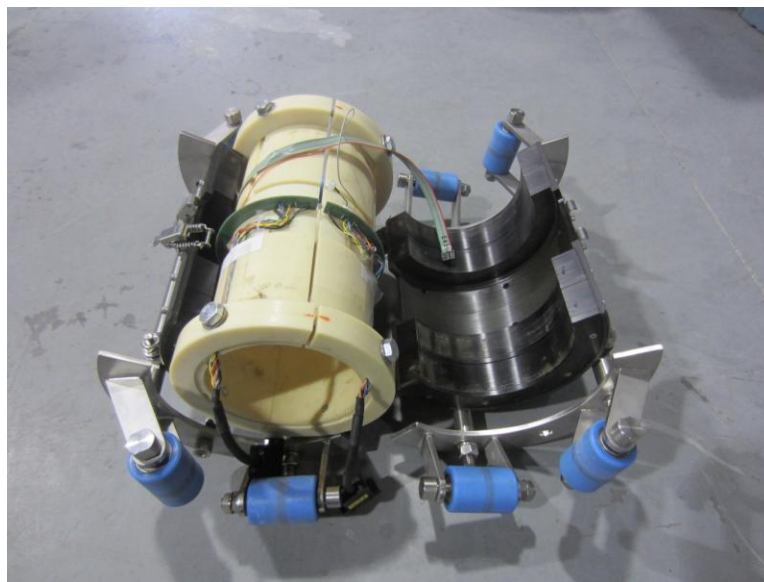


Figure 4. Interior view of the permanent magnet type MMFM magnetizer.



Figure 5. Rotary encoder type distance meter.

Two types of sensors are included in the magnetizer: search coils and Hall effect sensors. These sensors are accommodated in a sensor holder, which is placed inside the steel shell. The sensor holder consists of two half split pieces which allow quick installation around an external PT tendon. Figure 6 and Figure 7 show two sensor holder pieces being wrapped around a tendon and a close-up view of the assembled sensor holder, respectively.



Figure 6. Installing two half-split sensor holder pieces on a tendon.

In this study, two search coils were wrapped around the assembled sensor holder (see Figure 7). The search coil #1 (coil 5Turn) can detect up to ten percent section loss and the search coil #2 (coil 10Turn) up to five percent section loss.

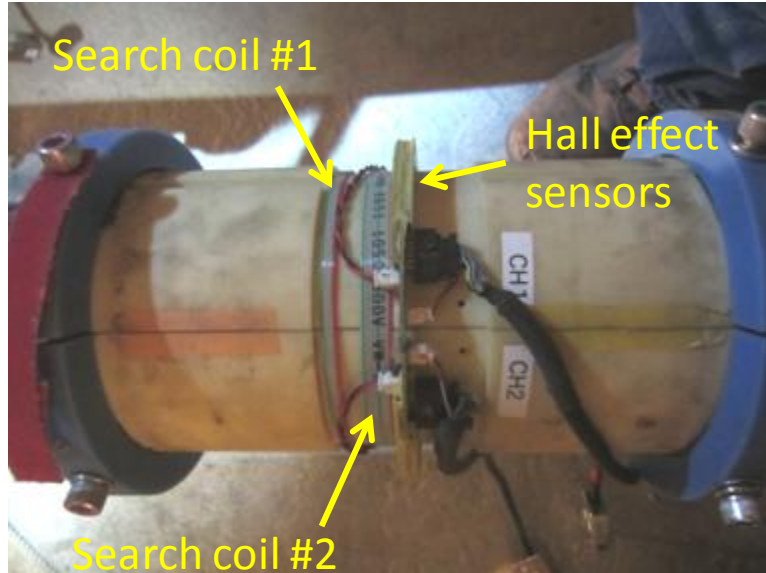


Figure 7. Assembled sensor holder.

A Hall effect sensor produces the voltage proportional to the intensity of magnetic field (H, or magnetic flux density) which passes through the sensor. A gauss meter measures the changes in the magnetic field via the Hall effect sensor. In order to collect the induced voltages at various positions, a total of 16 Hall effect sensors are set around the metal object: eight radial sensors face the center of the object and eight axial sensors face in the longitudinal direction. Figure 8 shows the Hall effect sensor arrangement schematically. Actual Hall effect sensors are installed on the half split rings that are shown in Figure 7.

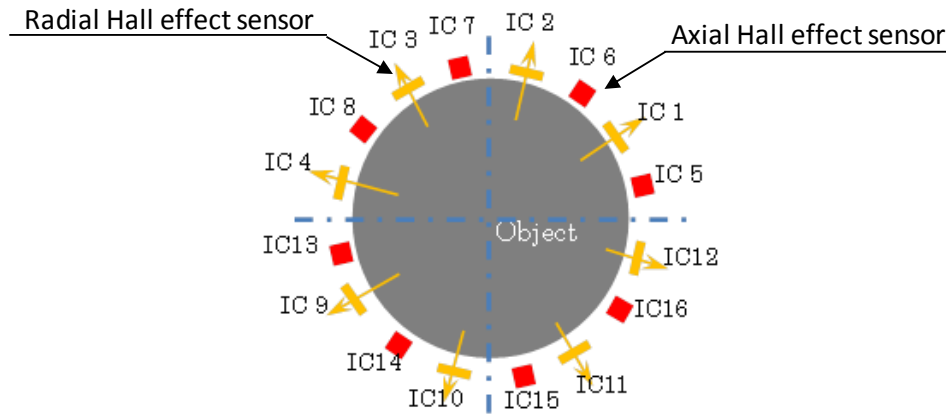


Figure 8. Arrangement of Hall effect sensors.

With such a sensor arrangement, no matter where a defect exists in the metal object, detecting a change of the magnetic flux can be ensured.

With help of Figure 3, the following describes how individual sensors respond when a permanent magnet type magnetizer moves through defect-free locations (point A and point C) and defect containing the location (point B) during a scan measurement. As magnetic flux leaks at the



defect (point B), the leaked magnetic flux is divided into vertical component (radial) and a horizontal component (axial). During this transition from defect-free → defect → defect-free conditions, change of magnetic flux influences the sensors as follows:

1. Search coils: direct voltage signals from two search coils are automatically integrated by the change of magnetic flux. These integrated voltages begin to decrease beyond point A, become the lowest at point B, and return to the normal value at point C and onward.
2. Upper region radial Hall effect sensors: After passing point A, magnet flux starts leaking and the vertical (i.e., perpendicular to the metal object) component of the leaked magnetic flux increases and then decreases until it becomes the normal value at point B. After passing point B, the vertical component of the leaked magnetic flux increases again in the opposite direction and then decreases until it becomes the normal value again at point C and onward.
3. Upper region axial Hall effect sensors: After passing point A, magnet flux starts leaking and the horizontal (i.e., parallel to the metal object) component of the leaked magnetic flux increases until it becomes the highest at point B. After passing point B, the horizontal component of the leaked magnetic flux decreases until it becomes the normal value at point C and onward.
4. Bottom region radial and axial Hall effect sensors: Because these Hall effect sensors are situated far away from the defect located in the upper region, the effect of the magnetic flux fluctuations is minimal.

From these sensor responses, the permanent magnet type MMFM system produces three types of data: induced voltage signals from the search coils, relative changes in magnetic flux by integrating voltages from the search coils, and voltage signals from the Hall effect sensors.

Once the sensor holder is installed, the steel outer shell is wrapped around the sensor holder and is closed using two spring-loaded clamps. Figure 9 shows the steel shell being wrapped around the sensor holder. Two black cables coming from the sensor holder go through a rectangular slot in the steel shell.



Figure 9. A steel outer shell being installed.



Tokyo Rope USA, Inc.

A key component of the permanent magnet type MMFM system is the controller. It operates with a 9-volt battery and the collecting data are transmitted wirelessly to the laptop computer. Figure 10 shows one type of the MMFM controller.

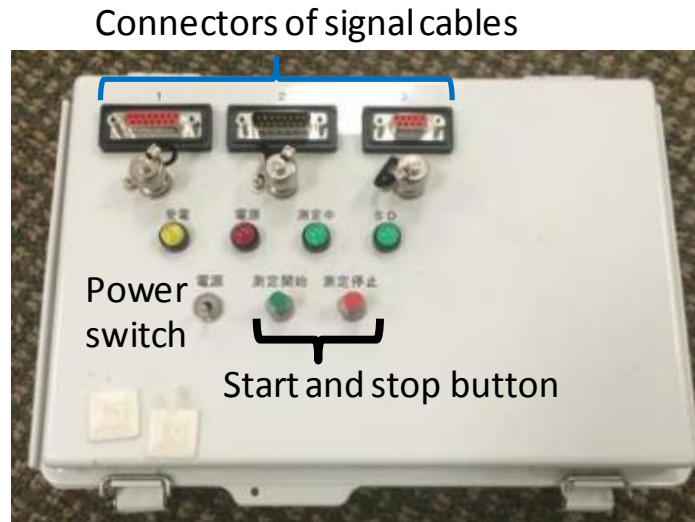


Figure 10. Controller.

The controller has the following functions:

1. Applying the driving voltage to Hall effect sensors.
2. Receiving the signal from each sensor and save it into SD card.
3. Integrating the signals from the search coils and save them into SD card.
4. Counting the pulse signal from the distance encoder and save it to SD card.
5. Sending the data stored on the SD card to the computer wirelessly.

OBJECTIVES

The Ringling Causeway Bridge (hereinafter Ringling Bridge) is a 3,100-ft long, multi-cell segmental box girder PT bridge over Sarasota Bay and the Intracoastal Waterway of the Gulf of Mexico. It was constructed with internal and external tendons and was completed in 2003. Half of a span between piers consists of twelve 12-ft long precast segments. The external PT tendons are 4-inch internal diameter with 22 of high strength 0.6 inch 7-wire strands. Corrosion failure of an external PT tendon was discovered in span 7 in January 2011 and another failed external tendon in span 9 in July 2011 after approximately eight years of service. Ultimately, a total of 17 external tendons were replaced.⁽³⁾

The objectives of this project were to evaluate field applicability and accuracy of the permanent magnet type MMFM system and to perform non-destructive evaluation of roughly 25 percent of the external PT tendons on the Ringling Bridge.



Tokyo Rope USA, Inc.

FIELD INVESTIGATION PROCEDURE

This section describes how the field investigation was carried out in two steps from February 5 through 22, 2018. The first step was to calibrate the permanent magnet type system and to confirm “ready-for-testing” condition of the system hardware. Following the calibration and system check, main field testing was performed in the second step on the bridge.

Off-site Testing of Two Field Tendon Samples

In order to ensure the accuracy and error-free condition of the MMFM systems, a half-day testing was performed for calibration and system check at the FDOT Manatee Operations Center in Bradenton, FL on February 5, 2018. For this testing, two 5-ft PT tendon samples retrieved from the Ringling Bridge were provided by FDOT. Since these tendon samples are identical to in-service tendons, they were considered the ideal specimens for calibration. Figure 11 shows the testing setup for tendon sample #1.



Figure 11. Calibration setup for tendon sample #1.

The calibration work was performed by introducing four levels of damage into 22 of 0.6-inch 7-wire strands (total 154 wires) in the tendon. The artificial damage simulating corrosion-induced section loss was created by removing 1, 7, 14, and 21 wire segments sequentially using an angle grinder. The average length of the removed wires was 6 inches. Although the center wire is slightly larger than the outer ones, a rough estimation was made by treating two wire types the same. From this, the removed wires were equivalent to 0.6, 4.5, 9.1, and 13.6 percent section loss, respectively.

The first scan was made for the intact (as-received) condition to collect baseline MMFM data. Following it, four consecutive scans were made after the next level damage was introduced. Based on the MMFM data generated with the progressively larger damage, a calibration chart was created to establish a relationship between the magnitude of the artificial damage and the corresponding magnetic flux.



Tokyo Rope USA, Inc.

Figure 12 shows a 6 x 3 inches cut-out area in preparation of the artificial damage. Center of the cut-out area was 27 inches away from one end of the sample.



Figure 12. Making a 6 x 3 inches duct opening (left) and as-exposed grout condition (right).

Figure 13 shows removed wires during the calibration work.



Figure 13. Removed wires for 0.6, 4.5, 9.1, and 13.6 percent section losses (clockwise from top left).

Upon completion of the calibration work, tendon sample #2 was tested for a system check.



Tokyo Rope USA, Inc.

Field Testing

Once calibration work was completed in the morning of February 5, 2018, field testing started on the bridge in the afternoon of the same day and continued for next 15 working days.

Preparation of Duplicate MMFM Systems

TRM prepared two MMFM systems to expedite the field testing. Figure 14 and Figure 15 show two complete MMFM systems and two magnetizers installed side by side on adjacent 4-inch external PT tendons on the bridge, respectively.

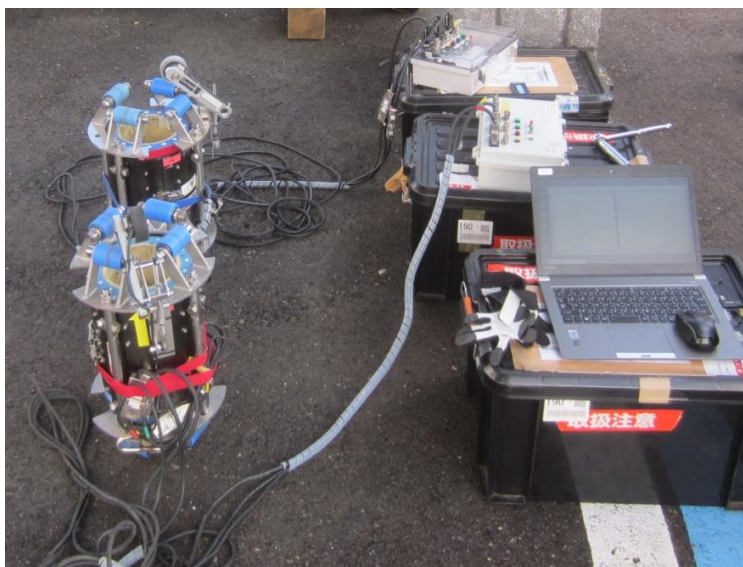


Figure 14. Two complete permanent magnet type MMFM systems.



Figure 15. Two permanent magnet type MMFM magnetizers installed on PT tendons.

During the scan measurement, the controllers were carried in cloth baskets that were attached to the magnetizers. This arrangement is also shown in Figure 15.



Tokyo Rope USA, Inc.

Selection of Test Tendons

Since the project contract requires that 25 percent of the external tendons are tested for three weeks, an original work plan was developed to test the external tendons in the center cell until 25 percent requirement was met. Due to little clearance between girder floor and the horizontal tendon sections running parallel to the girder floor, the MMFM testing was not done for the entire bottom horizontal tendon sections.

The scan measurement proceeded from pier 1 toward pier 12. Thanks to two MMFM systems, efficient field operations, and streamlined testing procedure, TRM accomplished the contract requirement ahead of the schedule and then decided to continue the testing for the remainder of the contract period. As a result, a total of 221 tendon sections in the entire center cells and additional ones in left and right cells of pier 8 – pier 9 and pier 9 – pier 10.

A systematic tendon section identification (ID) system was developed specifically for this project. A test section ID consists of three components, pier ID-tendon ID-section ID, and each component is classified as follows:

1. Pier ID: pier 1 through pier 12; the lower pier number represents a particular span, e.g., P2 is for the pier 2 – pier 3 span.
2. Tendon ID:
 - 2.1. Center cell - 401L, 402L, 401R, 402R (additional 303L and 303R in P5 – P6 and P7 – P8 spans only)
 - 2.2. Left cell – 403L, 404L, 405L, 406L (additional 301L and 302L in P5 – P6 and P7 – P8 spans only)
 - 2.3. Right cell – 403R, 404R, 405R, 406R (additional 301R and 302R in P5 – P6 and P7 – P8 spans only)
3. Section ID: ‘H’ stands for a horizontal section and ‘I’ stands for an inclined section;
 - 3.1. H1 – the first horizontal section from the starting pier diaphragm
 - 3.2. H2 – the second horizontal section from the starting pier diaphragm
 - 3.3. I1 – the first inclined section from the starting pier diaphragm
 - 3.4. I2 – the second inclined section from the starting pier diaphragm
 - 3.5. I3 & I4 – Additional inclined sections can exist when a tendon run into structural obstacles.

Figure 16 and Figure 17 show examples of four tendons (401L, 402L, 402R, and 401R) coming out of pier 4 center cell diaphragm and six tendons (401L, 402L, 402R, 401R, 301L, and 301R) coming out of pier 5 center cell diaphragm, respectively.



Tokyo Rope USA, Inc.



Figure 16. Typical tendon arrangement in the center cell (west face of pier 4 diaphragm).



Figure 17. Tendon arrangement having two extra tendons in the center cell (east face of pier 5 diaphragm).

Figure 18 shows an example of tendon deflection at an upper deviator that re-directs two horizontal sections to two inclined sections.



Figure 18. Tendons going through an upper deviator.

In some spans, severely corroded tendons were replaced with new ones which were installed in different locations. Figure 19 shows one example where two new tendons avoided the original tendon penetration points. In such a case, horizontal sections disappeared and only long inclined sections existed.



Figure 19. Two replaced tendons that bypassed an upper deviator.

Figure 20 and Figure 21 show bottom horizontal tendon sections going through a lower deviator and the same tendons at a mid-span anchor block, respectively. As mentioned earlier, these bottom horizontal sections were not scanned.



Figure 20. Horizontal tendon sections going through a lower deviator.

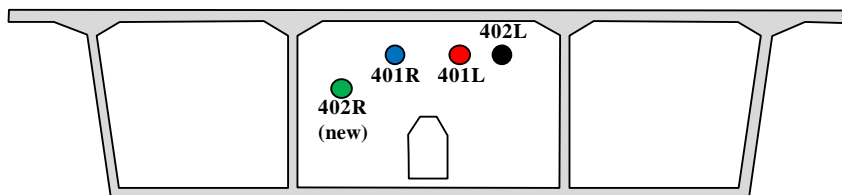


Figure 21. Horizontal tendon sections at an anchor block in the mid-span.

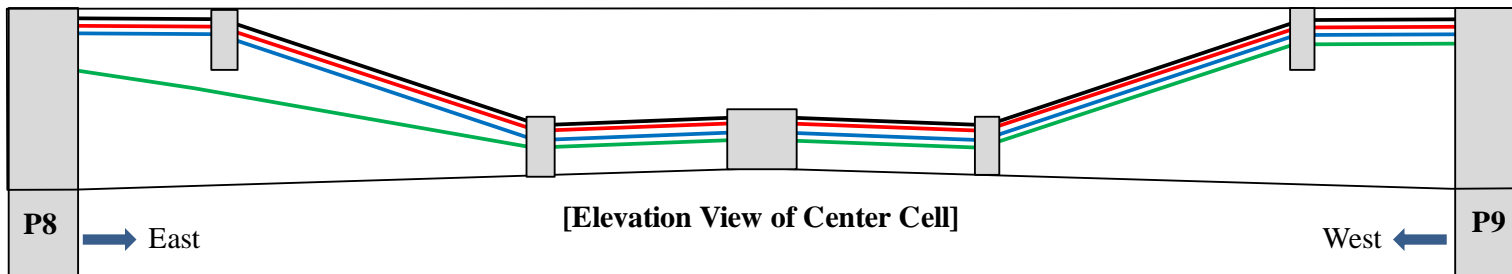
Figure 22 through Figure 24 present examples of schematic tendon arrangement and scanned sections of center cell, left cell, and right cell in P8 – P9 span, respectively. Schematic diagrams for all the spans are included in Appendix 1. Each figure consists of two opposite diaphragm faces and a tendon arrangement in elevation and plan views. Intermediate deviators dividing horizontal sections and inclined sections are also included in both views. Four tendon IDs are included in the diaphragm faces. When there is a replaced tendon, it is indicated by the original tendon ID (new). The scanned section IDs are included in the plan view. Since the bottom horizontal sections were not scanned, their IDs are not included. There was one tendon with no ID in the right cell and it is indicated with P8-40?R-I1 (new) in Figure 24.



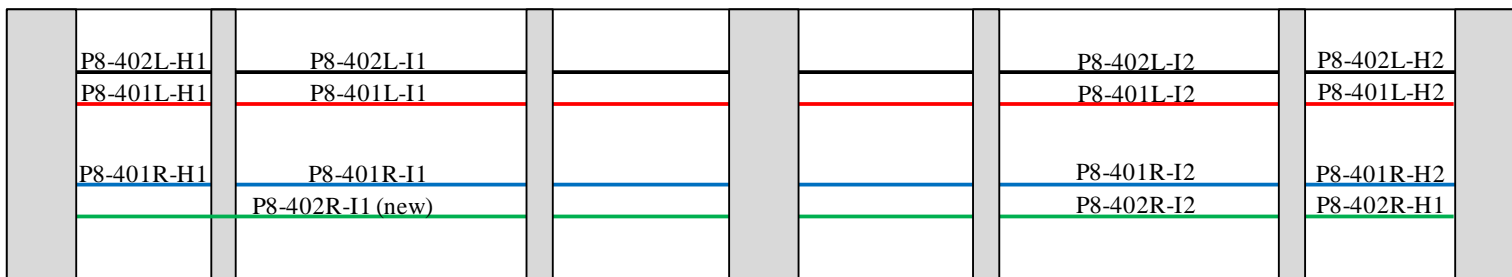
Tokyo Rope USA, Inc.



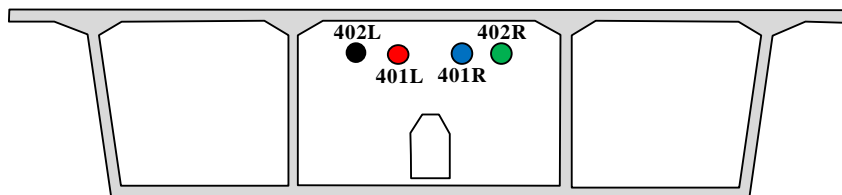
[Diaphragm: East Face at Pier 8]



[Elevation View of Center Cell]



[Plan View of Center Cell]

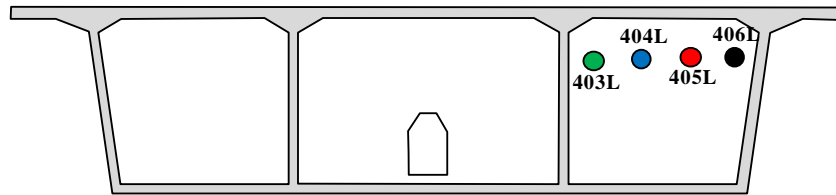


[Diaphragm: West Face at Pier 9]

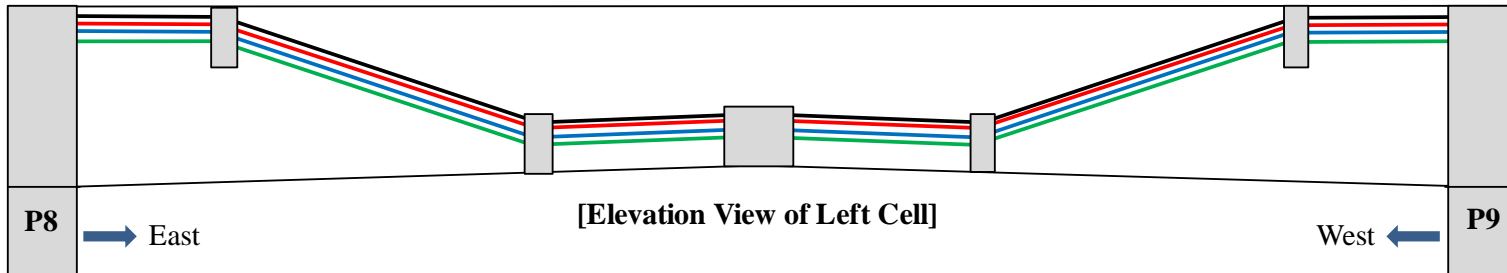
Figure 22. Scanned tendon sections in P8 – P9 (center cell).



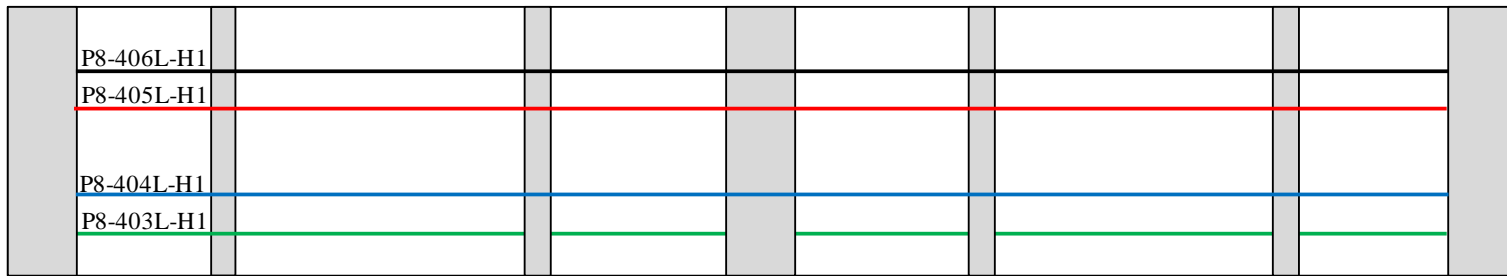
Tokyo Rope USA, Inc.



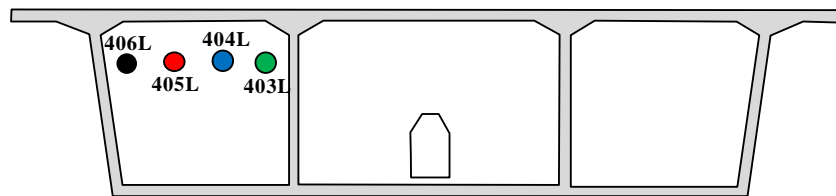
[Diaphragm: East Face at Pier 8]



[Elevation View of Left Cell]



[Plan View of Left Cell]

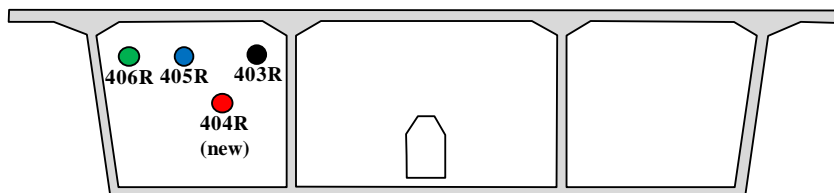


[Diaphragm: West Face at Pier 9]

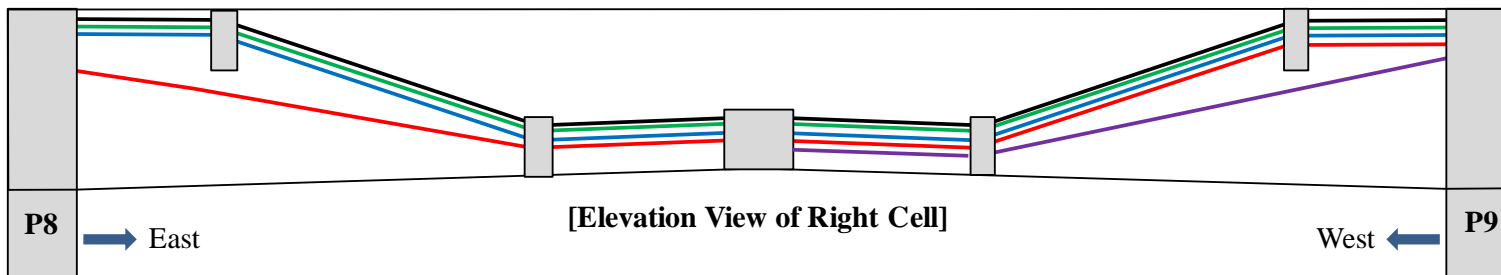
Figure 23. Scanned tendon sections in P8 – P9 (left cell).



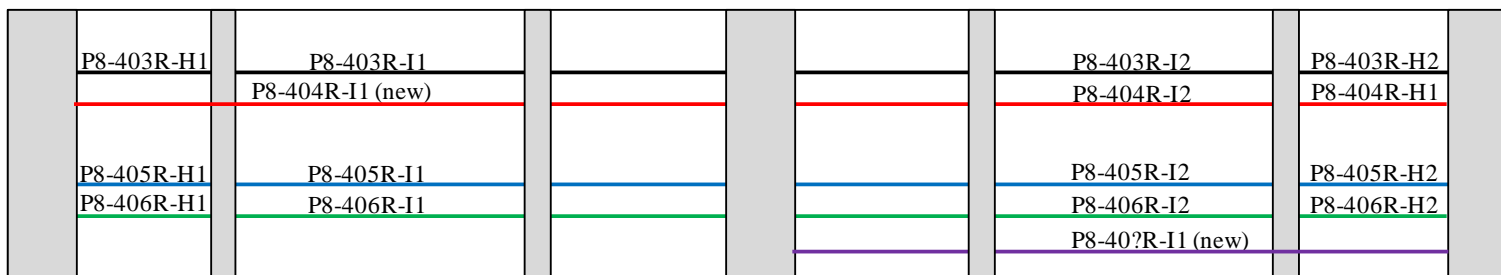
Tokyo Rope USA, Inc.



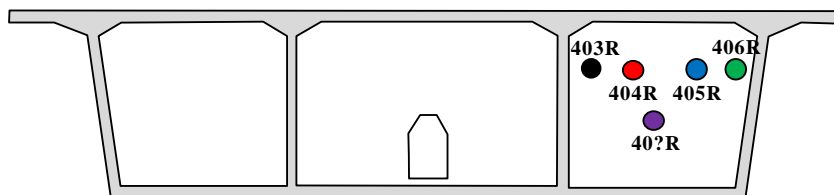
[Diaphragm: East Face at Pier 8]



[Elevation View of Right Cell]



[Plan View of Right Cell]



[Diaphragm: West Face at Pier 9]

Figure 24. Scanned tendon sections in P8 – P9 (right cell).



MMFM Testing Protocol

A continuous scan was made for each section, a part of a long tendon, which is divided by physical barriers such as diaphragms, deviators, transverse tendons, and anchor blocks. The following describes step by step procedure for the in-situ MMFM testing.

- Step 1: Installation of a steel clamp and a pulley

As shown in Figure 25, a steel clamp was attached to the highest point of an inclined section and a pulley was attached to the clamp. For every high elevation horizontal section, one more set of a clamp and a pulley was installed at the other end of the section.



Figure 25. Installing a steel clamp and a pulley.

- Step 2: Installation of the magnetizer

The sensor holder and the steel outer shell were installed on the tendon section. For the inclined section, this work was done at a low elevation for a better work environment. Figure 26 shows a sensor holder installation for the first magnetizer and a steel outer shell for the second magnetizer.



Figure 26. Installation of two magnetizers on the inclined sections at low elevation.



Tokyo Rope USA, Inc.

For the horizontal sections at high elevation, installation of the magnetizer was somewhat difficult due to lifting the magnetizer components and installing them on the ladders. Figure 27 and Figure 28 show the high elevation installation work in progress and the installed magnetizer, respectively. The latter shows the magnetizer installed at high elevation above a worker who is pulling the rope from the floor.

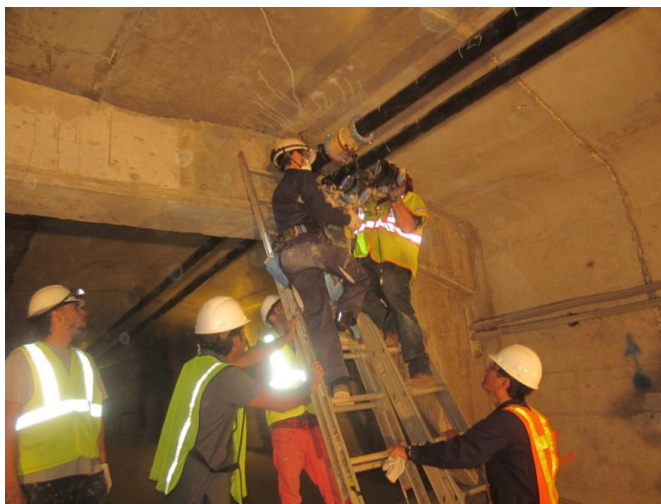


Figure 27. Installation of a magnetizer on a horizontal section at high elevation.

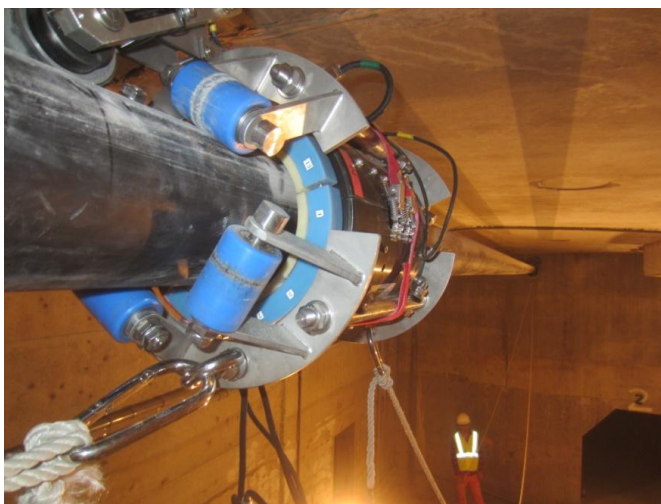


Figure 28. Installed magnetizer on a high elevation horizontal section.

- Step 3: Scan measurement

One end of the rope was tied to the magnetizer through the pulley and the signal cables from the sensors and the rotary encoder type distance meter were connected to the controller placed in the blue cloth basket. A scan measurement was performed by moving the magnetizer along the tendon section. For the inclined sections, the upward scan was made by pulling the other end of the rope and the downward scan was done by gravity while releasing the rope. Figure 29 shows this work.



Tokyo Rope USA, Inc.

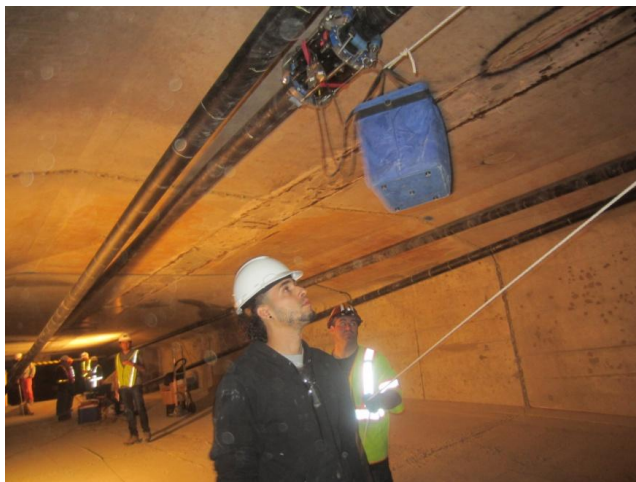


Figure 29. Scan measurement on an inclined tendon section.

For the horizontal sections at high elevation, the magnetizer was pulled in both directions with two separate ropes and pulleys as shown in Figure 30. A close-up view of the rope attachment to the magnetizer is also shown in Figure 28.



Figure 30. Magnetizer on a high elevation horizontal section.

Typically, a complete scan measurement was performed through five repetitive round trips of the magnetizer between the starting and ending points. The first three trips were to magnetize the test section and the remaining two trips for actual scan measurements. The first scan result was reviewed for data acceptance and the second one was for confirming the data reproducibility.

- Step 4: Measurement of total section length, starting position, and ending position
- Step 5: Data collection and preliminary data analysis

Once the scan measurement was completed, the wirelessly transmitted data from the controller to the laptop computer were analyzed to determine if the collected data were



Tokyo Rope USA, Inc.

acceptable or not. Additional scans might be required based on the preliminary data analysis results.

- Step 6: Dismantling the magnetizer from the test section

After it was determined that the collected data were acceptable, the magnetizer and the other components were dismantled and then moved them to next scheduled test section. Then, repeated Step 1 through Step 5.

Two problems were encountered during the field testing. The first problem was related to the extended dead zone (untestable area) created by lack of clearance between the magnetizer and the inclined test section end. Figure 31 shows one of these situations.

The second problem was extruded welding butt joints over the HDPE duct. One example is shown in Figure 32. Such a surface irregularity caused the magnetizer to jump and resulted in data disturbance in the waveforms.



Figure 31. A dead zone near the end of an inclined test section.



Figure 32. Extruded HDPE welding joint.



TEST RESULTS AND DISCUSSION

In this section, a brief explanation will be provided first how to understand the MMFM data, followed by presenting test results and discussion related to the FDOT tendon samples and field tendons on the bridge.

Understanding MMFM Data

There are four waveforms generated from each scanned tendon section. They include

1. Change of magnetic flux versus scan distance.
2. Signal of search coil versus scan distance.
3. Signal of radial Hall effect sensor versus scan distance.
4. Signal of axial Hall effect sensor versus scan distance.

The following explains the MMFM data with an example of a 3-wire cut case where the defect was located approximately 1.85 m (6.07 ft.) from the starting point. The first and second waveforms, i.e., change of magnetic flux versus distance and signal of search coil versus distance, are usually presented together in a single plot. Figure 33 shows magnified views of the change of magnetic flux (left) and the voltage signal of the search coil (right) at the defect location. The change of magnetic flux (left) is integration of the voltage signal of search coil (right). As illustrated in the figure, reduced magnetic flux corresponding to a section loss at the defect is measured from the bottom of the recessed curve to a straight line spanning over two adjacent highest points. The defect length can be estimated by measuring a peak-and-valley distance of the search coil signal associated with the reduced magnetic flux.

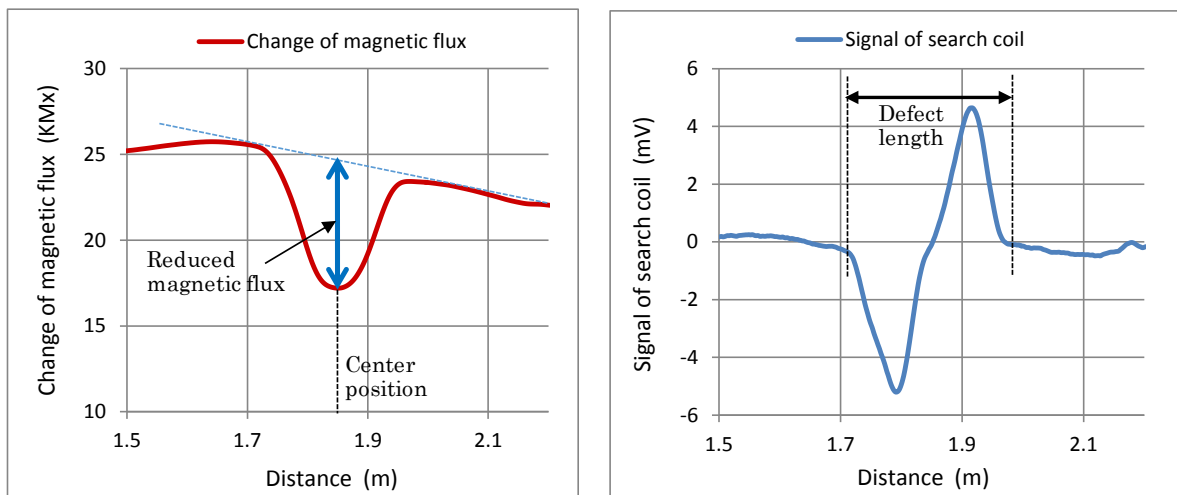


Figure 33. Examples of change of magnetic flux (left) and signal of search coil (right) plots.

The third waveform is related to axial Hall effect sensors. Figure 34 shows voltage signals coming from eight axial Hall effect sensors (left) and a magnified view of the IC7 sensor signal at the defect location (right) along the scan length. It can be seen in Figure 34 that some of the Hall effect sensors clearly responded to the defect location and the disturbed IC7 signal can be used to estimate the defect length.

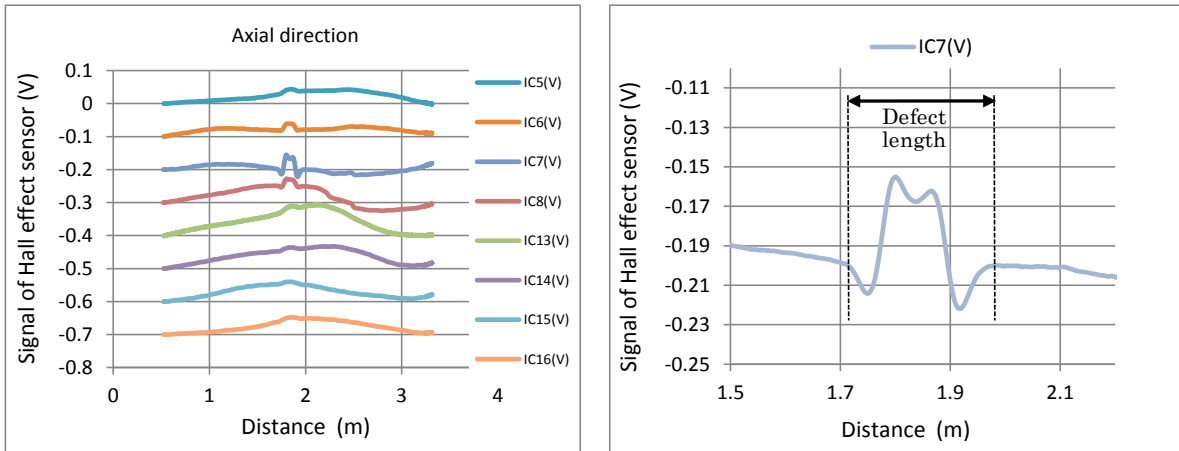


Figure 34. Example of axial Hall effect sensor signals (left) and a magnified view of IC7 sensor signal at the defect location (right).

The last waveform is related to radial Hall effect sensors. Figure 35 shows voltage signals coming from eight radial Hall effect sensors (left) and a magnified view of the IC3 sensor signal at the defect location (right) along the scan length. Similar to the axial Hall effect sensors, three radial Hall effect sensors clearly picked up the defect location and the disturbed IC3 signal can also provide estimated defect length.

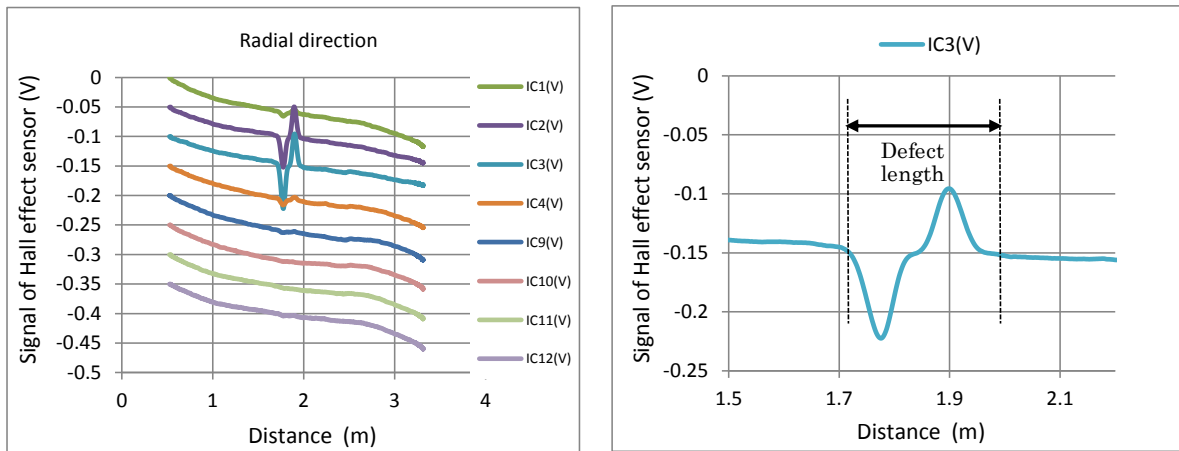


Figure 35. Example of radial Hall effect sensor signals (left) and a magnified view of IC3 sensor signal at the defect location (right).

By analyzing these waveforms simultaneously, experienced operators can identify defect locations immediately upon data collection and estimate section loss(es) through further data analyses in the laboratory.

Calibration Results from Tendon Sample #1

Figure 36 through Figure 40 show the MMFM data of tendon sample #1 having intact and four different artificial damage conditions. Each figure consists of four plots including two search coil data, one for 10 turns (labeled as Coil 10T) and the other for 5 turns (labeled as Coil 5T).

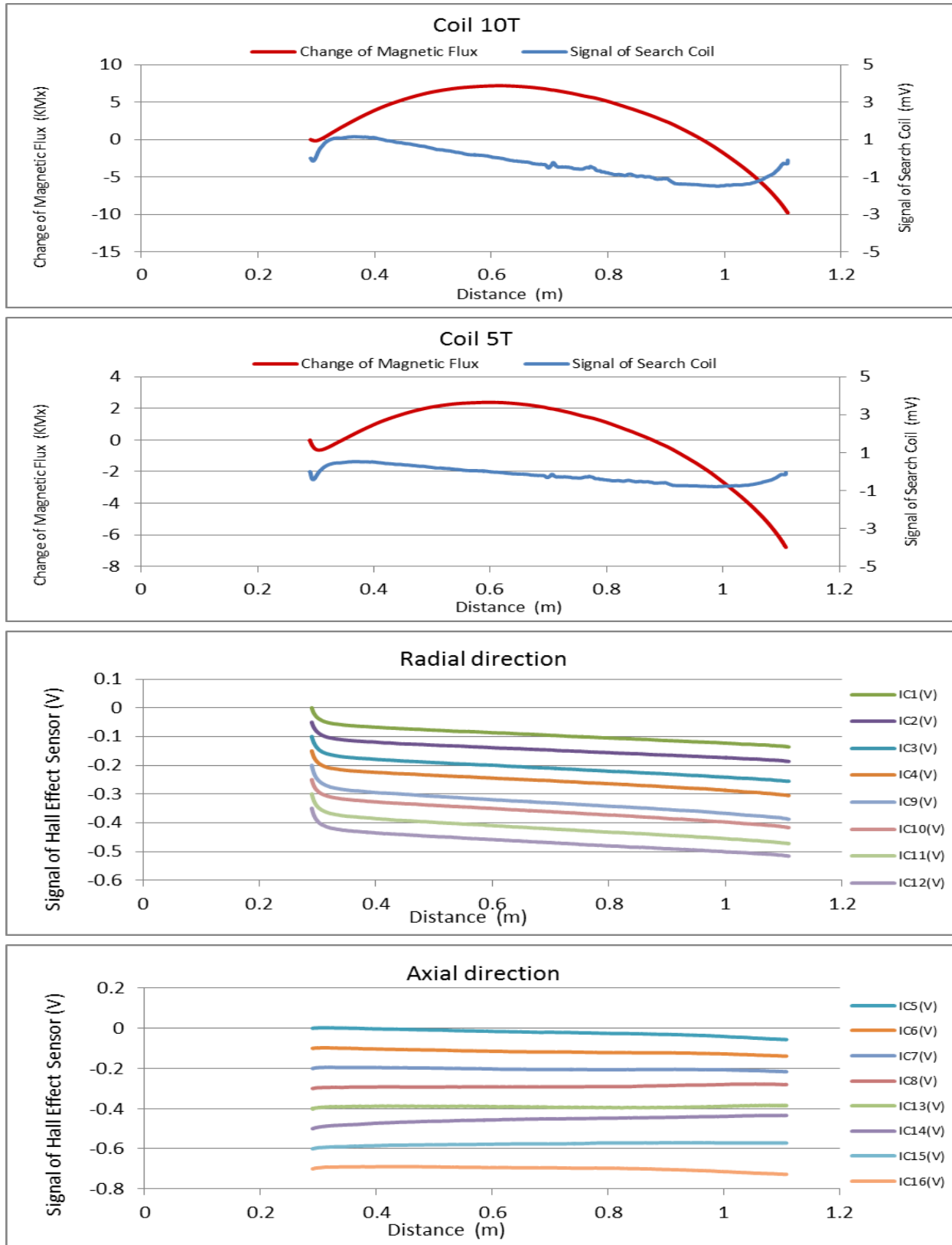


Figure 36. MMFM data for the intact condition of tendon sample #1.

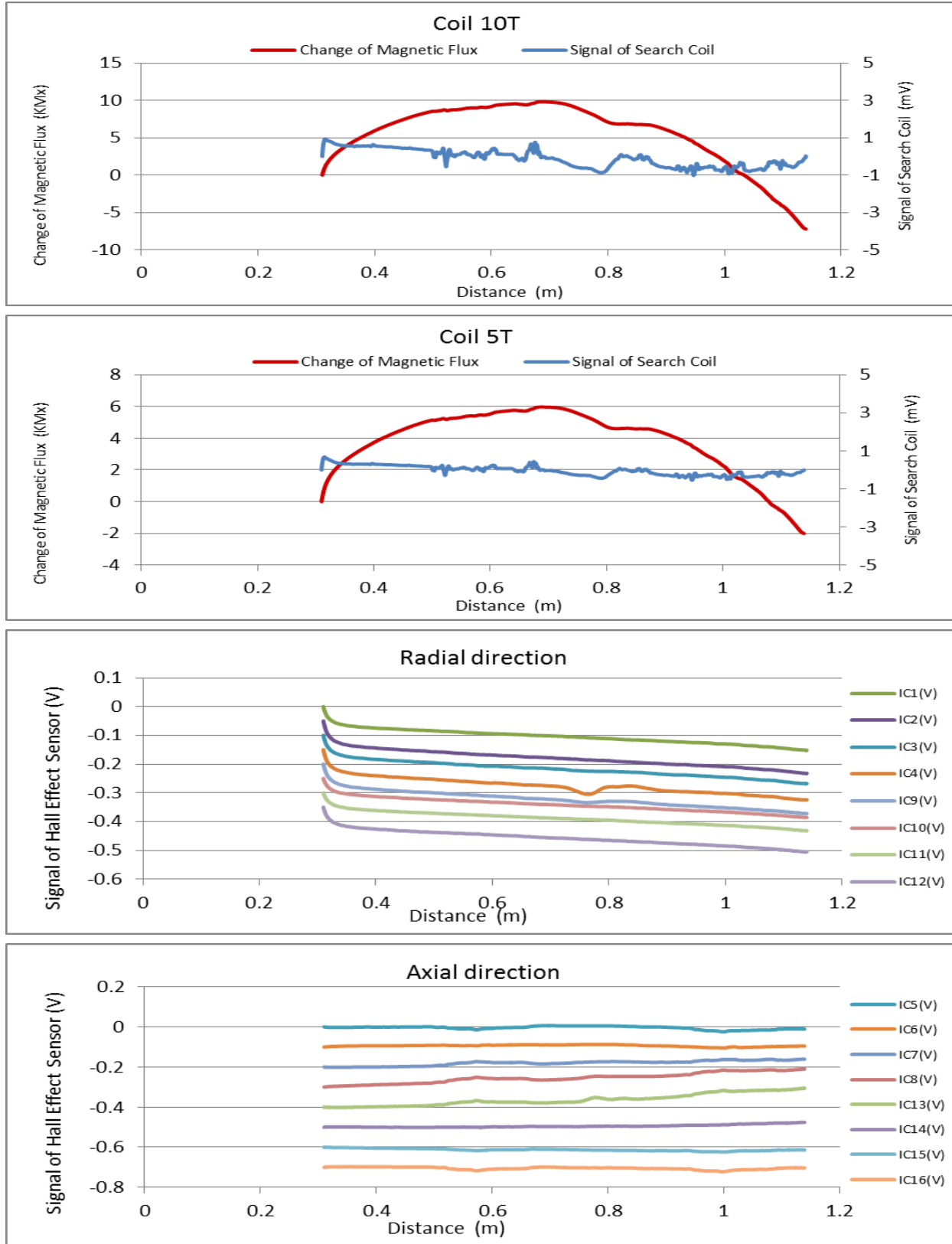


Figure 37. MMFM data for 0.6 percent damage (1 wire cut) of tendon sample #1.



Tokyo Rope USA, Inc.

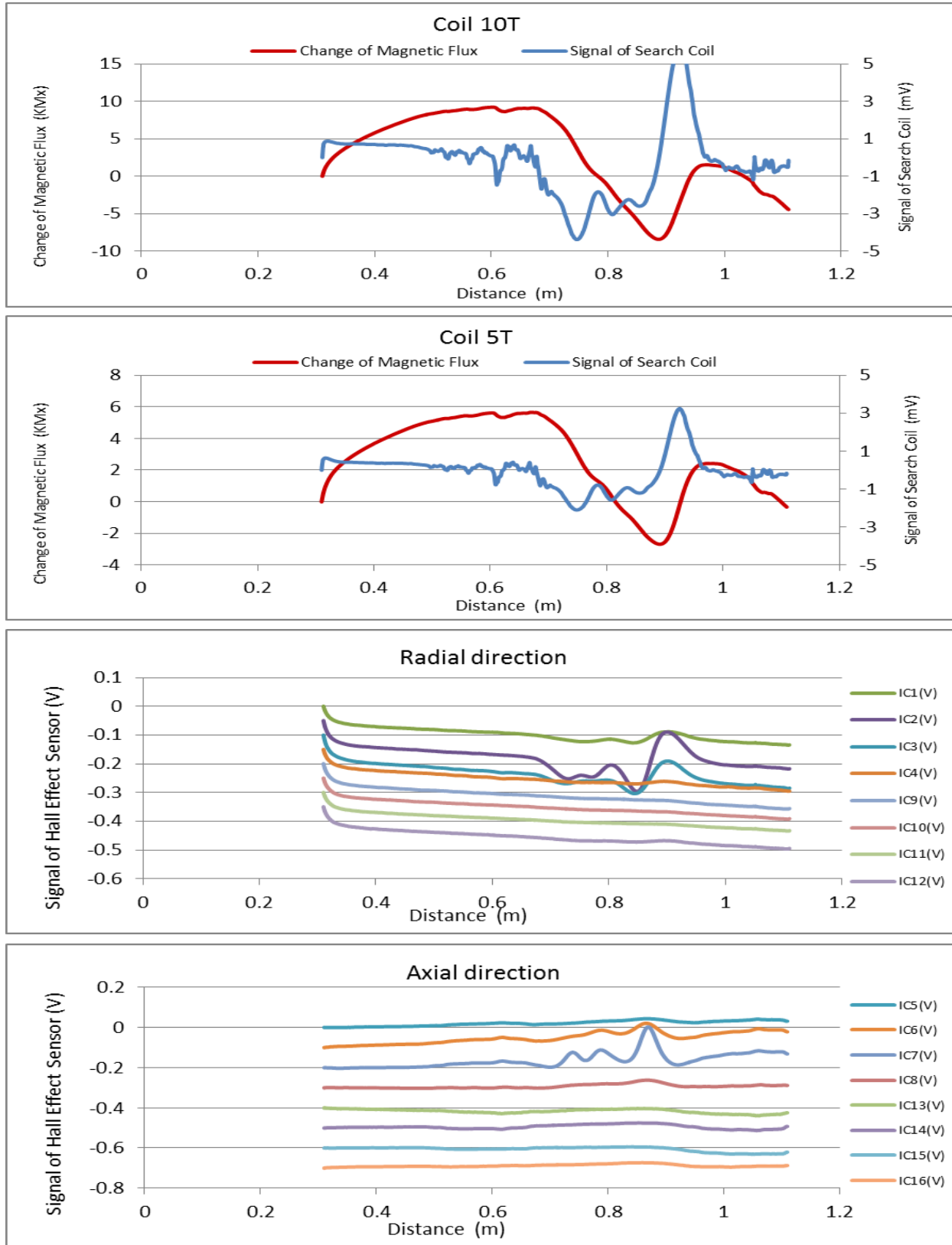


Figure 38. MMFM data for 4.5 percent damage (7 wires cut) of tendon sample #1.

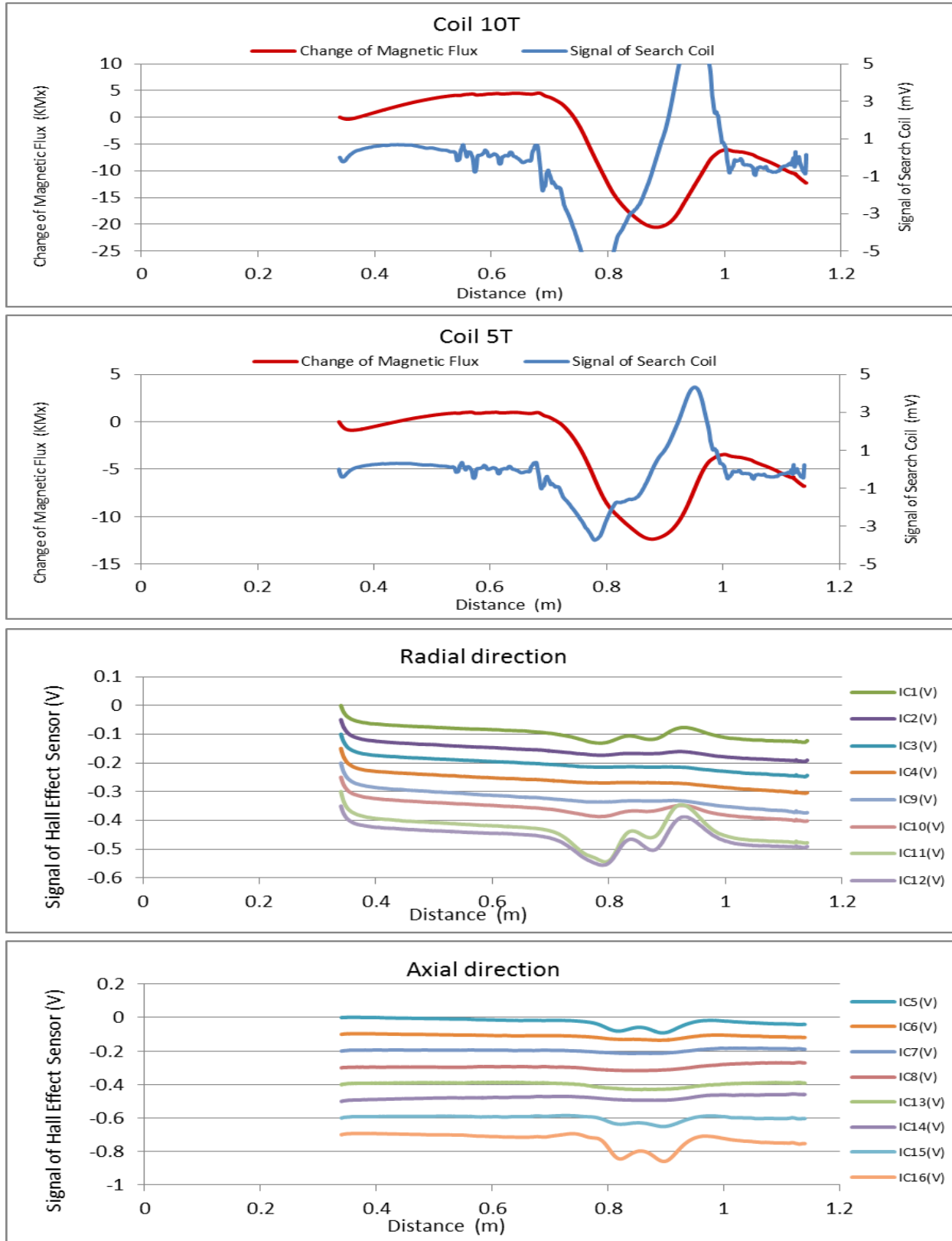


Figure 39. MMFM data for 9.1 percent damage (14 wires cut) of tendon sample #1.



Tokyo Rope USA, Inc.

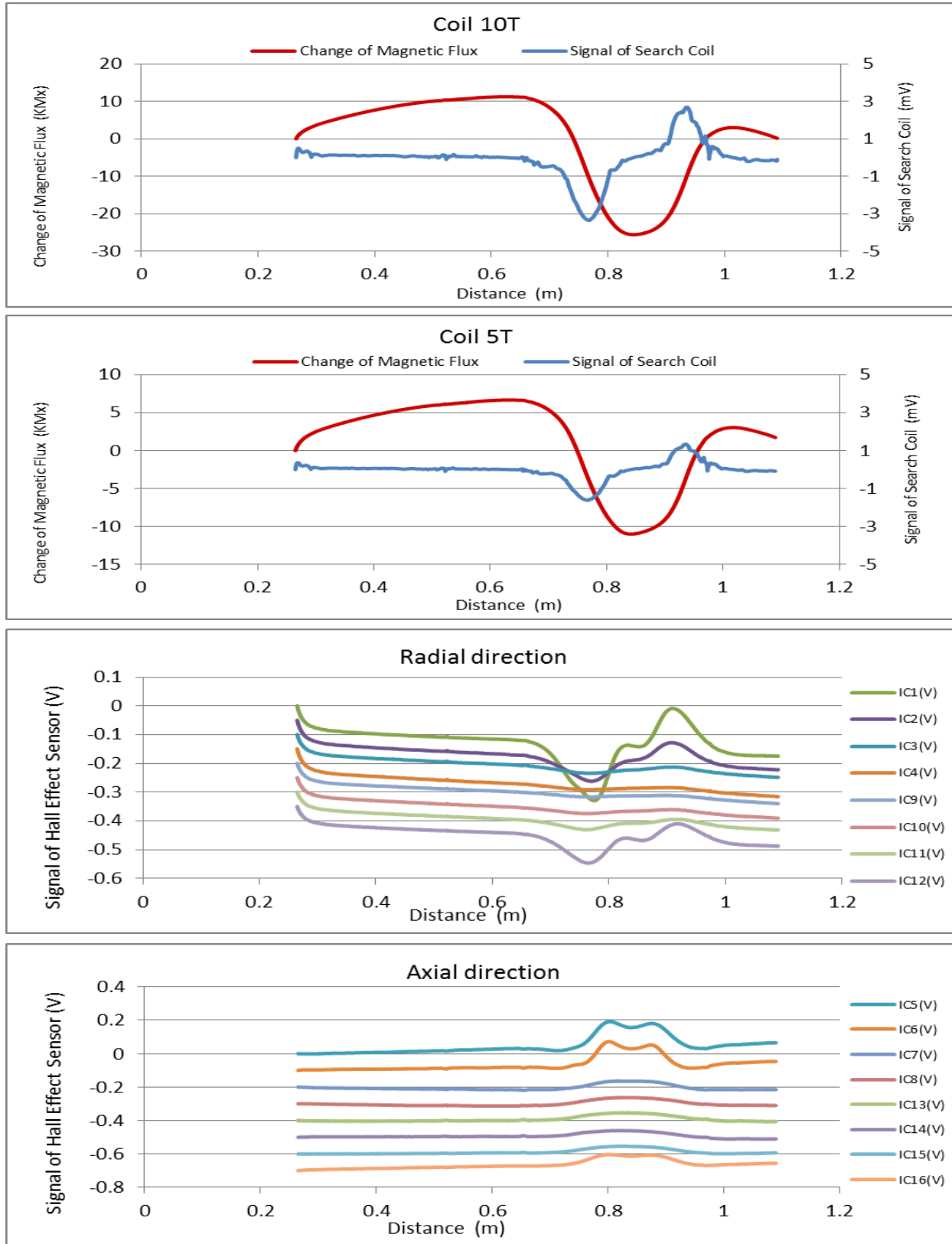


Figure 40. MMFM data for 13.6 percent damage (21 wires cut) of tendon sample #1.



Tokyo Rope USA, Inc.

It can be seen that these MMFM data reflect progressively increasing defect size by showing augmented signal changes. Based on changes of the magnetic flux (determined by the method illustrated in Figure 33) corresponding to the known section loss values, two calibration charts can be constructed as shown in Figure 41 and Figure 42. They show one-to-one relationships between section loss and change of magnetic flux sensed with 10-turn and 5-turn search coils, respectively. Both charts also include additional calibration data produced in the laboratory.

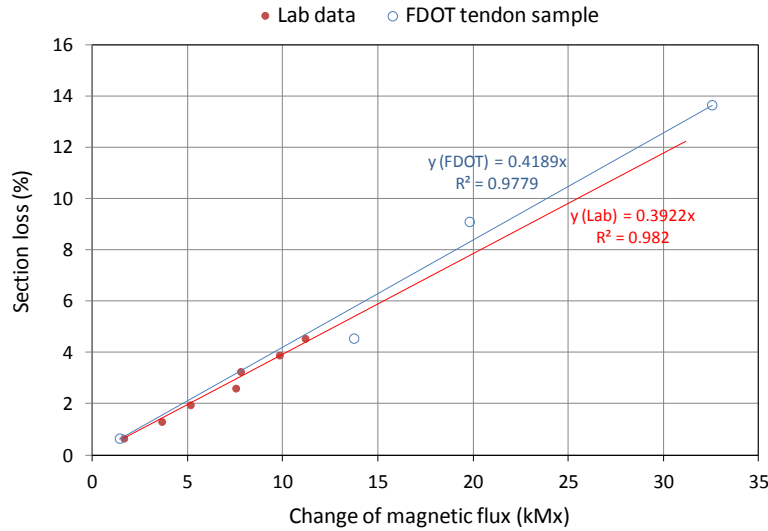


Figure 41. A calibration chart for 10T search coil.

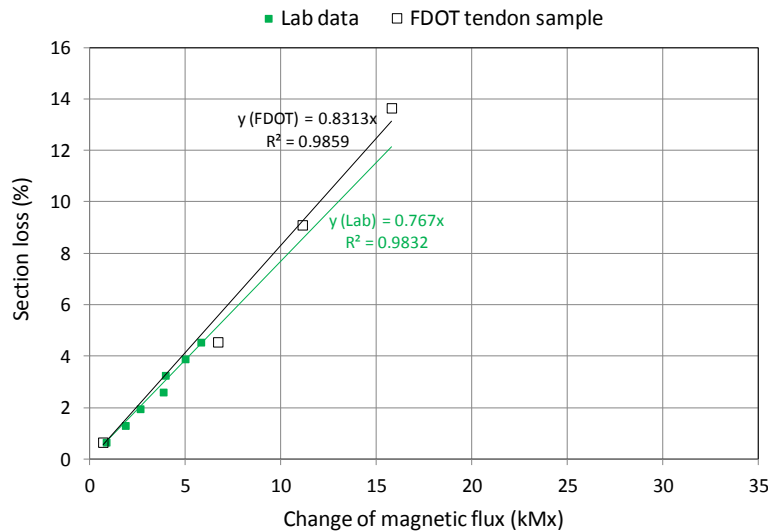


Figure 42. A calibration chart for 5T search coil.

Linear regression analysis results indicate that the calibration charts are accurate evidenced by high coefficient of determination (R^2) values and there is a reasonable agreement between the FDOT tendon sample data and the laboratory data in each chart. As shown in Figure 42, 5-turn search coil can handle larger flux changes and thus detect up to twice larger defect size compared to the 10-turn one.



MMFM Data and Autopsy of Tendon Sample #2

A very small section loss (estimated to be 0.3percent) was detected in an area between 16 and 22 inches (0.41 - 0.56 m) in the sample #2. Figure 43 shows the MMFM data of the sample #2.

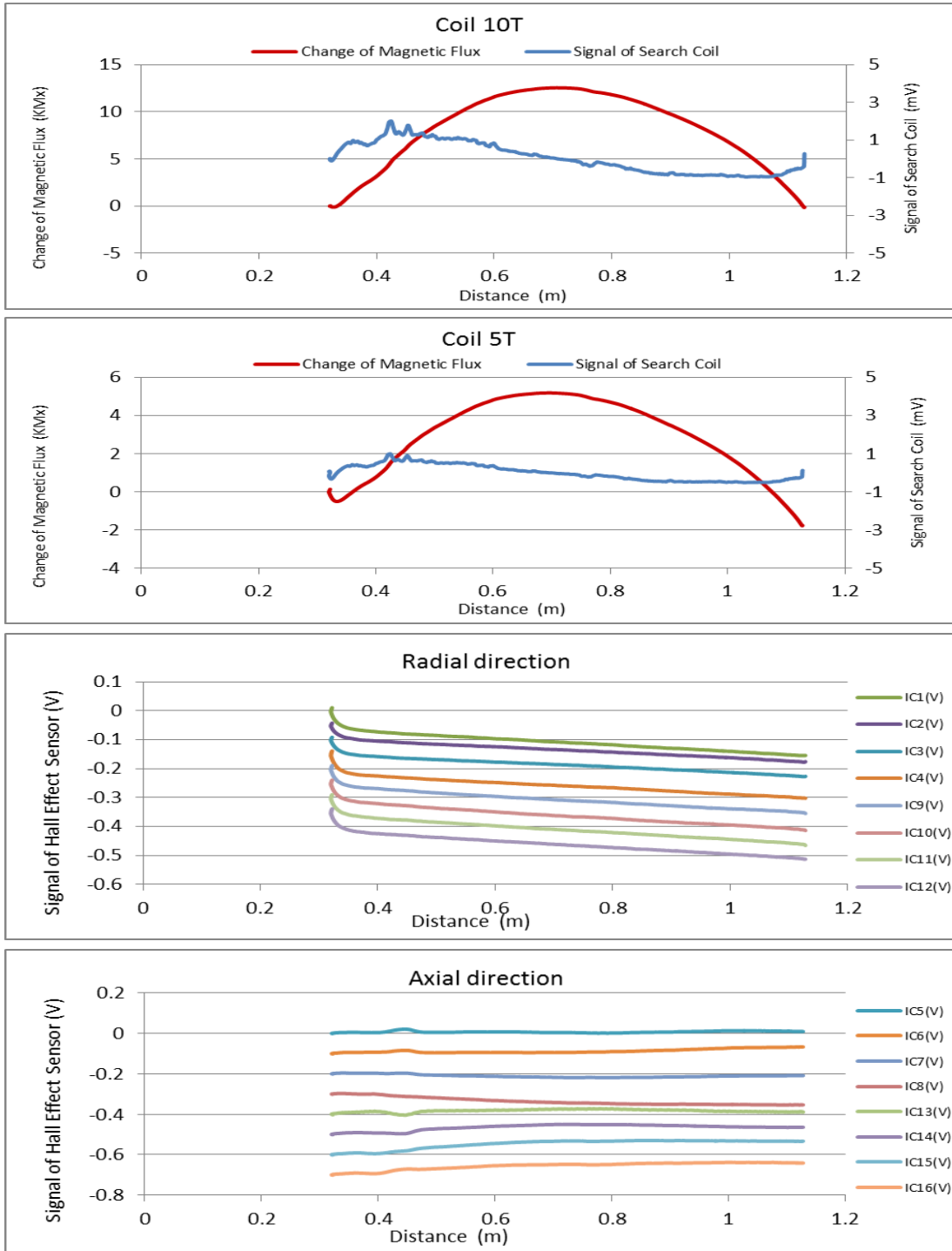


Figure 43. MMFM Data of tendon sample #2.



Tokyo Rope USA, Inc.

Upon reviewing the data, a 6-inch duct section was removed at the Manatee Operation Center to reveal the suspected area of damage. Figure 44 and Figure 45 show the exposed conditions soon after the duct was removed. When grout was partially removed, corrosion was apparent on the bottom side (Figure 45) compared to minor corrosion appeared on the top side (Figure 44). Even though 0.3 percent section loss is insignificant for naked eyes, none of the exposed strands appeared to contain the recognizable damage.

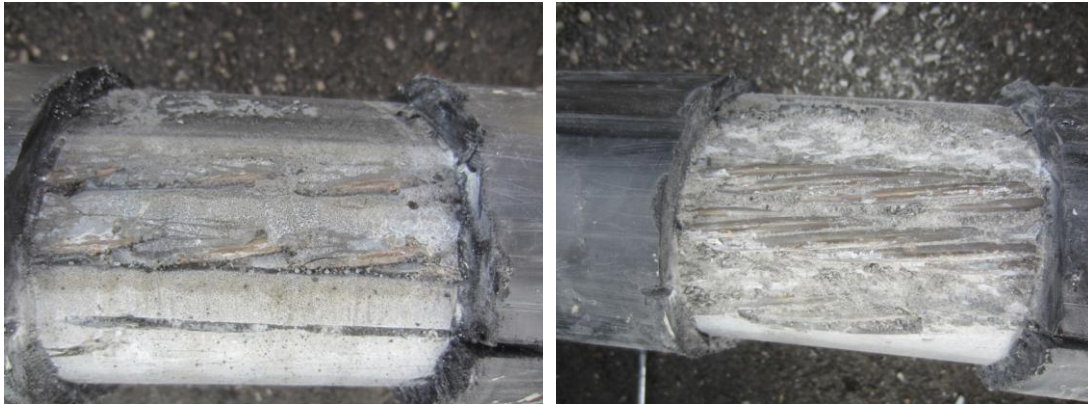


Figure 44. Front face of the suspected damage area as exposed (left) and after grout layer was partially removed (right).



Figure 45. Back face of the suspected damage area as exposed (left) and after grout layer was partially removed (right).

A further autopsy was performed in the laboratory to document strand condition after the entire sample #2 was dismantled. Figure 46 and Figure 47 show the sample condition before and after a full autopsy was performed, respectively.



Figure 46. Tendon sample #2 before full autopsy.



Tokyo Rope USA, Inc.

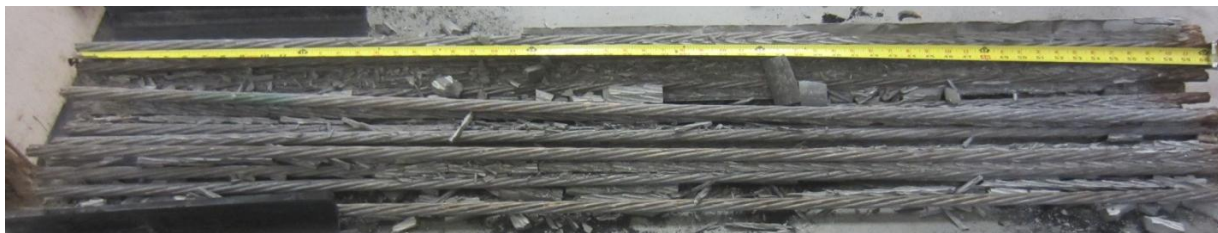


Figure 47. Tendon sample #2 after full autopsy.

None of 22 strands including the initially suspected damage area exhibited noticeable damage. From the autopsy result, it was learned that detecting small section loss with the permanent magnet type MMFM system was difficult. Even though the calibration data generated with controlled artificial damage support the lowest detection limit of 0.65 percent section loss, the official minimum detection limit of the permanent magnet type may be a higher value. Considering inherent various test conditions encountered in the field, 2.0 percent limit can be the threshold for the permanent magnet type MMFM system. Once more laboratory and field data are accumulated, more refined detection limit can be established.

Figure 48 shows three strands that appeared to be in the worst condition. When they were cleaned with a scrubbing pad, superficial corrosion was revealed.



Figure 48. Representative conditions of rusted strands.



Scan Results of Field Tendon Sections

A total of 175 tendon sections were scanned in the entire center cells on the bridge. Table 1 summarizes the scan results in terms of scan ID, tendon section ID, starting/ending points, center position/length of the identified damage, estimated section loss, and damage orientation. In addition, 46 tendon sections were also scanned in the left and right cells in P8 – P9 and P9 – P10 spans. Their scan results are summarized similarly in Table 2. The information in the tables is organized by the scan sequence. The replaced tendon sections (marked as ‘new’) were not tested due to their young age. The exact location of each scanned tendon section can be found in the schematic tendon arrangement diagrams provided in Appendix 1.

None of the MMFM data indicated 3.0 percent and larger section loss. Considering previous corrosion problems associated with this bridge, the absence of noticeable corrosion damage suggested by the present NDE technology is a very encouraging finding. For the purpose of validating the NDE data, four tendon sections containing 1.2 to 1.5 percent section losses are recommended for excavation and they are highlighted in green in Table 1 and Table 2. Interestingly, 21 tendon sections were estimated to have increased cross-sectional areas, instead of section loss. It might be caused by some foreign metal pieces installed in the duct prior to grouting. One of these sections showing 2.2 percent section increase is also recommended for excavation to investigate the cause. Figure 49 through Figure 53 show the MMFM data of five tendon sections recommended for destructive verification. Their opening locations are indicated by green dash lines in the figures.



Tokyo Rope USA, Inc.

Table 1. Summary of Scan Results in Center Cells

Scan ID	Pier ID-Tendon ID-Section ID	Section Length (m)	Scanned Length		Identified Damage			
			Starting Point (m)	Ending Point (m)	Center of Damage (m)	Length of Damage (m)	Estimated Section Loss (%)	Damage Orientation (Clock Position)
1	P1-401R-H1	20.8	0.6	20.5	11.7	1.7	1.5	Unknown
2	P1-402R-I1	20.5	0.6	19.1	18.12	0.2	-4.11	Unknown
3	P1-401L-H1	20.5	0.6	20.3	—	—	—	—
4	P1-402L-I1	20.4	0.6	18.9	10.3	2.8	2.7	Unknown
5	P1-401R-H2	21.7	0.2	21.1	—	—	—	—
6	P1-402R-I2	21.5	0.6	20.7	—	—	—	—
7	P1-401L-H2	21.3	0.1	20.7	—	—	—	—
8	P1-402L-I2	21.2	0.7	20.5	13.8	1.2	1.5	Unknown
9	P1-401R-H3	9.5	0.6	8.9	—	—	—	—
10	P1-402R-H1	9.5	0.6	8.9	—	—	—	—
11	P1-401L-H3	9.5	0.6	8.9	7.8	0.1	-2.4	12 to 2
12	P1-402L-H1	9.5	0.6	8.9	—	—	—	—
13	P2-401R-H1	9.5	0.6	8.8	—	—	—	—
14	P2-402R-H1	9.5	0.6	8.7	—	—	—	—
15	P2-401L-H1	9.4	0.6	8.7	8.2	0.2	-5.0	12 to 1
16	P2-402L-H1	9.4	0.6	8.7	—	—	—	—
17	P2-401R-I1	21.4	0.6	20.6	15.4	0.2	-3.8	8 to 11
18	P2-402R-I1	21.4	0.5	20.7	—	—	—	—
19	P2-401L-I1	21.4	0.6	20.7	—	—	—	—
20	P2-402L-I1	21.4	0.6	20.7	8.2	1.8	2.4	6 to 8
21	P2-401R-I2	21.5	0.7	20.9	—	—	—	—
22	P2-402R-I2	21.5	0.7	20.9	6.9	0.1	-2.3	11 to 1
					14.3	0.2	-1.9	9 to 11
23	P2-401L-I2	21.5	0.7	20.9	—	—	—	—
24	P2-402L-I2	21.5	0.7	20.9	—	—	—	—
25	P2-401R-H2	9.4	0.7	8.8	—	—	—	—



Table 1. Summary of Scan Results in Center Cells (Continued)

Scan ID	Pier ID-Tendon ID- Section ID	Section Length (m)	Scanned Length		Identified Damage			
			Starting Point (m)	Ending Point (m)	Center of Damage (m)	Length of Damage (m)	Estimated Section Loss (%)	Damage Orientation (Clock Position)
26	P2-402R-H2	9.4	0.7	8.8	3.8	1.1	1.7	8 to 11
27	P2-401L-H2	9.4	0.8	8.9	—	—	—	—
28	P2-402L-H2	9.4	0.6	8.8	—	—	—	—
29	P3-401R-H1	9.4	0.6	8.6	—	—	—	—
30	P3-402R-H1	9.4	0.6	8.6	—	—	—	—
31	P3-401L-H1	9.5	0.6	8.7	—	—	—	—
32	P3-402L-H1	9.5	0.6	8.7	4.5	0.3	-1.5	1 to 4
33	P3-401R-I1	21.5	0.6	20.9	—	—	—	—
34	P3-402R-I1	21.5	0.6	20.8	—	—	—	—
35	P3-401L-I1	21.5	0.5	20.7	—	—	—	—
36	P3-402L-I1	21.5	1.6	20.7	—	—	—	—
37	P3-401R-I2	21.5	0.7	21.0	—	—	—	—
38	P3-402R-I2	21.5	0.7	20.9	—	—	—	—
39	P3-401L-I2	21.6	0.5	21.1	—	—	—	—
40	P3-402L-I2	21.6	0.5	21.2	—	—	—	—
41	P3-401R-H2	9.5	1.0	8.8	—	—	—	—
42	P3-402R-H2	9.5	0.7	8.9	—	—	—	—
43	P3-401L-H2	9.5	0.8	8.9	—	—	—	—
44	P3-402L-H2	9.5	0.8	9.0	—	—	—	—
45	P4-401R-H1	9.4	0.6	8.7	—	—	—	—
46	P4-402R-H1	9.4	0.6	8.6	3.5	0.7	1.7	12 to 3
47	P4-401L-H1	9.4	0.6	8.7	—	—	—	—
48	P4-402L-H1	9.4	0.5	8.6	5.9	0.9	1.0	12 to 2
49	P4-401R-I1	21.6	0.5	20.7	17.6	0.7	1.2	8 to 11
50	P4-402R-I1	21.6	0.6	20.8	—	—	—	—



Table 1. Summary of Scan Results in Center Cells (Continued)

Scan ID	Pier ID-Tendon ID- Section ID	Section Length (m)	Scanned Length		Identified Damage			
			Starting Point (m)	Ending Point (m)	Center of Damage (m)	Length of Damage (m)	Estimated Section Loss (%)	Damage Orientation (Clock Position)
51	P4-401L-I1	21.5	0.5	20.6	—	—	—	—
49	P4-401R-I1	21.6	0.5	20.7	17.6	0.7	1.2	8 to 11
50	P4-402R-I1	21.6	0.6	20.8	—	—	—	—
51	P4-401L-I1	21.5	0.5	20.6	—	—	—	—
52	P4-402L-I1	21.5	0.5	20.8	—	—	—	—
53	P4-401R-I2	21.5	0.7	20.9	19.8	0.1	-1.8	2 to 4
54	P4-402R-I2	21.5	0.7	20.9	—	—	—	—
55	P4-401L-I2	21.5	0.8	20.9	9.1	0.2	-2.2	12 to 2
56	P4-402L-I2	21.5	0.7	20.9	—	—	—	—
57	P4-401R-H2	9.4	0.7	8.8	—	—	—	—
58	P4-402R-H2	9.4	0.8	8.8	—	—	—	—
59	P4-401L-H2	9.4	0.8	8.9	—	—	—	—
60	P4-401L-H2	9.4	0.8	8.8	3.3	0.8	1.0	1 to 4
61	P5-401R-H1	9.4	0.6	8.8	—	—	—	—
62	P5-402R-H1	9.4	0.6	8.5	—	—	—	—
63	P5-303R-I1	9.6	0.6	9.2	—	—	—	—
64	P5-401L-H1	9.3	0.7	8.5	—	—	—	—
65	P5-402L-H1	9.3	0.7	8.4	7.5	1.4	1.3	8 to 11
66	P5-303L-I1	9.4	0.5	9.0	—	—	—	—
67	P5-401R-I1	21.5	0.9	20.6	2.3	0.6	1.4	3 to 9
68	P5-402R-I1	21.5	1.6	20.8	2.4	0.1	-2.8	6 to 10
					18.8	0.6	1.2	7 to 11
69	P5-303R-I2	21.6	0.4	21.3	—	—	—	—
	P5-303R-I2-1		0.4	14.3	—	—	—	—
	P5-303R-I2-2		14.9	21.3	—	—	—	—
70	P5-401L-I1	21.5	0.7	20.7	9.6	0.1	-1.7	6 to 9



Table 1. Summary of Scan Results in Center Cells (Continued)

Scan ID	Pier ID-Tendon ID- Section ID	Section Length (m)	Scanned Length		Identified Damage			
			Starting Point (m)	Ending Point (m)	Center of Damage (m)	Length of Damage (m)	Estimated Section Loss (%)	Damage Orientation (Clock Position)
71	P5-402L-I1	21.5	0.6	20.6	4.0	0.2	-3.0	5 to 7
					12.2	0.4	-3.1	10 to 12
72	P5-303L-I2	21.7	0.2	21.3	—	—	—	—
73	P5-401R-I2	21.5	0.8	20.9	—	—	—	—
74	P5-402R-I2	21.5	0.8	20.8	—	—	—	—
75	P5-303R-I3	21.6	0.3	21.3	—	—	—	—
76	P5-401L-I2	21.4	0.7	20.8	—	—	—	—
77	P5-402L-I2	21.4	0.9	20.9	—	—	—	—
78	P5-303L-I3	21.6	0.3	21.3	—	—	—	—
79	P5-401R-H2	9.4	0.7	8.9	—	—	—	—
80	P5-402R-H2	9.4	0.7	8.8	—	—	—	—
81	P5-303R-I4	9.5	0.3	9.0	—	—	—	—
82	P5-401L-H2	9.4	0.8	8.7	—	—	—	—
83	P5-402L-H2	9.4	0.8	8.7	—	—	—	—
84	P5-303L-I4	9.6	0.3	8.6	5.8	0.2	-2.2	4 to 7
85	P6-401R-H1	9.4	0.7	8.7	—	—	—	—
86	P6-402R-H1	9.4	0.7	8.7	—	—	—	—
87	P6-401L-H1	9.4	0.5	8.6	—	—	—	—
88	P6-402L-H1	9.4	0.6	8.7	—	—	—	—
89	P6-401R-I1	21.5	0.7	20.4	—	—	—	—
90	P6-402R-I1	21.5	0.8	20.5	—	—	—	—
91	P6-401L-I1	21.4	0.6	20.7	—	—	—	—
92	P6-402L-I1	21.4	0.6	20.6	—	—	—	—
93	P6-401R-I2	31.3	2.2	30.7	—	—	—	—
94	P6-402R-I2	21.5	0.7	20.6	—	—	—	—



Tokyo Rope USA, Inc.

Table 1. Summary of Scan Results in Center Cells (Continued)

Scan ID	Pier ID-Tendon ID- Section ID	Section Length (m)	Scanned Length		Identified Damage			
			Starting Point (m)	Ending Point (m)	Center of Damage (m)	Length of Damage (m)	Estimated Section Loss (%)	Damage Orientation (Clock Position)
95	P6-401L-I2	31.3	2.0	30.7	—	—	—	—
96	P6-402L-I2	31.3	2.1	30.8	—	—	—	—
97	P6-402R-H2	9.4	0.8	8.8	3.7	1.4	1.4	5 to 9
98	P7-401R-H1	9.4	0.5	8.5	—	—	—	—
99	P7-402R-H1	9.4	0.5	7.8	—	—	—	—
100	P7-303R-I1	9.5	2.0	9.2	—	—	—	—
101	P7-401L-H1	9.4	0.5	8.6	—	—	—	—
102	P7-402L-H1	9.4	0.6	8.6	—	—	—	—
103	P7-303L-I1	9.5	0.4	9.2	—	—	—	—
104	P7-401R-I1	21.4	0.5	20.6	—	—	—	—
105	P7-402R-I1	21.4	0.7	20.7	—	—	—	—
106	P7-303R-I2	21.7	0.2	20.8	—	—	—	—
107	P7-401L-I1	21.4	0.7	20.6	—	—	—	—
108	P7-402L-I1	21.4	1.0	20.6	—	—	—	—
109	P7-303L-I2	21.6	0.3	21.3	—	—	—	—
110	P7-401R-I2	21.5	0.9	20.9	—	—	—	—
111	P7-402R-I2	31.4	2.3	31.0	—	—	—	—
112	P7-303R-I3	21.6	0.3	21.3	—	—	—	—
113	P7-401L-I2	21.5	0.8	21.0	11.8	0.2	-2.6	9 to 12
114	P7-402L-I2	21.5	0.7	21.0	15.9	0.2	-2.5	11 to 1
115	P7-303L-I3	21.7	0.3	21.0	—	—	—	—
116	P7-401R-H2	9.4	0.9	8.8	—	—	—	—
117	P7-303R-I4	9.5	0.3	9.1	—	—	—	—
118	P7-401L-H2	9.4	0.7	9.0	—	—	—	—
119	P7-402L-H2	9.4	0.7	8.9	—	—	—	—



Table 1. Summary of Scan Results in Center Cells (Continued)

Scan ID	Pier ID-Tendon ID- Section ID	Section Length (m)	Scanned Length		Identified Damage			
			Starting Point (m)	Ending Point (m)	Center of Damage (m)	Length of Damage (m)	Estimated Section Loss (%)	Damage Orientation (Clock Position)
120	P7-303L-I4	9.5	0.3	9.0	—	—	—	—
121	P8-401R-H1	9.5	0.9	8.7	—	—	—	—
122	P8-402R-I1	31.3	0.4	29.4	—	—	—	—
123	P8-401L-H1	9.5	0.6	8.8	—	—	—	—
124	P8-402L-H1	9.5	0.5	8.7	—	—	—	—
125	P8-401R-I1	21.5	0.6	20.5	—	—	—	—
126	P8-401L-I1	21.5	0.6	20.2	—	—	—	—
127	P8-402L-I1	21.5	0.7	20.2	—	—	—	—
128	P8-401R-I2	21.5	0.7	20.7	—	—	—	—
129	P8-402R-I2	21.5	0.7	20.8	—	—	—	—
130	P8-401L-I2	21.5	0.7	21.0	—	—	—	—
131	P8-402L-I2	21.5	0.7	20.9	—	—	—	—
132	P8-401R-H2	9.3	1.3	8.8	—	—	—	—
133	P8-402R-H1	9.3	1.0	8.9	—	—	—	—
134	P8-401L-H2	9.4	0.6	9.0	—	—	—	—
135	P8-402L-H2	9.4	0.7	8.8	—	—	—	—
136	P9-401R-H1	9.3	0.7	8.7	—	—	—	—
137	P9-402R-H1	9.3	0.8	8.5	—	—	—	—
138	P9-401L-H1	9.3	0.5	8.4	—	—	—	—
139	P9-402L-H1	9.3	0.5	8.4	—	—	—	—
140	P9-401R-I1	21.6	0.6	20.8	9.4	0.3	-0.9	6 to 9
141	P9-402R-I1	21.6	0.6	20.9	—	—	—	—
142	P9-401L-I1	21.5	0.5	20.5	—	—	—	—
143	P9-402L-I1	21.5	0.6	20.8	12.3	3.2	1.6	3 to 9
144	P9-401R-I2	31.3	1.9	30.7	—	—	—	—



Table 1. Summary of Scan Results in Center Cells (Continued)

Scan ID	Pier ID-Tendon ID- Section ID	Section Length (m)	Scanned Length		Identified Damage			
			Starting Point (m)	Ending Point (m)	Center of Damage (m)	Length of Damage (m)	Estimated Section Loss (%)	Damage Orientation (Clock Position)
145	P9-402R-I2	21.5	0.6	20.4	10.3	2.6	1.5	5 to 10
146	P9-401L-I2	21.5	0.5	20.4	—	—	—	—
147	P9-402L-I2	31.3	1.8	30.8	—	—	—	—
148	P9-402R-H2	9.4	1.0	8.9	—	—	—	—
149	P9-401L-H2	9.4	1.5	8.9	3.2	0.1	0.5	11 to 3
150	P10-402R-H1	9.4	0.6	8.6	—	—	—	—
151	P10-401L-H1	9.5	0.6	8.8	—	—	—	—
152	P10-402L-I1	31.4	0.5	29.3	—	—	—	—
153	P10-401R-I1	31.3	0.4	29.2	—	—	—	—
154	P10-401L-I1	21.5	0.6	20.6	6.3	0.2	-3.0	11 to 3
155	P10-402R-I1	21.5	0.5	20.8	—	—	—	—
156	P10-401R-I2	21.4	0.7	20.7	—	—	—	—
157	P10-402R-I2	21.4	0.7	19.9	—	—	—	—
158	P10-401L-I2	21.5	0.7	19.9	—	—	—	—
159	P10-402L-I2	21.5	0.7	19.1	2.1	0.2	-3.4	7 to 10
					9.2	0.2	-3.0	4 to 8
160	P10-401R-H1	9.3	0.6	8.9	—	—	—	—
161	P10-402R-H2	9.3	0.6	8.9	—	—	—	—
162	P10-401L-H2	9.4	0.7	8.9	—	—	—	—
163	P10-402L-H1	9.4	0.8	8.9	—	—	—	—
164	P11-401R-H1	9.4	0.8	8.5	—	—	—	—
165	P11-402R-H1	9.4	0.5	8.5	—	—	—	—
166	P11-402L-H1	9.4	0.5	8.5	—	—	—	—
167	P11-401L-H1	9.4	0.5	8.4	—	—	—	—
168	P11-402R-I1	21.4	0.5	20.5	—	—	—	—



Tokyo Rope USA, Inc.

Table 1. Summary of Scan Results in Center Cells (Continued)

Scan ID	Pier ID-Tendon ID- Section ID	Section Length (m)	Scanned Length		Identified Damage			
			Starting Point (m)	Ending Point (m)	Center of Damage (m)	Length of Damage (m)	Estimated Section Loss (%)	Damage Orientation (Clock Position)
169	P11-401R-I1	21.5	0.5	21.3	—	—	—	—
170	P11-402L-I1	21.6	0.5	21.0	—	—	—	—
171	P11-401L-I1	21.6	0.5	21.4	—	—	—	—
172	P11-402R-I2	28.5	2.6	28.0	15.0	2.5	1.5	10 to 2
173	P11-401R-I2	28.6	0.0	28.1	—	—	—	—
174	P11-402L-I2	28.5	1.9	28.0	7.0	1.6	1.3	3 to 9
					12.4	2.1	1.8	3 to 9
175	P11-401L-I2	28.6	0.0	28.2	—	—	—	—



Table 2. Summary of Scan Results in Left and Right Cells in P8 – P9 and P9 – P10 Spans

Scan ID	Pier ID-Tendon ID-Section ID	Section Length (m)	Scanned Length		Identified Damage			
			Starting Point (m)	Ending Point (m)	Center of Damage (m)	Length of Damage (m)	Estimated Section Loss (%)	Damage Orientation (Clock Position)
176	P9-404L-H1	9.5	0.5	8.7	—	—	—	—
177	P9-403L-H1	9.5	0.4	8.6	—	—	—	—
178	P9-405L-H1	9.4	0.6	8.8	—	—	—	—
179	P9-406L-H1	9.4	0.5	8.7	3.7	1.0	0.8	10 to 4
180	P9-403L-I1	21.5	0.5	20.7	—	—	—	—
181	P9-404L-I1	21.5	0.5	20.8	—	—	—	—
182	P9-405L-I1	21.5	0.4	20.8	—	—	—	—
183	P9-406L-I1	21.5	0.5	20.8	3.9	1.1	1.4	2 to 4
					16.5	0.7	1.2	12 to 3
	P9-403L-I2(new)	Due to new condition, scan was not made.						
184	P9-404L-I2	21.5	0.8	21.0	—	—	—	—
	P9-405L-I2(new)	Due to new condition, scan was not made.						
185	P9-406L-I2	21.5	0.8	14.4	—	—	—	—
186	P9-404L-H2	9.4	0.6	8.8	—	—	—	—
187	P9-406L-H2	9.4	0.7	8.8	—	—	—	—
188	P9-406R-H2	9.4	0.6	9.0	—	—	—	—
189	P9-405R-H2	9.4	0.7	8.9	—	—	—	—
190	P9-404R-H2	9.4	0.7	9.0	—	—	—	—
191	P9-403R-H2	9.4	0.8	8.9	5.2	0.6	0.8	7 to 1
192	P9-406R-I2	21.5	0.5	19.4	—	—	—	—
193	P9-405R-I2	21.5	0.5	21.0	18.4	1.3	1.5	10 to 4
194	P9-404R-I2	21.5	0.5	21.0	—	—	—	—
195	P9-403R-I2	21.5	0.6	20.9	7.2	0.2	-2.4	6 to 9
					12.5	0.4	-3.9	6 to 9
196	P9-406R-I1	21.5	0.4	20.7	11.6	3.3	1.1	11 to 4
197	P9-405R-I1	21.5	0.4	20.7	—	—	—	—



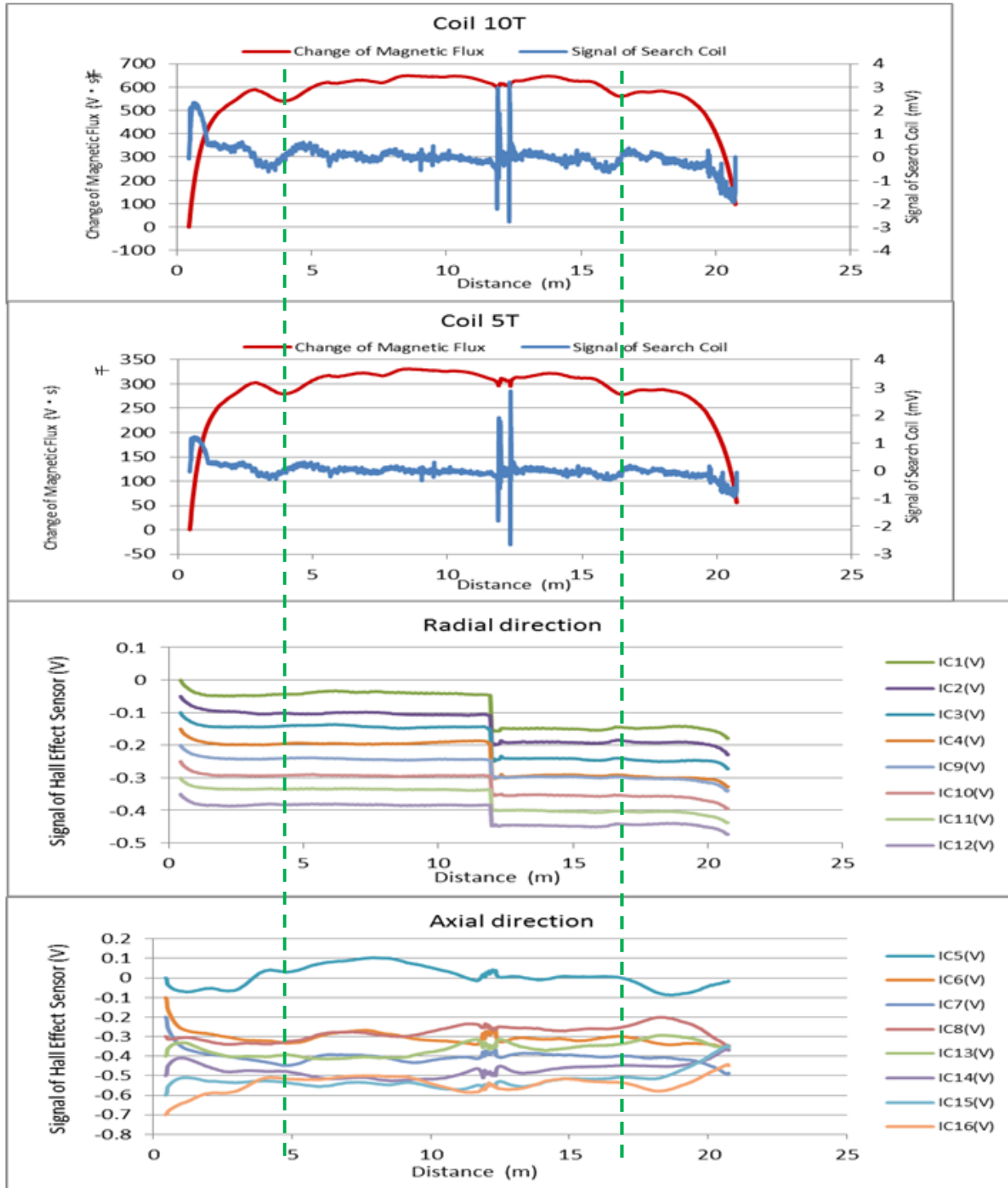
Tokyo Rope USA, Inc.

**Table 2. Summary of Scan Results in Left and Right Cells in P8 – P9 and P9 – P10 Spans
(Continued)**

Scan ID	Pier ID-Tendon ID- Section ID	Section Length (m)	Scanned Length		Identified Damage			
			Starting Point (m)	Ending Point (m)	Center of Damage (m)	Length of Damage (m)	Estimated Section Loss (%)	Damage Orientation (Clock Position)
198	P9-404R-I1	21.4	0.4	20.8	1.3	0.1	-2.2	6 to 12
199	P9-403R-I1	21.5	0.4	20.9	—	—	—	—
200	P9-403R-H1	9.3	1.5	8.1	—	—	—	—
201	P9-404R-H1	9.3	0.5	8.5	—	—	—	—
202	P9-405R-H1	9.3	0.5	8.5	—	—	—	—
203	P9-406R-H1	9.3	0.8	8.6	—	—	—	—
204	P8-406R-H2	9.4	0.8	8.8	—	—	—	—
205	P8-405R-H2	9.4	0.6	8.8	—	—	—	—
206	P8-404R-H1	9.4	0.6	8.9	—	—	—	—
207	P8-403R-H2	9.4	0.6	8.9	—	—	—	—
208	P8-406R-I2	21.4	0.7	20.6	—	—	—	—
209	P8-405R-I2	21.4	0.6	21.0	3.3	0.3	-3.1	6 to 10
210	P8-404R-I2	21.4	0.7	20.6	—	—	—	—
211	P8-403R-I2	21.4	0.7	20.6	—	—	—	—
212	P8-406R-I1	21.4	0.4	20.4	16.8	1.0	1.0	4 to 10
213	P8-405R-I1	21.4	0.4	20.4	14.9	1.7	1.3	10 to 4
214	P8-403R-I1	21.4	0.5	20.4	—	—	—	—
215	P8-406R-H1	9.3	0.5	8.5	—	—	—	—
216	P8-405R-H1	9.3	0.4	8.5	—	—	—	—
217	P8-403R-H1	9.3	0.5	8.6	2.6	0.8	1.5	10 to 12
	P8-404?R-I1 (new)	Due to new condition, scan was not made.						
218	P8-403L-H1	9.4	0.7	8.7	—	—	—	—
219	P8-404L-H1	9.4	0.6	8.8	2.6	0.6	0.7	10 to 1
220	P8-405L-H1	9.5	0.5	8.8	—	—	—	—
221	P8-406L-H1	9.5	0.4	8.8	—	—	—	—



Tokyo Rope USA, Inc.

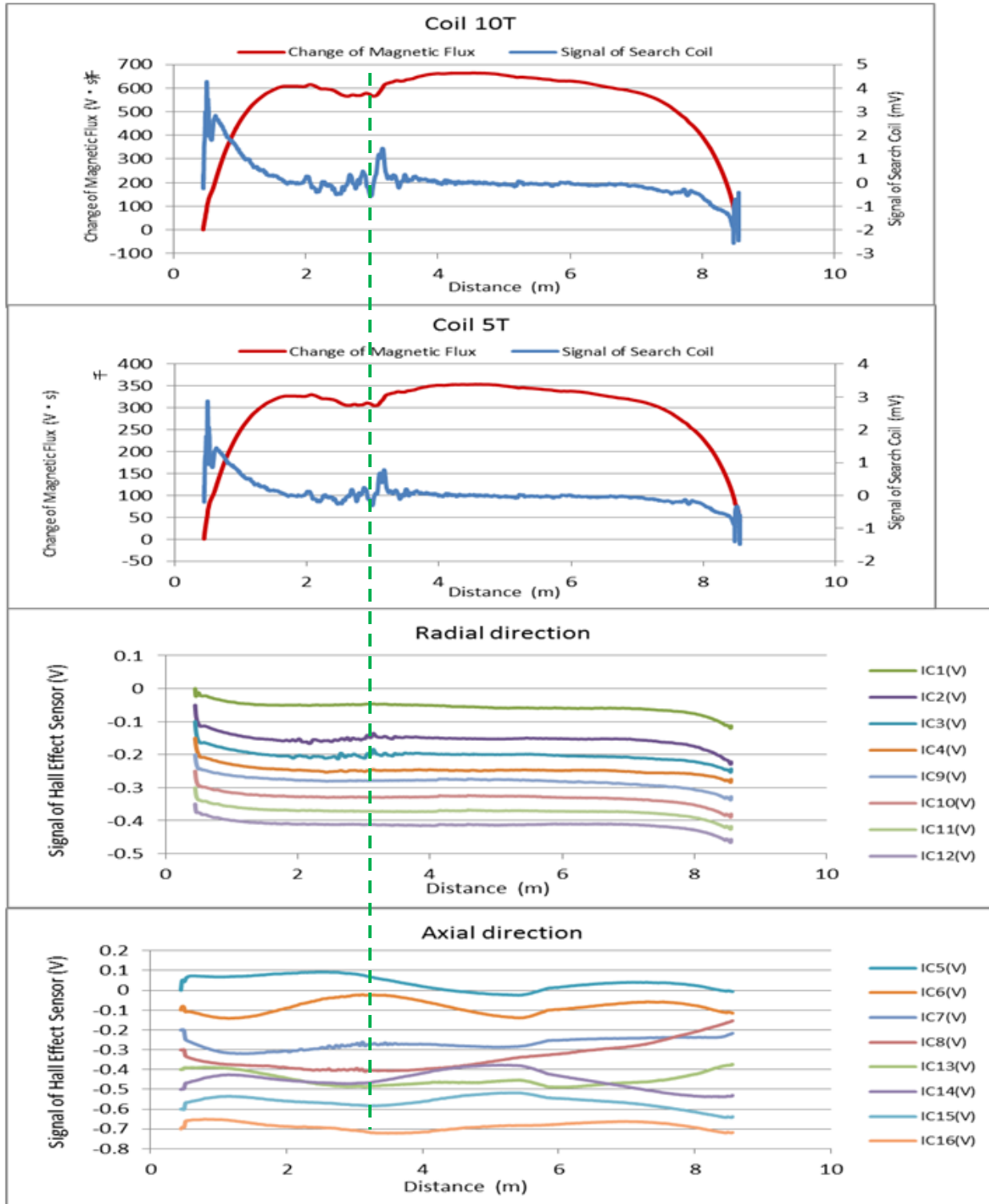


* Coil 10T = search coil 10 Turns; Coil 5T = search coil 5 Turns.

Figure 49. MMFM data for P9-406L-I1 (estimated section loss = 1.4 and 1.2 percent).



Tokyo Rope USA, Inc.

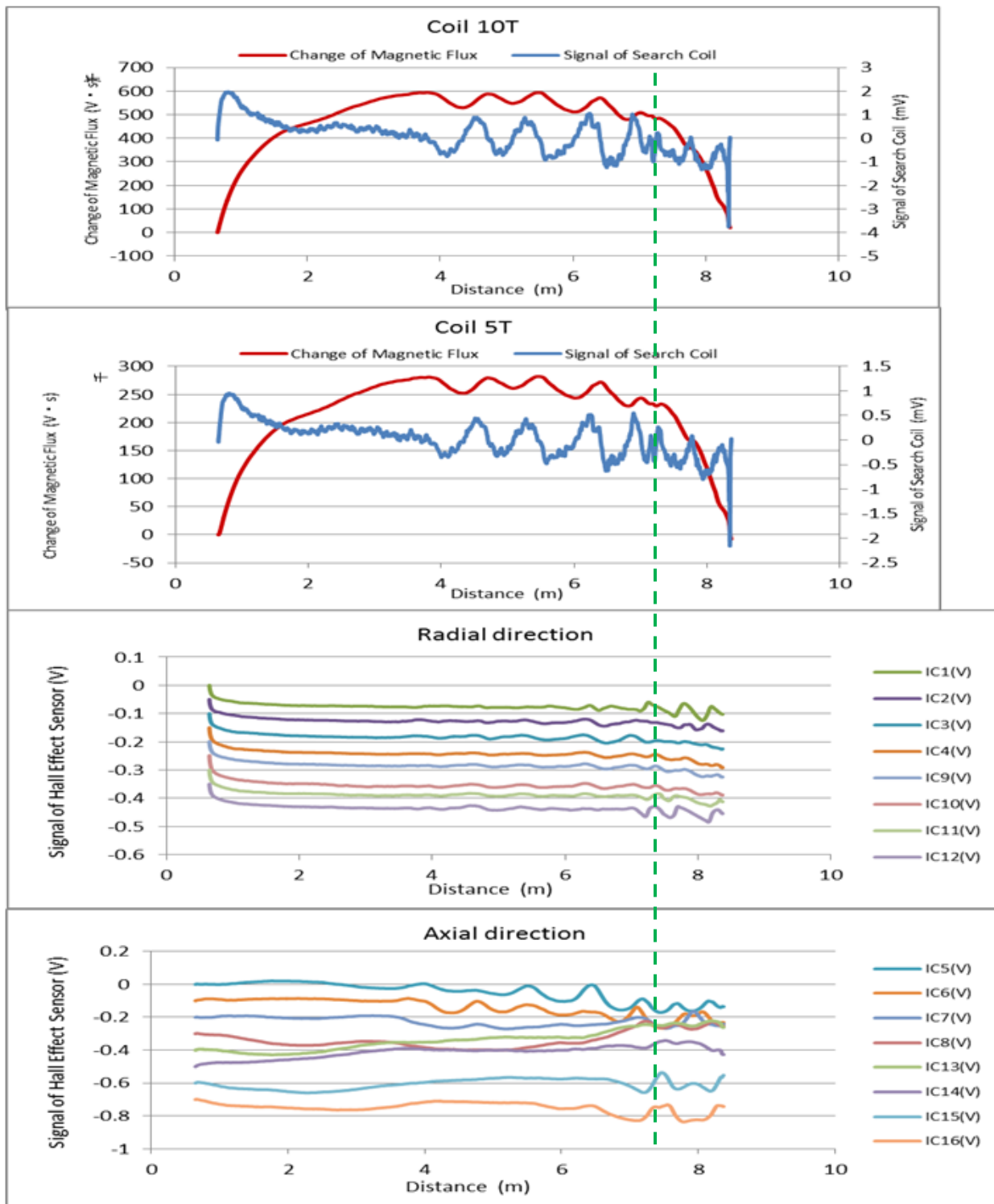


* Coil 10T = search coil 10 Turns; Coil 5T = search coil 5 Turns.

Figure 50. MMFM data for P8-403R-H1 (estimated section loss = 1.5 percent).



Tokyo Rope USA, Inc.

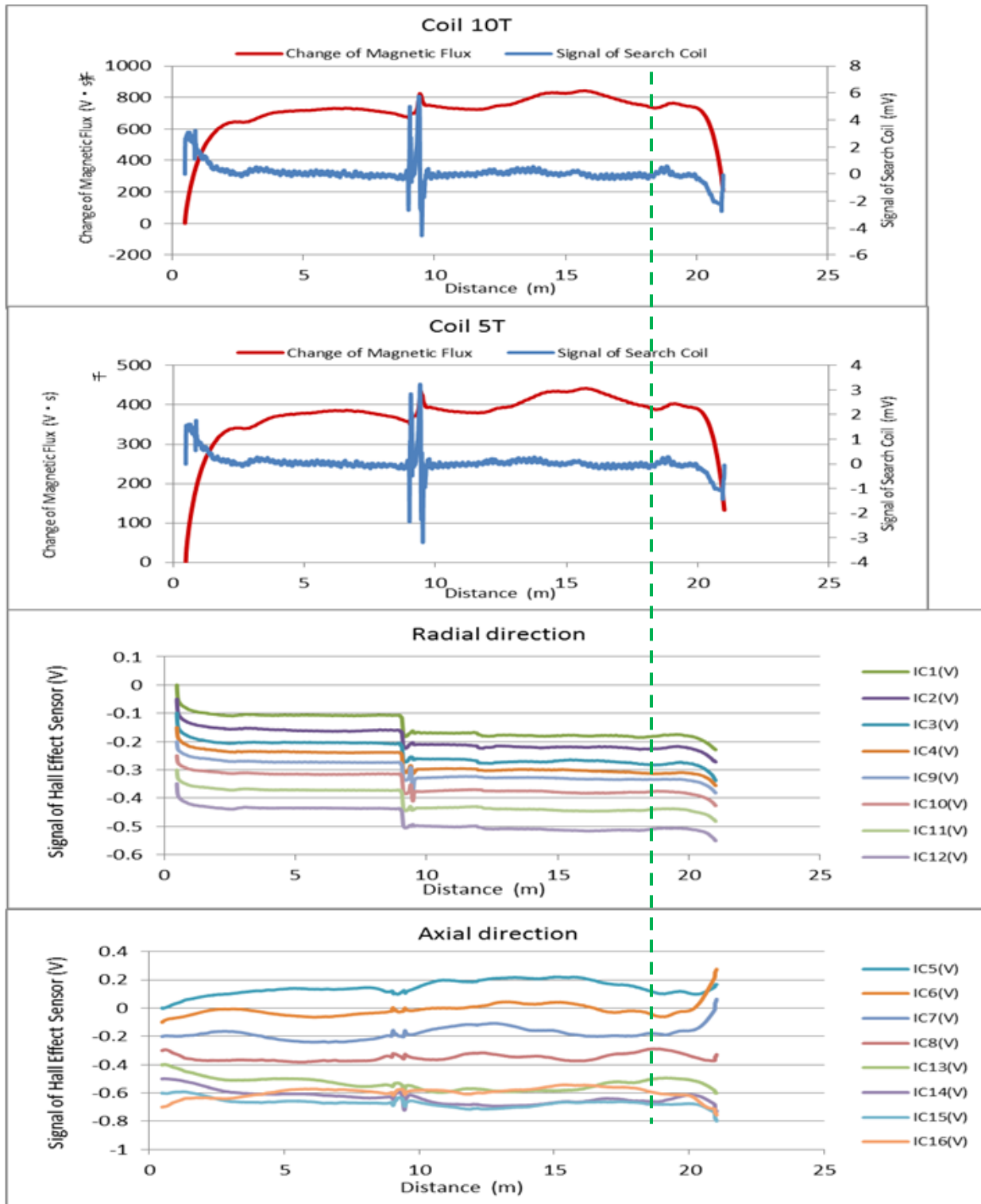


* Coil 10T = search coil 10 Turns; Coil 5T = search coil 5 Turns.

Figure 51. MMFM data for P5-402L-H1 (estimated section loss = 1.3 percent).



Tokyo Rope USA, Inc.

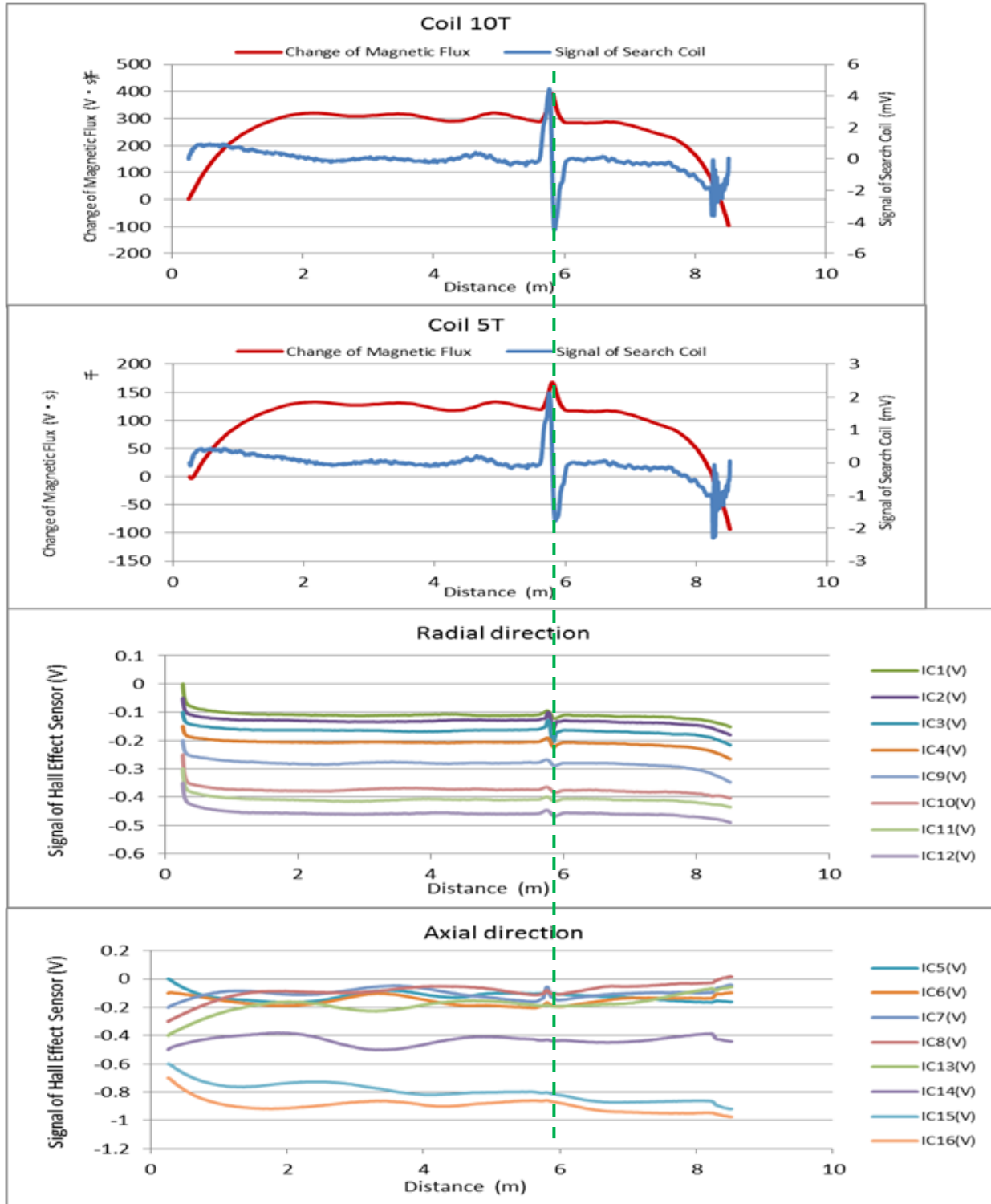


* Coil 10T = search coil 10 Turns; Coil 5T = search coil 5 Turns.

Figure 52. MMFM data for P9-405L-I2 (estimated section loss = 1.5 percent).



Tokyo Rope USA, Inc.



* Coil 10T = search coil 10 Turns; Coil 5T = search coil 5 Turns.

Figure 53. MMFM data for P5-303L-I4 (estimated section increase = 2.2 percent).



Tokyo Rope USA, Inc.

CONCLUSIONS

Based on the analysis results of field MMFM data collected from 217 tendon sections, the following conclusions are made:

1. Overall condition of the scanned tendon sections is judged to be good with no immediate maintenance actions required at the time of measurement.
2. None of the scanned tendon sections exhibited any indication of having larger than 3.0 percent section loss which is equivalent to losing 66 percent of the nominal cross-sectional area of one 0.6-inch strand out of all 22 strands.
3. Only two test sections contained larger than 2.0 percent section loss. Other 29 sections contained minor damage ranging from 0.5 to 1.8 percent section loss. Tokyo Rope NDE team recommends that FDOT open and examine five tendon sections including one with the increased sectional area.

REFERENCES

1. Federal Highway Administration, "Transportation System Preservation Research, Development, and Implementation Roadmap," <https://www.pavementpreservation.org/fhwa-resources/tsp-research-roadmap/>, January 2008.
2. Masamichi Sugahara et al., "Non-Destructive Evaluation of Bridge Cables and Strands Using the Magnetic Main Flux Method (MMFM)," Conference Proceedings at 2010 FHWA Bridge Engineering Conference: Highways for LIFE and Accelerated Bridge Construction" in Orlando, Florida, April 8-9, 2010.
3. Kingsley Lau, Ivan Lasa, and Mario Paredes, "Corrosion Development of Pt Tendons with Deficient Grout: Corrosion Failure In Ringling Causeway Bridge," Draft Report, Florida Department of Transportation, December 201

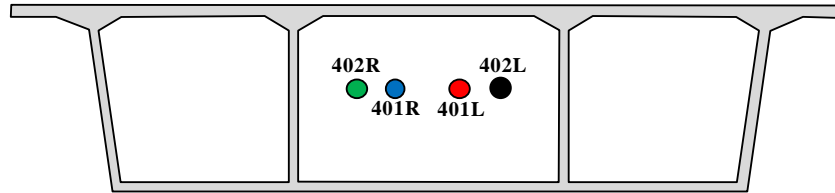


Tokyo Rope USA, Inc.

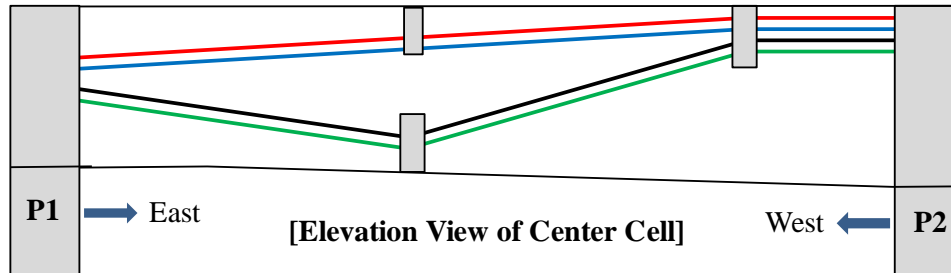
APPENDIX 1. Schematic Diagrams of Scanned Tendon Sections



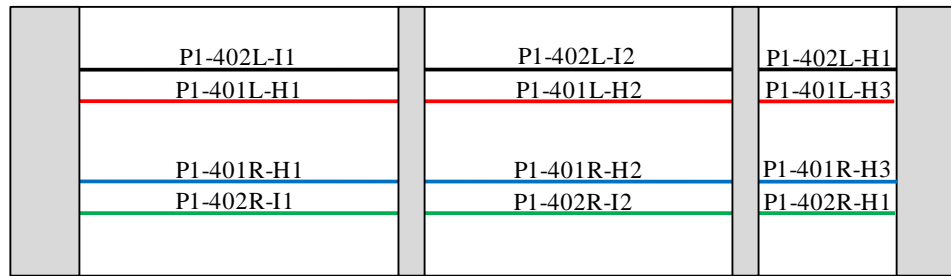
Tokyo Rope USA, Inc.



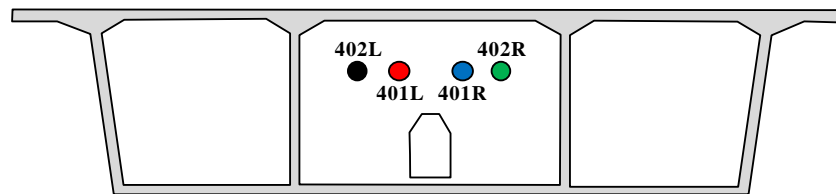
[Diaphragm: East Face at Pier 1 (Abutment)]



[Elevation View of Center Cell]



[Plan View of Center Cell]

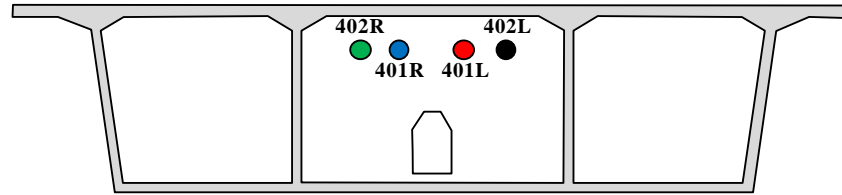


[Diaphragm: West Face at Pier 2]

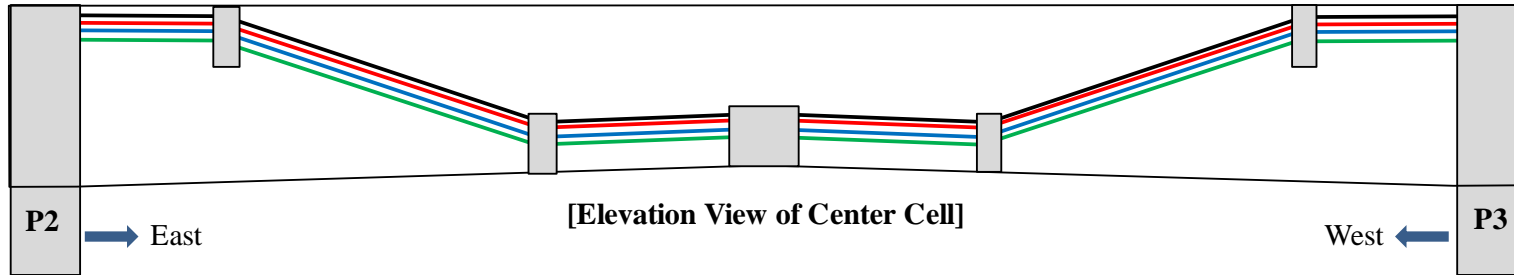
Figure A1. Scanned tendon sections in P1 – P2 (center cell).



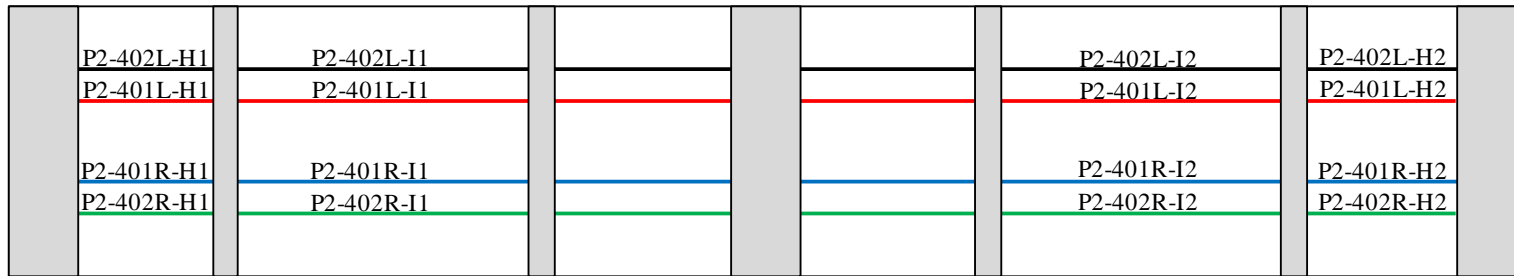
Tokyo Rope USA, Inc.



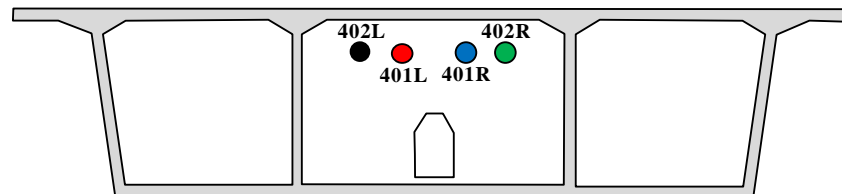
[Diaphragm: East Face at Pier 2]



[Elevation View of Center Cell]



[Plan View of Center Cell]

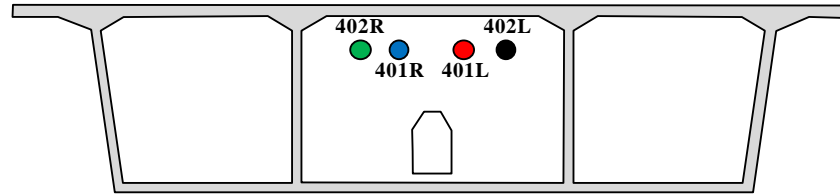


[Diaphragm: West Face at Pier 3]

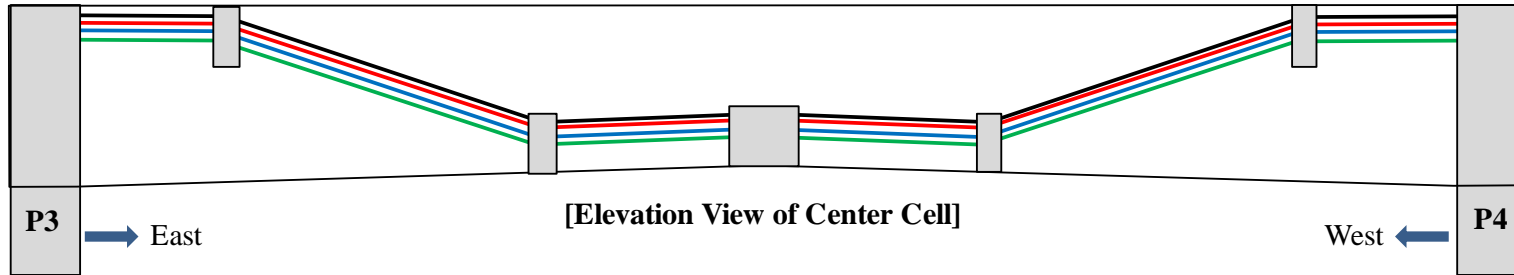
Figure A2. Scanned tendon sections in P2 – P3 (center cell).



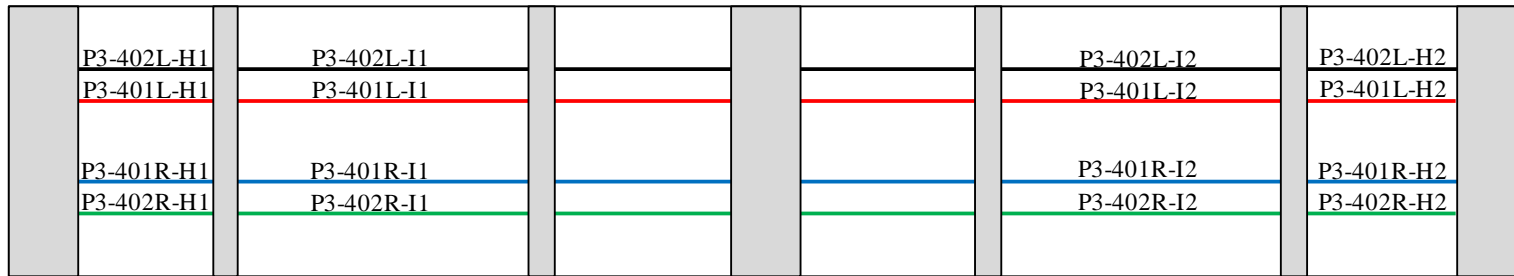
Tokyo Rope USA, Inc.



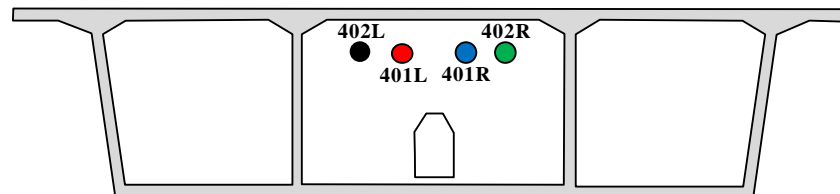
[Diaphragm: East Face at Pier 3]



[Elevation View of Center Cell]



[Plan View of Center Cell]

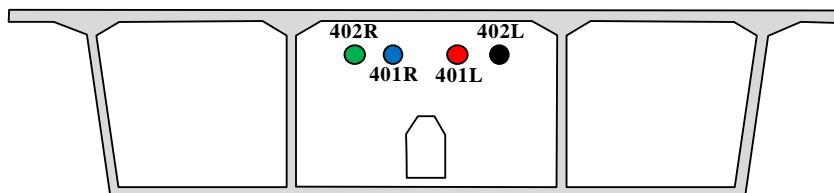


[Diaphragm: West Face at Pier 4]

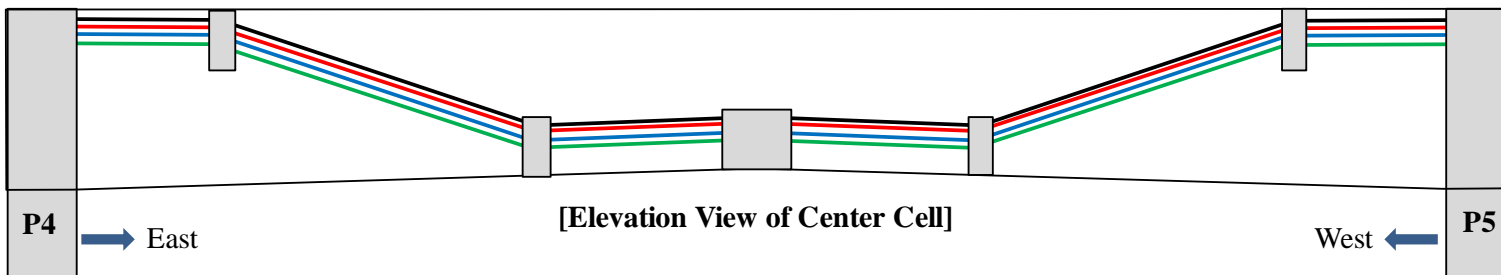
Figure A3. Scanned tendon sections in P3 – P4 (center cell).



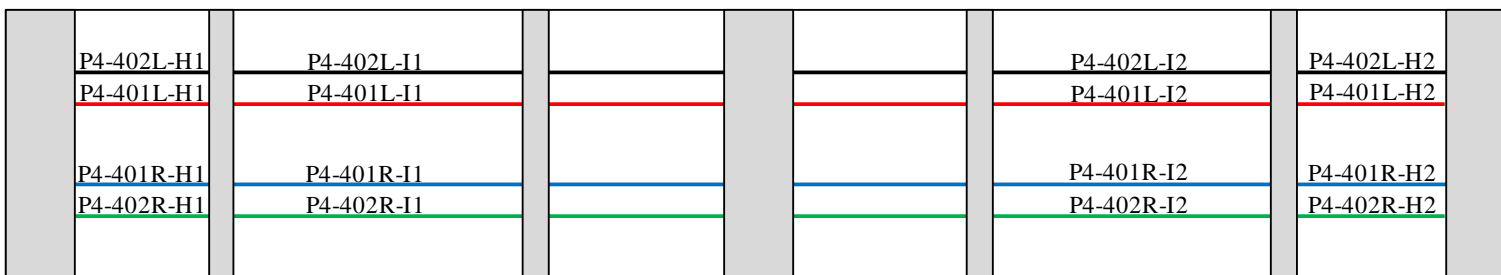
Tokyo Rope USA, Inc.



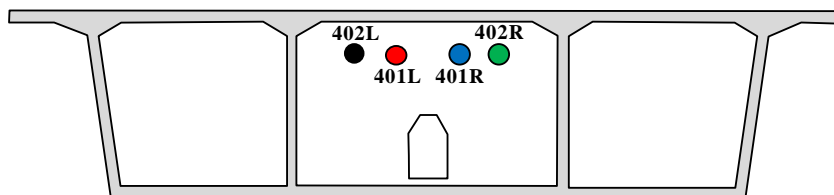
[Diaphragm: East Face at Pier 4]



[Elevation View of Center Cell]



[Plan View of Center Cell]

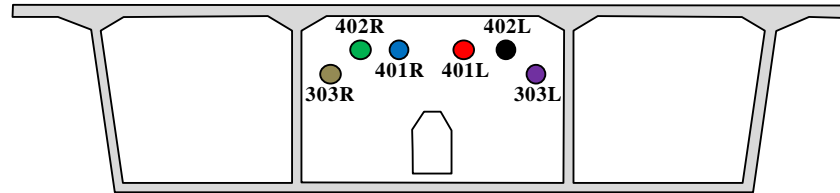


[Diaphragm: West Face at Pier 5]

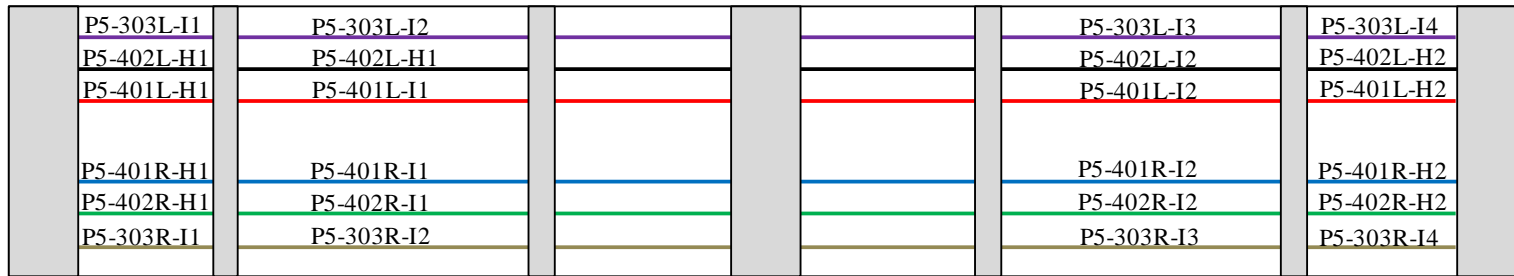
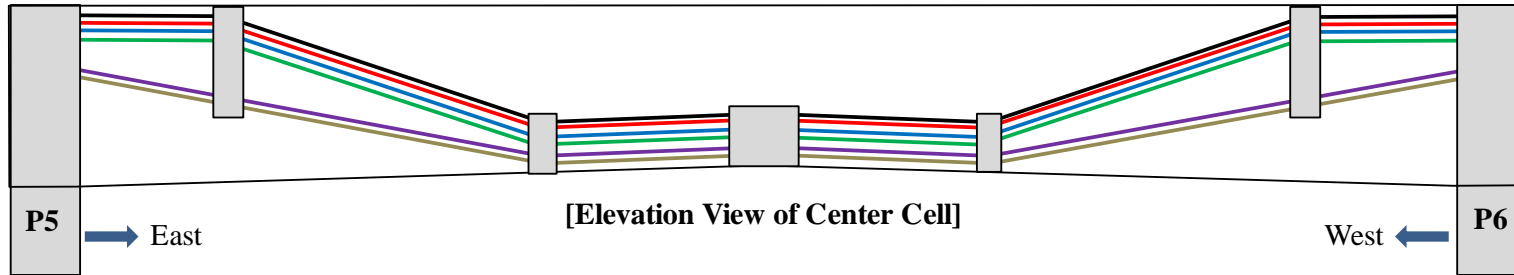
Figure A4. Scanned tendon sections in P4 – P5 (center cell).



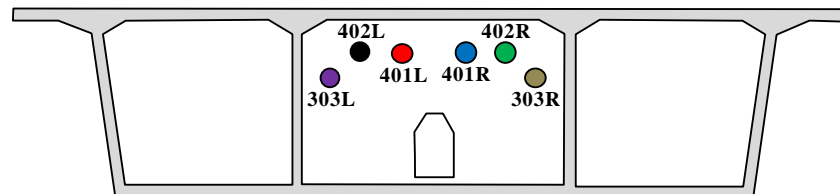
Tokyo Rope USA, Inc.



[Diaphragm: East Face at Pier 5]



[Plan View of Center Cell]

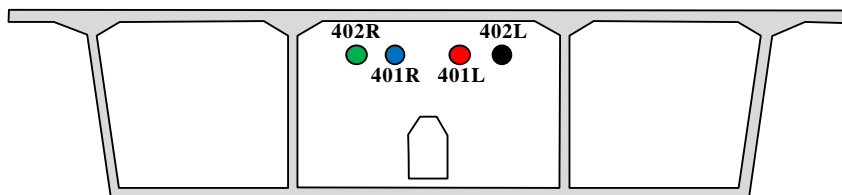


[Diaphragm: West Face at Pier 6]

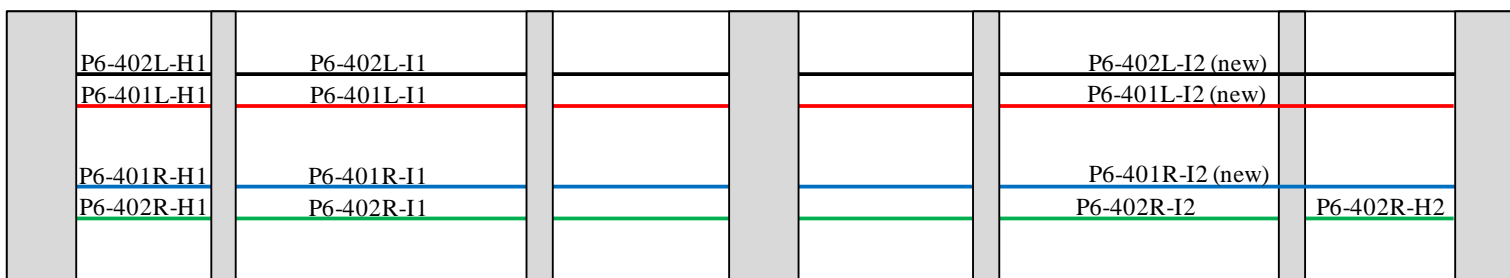
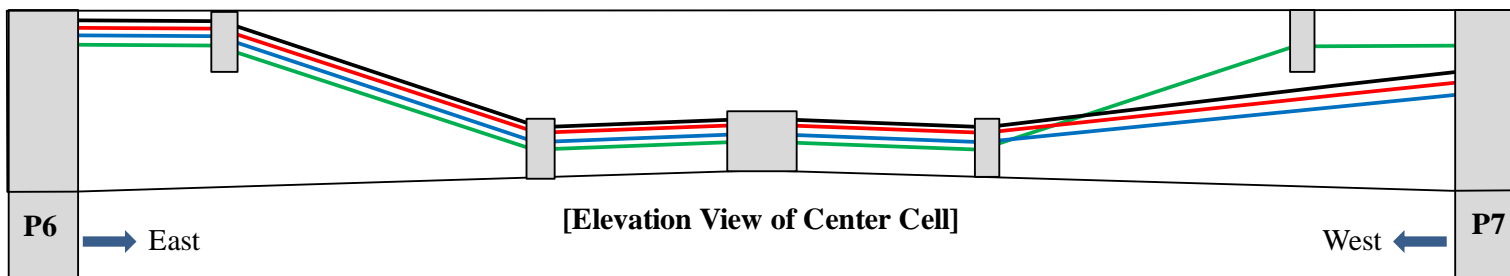
Figure A5. Scanned tendon sections in P5 – P6 (center cell).



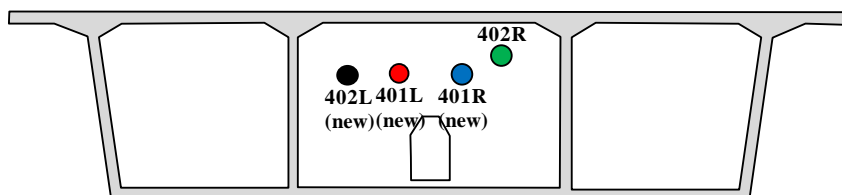
Tokyo Rope USA, Inc.



[Diaphragm: East Face at Pier 6]



[Plan View of Center Cell]

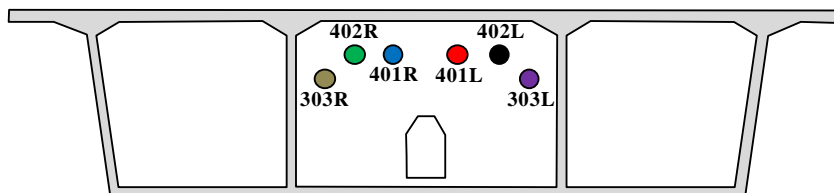


[Diaphragm: West Face at Pier 7]

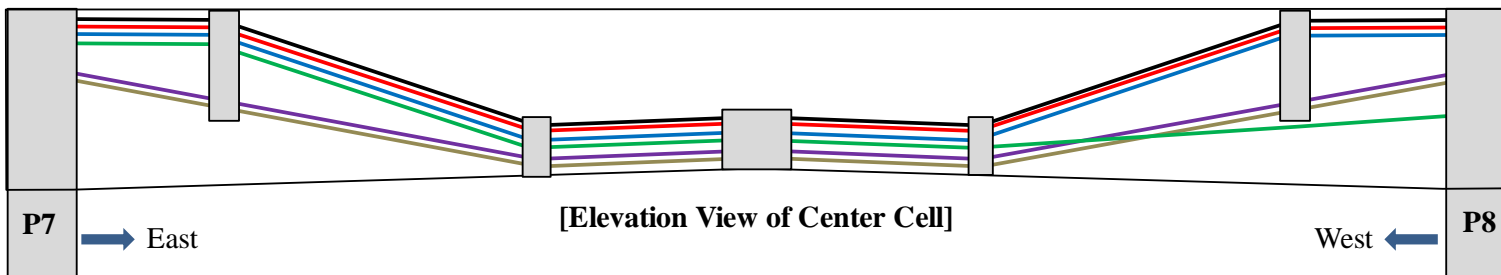
Figure A6. Scanned tendon sections in P6 – P7 (center cell).



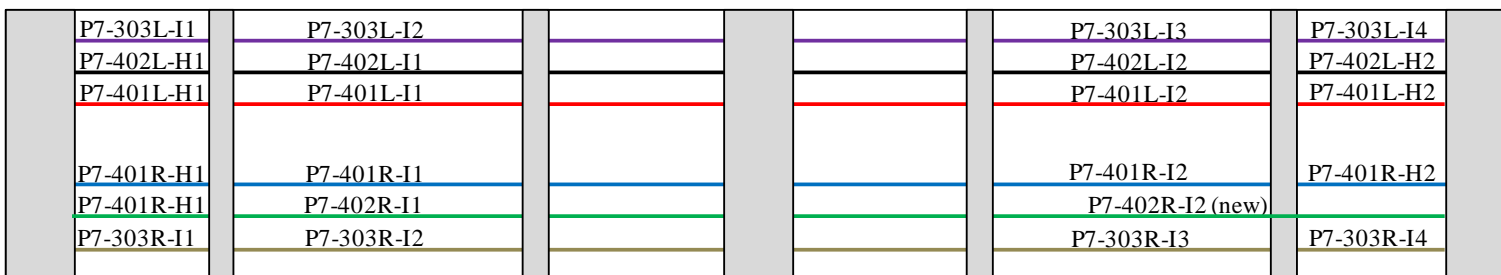
Tokyo Rope USA, Inc.



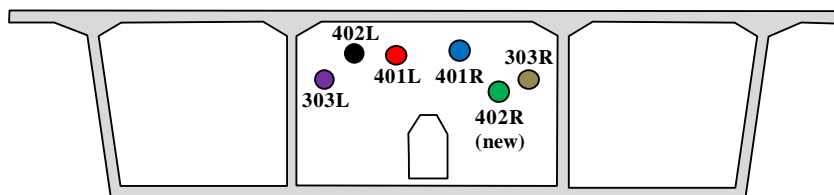
[Diaphragm: East Face at Pier 7]



[Elevation View of Center Cell]



[Plan View of Center Cell]

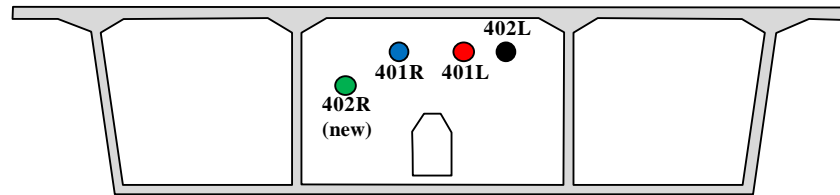


[Diaphragm: West Face at Pier 8]

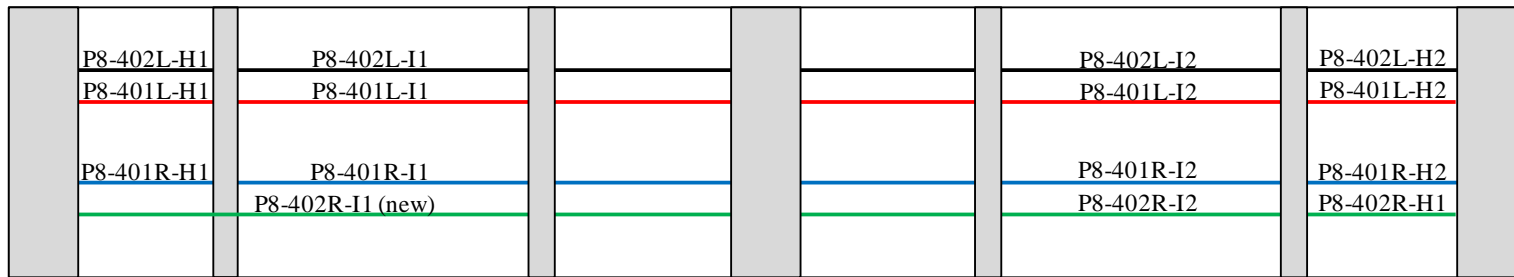
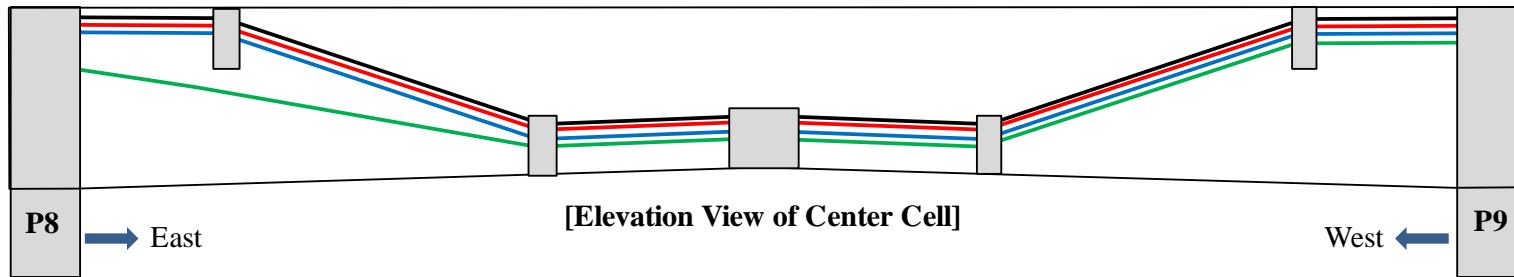
Figure A7. Scanned tendon sections in P7 – P8 (center cell).



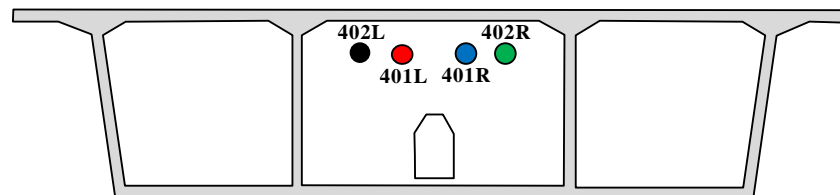
Tokyo Rope USA, Inc.



[Diaphragm: East Face at Pier 8]



[Plan View of Center Cell]

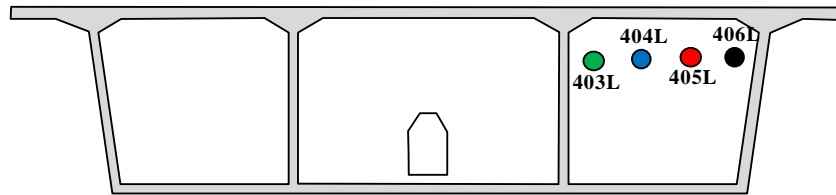


[Diaphragm: West Face at Pier 9]

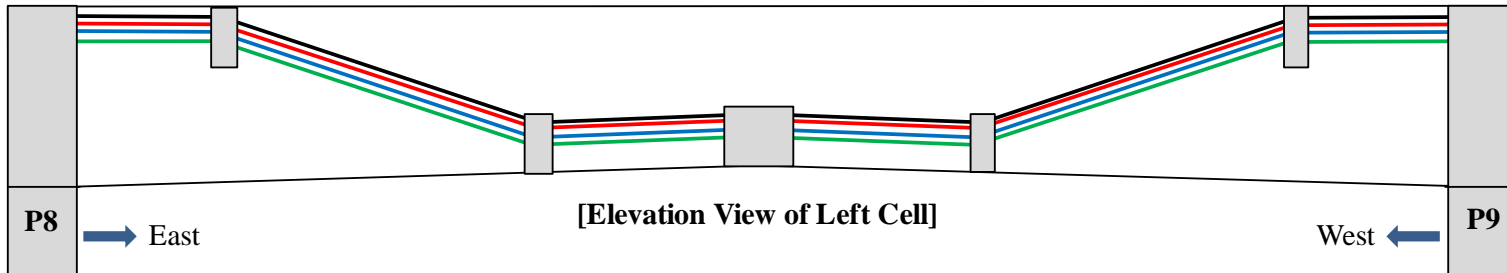
Figure A8. Scanned tendon sections in P8 – P9 (center cell).



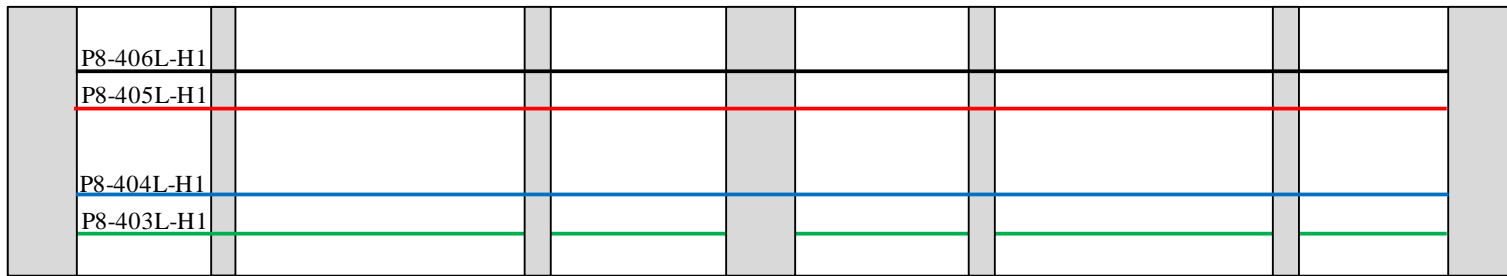
Tokyo Rope USA, Inc.



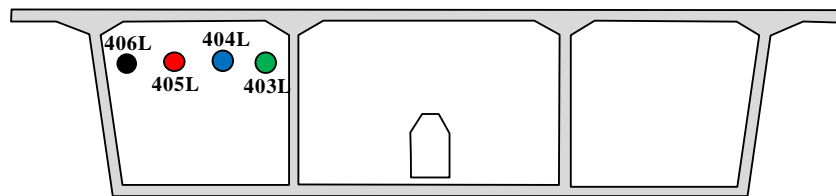
[Diaphragm: East Face at Pier 8]



[Elevation View of Left Cell]



[Plan View of Left Cell]

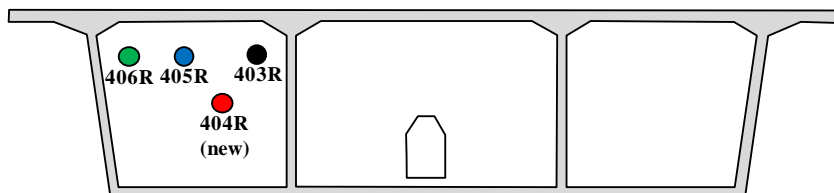


[Diaphragm: West Face at Pier 9]

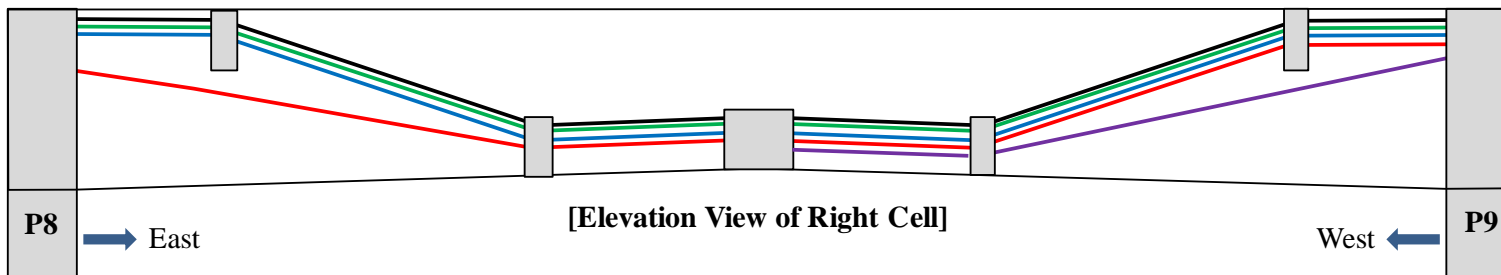
Figure A9. Scanned tendon sections in P8 – P9 (left cell).



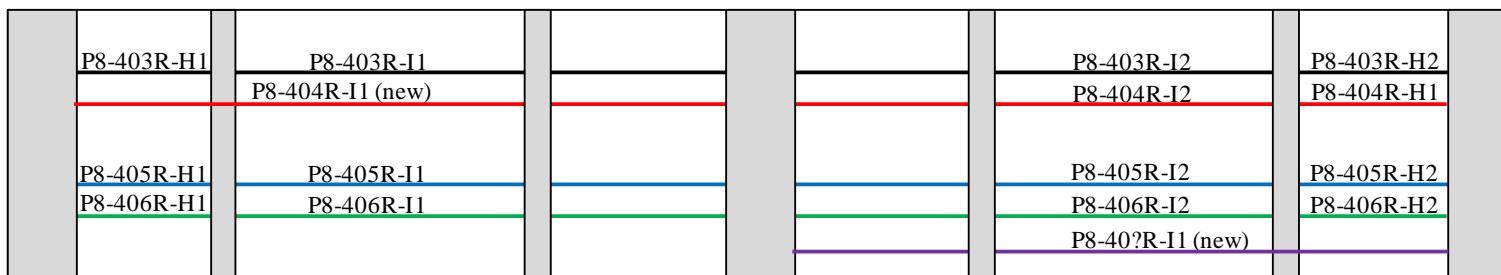
Tokyo Rope USA, Inc.



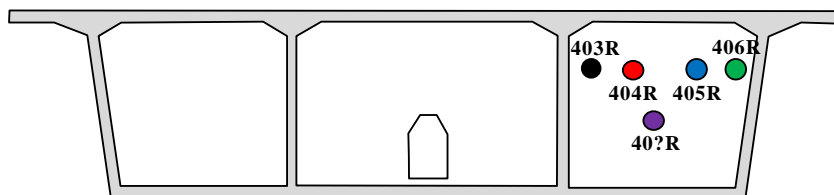
[Diaphragm: East Face at Pier 8]



[Elevation View of Right Cell]



[Plan View of Right Cell]

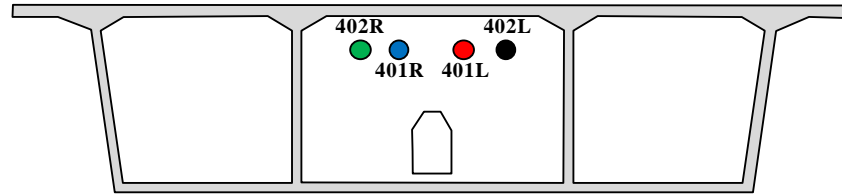


[Diaphragm: West Face at Pier 9]

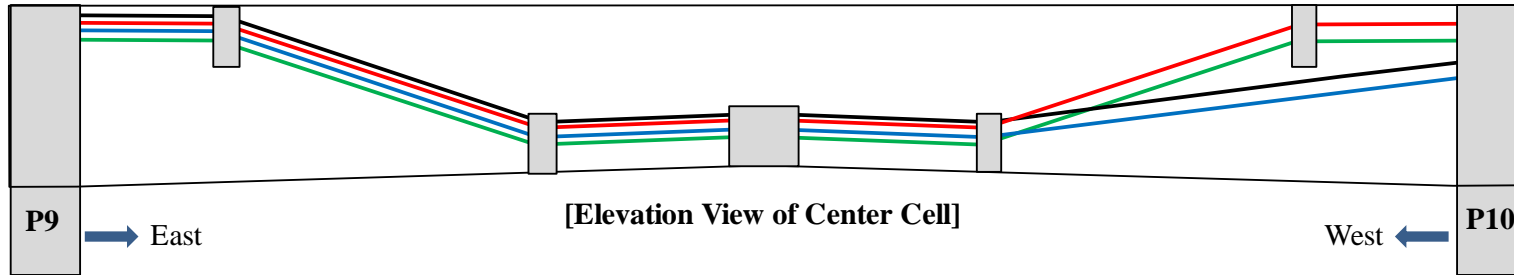
Figure A10. Scanned tendon sections in P8 – P9 (right cell).



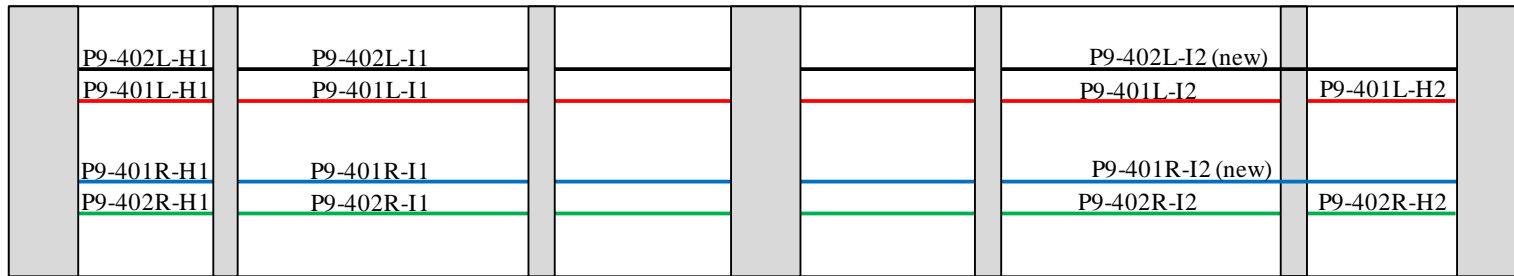
Tokyo Rope USA, Inc.



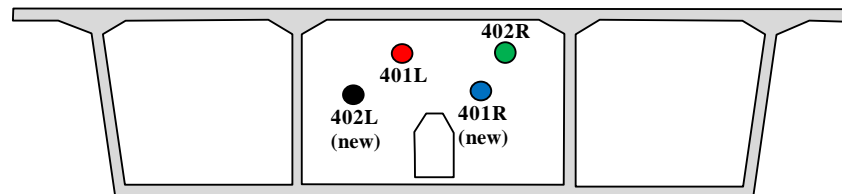
[Diaphragm: East Face at Pier 9]



[Elevation View of Center Cell]



[Plan View of Center Cell]

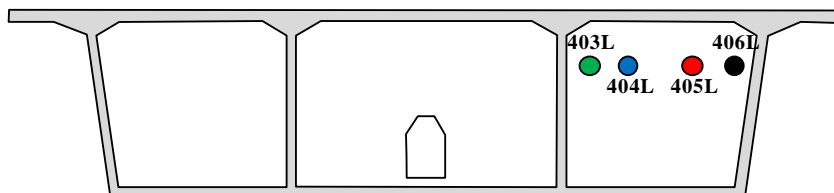


[Diaphragm: West Face at Pier 10]

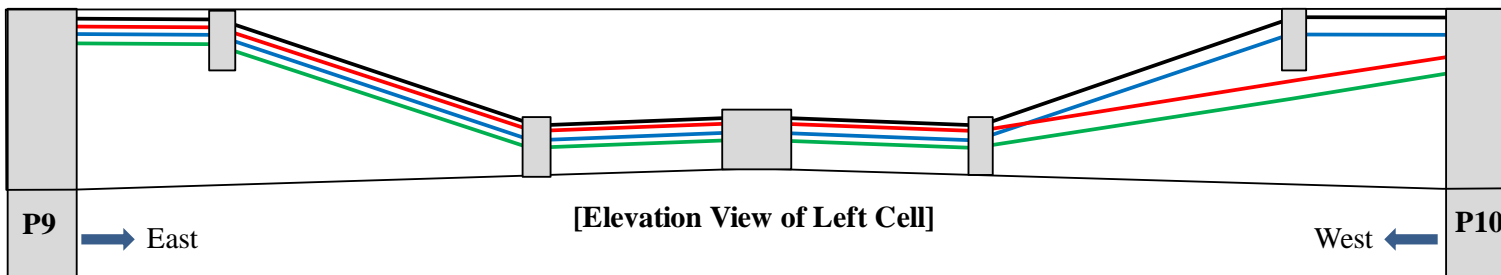
Figure A11. Scanned tendon sections in P9 – P10 (center cell).



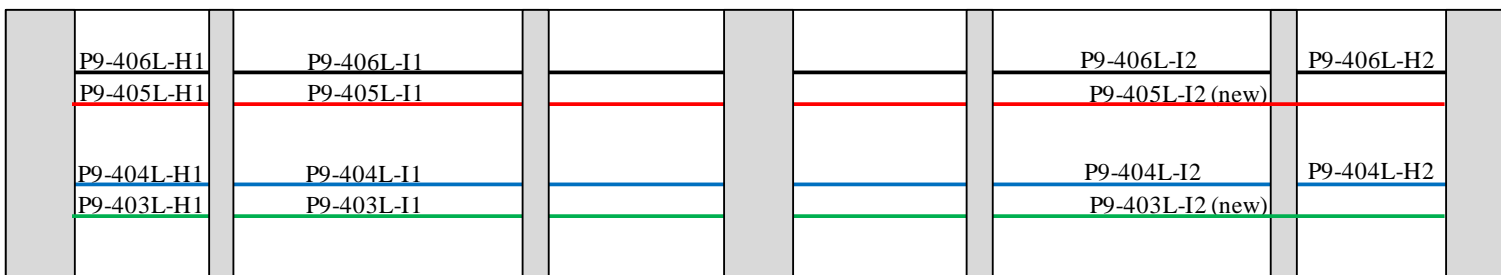
Tokyo Rope USA, Inc.



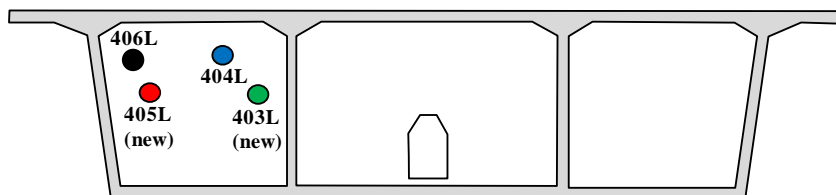
[Diaphragm: East Face at Pier 9]



[Elevation View of Left Cell]



[Plan View of Left Cell]

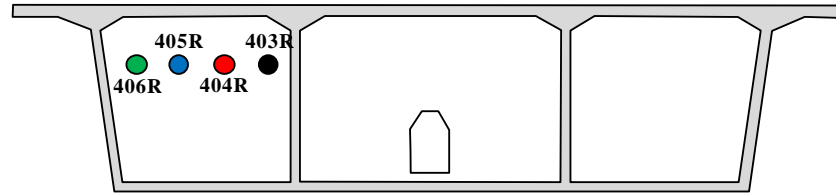


[Diaphragm: West Face at Pier 10]

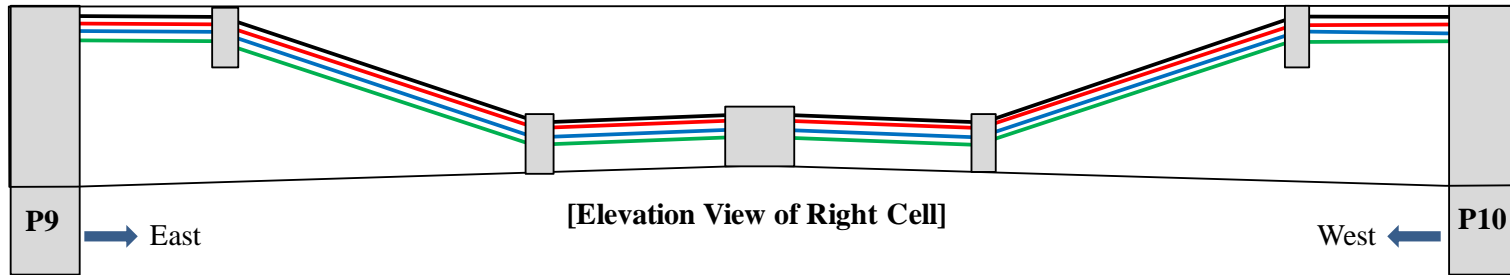
Figure A12. Scanned tendon sections in P9 – P10 (left cell).



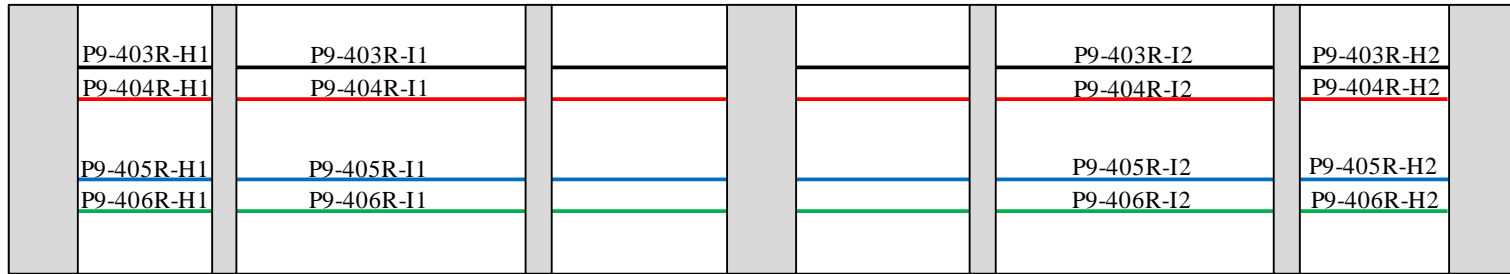
Tokyo Rope USA, Inc.



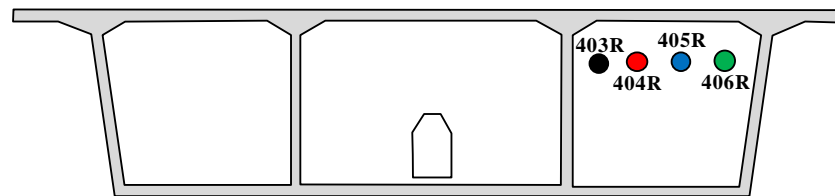
[Diaphragm: East Face at Pier 9]



[Elevation View of Right Cell]



[Plan View of Right Cell]

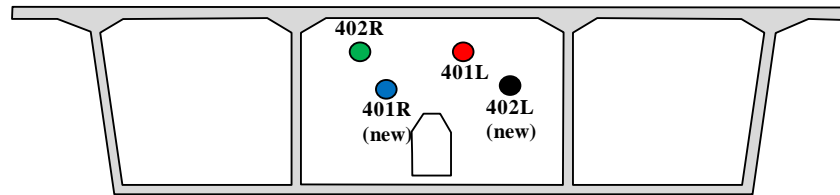


[Diaphragm: West Face at Pier 10]

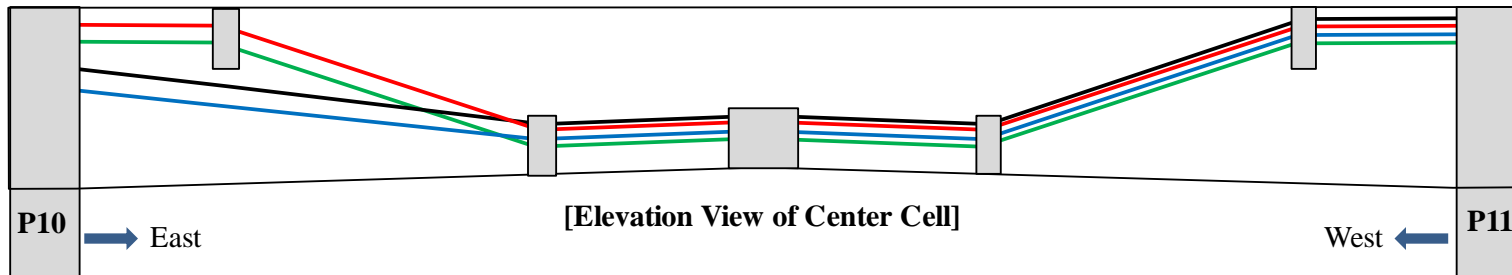
Figure A13. Scanned tendon sections in P9 – P10 (right cell).



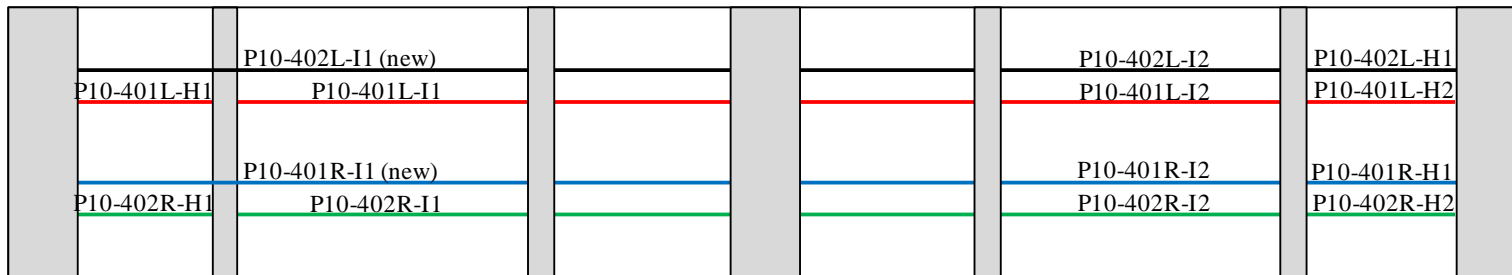
Tokyo Rope USA, Inc.



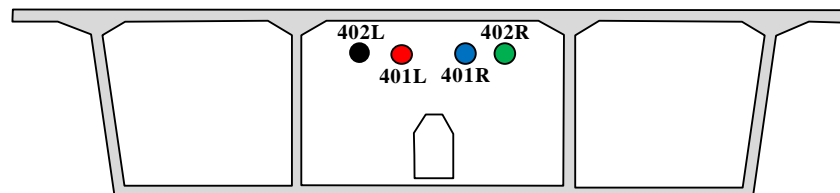
[Diaphragm: East Face at Pier 10]



[Elevation View of Center Cell]



[Plan View of Center Cell]

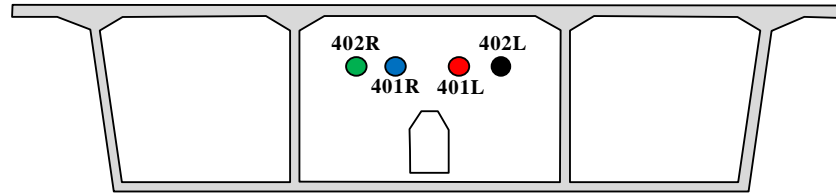


[Diaphragm: West Face at Pier 11]

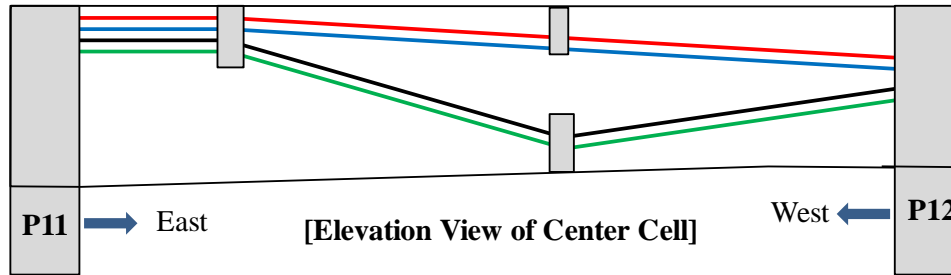
Figure A14. Scanned tendon sections in P10 – P11 (center cell).



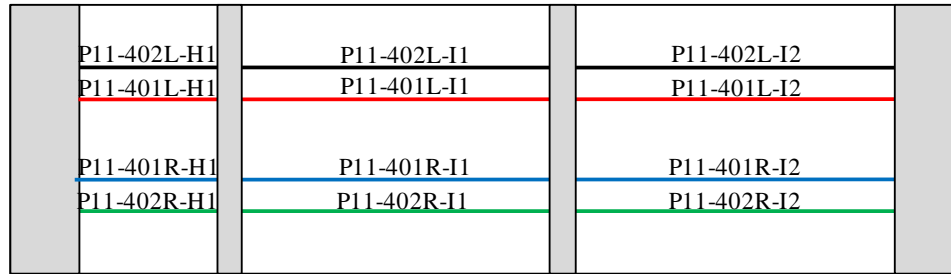
Tokyo Rope USA, Inc.



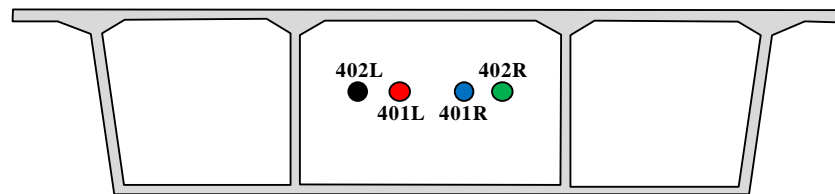
[Diaphragm: East Face at Pier 11]



[Elevation View of Center Cell]



[Plan View of Center Cell]



[Diaphragm: West Face at Pier 12 (Abutment)]

Figure A15. Scanned tendon sections in P11 – P12 (center cell)



Tokyo Rope USA, Inc.

APPENDIX 2. Collection of MMFM Data Containing Damage



Tokyo Rope USA, Inc.

File Name 【Pier-Tendon-Section】	Section Total Length (m)	Scanned Length		Note			
		Starting Point (m)	Ending Point (m)				
P1-401R-H1	20.8	0.56	20.46	Joint position : 12.7 mm Repair tape position : 7.64 m			
Identified Damage 1				Identified Damage 2			
Max Loss Point (m)	Section Loss (%)	Damage Length (m)	Damage Orientation	Max Loss Point (m)	Section Loss (%)	Damage Length (m)	Damage Orientation
11.7	1.5	1.7	—	—	—	—	—

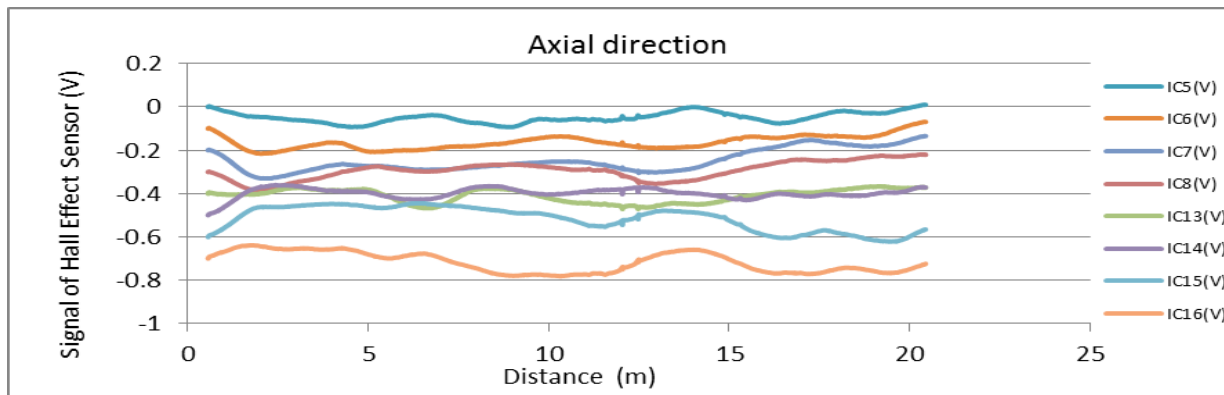
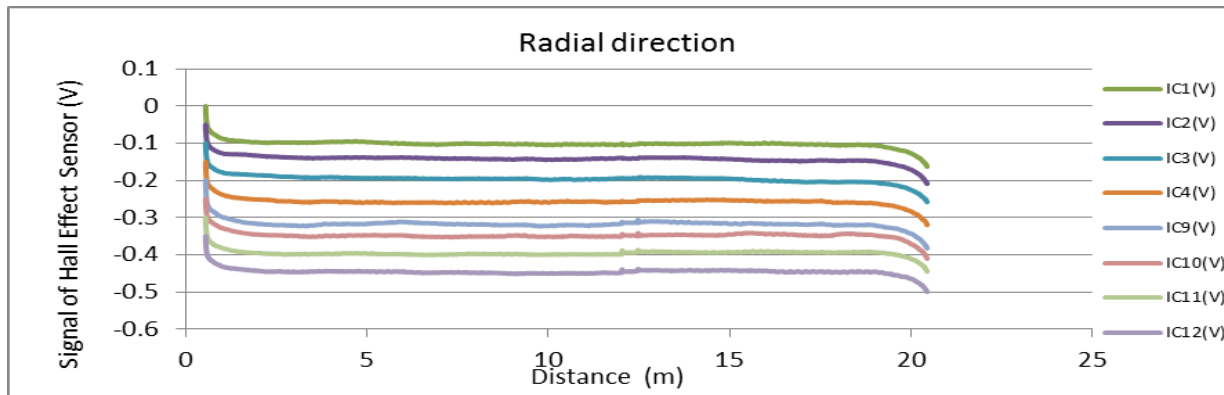
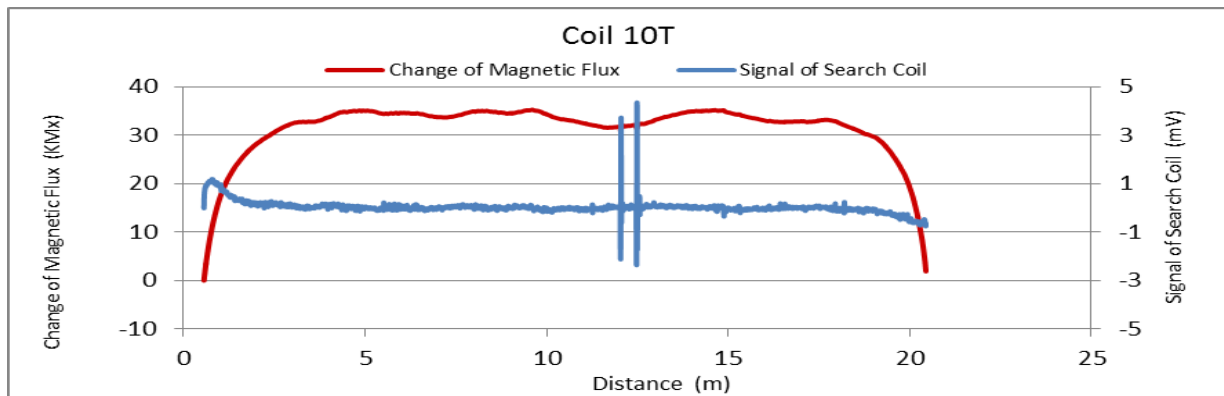


Figure A16. MMFM data of P1-401R-H1 tendon section.



Tokyo Rope USA, Inc.

File Name 【Pier-Tendon-Section】	Section Total Length (m)	Scanned Length		Note			
		Starting Point (m)	Ending Point (m)				
P1-402R-I1	20.5	0.56	19.14	Joint position : 12.3 m Identified damage 1 : Increase of magnetic flux Repair tape position : 18.05 m			
Identified Damage 1				Identified Damage 2			
Max Loss Point (m)	Loss (%)	Length (m)	Damage Orientation	Max Loss Point (m)	Loss (%)	Length (m)	Damage Orientation
18.1	-4.1	0.2	—	—	—	—	—

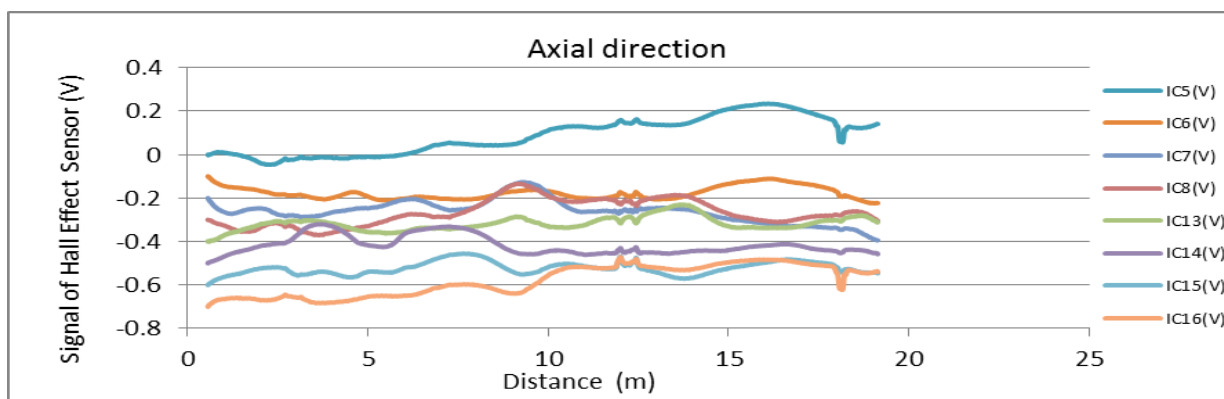
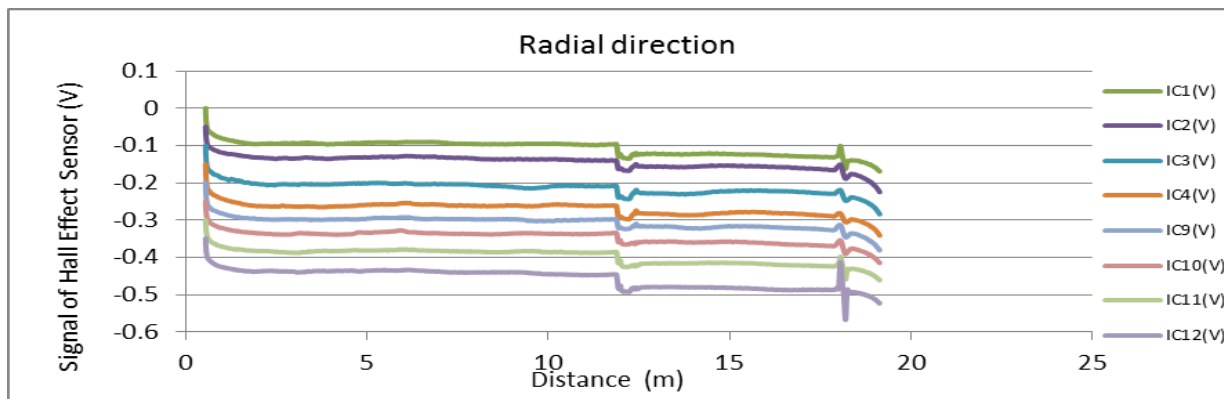
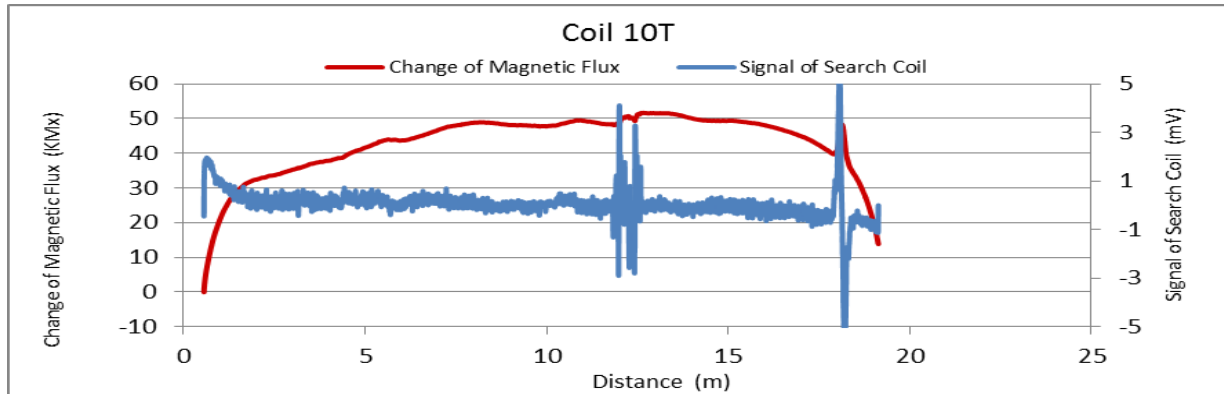


Figure A17. MMFM data of P1-402R-I1 tendon section.



Tokyo Rope USA, Inc.

File Name 【Pier-Tendon-Section】	Section Total Length (m)	Scanned Length		Note			
		Starting Point (m)	Ending Point (m)				
P1-402L-I1	20.4	0.55	18.88	Joint position : 12.3 m Starting point of damage 1 : 8.61 m Starting point of damage 2 : 14.4 m			
Identified Damage 1				Identified Damage 2			
Max Loss Point (m)	Loss (%)	Length (m)	Damage Orientation	Max Loss Point (m)	Loss (%)	Length (m)	Damage Orientation
10.3	2.7	2.8	—	15.0	1.5	0.9	—

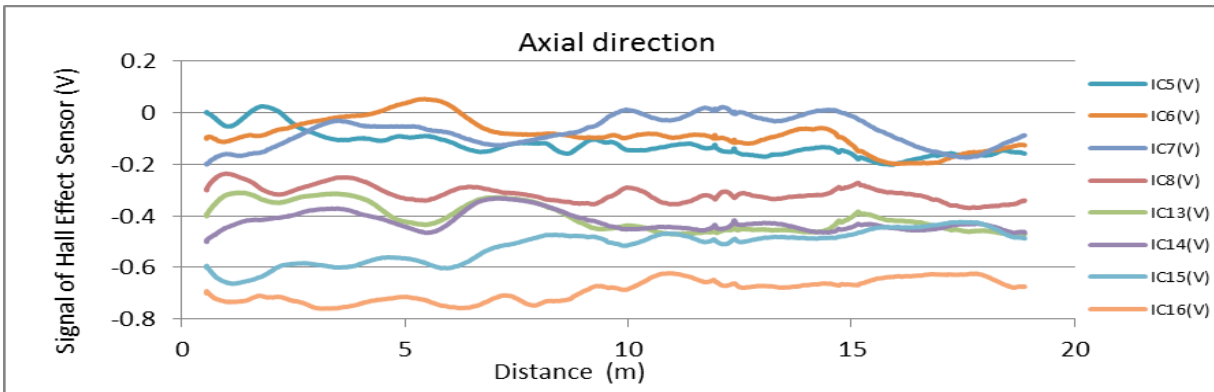
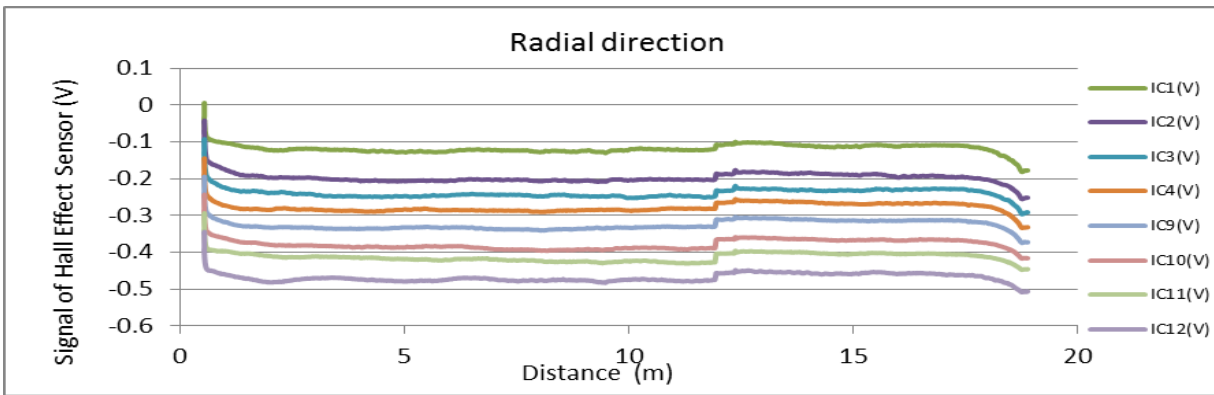
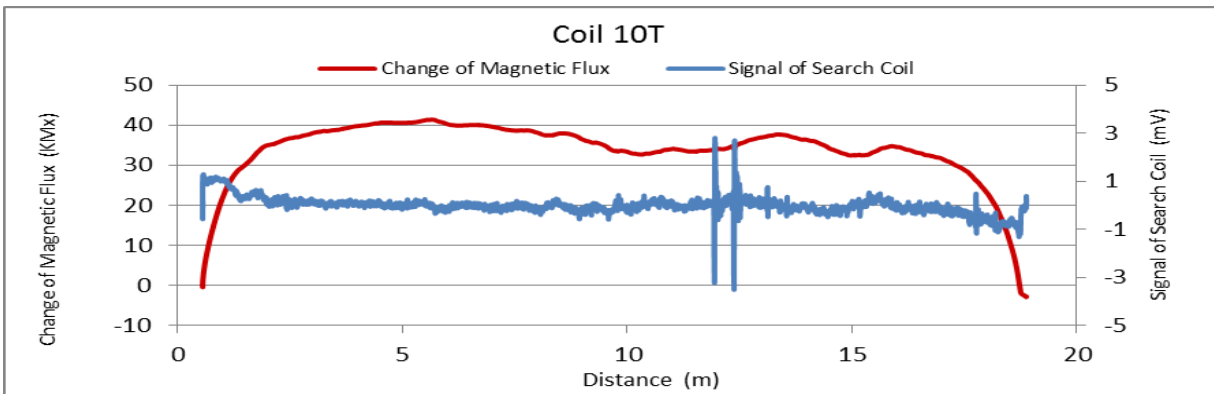


Figure A18. MMFM data of P1-402L-I1 tendon section.



Tokyo Rope USA, Inc.

File Name 【Pier-Tendon-Section】	Section Total Length (m)	Scanned Length		Note Joint position : 9.1 m Starting point of damage 1 : 13.15 m			
		Starting Point (m)	Ending Point (m)				
P1-402L-I2	21.19	0.72	20.54				
Identified Damage 1				Identified Damage 2			
Max Loss Point (m)	Loss (%)	Length (m)	Damage Orientation	Max Loss Point (m)	Loss (%)	Length (m)	Damage Orientation
13.8	1.5	1.2	—	—	—	—	—

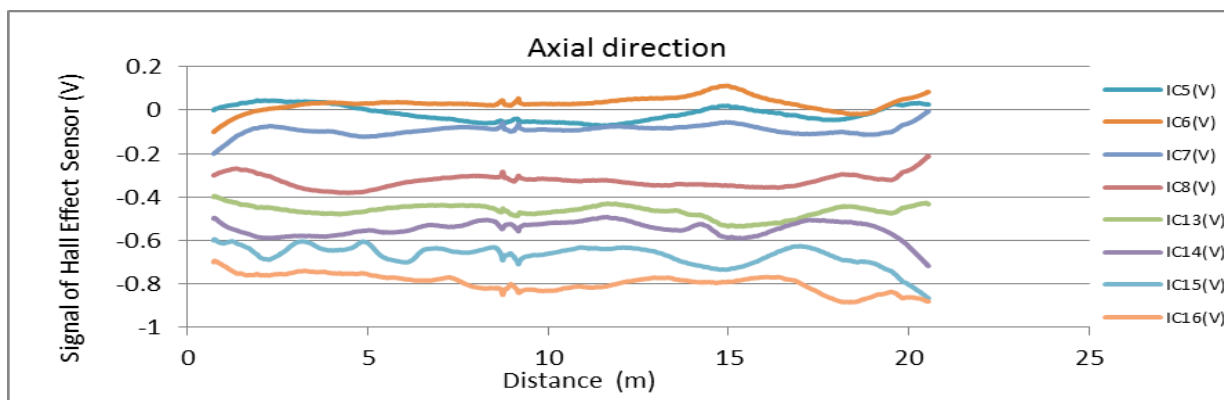
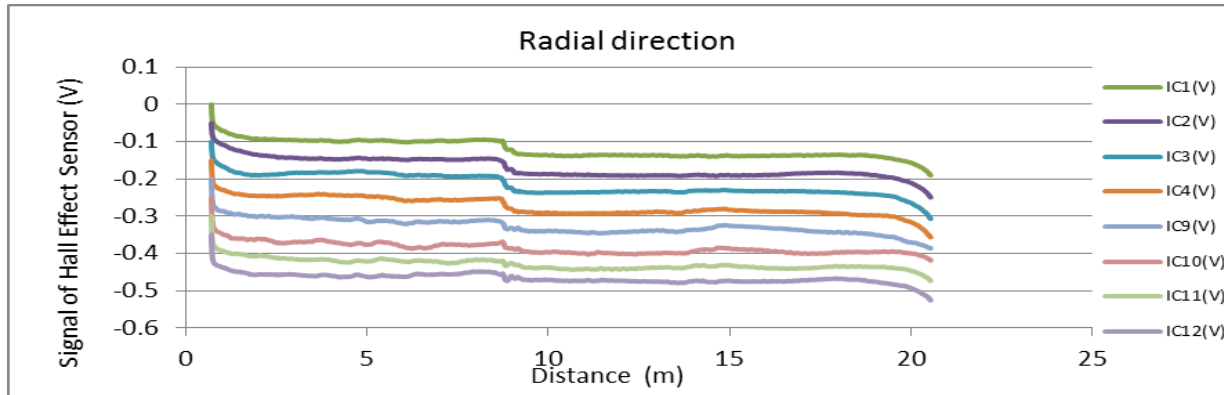
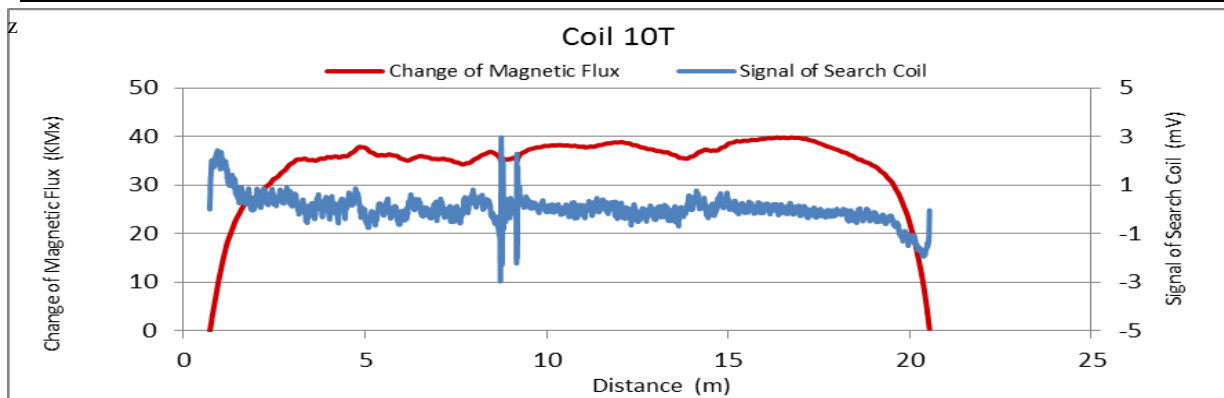


Figure A19. MMFM data of P1-402L-I2 tendon section.



Tokyo Rope USA, Inc.

File Name 【Pier-Tendon-Section】	Section Total Length (m)	Scanned Length		Note			
		Starting Point (m)	Ending Point (m)				
P1-401L-H3	9.45	0.63	8.88	Identified damage 1 : Increase of magnetic flux Starting point of damage 1 : 7.74 m			
Identified Damage 1				Identified Damage 2			
Max Loss Point (m)	Loss (%)	Length (m)	Damage Orientation	Max Loss Point (m)	Loss (%)	Length (m)	Damage Orientation
7.8	-2.4	0.13	12~2 o'clock	—	—	—	—

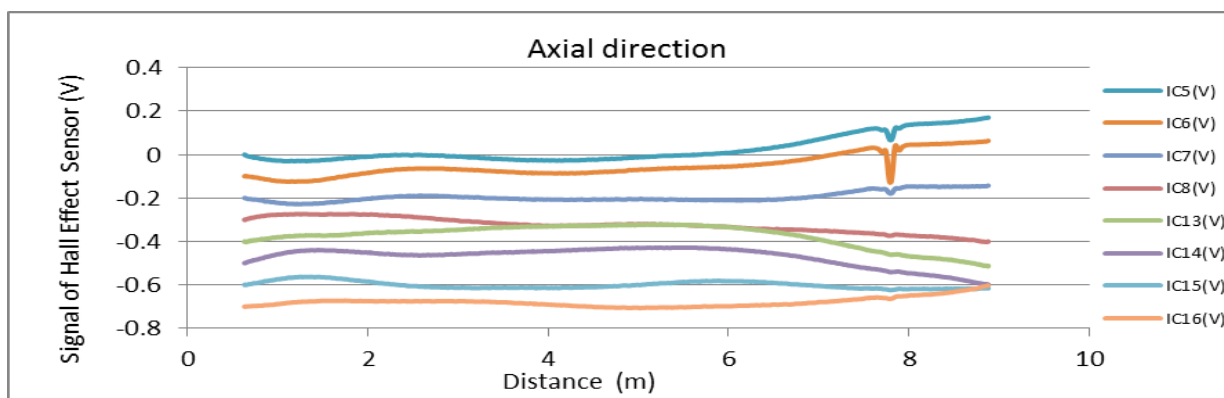
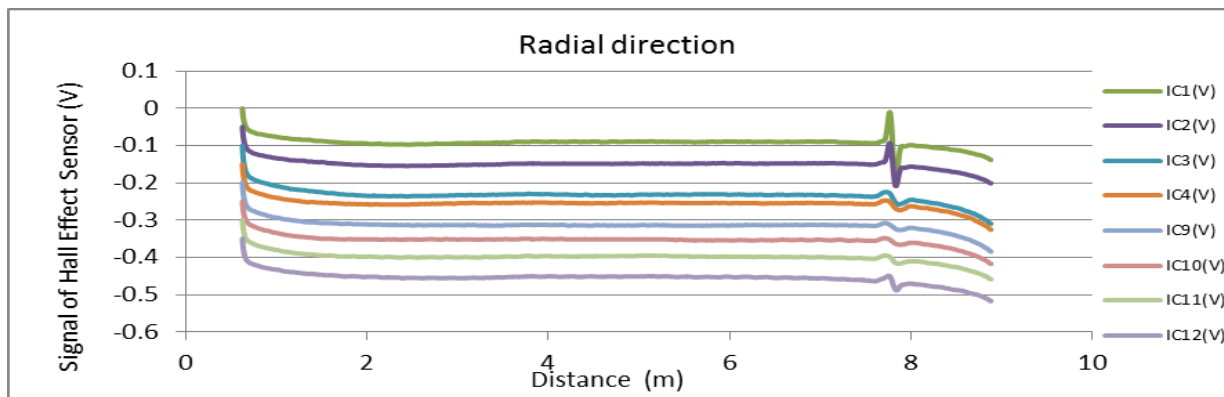
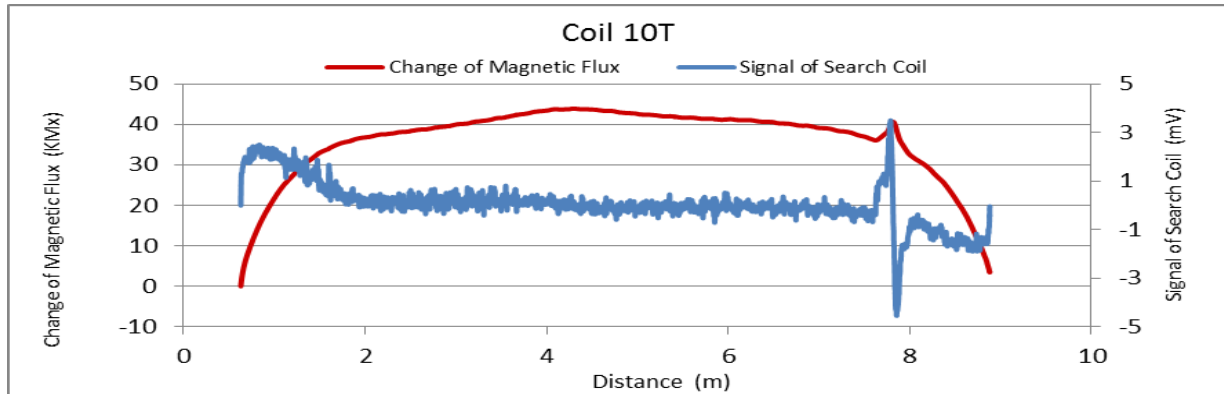


Figure A20. MMFM data of P1-401L-H3 tendon section.



Tokyo Rope USA, Inc.

File Name 【Pier-Tendon-Section】	Section Total Length (m)	Scanned Length		Note			
		Starting Point (m)	Ending Point (m)				
P2-401L-H1	9.38	0.63	8.73	Identified damage 1 : Increase of magnetic flux Starting point of damage 1 : 8.13 m			
Identified Damage 1				Identified Damage 2			
Max Loss Point (m)	Loss (%)	Length (m)	Damage Orientation	Max Loss Point (m)	Loss (%)	Length (m)	Damage Orientation
8.2	-5.0	0.18	12~1 o'clock	—	—	—	—

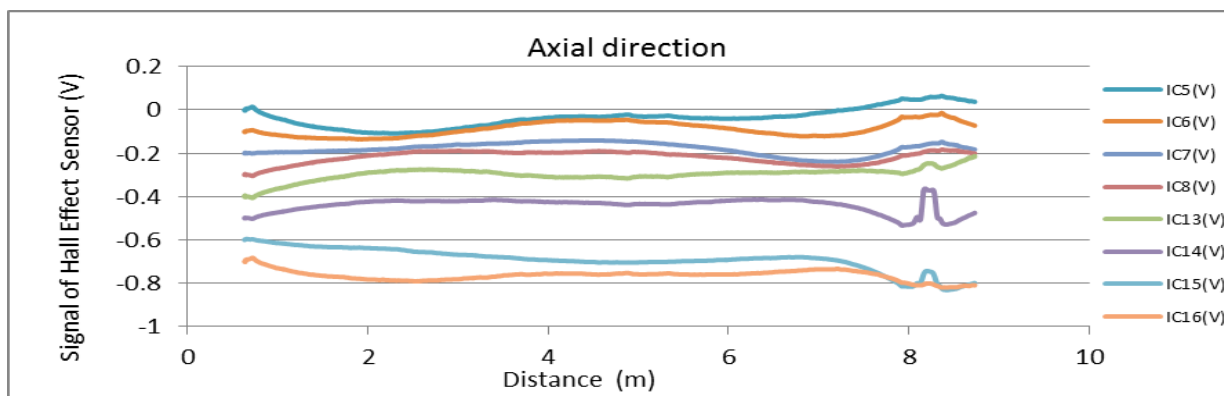
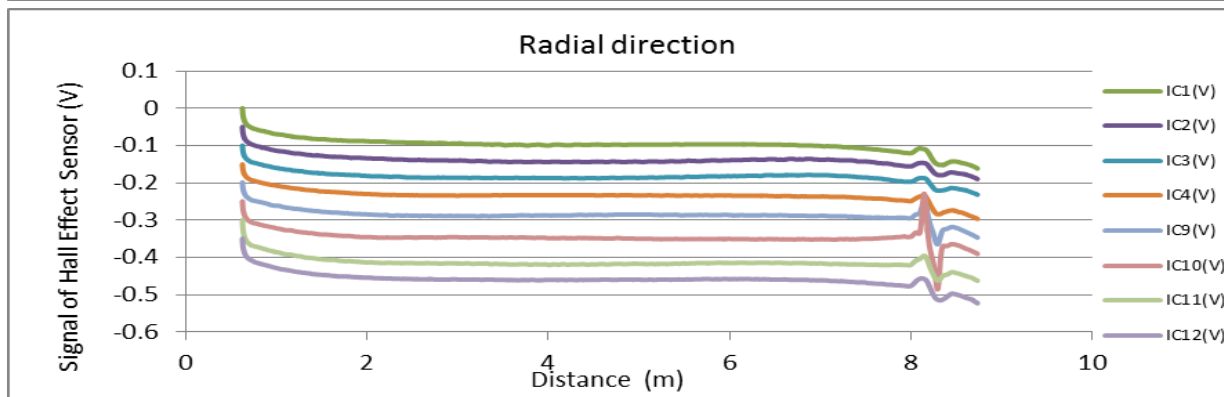
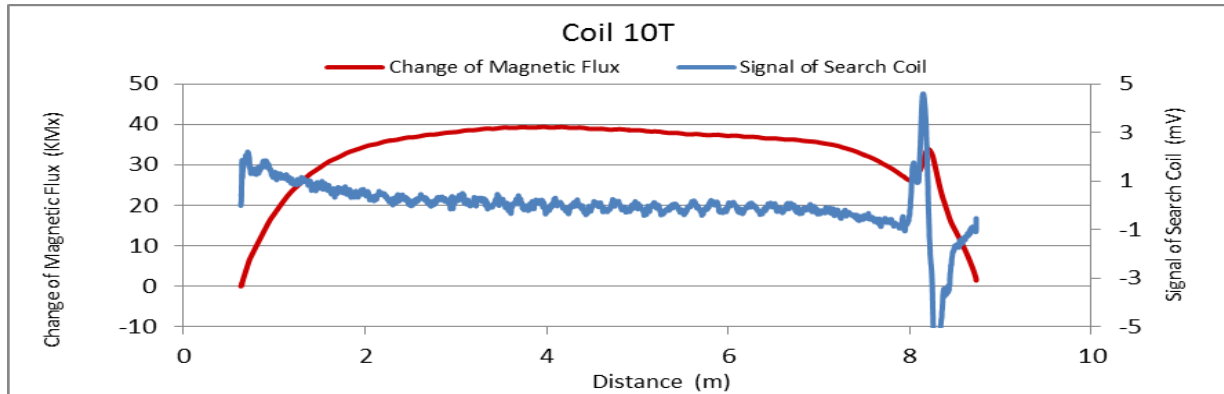


Figure A21. MMFM data of P2-401L-H1 tendon section.



Tokyo Rope USA, Inc.

File Name 【Pier-Tendon-Section】	Section Total Length (m)	Scanned Length		Note			
		Starting Point (m)	Ending Point (m)				
P2-401R-I1	21.43	0.56	20.64	Joint position : 12.2 m Identified damage 1 : Increase of magnetic flux Starting point of damage 1 : 15.33 m			
Identified Damage 1				Identified Damage 2			
Max Loss Point (m)	Loss (%)	Length (m)	Damage Orientation	Max Loss Point (m)	Loss (%)	Length (m)	Damage Orientation
15.4	-3.8	0.17	8~12 o'clock	—	—	—	—

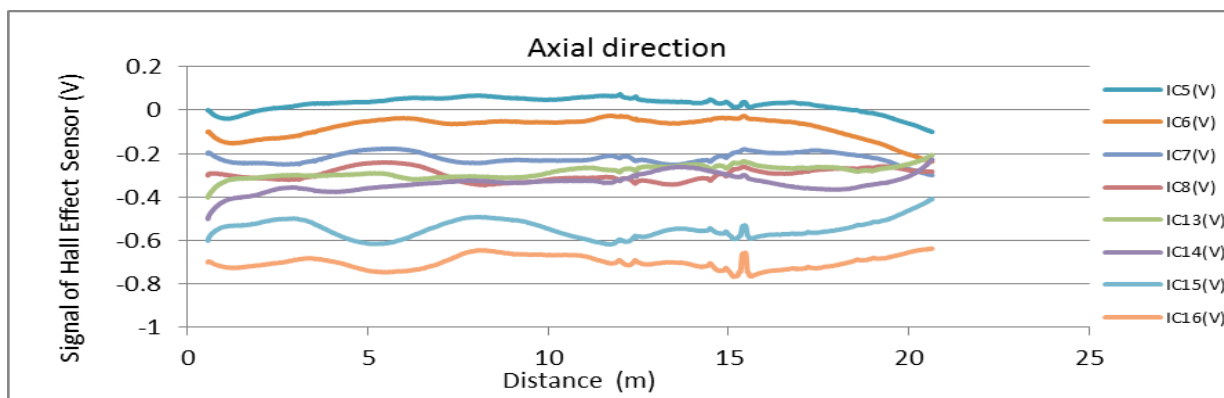
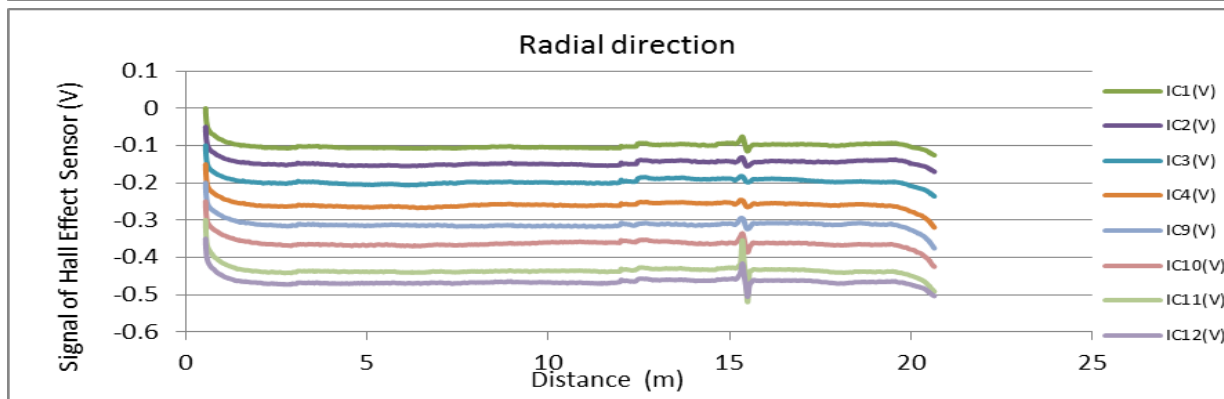
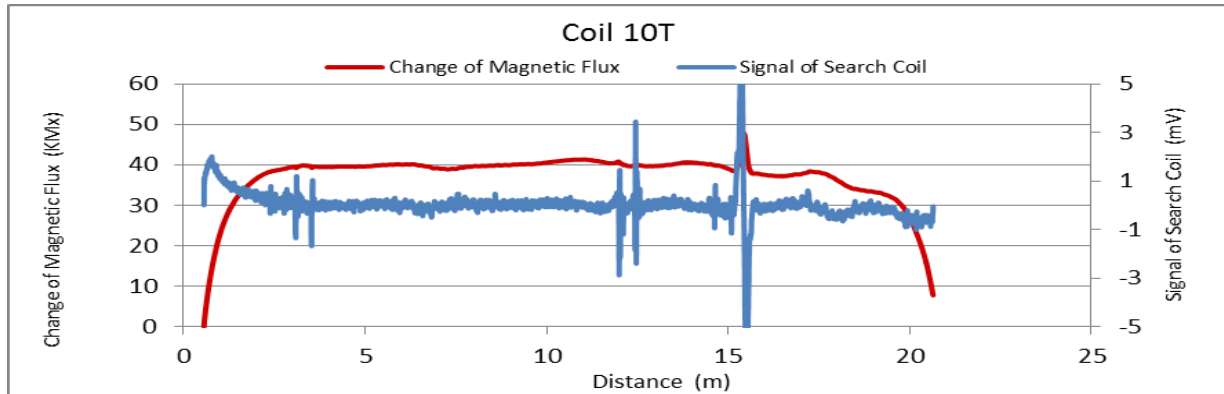


Figure A22. MMFM data of P2-401R-I1 tendon section.



Tokyo Rope USA, Inc.

File Name 【Pier-Tendon-Section】	Section Total Length (m)	Scanned Length		Note Joint position : 12.3 m Starting point of damage 1 : 7.15 m			
		Starting Point (m)	Ending Point (m)				
P2-402L-I1	21.37	0.59	20.68				
Identified Damage 1				Identified Damage 2			
Max Loss Point (m)	Loss (%)	Length (m)	Damage Orientation	Max Loss Point (m)	Loss (%)	Length (m)	Damage Orientation
8.2	2.4	1.78	6~8 o'clock	—	—	—	—

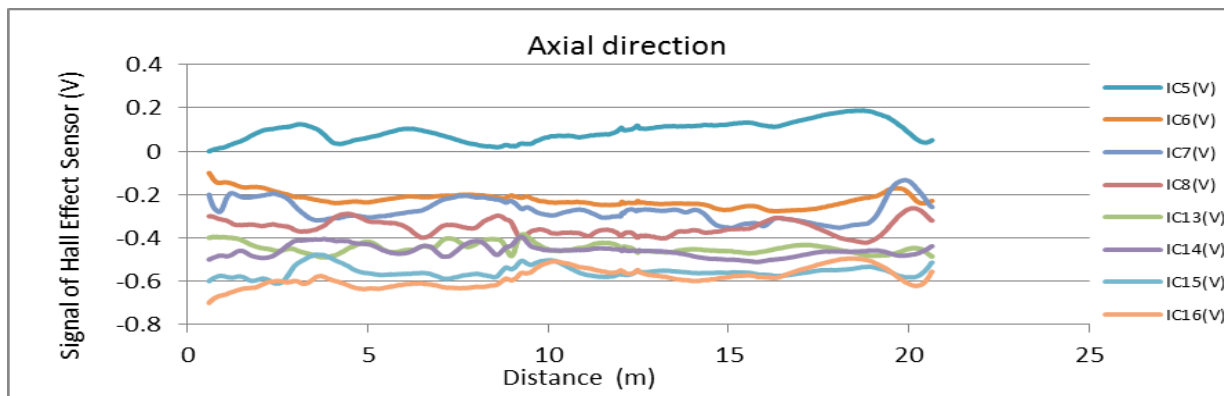
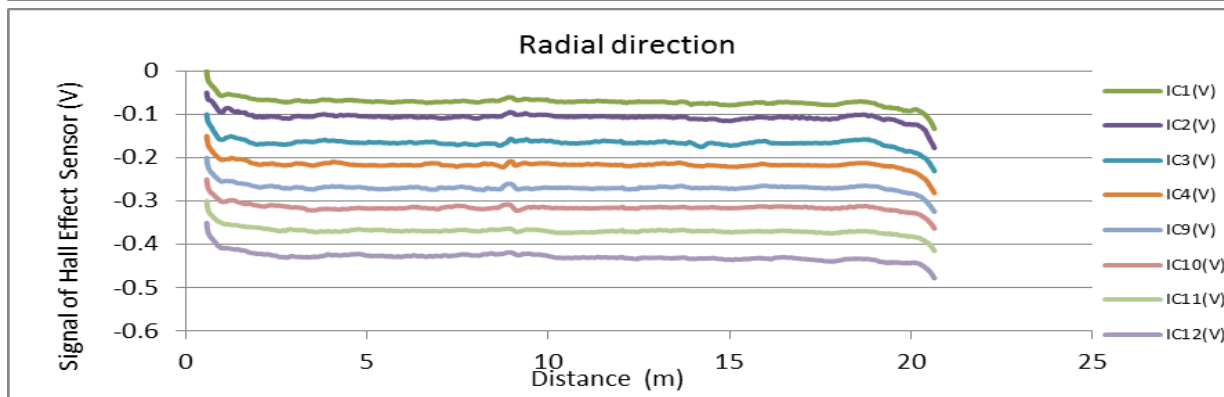
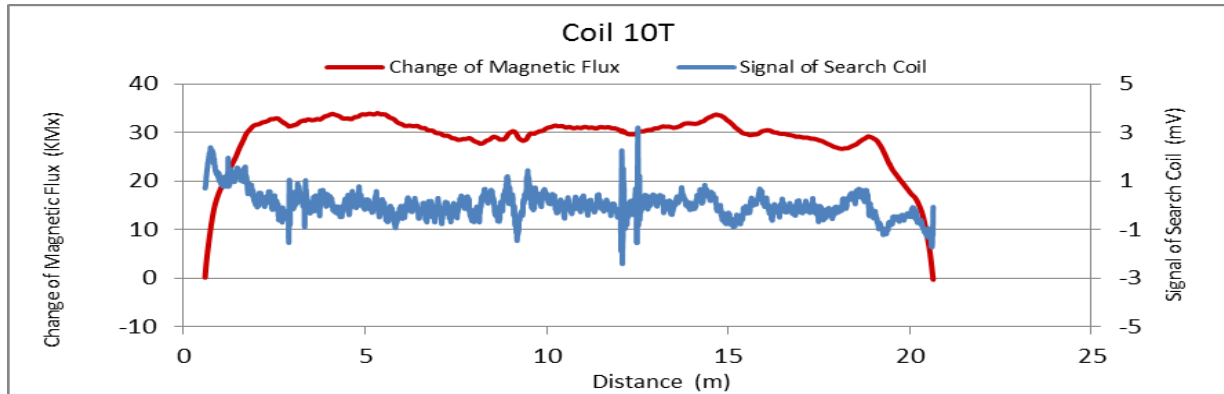


Figure A23. MMFM data of P2-402L-I1 tendon section.



Tokyo Rope USA, Inc.

File Name 【Pier-Tendon-Section】	Section Total Length (m)	Scanned Length		Note			
		Starting Point (m)	Ending Point (m)				
P2-402R-I2	21.47	0.65	20.87	Joint position : 12.3 m Identified damage 1&2 : Increase of magnetic flux Starting point of damage 1 : 6.85 m Starting point of damage 2 : 14.2 m			
Identified Damage 1				Identified Damage 2			
Max Loss Point (m)	Loss (%)	Length (m)	Damage Orientation	Max Loss Point (m)	Loss (%)	Length (m)	Damage Orientation
6.9	-2.3	0.15	11~1 o'clock	14.3	-1.9	0.16	9~11 o'clock

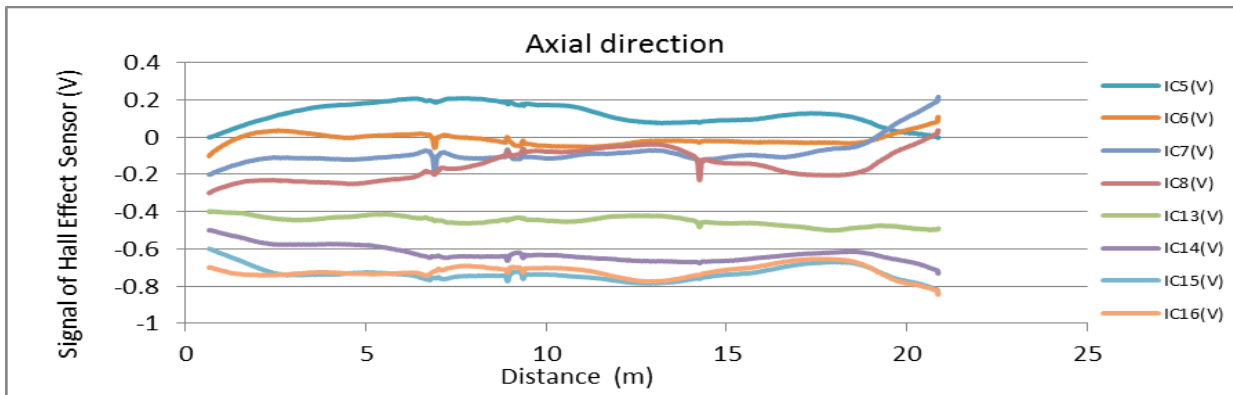
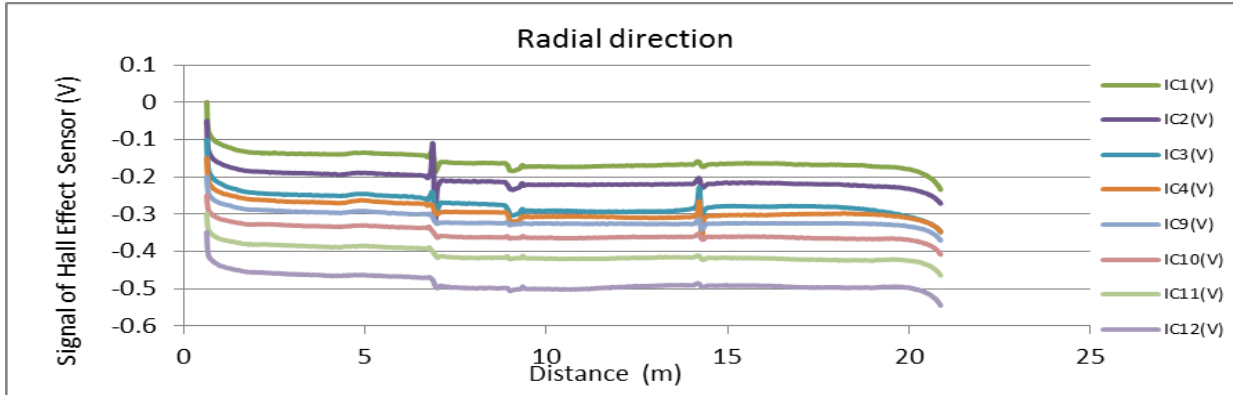
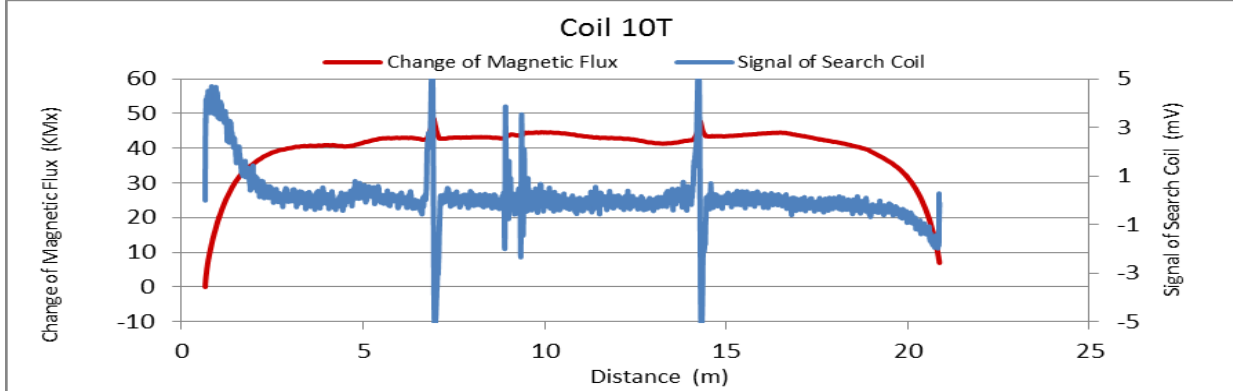


Figure A24. MMFM data of P2-402R-I2 tendon section.



Tokyo Rope USA, Inc.

File Name 【Pier-Tendon-Section】	Section Total Length (m)	Scanned Length		Note Starting point of damage 1 : 3.31 m			
		Starting Point (m)	Ending Point (m)				
P2-402R-H2	9.43	0.67	8.83				
Identified Damage 1				Identified Damage 2			
Max Loss Point (m)	Loss (%)	Length (m)	Damage Orientation	Max Loss Point (m)	Loss (%)	Length (m)	Damage Orientation
3.8	1.7	1.14	8~11 o'clock	—	—	—	—

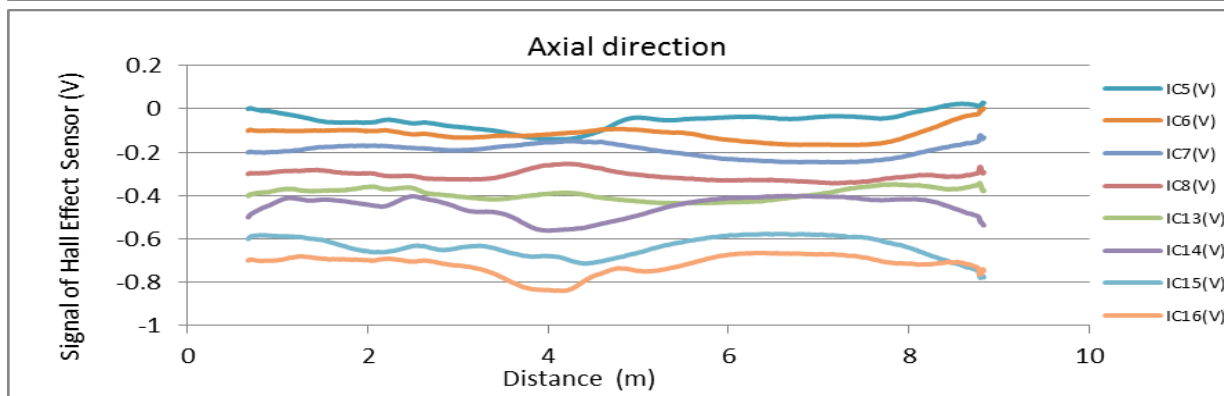
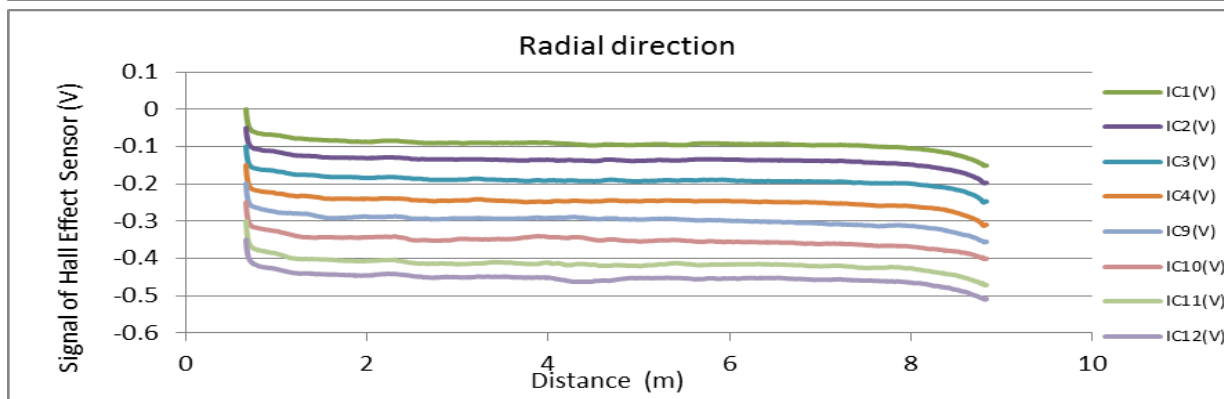
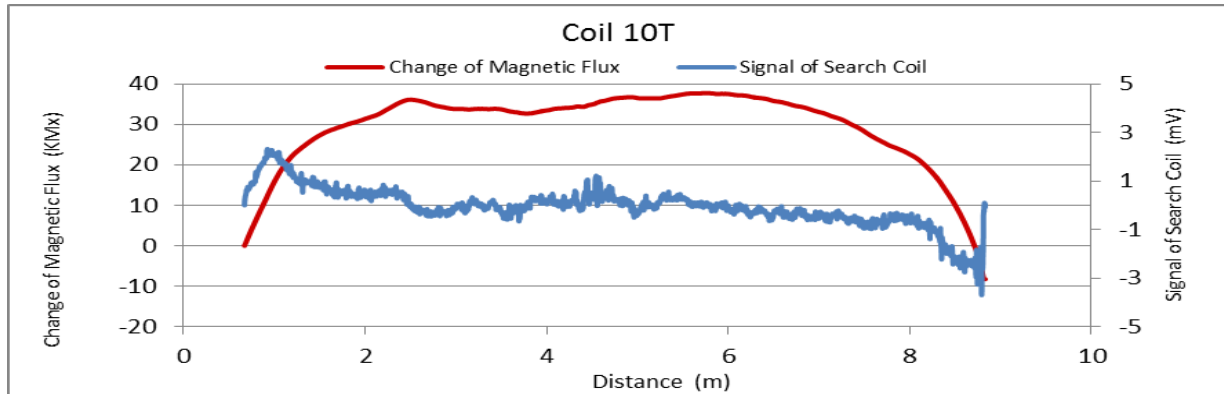


Figure A25. MMFM data of P2-402R-H2 tendon section.



Tokyo Rope USA, Inc.

File Name 【Pier-Tendon-Section】	Section Total Length (m)	Scanned Length		Note Identified damage 1 : Increase of magnetic flux Starting point of damage 1 : 4.43 m			
		Starting Point (m)	Ending Point (m)				
P3-402L-H1	21.43	0.56	20.64				
Identified Damage 1				Identified Damage 2			
Max Loss Point (m)	Loss (%)	Length (m)	Damage Orientation	Max Loss Point (m)	Loss (%)	Length (m)	Damage Orientation
4.5	-1.5	0.27	1~4 o'clock	—	—	—	—

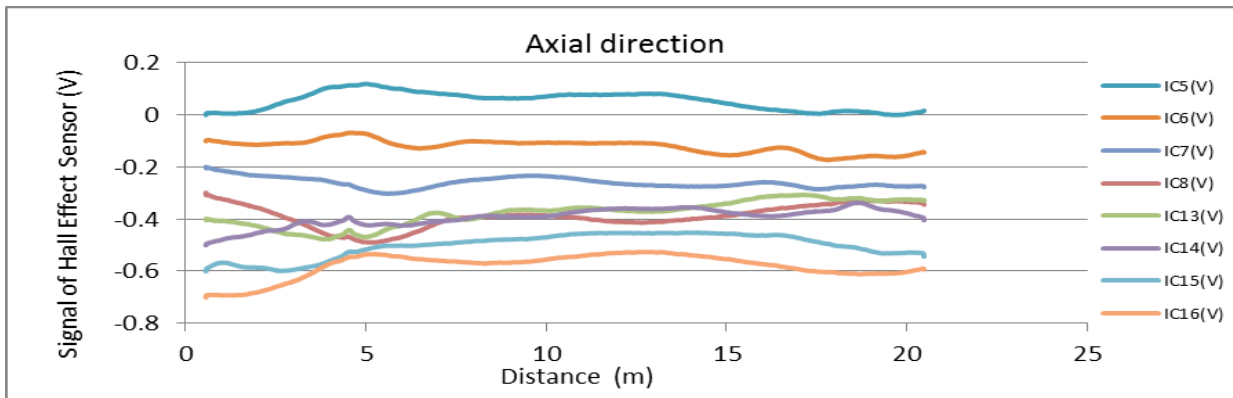
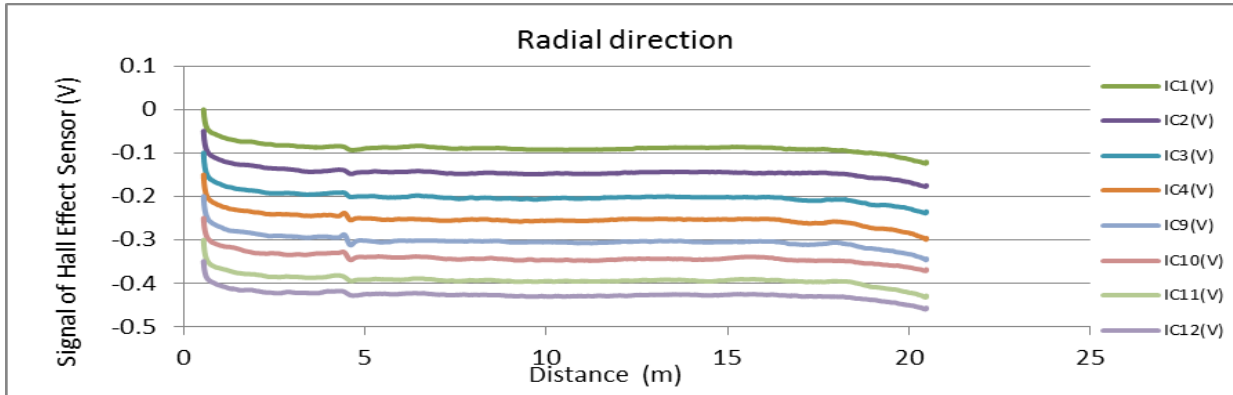
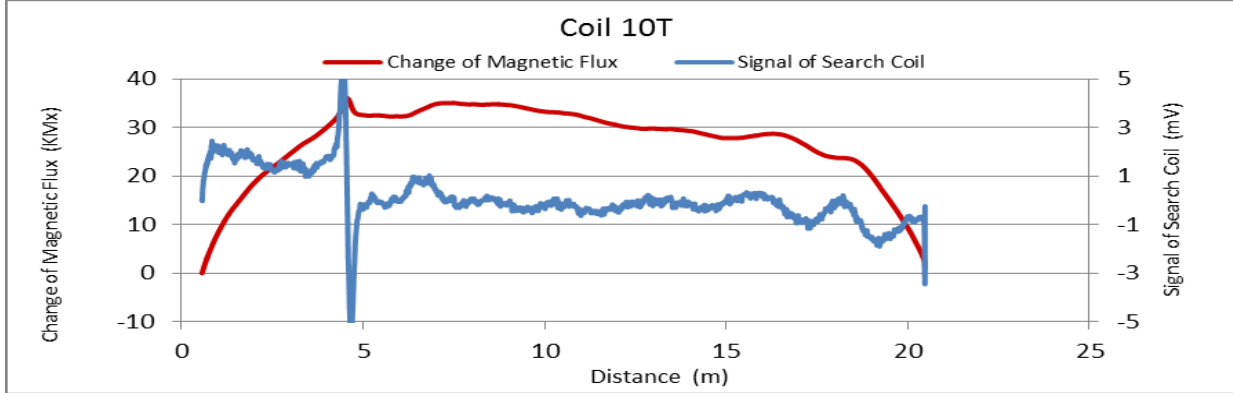


Figure A26. MMFM data of P3-402L-H1 tendon section.



Tokyo Rope USA, Inc.

File Name 【Pier-Tendon-Section】	Section Total Length (m)	Scanned Length		Note Starting point of damage 1 : 3.24 m			
		Starting Point (m)	Ending Point (m)				
P4-402R-H1	9.35	0.57	8.56				
Identified Damage 1				Identified Damage 2			
Max Loss Point (m)	Loss (%)	Length (m)	Damage Orientation	Max Loss Point (m)	Loss (%)	Length (m)	Damage Orientation
3.5	1.7	0.71	12~3 o'clock	—	—	—	—

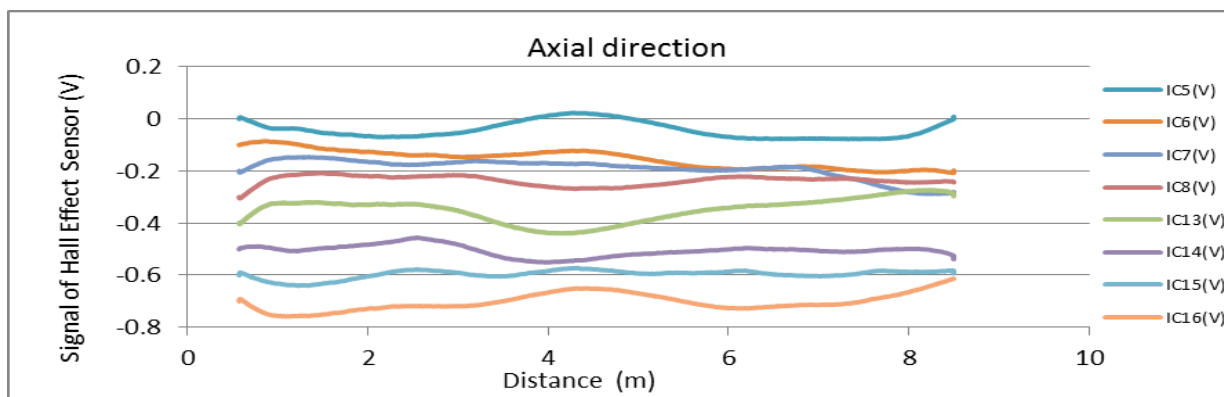
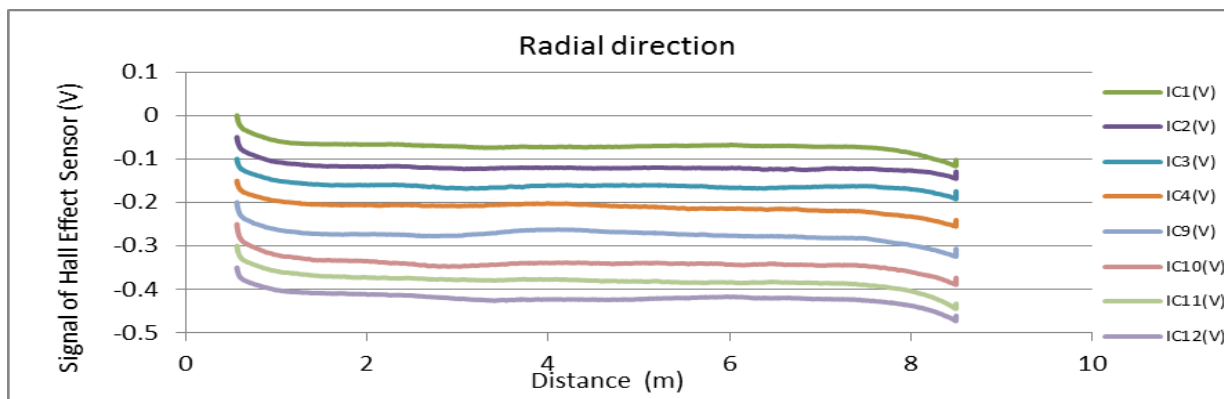
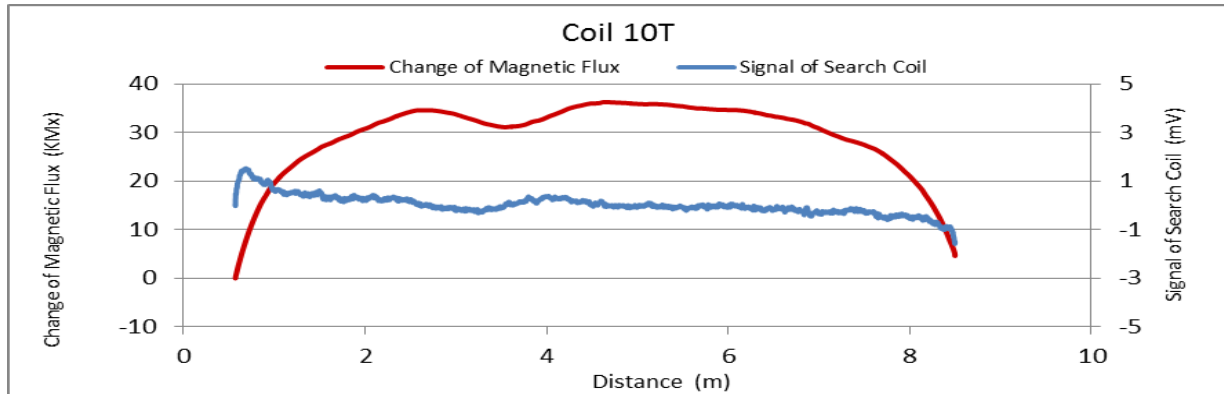


Figure A27. MMFM data of P4-402R-H1 tendon section.



Tokyo Rope USA, Inc.

File Name 【Pier-Tendon-Section】	Section Total Length (m)	Scanned Length		Note Starting point of damage 1 : 5.26 m			
		Starting Point (m)	Ending Point (m)				
P4-402L-H1	9.36	0.46	8.64				
Identified Damage 1				Identified Damage 2			
Max Loss Point (m)	Loss (%)	Length (m)	Damage Orientation	Max Loss Point (m)	Loss (%)	Length (m)	Damage Orientation
5.9	1.0	0.86	12~2 o'clock	—	—	—	—

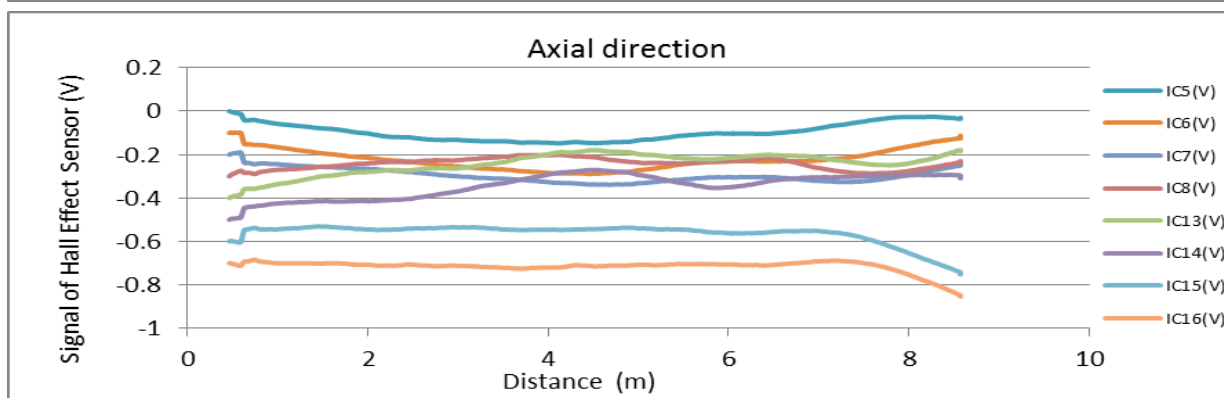
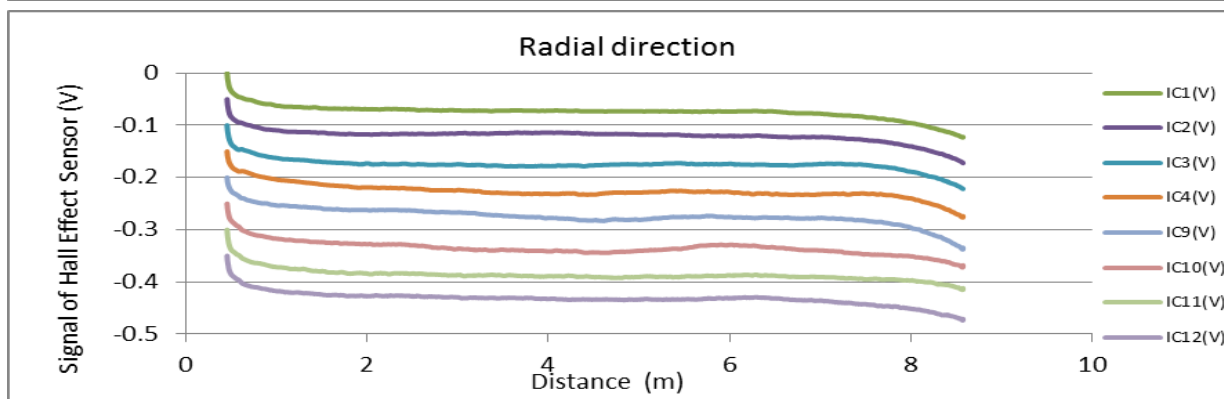
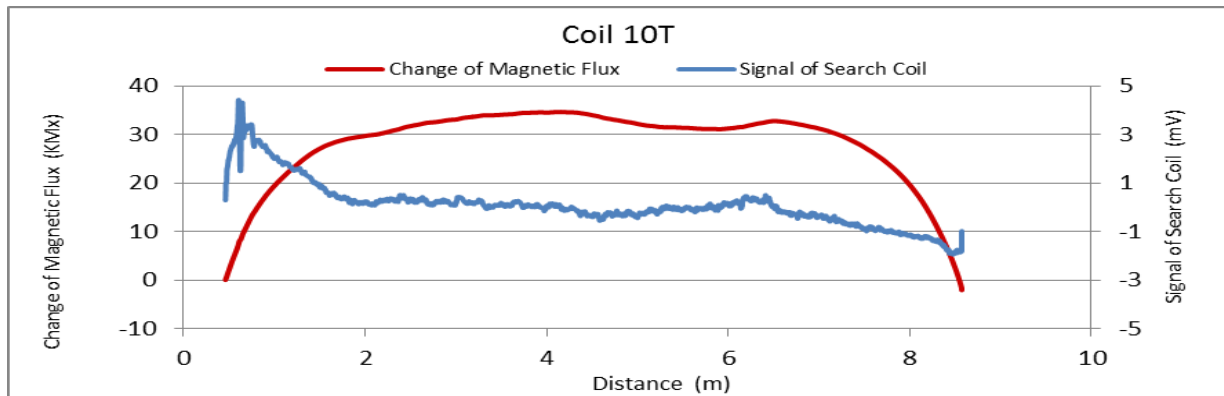


Figure A28. MMFM data of P4-402L-H1 tendon section.



Tokyo Rope USA, Inc.

File Name		Section	Scanned Length		Note		
【Pier-Tendon-Section】		Total Length (m)	Starting Point (m)	Ending Point (m)	Joint position: 12.37 m Starting point of damage 1: 17.15 m		
P4-401R-II		21.57	0.52	20.65			
Identified Damage 1				Identified Damage 2			
Max Loss Point (m)	Loss (%)	Length (m)	Damage Orientation	Max Loss Point (m)	Loss (%)	Length (m)	Damage Orientation
17.6	1.2	0.74	8~11 o'clock	—	—	—	—

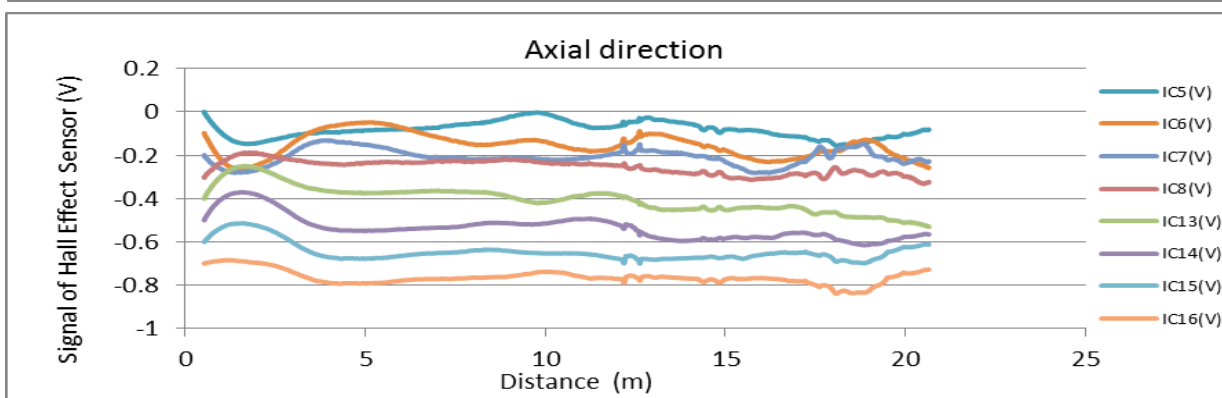
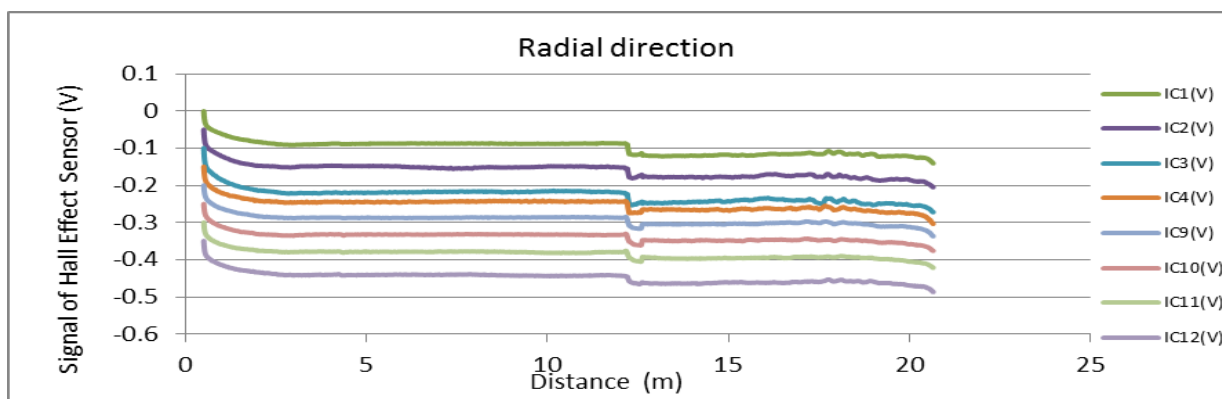
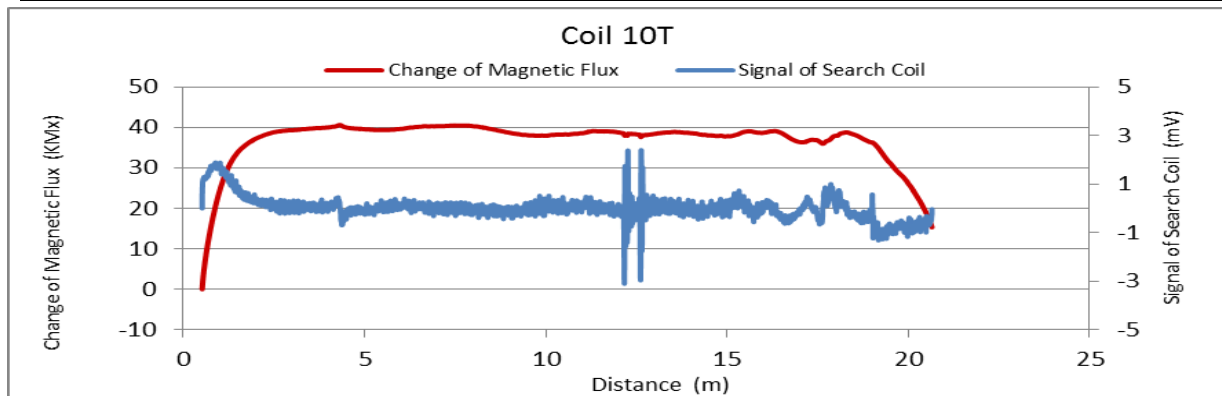


Figure A29. MMFM data of P4-401R-II tendon section.



Tokyo Rope USA, Inc.

File Name 【Pier-Tendon-Section】	Section Total Length (m)	Scanned Length		Note			
		Starting Point (m)	Ending Point (m)				
P4-401R-I2	21.46	0.7	20.88	Joint position : 9.14 m Identified damage 1 : Increase of magnetic flux Starting point of damage 1 : 19.71 m			
Identified Damage 1				Identified Damage 2			
Max Loss Point (m)	Section Loss (%)	Damage Length (m)	Damage Orientation	Max Loss Point (m)	Section Loss (%)	Damage Length (m)	Damage Orientation
19.8	-1.8	0.13	2~4 o'clock	—	—	—	—

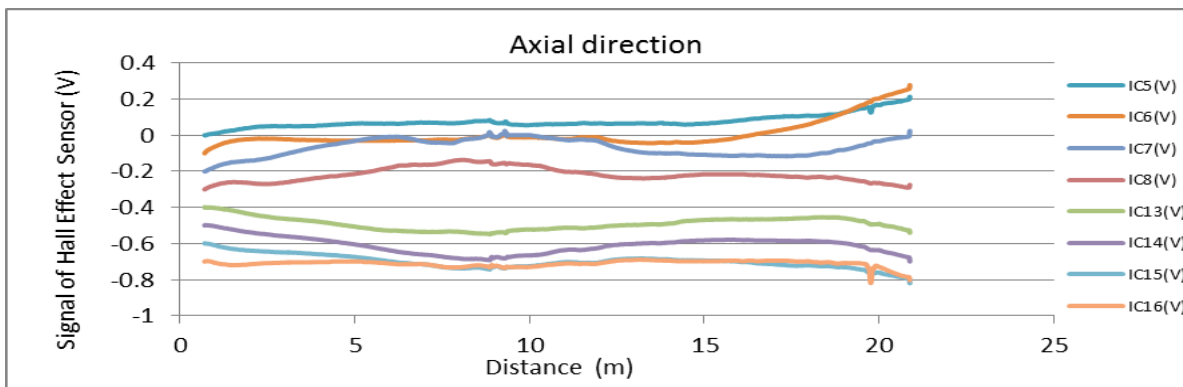
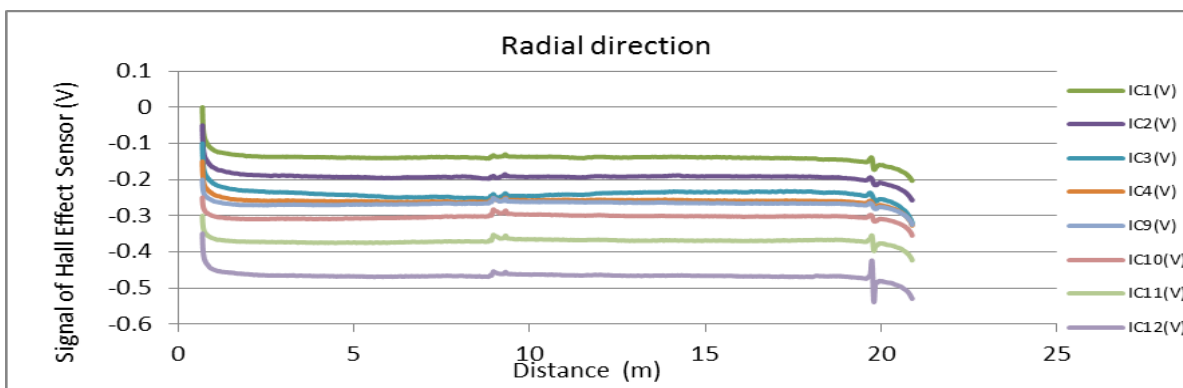
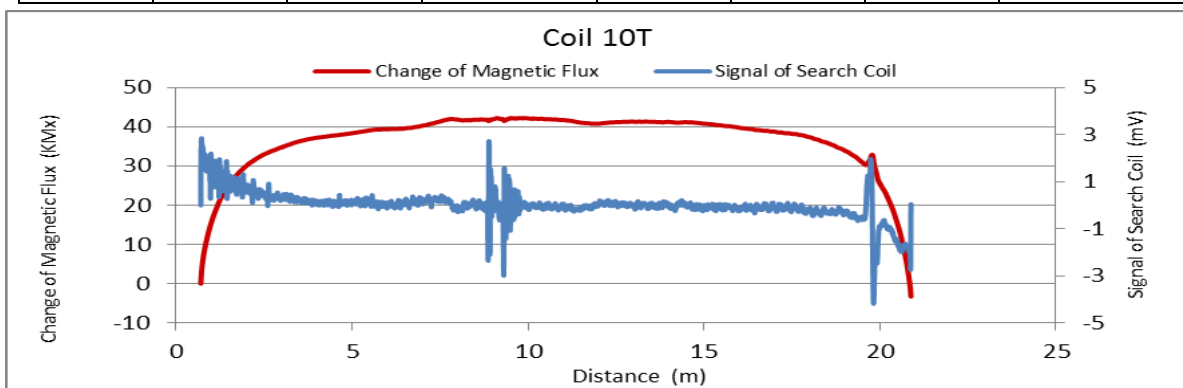


Figure A30. MMFM data of P4-401R-I2 tendon section.



Tokyo Rope USA, Inc.

File Name 【Pier-Tendon-Section】	Section Total Length (m)	Scanned Length		Note Joint position: 9.18 m Identified damage 1 : Increase of magnetic flux Starting point of damage 1 : 9.07 m			
		Starting Point (m)	Ending Point (m)				
P4-401L-I2	21.5	0.78	20.85				
Identified Damage 1				Identified Damage 2			
Max Loss Point (m)	Loss (%)	Length (m)	Damage Orientation	Max Loss Point (m)	Loss (%)	Length (m)	Damage Orientation
9.1	-2.2	0.17	12~2 o'clock	—	—	—	—

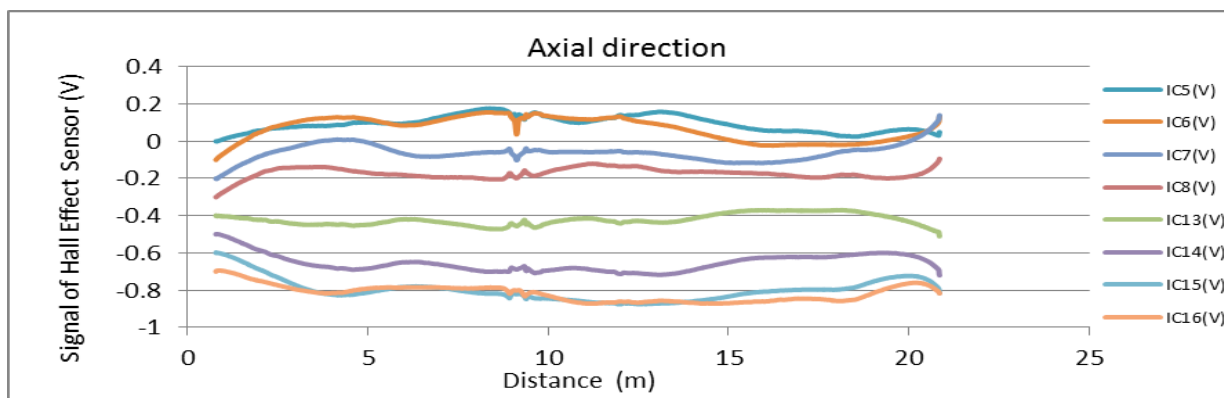
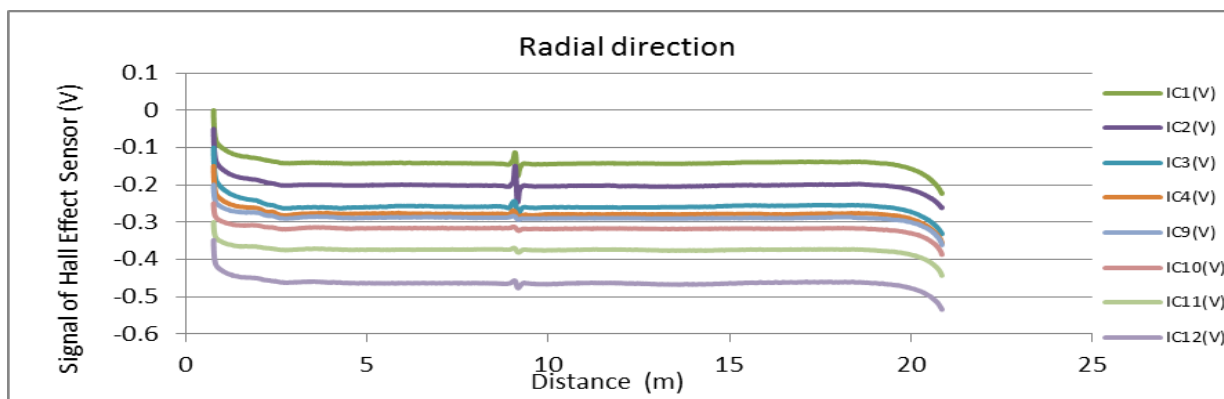
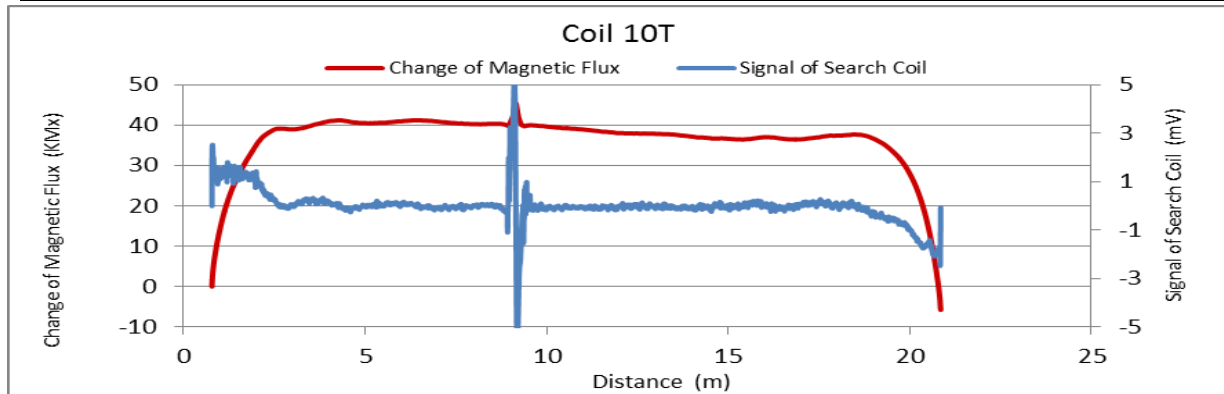


Figure A31. MMFM data of P4-401L-I2 tendon section.



Tokyo Rope USA, Inc.

File Name 【Pier-Tendon-Section】	Section Total Length (m)	Scanned Length		Note Repair tape position : 7.64 m Starting point of damage 1 : 2.97 m			
		Starting Point (m)	Ending Point (m)				
P4-402L-H2	9.39	0.8	8.81				
Identified Damage 1				Identified Damage 2			
Max Loss Point (m)	Loss (%)	Length (m)	Damage Orientation	Max Loss Point (m)	Loss (%)	Length (m)	Damage Orientation
3.3	1.0	0.83	1~4 o'clock	—	—	—	—

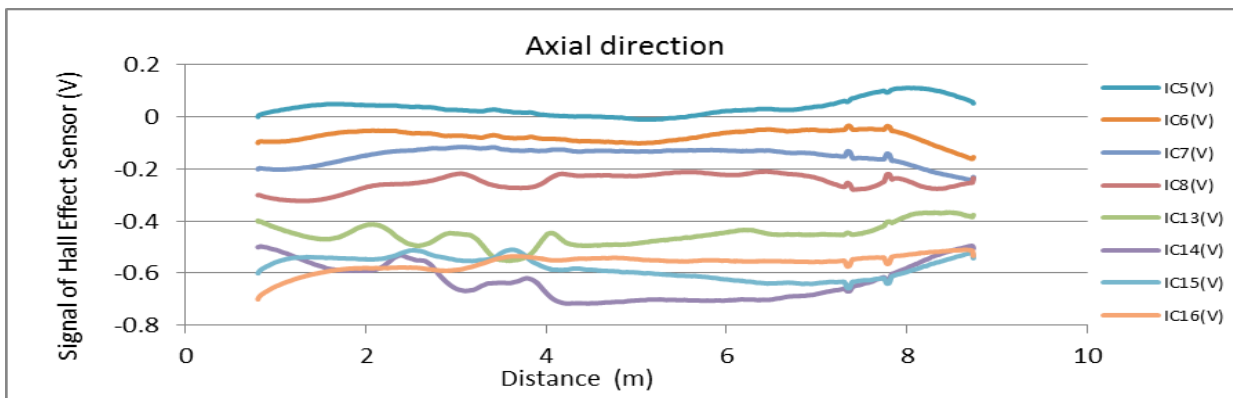
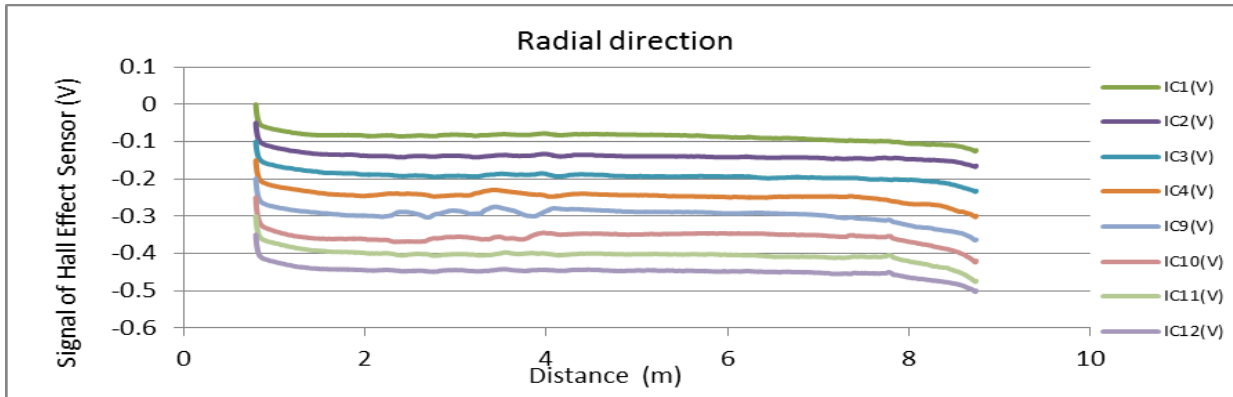
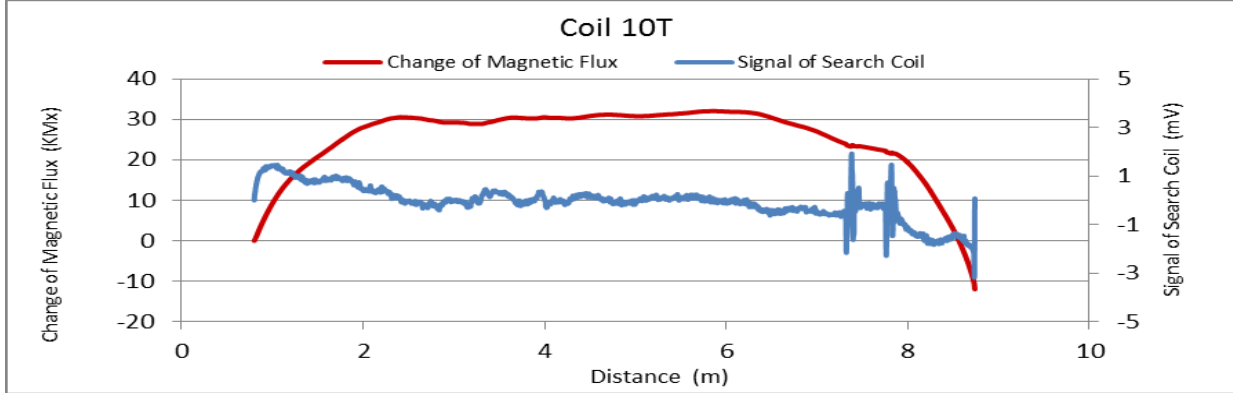


Figure A32. MMFM data of P4-402L-H2 tendon section.



Tokyo Rope USA, Inc.

File Name 【Pier-Tendon-Section】	Section Total Length (m)	Scanned Length		Note Joint position : 12.24 m Starting point of damage 1 : 2.29 m			
		Starting Point (m)	Ending Point (m)				
P5-401R-II	21.45	0.86	20.58				
Identified Damage 1				Identified Damage 2			
Max Loss Point (m)	Loss (%)	Length (m)	Damage Orientation	Max Loss Point (m)	Loss (%)	Length (m)	Damage Orientation
2.3	1.5	0.61	3~9 o'clock	—	—	—	—

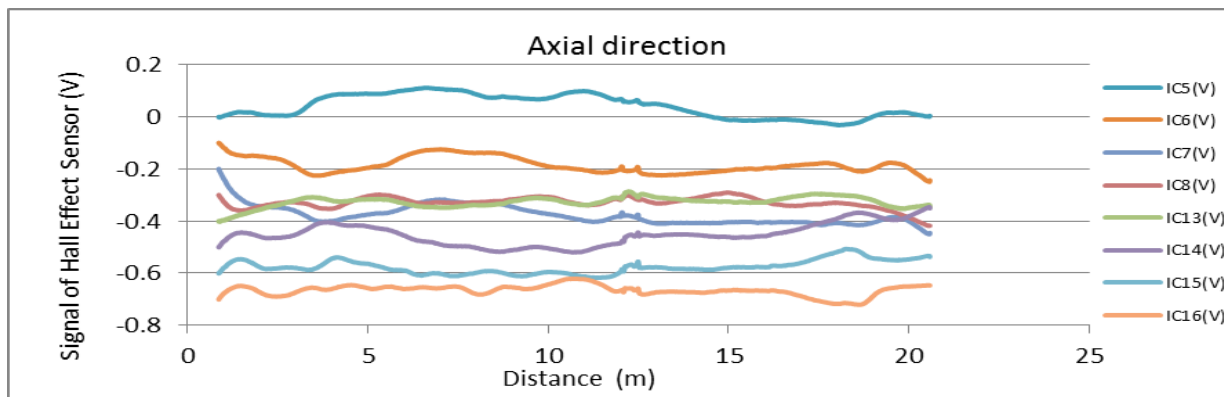
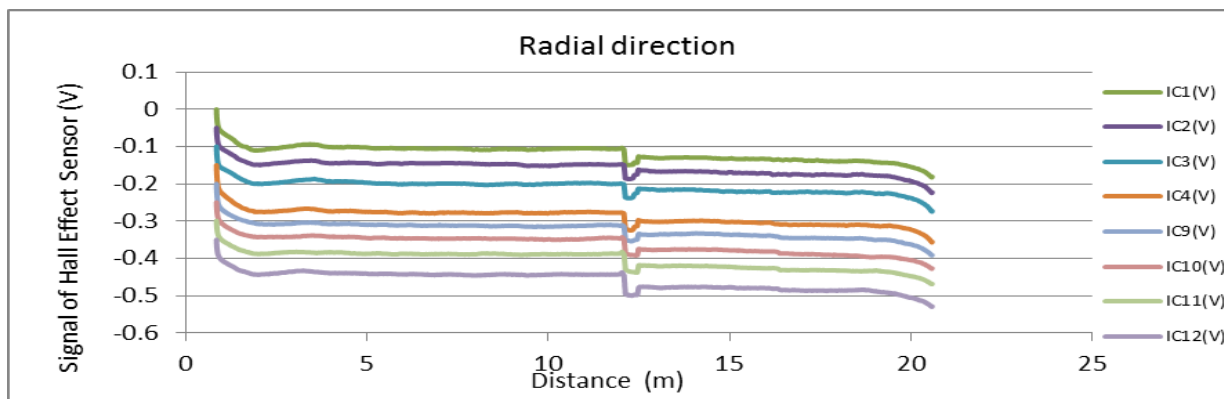
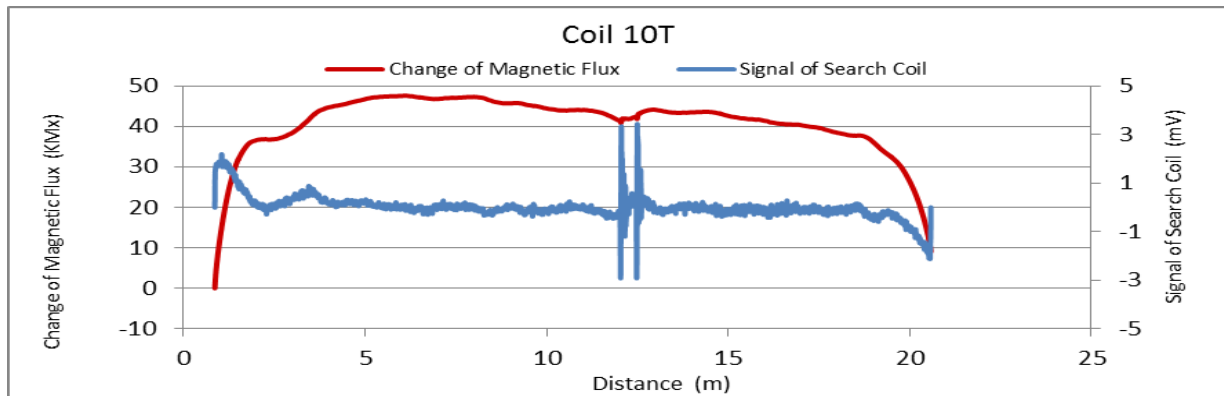


Figure A33. MMFM data of P5-401R-II tendon section.



Tokyo Rope USA, Inc.

File Name 【Pier-Tendon-Section】	Section Total Length (m)	Scanned Length		Note			
		Starting Point (m)	Ending Point (m)				
P5-402R-I1	21.45	1.55	20.83	Joint position: 12.56 m Identified damage 1: Increase of magnetic flux Identified damage 2: Elliptical deformed duct Starting point of damage 1: 2.34 m Starting point of damage 2: 18.5 m			
Identified Damage 1				Identified Damage 2			
Max Loss Point (m)	Loss (%)	Length (m)	Damage Orientation	Max Loss Point (m)	Loss (%)	Length (m)	Damage Orientation
2.4	-2.3	0.08	6~10 o'clock	18.8	1.2	0.6	7~11 o'clock

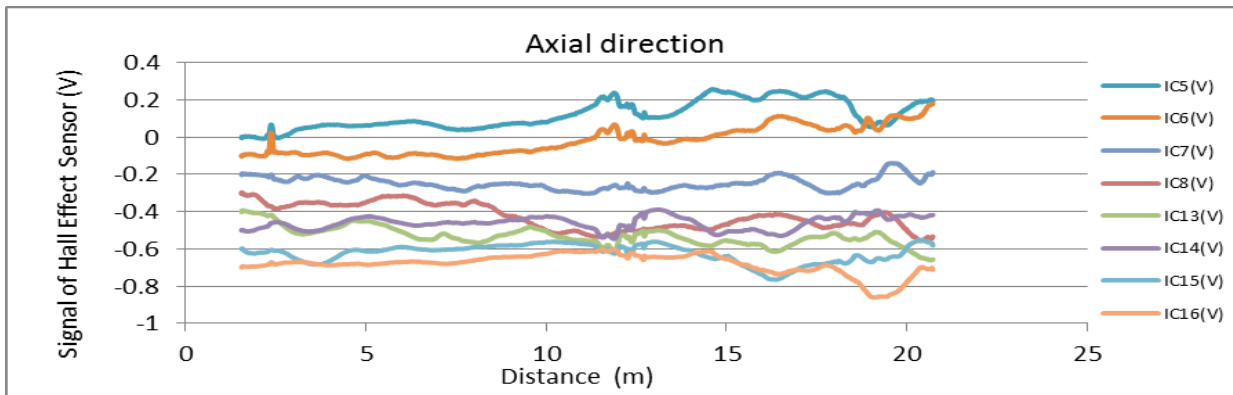
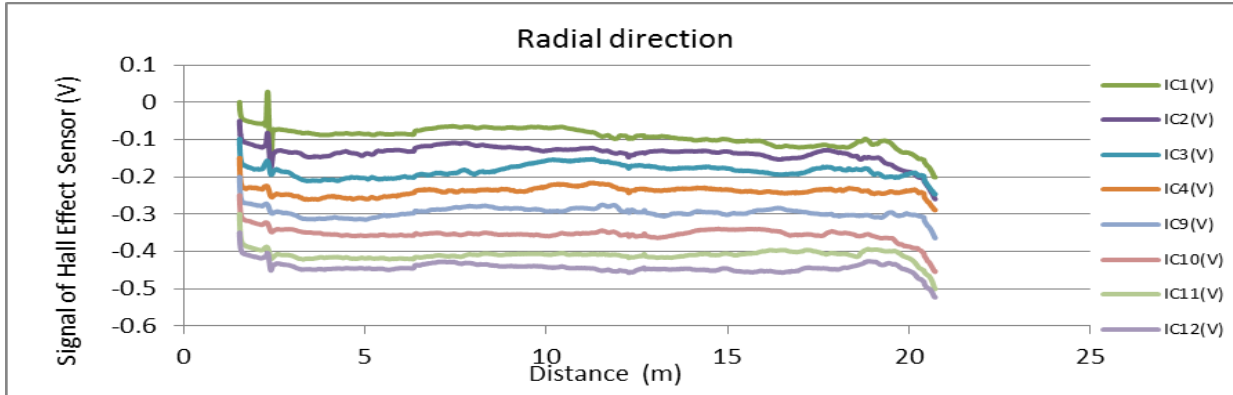
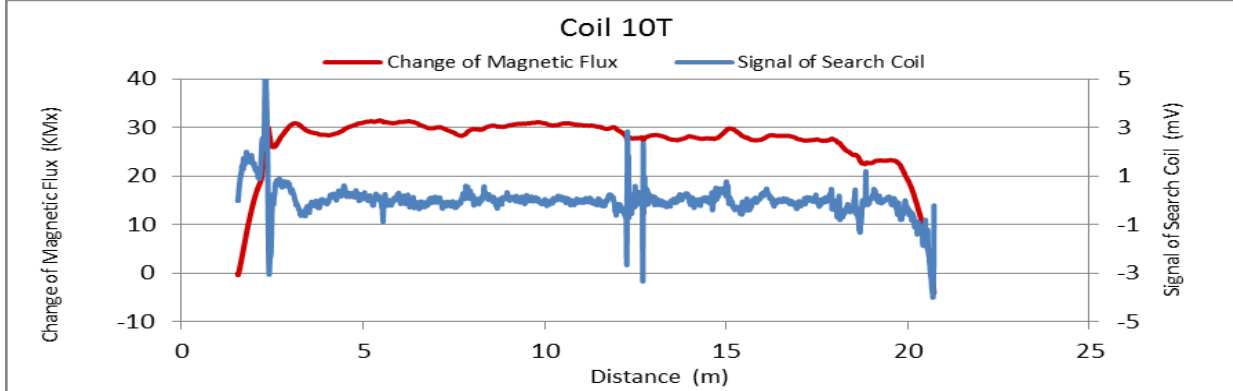


Figure A34. MMFM data of P5-402R-I1 tendon section.



Tokyo Rope USA, Inc.

File Name 【Pier-Tendon-Section】	Section Total Length (m)	Scanned Length		Note Joint or repair position : 12.28 m Identified damage 1 : Increase of magnetic flux Starting point of damage 1 : 9.56 m			
		Starting Point (m)	Ending Point (m)				
P5-401L-I1	21.51	0.71	20.73				
Identified Damage 1				Identified Damage 2			
Max Loss Point (m)	Loss (%)	Length (m)	Damage Orientation	Max Loss Point (m)	Loss (%)	Length (m)	Damage Orientation
9.6	-1.7	0.14	6~9 o'clock	—	—	—	—

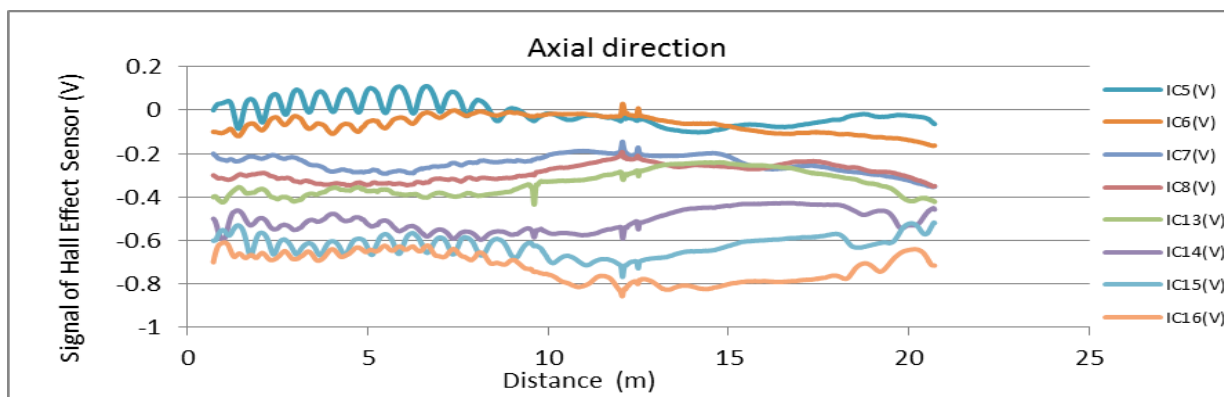
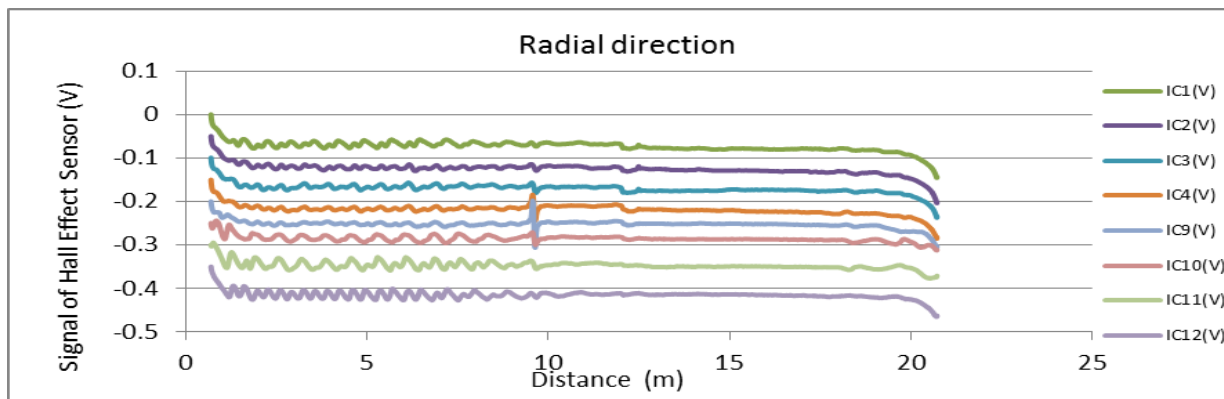
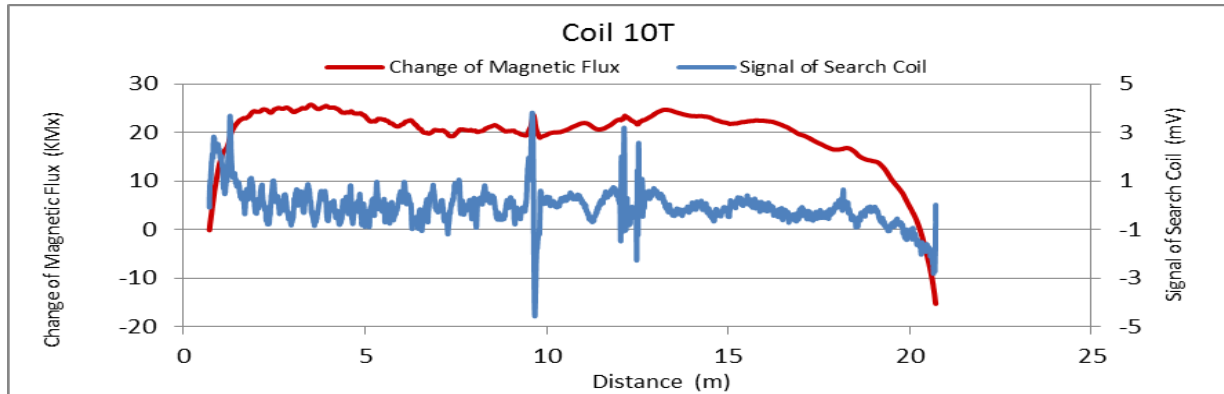


Figure A35. MMFM data of P5-401L-I1 tendon section.



Tokyo Rope USA, Inc.

File Name 【Pier-Tendon-Section】	Section Total Length (m)	Scanned Length		Note			
		Starting Point (m)	Ending Point (m)				
P5-402L-I1	21.51	0.62	20.62	Joint or repair position : 12.28 m Identified damage 1&2 : Increase of magnetic flux Starting point of damage 1 : 3.94 m Starting point of damage 2 : 12.13 m			
Identified Damage 1				Identified Damage 2			
Max Loss Point (m)	Loss (%)	Length (m)	Damage Orientation	Max Loss Point (m)	Loss (%)	Length (m)	Damage Orientation
4.0	-2.3	0.15	5~7 o'clock	12.2	-3.1	0.2	10~12 o'clock

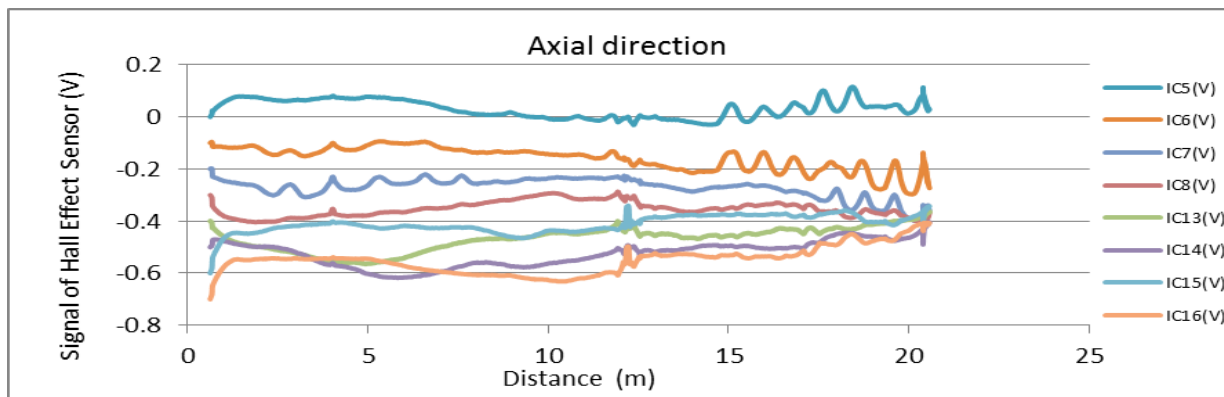
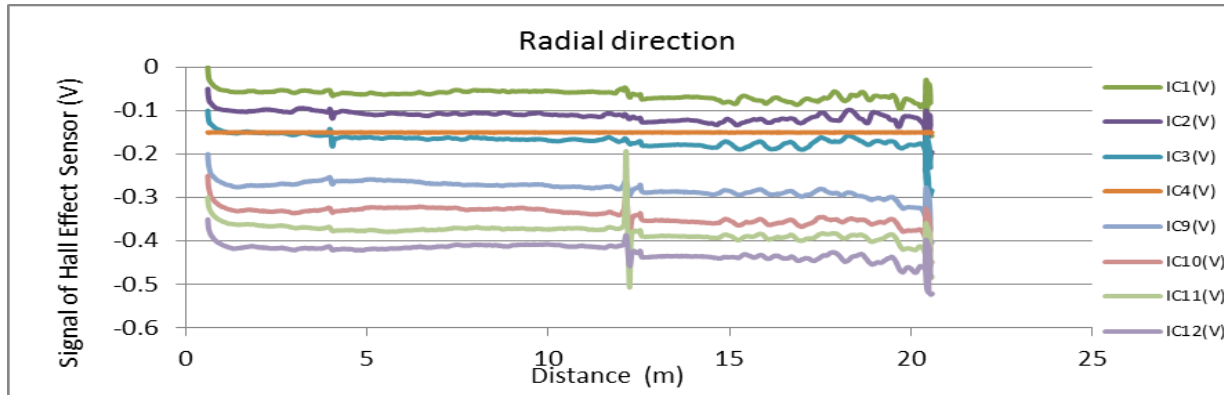
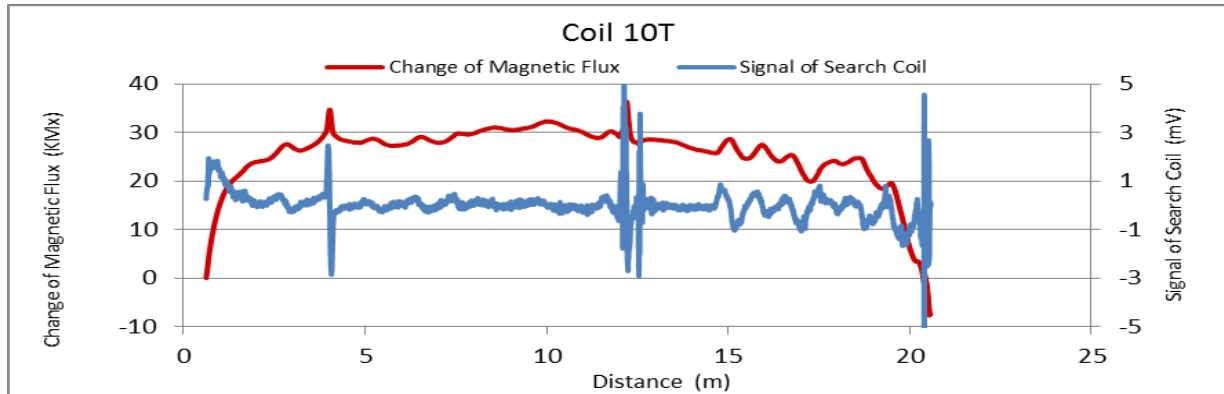


Figure A36. MMFM data of P5-402L-I1 tendon section.



Tokyo Rope USA, Inc.

File Name 【Pier-Tendon-Section】	Section Total Length (m)	Scanned Length		Note Starting point of damage 1 : 3.28 m			
		Starting Point (m)	Ending Point (m)				
P6-402R-H2	9.36	0.78	8.83				
Identified Damage 1				Identified Damage 2			
Max Loss Point (m)	Loss (%)	Length (m)	Damage Orientation	Max Loss Point (m)	Loss (%)	Length (m)	Damage Orientation
3.7	1.3	1.34	5~9 o'clock	—	—	—	—

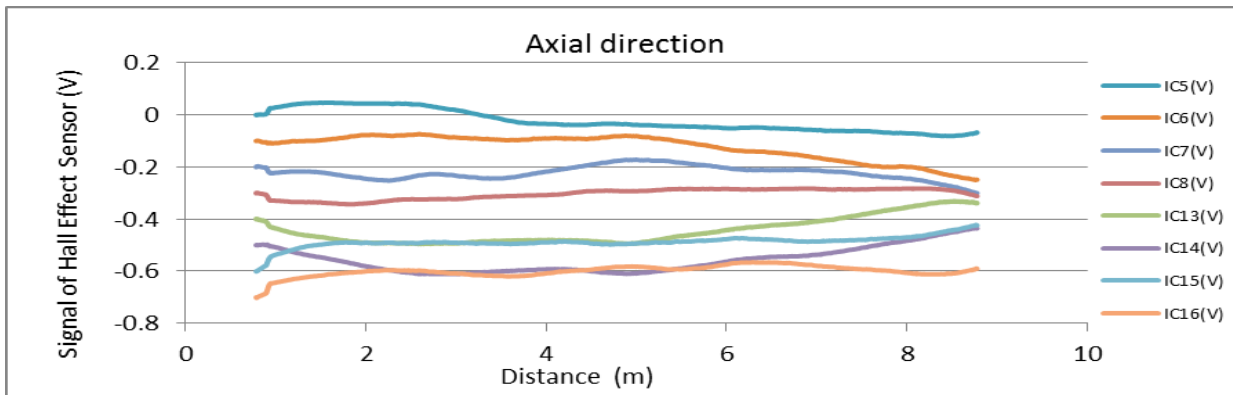
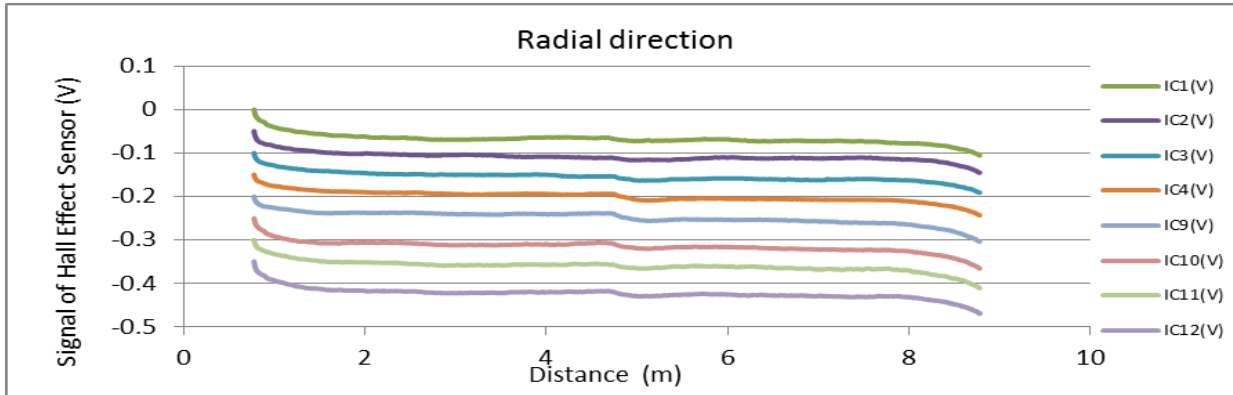
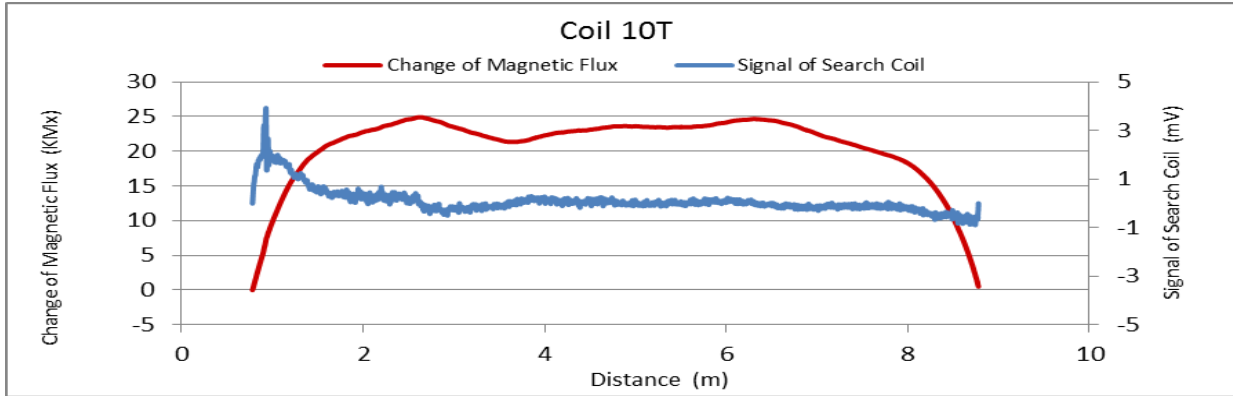


Figure A37. MMFM data of P6-402R-H2 tendon section.



Tokyo Rope USA, Inc.

File Name		Section	Scanned Length		Note		
【Pier-Tendon-Section】		Total Length (m)	Starting Point (m)	Ending Point (m)	Joint position: 9.23m Identified damage 1 : Increase of magnetic flux Starting point of damage 1 : 11.77 m		
P7-401L-I2		21.51	0.8	20.95			
Identified Damage 1				Identified Damage 2			
Max Loss Point (m)	Loss (%)	Length (m)	Damage Orientation	Max Loss Point (m)	Loss (%)	Length (m)	Damage Orientation
11.8	-2.6	0.17	9~12 o'clock	—	—	—	—

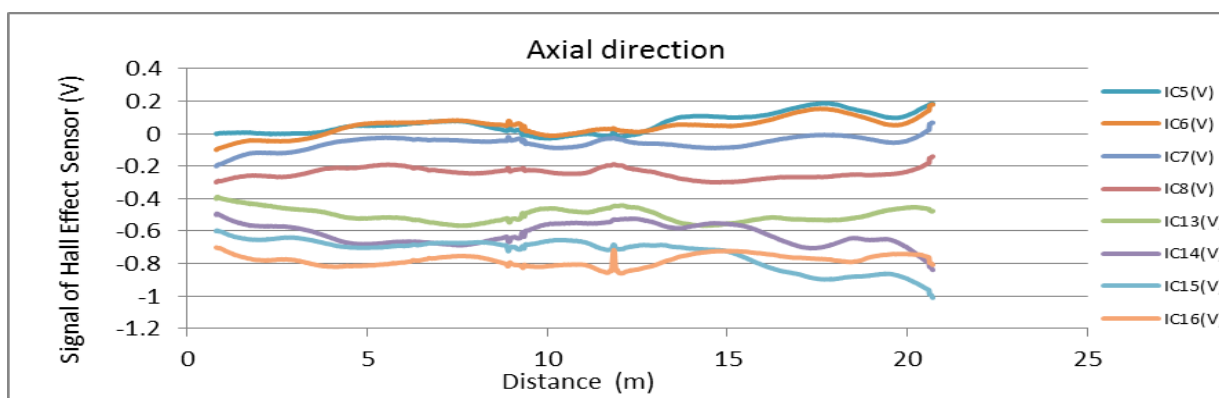
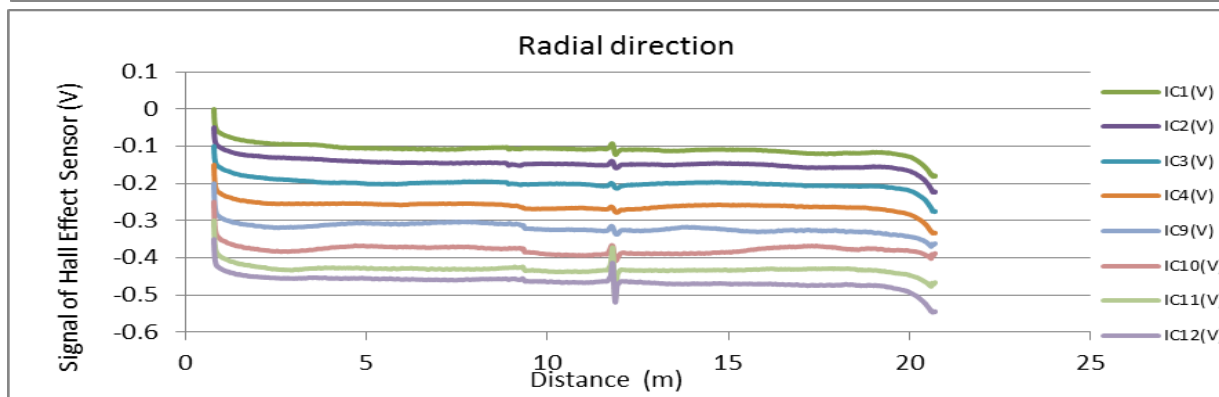
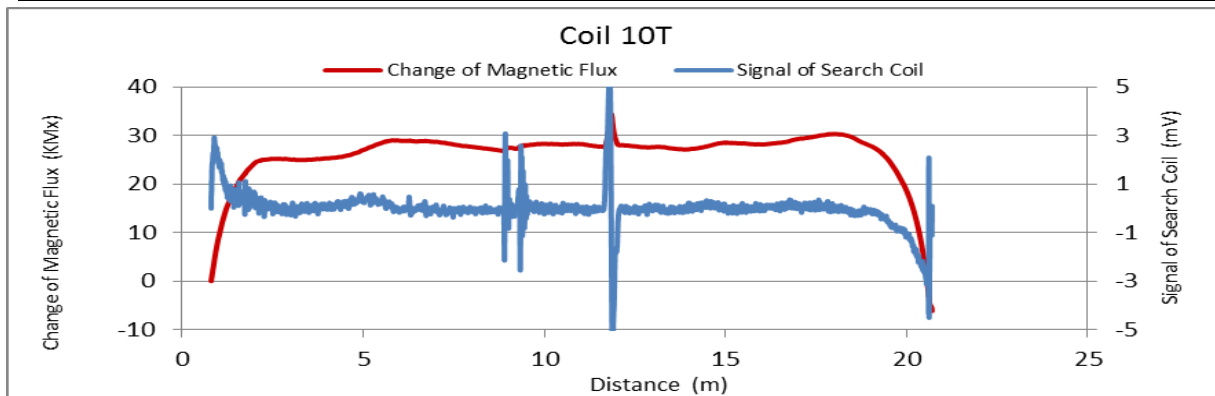


Figure A38. MMFM data of P7-401L-I2 tendon section.



Tokyo Rope USA, Inc.

File Name 【Pier-Tendon-Section】	Section Total Length (m)	Scanned Length		Note Joint position: 9.2 m Identified damage 1 : Increase of magnetic flux Starting point of damage 1 : 15.87 m			
		Starting Point (m)	Ending Point (m)				
P7-402L-I2	21.51	0.72	20.97				
Identified Damage 1				Identified Damage 2			
Max Loss Point (m)	Loss (%)	Length (m)	Damage Orientation	Max Loss Point (m)	Loss (%)	Length (m)	Damage Orientation
15.9	-2.5	0.17	11~1 o'clock	—	—	—	—

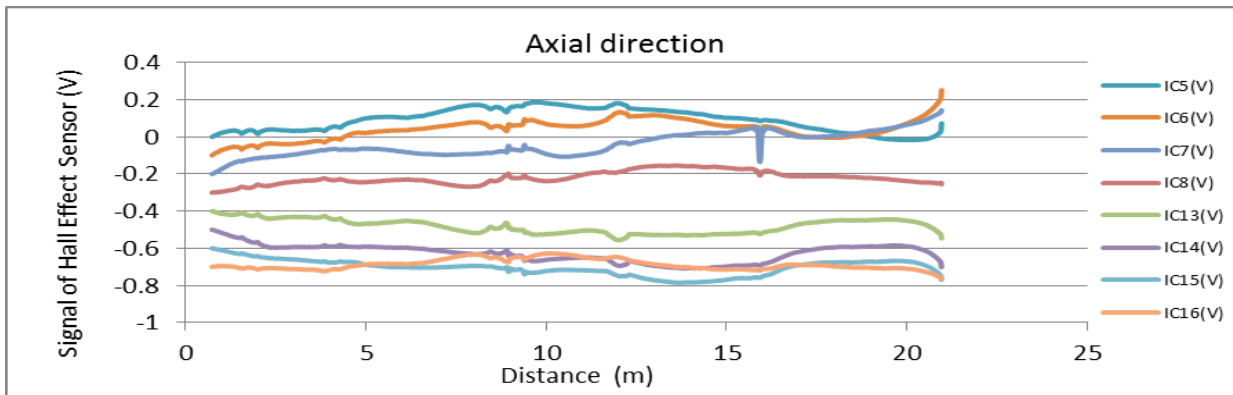
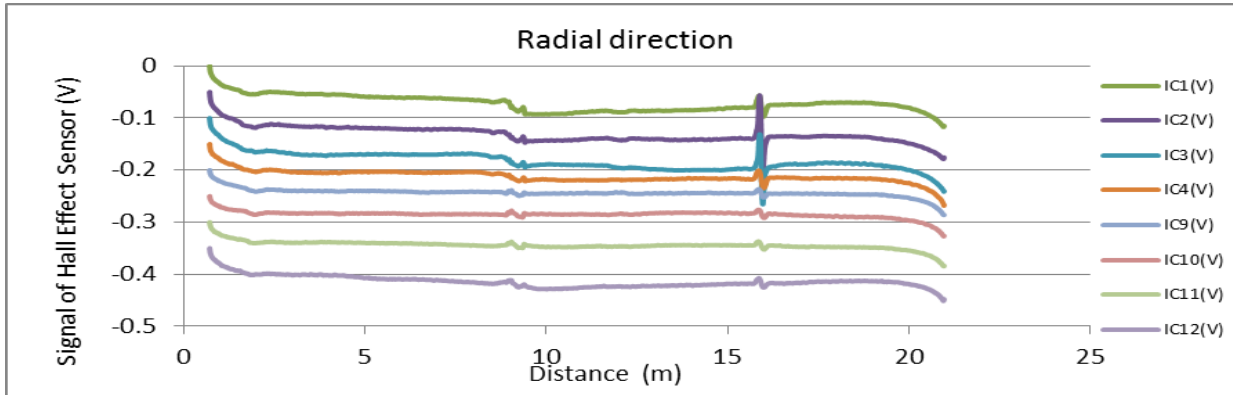
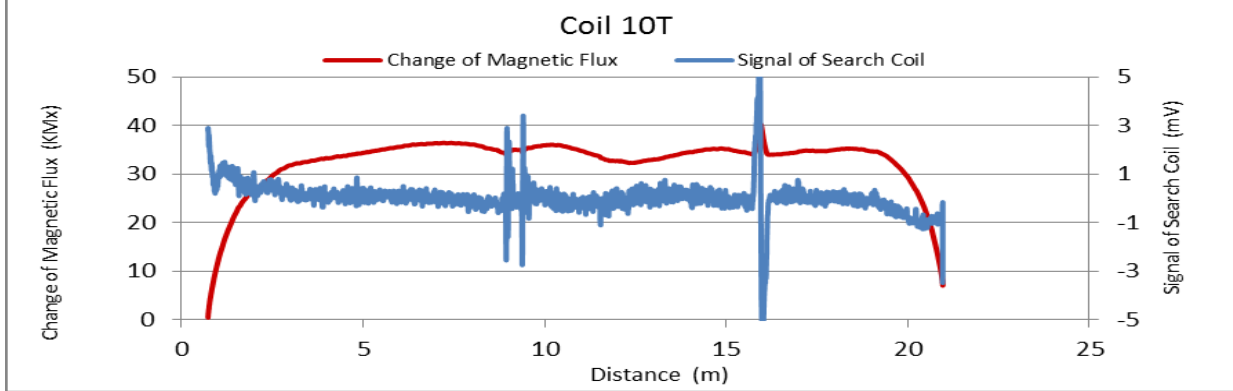


Figure A39. MMFM data of P7-402L-I2 tendon section.



Tokyo Rope USA, Inc.

File Name 【Pier-Tendon-Section】	Section Total Length (m)	Scanned Length		Note Joint position: 12.29 m, 18.9 m Identified damage 1: Increase of magnetic flux Starting point of damage 1: 9.31 m			
		Starting Point (m)	Ending Point (m)				
P9-401R-I1	21.57	0.61	20.82				
Identified Damage 1				Identified Damage 2			
Max Loss Point (m)	Loss (%)	Length (m)	Damage Orientation	Max Loss Point (m)	Loss (%)	Length (m)	Damage Orientation
9.4	-0.9	0.28	6~9 o'clock	—	—	—	—

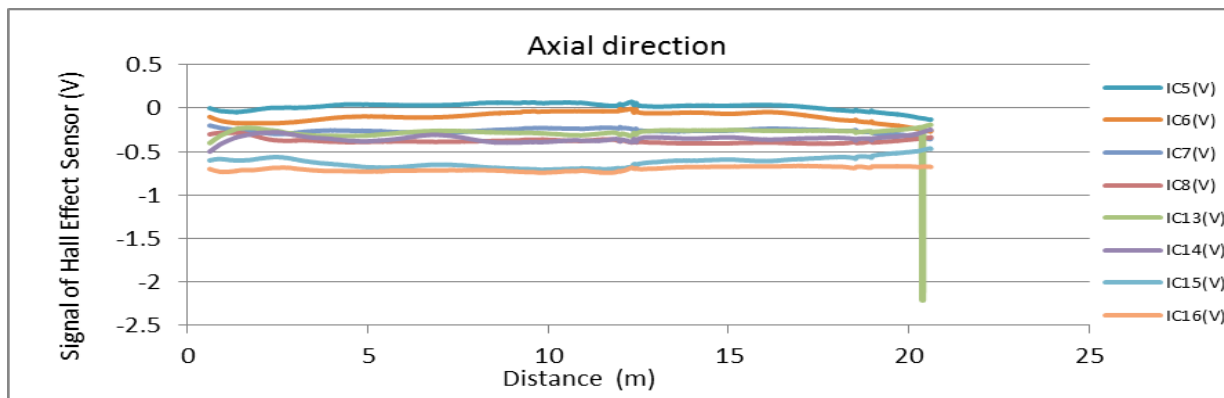
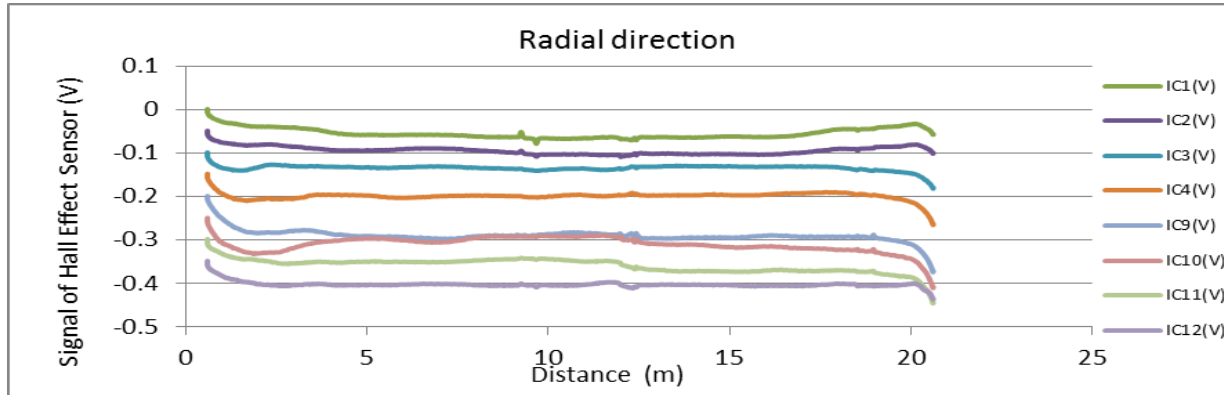
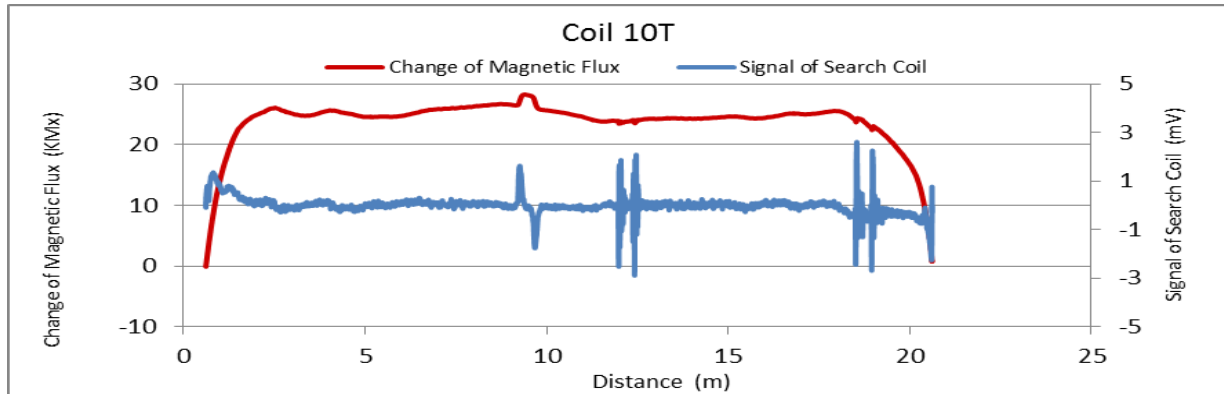


Figure A40. MMFM data of P9-401R-I1 tendon section.



Tokyo Rope USA, Inc.

File Name 【Pier-Tendon-Section】	Section Total Length (m)	Scanned Length		Note Joint position : 12.3 m Starting point of damage 1 : 11.2 m			
		Starting Point (m)	Ending Point (m)				
P9-402L-I1	21.48	0.58	20.78				
Identified Damage 1				Identified Damage 2			
Max Loss Point (m)	Loss (%)	Length (m)	Damage Orientation	Max Loss Point (m)	Loss (%)	Length (m)	Damage Orientation
12.3	1.6	3.13	3~9 o'clock	—	—	—	—

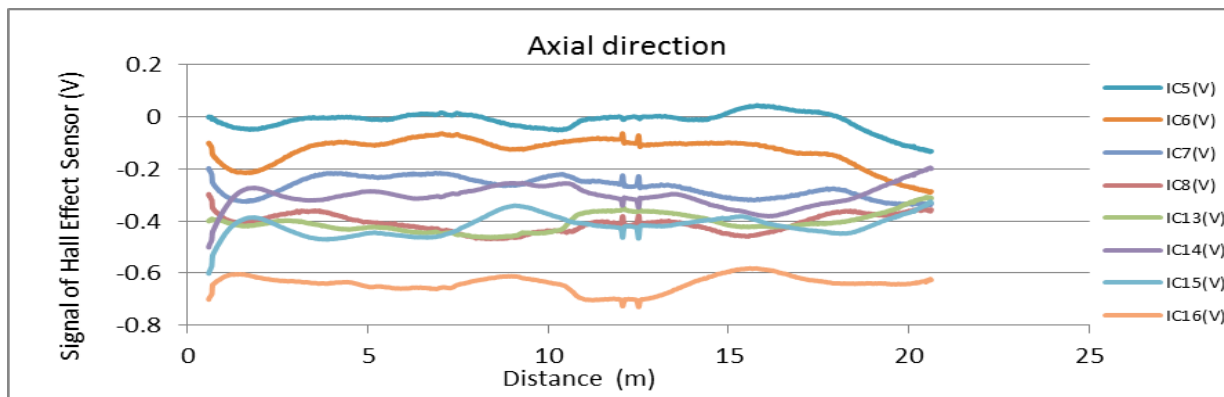
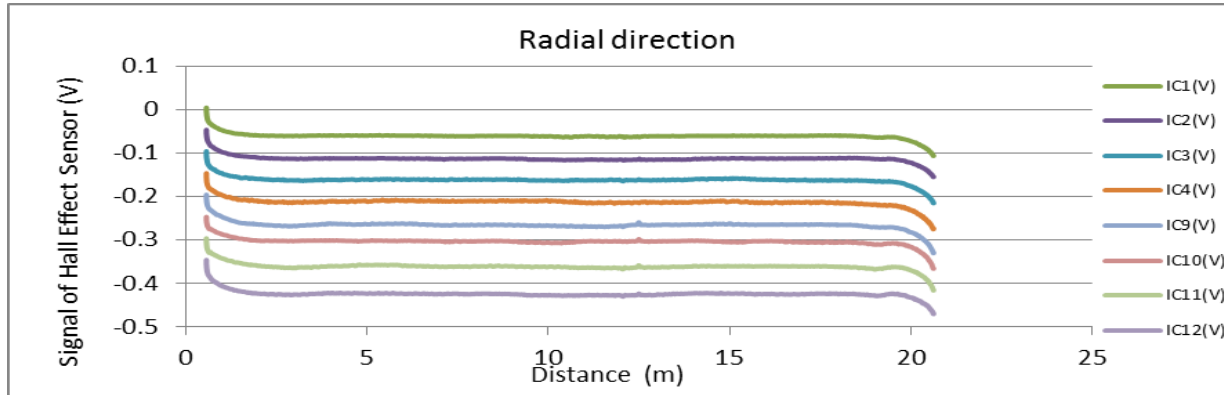
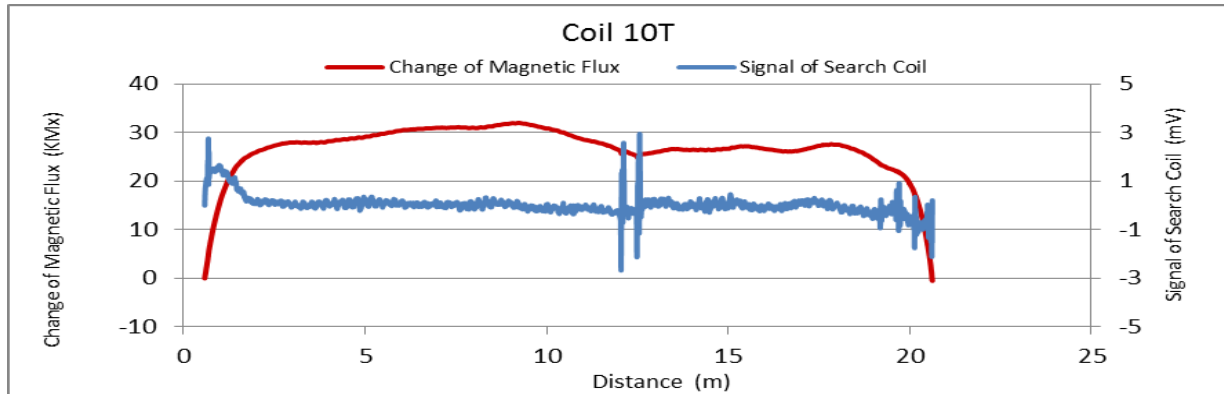


Figure A41. MMFM data of P9-402L-I1 tendon section.



Tokyo Rope USA, Inc.

File Name 【Pier-Tendon-Section】	Section Total Length (m)	Scanned Length		Note Joint position : 9.24 m Starting point of damage 1 : 8.55 m			
		Starting Point (m)	Ending Point (m)				
P9-402R-I2	21.47	0.55	20.42				
Identified Damage 1				Identified Damage 2			
Max Loss Point (m)	Loss (%)	Length (m)	Damage Orientation	Max Loss Point (m)	Loss (%)	Length (m)	Damage Orientation
10.3	1.5	2.52	5~10 o'clock	—	—	—	—

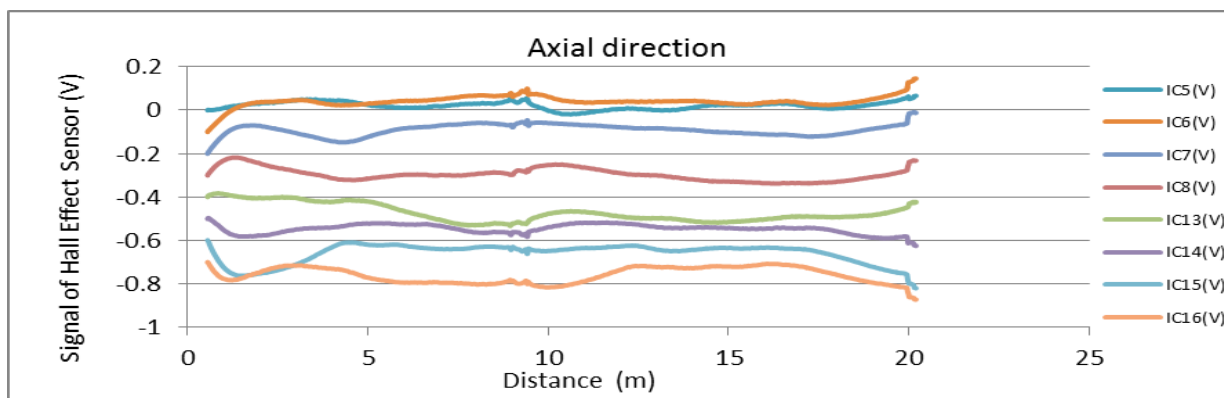
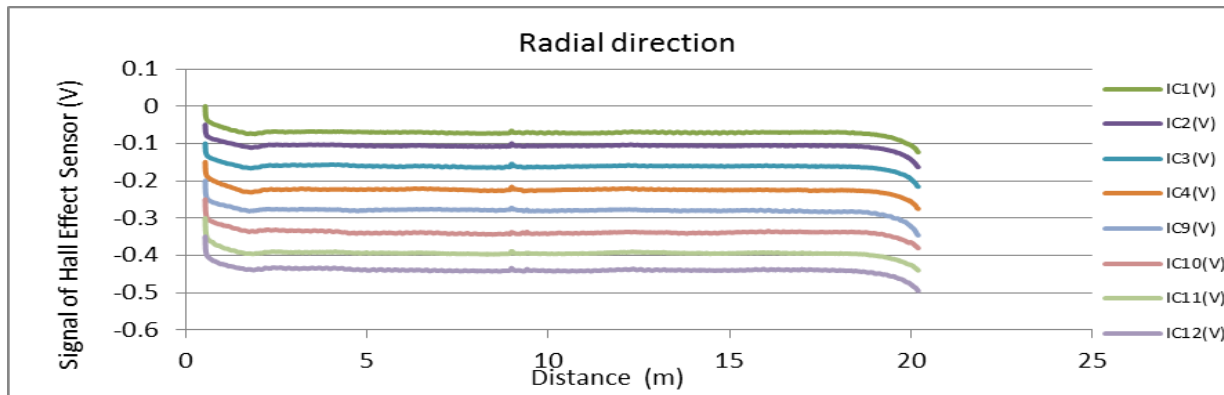
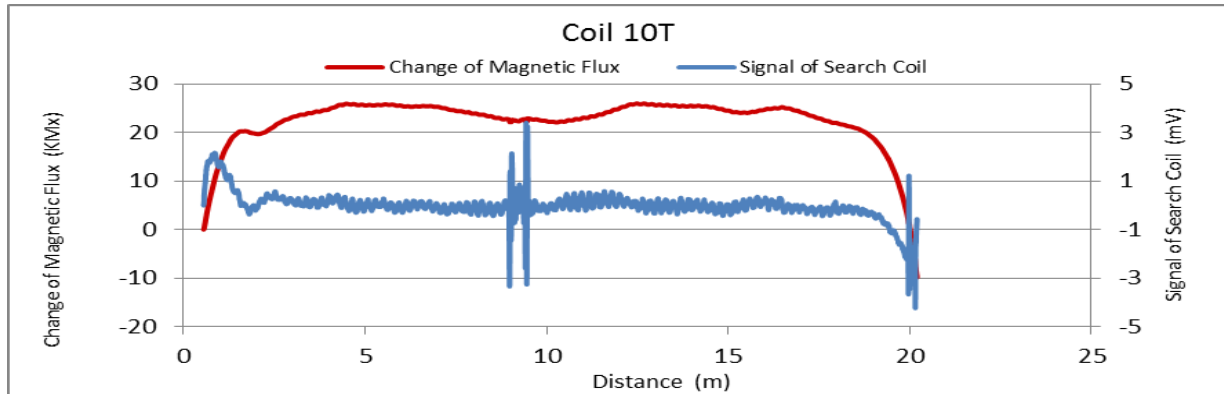


Figure A42. MMFM data of P9-402R-I2 tendon section.



Tokyo Rope USA, Inc.

File Name 【Pier-Tendon-Section】	Section Total Length (m)	Scanned Length		Note Starting point of damage 1 : 3.2 m			
		Starting Point (m)	Ending Point (m)				
P9-401L-H2	9.37	1.51	8.91				
Identified Damage 1				Identified Damage 2			
Max Loss Point (m)	Loss (%)	Length (m)	Damage Orientation	Max Loss Point (m)	Loss (%)	Length (m)	Damage Orientation
3.2	0.5	0.11	11~3 o'clock	—	—	—	—

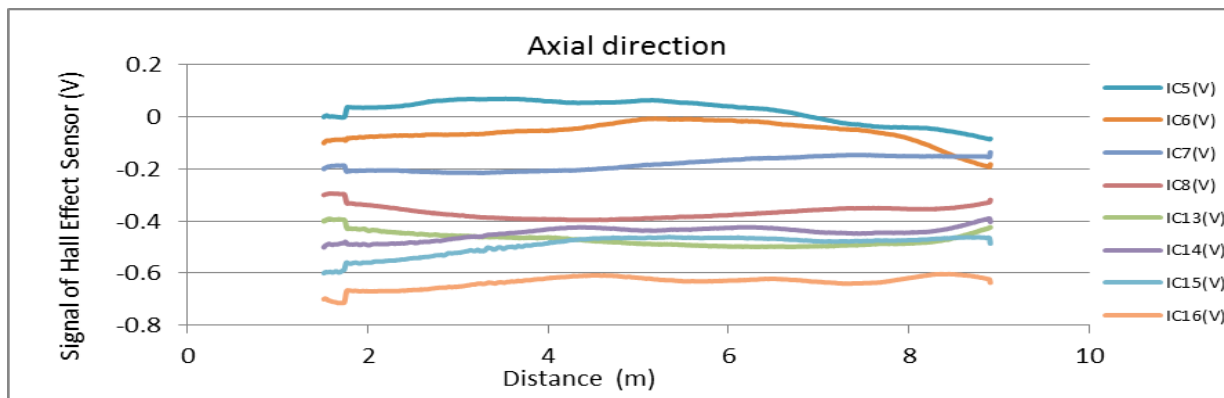
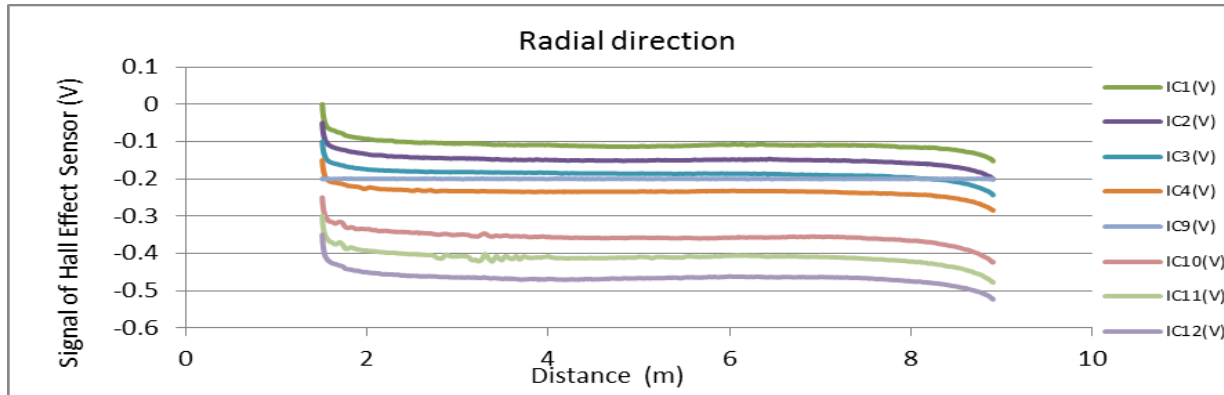
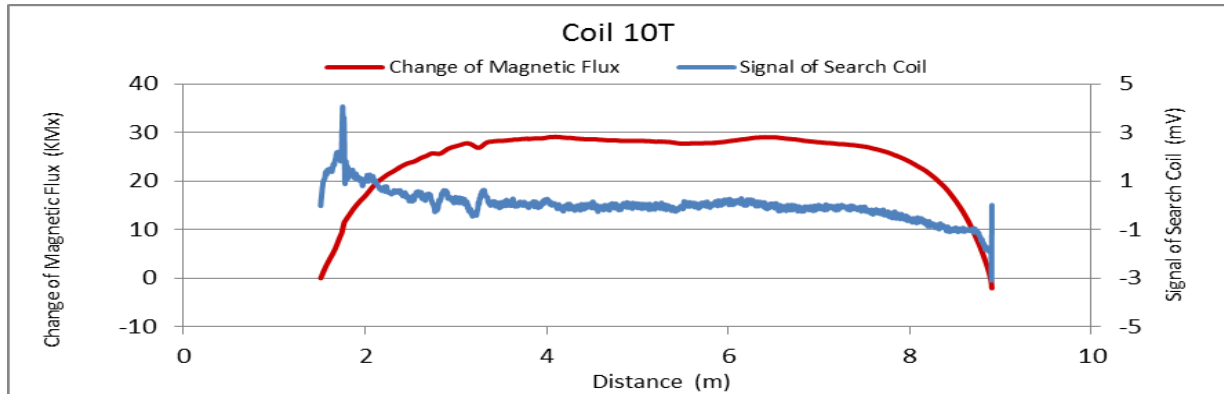


Figure A43. MMFM data of P9-401L-H2 tendon section.



Tokyo Rope USA, Inc.

File Name 【Pier-Tendon-Section】	Section Total Length (m)	Scanned Length		Note Joint position: 12.23 m, 19.6 m Identified damage 1 : Increase of magnetic flux Starting point of damage 1 : 6.25 m			
		Starting Point (m)	Ending Point (m)				
P10-401L-I1	21.47	0.56	20.63				
Identified Damage 1				Identified Damage 2			
Max Loss Point (m)	Loss (%)	Length (m)	Damage Orientation	Max Loss Point (m)	Loss (%)	Length (m)	Damage Orientation
6.3	-3.0	0.23	11~3 o'clock	—	—	—	—

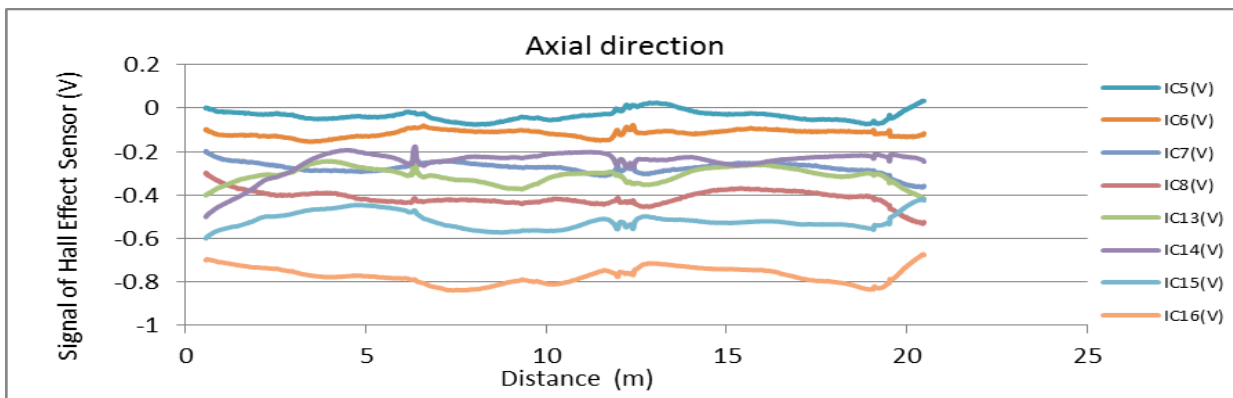
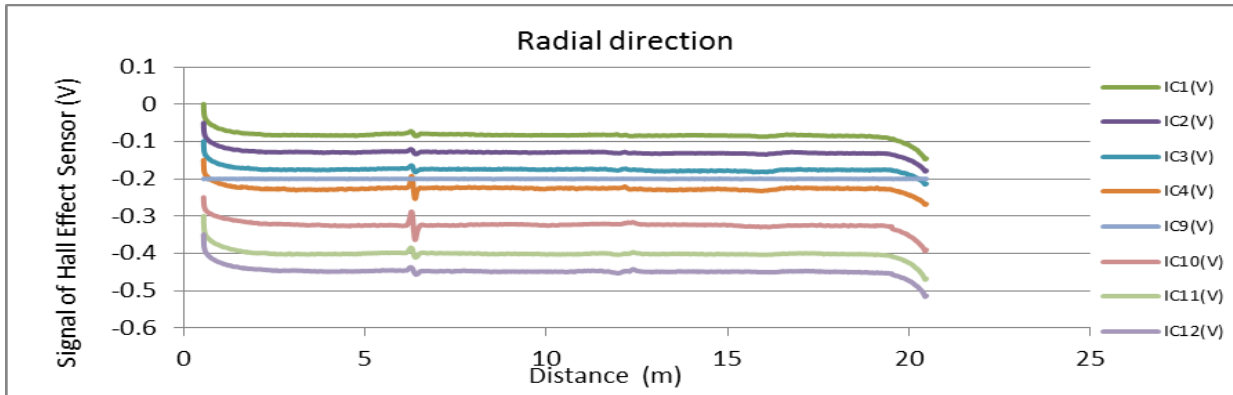
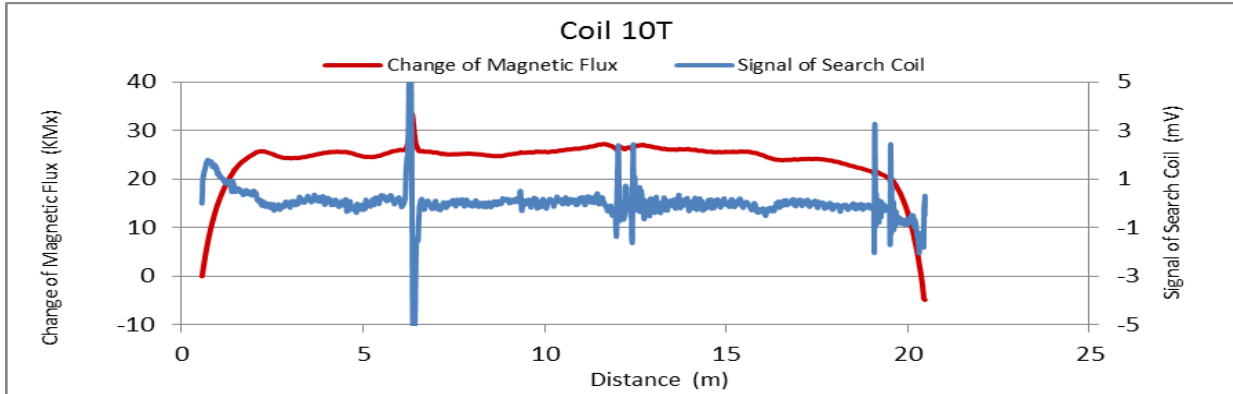


Figure A44. MMFM data of P10-401L-I1 tendon section.



Tokyo Rope USA, Inc.

File Name 【Pier-Tendon-Section】	Section Total Length (m)	Scanned Length		Note			
		Starting Point (m)	Ending Point (m)				
P10-402L-I2	21.54	0.72	19.11	Joint position: 9.15 m Identified damage 1&2: Increase of magnetic flux Starting point of damage 1: 2.0 m Starting point of damage 2: 9.12 m			
Identified Damage 1				Identified Damage 2			
Max Loss Point (m)	Loss (%)	Length (m)	Damage Orientation	Max Loss Point (m)	Loss (%)	Length (m)	Damage Orientation
2.1	-3.4	0.19	7~10 o'clock	9.2	-3.0	0.23	4~8 o'clock

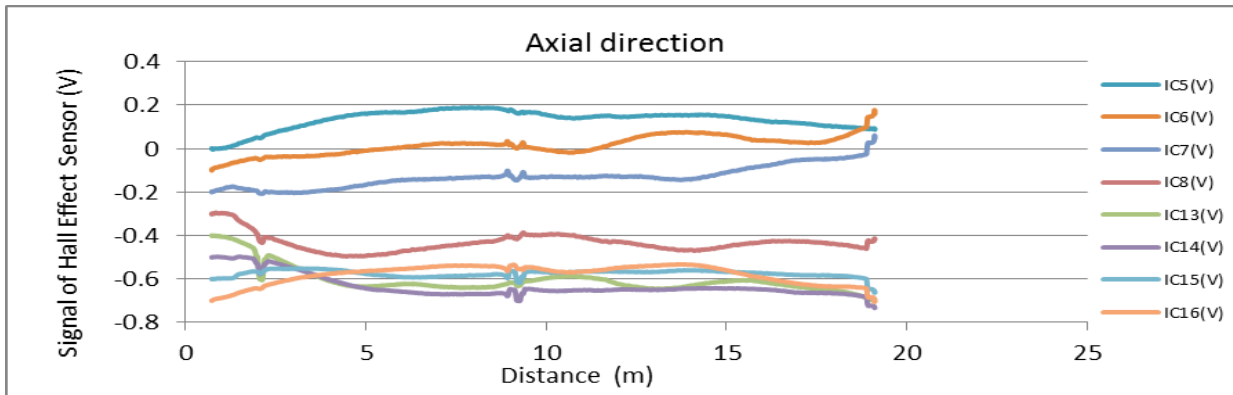
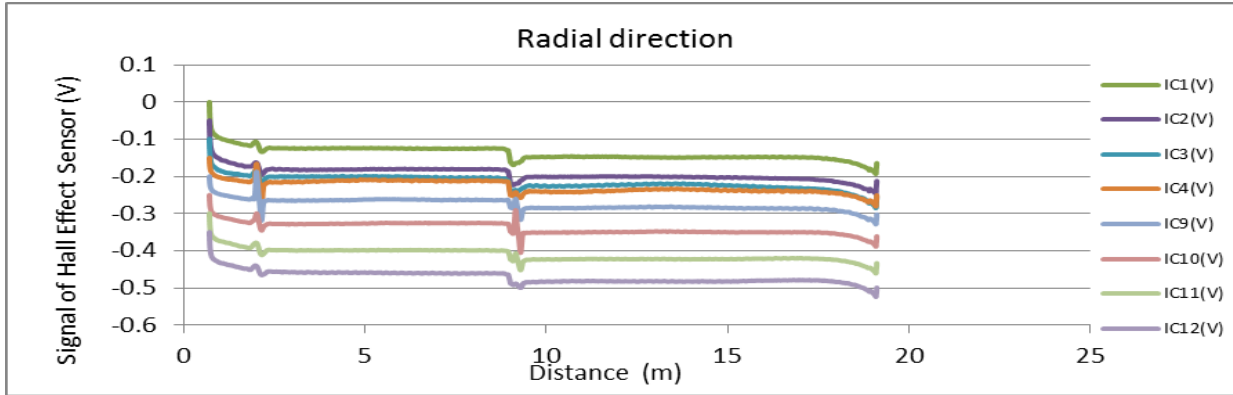
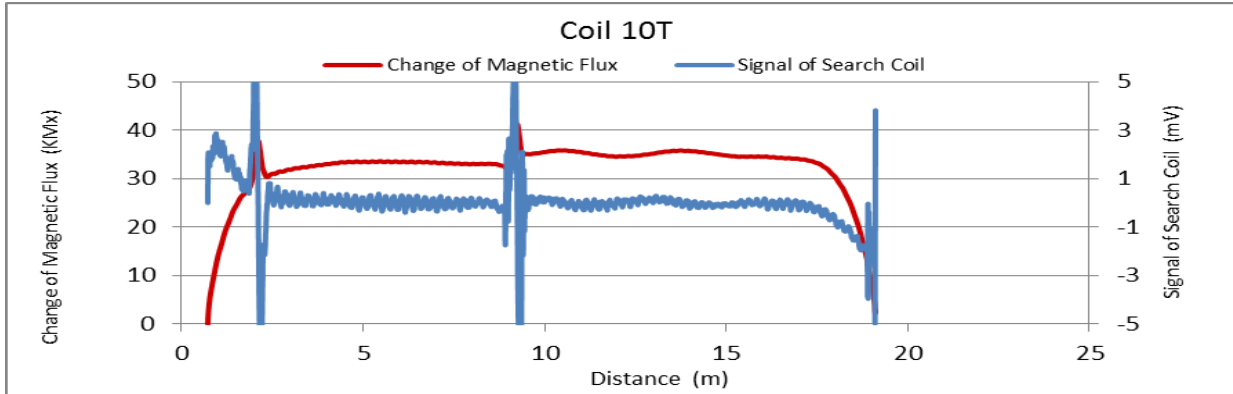


Figure A45. MMFM data of P10-402L-I2 tendon section.



Tokyo Rope USA, Inc.

File Name 【Pier-Tendon-Section】	Section Total Length (m)	Scanned Length		Note Joint position : 12.3 m, 24.47 m Starting point of damage 1 : 13.2 m			
		Starting Point (m)	Ending Point (m)				
P11-402R-I2	28.49	2.58	28.02				
Identified Damage 1				Identified Damage 2			
Max Loss Point (m)	Loss (%)	Length (m)	Damage Orientation	Max Loss Point (m)	Loss (%)	Length (m)	Damage Orientation
15.0	1.5	3.85	10~2 o'clock	—	—	—	—

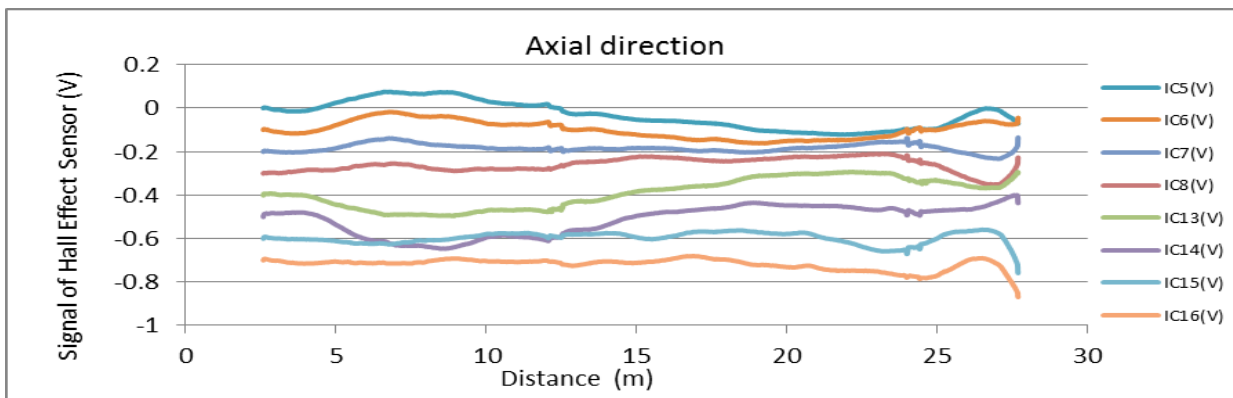
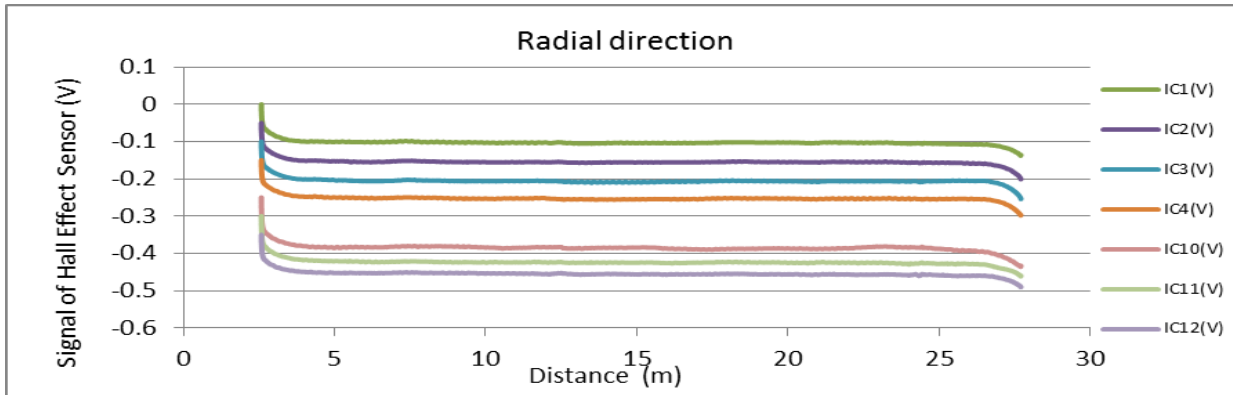
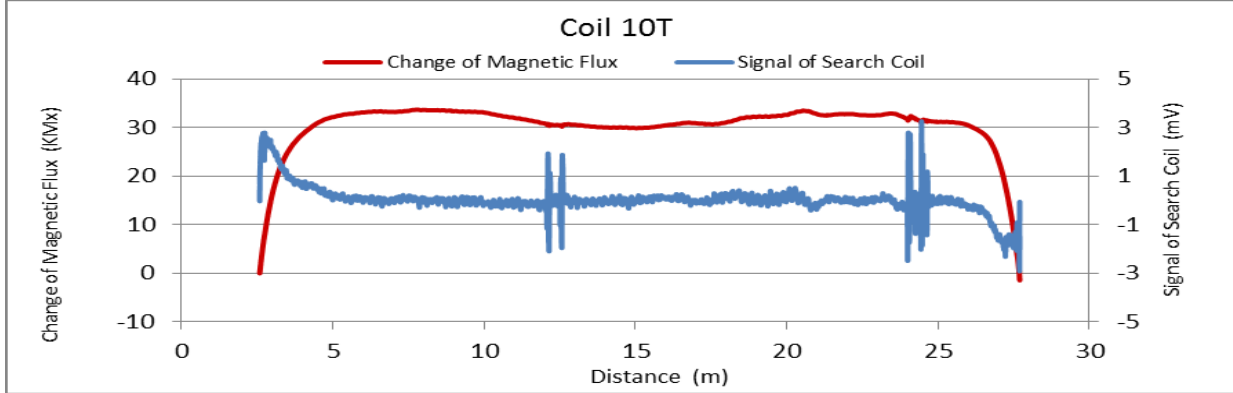


Figure A46. MMFM data of P11-402R-I2 tendon section.



Tokyo Rope USA, Inc.

File Name 【Pier-Tendon-Section】	Section Total Length (m)	Scanned Length		Note Joint position : 12.26 m, 24.42 m Starting point of damage 1 : 6.25 m Starting point of damage 2 : 11.73 m			
		Starting Point (m)	Ending Point (m)				
P11-402L-I2	28.46	1.9	27.97				
Identified Damage 1				Identified Damage 2			
Max Loss Point (m)	Loss (%)	Length (m)	Damage Orientation	Max Loss Point (m)	Loss (%)	Length (m)	Damage Orientation
7.0	1.3	2.06	3~9 o'clock	12.4	1.8	3.04	3~9 o'clock

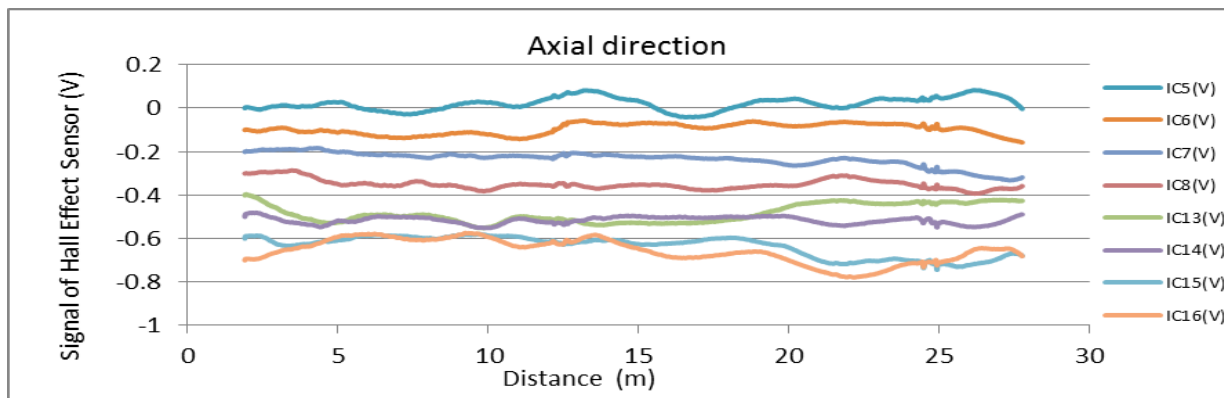
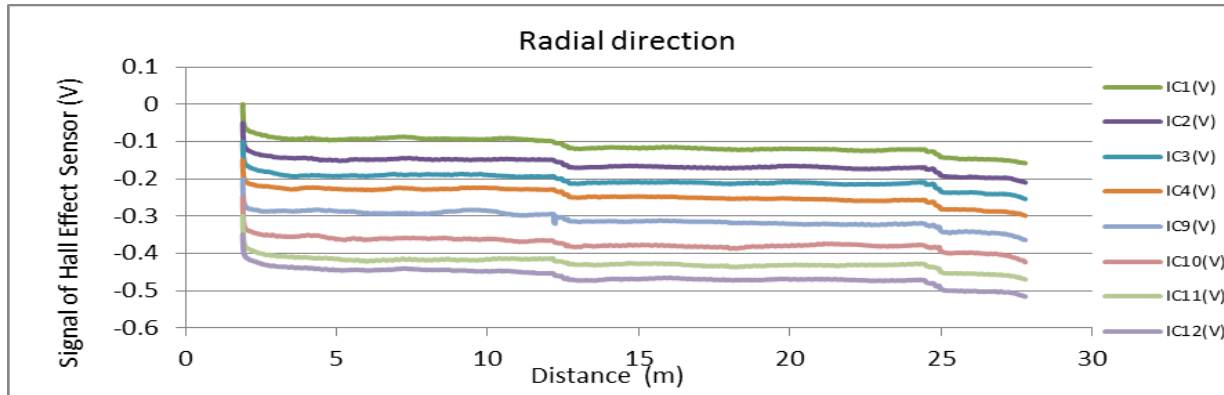
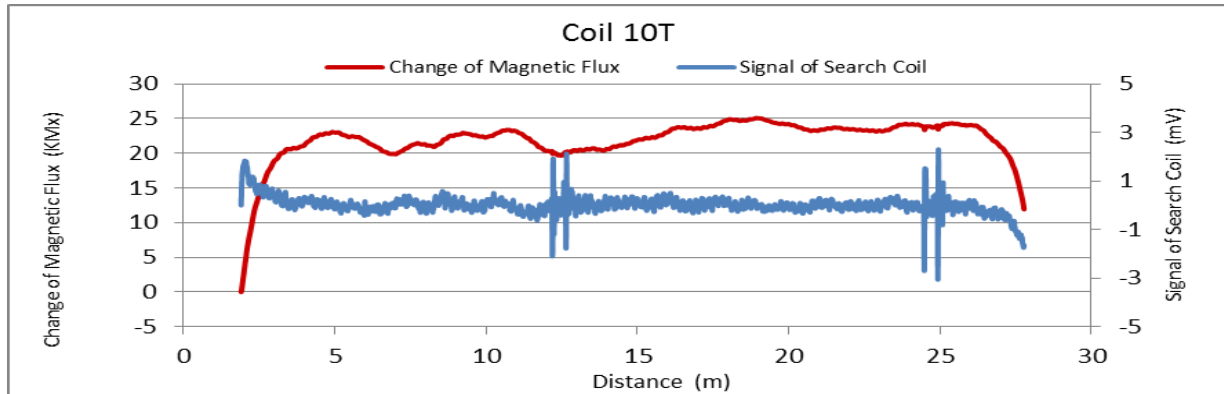


Figure A47. MMFM data of P11-402L-I2 tendon section.



Tokyo Rope USA, Inc.

File Name 【Pier-Tendon-Section】	Section Total Length (m)	Scanned Length		Note			
		Starting Point (m)	Ending Point (m)				
P9-406L-H1	9.43	0.49	8.65	Starting point of damage 1 : 3.43 m			
Identified Damage 1				Identified Damage 2			
Max Loss Point (m)	Loss (%)	Length (m)	Damage Orientation	Max Loss Point (m)	Loss (%)	Length (m)	Damage Orientation
3.7	0.8	1.01	10~4 o'clock	—	—	—	—

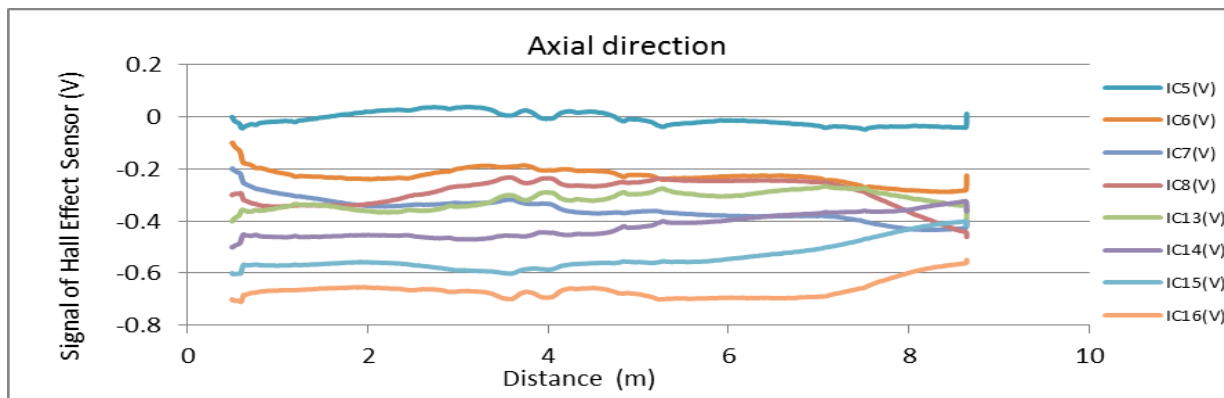
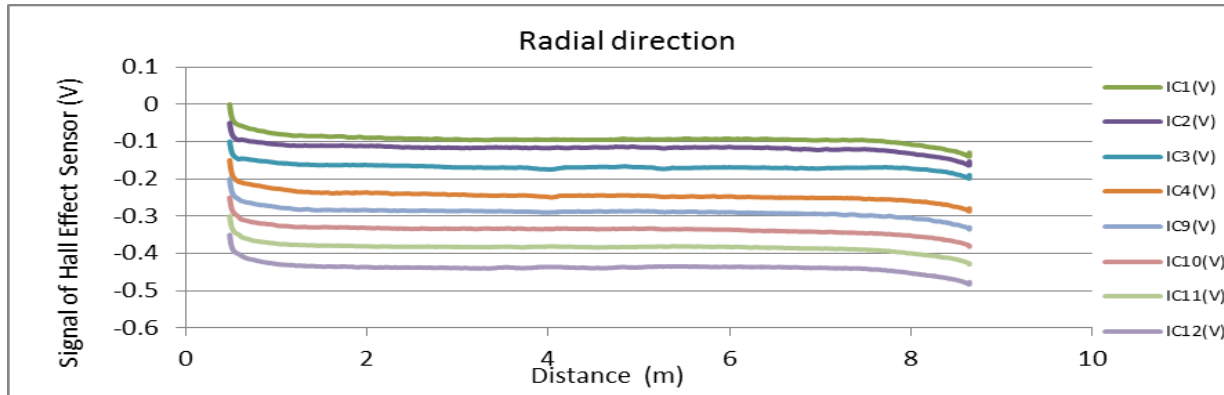
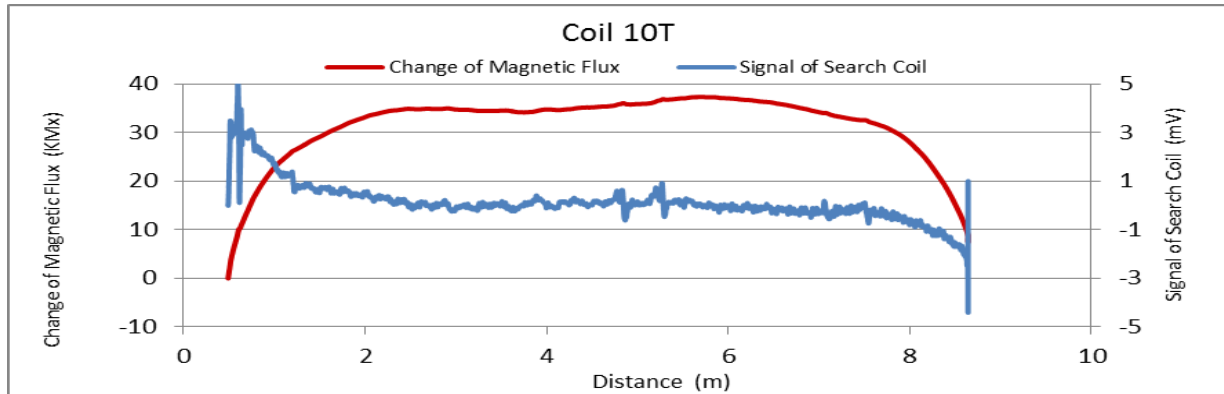


Figure A48. MMFM data of P9-406L-H1 tendon section.



Tokyo Rope USA, Inc.

File Name 【Pier-Tendon-Section】	Section Total Length (m)	Scanned Length		Note			
		Starting Point (m)	Ending Point (m)	Starting point of damage 1 : 4.83 m			
P9-403R-H2	9.4	0.78	8.92				
Identified Damage 1				Identified Damage 2			
Max Loss Point (m)	Loss (%)	Length (m)	Damage Orientation	Max Loss Point (m)	Loss (%)	Length (m)	Damage Orientation
5.2	0.8	0.63	7~1 o'clock	—	—	—	—

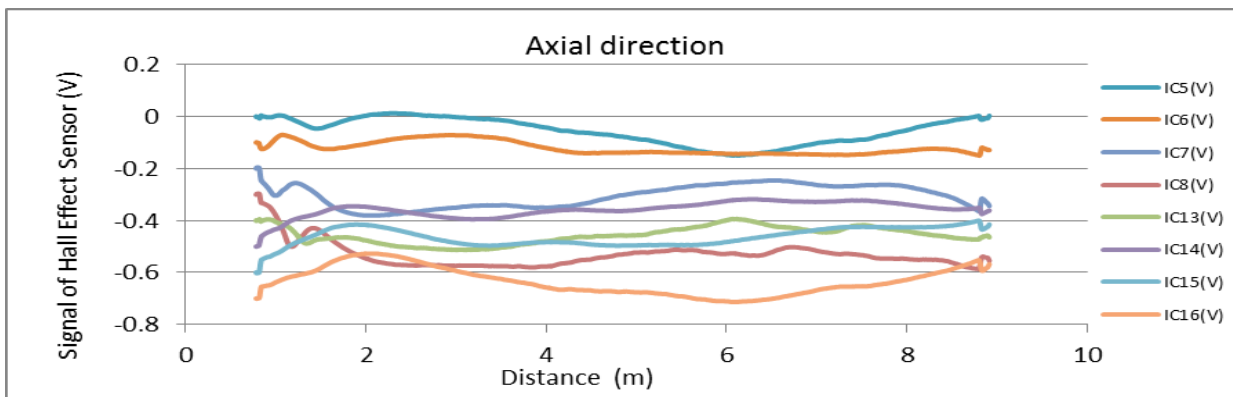
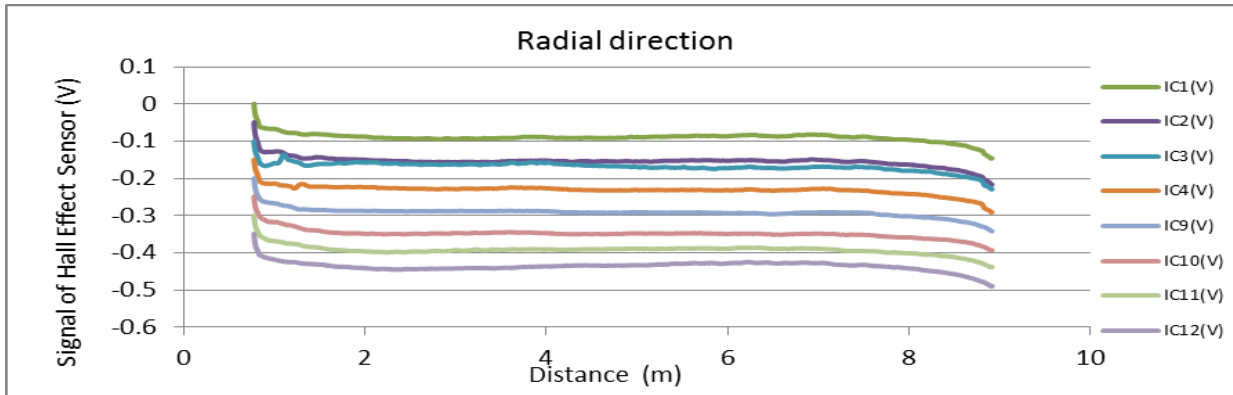
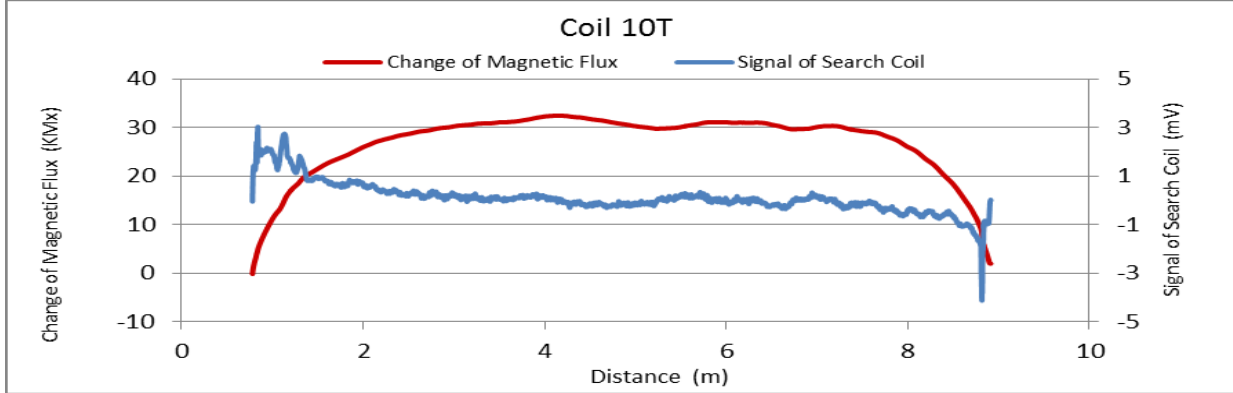


Figure A49. MMFM data of P9-403R-H2 tendon section.



Tokyo Rope USA, Inc.

File Name 【Pier-Tendon-Section】	Section Total Length (m)	Scanned Length		Note			
		Starting Point (m)	Ending Point (m)				
P9-403R-I2	21.49	0.57	20.94	Joint position: 12.3 m Identified damage 1&2: Increase of magnetic flux Starting point of damage 1: 7.1 m Starting point of damage 2: 12.32 m			
Identified Damage 1				Identified Damage 2			
Max Loss Point (m)	Loss (%)	Length (m)	Damage Orientation	Max Loss Point (m)	Loss (%)	Length (m)	Damage Orientation
7.2	-2.4	0.17	6~9 o'clock	12.5	-3.9	0.39	6~9 o'clock

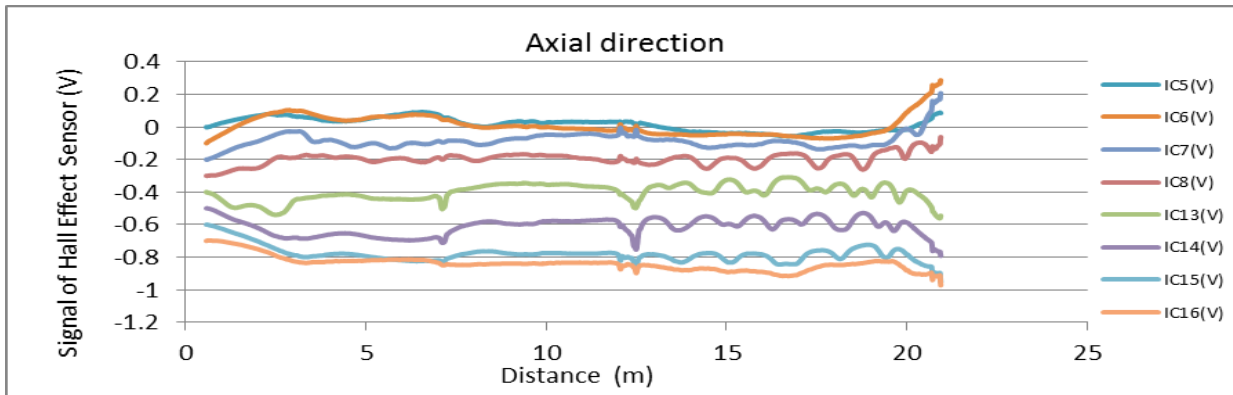
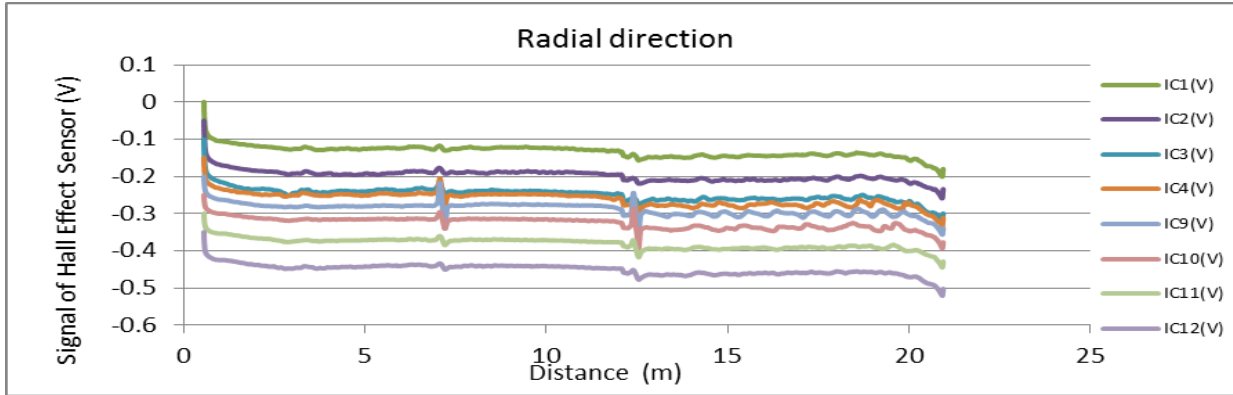
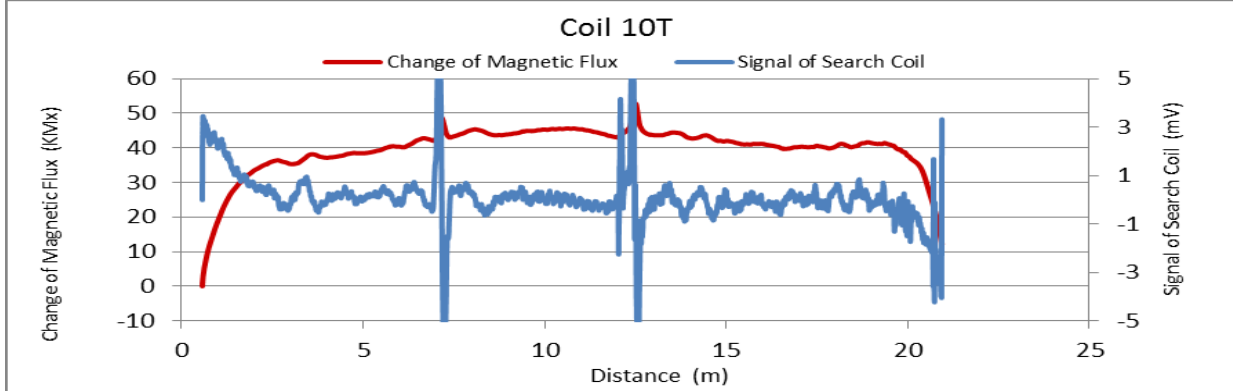


Figure A50. MMFM data of P9-403R-I2 tendon section.



Tokyo Rope USA, Inc.

File Name 【Pier-Tendon-Section】	Section Total Length (m)	Scanned Length		Note Joint position : 12.26 m Starting point of damage 1 : 10.66 m			
		Starting Point (m)	Ending Point (m)				
P9-406R-I1	21.47	0.39	20.74				
Identified Damage 1				Identified Damage 2			
Max Loss Point (m)	Loss (%)	Length (m)	Damage Orientation	Max Loss Point (m)	Loss (%)	Length (m)	Damage Orientation
11.6	1.4	1.54	11~4 o'clock	—	—	—	—

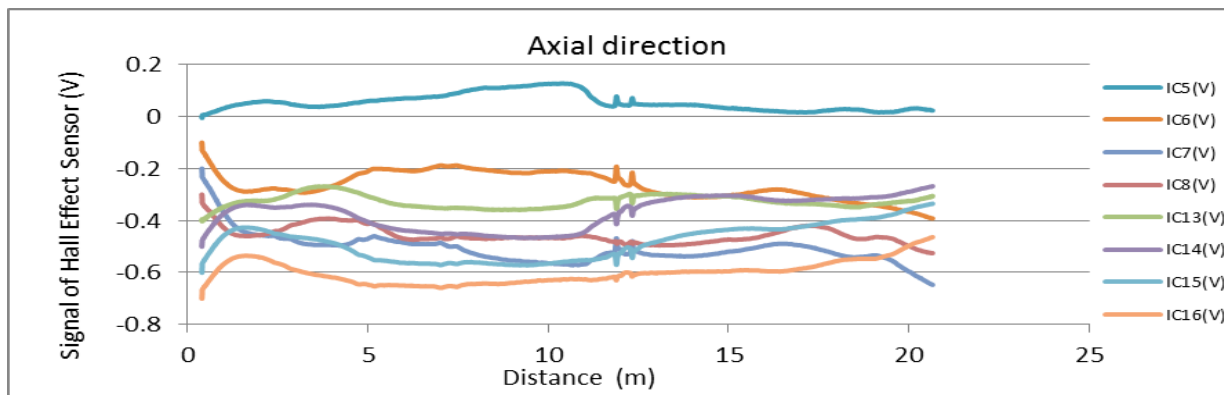
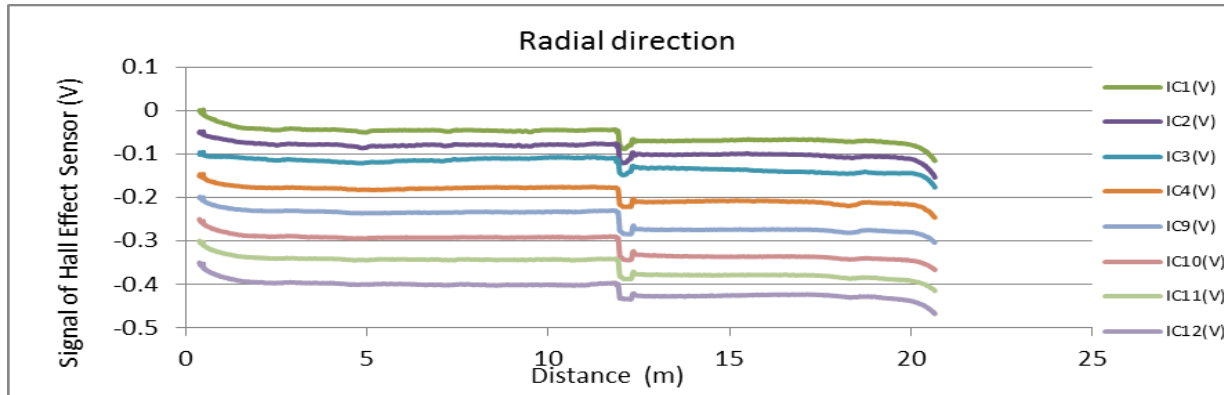
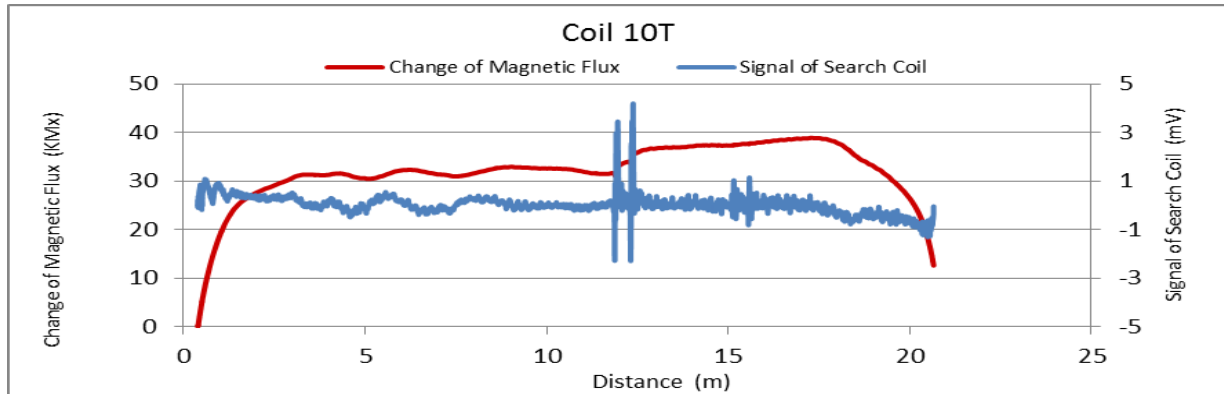


Figure A51. MMFM data of P9-406R-I1 tendon section.



Tokyo Rope USA, Inc.

File Name 【Pier-Tendon-Section】	Section Total Length (m)	Scanned Length		Note Joint position : 12.28 m Identified damage 1 : Increase of magnetic flux Starting point of damage 1 : 1.26 m			
		Starting Point (m)	Ending Point (m)				
P9-404R-I1	21.44	0.39	20.79				
Identified Damage 1				Identified Damage 2			
Max Loss Point (m)	Loss (%)	Length (m)	Damage Orientation	Max Loss Point (m)	Loss (%)	Length (m)	Damage Orientation
1.3	-2.2	0.12	6~12 o'clock	—	—	—	—

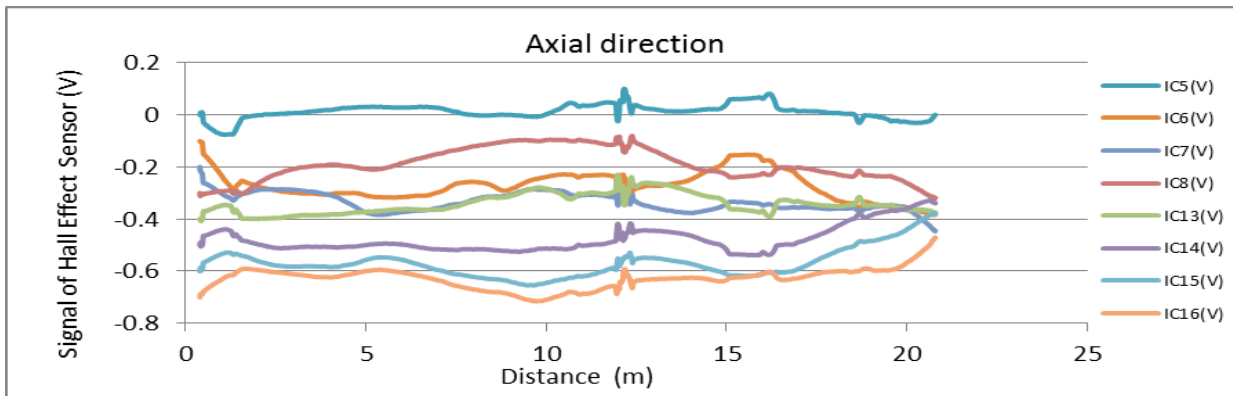
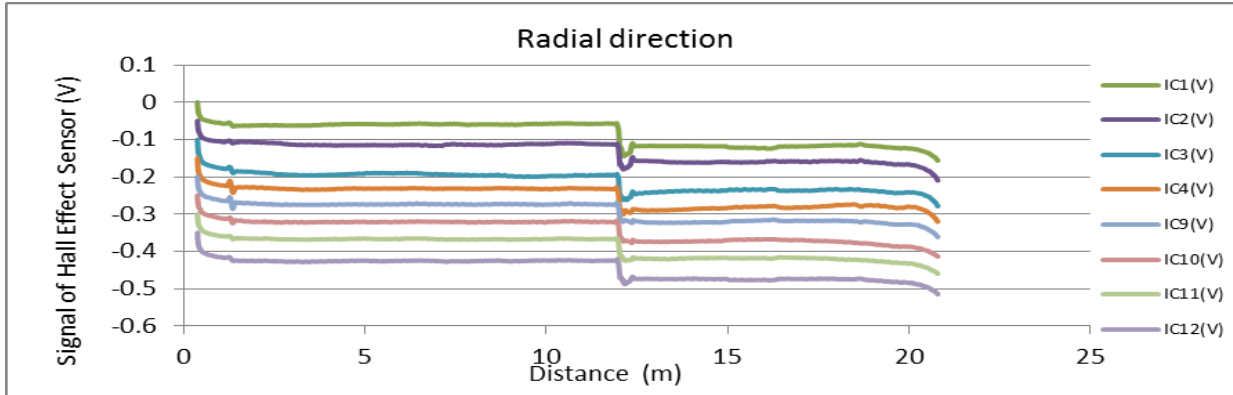
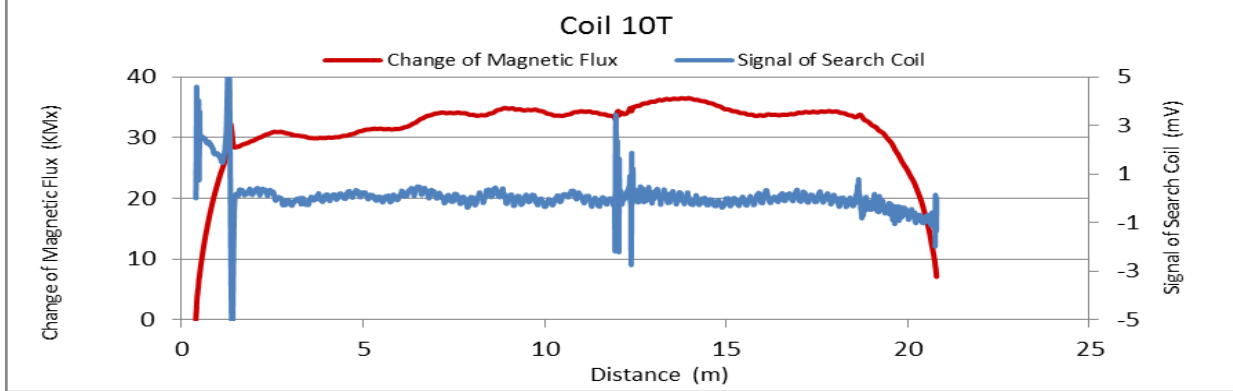


Figure A52. MMFM data of P9-404R-I1 tendon section.



Tokyo Rope USA, Inc.

File Name 【Pier-Tendon-Section】	Section Total Length (m)	Scanned Length		Note Joint position: 9.1 m Identified damage 1 : Increase of magnetic flux Starting point of damage 1 : 3.14 m			
		Starting Point (m)	Ending Point (m)				
P8-405R-I2	21.43	0.63	20.95				
Identified Damage 1				Identified Damage 2			
Max Loss Point (m)	Loss (%)	Length (m)	Damage Orientation	Max Loss Point (m)	Loss (%)	Length (m)	Damage Orientation
3.3	-3.1	0.33	6~10 o'clock	—	—	—	—

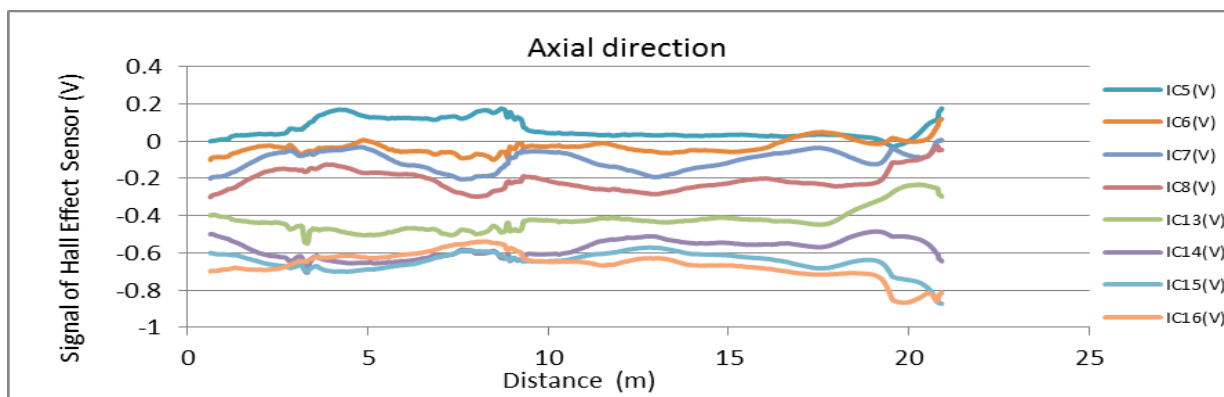
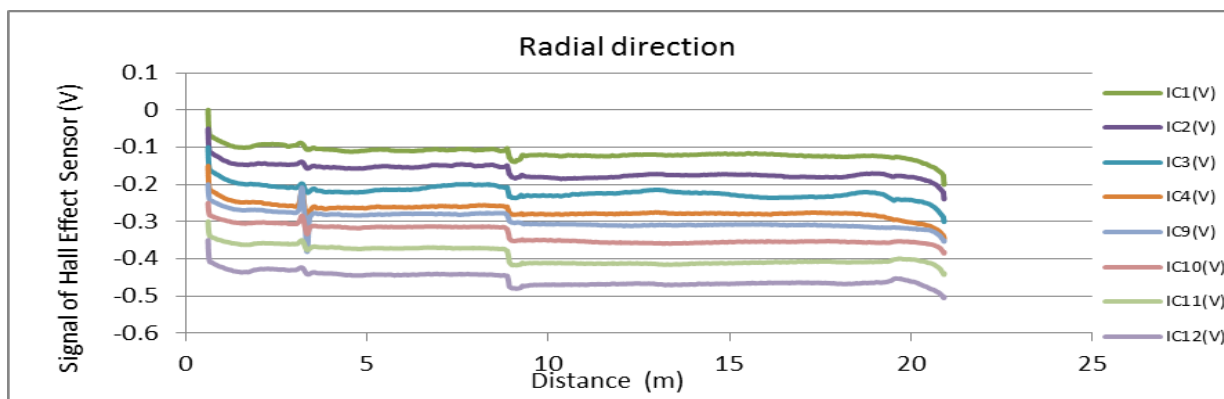
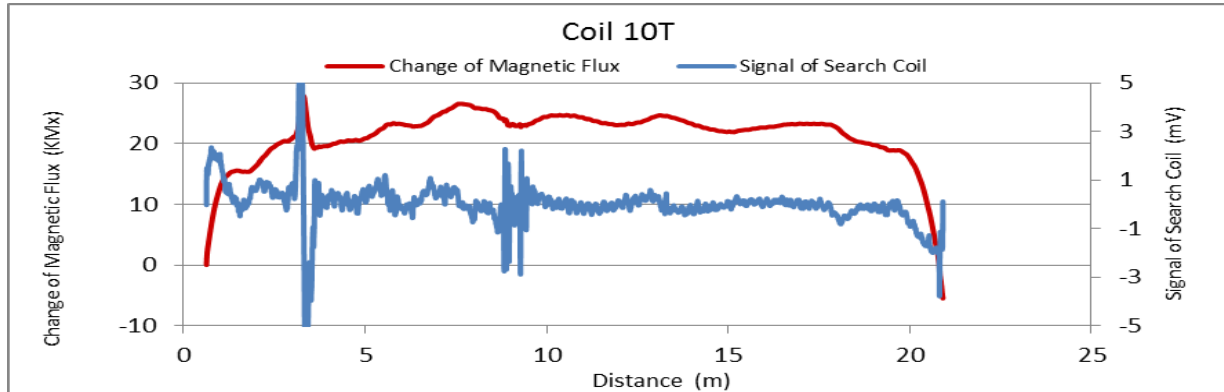


Figure A53. MMFM data of P8-405R-I2 tendon section.



Tokyo Rope USA, Inc.

File Name 【Pier-Tendon-Section】	Section Total Length (m)	Scanned Length		Note Joint position : 12.24 m Starting point of damage 1 : 16.21 m			
		Starting Point (m)	Ending Point (m)				
P8-406R-I1	21.4	0.4	20.39				
Identified Damage 1				Identified Damage 2			
Max Loss Point (m)	Loss (%)	Length (m)	Damage Orientation	Max Loss Point (m)	Loss (%)	Length (m)	Damage Orientation
16.8	1.0	1.01	4~10 o'clock	—	—	—	—

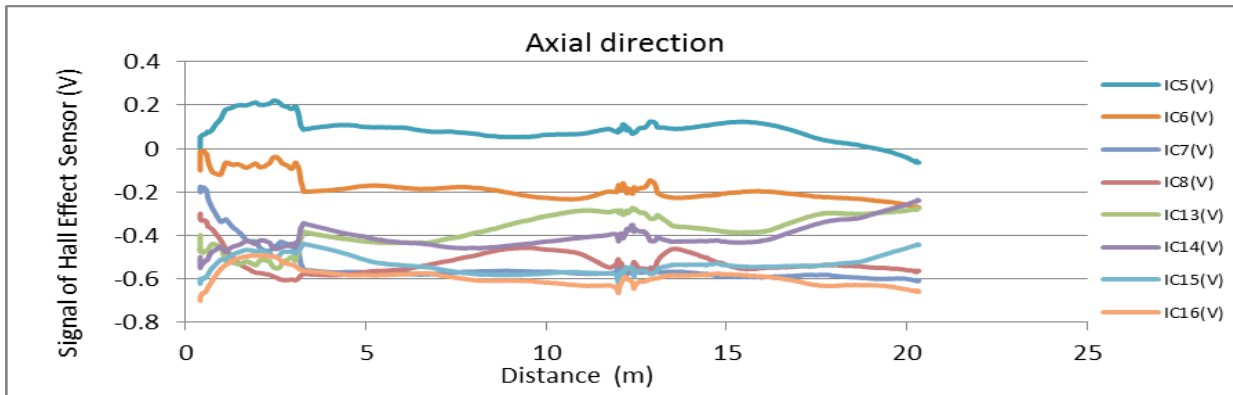
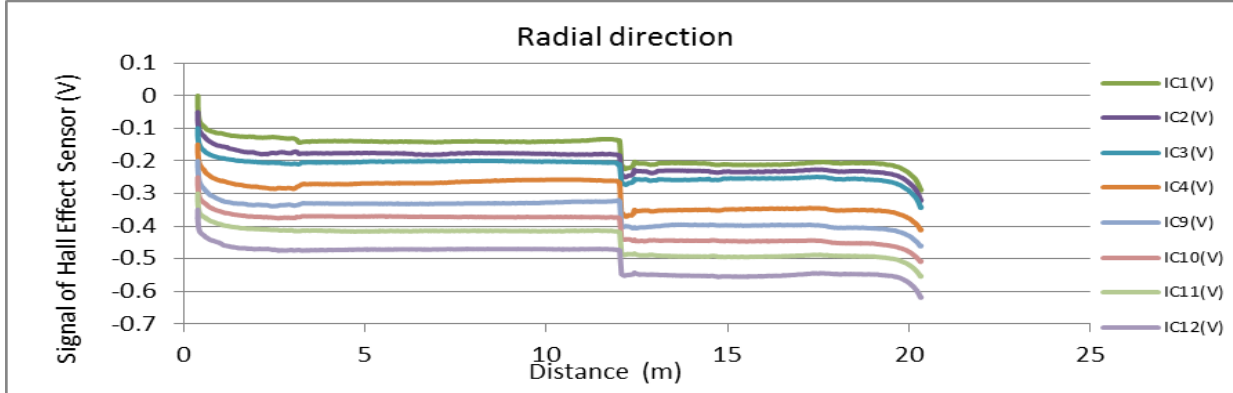
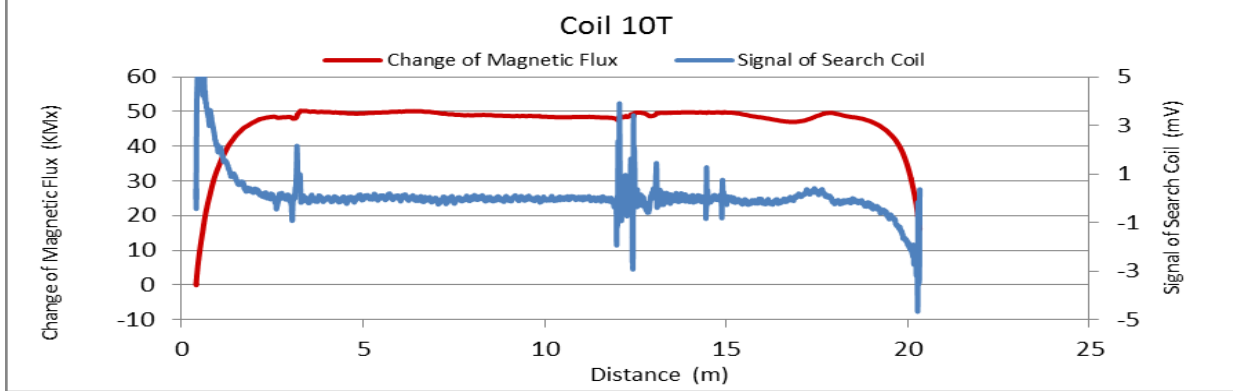


Figure A54. MMFM data of P8-406R-I1 tendon section.



Tokyo Rope USA, Inc.

File Name 【Pier-Tendon-Section】	Section Total Length (m)	Scanned Length		Note Joint position : 12.3 m Starting point of damage 1 : 14.07 m			
		Starting Point (m)	Ending Point (m)				
P8-405R-I1	21.4	0.36	20.37				
Identified Damage 1				Identified Damage 2			
Max Loss Point (m)	Loss (%)	Length (m)	Damage Orientation	Max Loss Point (m)	Loss (%)	Length (m)	Damage Orientation
14.9	1.3	1.64	10~4 o'clock	—	—	—	—

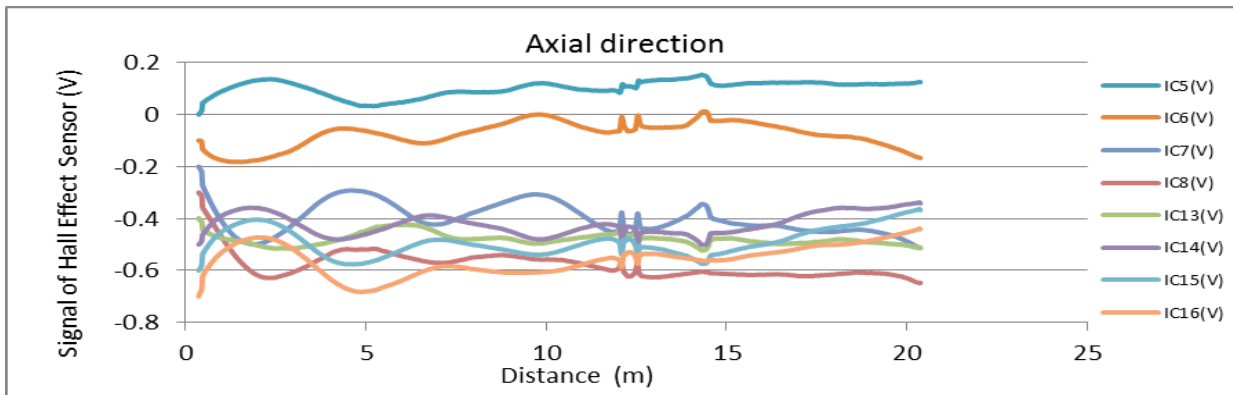
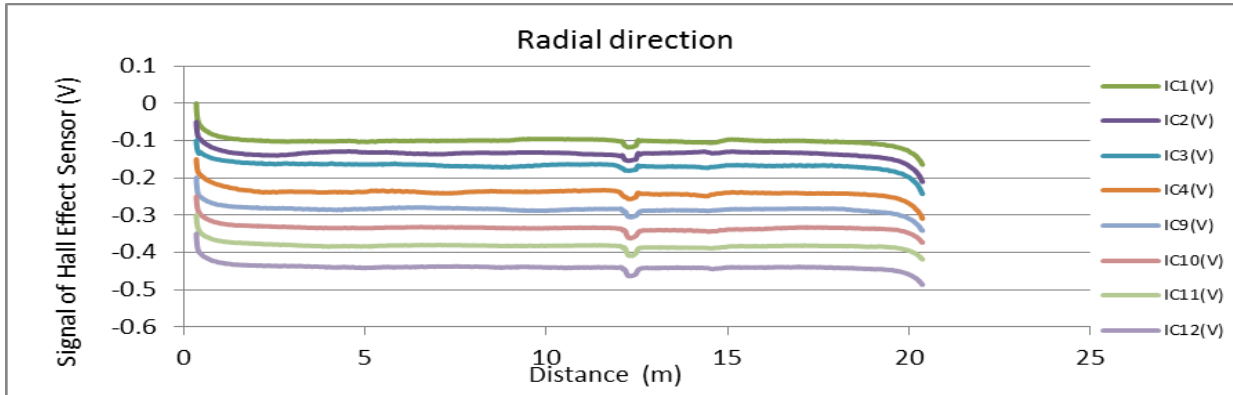
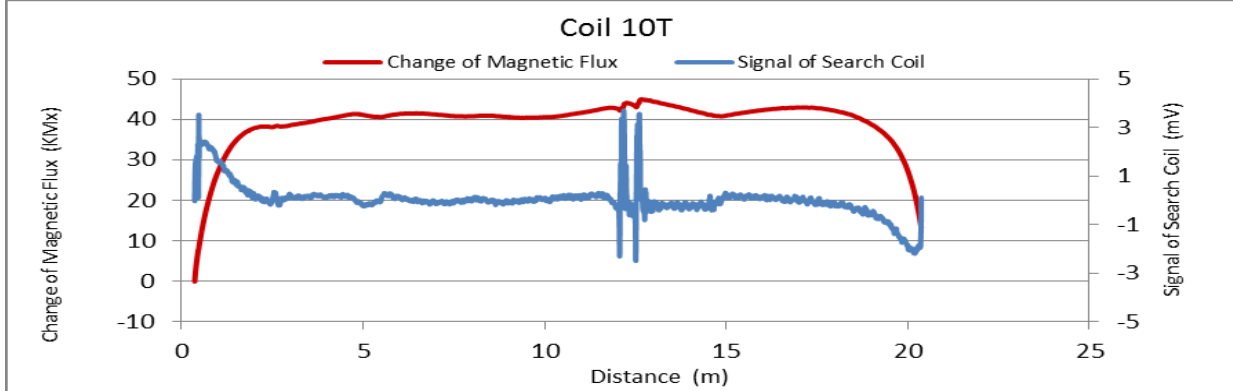


Figure A55. MMFM data of P8-405R-I1 tendon section.



Tokyo Rope USA, Inc.

File Name 【Pier-Tendon-Section】	Section Total Length (m)	Scanned Length		Note Starting point of damage 1 : 2.32 m			
		Starting Point (m)	Ending Point (m)				
P8-404L-H1	9.44	0.59	8.75				
Identified Damage 1				Identified Damage 2			
Max Loss Point (m)	Loss (%)	Length (m)	Damage Orientation	Max Loss Point (m)	Loss (%)	Length (m)	Damage Orientation
2.6	0.7	0.59	10~1 o'clock	—	—	—	—

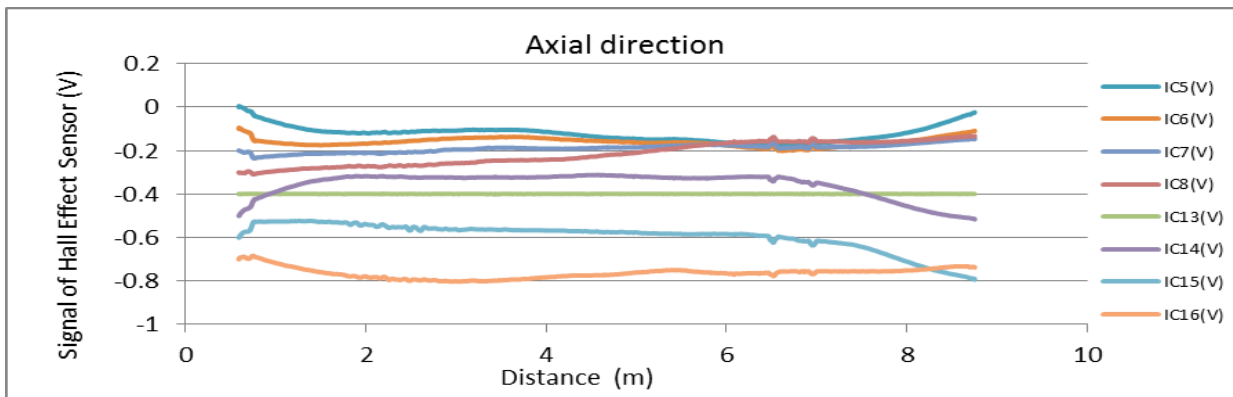
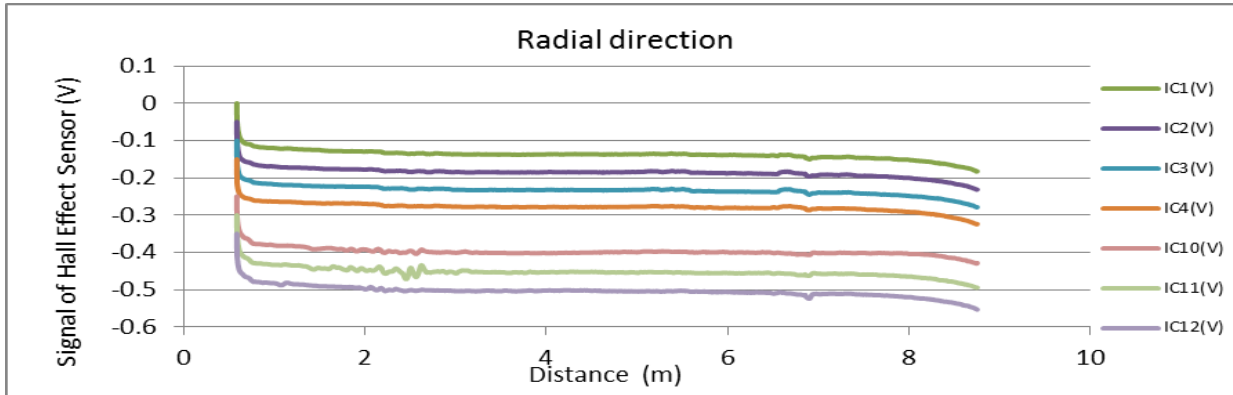
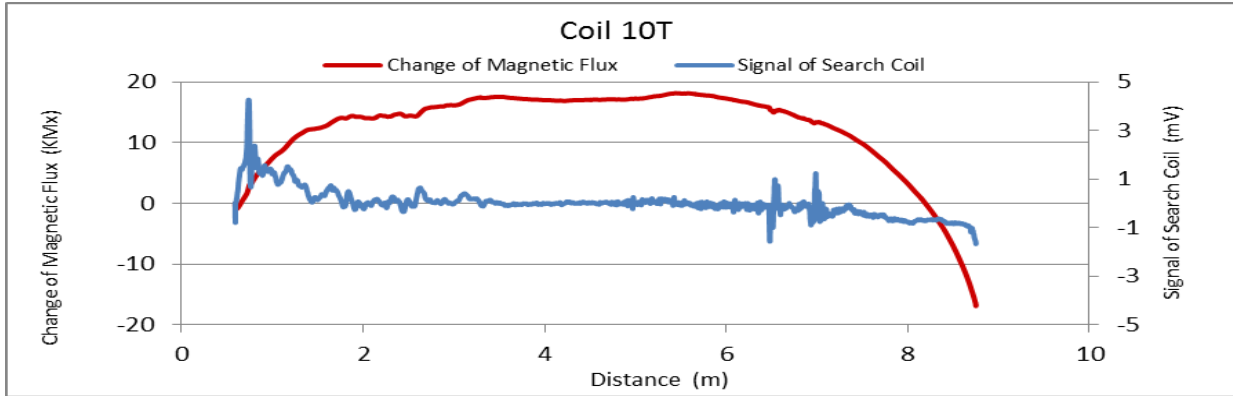


Figure A56. MMFM data of P8-404L-H1 tendon section.



Tokyo Rope USA, Inc.

APPENDIX 3. Collection of MMFM Data Containing No Damage



Tokyo Rope USA, Inc.

File Name 【Pier-Tendon-Section】	Section Total Length (m)	Scanned Length		Note			
		Starting Point (m)	Ending Point (m)				
P1-401L-H1	20.5	0.61	20.28	Joint position: 12.3 m			
Identified Damage 1				Identified Damage 2			
Max Loss Point (m)	Section Loss (%)	Damage Length (m)	Damage Orientation	Max Loss Point (m)	Section Loss (%)	Damage Length (m)	Damage Orientation
—	—	—	—	—	—	—	—

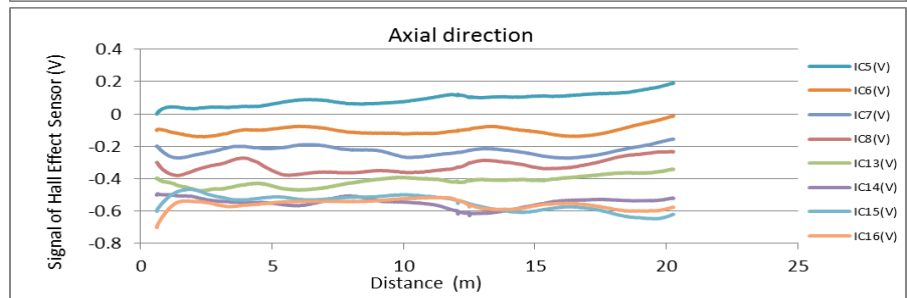
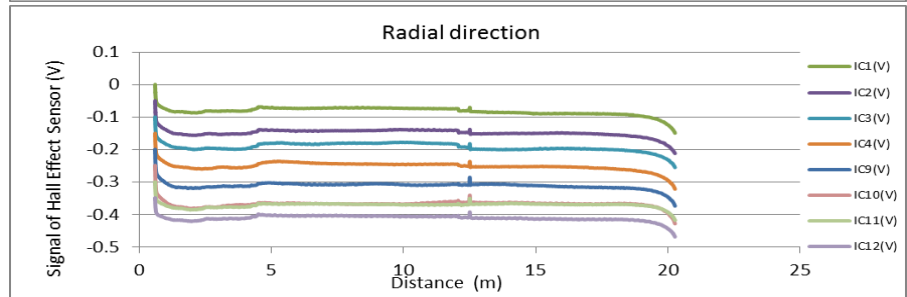
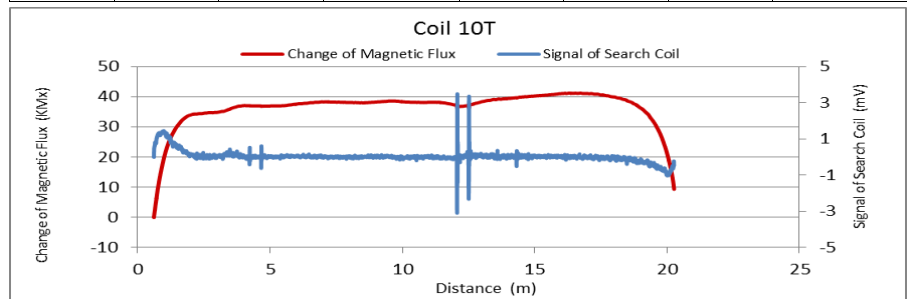


Figure A57. MMFM data of P1-401L-H1 tendon section.

File Name 【Pier-Tendon-Section】	Section Total Length (m)	Scanned Length		Note			
		Starting Point (m)	Ending Point (m)				
P1-401R-H2	21.65	0.17	21.07	Joint position: 3.5 m, 15.6 m			
Identified Damage 1				Identified Damage 2			
Max Loss Point (m)	Section Loss (%)	Damage Length (m)	Damage Orientation	Max Loss Point (m)	Section Loss (%)	Damage Length (m)	Damage Orientation
—	—	—	—	—	—	—	—

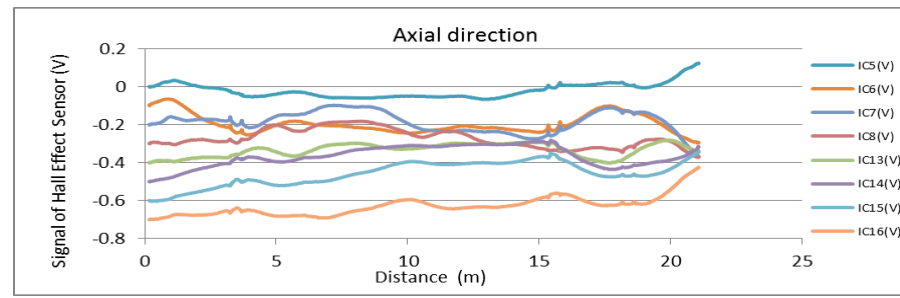
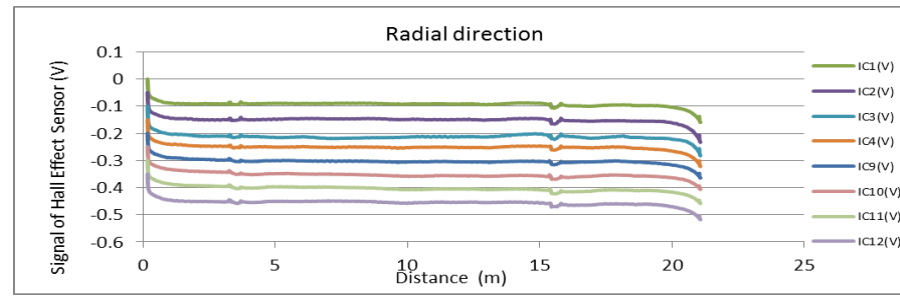
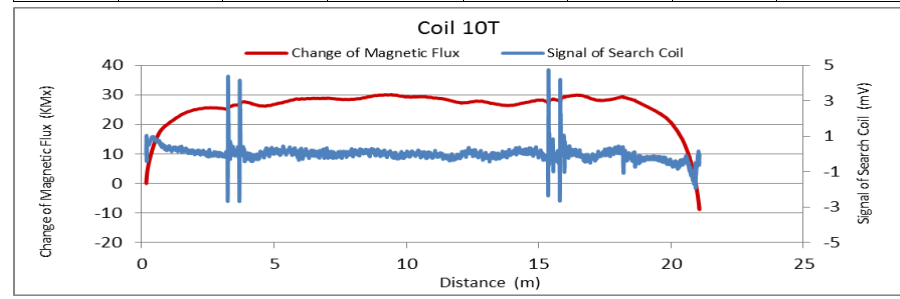


Figure A58. MMFM data of P1-401R-H2 tendon section.



Tokyo Rope USA, Inc.

File Name 【Pier-Tendon-Section】	Section Total Length (m)	Scanned Length		Note			
		Starting Point (m)	Ending Point (m)				
P1-402R-I2	21.5	0.6	20.73	Joint position: 9.1 m			
Identified Damage 1				Identified Damage 2			
Max Loss Point (m)	Section Loss (%)	Damage Length (m)	Damage Orientation	Max Loss Point (m)	Section Loss (%)	Damage Length (m)	Damage Orientation
—	—	—	—	—	—	—	—

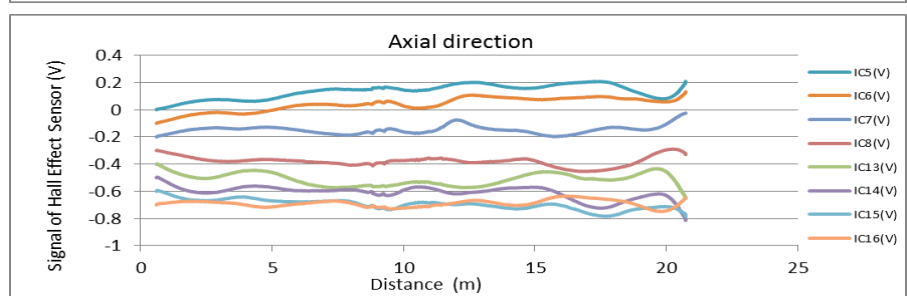
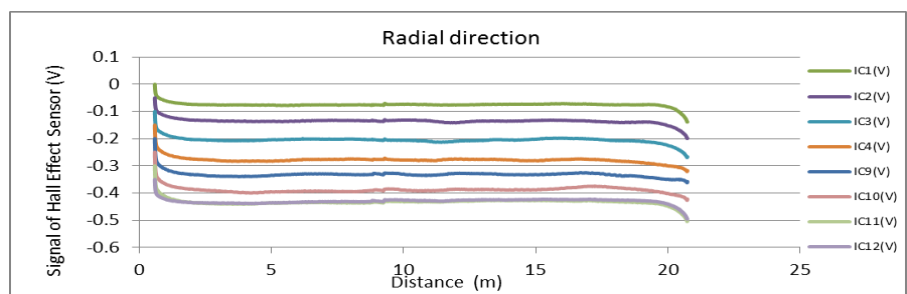
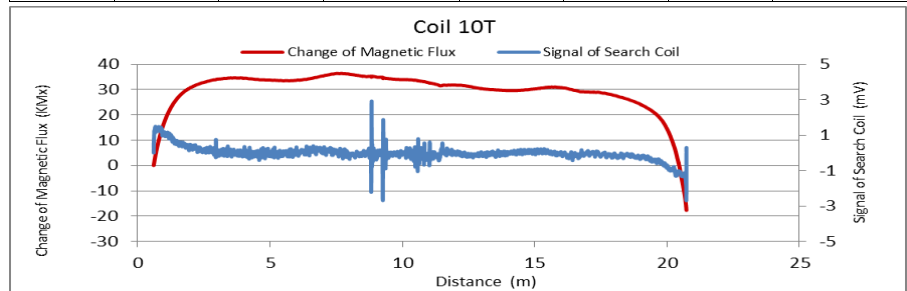


Figure A59. MMFM data of P1-402R-I2 tendon section.

File Name 【Pier-Tendon-Section】	Section Total Length (m)	Scanned Length		Note			
		Starting Point (m)	Ending Point (m)				
P1-401L-H2	21.34	0.13	20.73	Joint position: 3.6 m, 15.7 m			
Identified Damage 1				Identified Damage 2			
Max Loss Point (m)	Section Loss (%)	Damage Length (m)	Damage Orientation	Max Loss Point (m)	Section Loss (%)	Damage Length (m)	Damage Orientation
—	—	—	—	—	—	—	—

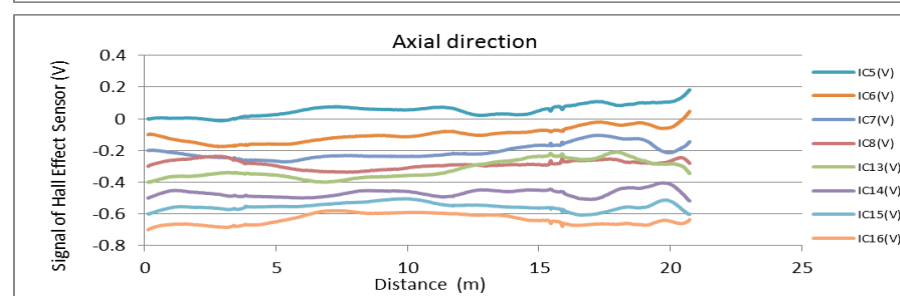
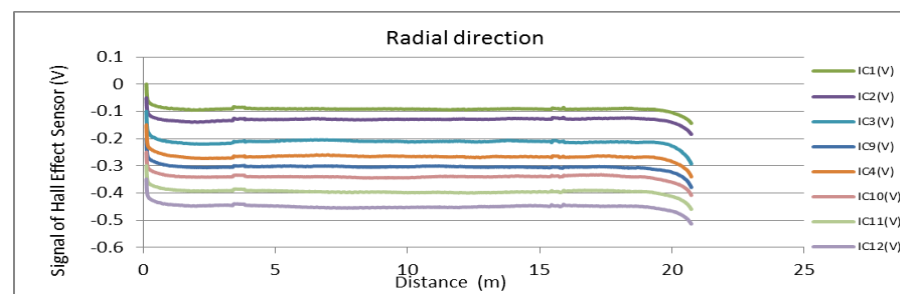
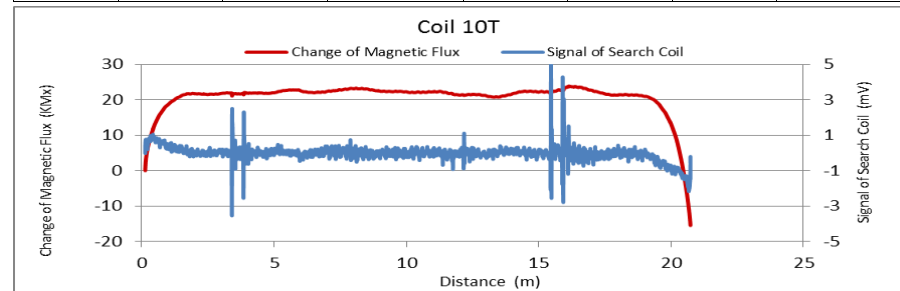


Figure A60. MMFM data of P1-401L-H2 tendon section.



Tokyo Rope USA, Inc.

File Name 【Pier-Tendon-Section】	Section Total Length (m)	Scanned Length		Note			
		Starting Point (m)	Ending Point (m)				
P1-401R-H3	9.45	0.62	8.88				
Identified Damage 1				Identified Damage 2			
Max Loss Point (m)	Section Loss (%)	Damage Length (m)	Damage Orientation	Max Loss Point (m)	Section Loss (%)	Damage Length (m)	Damage Orientation
—	—	—	—	—	—	—	—

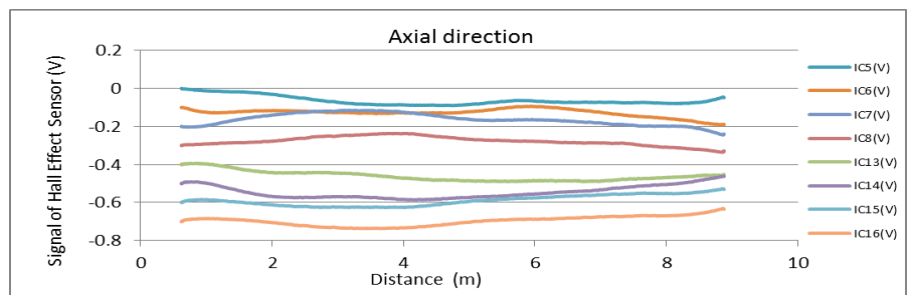
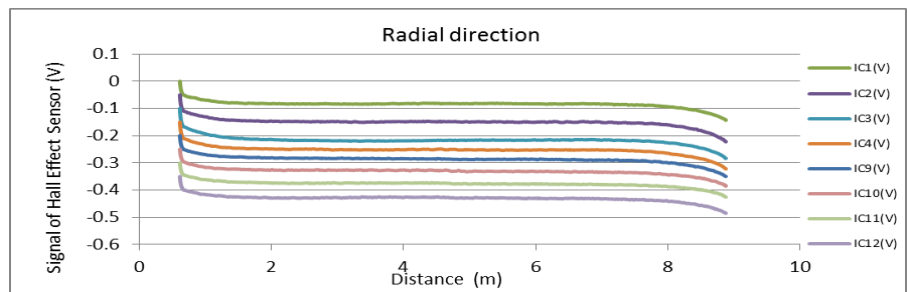
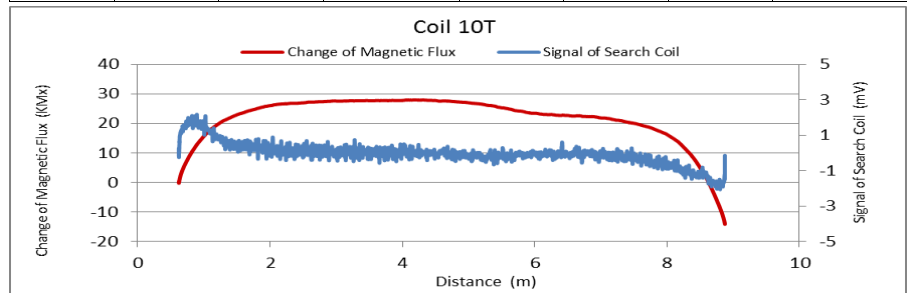


Figure A61. MMFM data of P1-401R-H3 tendon section.

File Name 【Pier-Tendon-Section】	Section Total Length (m)	Scanned Length		Note			
		Starting Point (m)	Ending Point (m)				
P1-402R-H1	9.45	0.63	8.88				
Identified Damage 1				Identified Damage 2			
Max Loss Point (m)	Section Loss (%)	Damage Length (m)	Damage Orientation	Max Loss Point (m)	Section Loss (%)	Damage Length (m)	Damage Orientation
—	—	—	—	—	—	—	—

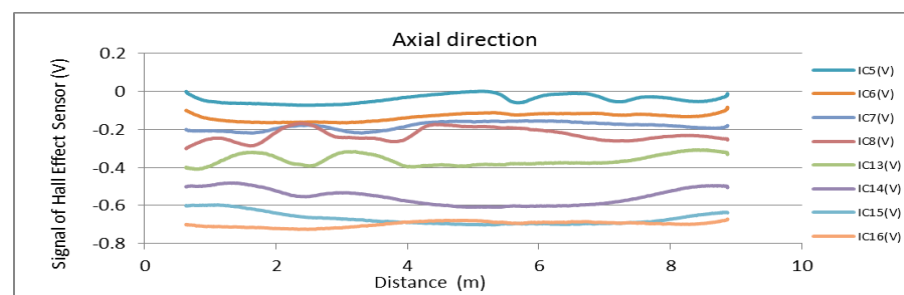
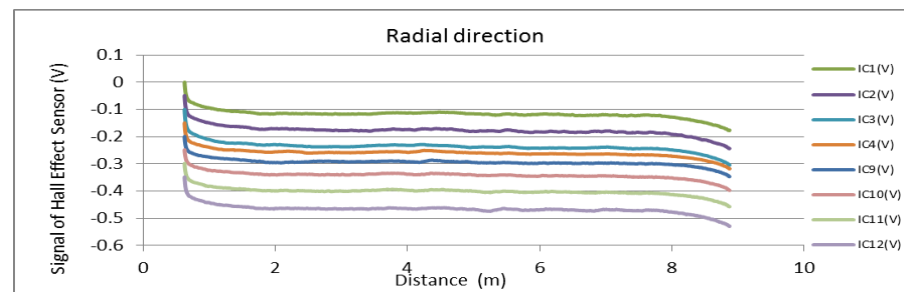
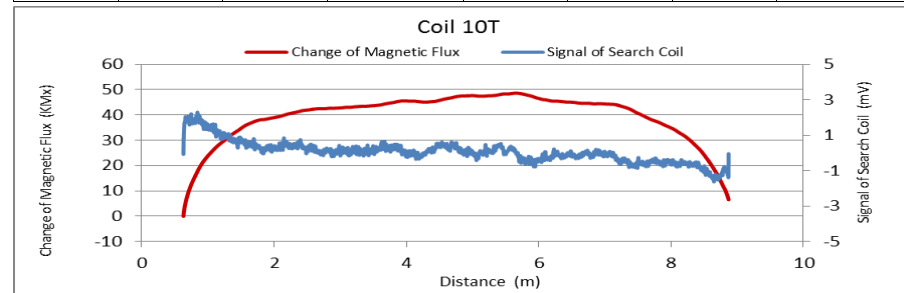


Figure A62. MMFM data of P1-402R-H1 tendon section.



Tokyo Rope USA, Inc.

File Name 【Pier-Tendon-Section】	Section Total Length (m)	Scanned Length		Note			
		Starting Point (m)	Ending Point (m)				
P1-402L-H1	9.45	0.63	8.88				
Identified Damage 1				Identified Damage 2			
Max Loss Point (m)	Section Loss (%)	Damage Length (m)	Damage Orientation	Max Loss Point (m)	Section Loss (%)	Damage Length (m)	Damage Orientation
—	—	—	—	—	—	—	—

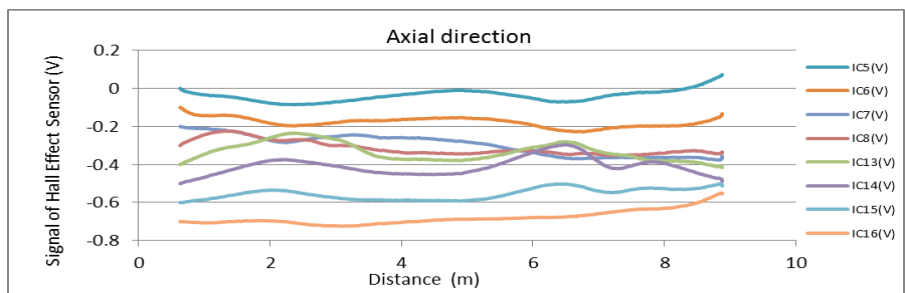
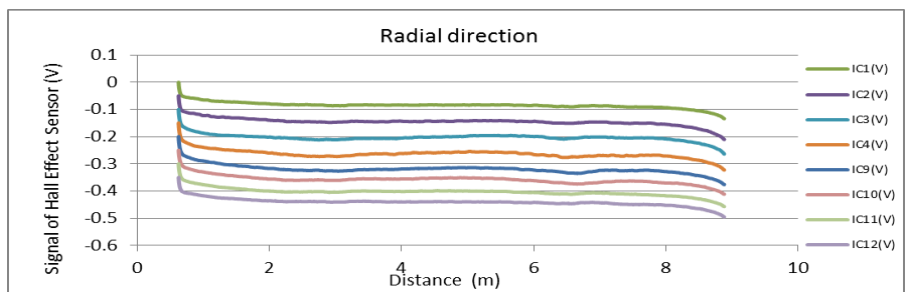
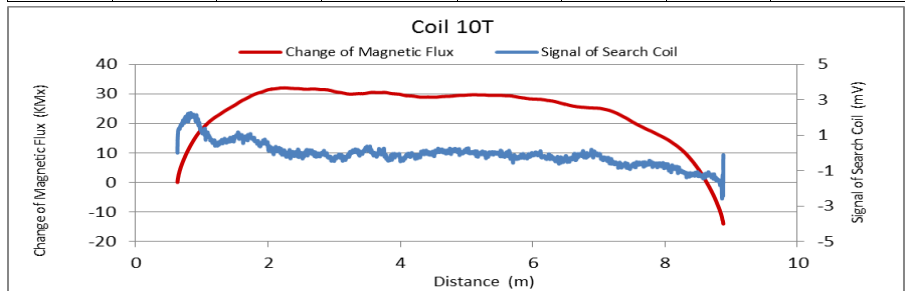


Figure A63. MMFM data of P1-402L-H1 tendon section.

File Name 【Pier-Tendon-Section】	Section Total Length (m)	Scanned Length		Note			
		Starting Point (m)	Ending Point (m)				
P2-401R-H1	9.45	0.63	8.75				
Identified Damage 1				Identified Damage 2			
Max Loss Point (m)	Section Loss (%)	Damage Length (m)	Damage Orientation	Max Loss Point (m)	Section Loss (%)	Damage Length (m)	Damage Orientation
—	—	—	—	—	—	—	—

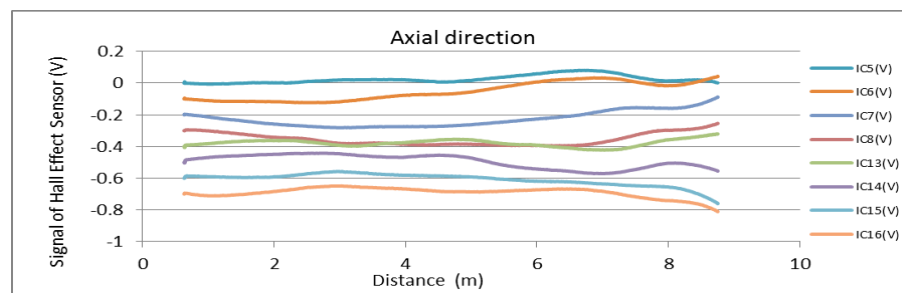
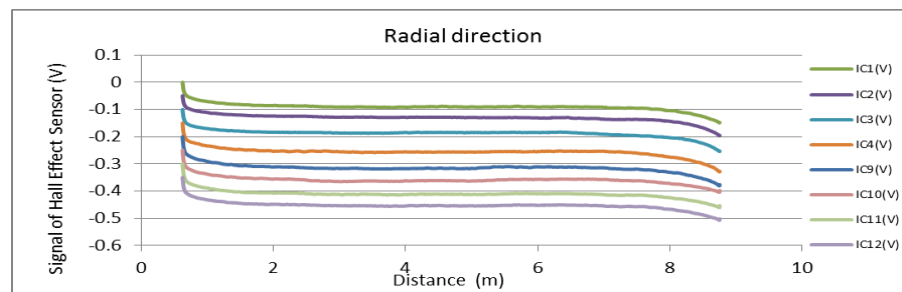
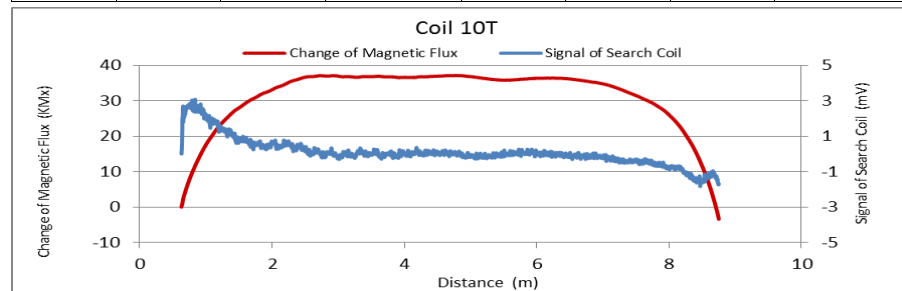


Figure A64. MMFM data of P2-401R-H1 tendon section.



Tokyo Rope USA, Inc.

File Name 【Pier-Tendon-Section】	Section Total Length (m)	Scanned Length		Note			
		Starting Point (m)	Ending Point (m)				
P2-402R-H1	9.45	0.63	8.71				
Identified Damage 1				Identified Damage 2			
Max Loss Point (m)	Section Loss (%)	Damage Length (m)	Damage Orientation	Max Loss Point (m)	Section Loss (%)	Damage Length (m)	Damage Orientation
—	—	—	—	—	—	—	—

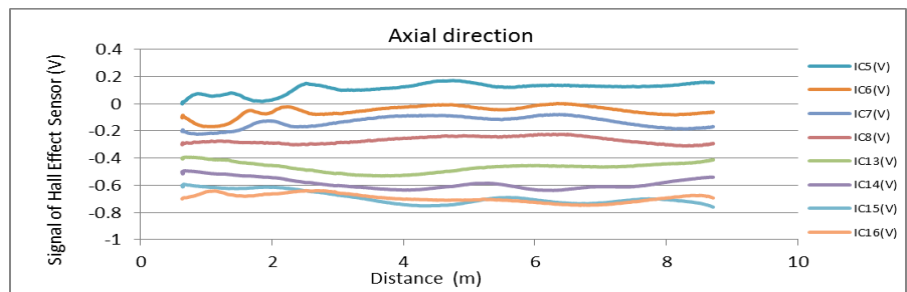
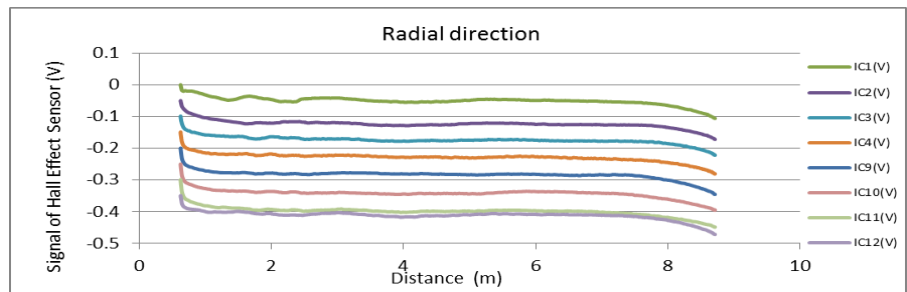
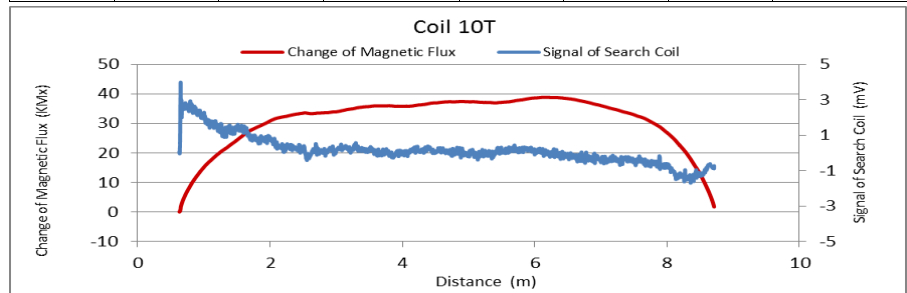


Figure A65. MMFM data of P2-402R-H1 tendon section.

File Name 【Pier-Tendon-Section】	Section Total Length (m)	Scanned Length		Note			
		Starting Point (m)	Ending Point (m)				
P2-402L-H1	9.38	0.59	8.66	The grout sticks to the duct and has irregularities.			
Identified Damage 1				Identified Damage 2			
Max Loss Point (m)	Section Loss (%)	Damage Length (m)	Damage Orientation	Max Loss Point (m)	Section Loss (%)	Damage Length (m)	Damage Orientation
—	—	—	—	—	—	—	—

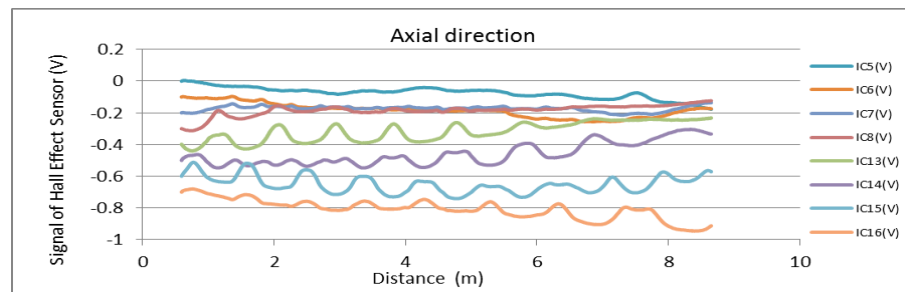
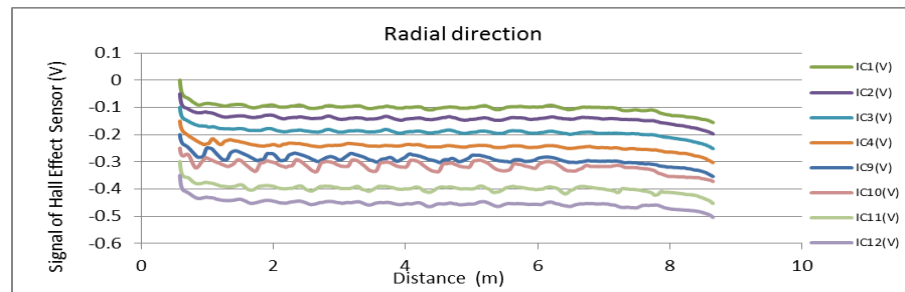
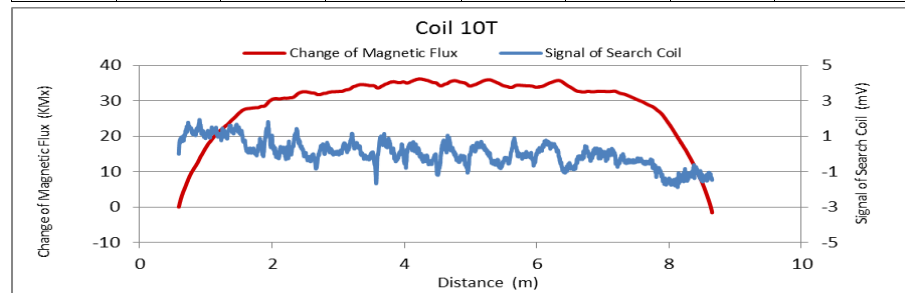


Figure A66. MMFM data of P2-402L-H1 tendon section.



Tokyo Rope USA, Inc.

File Name 【Pier-Tendon-Section】	Section Total Length (m)	Scanned Length		Note			
		Starting Point (m)	Ending Point (m)				
P2-402R-I1	21.43	0.53	20.69	Joint position: 12.2 m			
Identified Damage 1				Identified Damage 2			
Max Loss Point (m)	Section Loss (%)	Damage Length (m)	Damage Orientation	Max Loss Point (m)	Section Loss (%)	Damage Length (m)	Damage Orientation
—	—	—	—	—	—	—	—

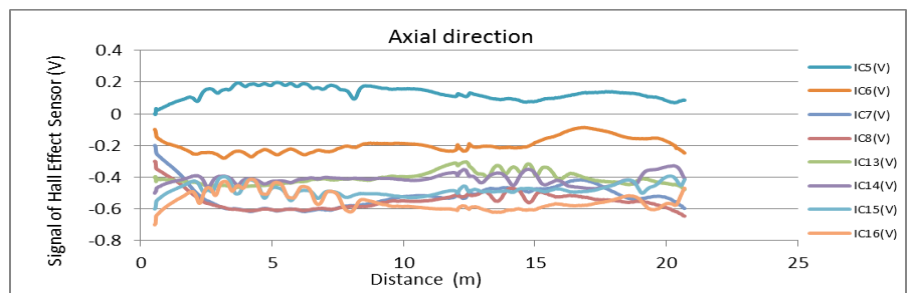
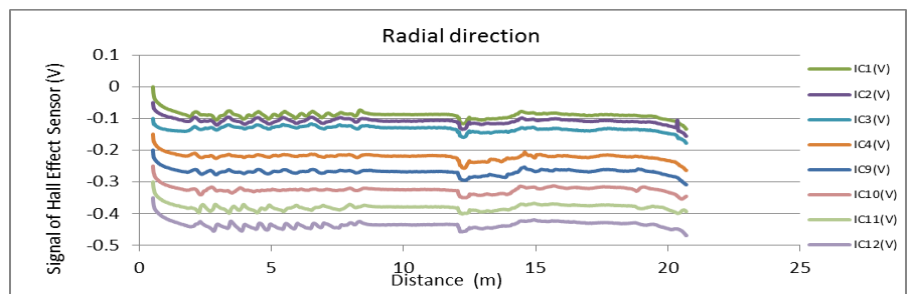
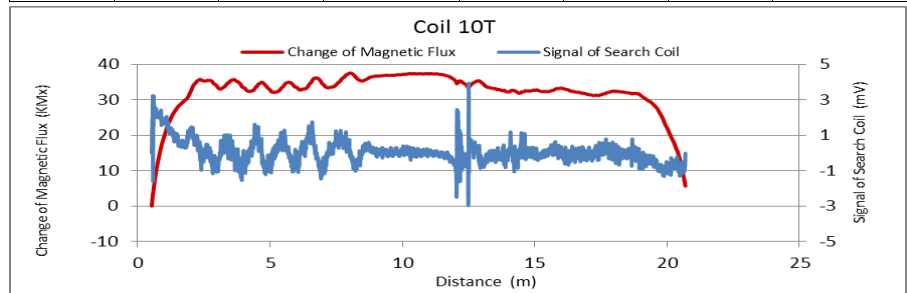


Figure A67. MMFM data of P2-402R-I1 tendon section.

File Name 【Pier-Tendon-Section】	Section Total Length (m)	Scanned Length		Note			
		Starting Point (m)	Ending Point (m)				
P2-401L-I1	21.37	0.59	20.68	Joint position: 12.3 m			
Identified Damage 1				Identified Damage 2			
Max Loss Point (m)	Section Loss (%)	Damage Length (m)	Damage Orientation	Max Loss Point (m)	Section Loss (%)	Damage Length (m)	Damage Orientation
—	—	—	—	—	—	—	—

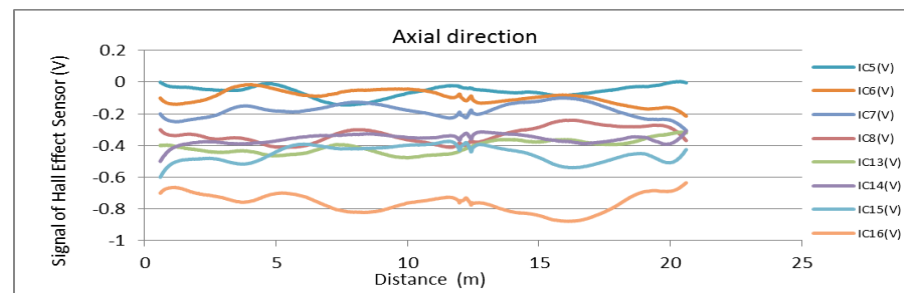
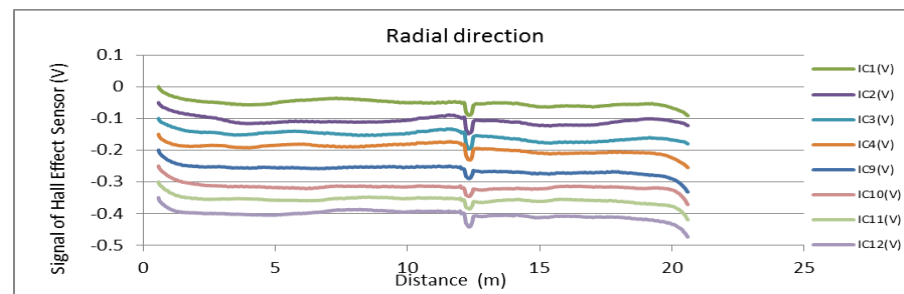
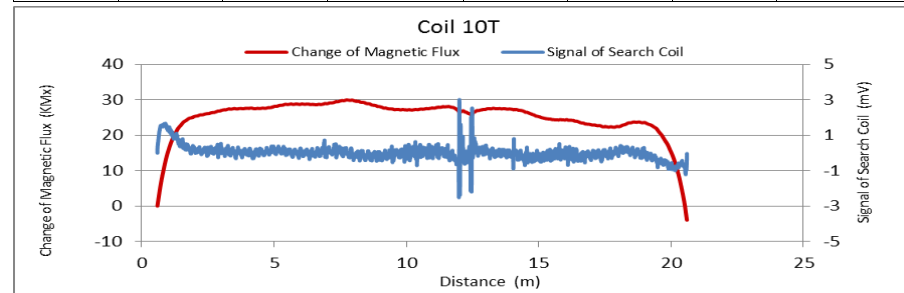


Figure A68. MMFM data of P2-401L-I1 tendon section.



Tokyo Rope USA, Inc.

File Name 【Pier-Tendon-Section】	Section Total Length (m)	Scanned Length		Note			
		Starting Point (m)	Ending Point (m)				
P2-401R-I2	21.47	0.67	20.87	Joint position: 4 m, 7 m, 9.1 m, 10 m			
Identified Damage 1				Identified Damage 2			
Max Loss Point (m)	Section Loss (%)	Damage Length (m)	Damage Orientation	Max Loss Point (m)	Section Loss (%)	Damage Length (m)	Damage Orientation
—	—	—	—	—	—	—	—

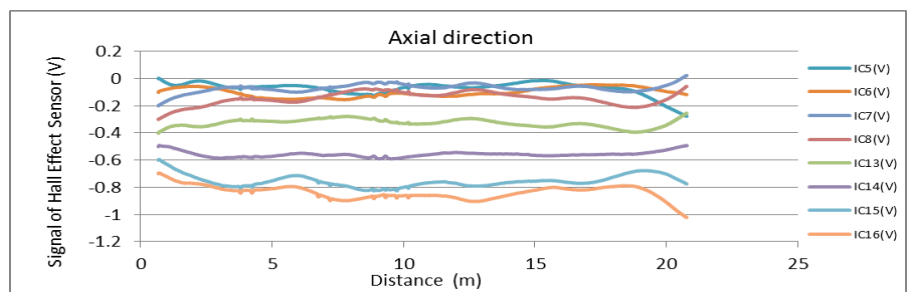
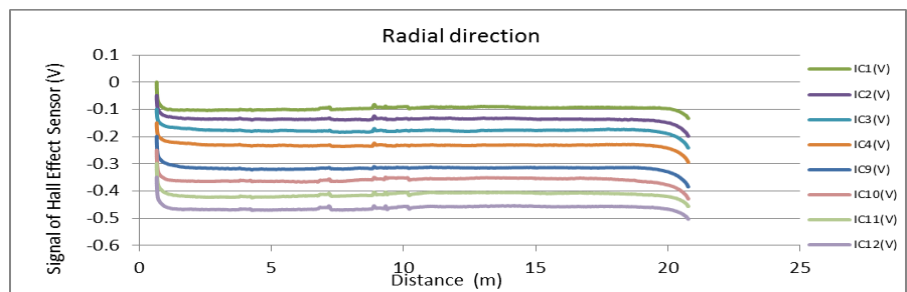
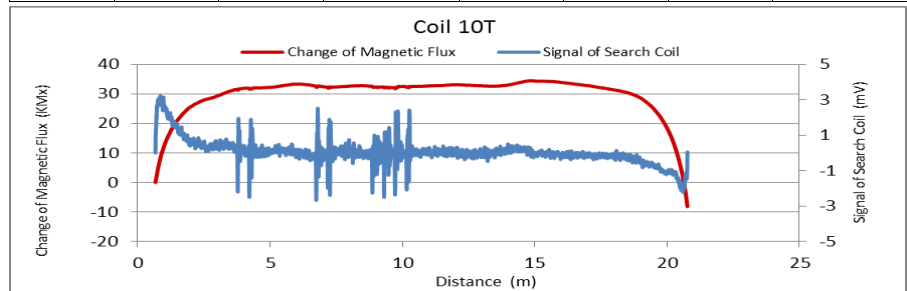


Figure A69. MMFM data of P2-402R-I2 tendon section.

File Name 【Pier-Tendon-Section】	Section Total Length (m)	Scanned Length		Note			
		Starting Point (m)	Ending Point (m)				
P2-401L-I2	21.5	0.73	20.93	Joint position: 9.3 m			
Identified Damage 1				Identified Damage 2			
Max Loss Point (m)	Section Loss (%)	Damage Length (m)	Damage Orientation	Max Loss Point (m)	Section Loss (%)	Damage Length (m)	Damage Orientation
—	—	—	—	—	—	—	—

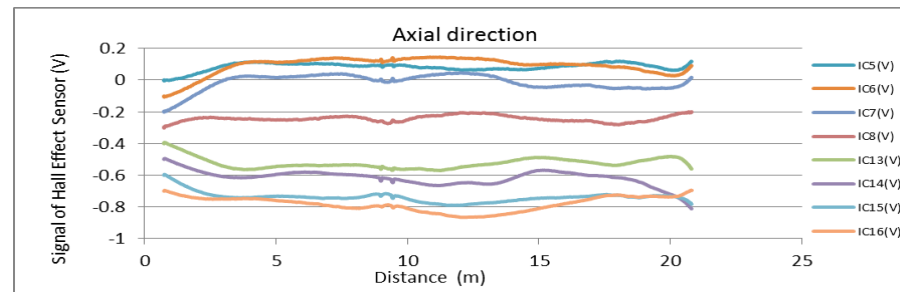
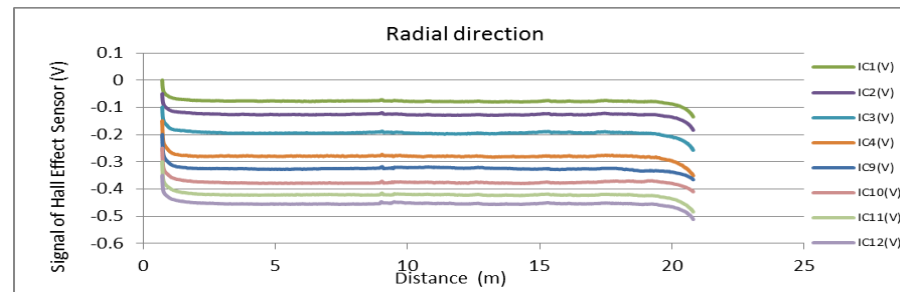
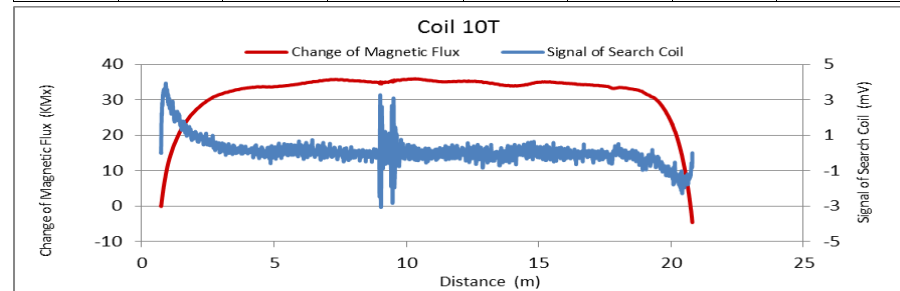


Figure A70. MMFM data of P2-401L-I2 tendon section.



Tokyo Rope USA, Inc.

File Name 【Pier-Tendon-Section】	Section Total Length (m)	Scanned Length		Note			
		Starting Point (m)	Ending Point (m)				
P2-402L-I2	21.5	0.73	20.93	Joint position: 9.3 m			
Identified Damage 1				Identified Damage 2			
Max Loss Point (m)	Section Loss (%)	Damage Length (m)	Damage Orientation	Max Loss Point (m)	Section Loss (%)	Damage Length (m)	Damage Orientation
—	—	—	—	—	—	—	—

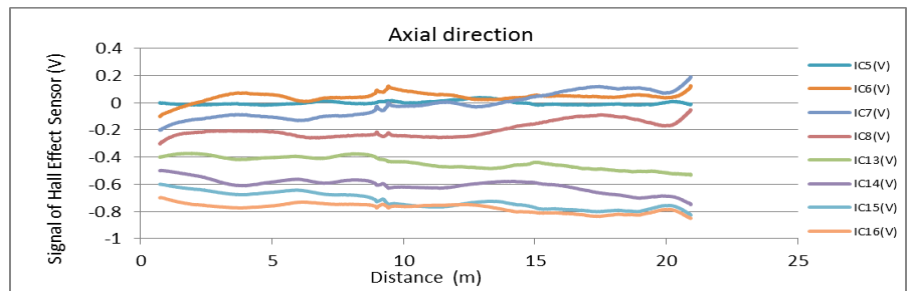
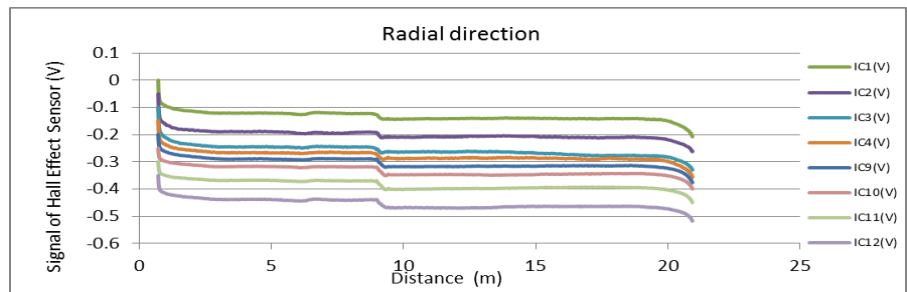
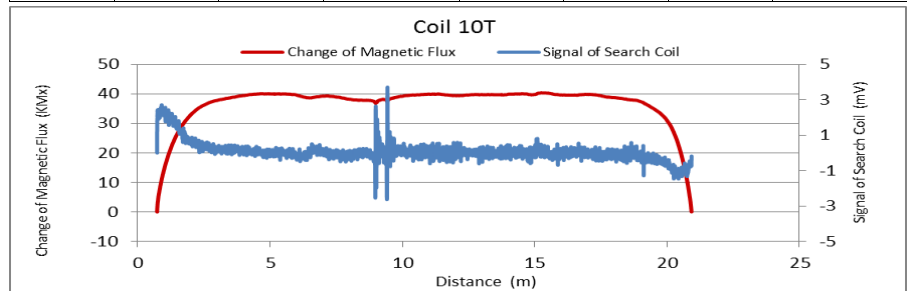


Figure A71. MMFM data of P2-402L-I2 tendon section.

File Name 【Pier-Tendon-Section】	Section Total Length (m)	Scanned Length		Note			
		Starting Point (m)	Ending Point (m)				
P2-401R-H2	9.43	0.73	8.83				
Identified Damage 1				Identified Damage 2			
Max Loss Point (m)	Section Loss (%)	Damage Length (m)	Damage Orientation	Max Loss Point (m)	Section Loss (%)	Damage Length (m)	Damage Orientation
—	—	—	—	—	—	—	—

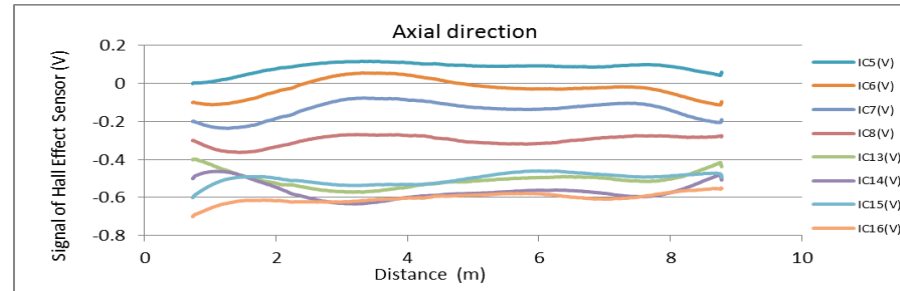
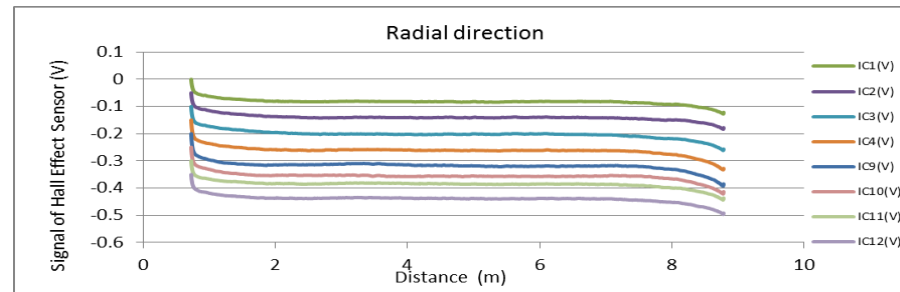
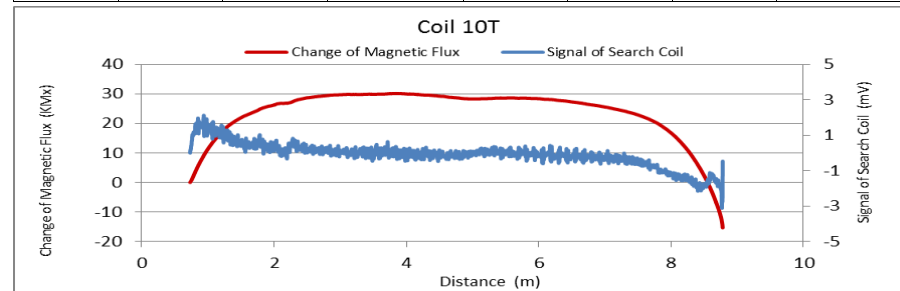


Figure A72. MMFM data of P2-401R-H2 tendon section.



Tokyo Rope USA, Inc.

File Name 【Pier-Tendon-Section】	Section Total Length (m)	Scanned Length		Note			
		Starting Point (m)	Ending Point (m)				
P2-401L-H2	9.4	0.81	8.9				
Identified Damage 1				Identified Damage 2			
Max Loss Point (m)	Section Loss (%)	Damage Length (m)	Damage Orientation	Max Loss Point (m)	Section Loss (%)	Damage Length (m)	Damage Orientation
—	—	—	—	—	—	—	—

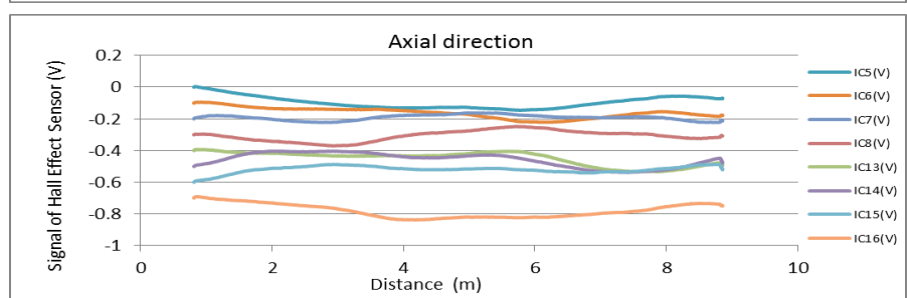
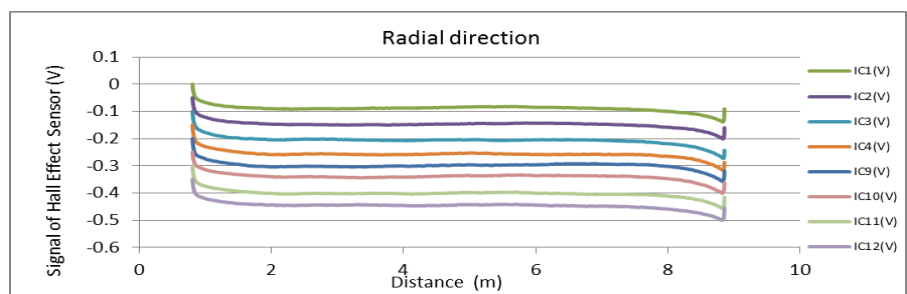
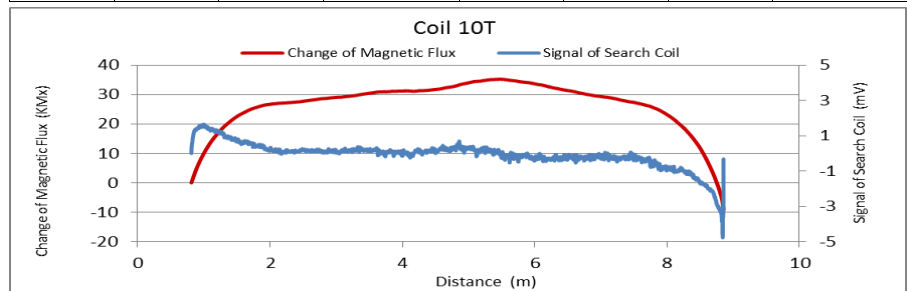


Figure A73. MMFM data of P2-401L-H2 tendon section.

File Name 【Pier-Tendon-Section】	Section Total Length (m)	Scanned Length		Note			
		Starting Point (m)	Ending Point (m)				
P2-402L-H2	9.4	0.57	8.84				
Identified Damage 1				Identified Damage 2			
Max Loss Point (m)	Section Loss (%)	Damage Length (m)	Damage Orientation	Max Loss Point (m)	Section Loss (%)	Damage Length (m)	Damage Orientation
—	—	—	—	—	—	—	—

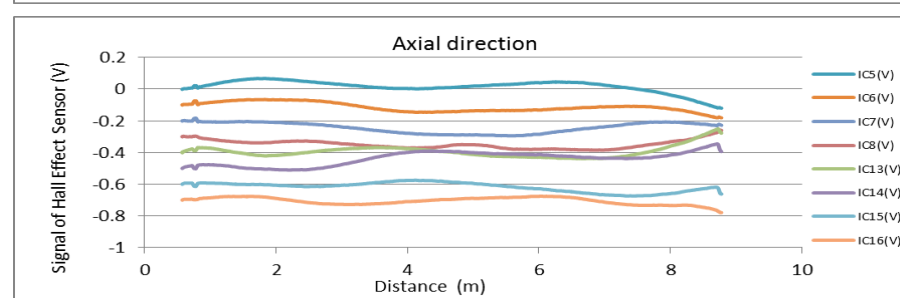
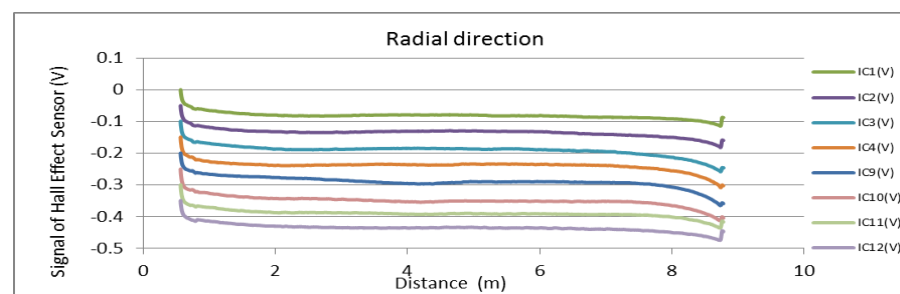
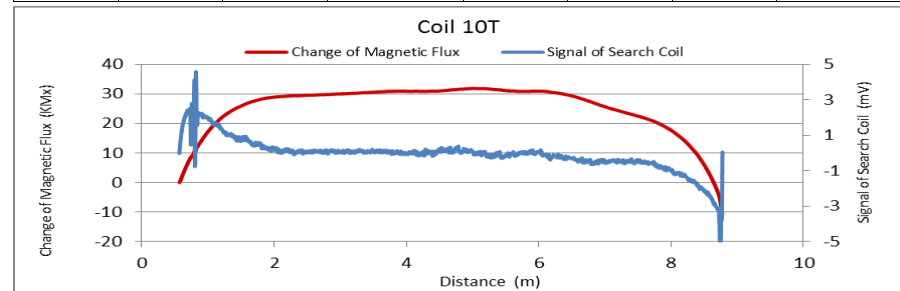


Figure A74. MMFM data of P2-402L-H2 tendon section.



Tokyo Rope USA, Inc.

File Name 【Pier-Tendon-Section】	Section Total Length (m)	Scanned Length		Note			
		Starting Point (m)	Ending Point (m)				
P3-401R-H1	9.43	0.59	8.63				
Identified Damage 1				Identified Damage 2			
Max Loss Point (m)	Section Loss (%)	Damage Length (m)	Damage Orientation	Max Loss Point (m)	Section Loss (%)	Damage Length (m)	Damage Orientation
—	—	—	—	—	—	—	—

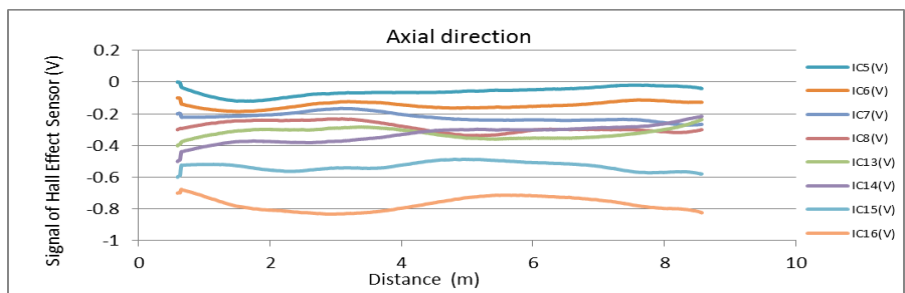
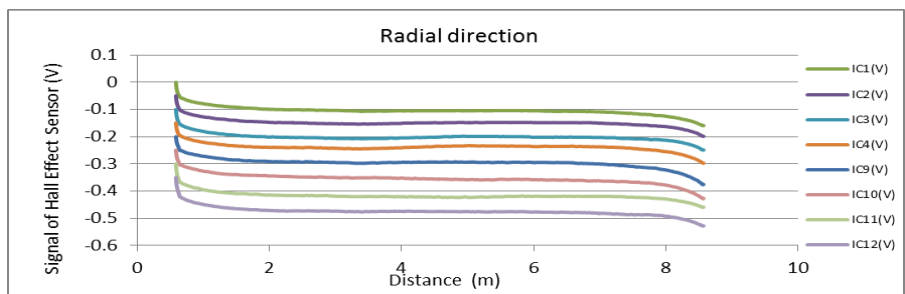
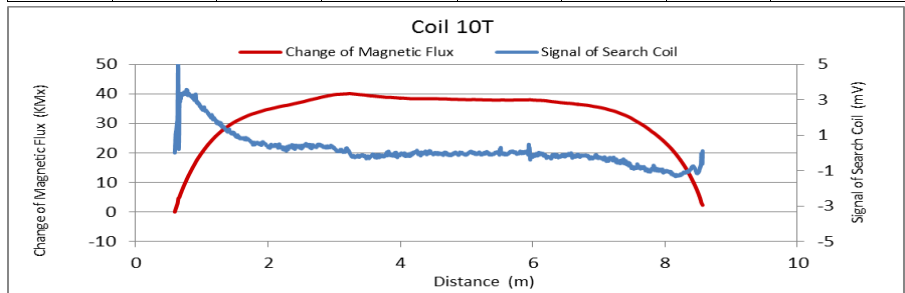


Figure A75. MMFM data of P3-401R-H1 tendon section.

File Name 【Pier-Tendon-Section】	Section Total Length (m)	Scanned Length		Note			
		Starting Point (m)	Ending Point (m)				
P3-402R-H1	9.43	0.57	8.62				
Identified Damage 1				Identified Damage 2			
Max Loss Point (m)	Section Loss (%)	Damage Length (m)	Damage Orientation	Max Loss Point (m)	Section Loss (%)	Damage Length (m)	Damage Orientation
—	—	—	—	—	—	—	—

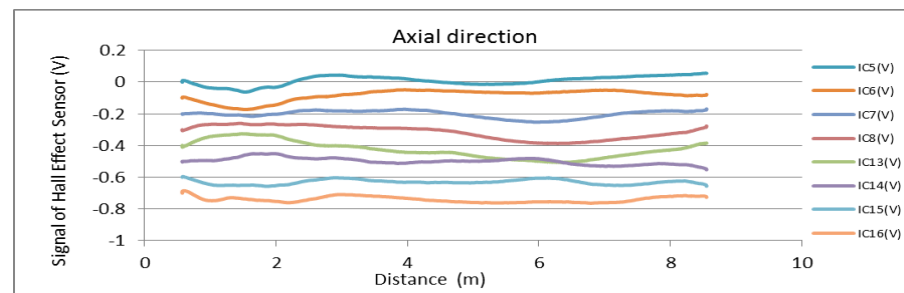
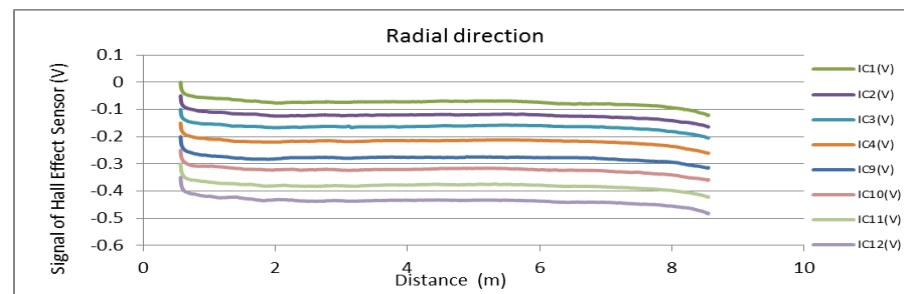
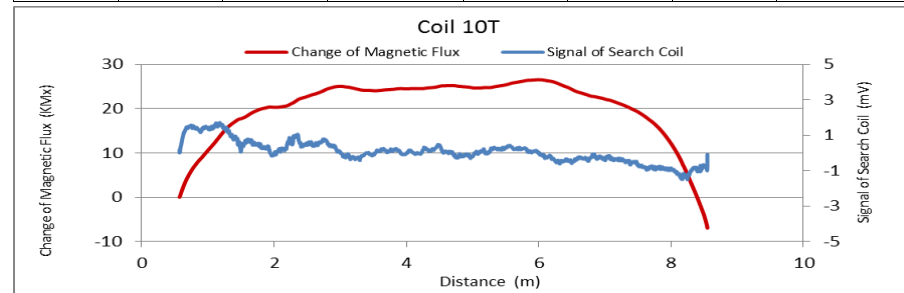


Figure A76. MMFM data of P3-402R-H1 tendon section.



Tokyo Rope USA, Inc.

File Name 【Pier-Tendon-Section】	Section Total Length (m)	Scanned Length		Note			
		Starting Point (m)	Ending Point (m)				
P3-401L-H1	9.49	0.62	8.74				
Identified Damage 1				Identified Damage 2			
Max Loss Point (m)	Section Loss (%)	Damage Length (m)	Damage Orientation	Max Loss Point (m)	Section Loss (%)	Damage Length (m)	Damage Orientation
—	—	—	—	—	—	—	—

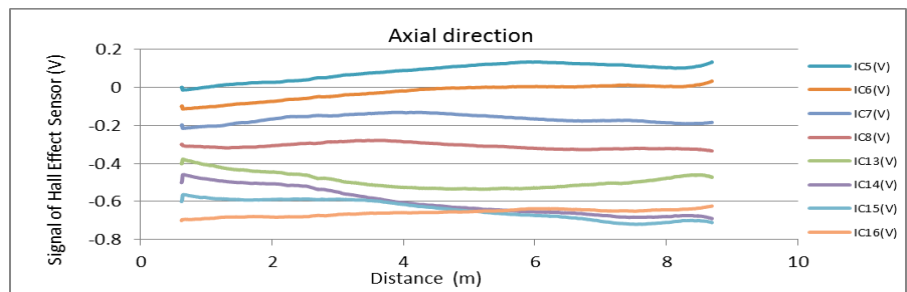
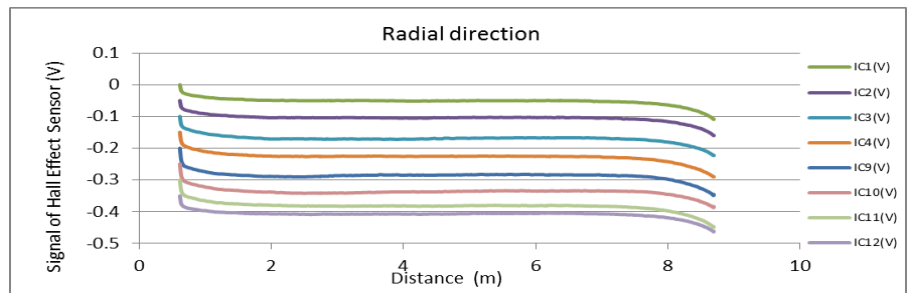
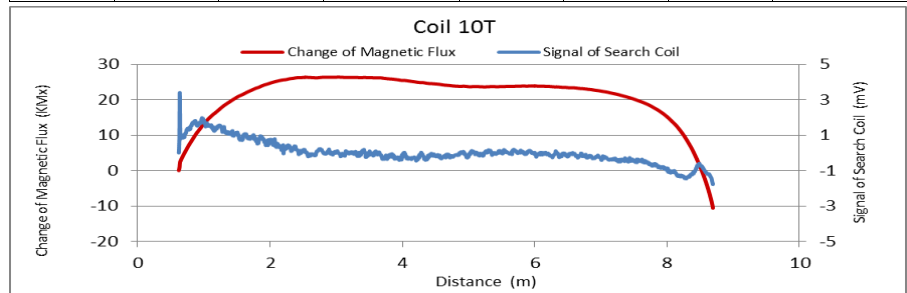


Figure A77. MMFM data of P3-401L-H1 tendon section.

File Name 【Pier-Tendon-Section】	Section Total Length (m)	Scanned Length		Note			
		Starting Point (m)	Ending Point (m)				
P3-401R-I1	21.53	0.57	20.92				
Identified Damage 1				Identified Damage 2			
Max Loss Point (m)	Section Loss (%)	Damage Length (m)	Damage Orientation	Max Loss Point (m)	Section Loss (%)	Damage Length (m)	Damage Orientation
—	—	—	—	—	—	—	—

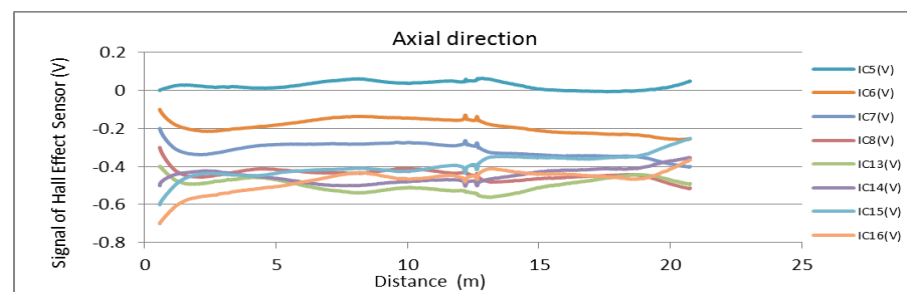
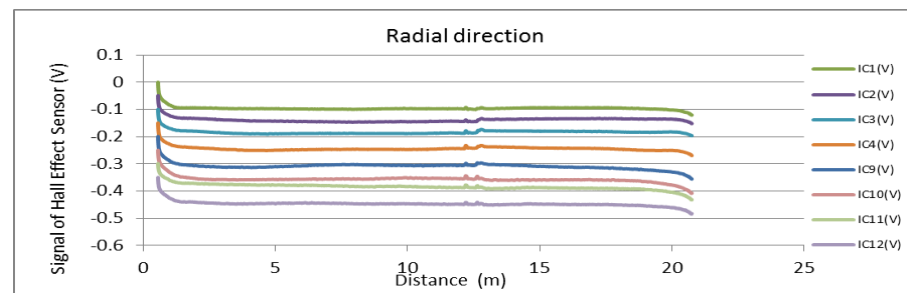
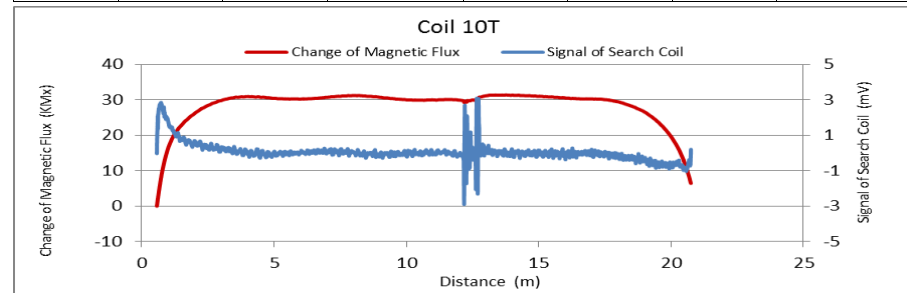


Figure A78. MMFM data of P3-401R-I1 tendon section.



Tokyo Rope USA, Inc.

File Name 【Pier-Tendon-Section】	Section Total Length (m)	Scanned Length		Note			
		Starting Point (m)	Ending Point (m)				
P3-402R-I1	21.53	0.58	20.81	Joint position: 13.3 m			
Identified Damage 1				Identified Damage 2			
Max Loss Point (m)	Section Loss (%)	Damage Length (m)	Damage Orientation	Max Loss Point (m)	Section Loss (%)	Damage Length (m)	Damage Orientation
—	—	—	—	—	—	—	—

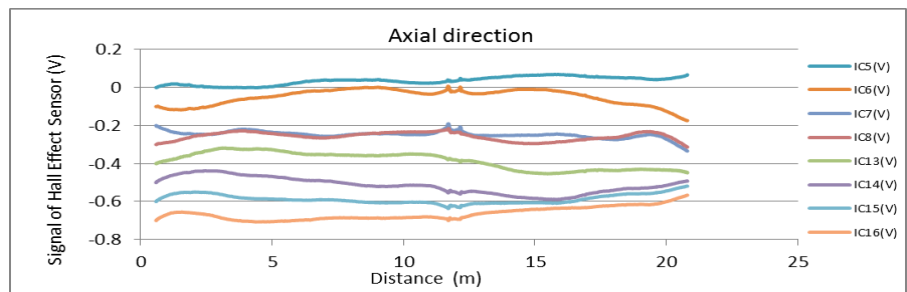
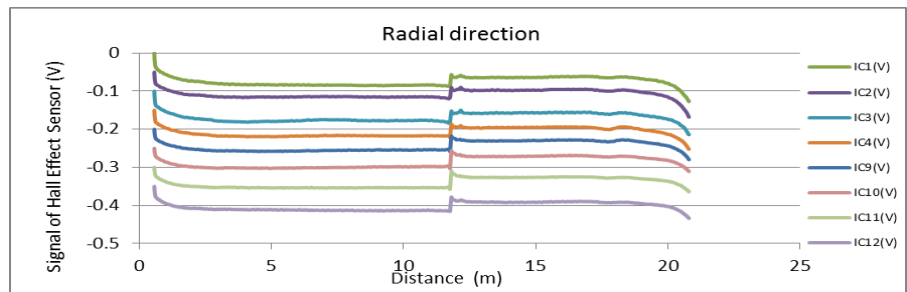
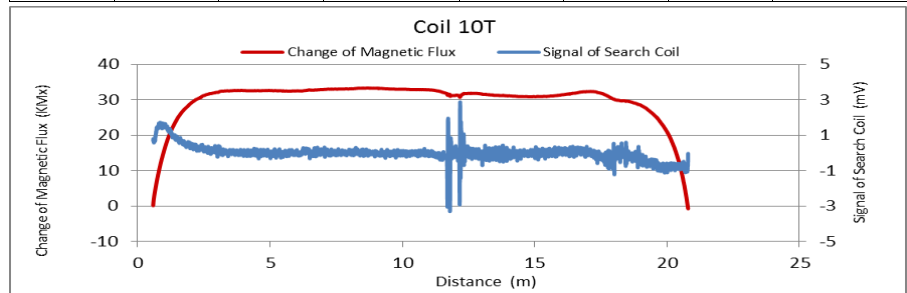


Figure A79. MMFM data of P3-402R-I1 tendon section.

File Name 【Pier-Tendon-Section】	Section Total Length (m)	Scanned Length		Note			
		Starting Point (m)	Ending Point (m)				
P3-401L-I1	21.53	0.48	20.68	Joint position: 12.2 m			
Identified Damage 1				Identified Damage 2			
Max Loss Point (m)	Section Loss (%)	Damage Length (m)	Damage Orientation	Max Loss Point (m)	Section Loss (%)	Damage Length (m)	Damage Orientation
—	—	—	—	—	—	—	—

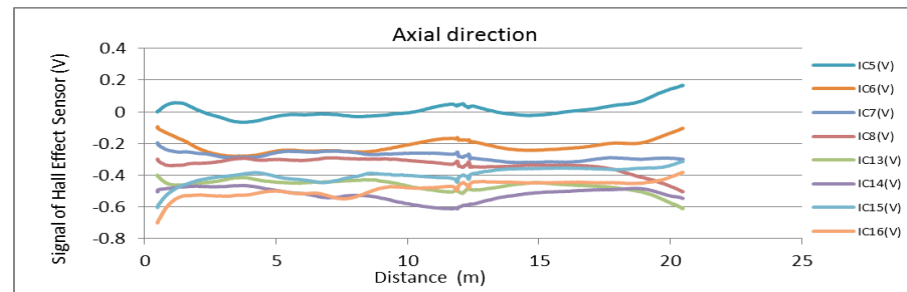
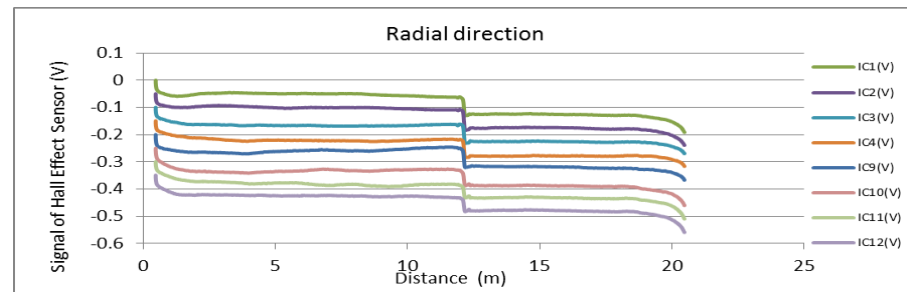
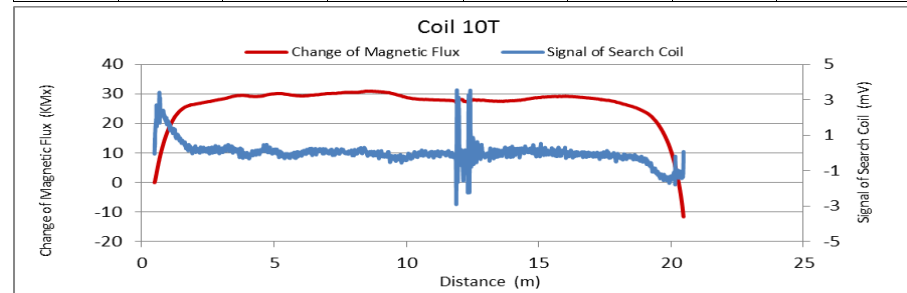


Figure A80. MMFM data of P3-401L-I1 tendon section.



Tokyo Rope USA, Inc.

File Name 【Pier-Tendon-Section】	Section Total Length (m)	Scanned Length		Note			
		Starting Point (m)	Ending Point (m)				
P3-402L-I1	21.53	1.59	20.75	Joint position: 8.02 m, 12.35 m			
Identified Damage 1				Identified Damage 2			
Max Loss Point (m)	Section Loss (%)	Damage Length (m)	Damage Orientation	Max Loss Point (m)	Section Loss (%)	Damage Length (m)	Damage Orientation
—	—	—	—	—	—	—	—

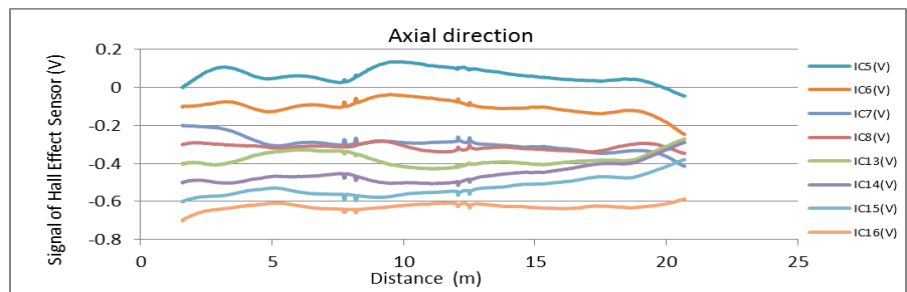
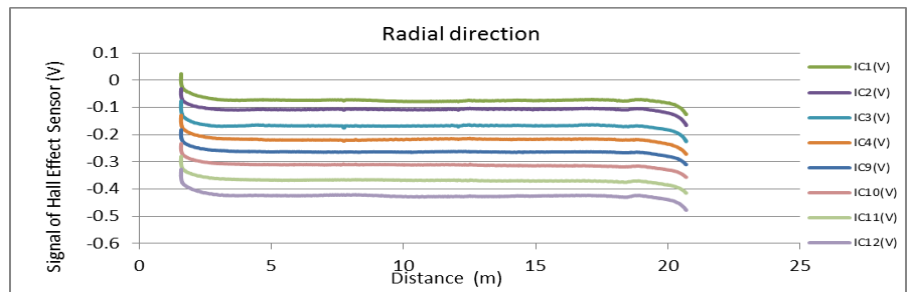
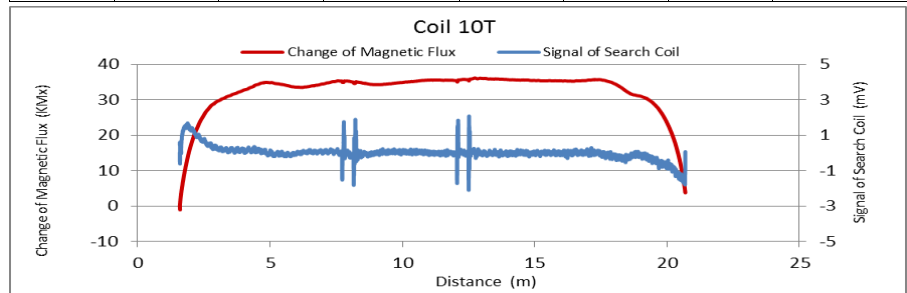


Figure A81. MMFM data of P3-402L-I1 tendon section.

File Name 【Pier-Tendon-Section】	Section Total Length (m)	Scanned Length		Note			
		Starting Point (m)	Ending Point (m)				
P3-401R-I2	21.5	0.74	20.95	Joint position: 9.3 m			
Identified Damage 1				Identified Damage 2			
Max Loss Point (m)	Section Loss (%)	Damage Length (m)	Damage Orientation	Max Loss Point (m)	Section Loss (%)	Damage Length (m)	Damage Orientation
—	—	—	—	—	—	—	—

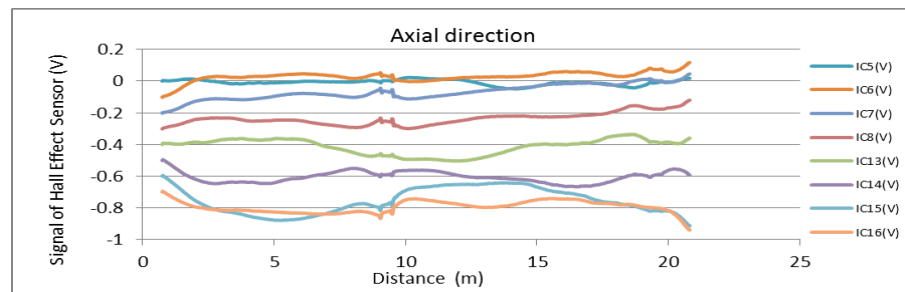
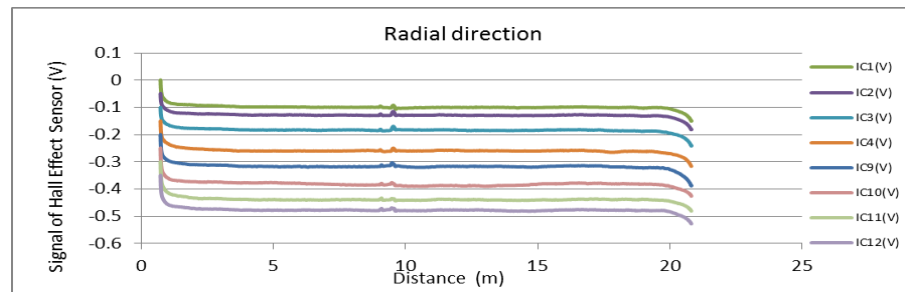
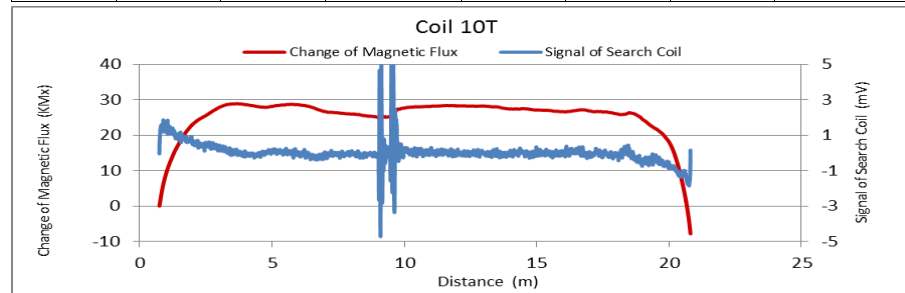


Figure A82. MMFM data of P3-401R-I2 tendon section.



Tokyo Rope USA, Inc.

File Name 【Pier-Tendon-Section】	Section Total Length (m)	Scanned Length		Note			
		Starting Point (m)	Ending Point (m)				
P3-402R-I2	21.5	0.55	20.91	Joint position: 9.2 m			
Identified Damage 1				Identified Damage 2			
Max Loss Point (m)	Section Loss (%)	Damage Length (m)	Damage Orientation	Max Loss Point (m)	Section Loss (%)	Damage Length (m)	Damage Orientation
—	—	—	—	—	—	—	—

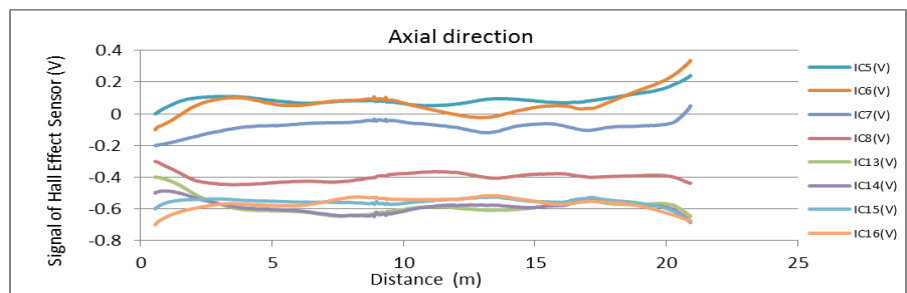
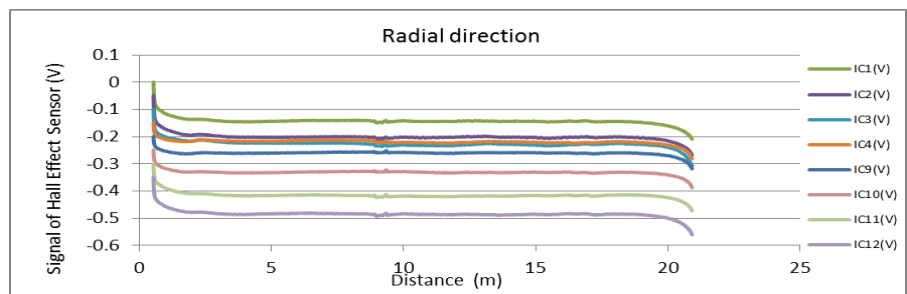
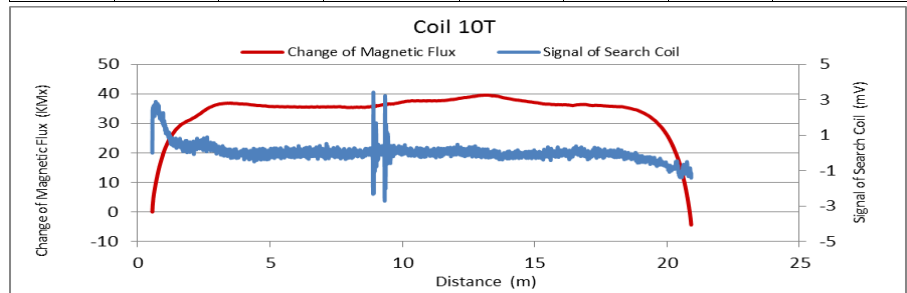


Figure A83. MMFM data of P3-402R-I2 tendon section.

File Name 【Pier-Tendon-Section】	Section Total Length (m)	Scanned Length		Note			
		Starting Point (m)	Ending Point (m)				
P3-401L-I2	21.6	0.5	21.05	Joint position: 9.34 m			
Identified Damage 1				Identified Damage 2			
Max Loss Point (m)	Section Loss (%)	Damage Length (m)	Damage Orientation	Max Loss Point (m)	Section Loss (%)	Damage Length (m)	Damage Orientation
—	—	—	—	—	—	—	—

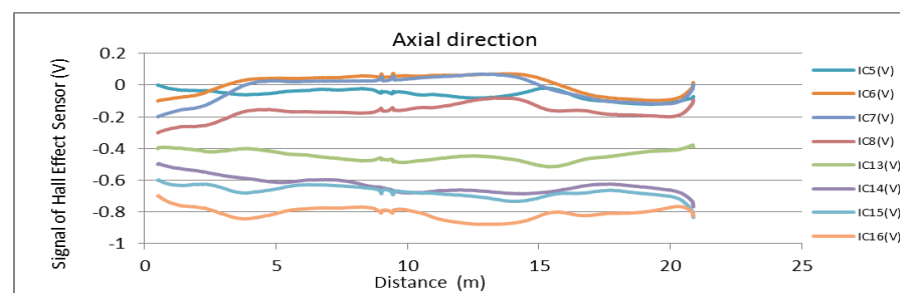
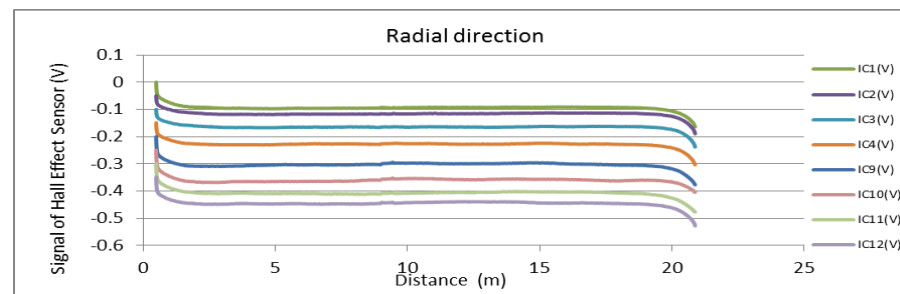
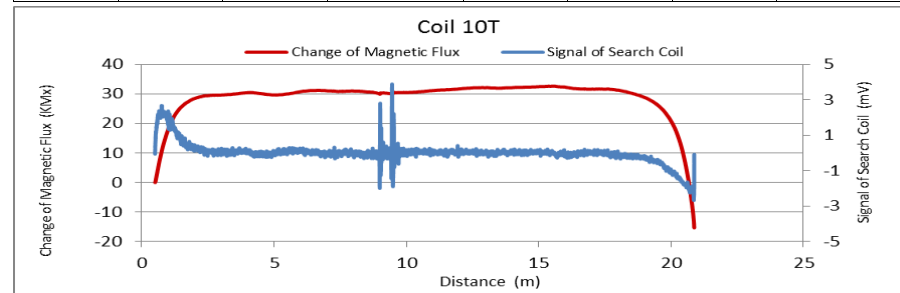


Figure A84. MMFM data of P3-401L-I2 tendon section.



Tokyo Rope USA, Inc.

File Name 【Pier-Tendon-Section】	Section Total Length (m)	Scanned Length		Note			
		Starting Point (m)	Ending Point (m)				
P3-402L-I2	21.6	0.53	21.16	Joint position:9.34 m			
Identified Damage 1				Identified Damage 2			
Max Loss Point (m)	Section Loss (%)	Damage Length (m)	Damage Orientation	Max Loss Point (m)	Section Loss (%)	Damage Length (m)	Damage Orientation
—	—	—	—	—	—	—	—

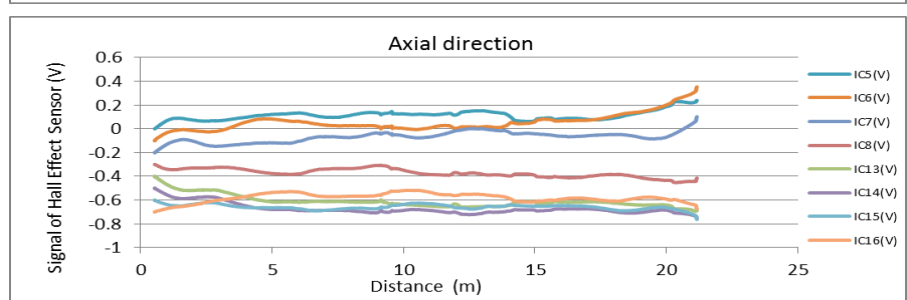
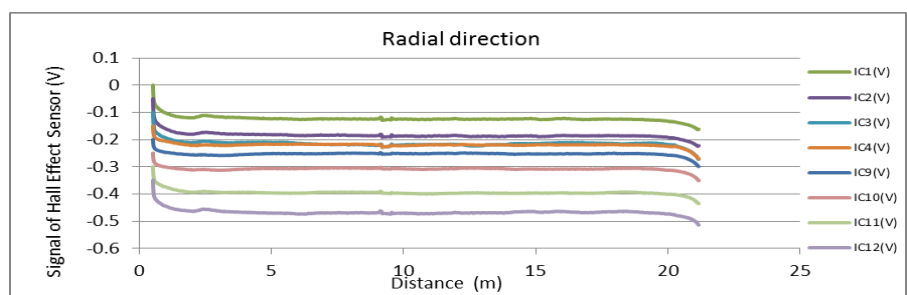
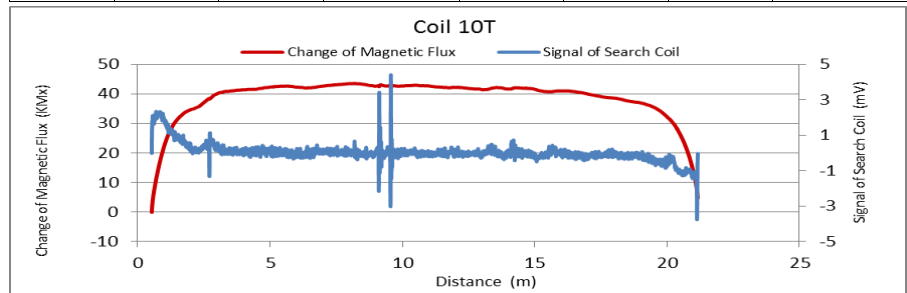


Figure A85. MMFM data of P3-402L-I2 tendon section.

File Name 【Pier-Tendon-Section】	Section Total Length (m)	Scanned Length		Note			
		Starting Point (m)	Ending Point (m)				
P3-401R-H2	9.45	1	8.79				
Identified Damage 1				Identified Damage 2			
Max Loss Point (m)	Section Loss (%)	Damage Length (m)	Damage Orientation	Max Loss Point (m)	Section Loss (%)	Damage Length (m)	Damage Orientation
—	—	—	—	—	—	—	—

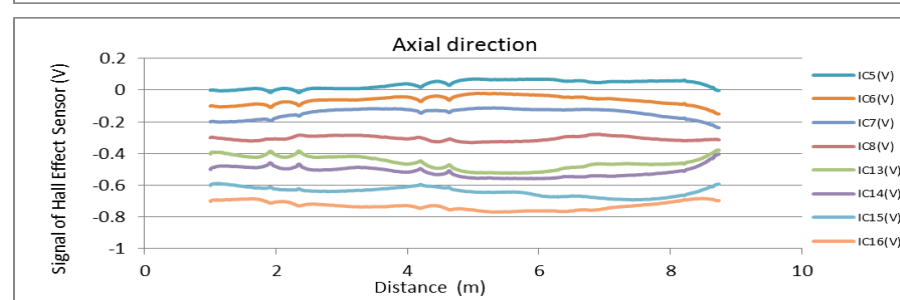
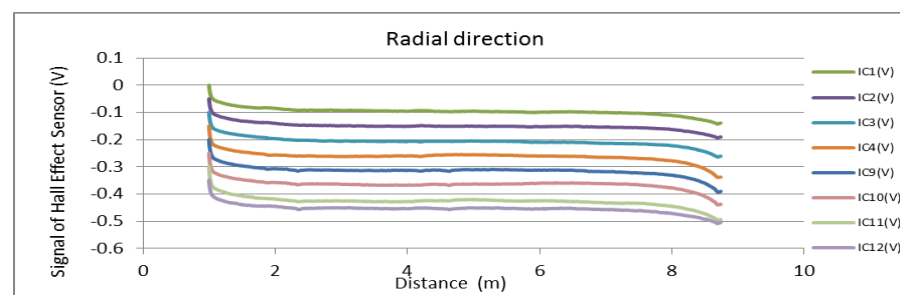
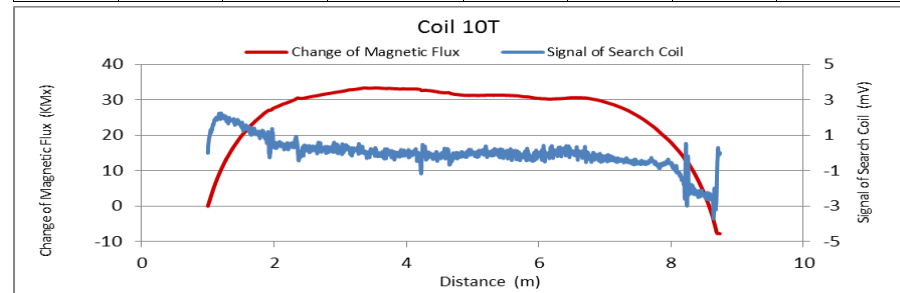


Figure A86. MMFM data of P3-401R-H2 tendon section.



Tokyo Rope USA, Inc.

File Name 【Pier-Tendon-Section】	Section Total Length (m)	Scanned Length		Note			
		Starting Point (m)	Ending Point (m)				
P3-402R-H2	9.45	0.71	8.85				
Identified Damage 1				Identified Damage 2			
Max Loss Point (m)	Section Loss (%)	Damage Length (m)	Damage Orientation	Max Loss Point (m)	Section Loss (%)	Damage Length (m)	Damage Orientation
—	—	—	—	—	—	—	—

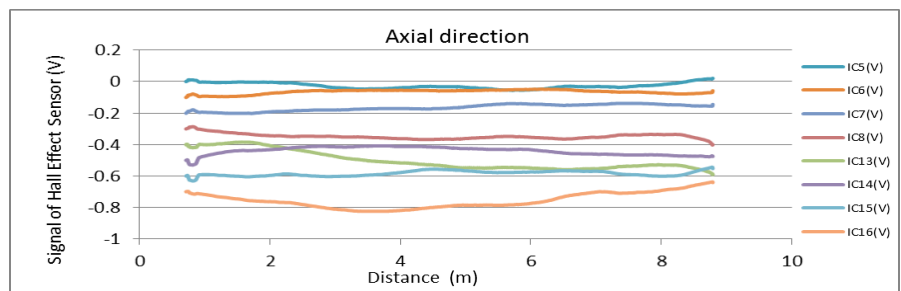
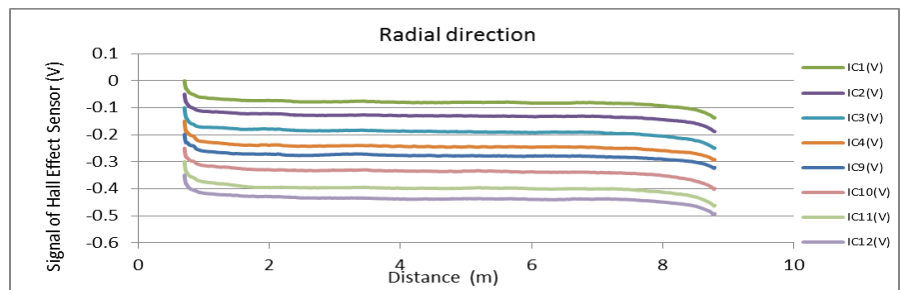
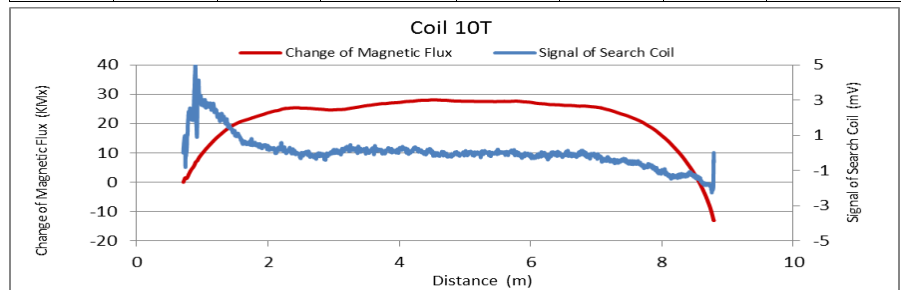


Figure A87. MMFM data of P3-402R-H2 tendon section.

File Name 【Pier-Tendon-Section】	Section Total Length (m)	Scanned Length		Note			
		Starting Point (m)	Ending Point (m)				
P3-401L-H2	9.49	0.79	8.91				
Identified Damage 1				Identified Damage 2			
Max Loss Point (m)	Section Loss (%)	Damage Length (m)	Damage Orientation	Max Loss Point (m)	Section Loss (%)	Damage Length (m)	Damage Orientation
—	—	—	—	—	—	—	—

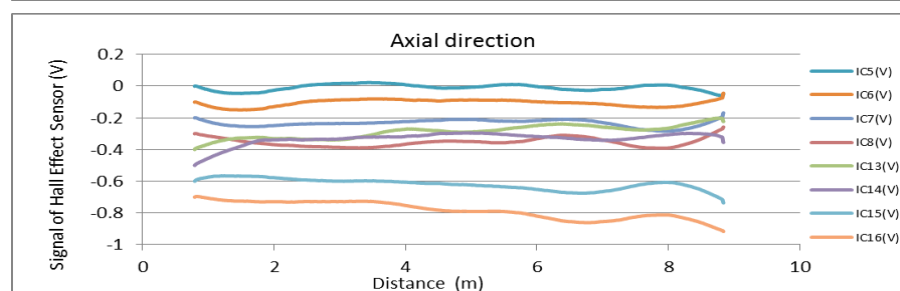
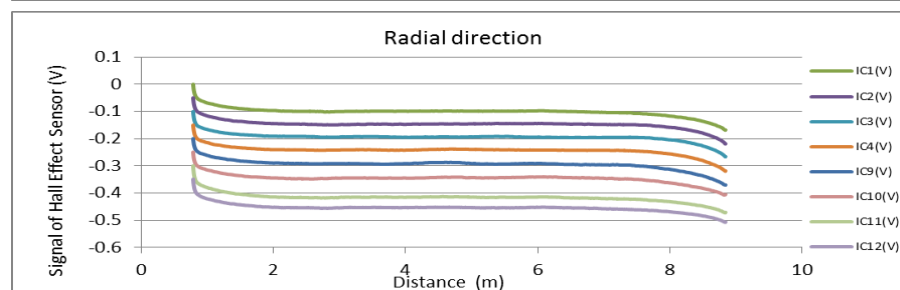
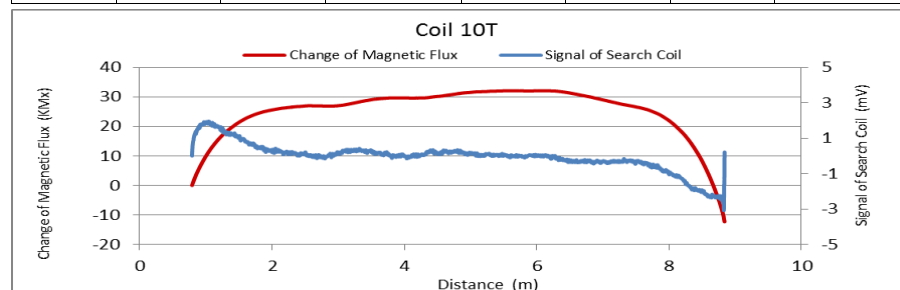


Figure A88. MMFM data of P3-401L-H2 tendon section.



Tokyo Rope USA, Inc.

File Name 【Pier-Tendon-Section】	Section Total Length (m)	Scanned Length		Note			
		Starting Point (m)	Ending Point (m)				
P3-402L-H2	9.49	0.77	8.96				
Identified Damage 1				Identified Damage 2			
Max Loss Point (m)	Section Loss (%)	Damage Length (m)	Damage Orientation	Max Loss Point (m)	Section Loss (%)	Damage Length (m)	Damage Orientation
—	—	—	—	—	—	—	—

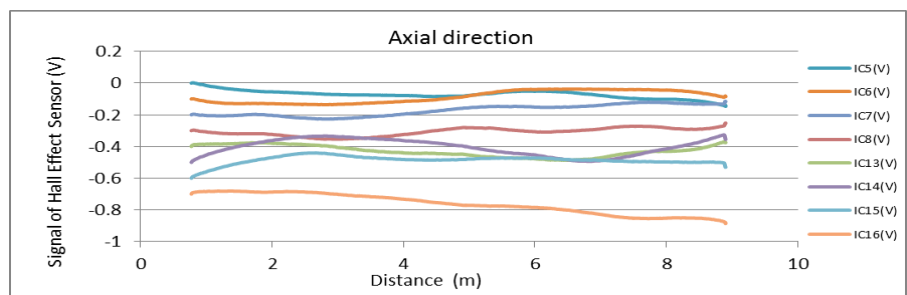
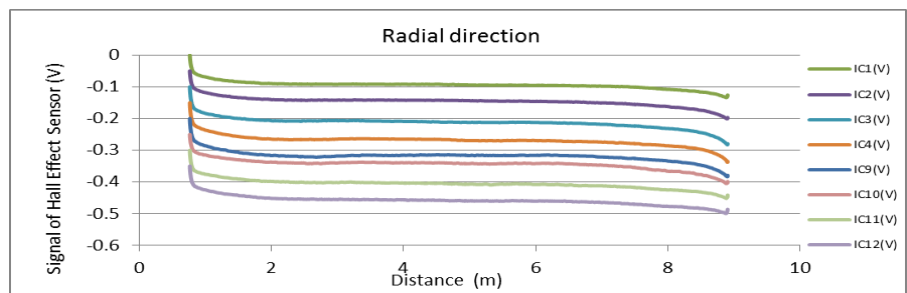
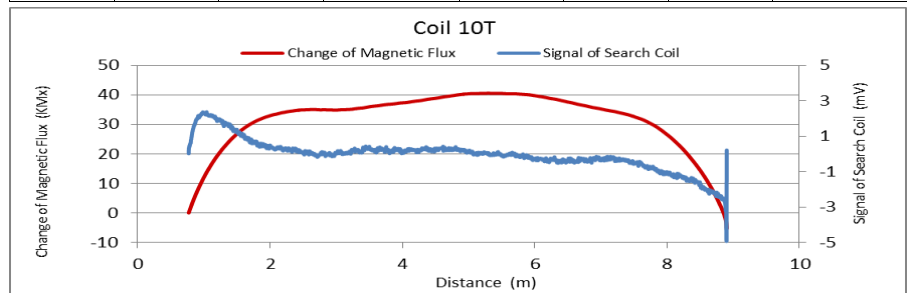


Figure A89. MMFM data of P3-402L-H2 tendon section.

File Name 【Pier-Tendon-Section】	Section Total Length (m)	Scanned Length		Note			
		Starting Point (m)	Ending Point (m)				
P4-401R-H1	9.35	0.55	8.66				
Identified Damage 1				Identified Damage 2			
Max Loss Point (m)	Section Loss (%)	Damage Length (m)	Damage Orientation	Max Loss Point (m)	Section Loss (%)	Damage Length (m)	Damage Orientation
—	—	—	—	—	—	—	—

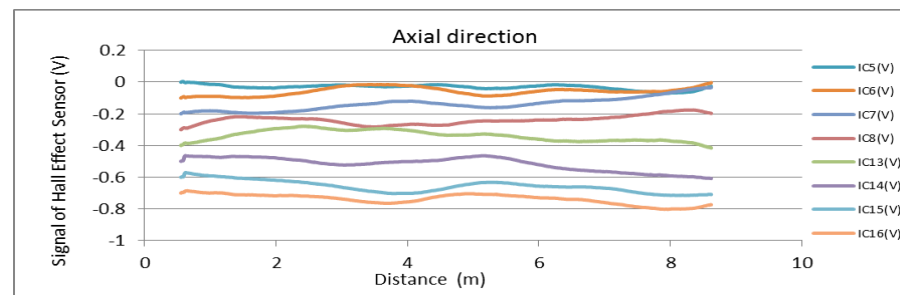
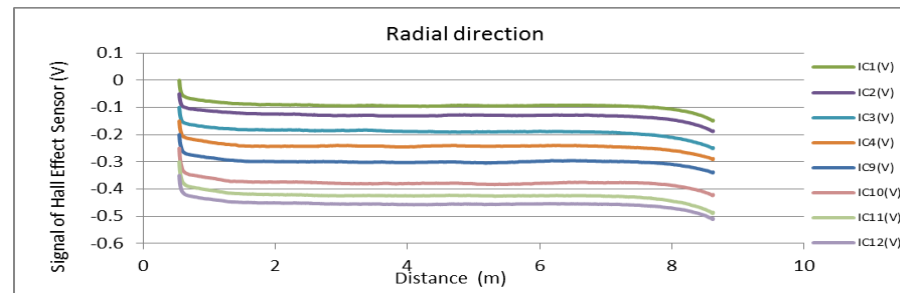
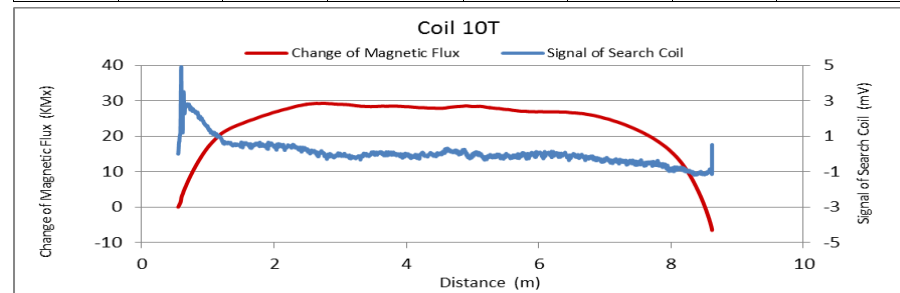


Figure A90. MMFM data of P4-401R-H1 tendon section.



Tokyo Rope USA, Inc.

File Name 【Pier-Tendon-Section】	Section Total Length (m)	Scanned Length		Note			
		Starting Point (m)	Ending Point (m)				
P4-401L-H1	9.36	0.57	8.66				
Identified Damage 1				Identified Damage 2			
Max Loss Point (m)	Section Loss (%)	Damage Length (m)	Damage Orientation	Max Loss Point (m)	Section Loss (%)	Damage Length (m)	Damage Orientation
—	—	—	—	—	—	—	—

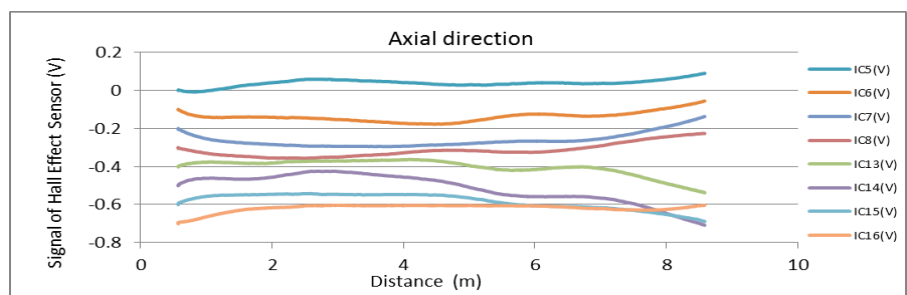
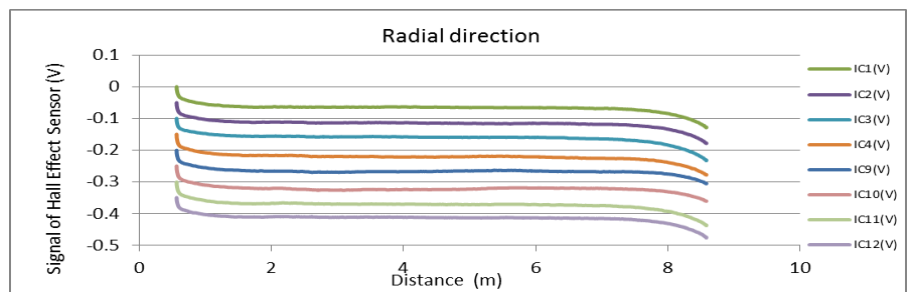
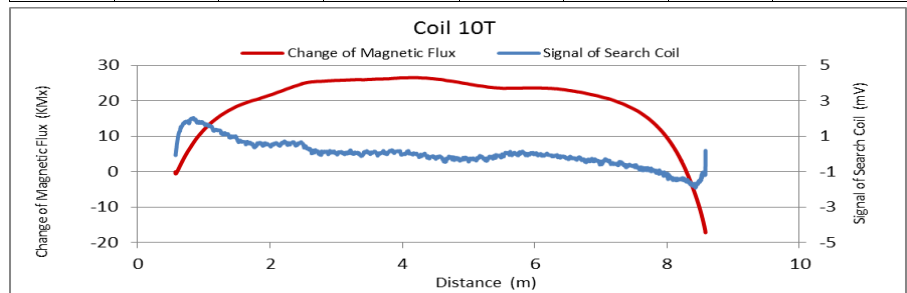


Figure A91. MMFM data of P4-401L-H1 tendon section.

File Name 【Pier-Tendon-Section】	Section Total Length (m)	Scanned Length		Note			
		Starting Point (m)	Ending Point (m)				
P4-402R-I1	21.57	0.58	20.78	Joint position: 12.27 m			
Identified Damage 1				Identified Damage 2			
Max Loss Point (m)	Section Loss (%)	Damage Length (m)	Damage Orientation	Max Loss Point (m)	Section Loss (%)	Damage Length (m)	Damage Orientation
—	—	—	—	—	—	—	—

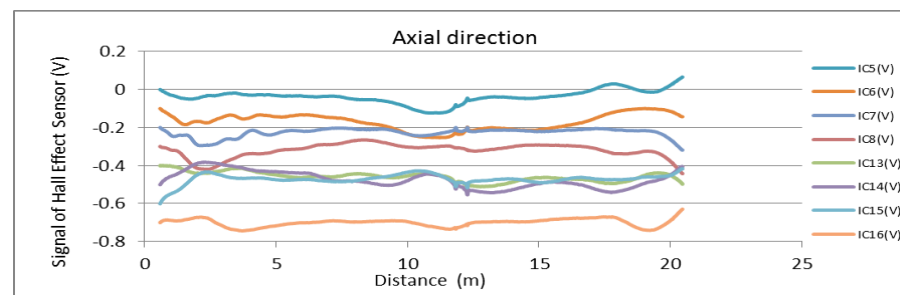
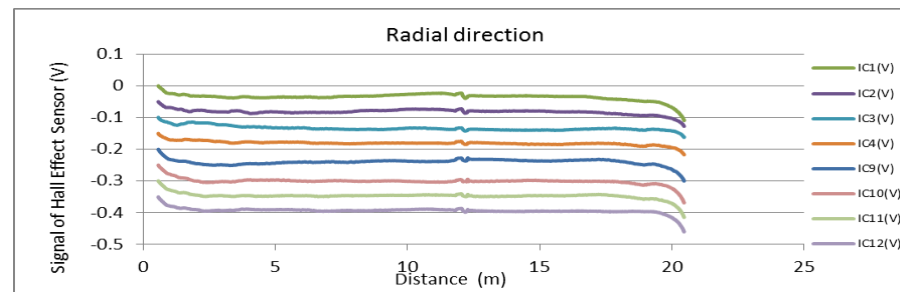
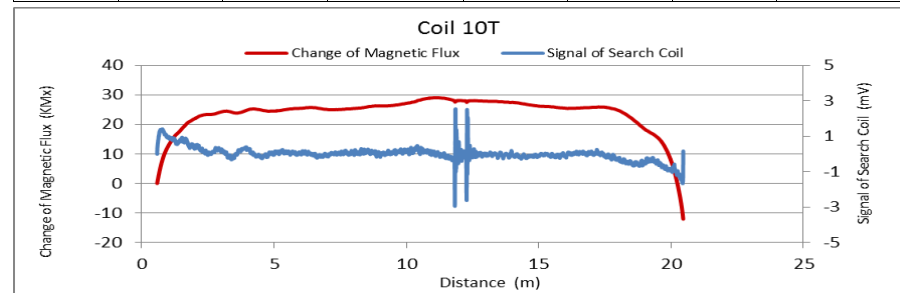


Figure A92. MMFM data of P4-402R-I1 tendon section.



Tokyo Rope USA, Inc.

File Name 【Pier-Tendon-Section】	Section Total Length (m)	Scanned Length		Note			
		Starting Point (m)	Ending Point (m)				
P4-401L-I1	21.5	0.54	20.61	Joint position: 12.27 m			
Identified Damage 1				Identified Damage 2			
Max Loss Point (m)	Section Loss (%)	Damage Length (m)	Damage Orientation	Max Loss Point (m)	Section Loss (%)	Damage Length (m)	Damage Orientation
—	—	—	—	—	—	—	—

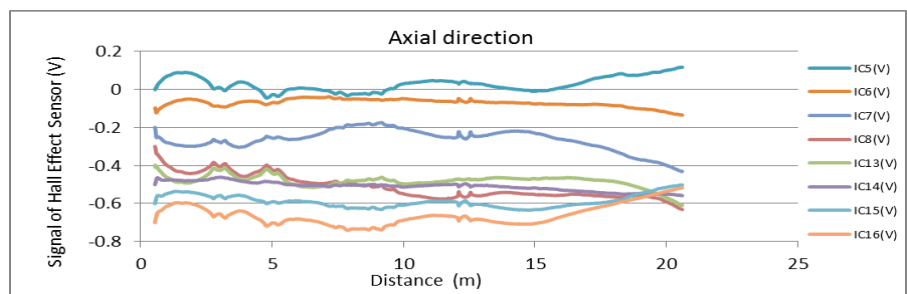
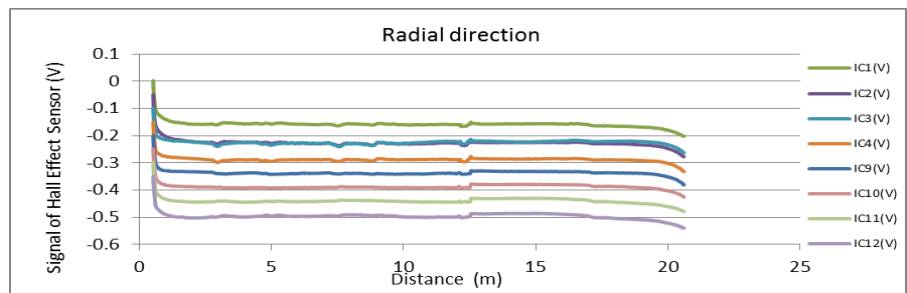
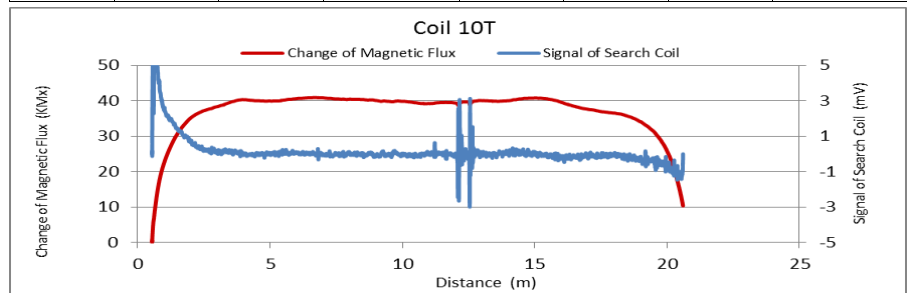


Figure A93. MMFM data of P4-401L-I1 tendon section.

File Name 【Pier-Tendon-Section】	Section Total Length (m)	Scanned Length		Note			
		Starting Point (m)	Ending Point (m)				
P4-402L-I1	21.5	0.5	20.75	Joint position: 12.27 m			
Identified Damage 1				Identified Damage 2			
Max Loss Point (m)	Section Loss (%)	Damage Length (m)	Damage Orientation	Max Loss Point (m)	Section Loss (%)	Damage Length (m)	Damage Orientation
—	—	—	—	—	—	—	—

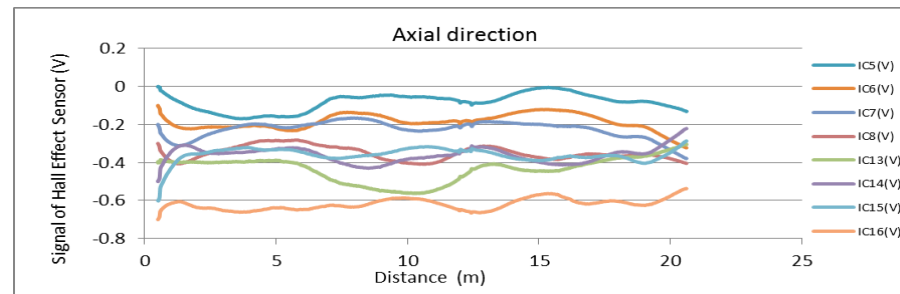
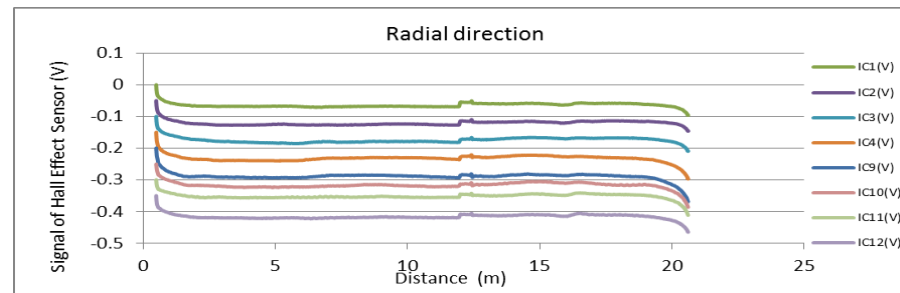
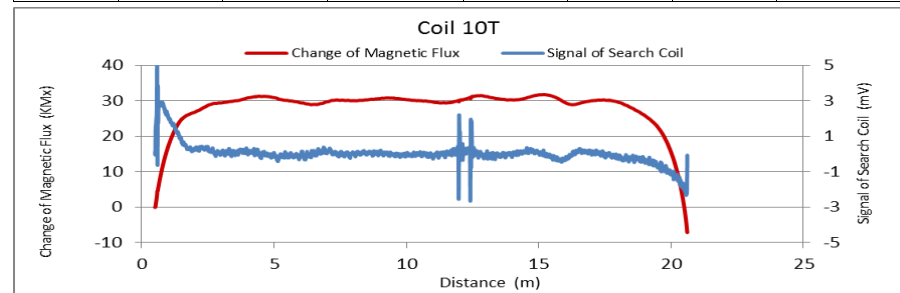


Figure A94. MMFM data of P4-402L-I1 tendon section.



Tokyo Rope USA, Inc.

File Name 【Pier-Tendon-Section】	Section Total Length (m)	Scanned Length		Note			
		Starting Point (m)	Ending Point (m)				
P4-402R-I2	21.46	0.69	20.92	Joint position: 9.38 m			
Identified Damage 1				Identified Damage 2			
Max Loss Point (m)	Section Loss (%)	Damage Length (m)	Damage Orientation	Max Loss Point (m)	Section Loss (%)	Damage Length (m)	Damage Orientation
—	—	—	—	—	—	—	—

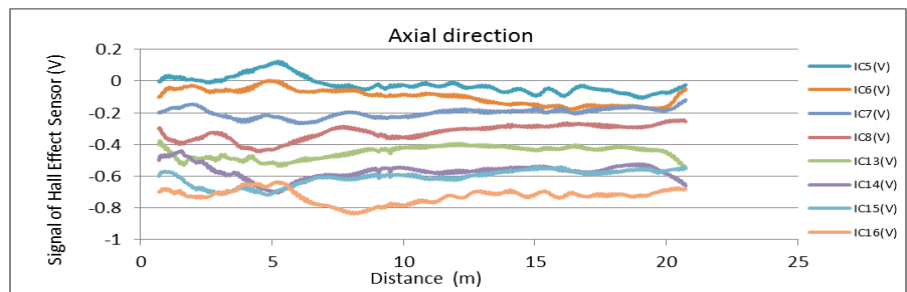
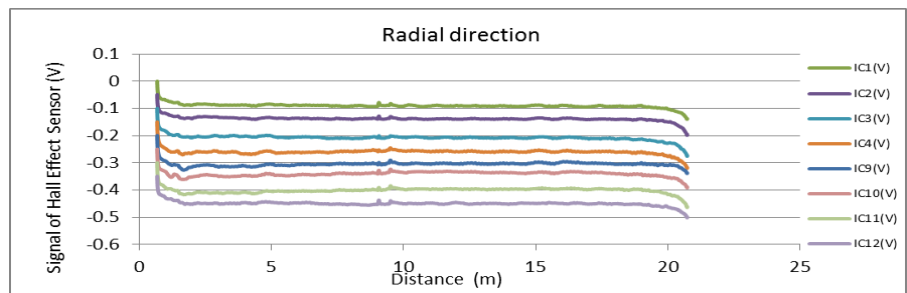
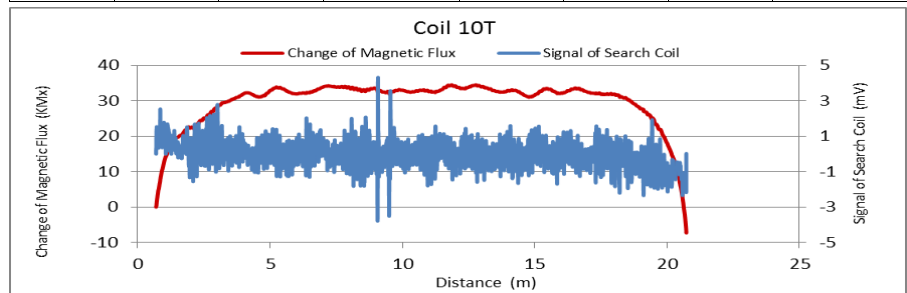


Figure A95. MMFM data of P4-402R-I2 tendon section.

File Name 【Pier-Tendon-Section】	Section Total Length (m)	Scanned Length		Note			
		Starting Point (m)	Ending Point (m)				
P4-402L-I2	21.5	0.78	20.85	Joint position: 9.18 m			
Identified Damage 1				Identified Damage 2			
Max Loss Point (m)	Section Loss (%)	Damage Length (m)	Damage Orientation	Max Loss Point (m)	Section Loss (%)	Damage Length (m)	Damage Orientation
—	—	—	—	—	—	—	—

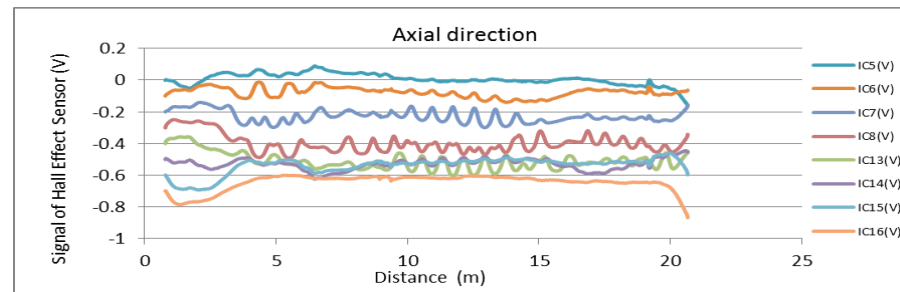
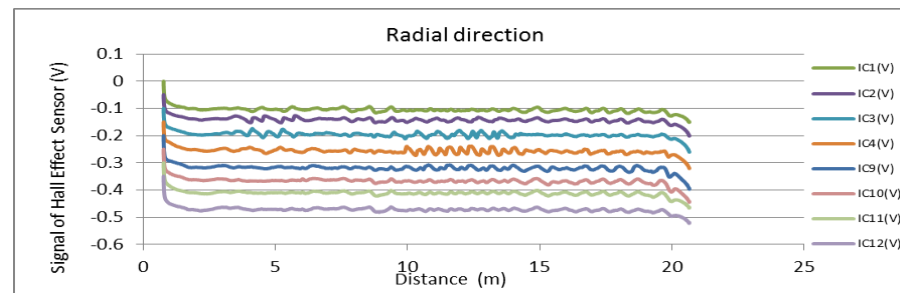
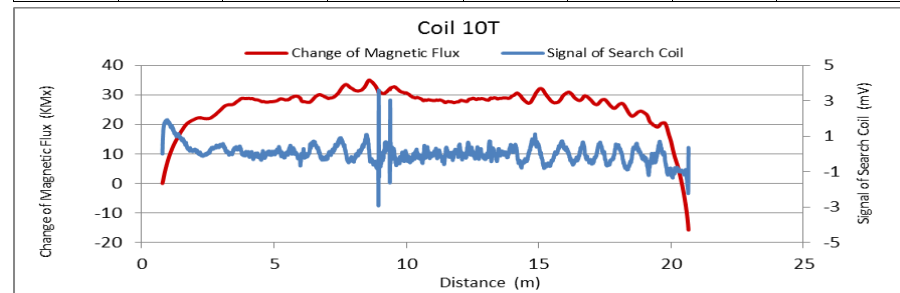


Figure A96. MMFM data of P4-402L-I2 tendon section.



Tokyo Rope USA, Inc.

File Name 【Pier-Tendon-Section】	Section Total Length (m)	Scanned Length		Note			
		Starting Point (m)	Ending Point (m)				
P4-401R-H2	9.38	0.72	8.84				
Identified Damage 1				Identified Damage 2			
Max Loss Point (m)	Section Loss (%)	Damage Length (m)	Damage Orientation	Max Loss Point (m)	Section Loss (%)	Damage Length (m)	Damage Orientation
—	—	—	—	—	—	—	—

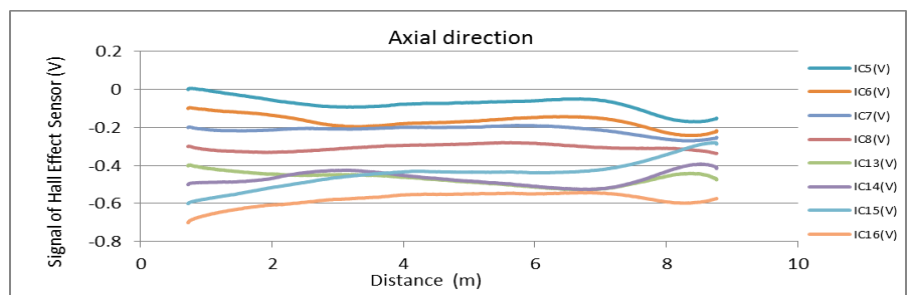
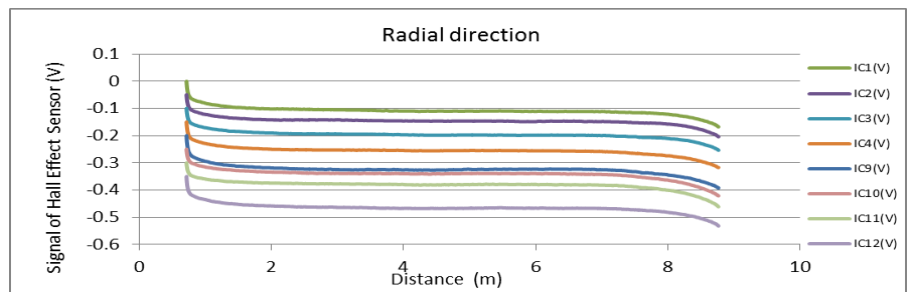
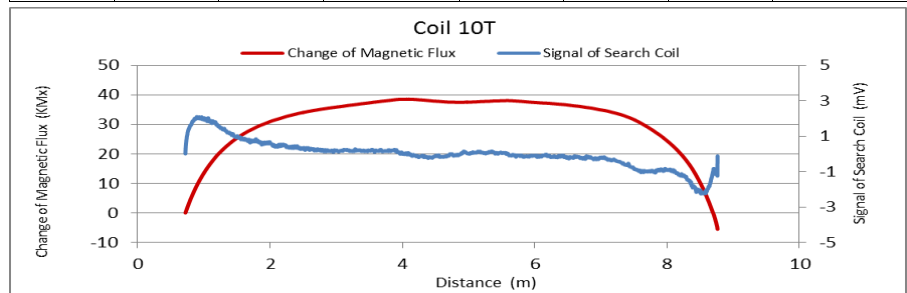


Figure A97. MMFM data of P4-401R-H2 tendon section.

File Name 【Pier-Tendon-Section】	Section Total Length (m)	Scanned Length		Note			
		Starting Point (m)	Ending Point (m)				
P4-402R-H2	9.38	0.8	8.77				
Identified Damage 1				Identified Damage 2			
Max Loss Point (m)	Section Loss (%)	Damage Length (m)	Damage Orientation	Max Loss Point (m)	Section Loss (%)	Damage Length (m)	Damage Orientation
—	—	—	—	—	—	—	—

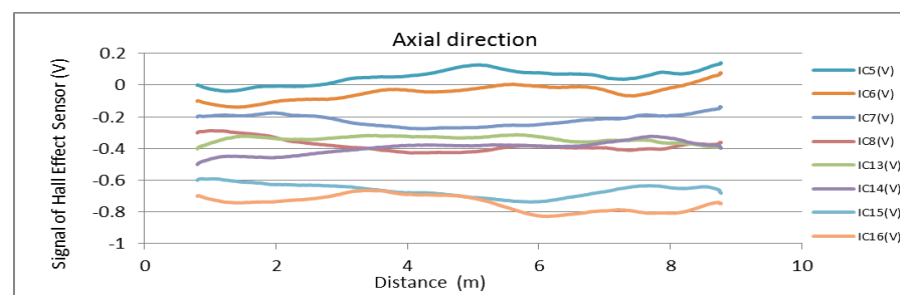
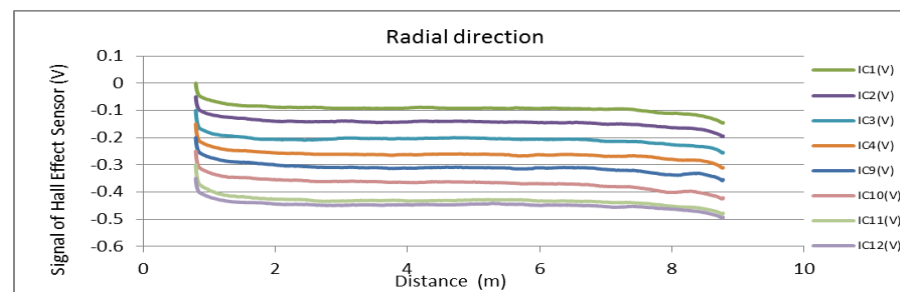
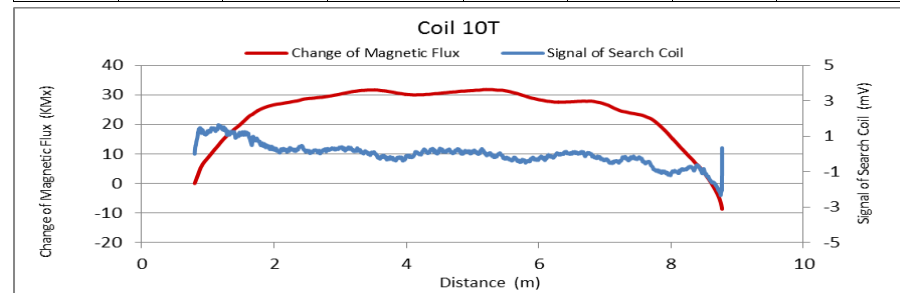


Figure A98. MMFM data of P4-402R-H2 tendon section.



Tokyo Rope USA, Inc.

File Name 【Pier-Tendon-Section】	Section Total Length (m)	Scanned Length		Note			
		Starting Point (m)	Ending Point (m)				
P4-401L-H2	9.39	0.82	8.86				
Identified Damage 1				Identified Damage 2			
Max Loss Point (m)	Section Loss (%)	Damage Length (m)	Damage Orientation	Max Loss Point (m)	Section Loss (%)	Damage Length (m)	Damage Orientation
—	—	—	—	—	—	—	—

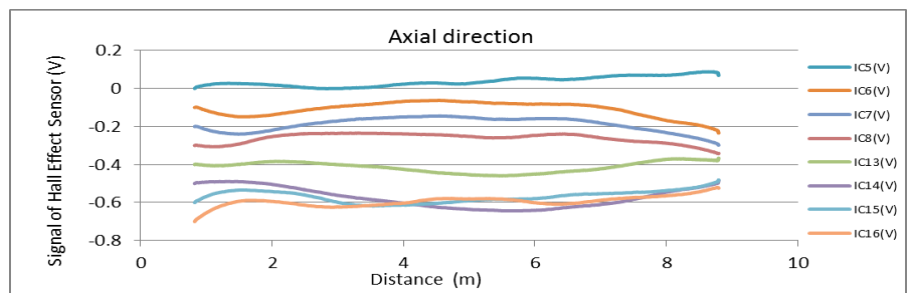
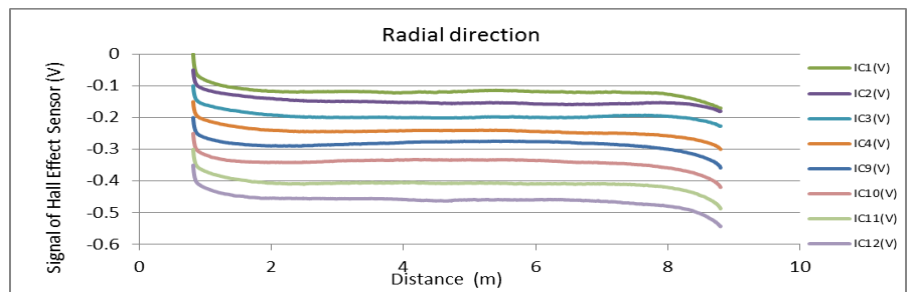
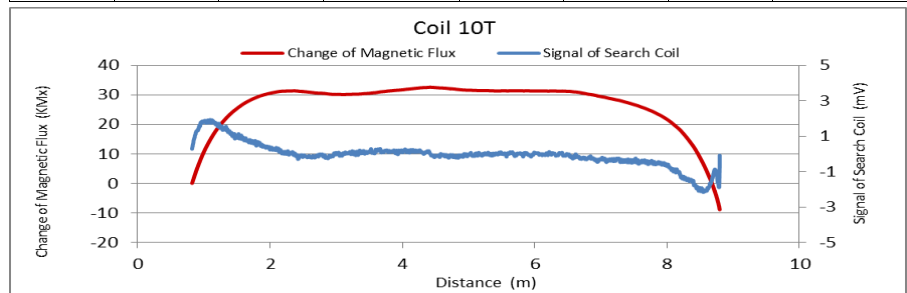


Figure A99. MMFM data of P4-401L-H2 tendon section.

File Name 【Pier-Tendon-Section】	Section Total Length (m)	Scanned Length		Note			
		Starting Point (m)	Ending Point (m)				
P5-401R-H1	9.35	0.57	8.76				
Identified Damage 1				Identified Damage 2			
Max Loss Point (m)	Section Loss (%)	Damage Length (m)	Damage Orientation	Max Loss Point (m)	Section Loss (%)	Damage Length (m)	Damage Orientation
—	—	—	—	—	—	—	—

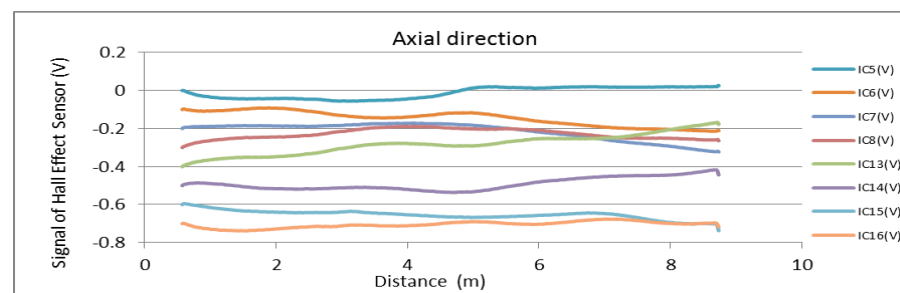
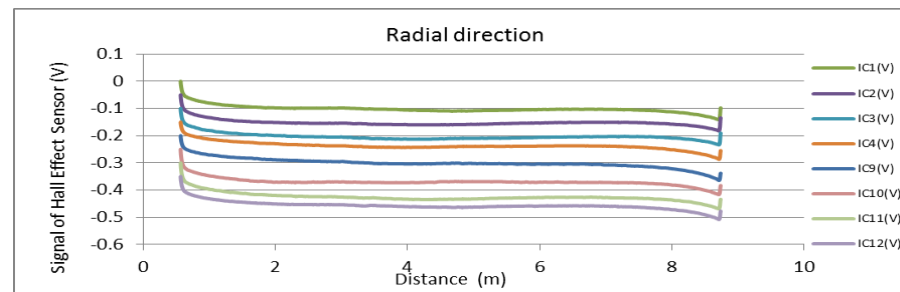
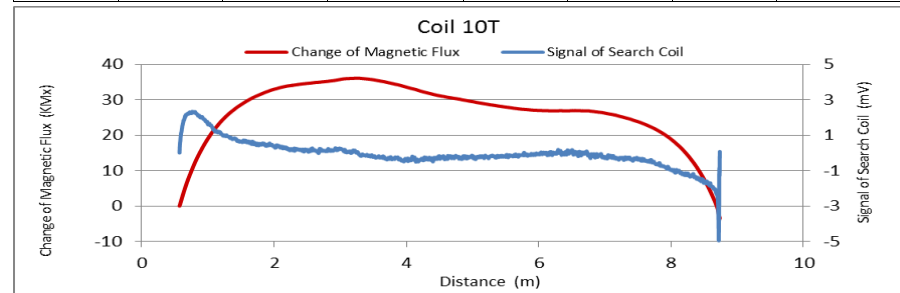


Figure A100. MMFM data of P5-401R-H1 tendon section.



Tokyo Rope USA, Inc.

File Name 【Pier-Tendon-Section】	Section Total Length (m)	Scanned Length		Note			
		Starting Point (m)	Ending Point (m)				
P5-402R-H1	9.35	0.59	8.49				
Identified Damage 1				Identified Damage 2			
Max Loss Point (m)	Section Loss (%)	Damage Length (m)	Damage Orientation	Max Loss Point (m)	Section Loss (%)	Damage Length (m)	Damage Orientation
—	—	—	—	—	—	—	—

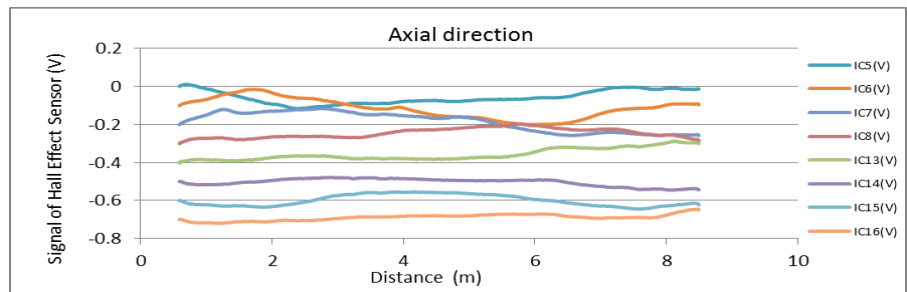
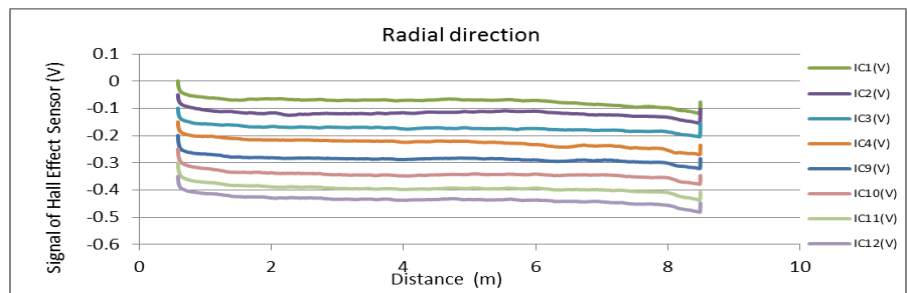
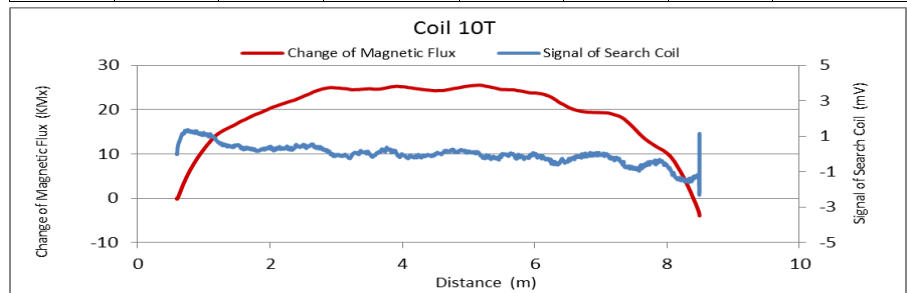


Figure A101. MMFM data of P5-402R-H1 tendon section.

File Name 【Pier-Tendon-Section】	Section Total Length (m)	Scanned Length		Note			
		Starting Point (m)	Ending Point (m)				
P5-303R-I1	9.6	0.59	9.19				
Identified Damage 1				Identified Damage 2			
Max Loss Point (m)	Section Loss (%)	Damage Length (m)	Damage Orientation	Max Loss Point (m)	Section Loss (%)	Damage Length (m)	Damage Orientation
—	—	—	—	—	—	—	—

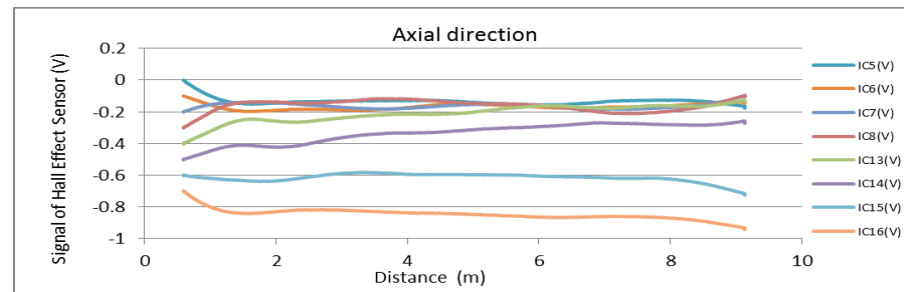
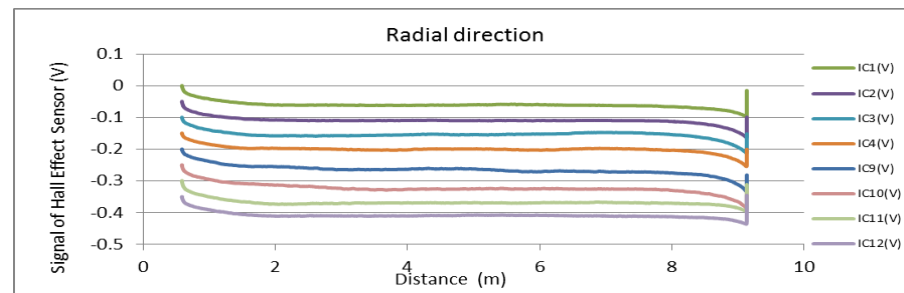
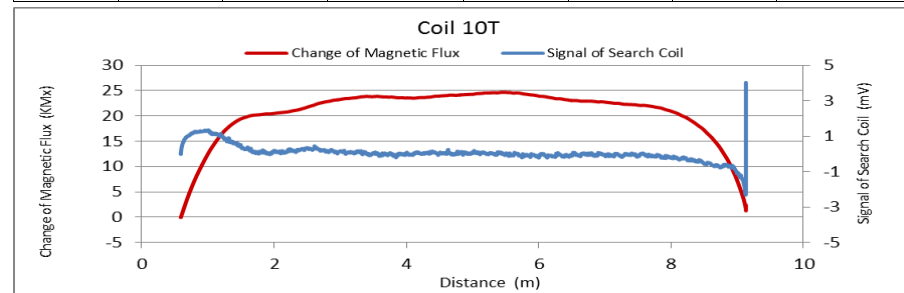


Figure A102. MMFM data of P5-303R-I1 tendon section.



Tokyo Rope USA, Inc.

File Name 【Pier-Tendon-Section】	Section Total Length (m)	Scanned Length		Note			
		Starting Point (m)	Ending Point (m)				
P5-401L-H1	9.28	0.65	8.45				
Identified Damage 1				Identified Damage 2			
Max Loss Point (m)	Section Loss (%)	Damage Length (m)	Damage Orientation	Max Loss Point (m)	Section Loss (%)	Damage Length (m)	Damage Orientation
—	—	—	—	—	—	—	—

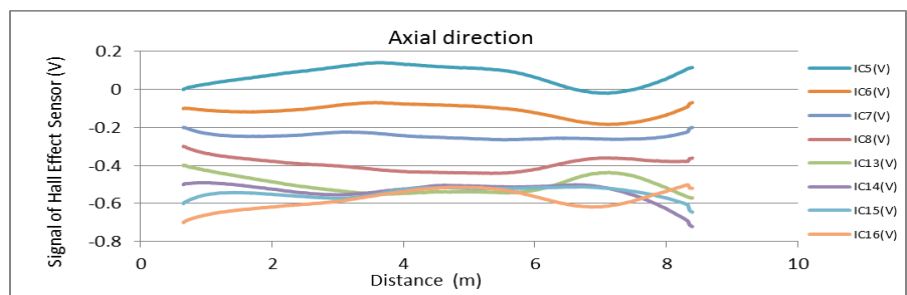
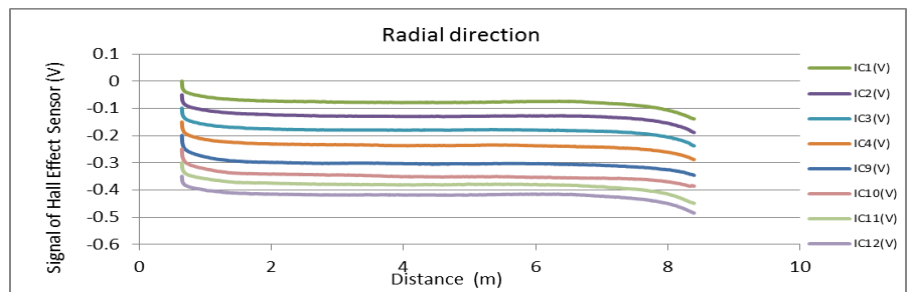
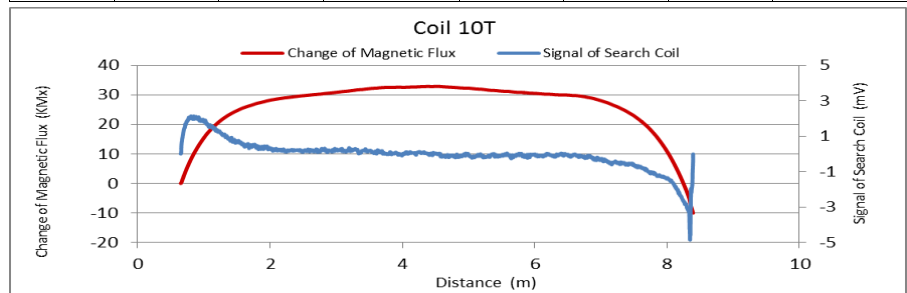


Figure A103. MMFM data of P5-401L-H1 tendon section.

File Name 【Pier-Tendon-Section】	Section Total Length (m)	Scanned Length		Note			
		Starting Point (m)	Ending Point (m)				
P5-303L-I1	9.39	0.52	9.01				
Identified Damage 1				Identified Damage 2			
Max Loss Point (m)	Section Loss (%)	Damage Length (m)	Damage Orientation	Max Loss Point (m)	Section Loss (%)	Damage Length (m)	Damage Orientation
—	—	—	—	—	—	—	—

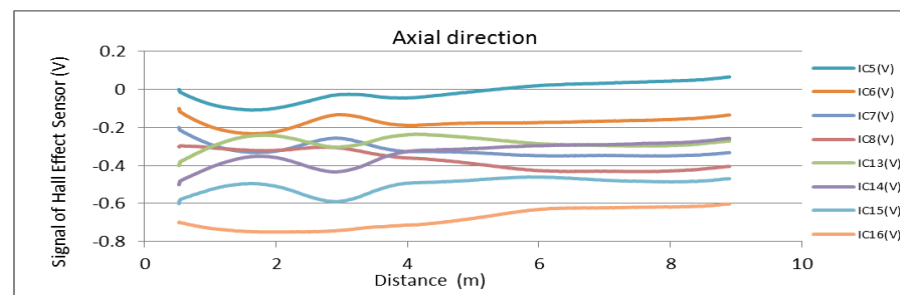
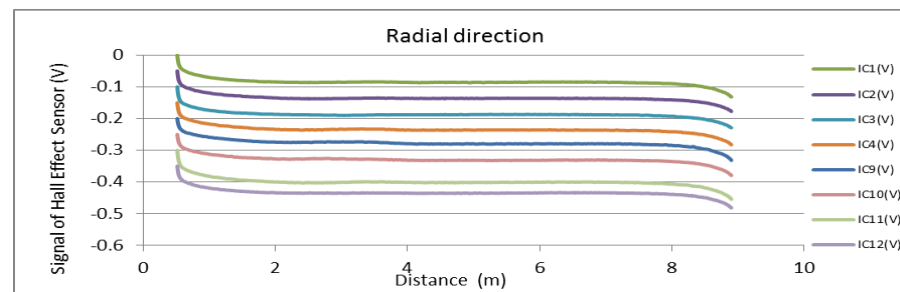
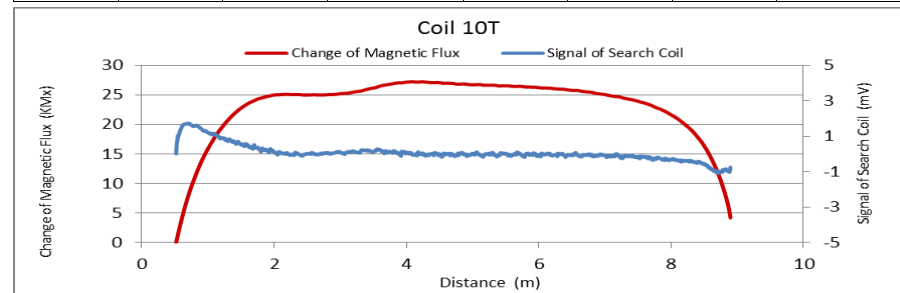


Figure A104. MMFM data of P5-303L-I1 tendon section.



Tokyo Rope USA, Inc.

File Name 【Pier-Tendon-Section】	Section Total Length (m)	Scanned Length		Note			
		Starting Point (m)	Ending Point (m)				
P5-303R-I2-1	21.62	0.38	14.3	Joint position : 8 m Has a large repair at 14.6 m position. Measured in two separate times			
Identified Damage 1				Identified Damage 2			
Max Loss Point (m)	Section Loss (%)	Damage Length (m)	Damage Orientation	Max Loss Point (m)	Section Loss (%)	Damage Length (m)	Damage Orientation
—	—	—	—	—	—	—	—

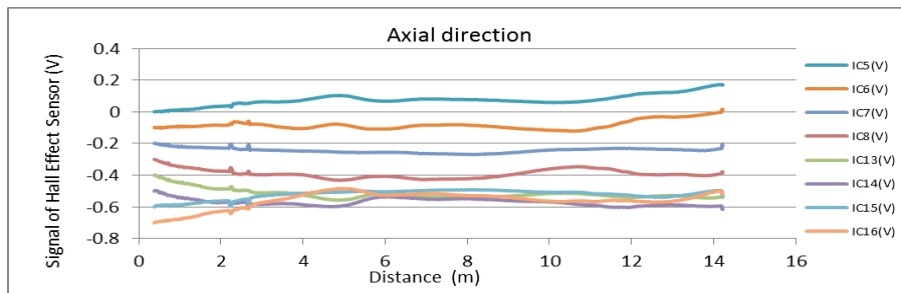
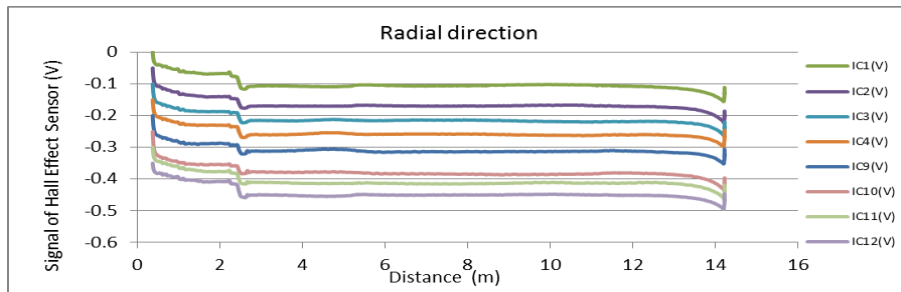
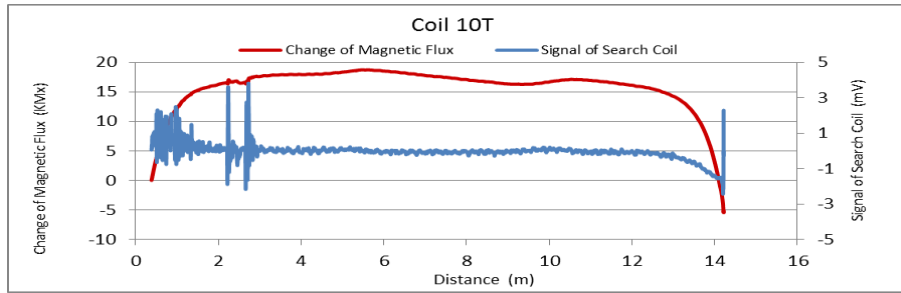


Figure A105. MMFM data of P5-303R-I2-1 tendon section.

File Name 【Pier-Tendon-Section】	Section Total Length (m)	Scanned Length		Note			
		Starting Point (m)	Ending Point (m)				
P5-303R-I2-2	21.62	14.93	21.31	Joint or repair position : 14.87 m, 15.26 m, 18.31 m Has a large repair 14.6 m position. Measured in two separate times			
Identified Damage 1				Identified Damage 2			
Max Loss Point (m)	Section Loss (%)	Damage Length (m)	Damage Orientation	Max Loss Point (m)	Section Loss (%)	Damage Length (m)	Damage Orientation
—	—	—	—	—	—	—	—

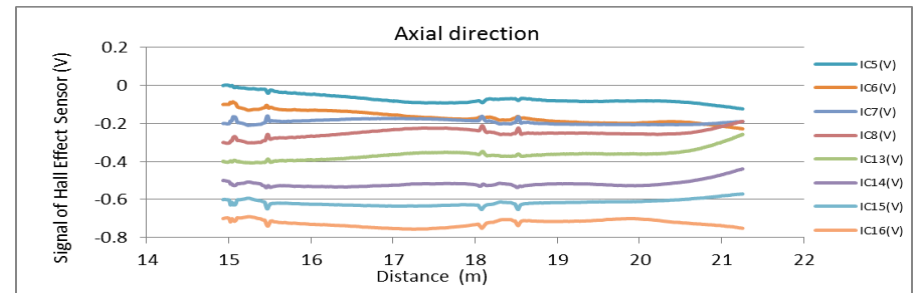
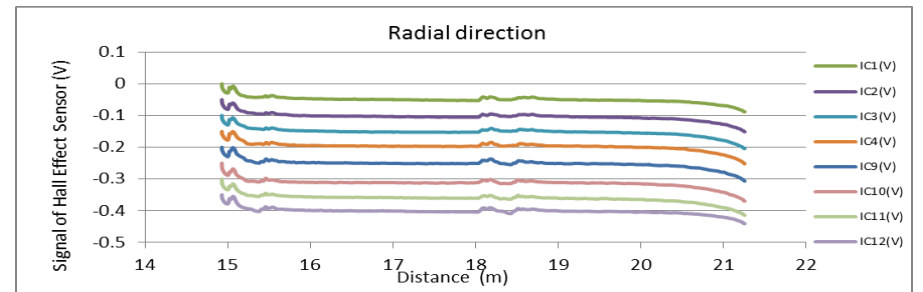
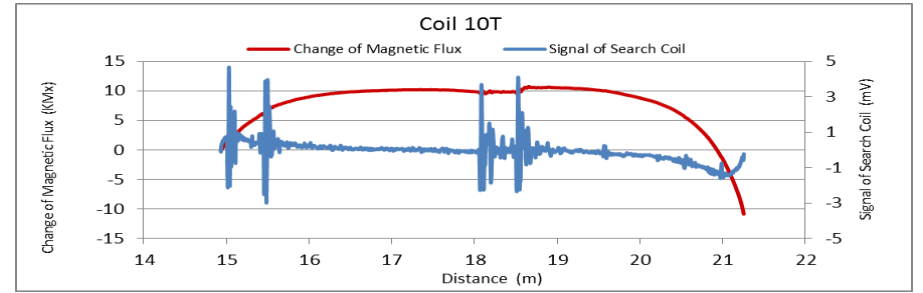


Figure A106. MMFM data of P5-303R-I2-2 tendon section.



Tokyo Rope USA, Inc.

File Name 【Pier-Tendon-Section】	Section Total Length (m)	Scanned Length		Note			
		Starting Point (m)	Ending Point (m)				
P5-303L-I2	21.65	0.22	21.28	Joint and repair position : 2.55 m, 14.68 m, 17.82 m			
Identified Damage 1				Identified Damage 2			
Max Loss Point (m)	Section Loss (%)	Damage Length (m)	Damage Orientation	Max Loss Point (m)	Section Loss (%)	Damage Length (m)	Damage Orientation
—	—	—	—	—	—	—	—

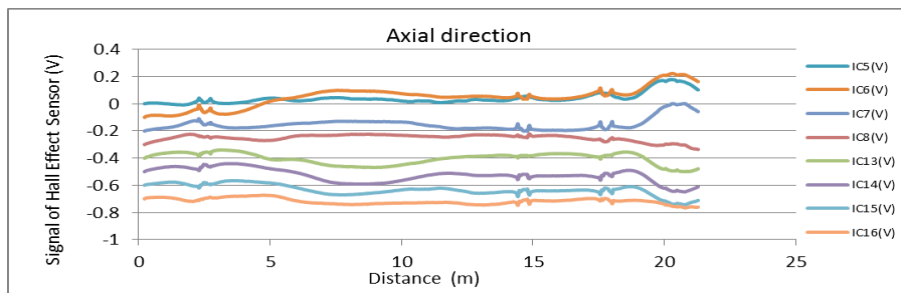
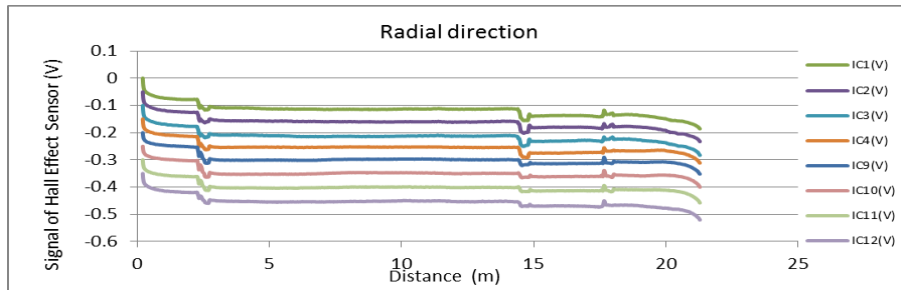
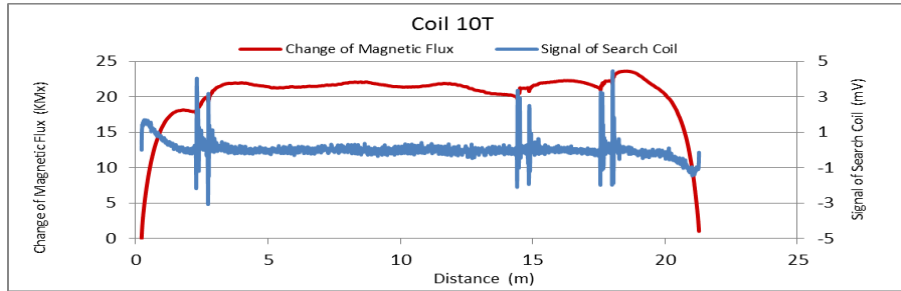


Figure A107. MMFM data of P5-303L-I2 tendon section.

File Name 【Pier-Tendon-Section】	Section Total Length (m)	Scanned Length		Note			
		Starting Point (m)	Ending Point (m)				
P5-401R-I2	21.47	0.84	20.87	Joint or Repair position : 9.2m			
Identified Damage 1				Identified Damage 2			
Max Loss Point (m)	Section Loss (%)	Damage Length (m)	Damage Orientation	Max Loss Point (m)	Section Loss (%)	Damage Length (m)	Damage Orientation
—	—	—	—	—	—	—	—

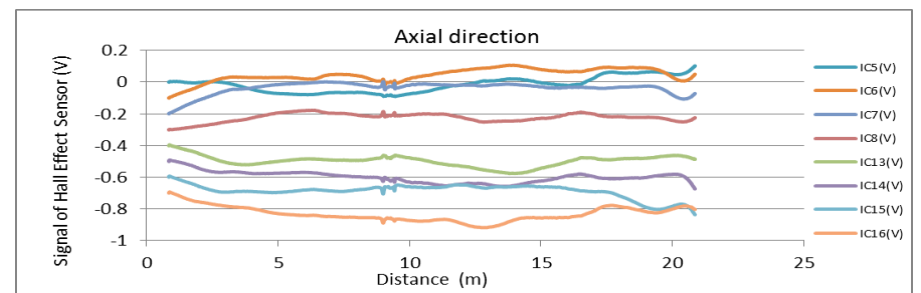
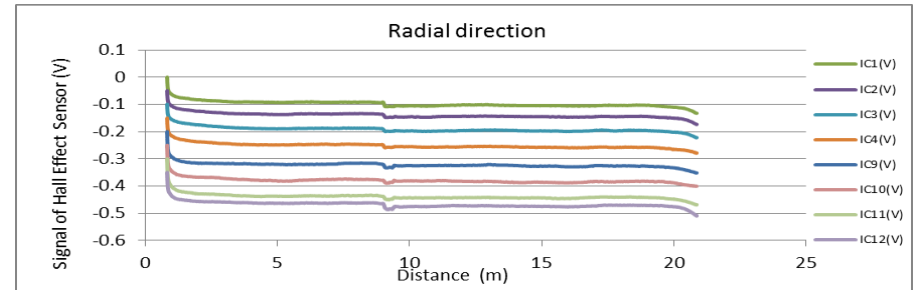
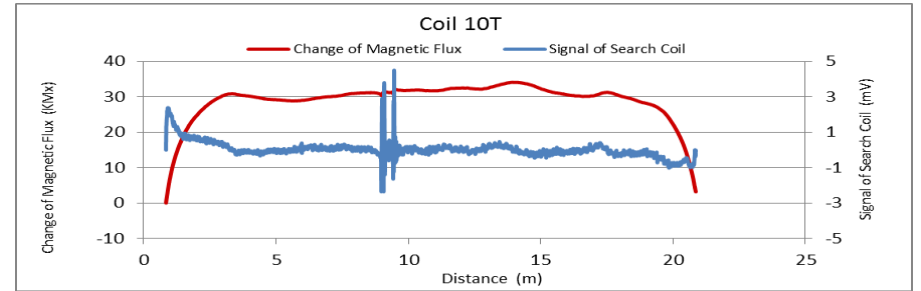


Figure A108. MMFM data of P5-401R-I2 tendon section.



Tokyo Rope USA, Inc.

File Name 【Pier-Tendon-Section】	Section Total Length (m)	Scanned Length		Note			
		Starting Point (m)	Ending Point (m)				
P5-402R-I2	21.47	0.77	20.79	Joint or repair position: 9.15 m			
Identified Damage 1				Identified Damage 2			
Max Loss Point (m)	Section Loss (%)	Damage Length (m)	Damage Orientation	Max Loss Point (m)	Section Loss (%)	Damage Length (m)	Damage Orientation
—	—	—	—	—	—	—	—

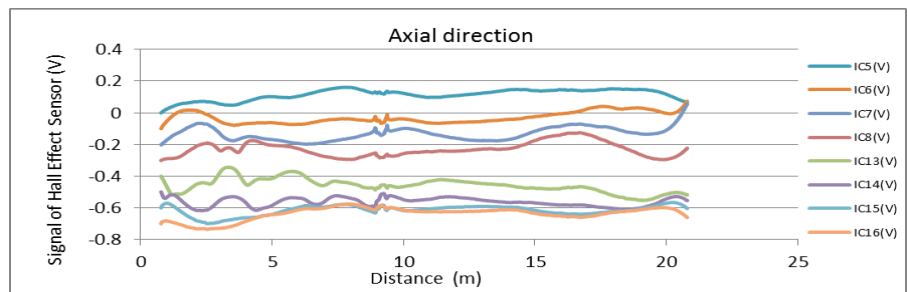
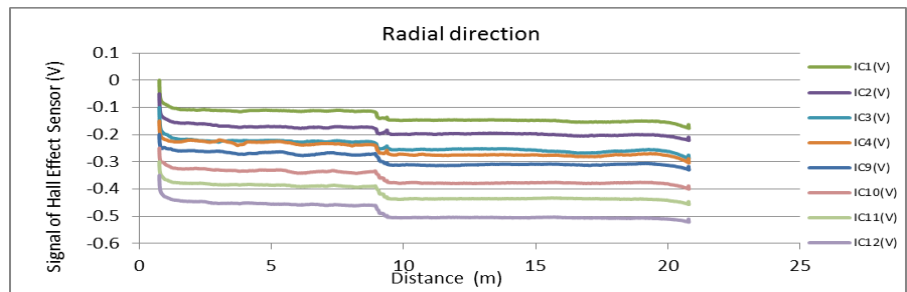
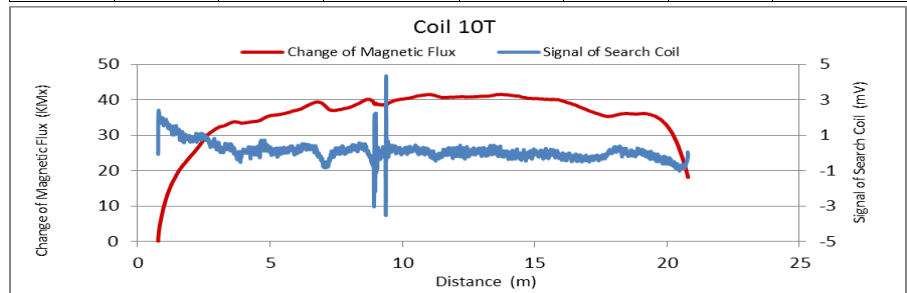


Figure A109. MMFM data of P5-402R-I2 tendon section.

File Name 【Pier-Tendon-Section】	Section Total Length (m)	Scanned Length		Note			
		Starting Point (m)	Ending Point (m)				
P5-303R-I3	21.6	0.33	21.27	Joint or repair position: 7.04 m, 19.18 m			
Identified Damage 1				Identified Damage 2			
Max Loss Point (m)	Section Loss (%)	Damage Length (m)	Damage Orientation	Max Loss Point (m)	Section Loss (%)	Damage Length (m)	Damage Orientation
—	—	—	—	—	—	—	—

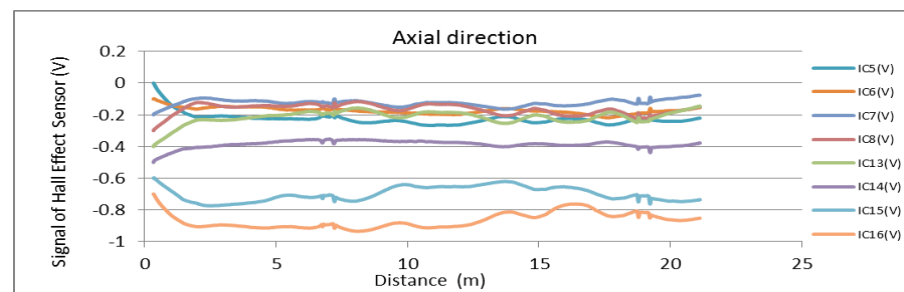
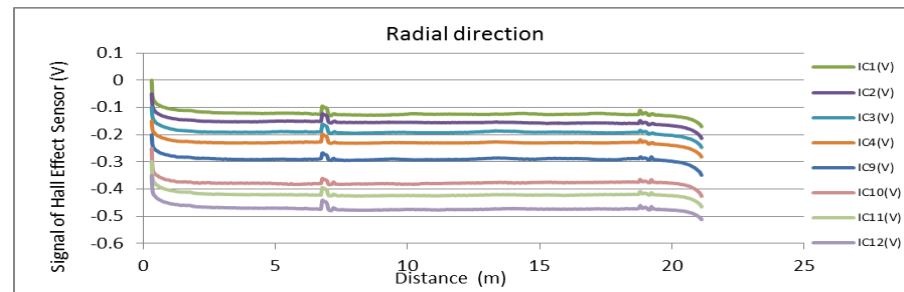
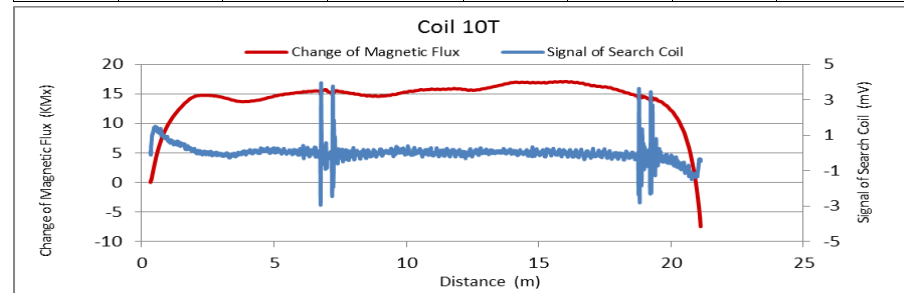


Figure A110. MMFM data of P5-303R-I3 tendon section.



Tokyo Rope USA, Inc.

File Name 【Pier-Tendon-Section】	Section Total Length (m)	Scanned Length		Note			
		Starting Point (m)	Ending Point (m)				
P5-401L-I2	21.43	0.65	20.84	Joint or repair position: 9.18 m			
Identified Damage 1				Identified Damage 2			
Max Loss Point (m)	Section Loss (%)	Damage Length (m)	Damage Orientation	Max Loss Point (m)	Section Loss (%)	Damage Length (m)	Damage Orientation
—	—	—	—	—	—	—	—

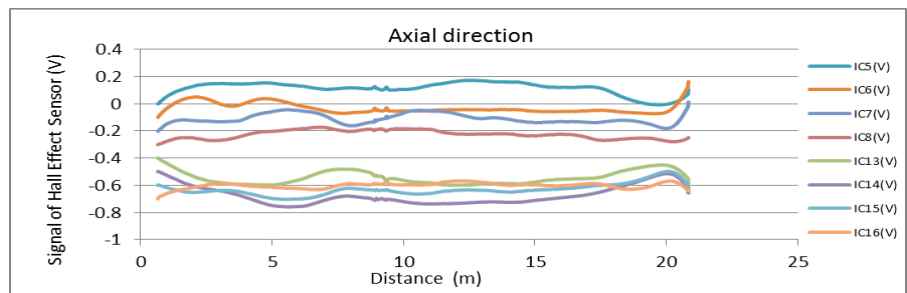
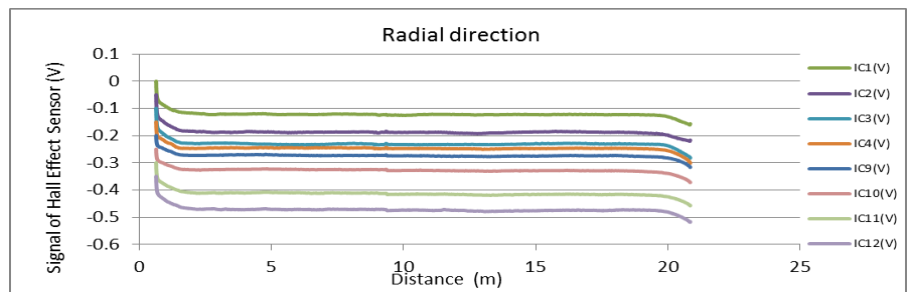
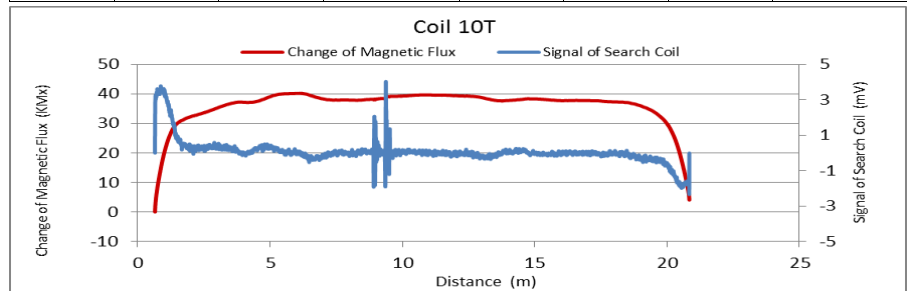


Figure A111. MMFM data of P5-401L-I2 tendon section.

File Name 【Pier-Tendon-Section】	Section Total Length (m)	Scanned Length		Note			
		Starting Point (m)	Ending Point (m)				
P5-402L-I2	21.43	0.85	20.85	Joint or repair position: 9.21 m			
Identified Damage 1				Identified Damage 2			
Max Loss Point (m)	Section Loss (%)	Damage Length (m)	Damage Orientation	Max Loss Point (m)	Section Loss (%)	Damage Length (m)	Damage Orientation
—	—	—	—	—	—	—	—

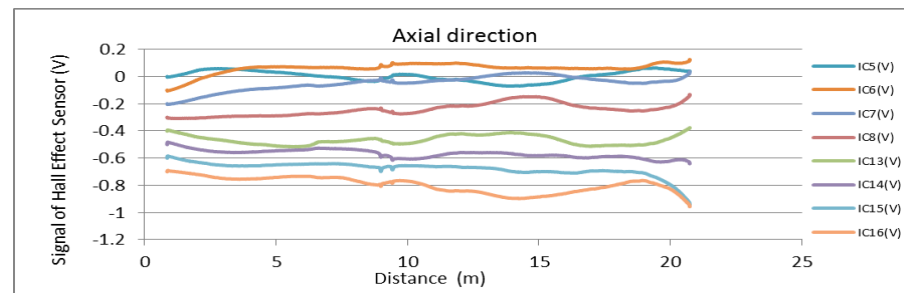
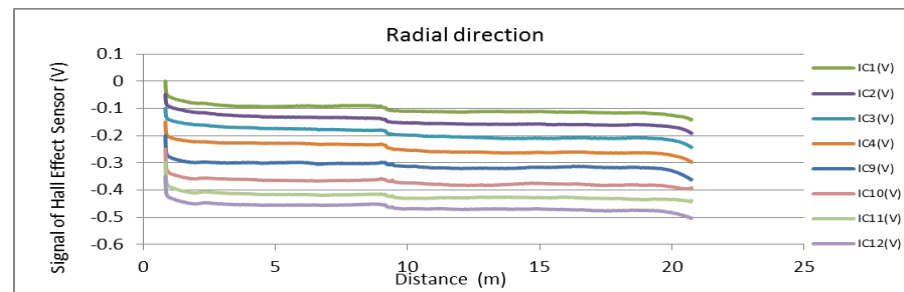
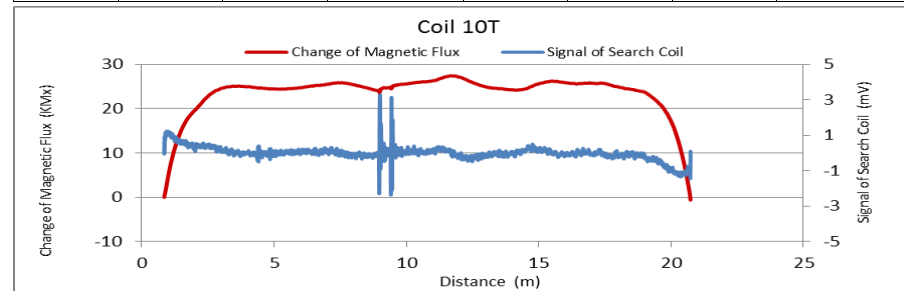


Figure A112. MMFM data of P5-402L-I2 tendon section.



Tokyo Rope USA, Inc.

File Name 【Pier-Tendon-Section】	Section Total Length (m)	Scanned Length		Note			
		Starting Point (m)	Ending Point (m)				
P5-303L-I3	21.6	0.26	21.26	Joint or repair position: 7.05 m, 19.18 m			
Identified Damage 1				Identified Damage 2			
Max Loss Point (m)	Section Loss (%)	Damage Length (m)	Damage Orientation	Max Loss Point (m)	Section Loss (%)	Damage Length (m)	Damage Orientation
—	—	—	—	—	—	—	—

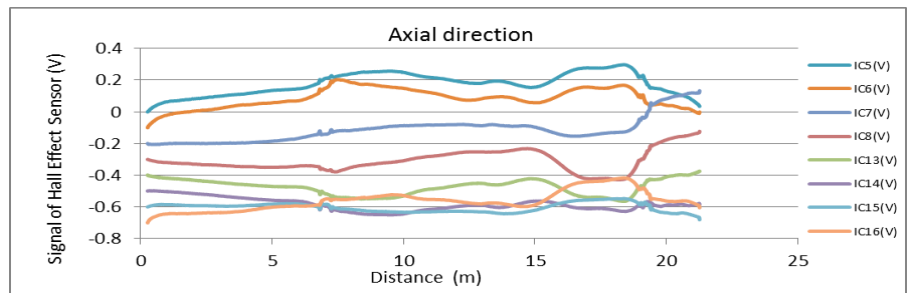
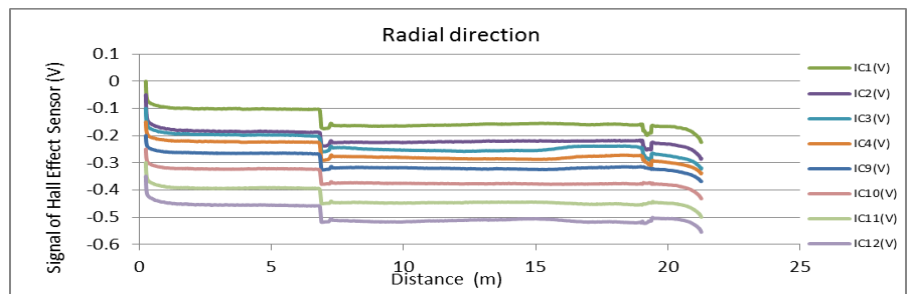
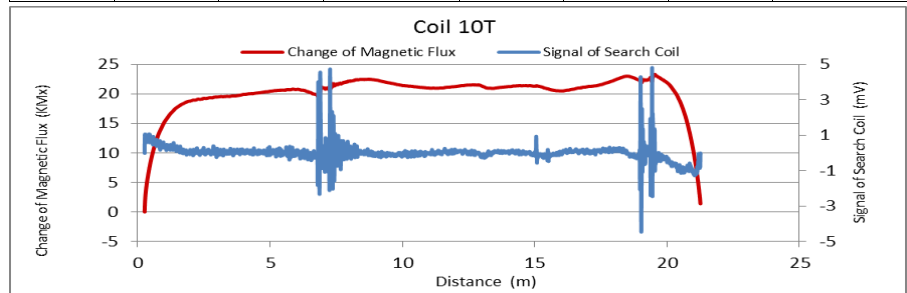


Figure A113. MMFM data of P5-303L-I3 tendon section.

File Name 【Pier-Tendon-Section】	Section Total Length (m)	Scanned Length		Note			
		Starting Point (m)	Ending Point (m)				
P5-401R-H2	9.37	0.74	8.86				
Identified Damage 1				Identified Damage 2			
Max Loss Point (m)	Section Loss (%)	Damage Length (m)	Damage Orientation	Max Loss Point (m)	Section Loss (%)	Damage Length (m)	Damage Orientation
—	—	—	—	—	—	—	—

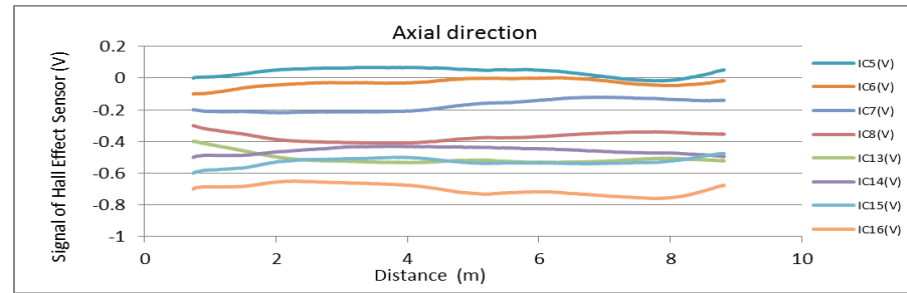
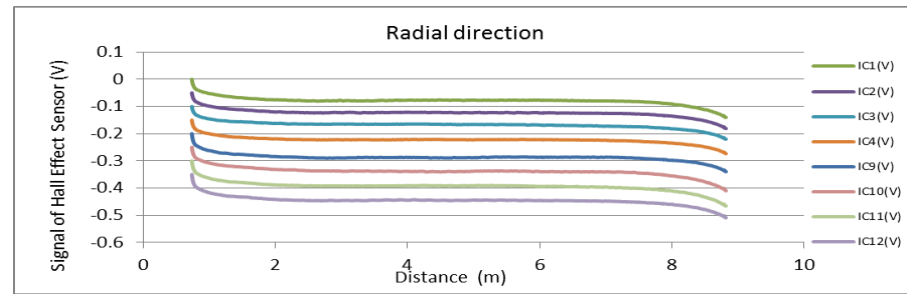
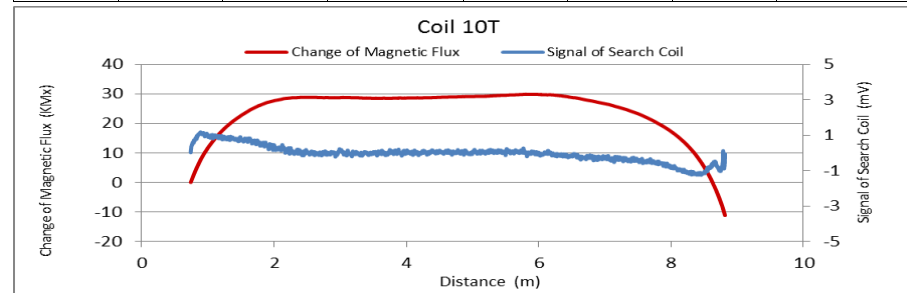
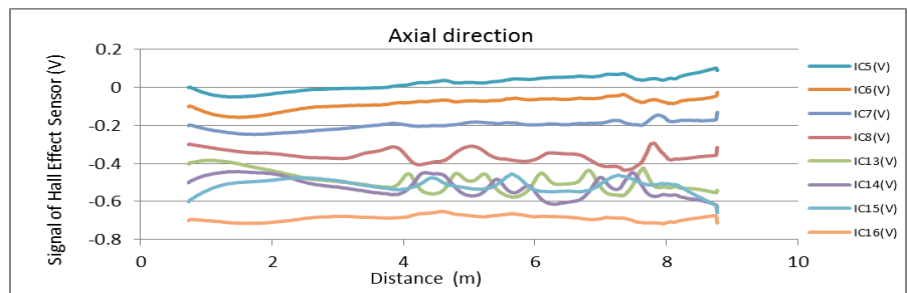
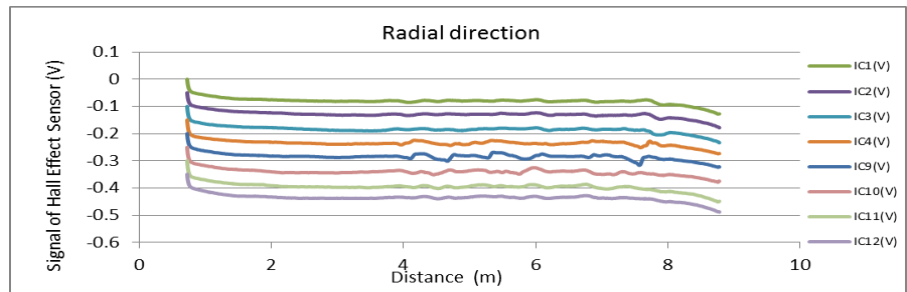
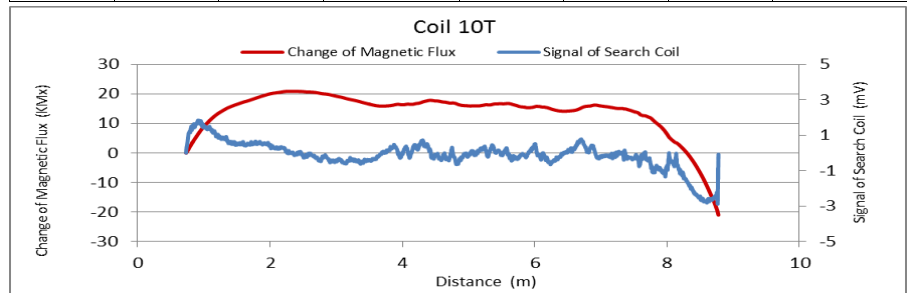


Figure A114. MMFM data of P5-401R-H2 tendon section.



Tokyo Rope USA, Inc.

File Name 【Pier-Tendon-Section】	Section Total Length (m)	Scanned Length		Note			
		Starting Point (m)	Ending Point (m)				
P5-402R-H2	9.37	0.73	8.81	There is a distortion at 8 m position.			
Identified Damage 1							
Max Loss Point (m)	Section Loss (%)	Damage Length (m)	Damage Orientation	Max Loss Point (m)	Section Loss (%)	Damage Length (m)	Damage Orientation
—	—	—	—	—	—	—	—



File Name 【Pier-Tendon-Section】	Section Total Length (m)	Scanned Length		Note			
		Starting Point (m)	Ending Point (m)				
P5-303R-I4	9.47	0.26	8.95				
Identified Damage 1							
Max Loss Point (m)	Section Loss (%)	Damage Length (m)	Damage Orientation	Max Loss Point (m)	Section Loss (%)	Damage Length (m)	Damage Orientation
—	—	—	—	—	—	—	—

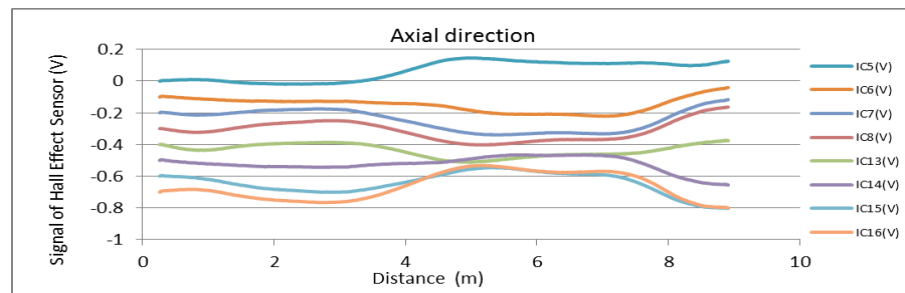
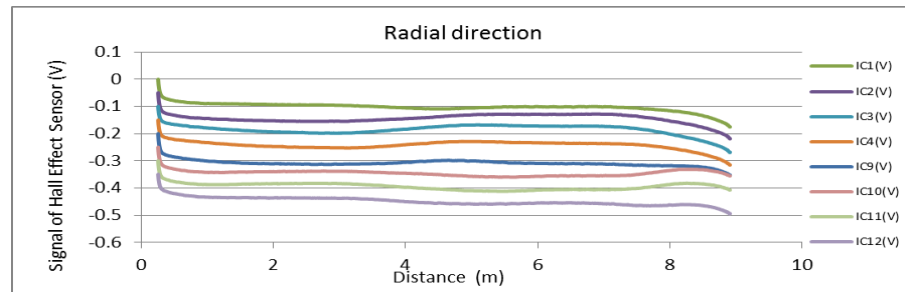
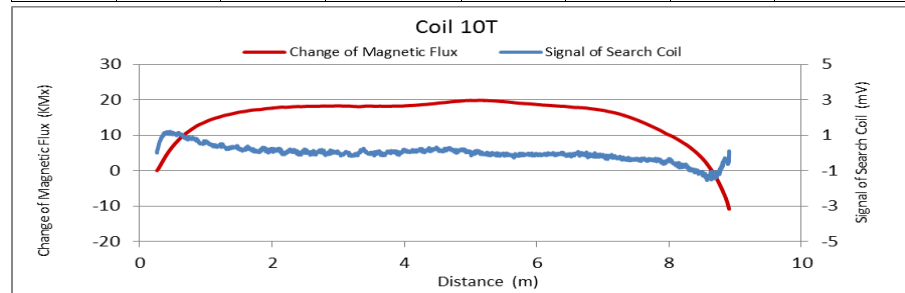


Figure A115. MMFM data of P5-402R-H2 tendon section.

Figure A116. MMFM data of P5-303R-I4 tendon section.



Tokyo Rope USA, Inc.

File Name 【Pier-Tendon-Section】	Section Total Length (m)	Scanned Length		Note			
		Starting Point (m)	Ending Point (m)				
P5-401L-H2	9.37	0.75	8.68				
Identified Damage 1				Identified Damage 2			
Max Loss Point (m)	Section Loss (%)	Damage Length (m)	Damage Orientation	Max Loss Point (m)	Section Loss (%)	Damage Length (m)	Damage Orientation
—	—	—	—	—	—	—	—

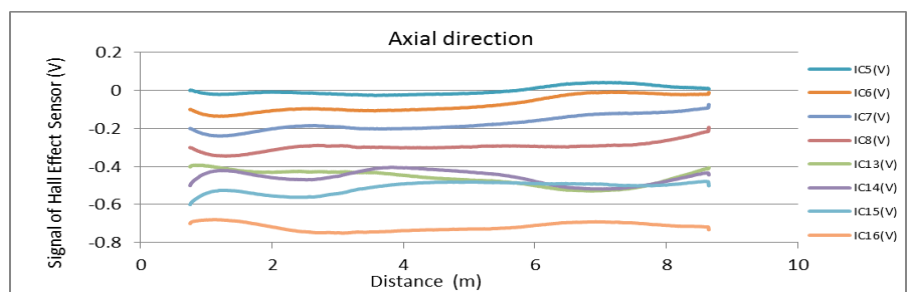
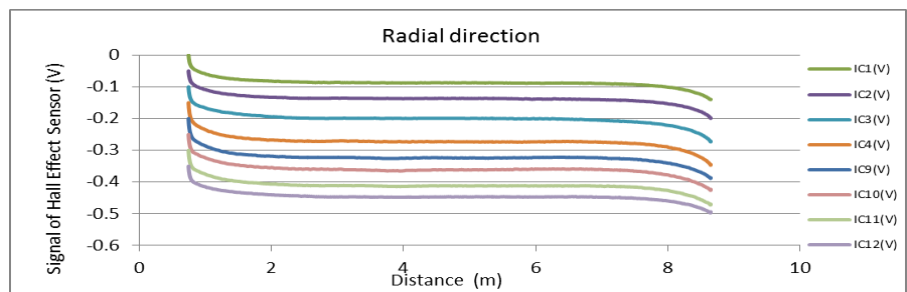
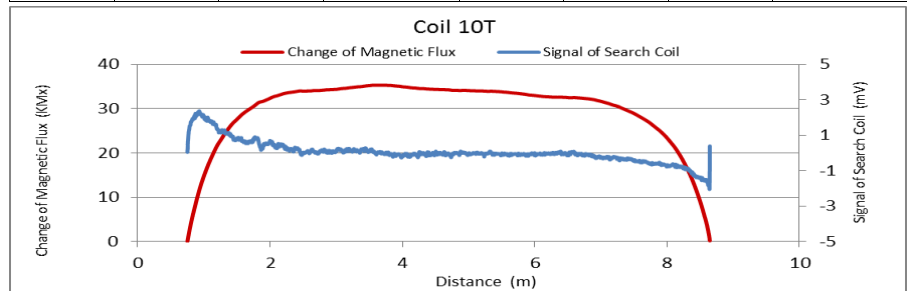


Figure A117. MMFM data of P5-401L-H2 tendon section.

File Name 【Pier-Tendon-Section】	Section Total Length (m)	Scanned Length		Note			
		Starting Point (m)	Ending Point (m)				
P5-402L-H2	9.37	0.75	8.7				
Identified Damage 1				Identified Damage 2			
Max Loss Point (m)	Section Loss (%)	Damage Length (m)	Damage Orientation	Max Loss Point (m)	Section Loss (%)	Damage Length (m)	Damage Orientation
—	—	—	—	—	—	—	—

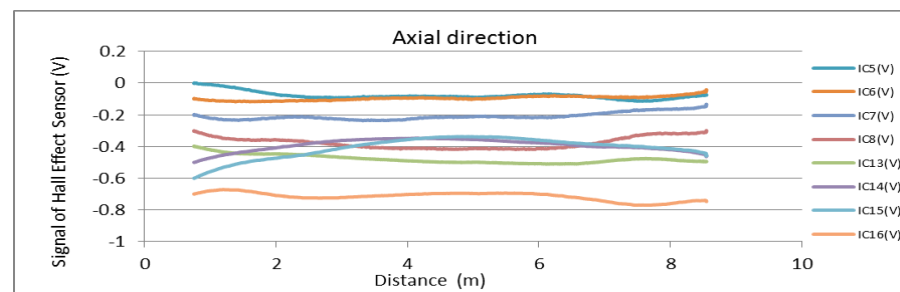
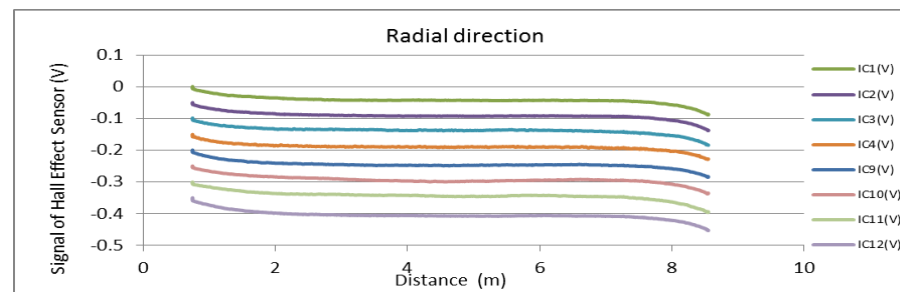
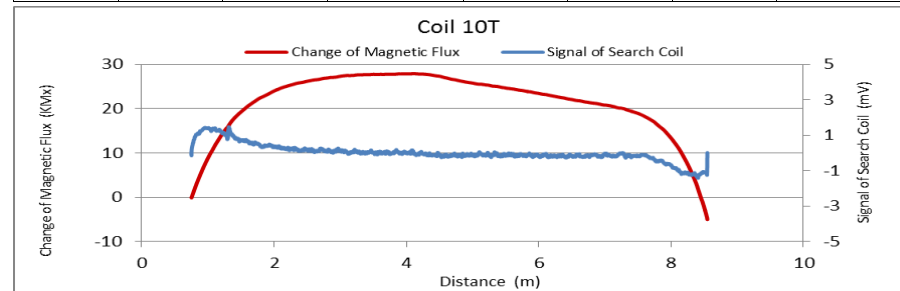


Figure A118. MMFM data of P5-402L-H2 tendon section.



Tokyo Rope USA, Inc.

File Name 【Pier-Tendon-Section】	Section Total Length (m)	Scanned Length		Note			
		Starting Point (m)	Ending Point (m)				
P6-401R-H1	9.43	0.66	8.67				
Identified Damage 1				Identified Damage 2			
Max Loss Point (m)	Section Loss (%)	Damage Length (m)	Damage Orientation	Max Loss Point (m)	Section Loss (%)	Damage Length (m)	Damage Orientation
—	—	—	—	—	—	—	—

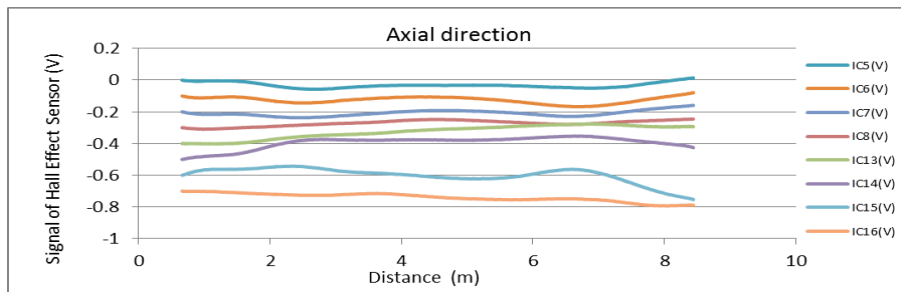
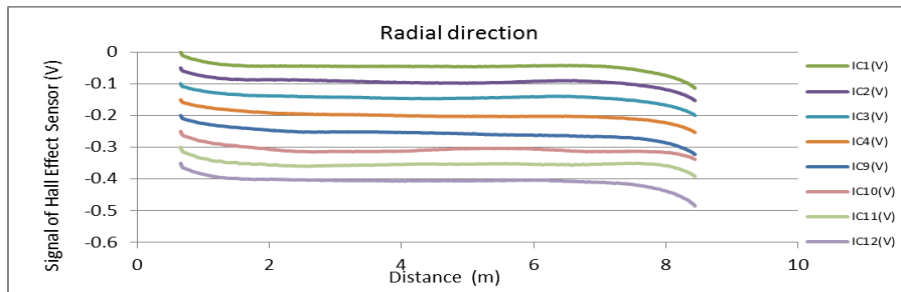
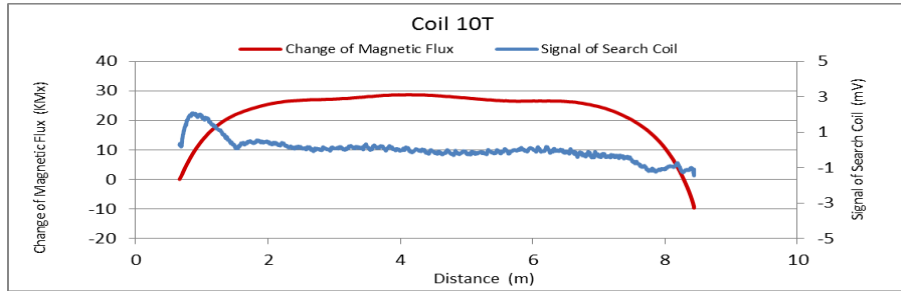


Figure A119. MMFM data of P6-401R-H1 tendon section.

File Name 【Pier-Tendon-Section】	Section Total Length (m)	Scanned Length		Note			
		Starting Point (m)	Ending Point (m)				
P6-402R-H1	9.43	0.65	8.65				
Identified Damage 1				Identified Damage 2			
Max Loss Point (m)	Section Loss (%)	Damage Length (m)	Damage Orientation	Max Loss Point (m)	Section Loss (%)	Damage Length (m)	Damage Orientation
—	—	—	—	—	—	—	—

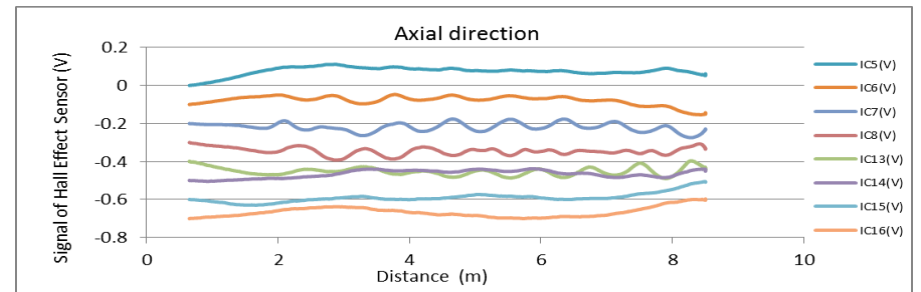
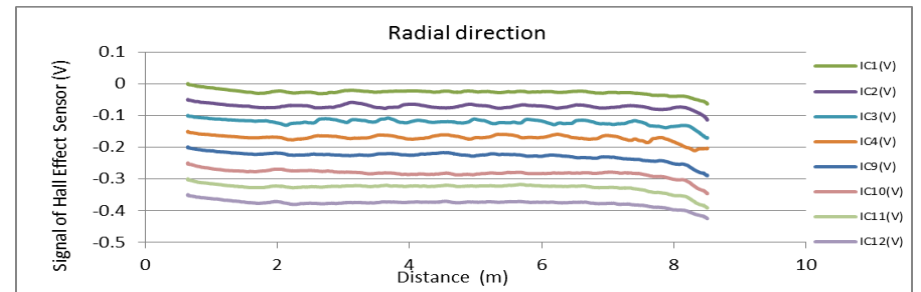
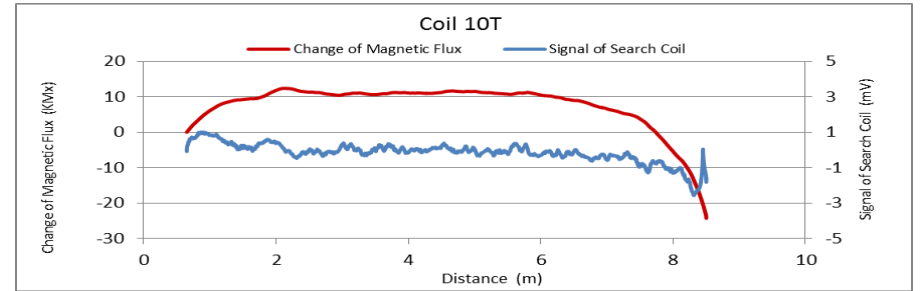


Figure A120. MMFM data of P6-402R-H1 tendon section.



Tokyo Rope USA, Inc.

File Name 【Pier-Tendon-Section】	Section Total Length (m)	Scanned Length		Note			
		Starting Point (m)	Ending Point (m)				
P6-401L-H1	9.41	0.52	8.62				
Identified Damage 1				Identified Damage 2			
Max Loss Point (m)	Section Loss (%)	Damage Length (m)	Damage Orientation	Max Loss Point (m)	Section Loss (%)	Damage Length (m)	Damage Orientation
—	—	—	—	—	—	—	—

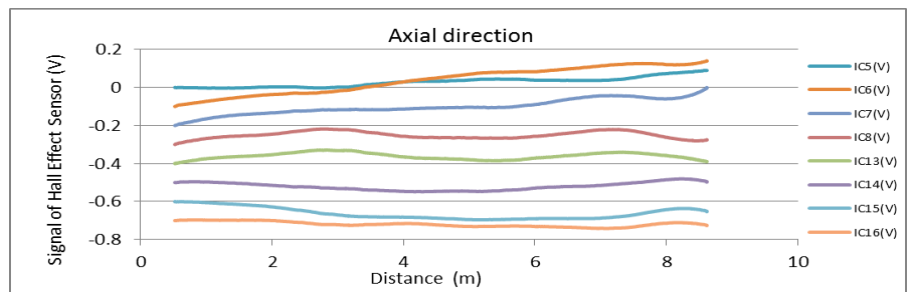
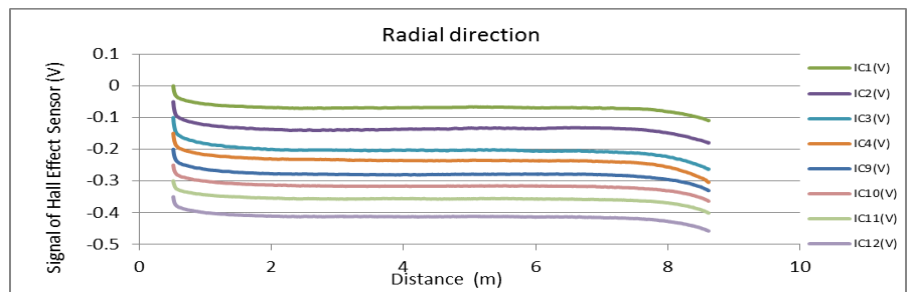
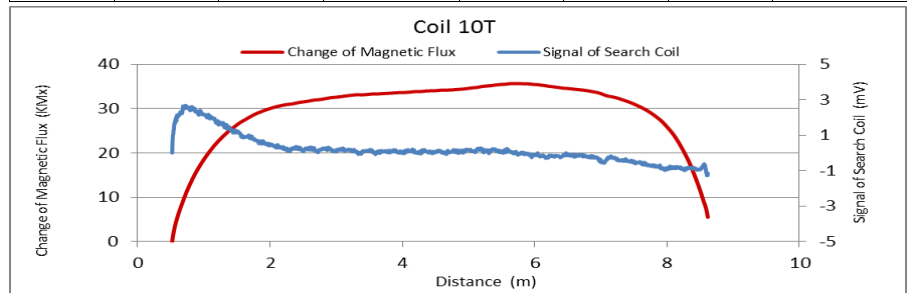


Figure A121. MMFM data of P6-401L-H1 tendon section.

File Name 【Pier-Tendon-Section】	Section Total Length (m)	Scanned Length		Note			
		Starting Point (m)	Ending Point (m)				
P6-402L-H1	9.41	0.57	8.69				
Identified Damage 1				Identified Damage 2			
Max Loss Point (m)	Section Loss (%)	Damage Length (m)	Damage Orientation	Max Loss Point (m)	Section Loss (%)	Damage Length (m)	Damage Orientation
—	—	—	—	—	—	—	—

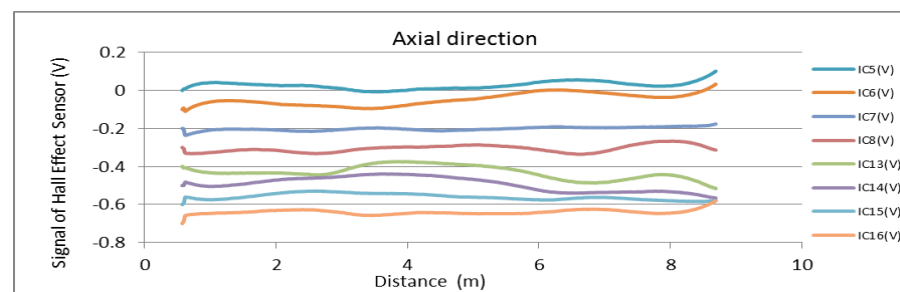
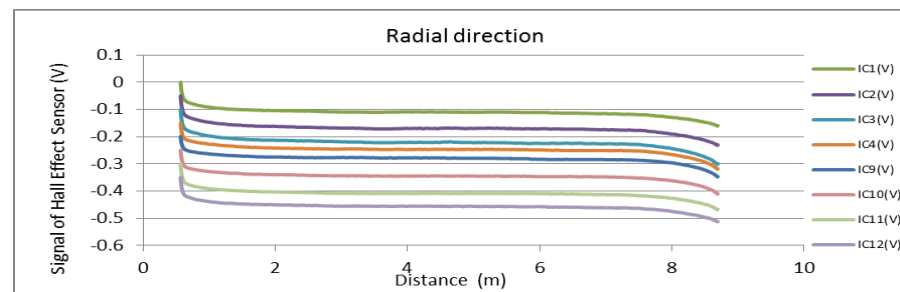
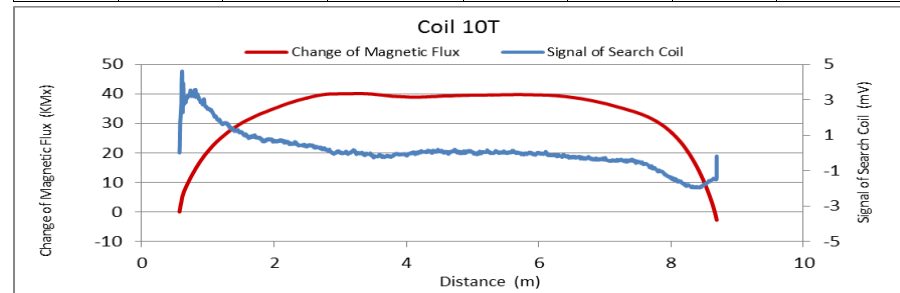


Figure A122. MMFM data of P6-402L-H1 tendon section.



Tokyo Rope USA, Inc.

File Name 【Pier-Tendon-Section】	Section Total Length (m)	Scanned Length		Note			
		Starting Point (m)	Ending Point (m)				
P6-401R-I1	21.5	0.71	20.42	Joint position: 12.4 m			
Identified Damage 1				Identified Damage 2			
Max Loss Point (m)	Section Loss (%)	Damage Length (m)	Damage Orientation	Max Loss Point (m)	Section Loss (%)	Damage Length (m)	Damage Orientation
—	—	—	—	—	—	—	—

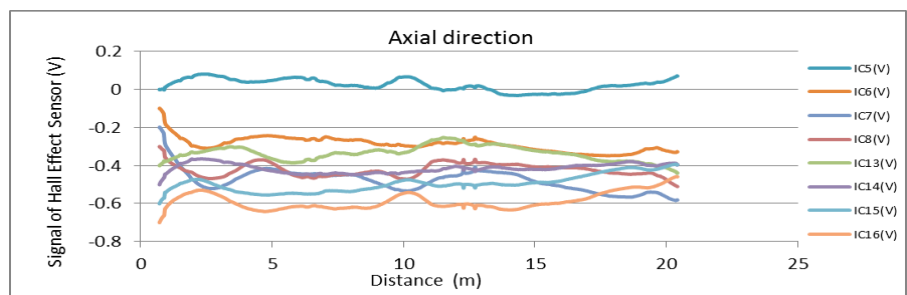
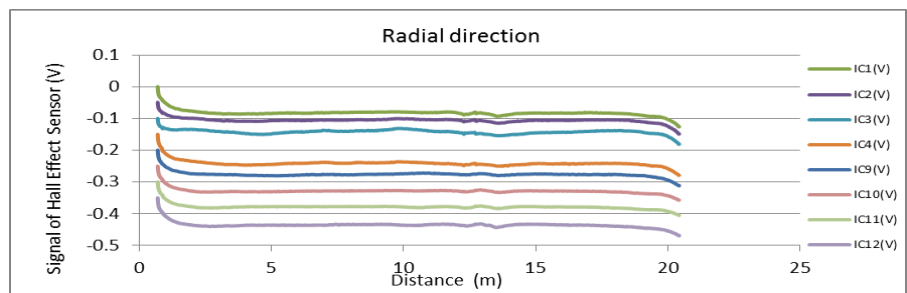
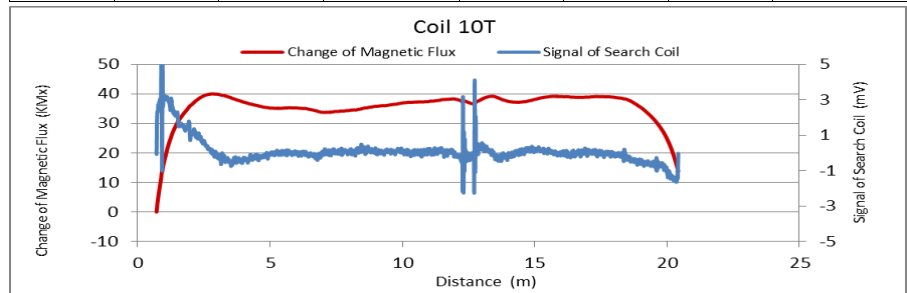


Figure A123. MMFM data of P6-401R-I1 tendon section.

File Name 【Pier-Tendon-Section】	Section Total Length (m)	Scanned Length		Note			
		Starting Point (m)	Ending Point (m)				
P6-402R-I1	21.5	0.75	20.52	Joint position: 12.35 m			
Identified Damage 1				Identified Damage 2			
Max Loss Point (m)	Section Loss (%)	Damage Length (m)	Damage Orientation	Max Loss Point (m)	Section Loss (%)	Damage Length (m)	Damage Orientation
—	—	—	—	—	—	—	—

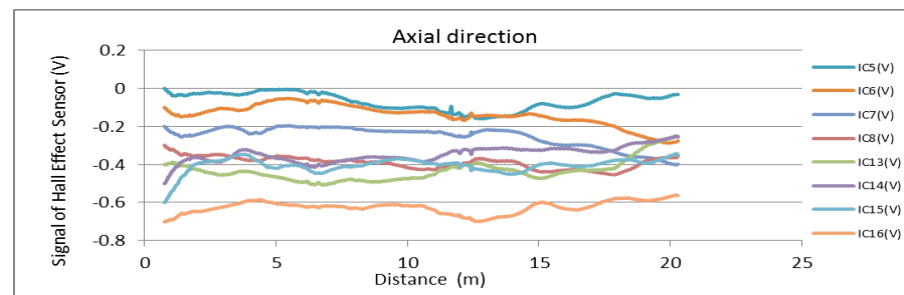
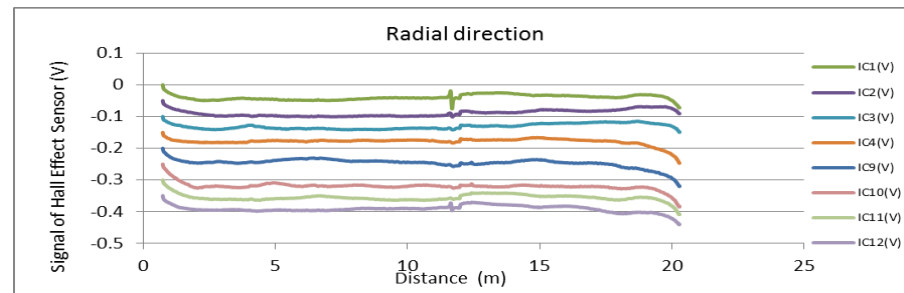
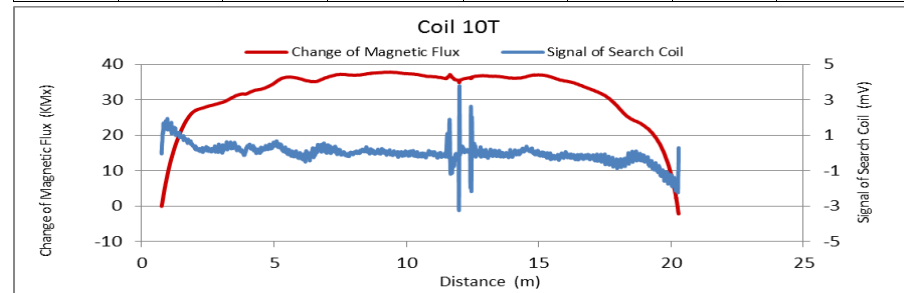


Figure A124. MMFM data of P6-402R-I1 tendon section.



Tokyo Rope USA, Inc.

File Name 【Pier-Tendon-Section】	Section Total Length (m)	Scanned Length		Note			
		Starting Point (m)	Ending Point (m)				
P6-401L-I1	21.44	0.56	20.67	Joint position: 12.23 m			
Identified Damage 1				Identified Damage 2			
Max Loss Point (m)	Section Loss (%)	Damage Length (m)	Damage Orientation	Max Loss Point (m)	Section Loss (%)	Damage Length (m)	Damage Orientation
—	—	—	—	—	—	—	—

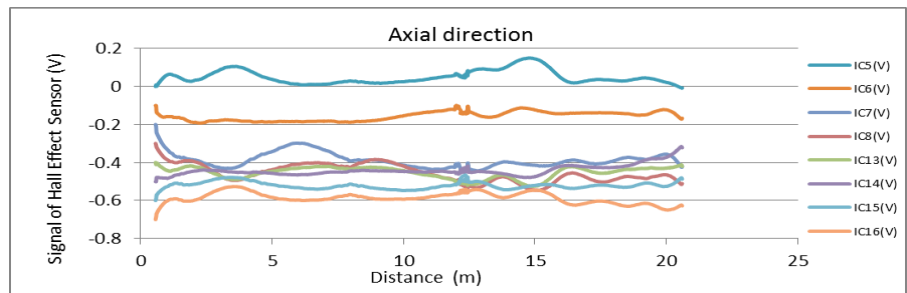
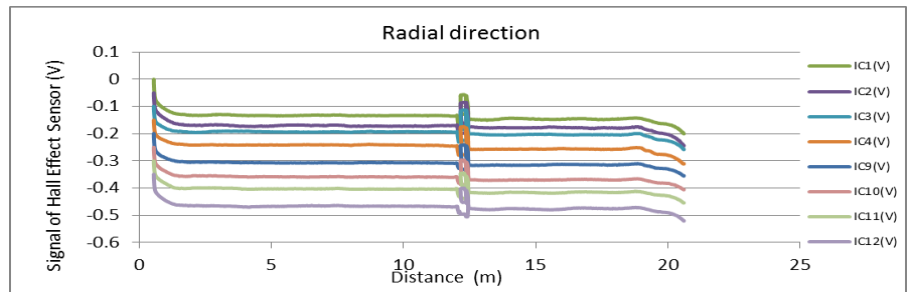
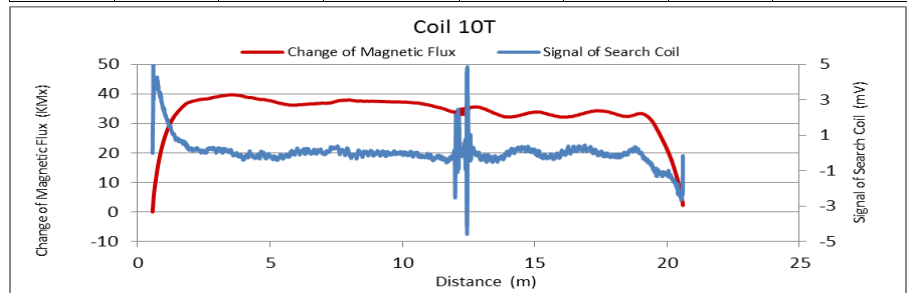


Figure A125. MMFM data of P6-401L-H1 tendon section.

File Name 【Pier-Tendon-Section】	Section Total Length (m)	Scanned Length		Note			
		Starting Point (m)	Ending Point (m)				
P6-402L-I1	21.44	0.61	20.6	Joint position: 12.32 m			
Identified Damage 1				Identified Damage 2			
Max Loss Point (m)	Section Loss (%)	Damage Length (m)	Damage Orientation	Max Loss Point (m)	Section Loss (%)	Damage Length (m)	Damage Orientation
—	—	—	—	—	—	—	—

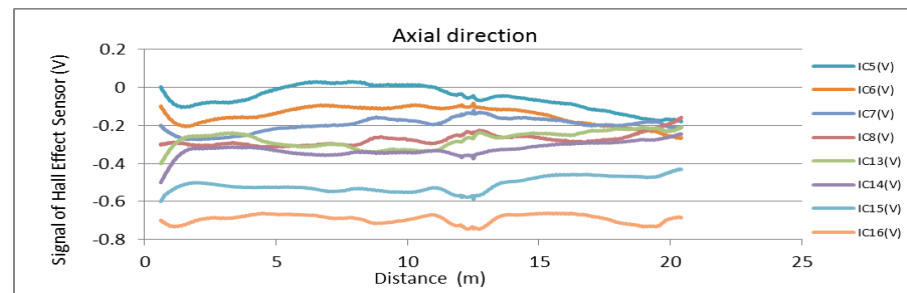
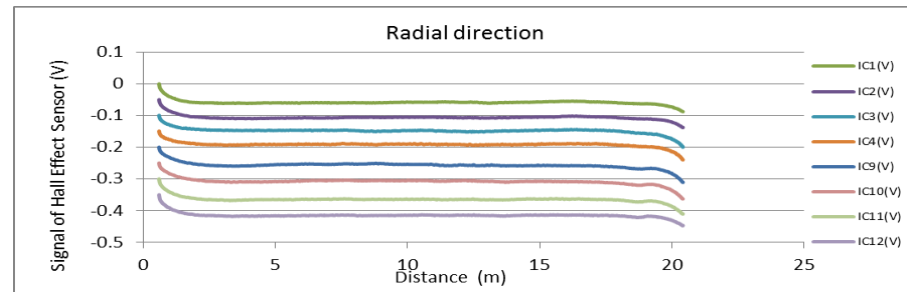
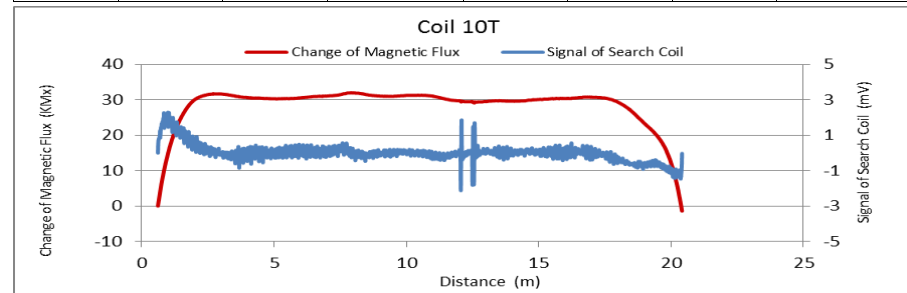


Figure A126. MMFM data of P6-402L-I1 tendon section.



Tokyo Rope USA, Inc.

File Name 【Pier-Tendon-Section】	Section Total Length (m)	Scanned Length		Note			
		Starting Point (m)	Ending Point (m)				
P6-401R-I2	31.31	2.17	30.66	Joint position: 9.67 m, 21.76 m			
Identified Damage 1				Identified Damage 2			
Max Loss Point (m)	Section Loss (%)	Damage Length (m)	Damage Orientation	Max Loss Point (m)	Section Loss (%)	Damage Length (m)	Damage Orientation
—	—	—	—	—	—	—	—

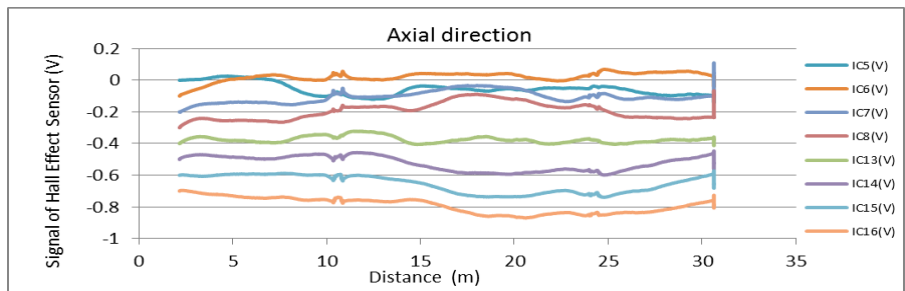
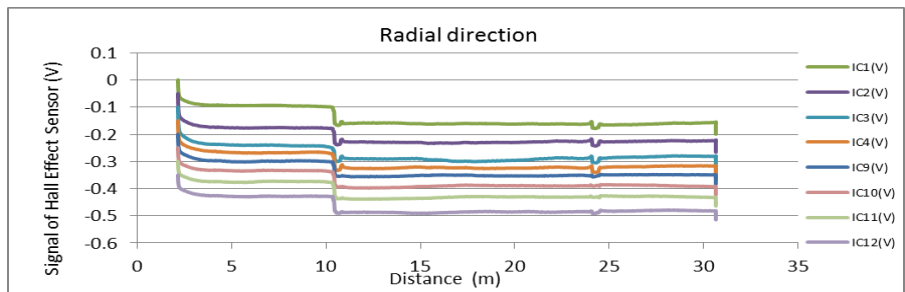
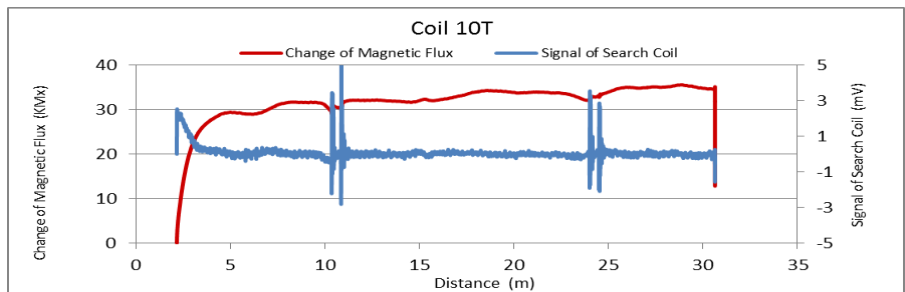


Figure A127. MMFM data of P6-401R-I2 tendon section.

File Name 【Pier-Tendon-Section】	Section Total Length (m)	Scanned Length		Note			
		Starting Point (m)	Ending Point (m)				
P6-402R-I2	21.46	0.68	20.6	Joint position: 9.18 m			
Identified Damage 1				Identified Damage 2			
Max Loss Point (m)	Section Loss (%)	Damage Length (m)	Damage Orientation	Max Loss Point (m)	Section Loss (%)	Damage Length (m)	Damage Orientation
—	—	—	—	—	—	—	—

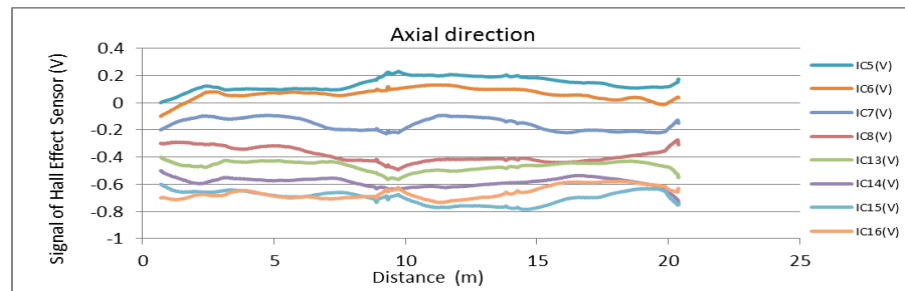
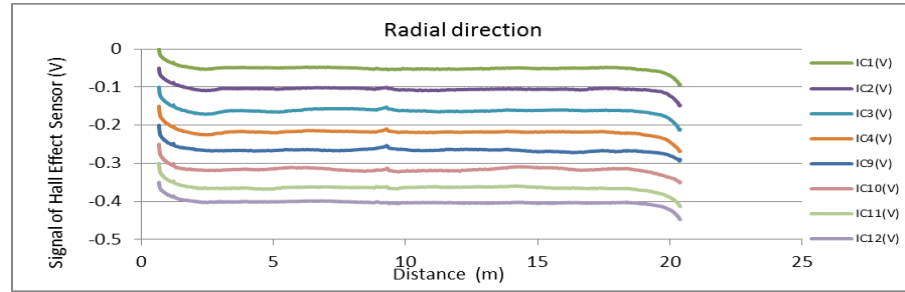
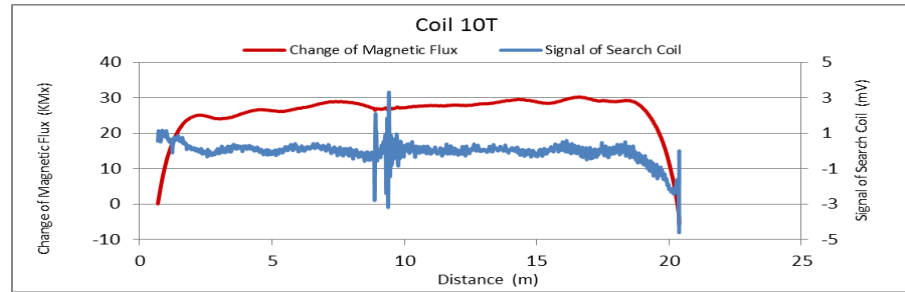


Figure A128. MMFM data of P6-402R-I2 tendon section.



Tokyo Rope USA, Inc.

File Name 【Pier-Tendon-Section】	Section Total Length (m)	Scanned Length		Note			
		Starting Point (m)	Ending Point (m)				
P6-401L-I2	31.3	1.97	30.68	Joint position: 9.51 m, 24.65 m			
Identified Damage 1				Identified Damage 2			
Max Loss Point (m)	Section Loss (%)	Damage Length (m)	Damage Orientation	Max Loss Point (m)	Section Loss (%)	Damage Length (m)	Damage Orientation
—	—	—	—	—	—	—	—

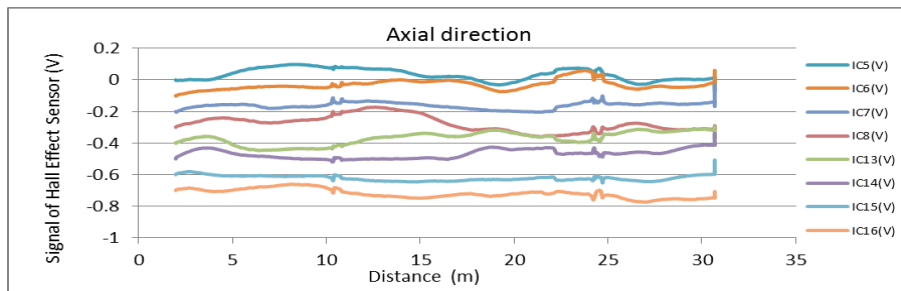
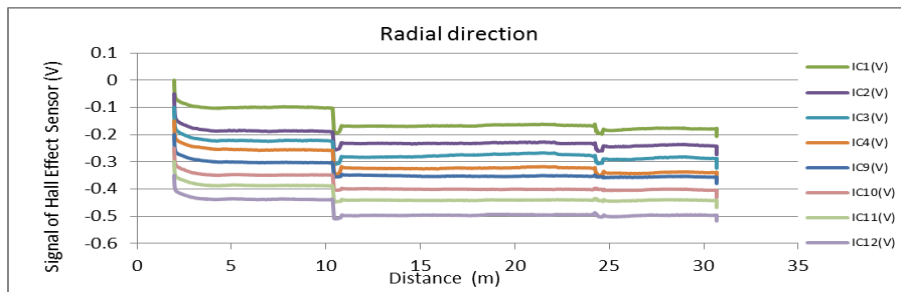
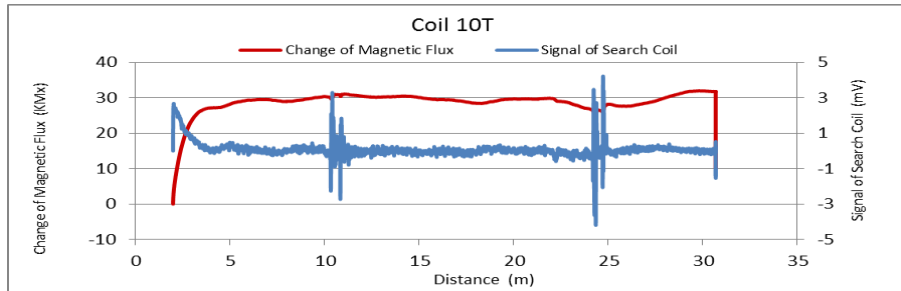


Figure A129. MMFM data of P6-401L-I2 tendon section.

File Name 【Pier-Tendon-Section】	Section Total Length (m)	Scanned Length		Note			
		Starting Point (m)	Ending Point (m)				
P6-402L-I2	31.3	2.07	30.82	Joint position: 9.58 m, 24.65 m			
Identified Damage 1				Identified Damage 2			
Max Loss Point (m)	Section Loss (%)	Damage Length (m)	Damage Orientation	Max Loss Point (m)	Section Loss (%)	Damage Length (m)	Damage Orientation
—	—	—	—	—	—	—	—

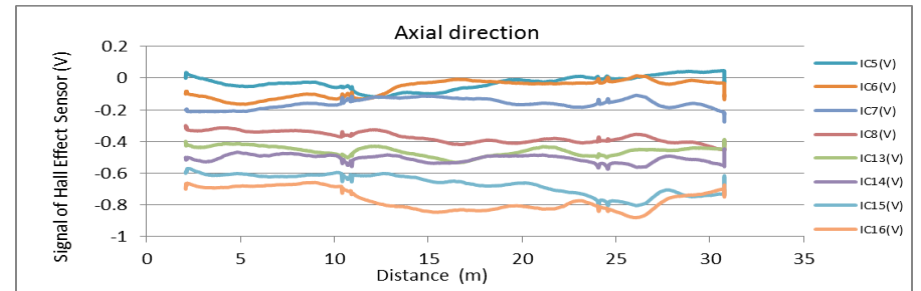
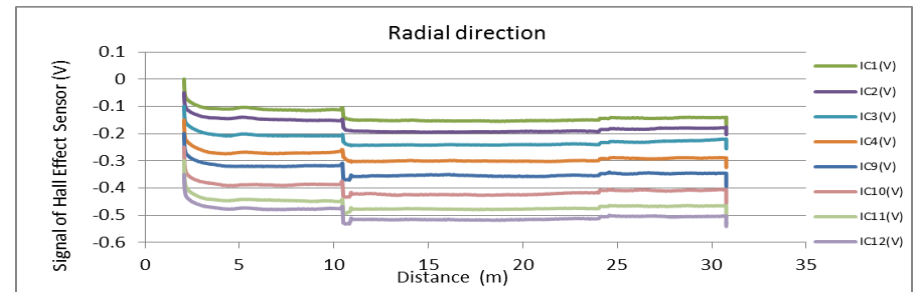
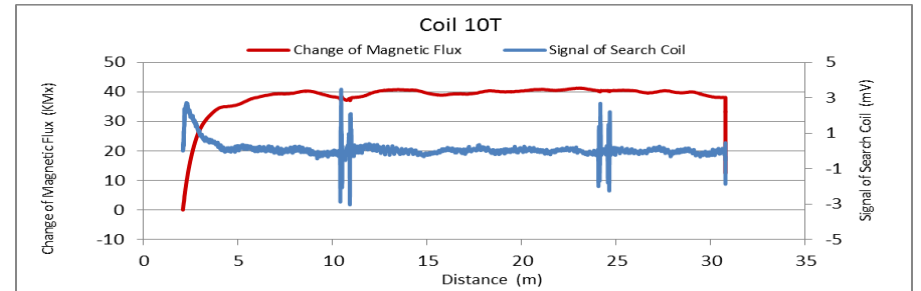


Figure A130. MMFM data of P6-402L-I2 tendon section.



Tokyo Rope USA, Inc.

File Name 【Pier-Tendon-Section】	Section Total Length (m)	Scanned Length		Note			
		Starting Point (m)	Ending Point (m)				
P7-401R-H1	9.35	0.51	8.54				
Identified Damage 1				Identified Damage 2			
Max Loss Point (m)	Section Loss (%)	Damage Length (m)	Damage Orientation	Max Loss Point (m)	Section Loss (%)	Damage Length (m)	Damage Orientation
—	—	—	—	—	—	—	—

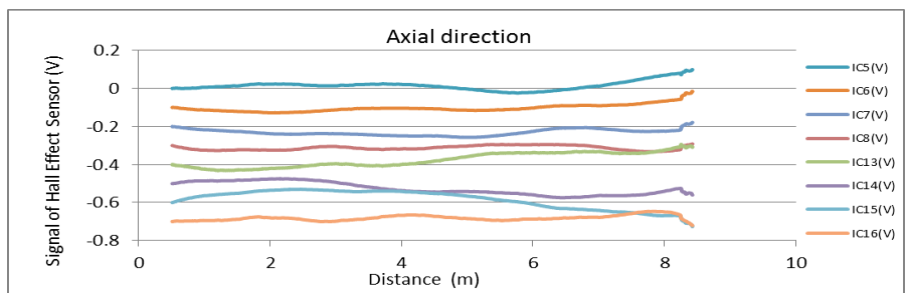
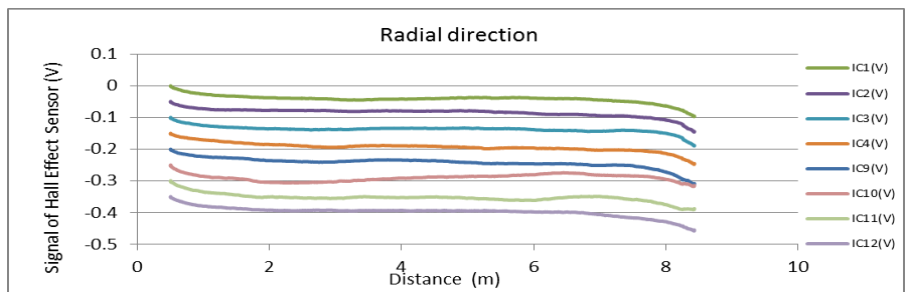
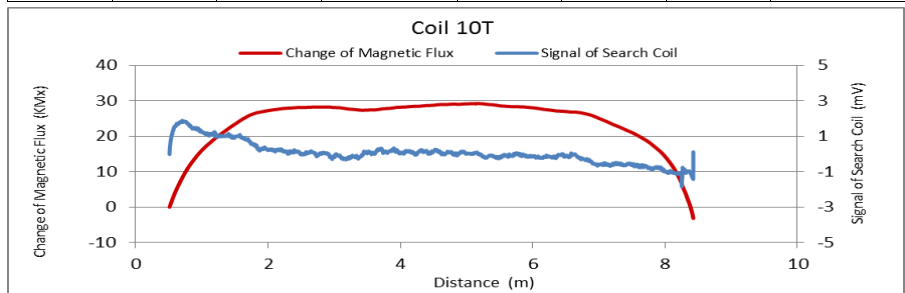


Figure A131. MMFM data of P7-401R-H1 tendon section.

File Name 【Pier-Tendon-Section】	Section Total Length (m)	Scanned Length		Note			
		Starting Point (m)	Ending Point (m)				
P7-402R-H1	9.35	0.54	7.78				
Identified Damage 1				Identified Damage 2			
Max Loss Point (m)	Section Loss (%)	Damage Length (m)	Damage Orientation	Max Loss Point (m)	Section Loss (%)	Damage Length (m)	Damage Orientation
—	—	—	—	—	—	—	—

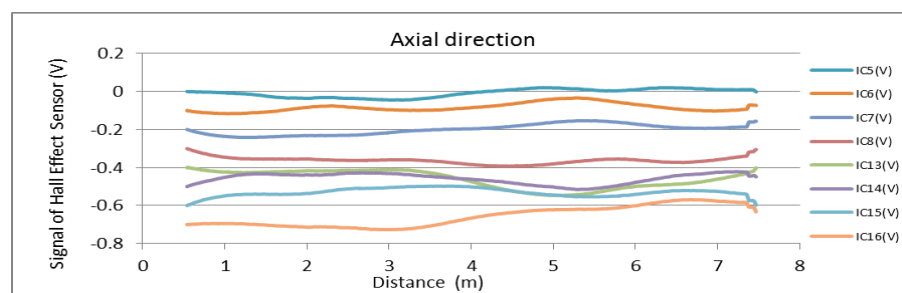
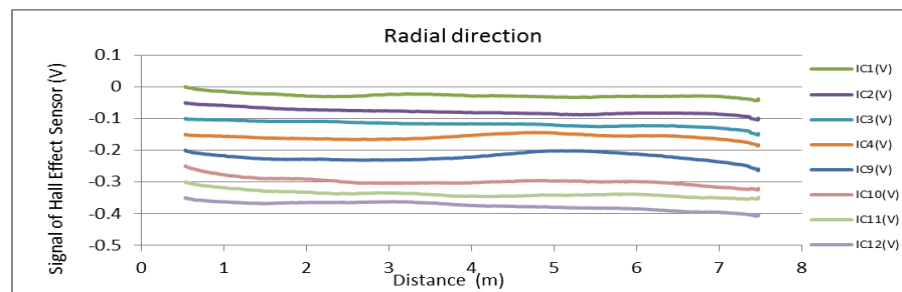
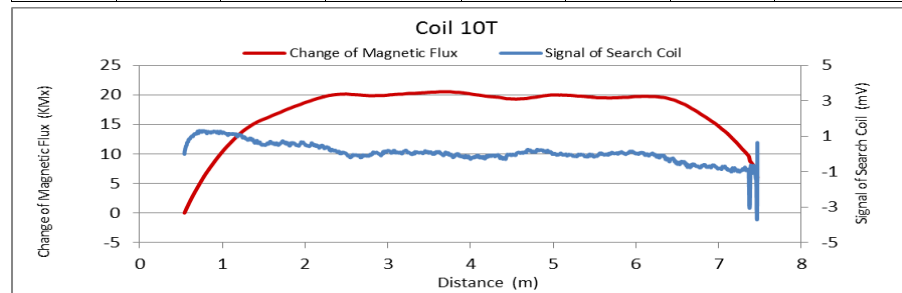


Figure A132. MMFM data of P7-402R-H1 tendon section.



Tokyo Rope USA, Inc.

File Name 【Pier-Tendon-Section】	Section Total Length (m)	Scanned Length		Note			
		Starting Point (m)	Ending Point (m)				
P7-303R-I1	9.48	1.97	9.17				
Identified Damage 1				Identified Damage 2			
Max Loss Point (m)	Section Loss (%)	Damage Length (m)	Damage Orientation	Max Loss Point (m)	Section Loss (%)	Damage Length (m)	Damage Orientation
—	—	—	—	—	—	—	—

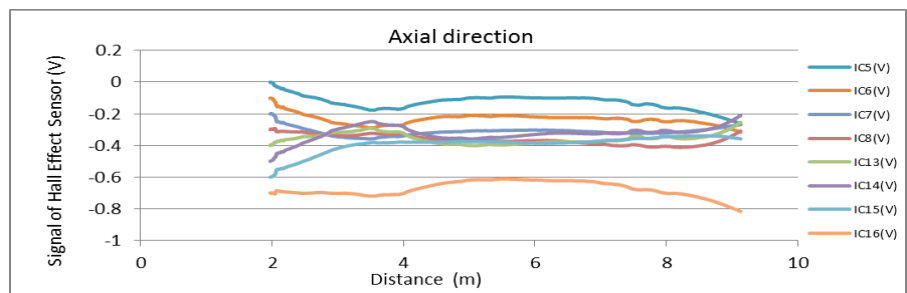
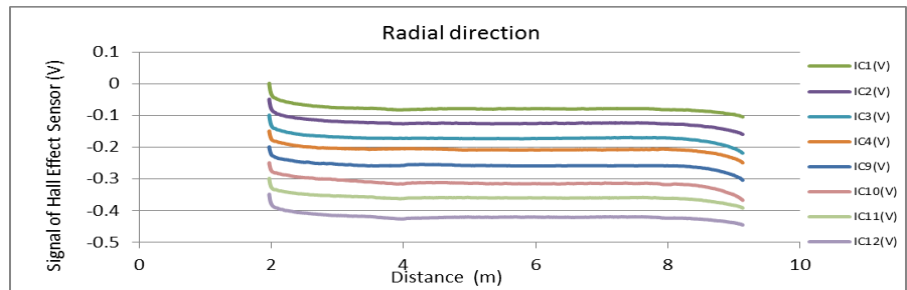
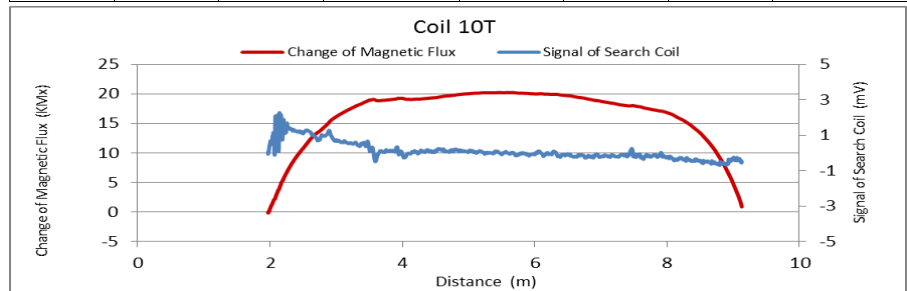


Figure A133. MMFM data of P7-303R-I1 tendon section.

File Name 【Pier-Tendon-Section】	Section Total Length (m)	Scanned Length		Note			
		Starting Point (m)	Ending Point (m)				
P7-401L-H1	9.37	0.53	8.64	Approximately 4 m from the beginning is distorted.			
Identified Damage 1				Identified Damage 2			
Max Loss Point (m)	Section Loss (%)	Damage Length (m)	Damage Orientation	Max Loss Point (m)	Section Loss (%)	Damage Length (m)	Damage Orientation
—	—	—	—	—	—	—	—

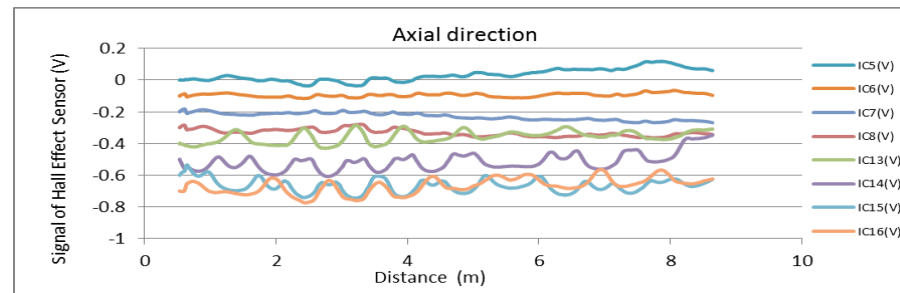
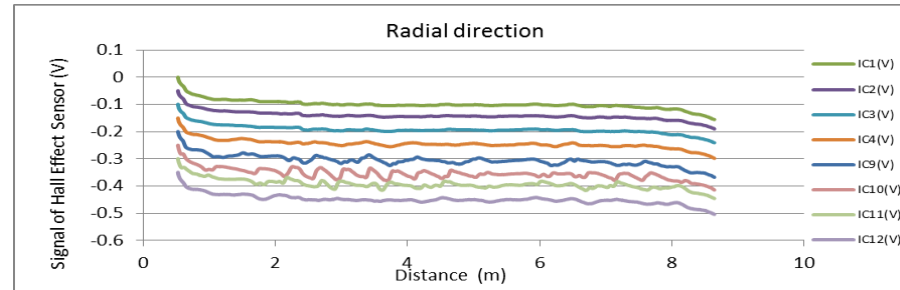
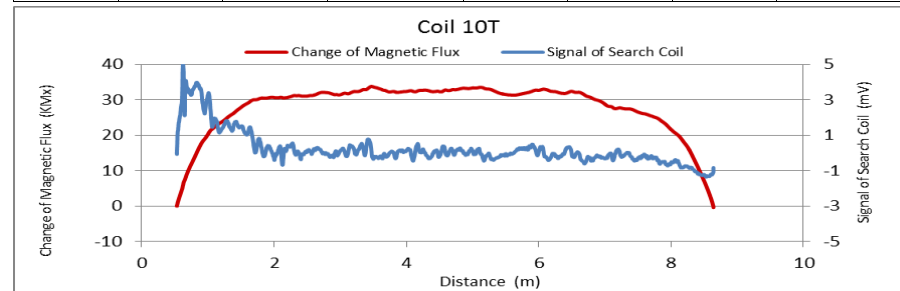


Figure A134. MMFM data of P7-401L-H1 tendon section.



Tokyo Rope USA, Inc.

File Name 【Pier-Tendon-Section】	Section Total Length (m)	Scanned Length		Note			
		Starting Point (m)	Ending Point (m)				
P7-402L-H1	9.37	0.56	8.58				
Identified Damage 1				Identified Damage 2			
Max Loss Point (m)	Section Loss (%)	Damage Length (m)	Damage Orientation	Max Loss Point (m)	Section Loss (%)	Damage Length (m)	Damage Orientation
—	—	—	—	—	—	—	—

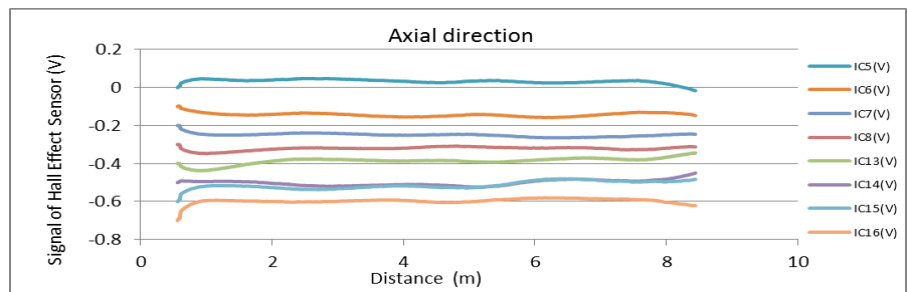
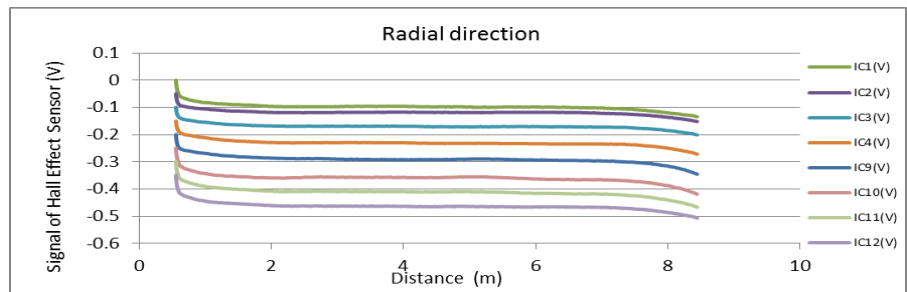
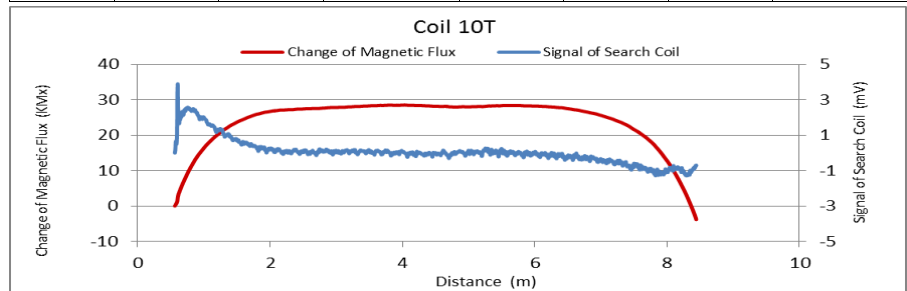


Figure A135. MMFM data of P7-402L-H1 tendon section.

File Name 【Pier-Tendon-Section】	Section Total Length (m)	Scanned Length		Note			
		Starting Point (m)	Ending Point (m)				
P7-303L-I1	9.52	0.43	9.19				
Identified Damage 1				Identified Damage 2			
Max Loss Point (m)	Section Loss (%)	Damage Length (m)	Damage Orientation	Max Loss Point (m)	Section Loss (%)	Damage Length (m)	Damage Orientation
—	—	—	—	—	—	—	—

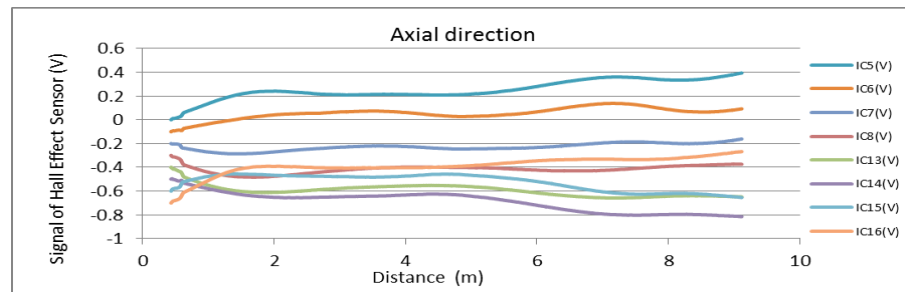
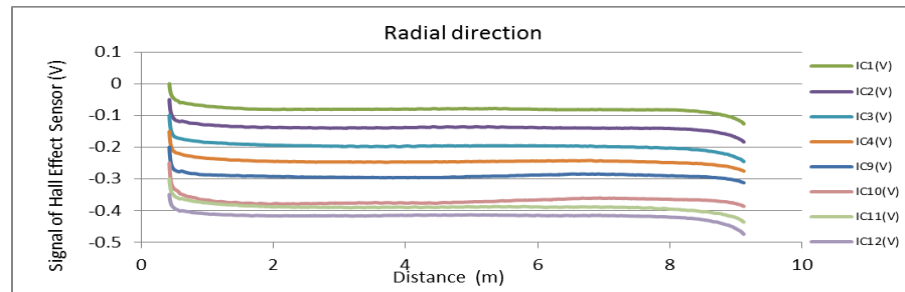
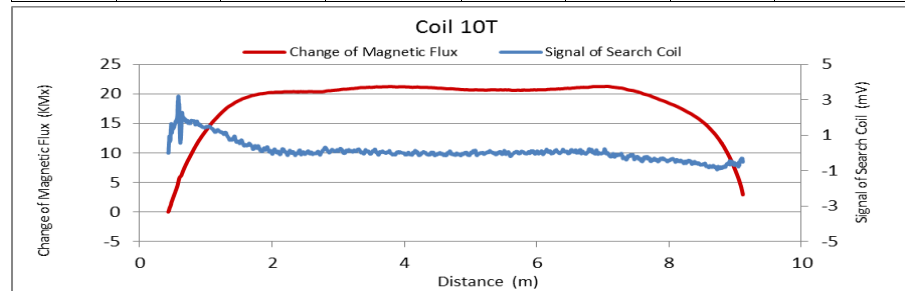


Figure A136. MMFM data of P7-303L-I1 tendon section.



Tokyo Rope USA, Inc.

File Name 【Pier-Tendon-Section】	Section Total Length (m)	Scanned Length		Note			
		Starting Point (m)	Ending Point (m)				
P7-401R-I1	21.44	0.54	20.62				
Identified Damage 1				Identified Damage 2			
Max Loss Point (m)	Section Loss (%)	Damage Length (m)	Damage Orientation	Max Loss Point (m)	Section Loss (%)	Damage Length (m)	Damage Orientation
—	—	—	—	—	—	—	—

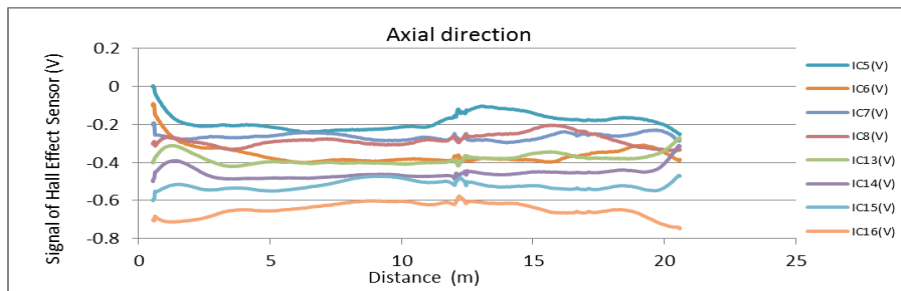
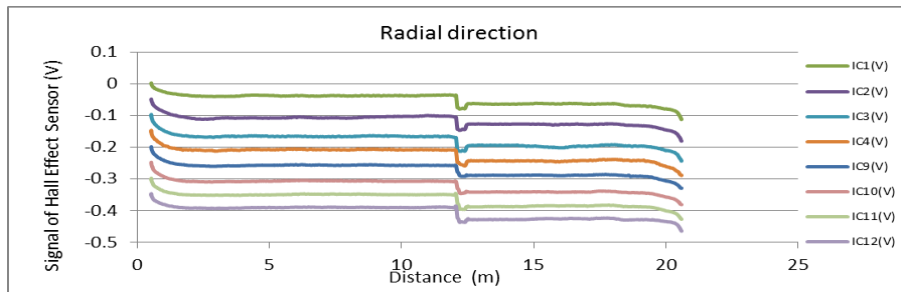
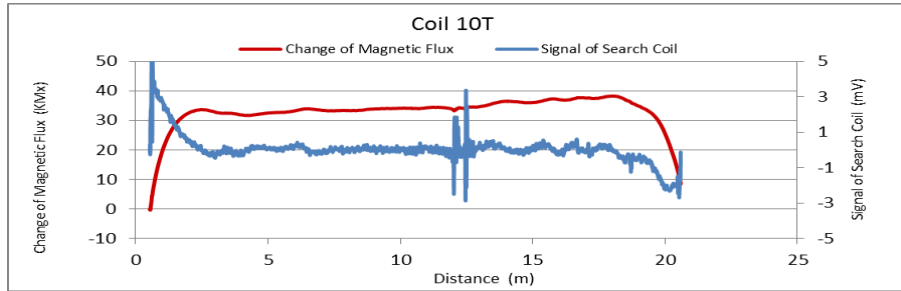


Figure A137. MMFM data of P7-401R-I1 tendon section.

File Name 【Pier-Tendon-Section】	Section Total Length (m)	Scanned Length		Note			
		Starting Point (m)	Ending Point (m)				
P7-402R-I1	21.44	0.66	20.66	Joint position: 12.35 m			
Identified Damage 1				Identified Damage 2			
Max Loss Point (m)	Section Loss (%)	Damage Length (m)	Damage Orientation	Max Loss Point (m)	Section Loss (%)	Damage Length (m)	Damage Orientation
—	—	—	—	—	—	—	—

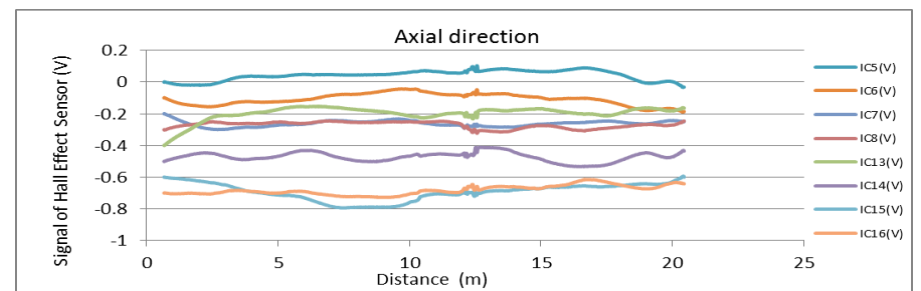
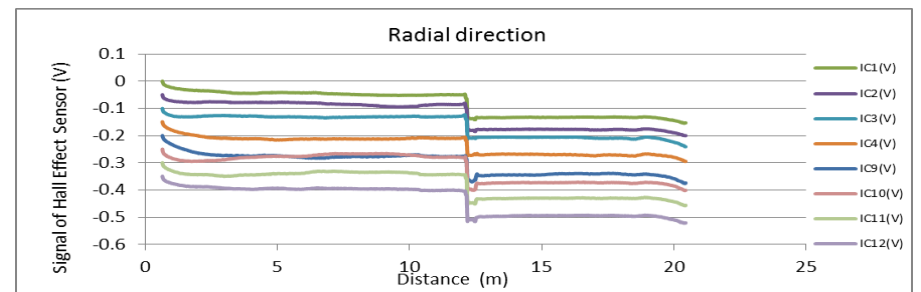
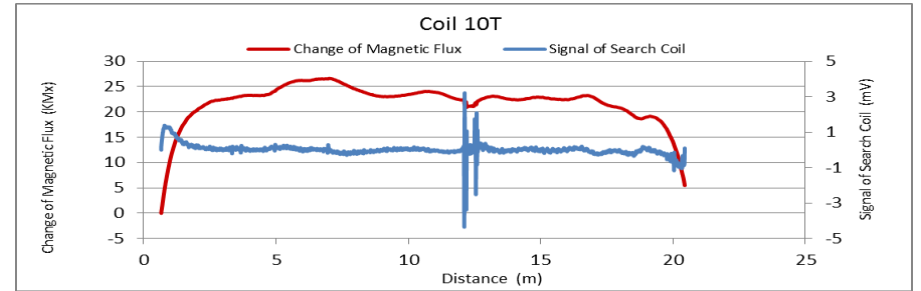


Figure A138. MMFM data of P7-402R-I1 tendon section.



Tokyo Rope USA, Inc.

File Name 【Pier-Tendon-Section】	Section Total Length (m)	Scanned Length		Note			
		Starting Point (m)	Ending Point (m)				
P7-303R-I2	21.65	0.22	20.83	Joint position : 2.5 m, 12.63 m			
Identified Damage 1				Identified Damage 2			
Max Loss Point (m)	Section Loss (%)	Damage Length (m)	Damage Orientation	Max Loss Point (m)	Section Loss (%)	Damage Length (m)	Damage Orientation
—	—	—	—	—	—	—	—

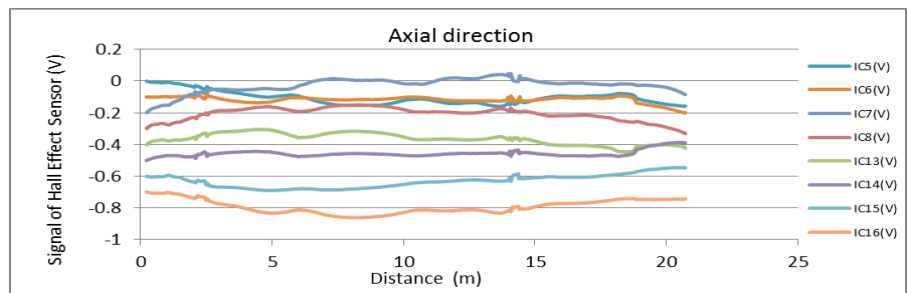
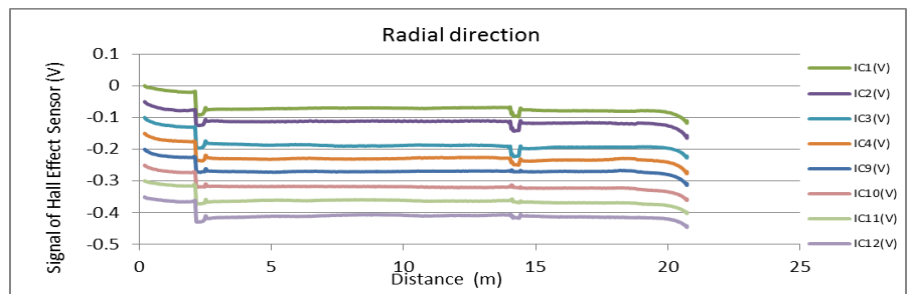
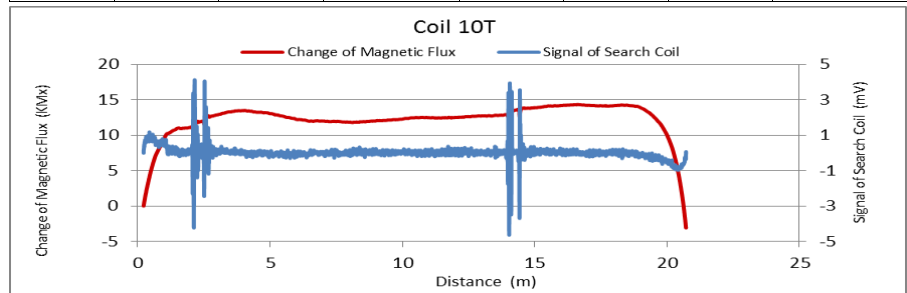


Figure A139. MMFM data of P7-303R-I2 tendon section.

File Name 【Pier-Tendon-Section】	Section Total Length (m)	Scanned Length		Note			
		Starting Point (m)	Ending Point (m)				
P7-401L-I1	21.37	0.66	20.6	Joint position : 12.3 m			
Identified Damage 1				Identified Damage 2			
Max Loss Point (m)	Section Loss (%)	Damage Length (m)	Damage Orientation	Max Loss Point (m)	Section Loss (%)	Damage Length (m)	Damage Orientation
—	—	—	—	—	—	—	—

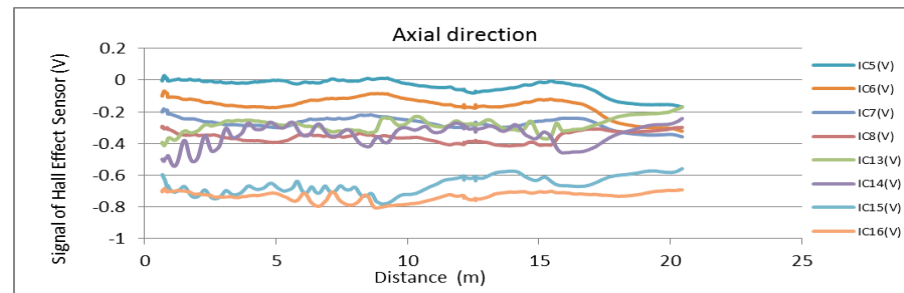
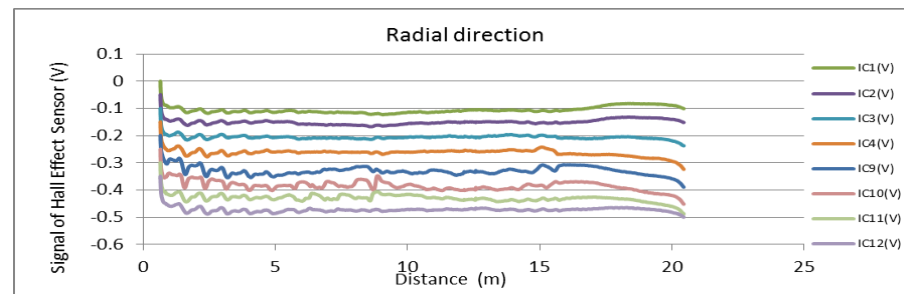
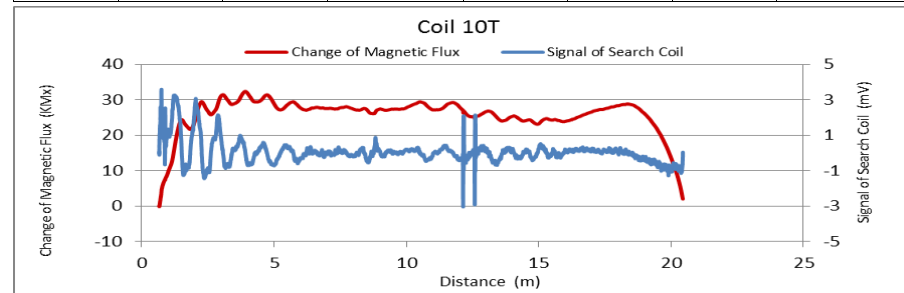


Figure A140. MMFM data of P7-401L-I1 tendon section.



Tokyo Rope USA, Inc.

File Name 【Pier-Tendon-Section】	Section Total Length (m)	Scanned Length		Note			
		Starting Point (m)	Ending Point (m)				
P7-402L-I1	21.37	0.96	20.55	Joint position : 12.23 m			
Identified Damage 1				Identified Damage 2			
Max Loss Point (m)	Section Loss (%)	Damage Length (m)	Damage Orientation	Max Loss Point (m)	Section Loss (%)	Damage Length (m)	Damage Orientation
—	—	—	—	—	—	—	—

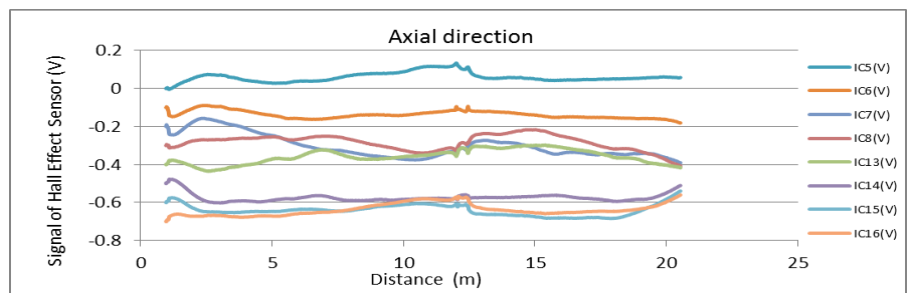
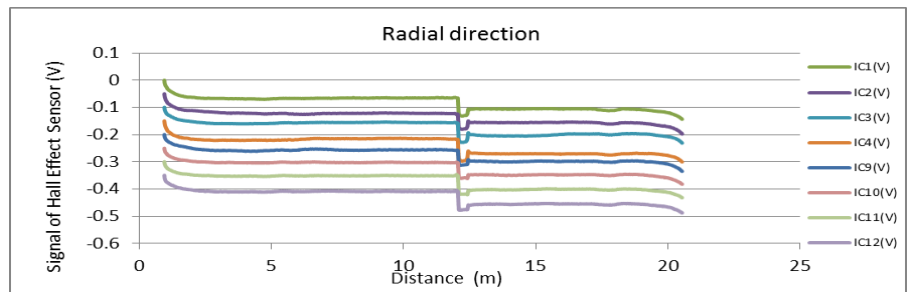
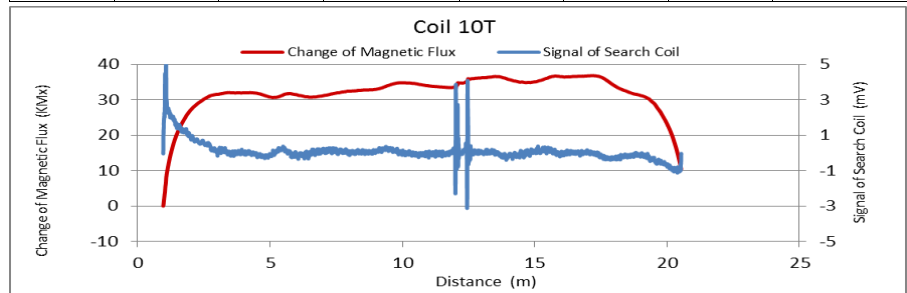


Figure A141. MMFM data of P7-402L-I1 tendon section.

File Name 【Pier-Tendon-Section】	Section Total Length (m)	Scanned Length		Note			
		Starting Point (m)	Ending Point (m)				
P7-303L-I2	21.56	0.26	21.25	Joint position : 2.47 m, 14.56 m			
Identified Damage 1				Identified Damage 2			
Max Loss Point (m)	Section Loss (%)	Damage Length (m)	Damage Orientation	Max Loss Point (m)	Section Loss (%)	Damage Length (m)	Damage Orientation
—	—	—	—	—	—	—	—

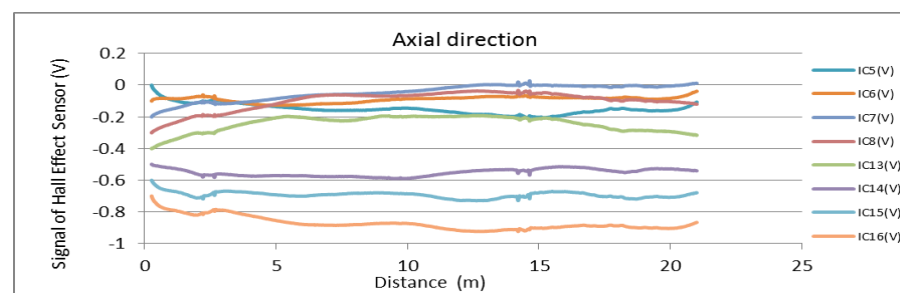
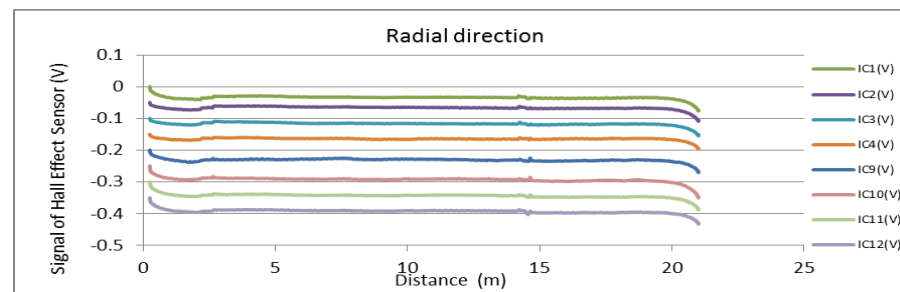
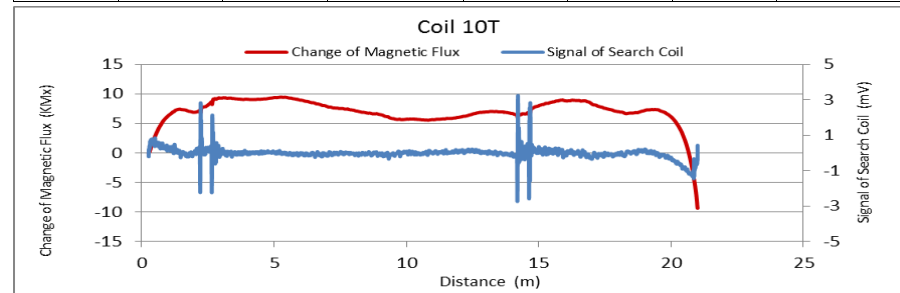


Figure A142. MMFM data of P7-303L-I2 tendon section.



Tokyo Rope USA, Inc.

File Name 【Pier-Tendon-Section】	Section Total Length (m)	Scanned Length		Note			
		Starting Point (m)	Ending Point (m)				
P7-401R-I2	21.52	0.86	20.92	Joint position: 9.18 m IC (1)-IC (8)-detection by poor contact			
Identified Damage 1				Identified Damage 2			
Max Loss Point (m)	Section Loss (%)	Damage Length (m)	Damage Orientation	Max Loss Point (m)	Section Loss (%)	Damage Length (m)	Damage Orientation
—	—	—	—	—	—	—	—

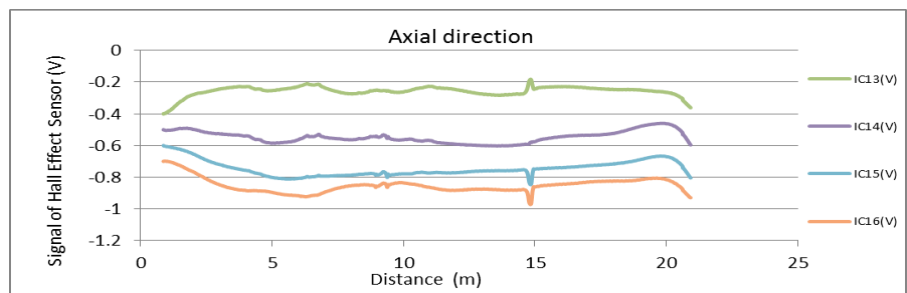
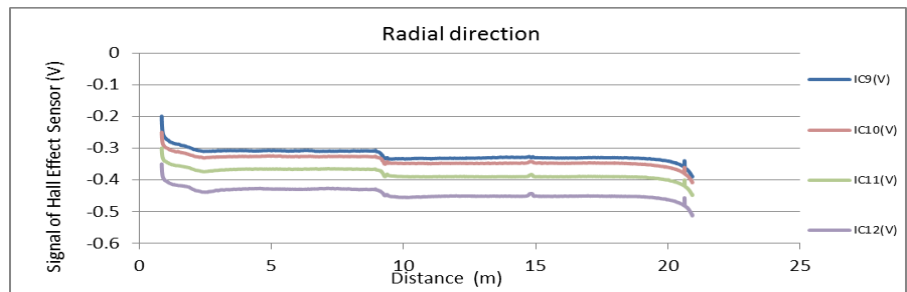
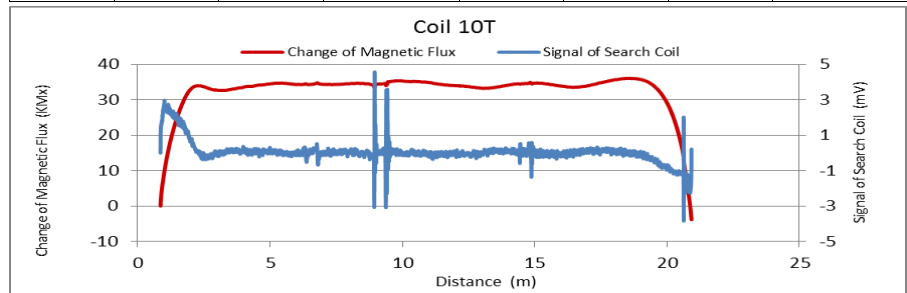


Figure A143. MMFM data of P7-401R-I2 tendon section.

File Name 【Pier-Tendon-Section】	Section Total Length (m)	Scanned Length		Note			
		Starting Point (m)	Ending Point (m)				
P7-402R-I2	31.35	2.25	30.95	Joint position: 12.25 m, 24.36 m Many distortions: 12m~			
Identified Damage 1				Identified Damage 2			
Max Loss Point (m)	Section Loss (%)	Damage Length (m)	Damage Orientation	Max Loss Point (m)	Section Loss (%)	Damage Length (m)	Damage Orientation
—	—	—	—	—	—	—	—

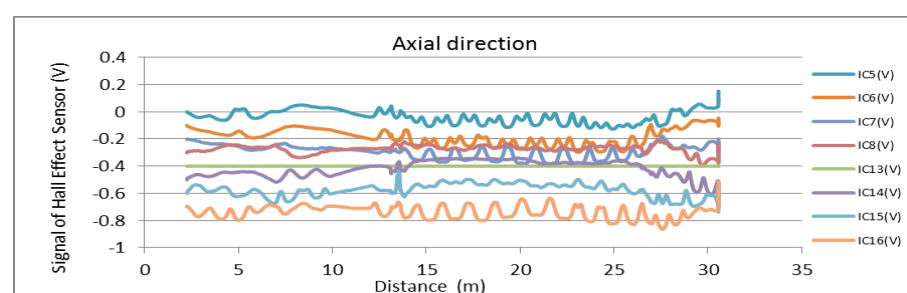
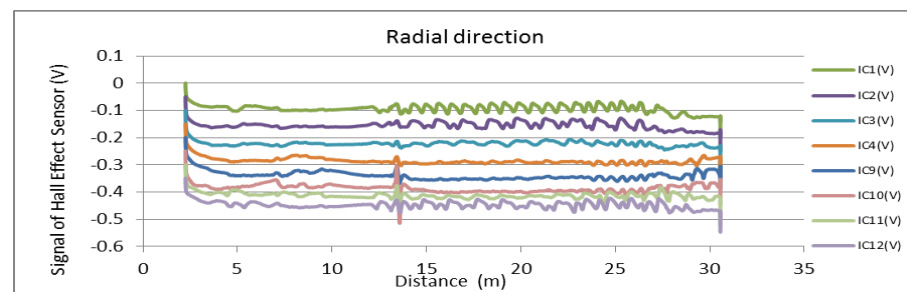
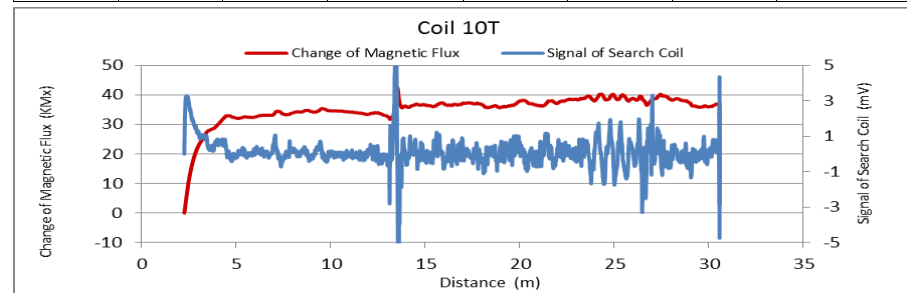


Figure A144. MMFM data of P7-402R-I2 tendon section.



Tokyo Rope USA, Inc.

File Name 【Pier-Tendon-Section】	Section Total Length (m)	Scanned Length		Note			
		Starting Point (m)	Ending Point (m)				
P7-303R-I3	21.64	0.26	21.31	Joint position: 7.04 m, 19.14 m			
Identified Damage 1				Identified Damage 2			
Max Loss Point (m)	Section Loss (%)	Damage Length (m)	Damage Orientation	Max Loss Point (m)	Section Loss (%)	Damage Length (m)	Damage Orientation
—	—	—	—	—	—	—	—

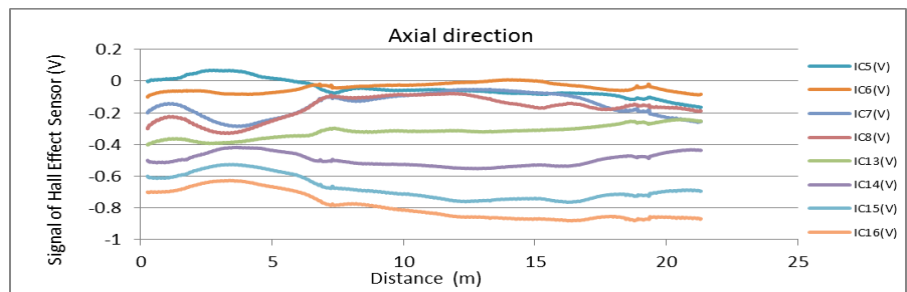
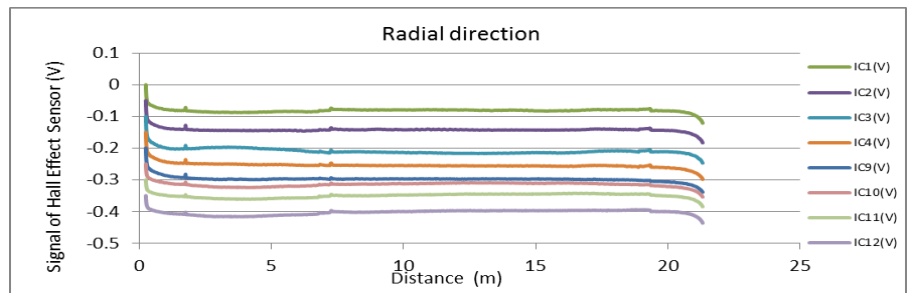
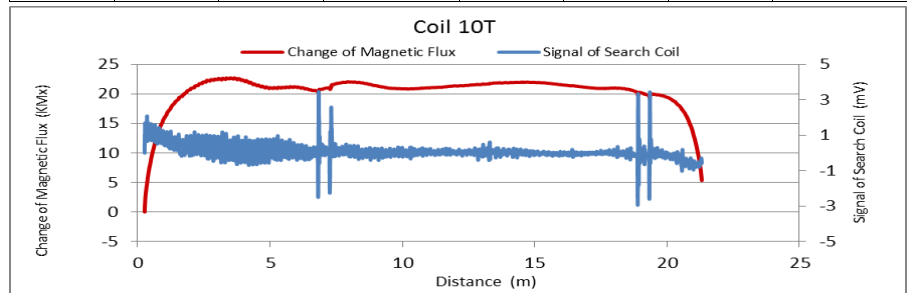


Figure A145. MMFM data of P7-303R-I3 tendon section.

File Name 【Pier-Tendon-Section】	Section Total Length (m)	Scanned Length		Note			
		Starting Point (m)	Ending Point (m)				
P7-401R-H2	9.38	0.9	8.84				
Identified Damage 1				Identified Damage 2			
Max Loss Point (m)	Section Loss (%)	Damage Length (m)	Damage Orientation	Max Loss Point (m)	Section Loss (%)	Damage Length (m)	Damage Orientation
—	—	—	—	—	—	—	—

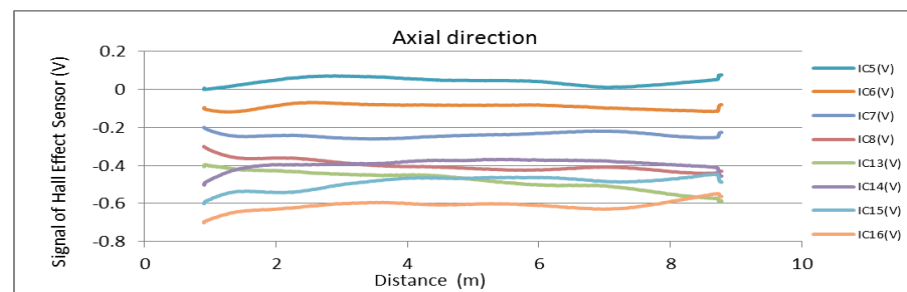
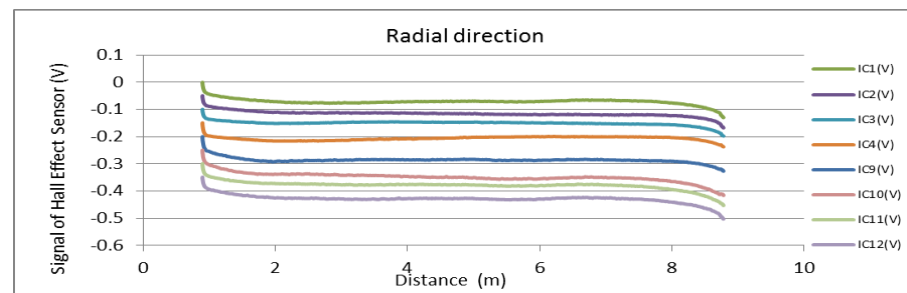
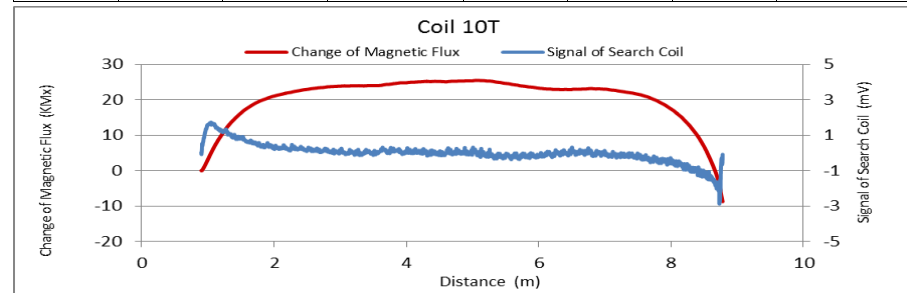


Figure A146. MMFM data of P7-401R-H2 tendon section.



Tokyo Rope USA, Inc.

File Name 【Pier-Tendon-Section】	Section Total Length (m)	Scanned Length		Note			
		Starting Point (m)	Ending Point (m)				
P7-303R-I4	9.47	0.26	9.06				
Identified Damage 1				Identified Damage 2			
Max Loss Point (m)	Section Loss (%)	Damage Length (m)	Damage Orientation	Max Loss Point (m)	Section Loss (%)	Damage Length (m)	Damage Orientation
—	—	—	—	—	—	—	—

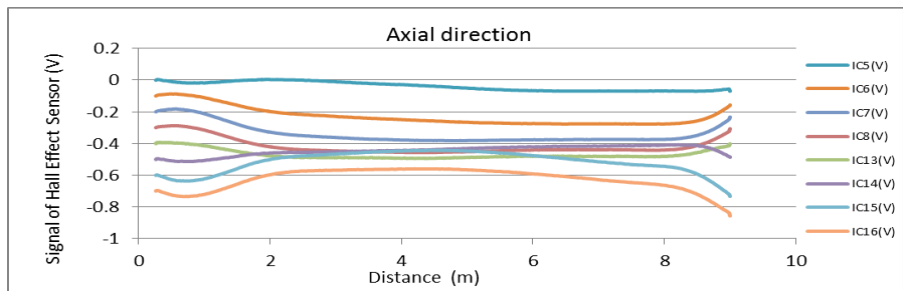
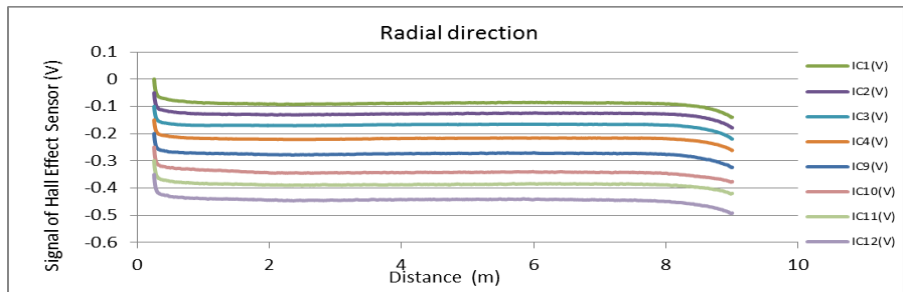
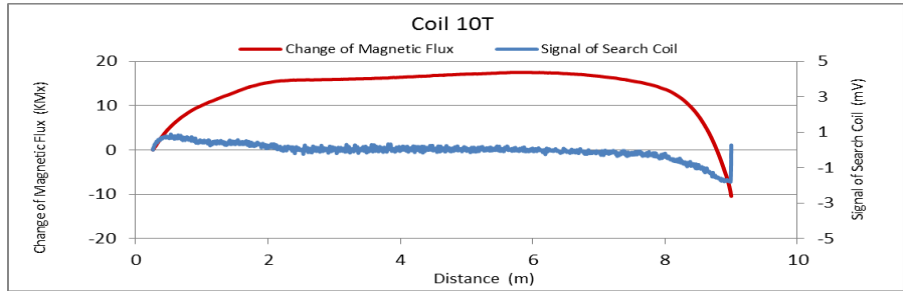


Figure A147. MMFM data of P7-303R-I4 tendon section.

File Name 【Pier-Tendon-Section】	Section Total Length (m)	Scanned Length		Note			
		Starting Point (m)	Ending Point (m)				
P7-401L-H2	9.41	0.72	8.95				
Identified Damage 1				Identified Damage 2			
Max Loss Point (m)	Section Loss (%)	Damage Length (m)	Damage Orientation	Max Loss Point (m)	Section Loss (%)	Damage Length (m)	Damage Orientation
—	—	—	—	—	—	—	—

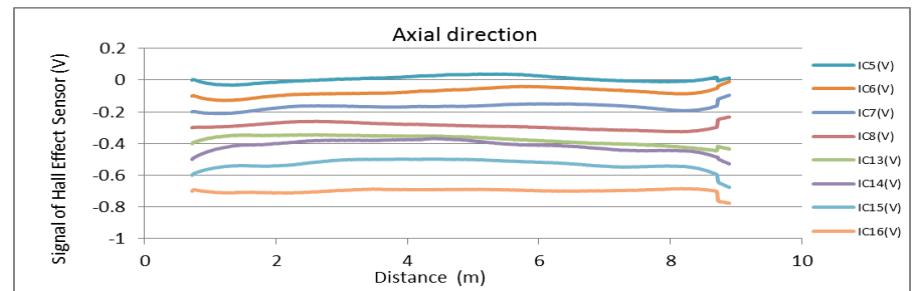
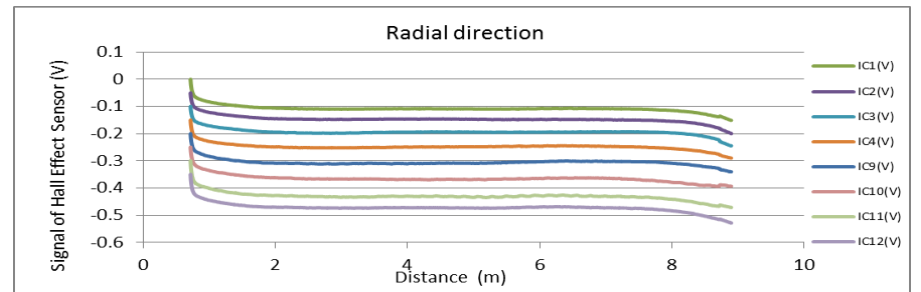
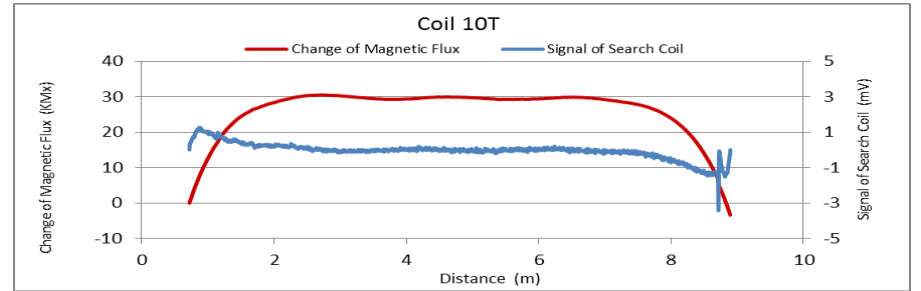


Figure A148. MMFM data of P7-401L-H2 tendon section.



Tokyo Rope USA, Inc.

File Name 【Pier-Tendon-Section】	Section Total Length (m)	Scanned Length		Note			
		Starting Point (m)	Ending Point (m)				
P7-402L-H2	9.41	0.74	8.92				
Identified Damage 1				Identified Damage 2			
Max Loss Point (m)	Section Loss (%)	Damage Length (m)	Damage Orientation	Max Loss Point (m)	Section Loss (%)	Damage Length (m)	Damage Orientation
—	—	—	—	—	—	—	—

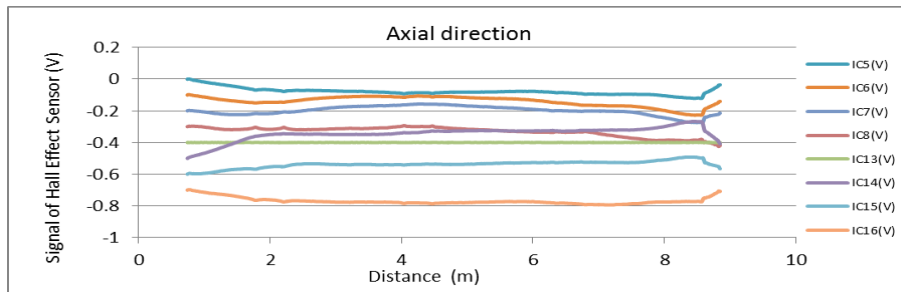
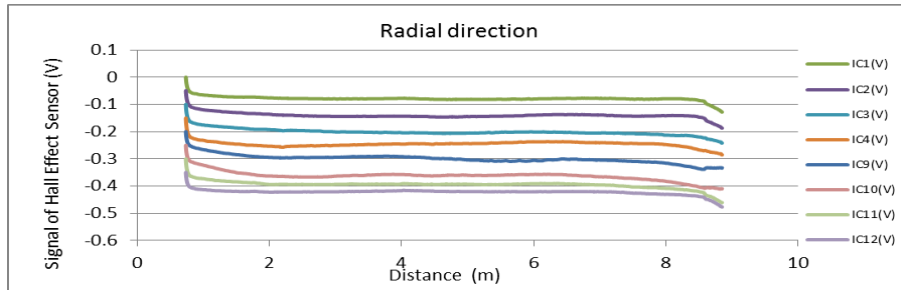
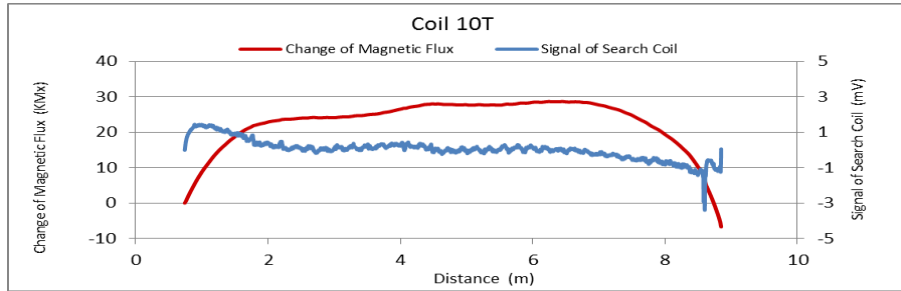


Figure A149. MMFM data of P7-402L-H2 tendon section.

File Name 【Pier-Tendon-Section】	Section Total Length (m)	Scanned Length		Note			
		Starting Point (m)	Ending Point (m)				
P7-303L-I4	9.46	0.26	9.01				
Identified Damage 1				Identified Damage 2			
Max Loss Point (m)	Section Loss (%)	Damage Length (m)	Damage Orientation	Max Loss Point (m)	Section Loss (%)	Damage Length (m)	Damage Orientation
—	—	—	—	—	—	—	—

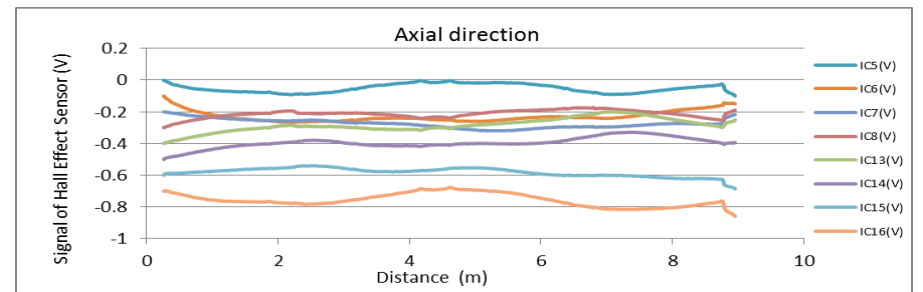
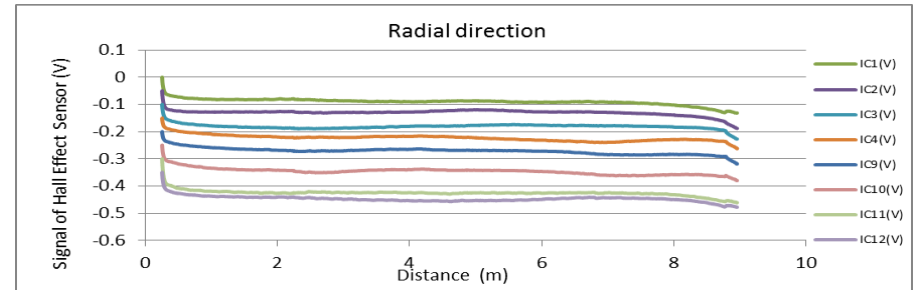
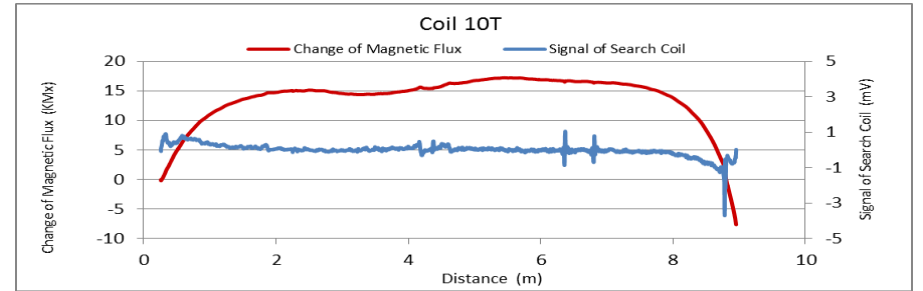


Figure A150. MMFM data of P7-303L-I4 tendon section.



Tokyo Rope USA, Inc.

File Name 【Pier-Tendon-Section】	Section Total Length (m)	Scanned Length		Note			
		Starting Point (m)	Ending Point (m)				
P8-401R-H1	9.49	0.88	8.67				
Identified Damage 1				Identified Damage 2			
Max Loss Point (m)	Section Loss (%)	Damage Length (m)	Damage Orientation	Max Loss Point (m)	Section Loss (%)	Damage Length (m)	Damage Orientation
—	—	—	—	—	—	—	—

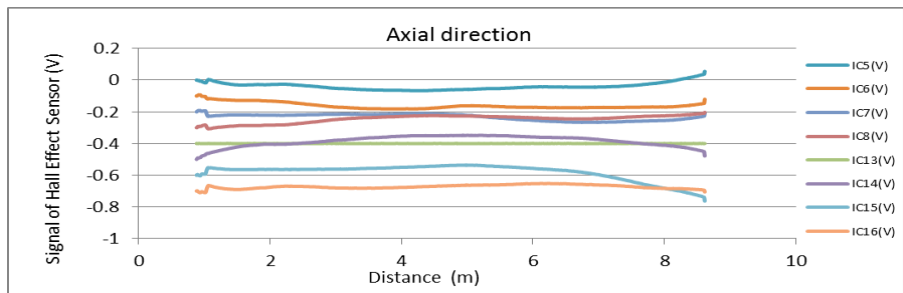
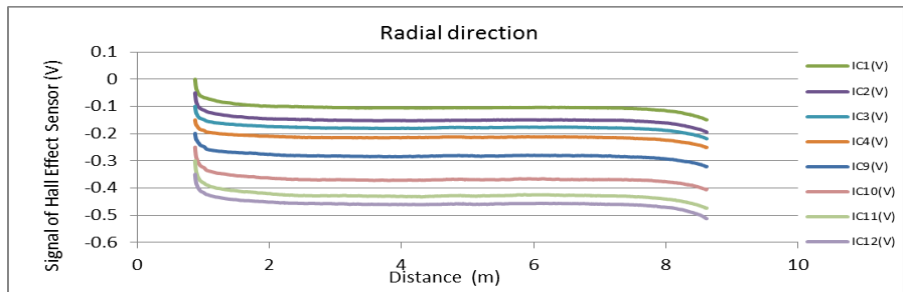
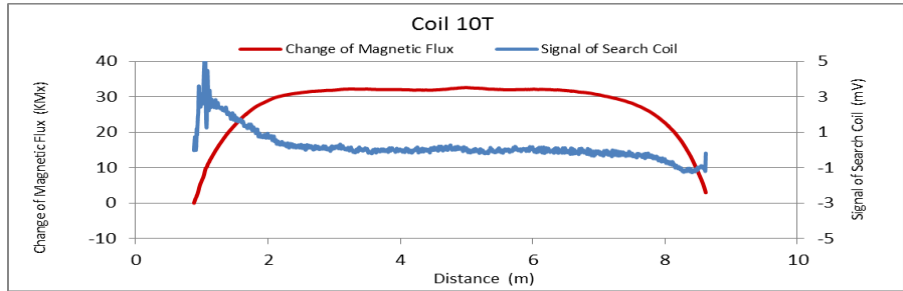


Figure A151. MMFM data of P8-401R-H1 tendon section.

File Name 【Pier-Tendon-Section】	Section Total Length (m)	Scanned Length		Note			
		Starting Point (m)	Ending Point (m)				
P8-402R-I1	31.34	0.36	29.36	Joint position : 2.67 m, 14.8 m, 26.93 m Have a lot of distortion			
Identified Damage 1				Identified Damage 2			
Max Loss Point (m)	Section Loss (%)	Damage Length (m)	Damage Orientation	Max Loss Point (m)	Section Loss (%)	Damage Length (m)	Damage Orientation
—	—	—	—	—	—	—	—

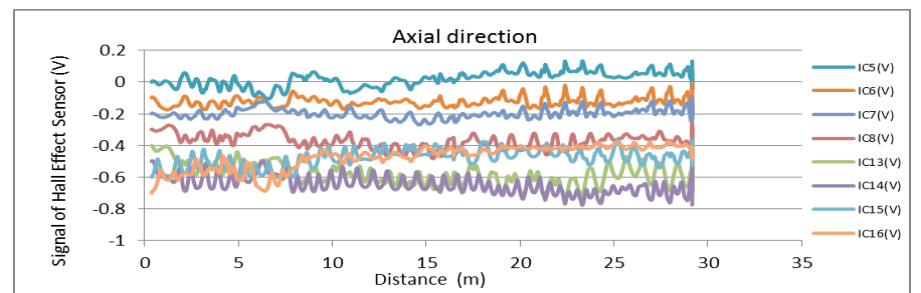
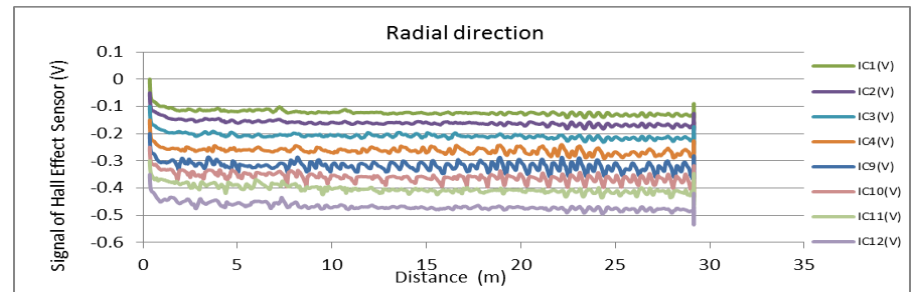
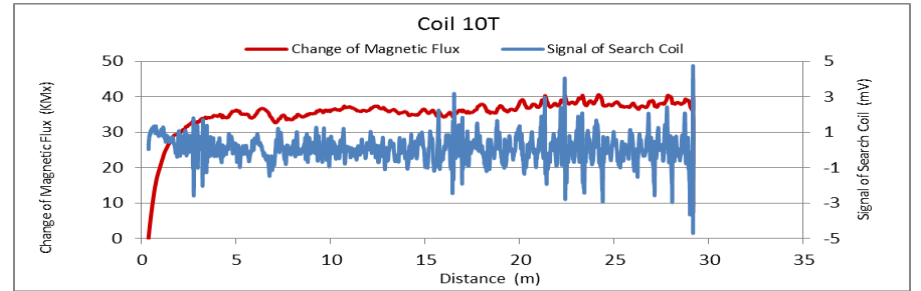


Figure A152. MMFM data of P8-402R-I1 tendon section.



Tokyo Rope USA, Inc.

File Name 【Pier-Tendon-Section】	Section Total Length (m)	Scanned Length		Note			
		Starting Point (m)	Ending Point (m)				
P8-401L-H1	9.45	0.59	8.78				
Identified Damage 1				Identified Damage 2			
Max Loss Point (m)	Section Loss (%)	Damage Length (m)	Damage Orientation	Max Loss Point (m)	Section Loss (%)	Damage Length (m)	Damage Orientation
—	—	—	—	—	—	—	—

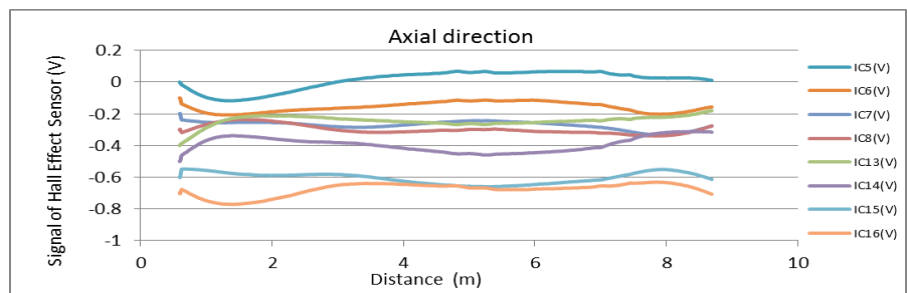
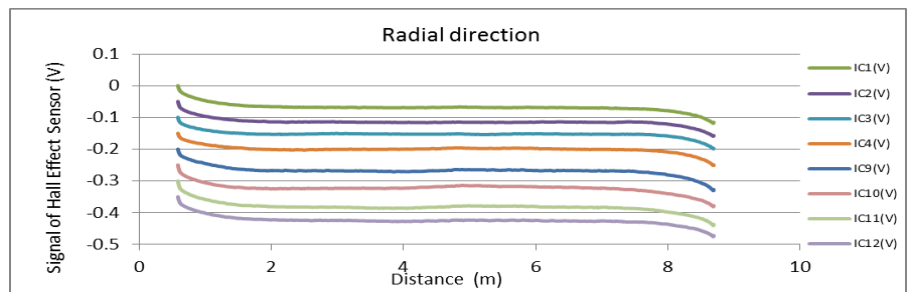
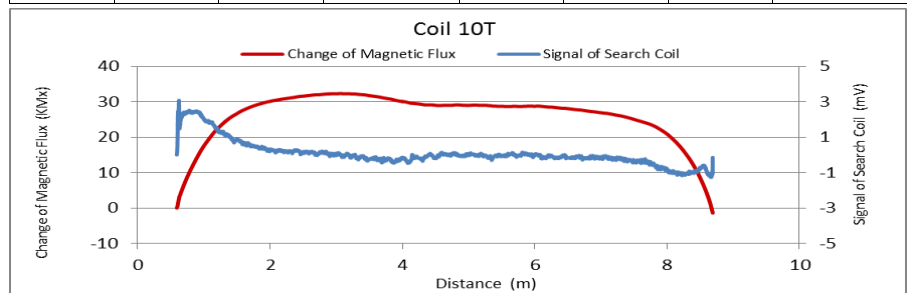


Figure A153. MMFM data of P8-401L-H1 tendon section.

File Name 【Pier-Tendon-Section】	Section Total Length (m)	Scanned Length		Note			
		Starting Point (m)	Ending Point (m)				
P8-402L-H1	9.45	0.48	8.69				
Identified Damage 1				Identified Damage 2			
Max Loss Point (m)	Section Loss (%)	Damage Length (m)	Damage Orientation	Max Loss Point (m)	Section Loss (%)	Damage Length (m)	Damage Orientation
—	—	—	—	—	—	—	—

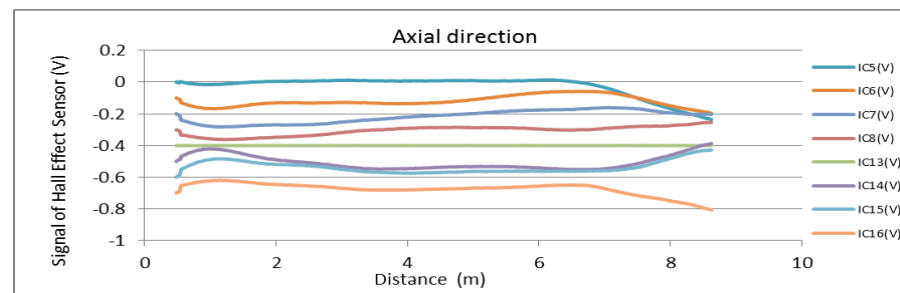
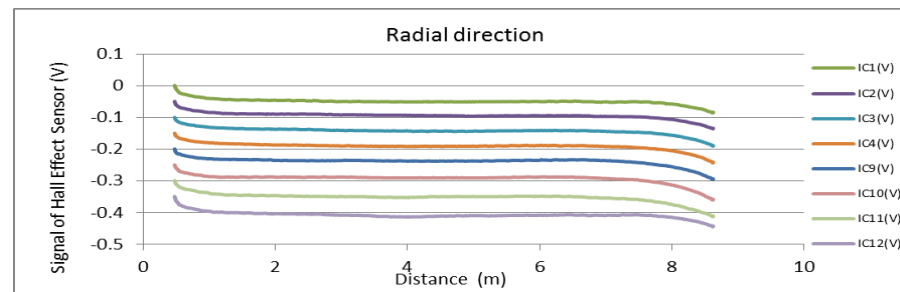
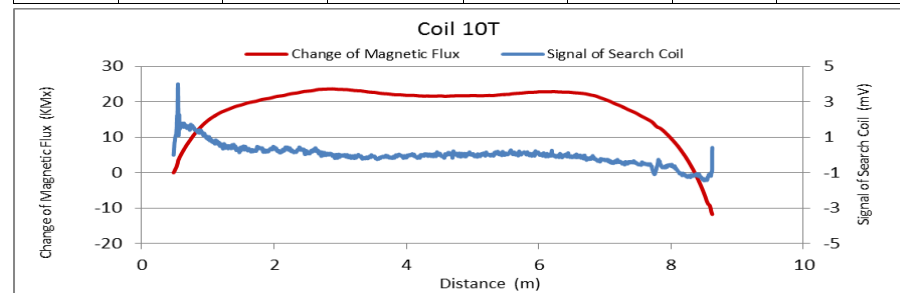


Figure A154. MMFM data of P8-402L-H1 tendon section.



Tokyo Rope USA, Inc.

File Name 【Pier-Tendon-Section】	Section Total Length (m)	Scanned Length		Note			
		Starting Point (m)	Ending Point (m)				
P8-401R-I1	21.49	0.6	20.49	Joint position: 12.31 m			
Identified Damage 1				Identified Damage 2			
Max Loss Point(m)	Section Loss (%)	Damage Length(m)	Damage Orientation	Max Loss Point(m)	Section Loss (%)	Damage Length(m)	Damage Orientation
—	—	—	—	—	—	—	—

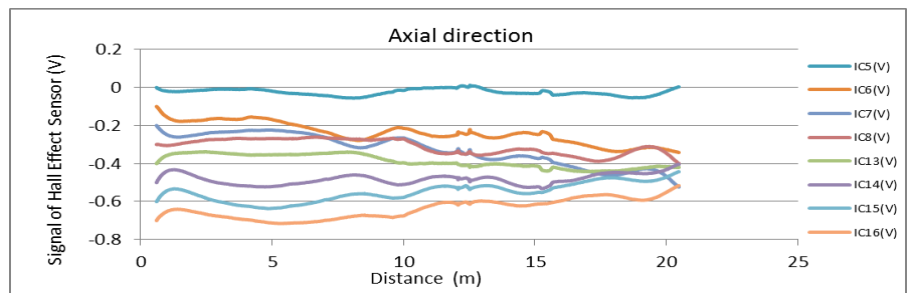
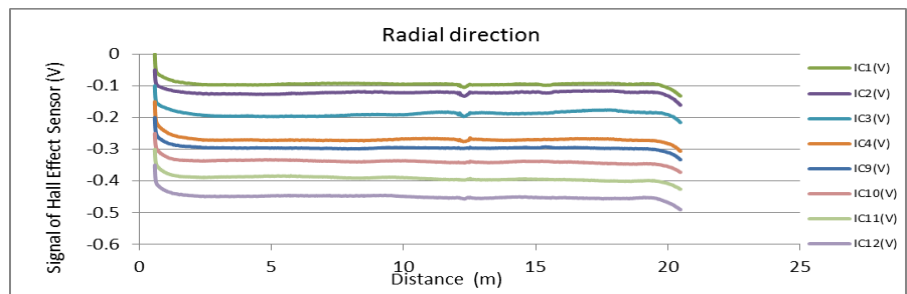
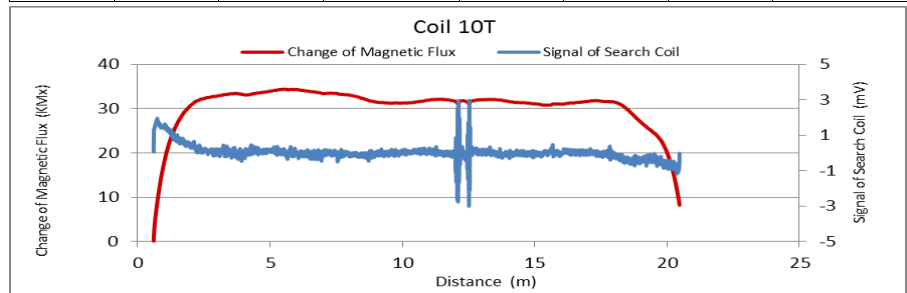


Figure A155. MMFM data of P8-401R-I1 tendon section.

File Name 【Pier-Tendon-Section】	Section Total Length (m)	Scanned Length		Note			
		Starting Point (m)	Ending Point (m)				
P8-401L-I1	21.48	0.59	20.24	Joint position: 12.37 m			
Identified Damage 1				Identified Damage 2			
Max Loss Point (m)	Section Loss (%)	Damage Length (m)	Damage Orientation	Max Loss Point (m)	Section Loss (%)	Damage Length (m)	Damage Orientation
—	—	—	—	—	—	—	—

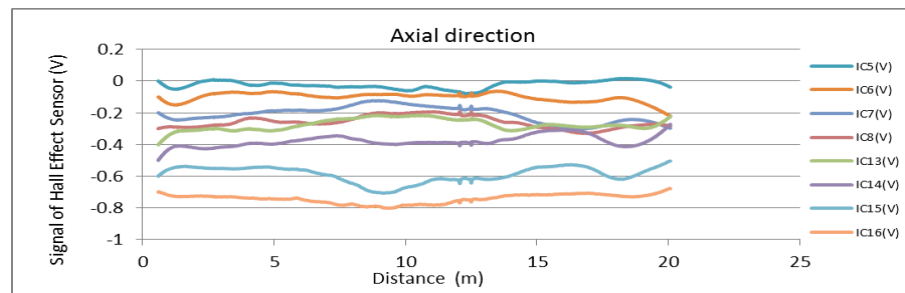
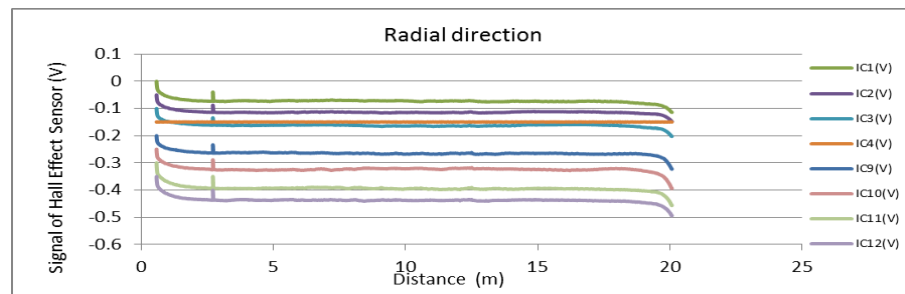
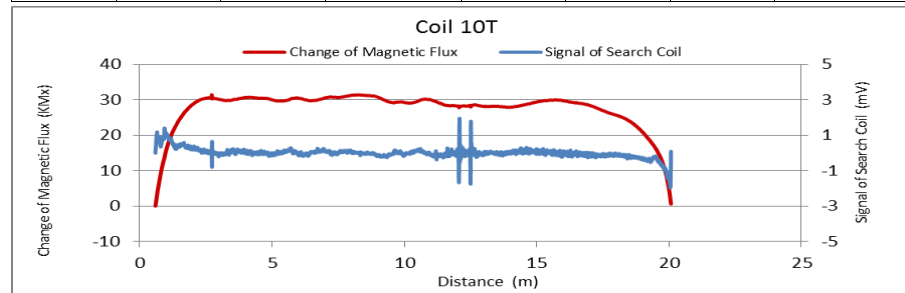


Figure A156. MMFM data of P8-401L-I1 tendon section.



Tokyo Rope USA, Inc.

File Name 【Pier-Tendon-Section】	Section Total Length (m)	Scanned Length		Note			
		Starting Point (m)	Ending Point (m)				
P8-402L-I1	21.48	0.67	20.22	Joint position: 12.3 m			
Identified Damage 1				Identified Damage 2			
Max Loss Point (m)	Section Loss (%)	Damage Length (m)	Damage Orientation	Max Loss Point (m)	Section Loss (%)	Damage Length (m)	Damage Orientation
—	—	—	—	—	—	—	—

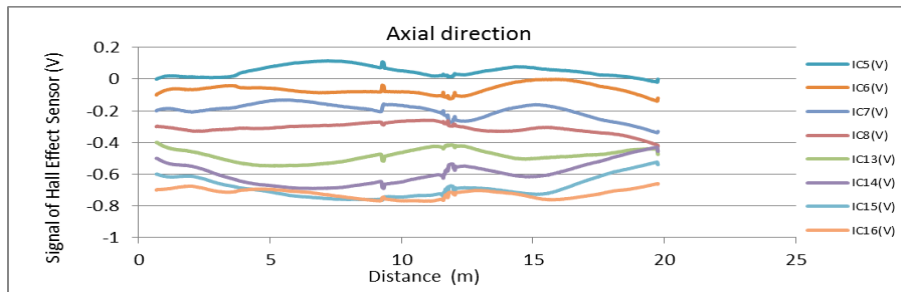
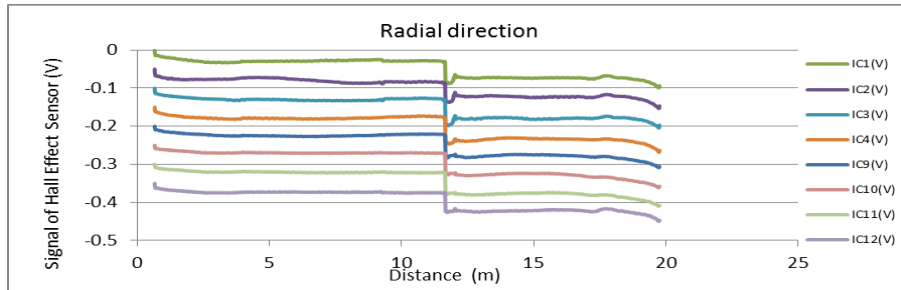
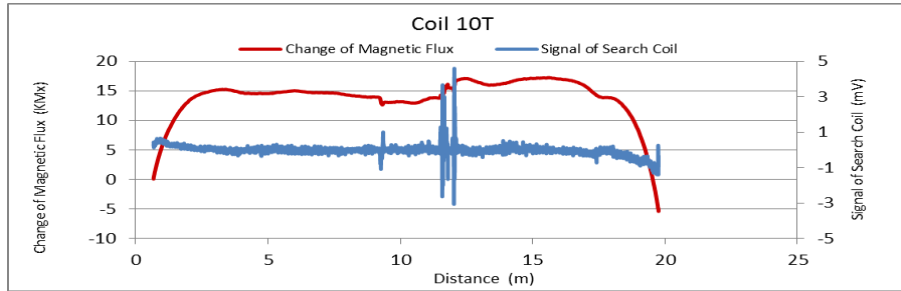


Figure A157. MMFM data of P8-402L-I1 tendon section.

File Name 【Pier-Tendon-Section】	Section Total Length (m)	Scanned Length		Note			
		Starting Point (m)	Ending Point (m)				
P8-401R-I2	21.48	0.74	20.72	Joint position: 9.2 m			
Identified Damage 1				Identified Damage 2			
Max Loss Point (m)	Section Loss (%)	Damage Length (m)	Damage Orientation	Max Loss Point (m)	Section Loss (%)	Damage Length (m)	Damage Orientation
—	—	—	—	—	—	—	—

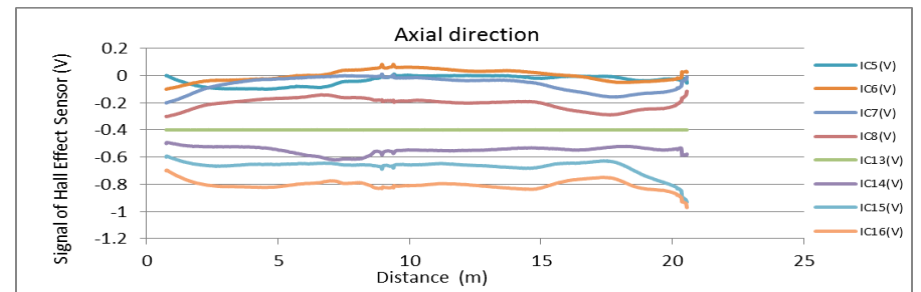
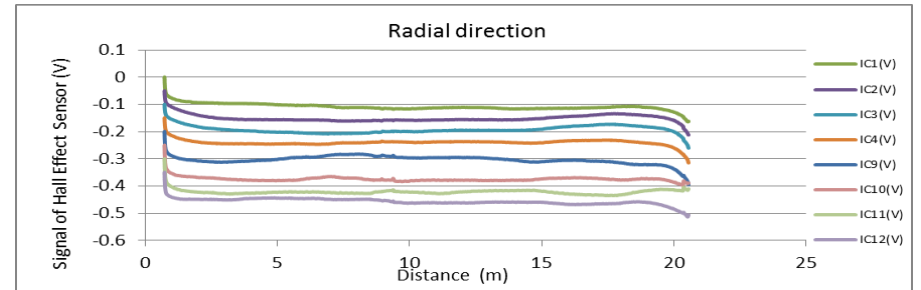
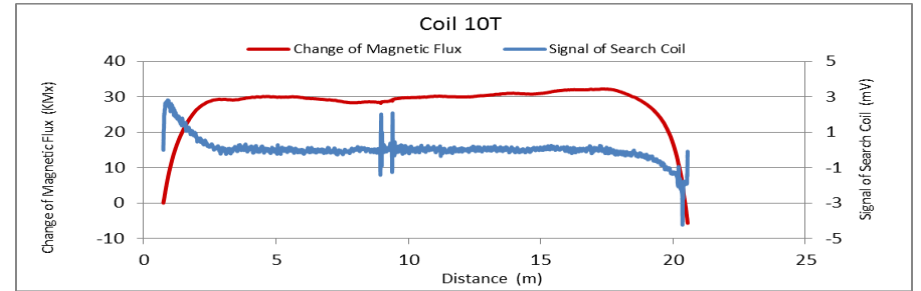


Figure A158. MMFM data of P8-401R-I2 tendon section.



Tokyo Rope USA, Inc.

File Name 【Pier-Tendon-Section】	Section Total Length (m)	Scanned Length		Note			
		Starting Point (m)	Ending Point (m)				
P8-402R-I2	21.48	0.7	20.8	Joint position: 9.2 m			
Identified Damage 1				Identified Damage 2			
Max Loss Point (m)	Section Loss (%)	Damage Length (m)	Damage Orientation	Max Loss Point (m)	Section Loss (%)	Damage Length (m)	Damage Orientation
—	—	—	—	—	—	—	—

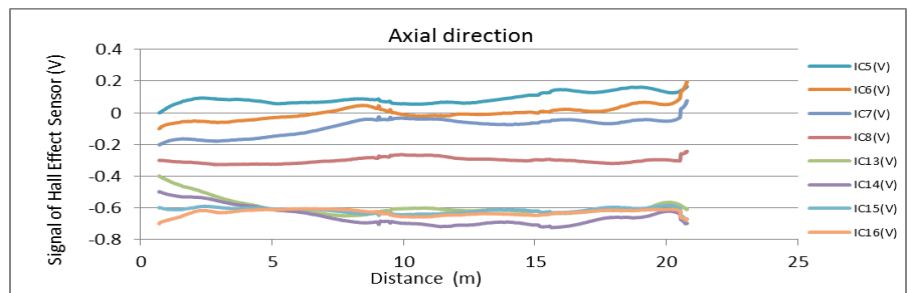
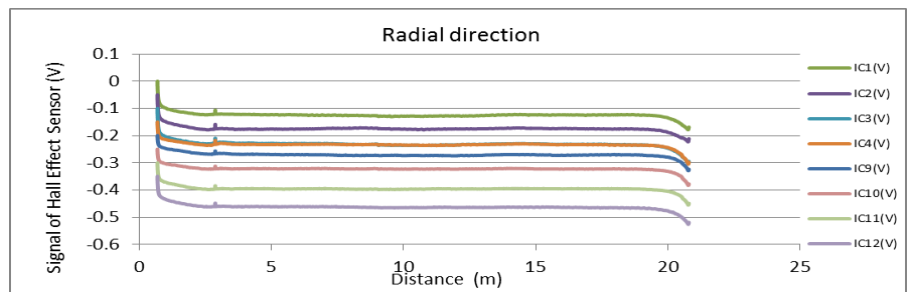
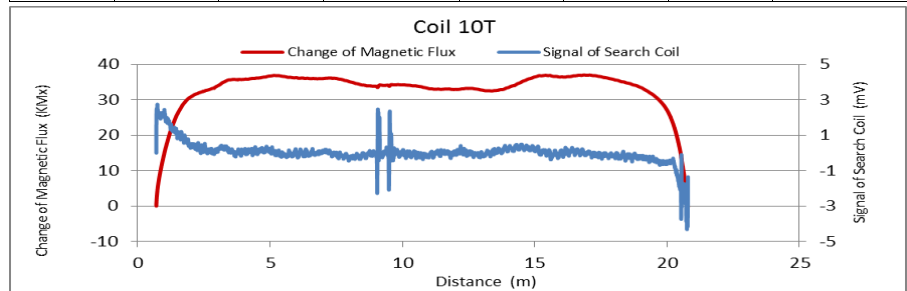


Figure A159. MMFM data of P8-402R-I2 tendon section.

File Name 【Pier-Tendon-Section】	Section Total Length (m)	Scanned Length		Note			
		Starting Point (m)	Ending Point (m)				
P8-401L-I2	21.47	0.73	21.01	Joint position: 9.17 m			
Identified Damage 1				Identified Damage 2			
Max Loss Point (m)	Section Loss (%)	Damage Length (m)	Damage Orientation	Max Loss Point (m)	Section Loss (%)	Damage Length (m)	Damage Orientation
—	—	—	—	—	—	—	—

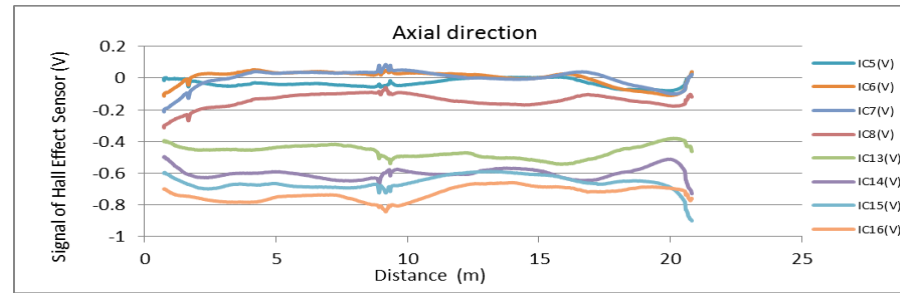
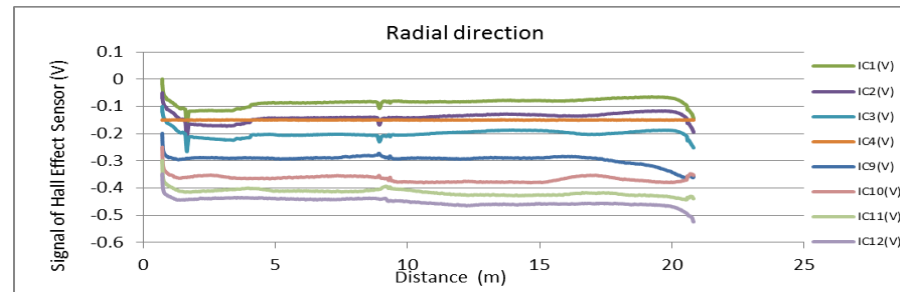
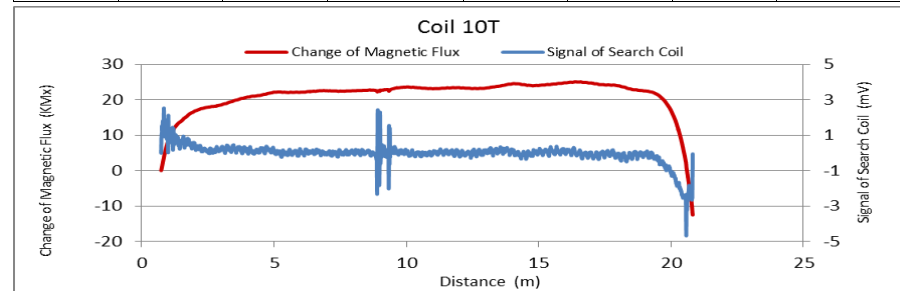


Figure A160. MMFM data of P8-401L-I2 tendon section.



Tokyo Rope USA, Inc.

File Name 【Pier-Tendon-Section】	Section Total Length (m)	Scanned Length		Note			
		Starting Point (m)	Ending Point (m)				
P8-402L-I2	21.47	0.69	20.93	Joint position: 9.2 m			
Identified Damage 1				Identified Damage 2			
Max Loss Point (m)	Section Loss (%)	Damage Length (m)	Damage Orientation	Max Loss Point (m)	Section Loss (%)	Damage Length (m)	Damage Orientation
—	—	—	—	—	—	—	—

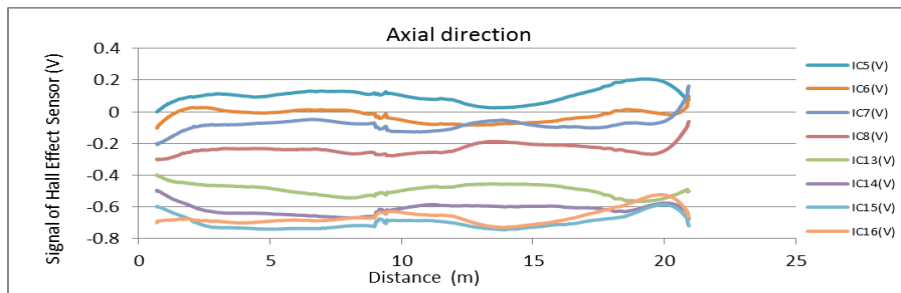
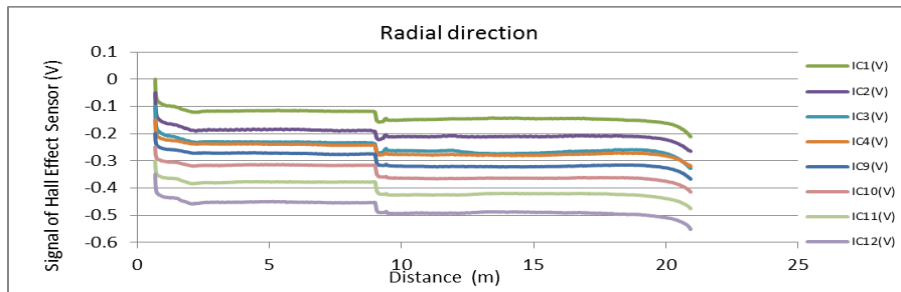
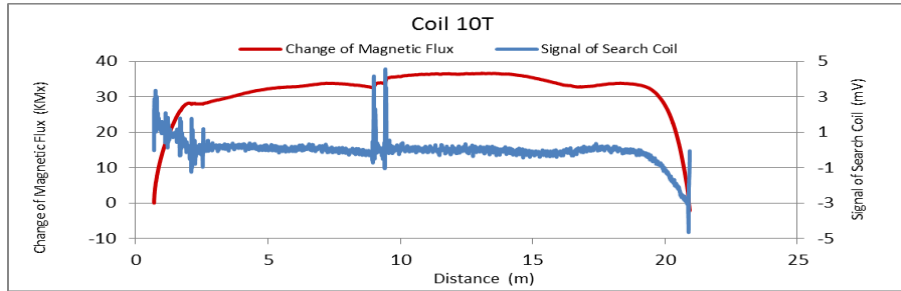


Figure A161. MMFM data of P8-402L-I2 tendon section.

File Name 【Pier-Tendon-Section】	Section Total Length (m)	Scanned Length		Note			
		Starting Point (m)	Ending Point (m)				
P8-401R-H2	9.34	1.25	8.82				
Identified Damage 1				Identified Damage 2			
Max Loss Point (m)	Section Loss (%)	Damage Length (m)	Damage Orientation	Max Loss Point (m)	Section Loss (%)	Damage Length (m)	Damage Orientation
—	—	—	—	—	—	—	—

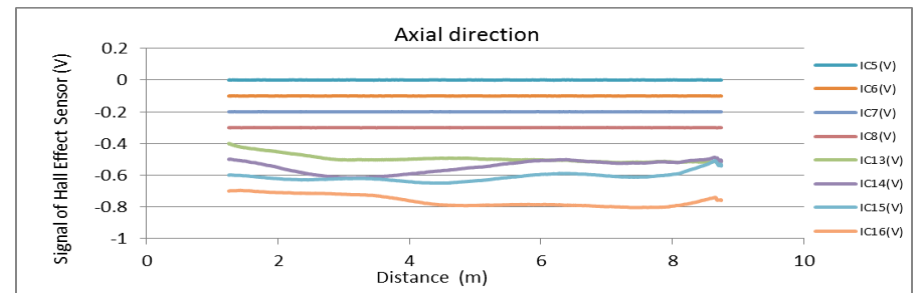
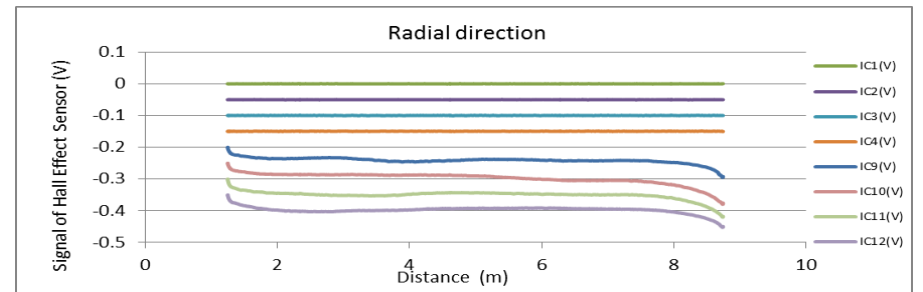
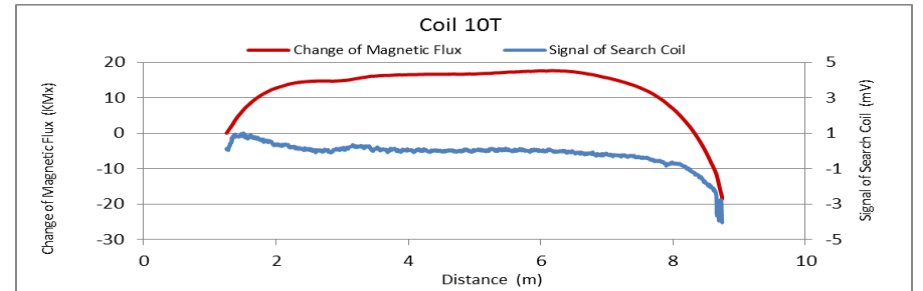


Figure A162. MMFM data of P8-401R-H2 tendon section.



Tokyo Rope USA, Inc.

File Name 【Pier-Tendon-Section】	Section Total Length (m)	Scanned Length		Note			
		Starting Point (m)	Ending Point (m)				
P8-402R-H1	9.34	0.95	8.92				
Identified Damage 1				Identified Damage 2			
Max Loss Point (m)	Section Loss (%)	Damage Length (m)	Damage Orientation	Max Loss Point (m)	Section Loss (%)	Damage Length (m)	Damage Orientation
—	—	—	—	—	—	—	—

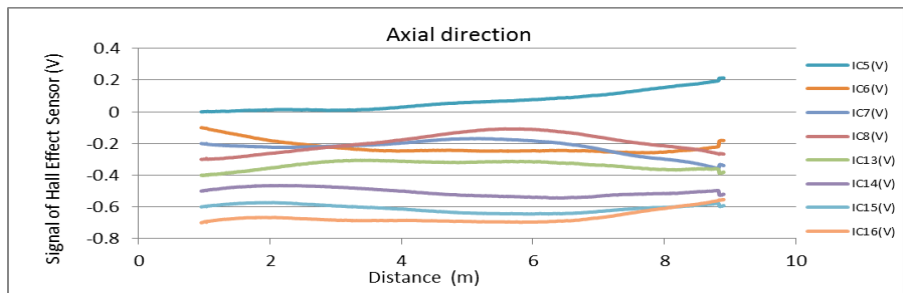
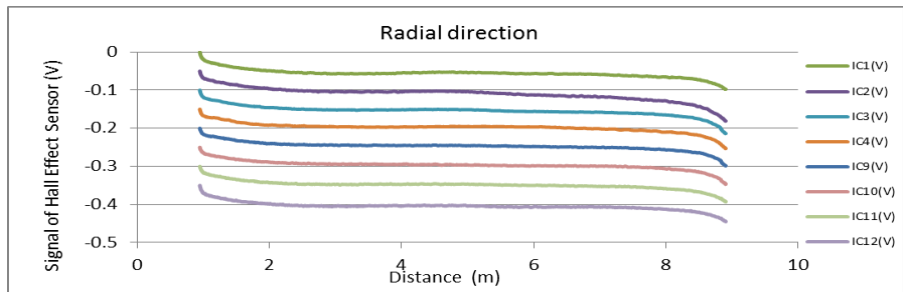
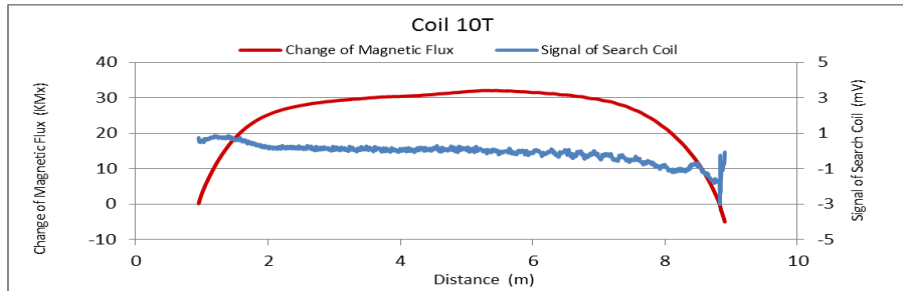


Figure A163. MMFM data of P8-402R-H1 tendon section.

File Name 【Pier-Tendon-Section】	Section Total Length (m)	Scanned Length		Note			
		Starting Point (m)	Ending Point (m)				
P8-401L-H2	9.36	0.62	8.97				
Identified Damage 1				Identified Damage 2			
Max Loss Point (m)	Section Loss (%)	Damage Length (m)	Damage Orientation	Max Loss Point (m)	Section Loss (%)	Damage Length (m)	Damage Orientation
—	—	—	—	—	—	—	—

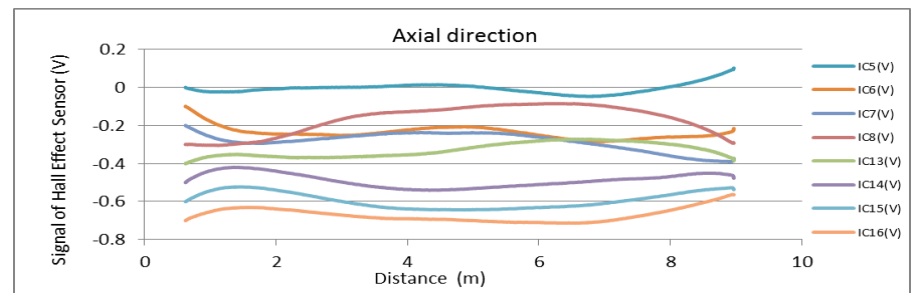
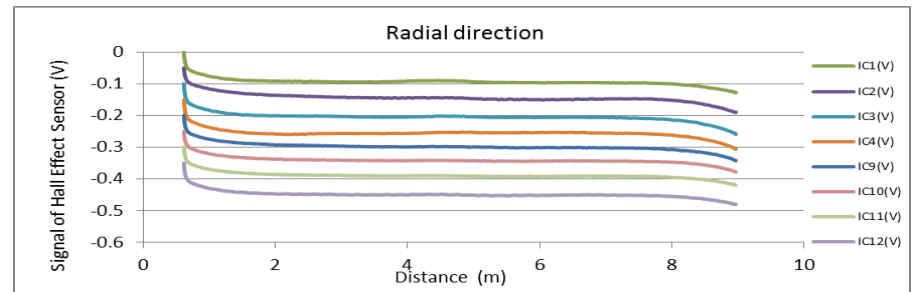
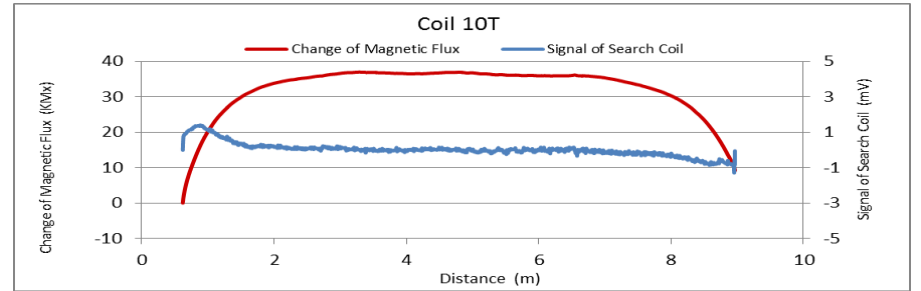


Figure A164. MMFM data of P8-401L-H2 tendon section.



Tokyo Rope USA, Inc.

File Name 【Pier-Tendon-Section】	Section Total Length (m)	Scanned Length		Note			
		Starting Point (m)	Ending Point (m)				
P8-402L-H2	9.36	0.68	8.77				
Identified Damage 1				Identified Damage 2			
Max Loss Point (m)	Section Loss (%)	Damage Length (m)	Damage Orientation	Max Loss Point (m)	Section Loss (%)	Damage Length (m)	Damage Orientation
—	—	—	—	—	—	—	—

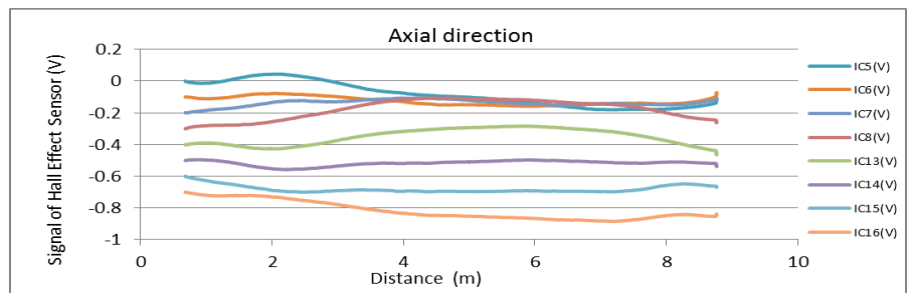
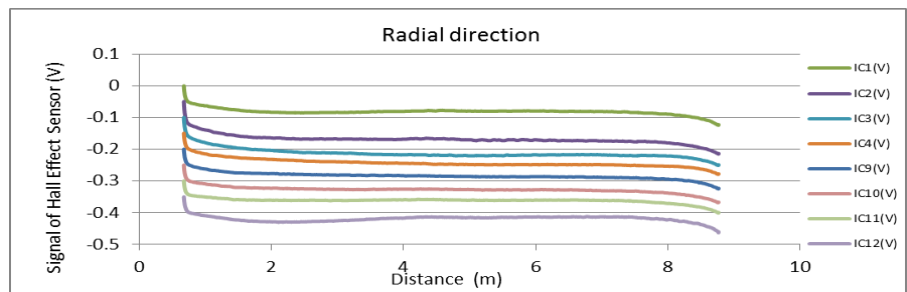
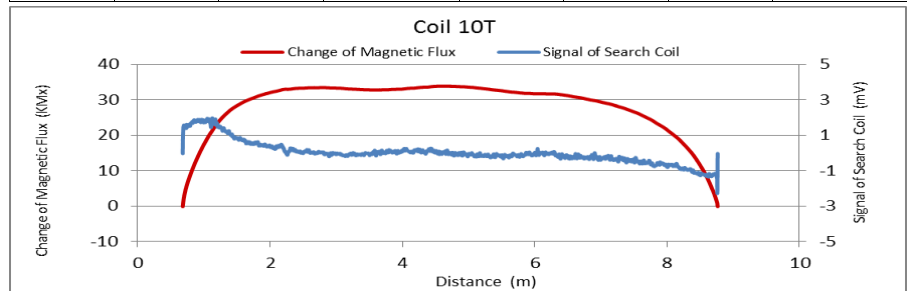


Figure A165. MMFM data of P8-402L-H2 tendon section.

File Name 【Pier-Tendon-Section】	Section Total Length (m)	Scanned Length		Note			
		Starting Point (m)	Ending Point (m)				
P9-401R-H1	9.33	0.74	8.7				
Identified Damage 1				Identified Damage 2			
Max Loss Point (m)	Section Loss (%)	Damage Length (m)	Damage Orientation	Max Loss Point (m)	Section Loss (%)	Damage Length (m)	Damage Orientation
—	—	—	—	—	—	—	—

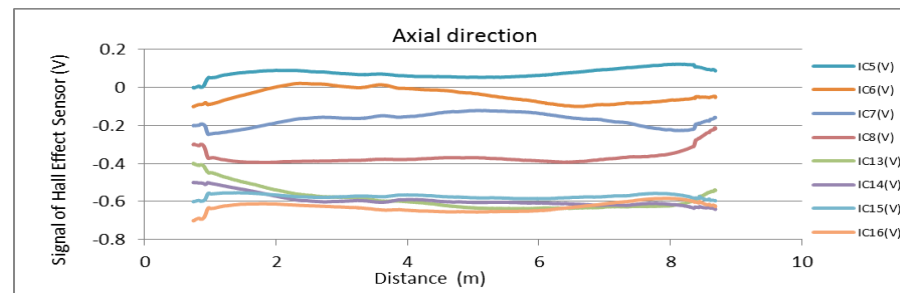
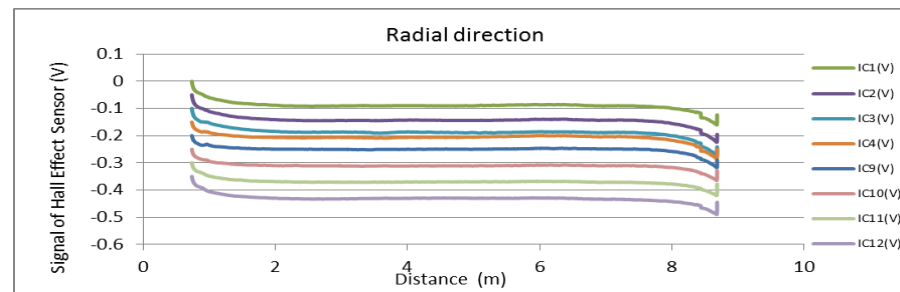
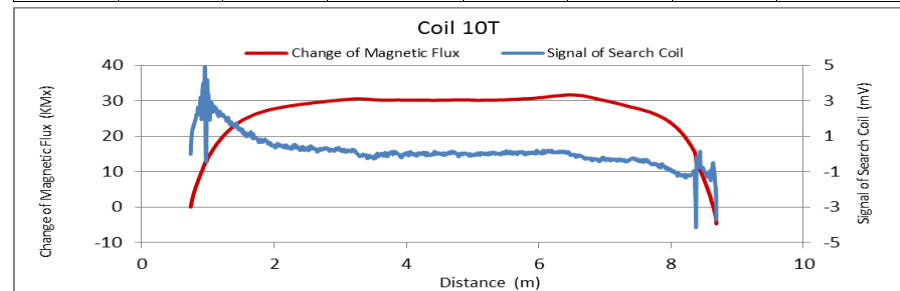


Figure A166. MMFM data of P9-401R-H1 tendon section.



Tokyo Rope USA, Inc.

File Name 【Pier-Tendon-Section】	Section Total Length (m)	Scanned Length		Note			
		Starting Point (m)	Ending Point (m)				
P9-402R-H1	9.33	0.81	8.49				
Identified Damage 1				Identified Damage 2			
Max Loss Point (m)	Section Loss (%)	Damage Length (m)	Damage Orientation	Max Loss Point (m)	Section Loss (%)	Damage Length (m)	Damage Orientation
—	—	—	—	—	—	—	—

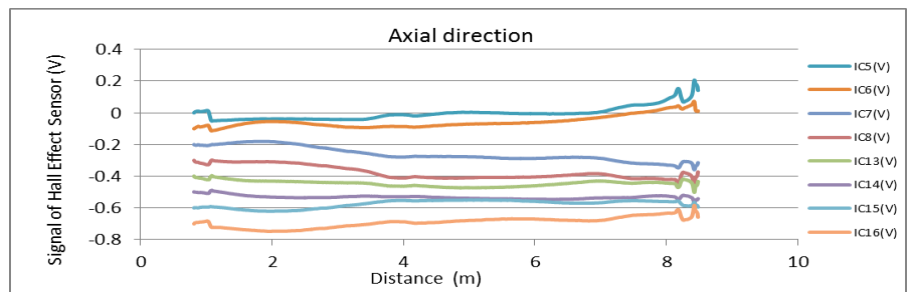
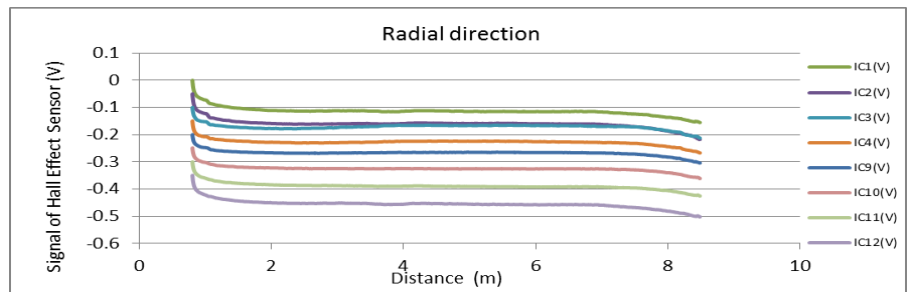
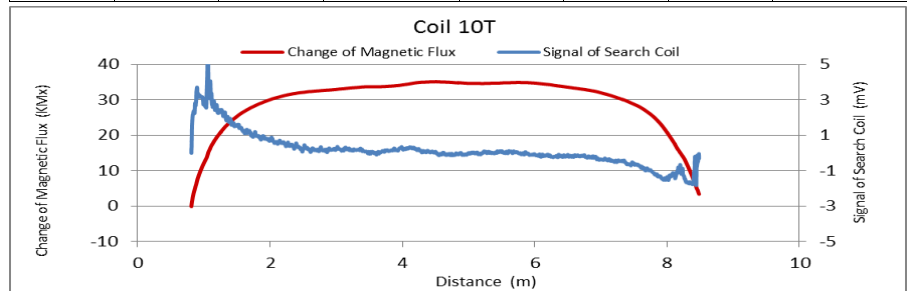


Figure A167. MMFM data of P9-402R-H1 tendon section.

File Name 【Pier-Tendon-Section】	Section Total Length (m)	Scanned Length		Note			
		Starting Point (m)	Ending Point (m)				
P9-401L-H1	9.28	0.45	8.43				
Identified Damage 1				Identified Damage 2			
Max Loss Point (m)	Section Loss (%)	Damage Length (m)	Damage Orientation	Max Loss Point (m)	Section Loss (%)	Damage Length (m)	Damage Orientation
—	—	—	—	—	—	—	—

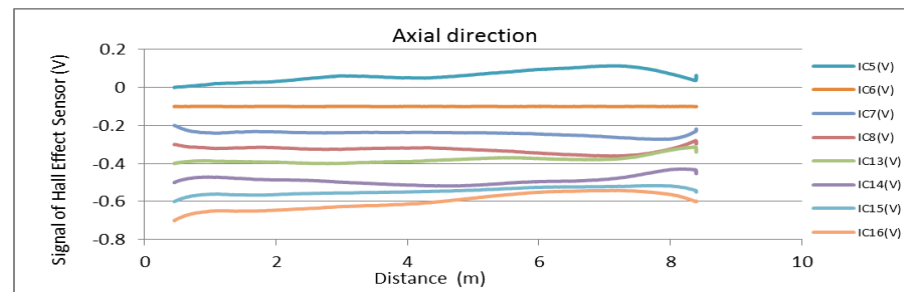
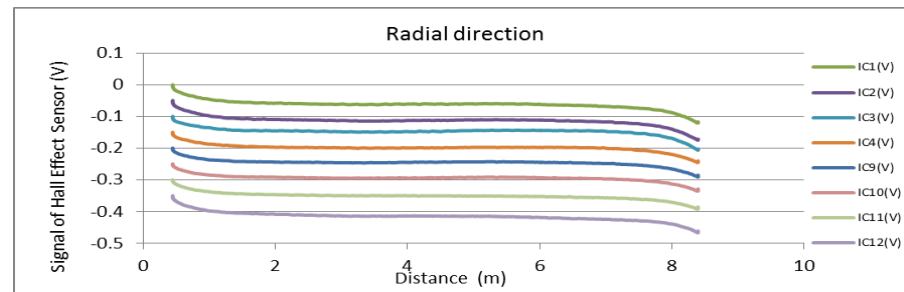
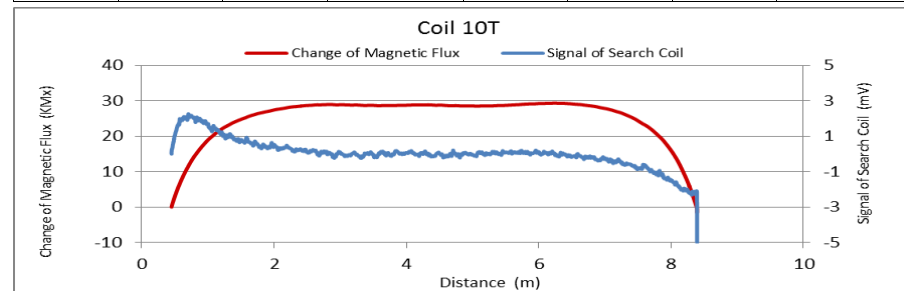


Figure A168. MMFM data of P9-401L-H1 tendon section.



Tokyo Rope USA, Inc.

File Name 【Pier-Tendon-Section】	Section Total Length (m)	Scanned Length		Note			
		Starting Point (m)	Ending Point (m)				
P9-402L-H1	9.28	0.47	8.43				
Identified Damage 1				Identified Damage 2			
Max Loss Point (m)	Section Loss (%)	Damage Length (m)	Damage Orientation	Max Loss Point (m)	Section Loss (%)	Damage Length (m)	Damage Orientation
—	—	—	—	—	—	—	—

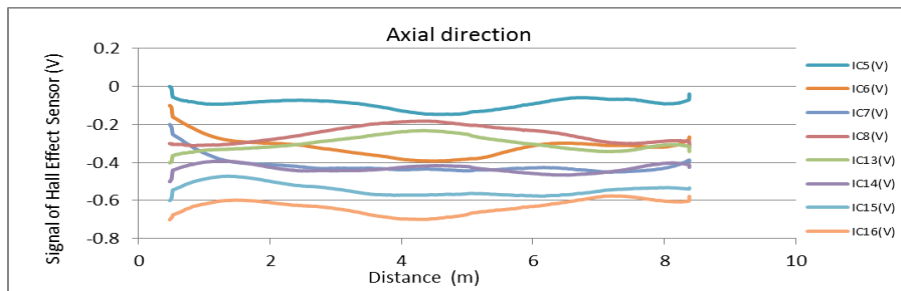
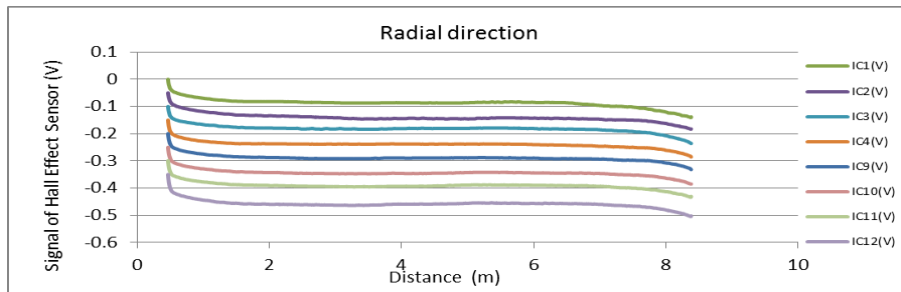
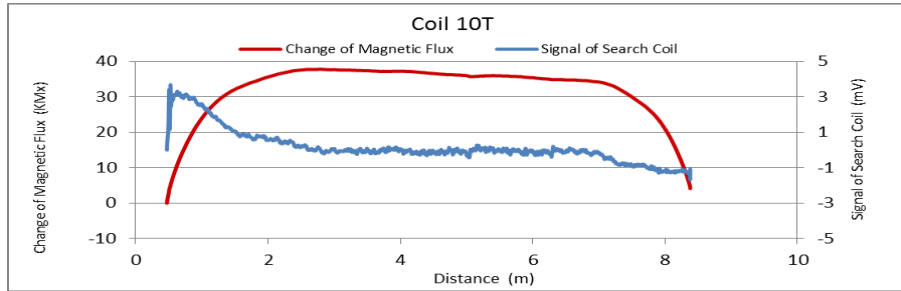


Figure A169. MMFM data of P9-402L-H1 tendon section.

File Name 【Pier-Tendon-Section】	Section Total Length (m)	Scanned Length		Note			
		Starting Point (m)	Ending Point (m)				
P9-402R-I1	21.57	0.57	20.86	Joint position: 12.26 m			
Identified Damage 1				Identified Damage 2			
Max Loss Point (m)	Section Loss (%)	Damage Length (m)	Damage Orientation	Max Loss Point (m)	Section Loss (%)	Damage Length (m)	Damage Orientation
—	—	—	—	—	—	—	—

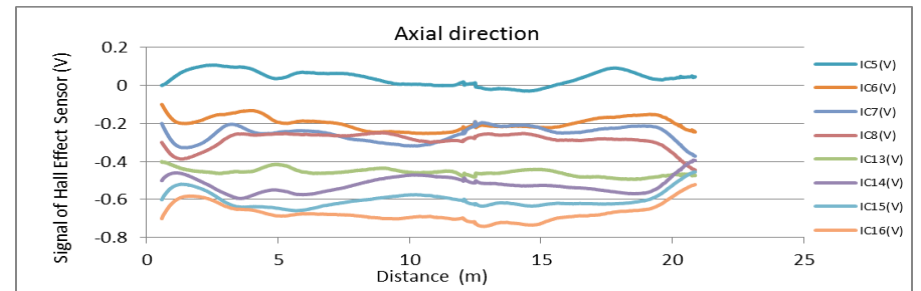
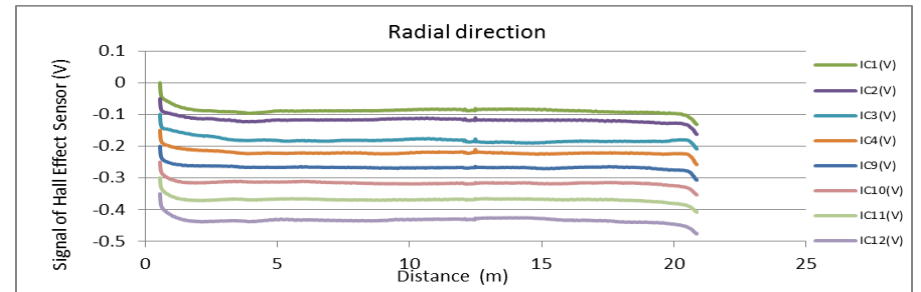
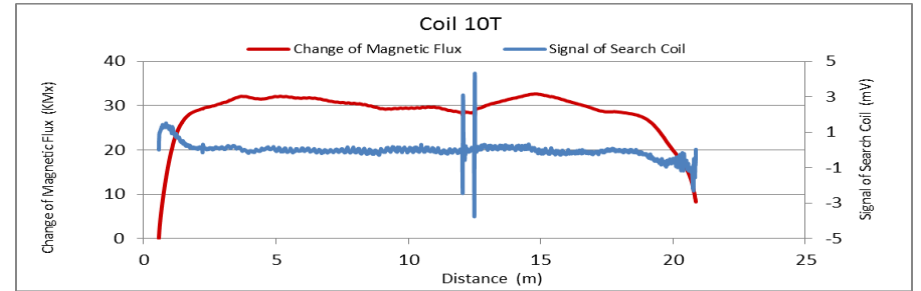


Figure A170. MMFM data of P9-402R-I1 tendon section.



Tokyo Rope USA, Inc.

File Name 【Pier-Tendon-Section】	Section Total Length (m)	Scanned Length		Note			
		Starting Point (m)	Ending Point (m)				
P9-401L-I1	21.53	0.47	20.48	Joint position: 12.28 m			
Identified Damage 1				Identified Damage 2			
Max Loss Point (m)	Section Loss (%)	Damage Length (m)	Damage Orientation	Max Loss Point (m)	Section Loss (%)	Damage Length (m)	Damage Orientation
—	—	—	—	—	—	—	—

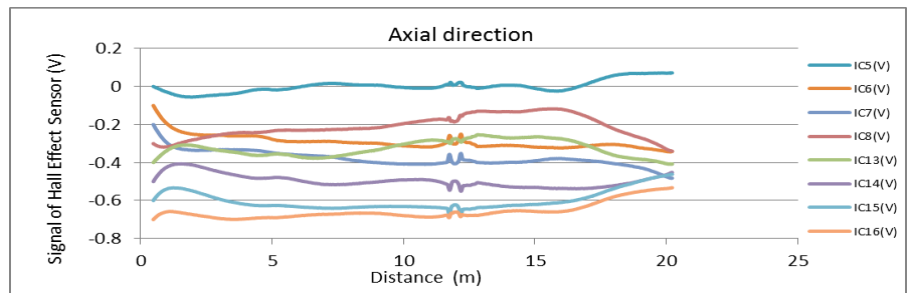
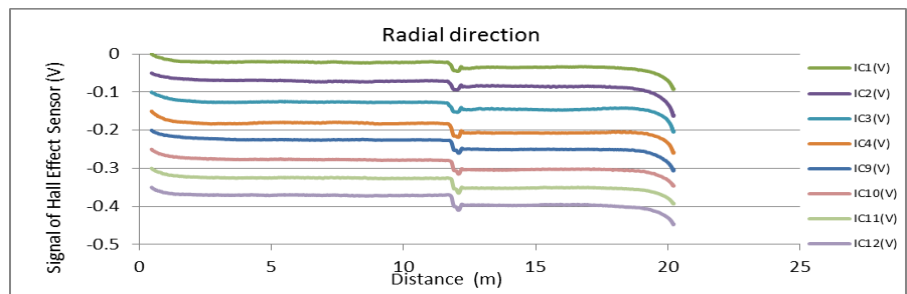
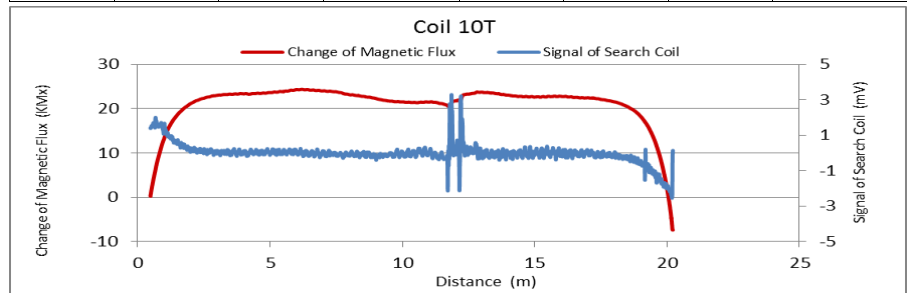


Figure A171. MMFM data of P9-401L-I1 tendon section.

File Name 【Pier-Tendon-Section】	Section Total Length (m)	Scanned Length		Note			
		Starting Point (m)	Ending Point (m)				
P9-401R-I2	31.33	1.85	30.72	Joint position: 4.51 m, 16.61 m			
Identified damage 1				Identified damage 2			
Max Loss Point (m)	Section Loss (%)	Damage Length (m)	Damage Orientation	Max Loss Point (m)	Section Loss (%)	Damage Length (m)	Damage Orientation
—	—	—	—	—	—	—	—

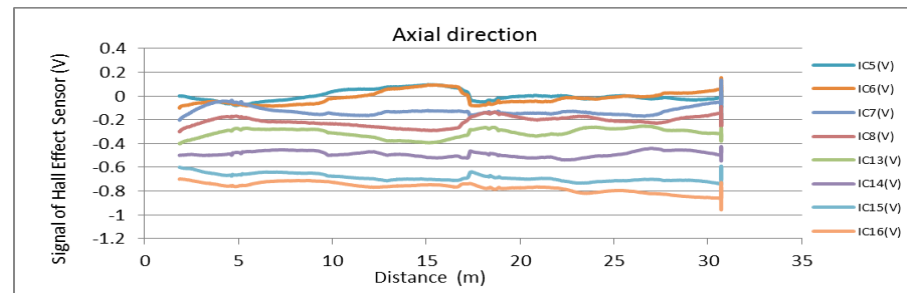
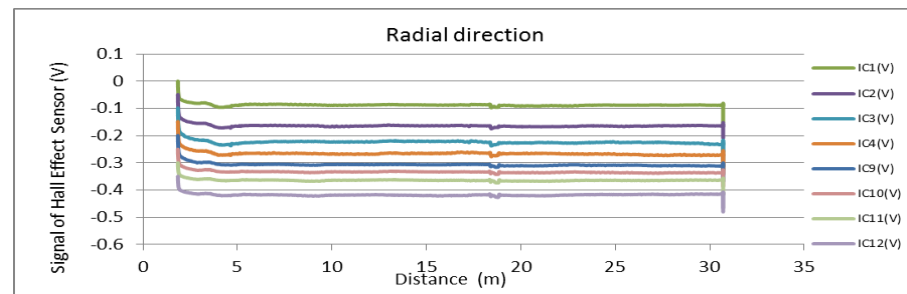
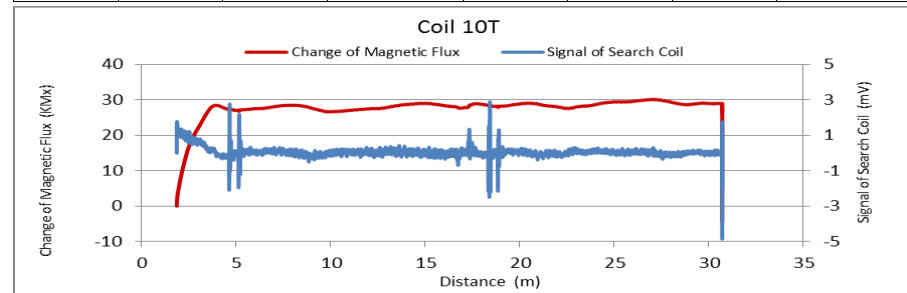


Figure A172. MMFM data of P9-401R-I2 tendon section.



Tokyo Rope USA, Inc.

File Name 【Pier-Tendon-Section】	Section Total Length (m)	Scanned Length		Note			
		Starting Point (m)	Ending Point (m)				
P9-401L-I2	21.51	0.52	20.44	Joint position: 9.27 m			
Identified Damage 1				Identified Damage 2			
Max Loss Point (m)	Section Loss (%)	Damage Length (m)	Damage Orientation	Max Loss Point (m)	Section Loss (%)	Damage Length (m)	Damage Orientation
—	—	—	—	—	—	—	—

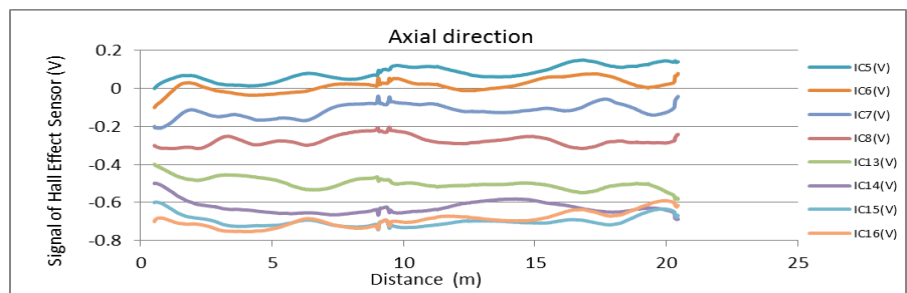
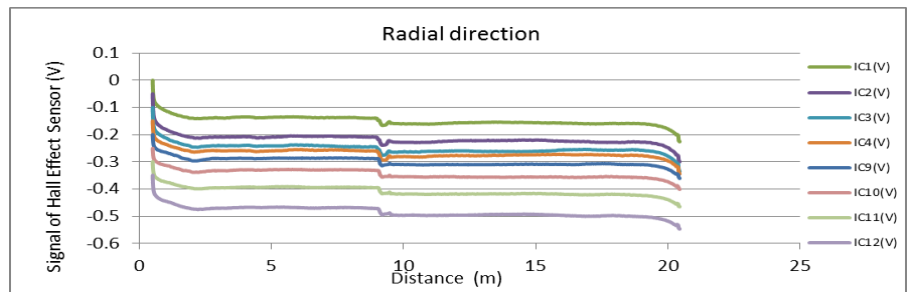
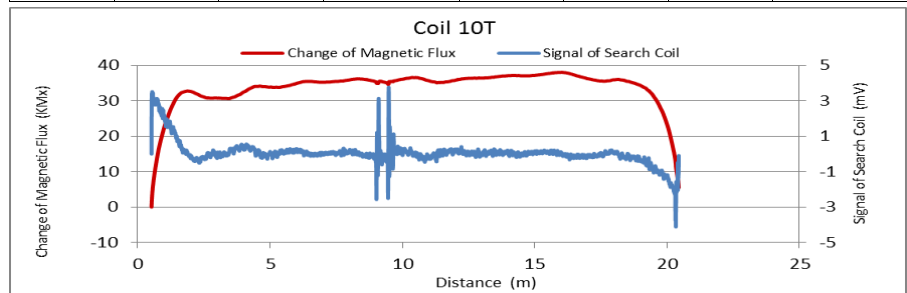


Figure A173. MMFM data of P9-401L-I2 tendon section.

File Name 【Pier-Tendon-Section】	Section Total Length (m)	Scanned Length		Note			
		Starting Point (m)	Ending Point (m)				
P9-402L-I2	31.34	1.75	30.8	Joint position: 13.65 m, 27.25 m			
Identified Damage 1				Identified Damage 2			
Max Loss Point (m)	Section Loss (%)	Damage Length (m)	Damage Orientation	Max Loss Point (m)	Section Loss (%)	Damage Length (m)	Damage Orientation
—	—	—	—	—	—	—	—

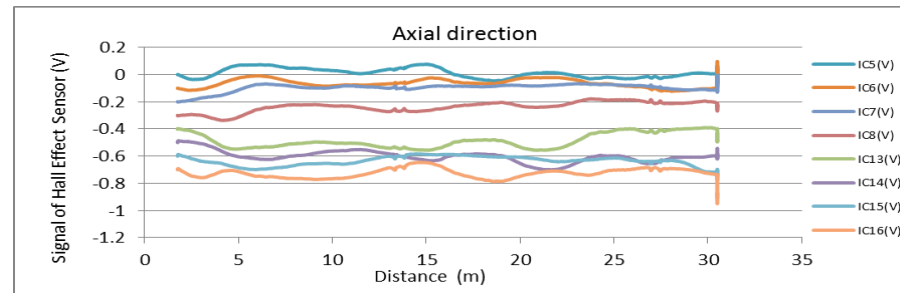
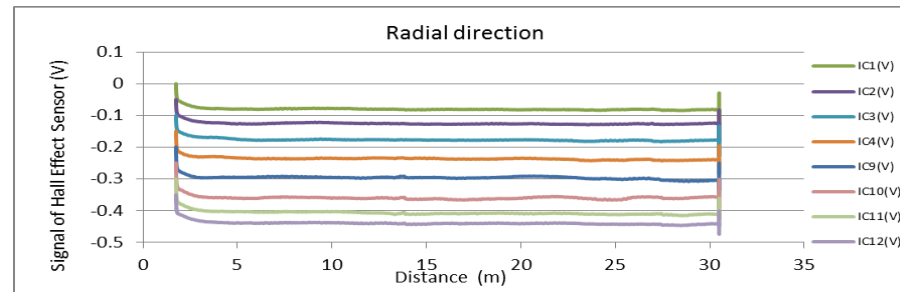
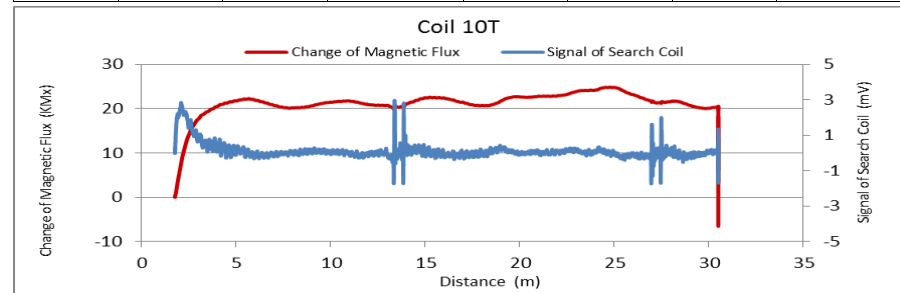


Figure A174. MMFM data of P9-402L-I2 tendon section.



Tokyo Rope USA, Inc.

File Name 【Pier-Tendon-Section】	Section Total Length (m)	Scanned Length		Note			
		Starting Point (m)	Ending Point (m)				
P9-402R-H2	9.38	0.95	8.88				
Identified Damage 1				Identified Damage 2			
Max Loss Point (m)	Section Loss (%)	Damage Length (m)	Damage Orientation	Max Loss Point (m)	Section Loss (%)	Damage Length (m)	Damage Orientation
—	—	—	—	—	—	—	—

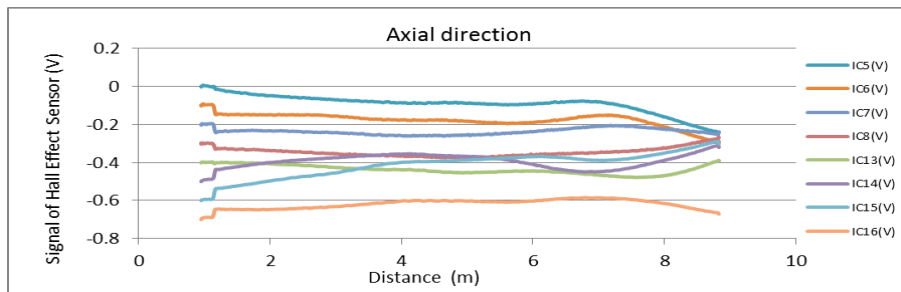
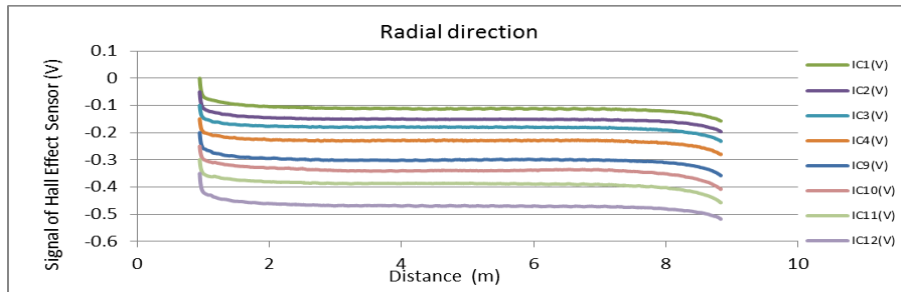
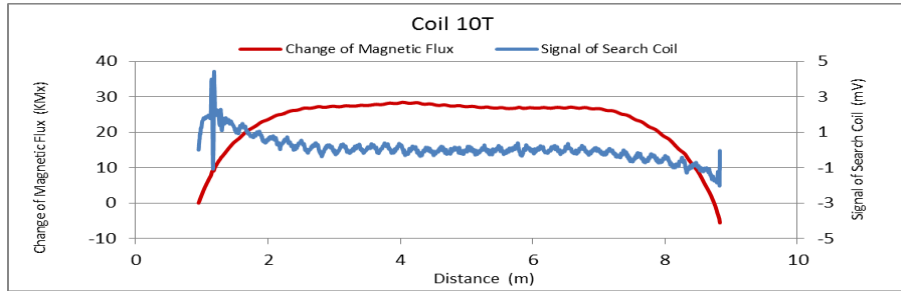


Figure A175. MMFM data of P9-402R-H2 tendon section.

File Name 【Pier-Tendon-Section】	Section Total Length (m)	Scanned Length		Note			
		Starting Point (m)	Ending Point (m)				
P10-402R-H1	9.4	0.62	8.59				
Identified Damage 1				Identified Damage 2			
Max Loss Point (m)	Section Loss (%)	Damage Length (m)	Damage Orientation	Max Loss Point (m)	Section Loss (%)	Damage Length (m)	Damage Orientation
—	—	—	—	—	—	—	—

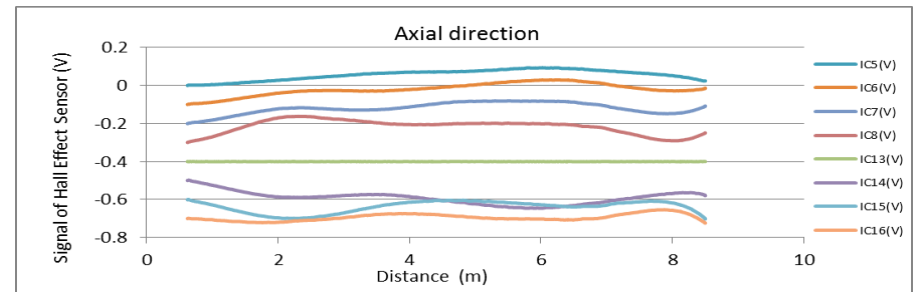
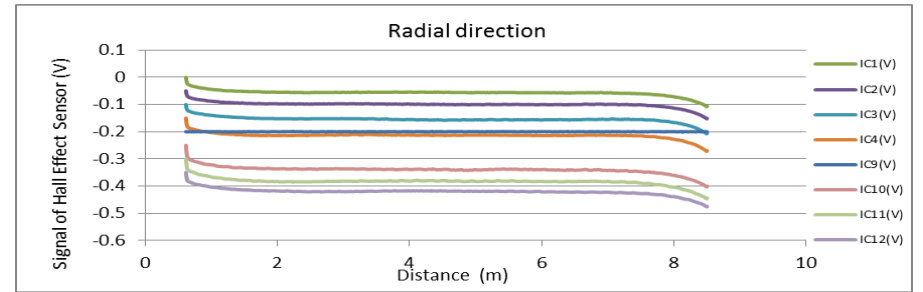
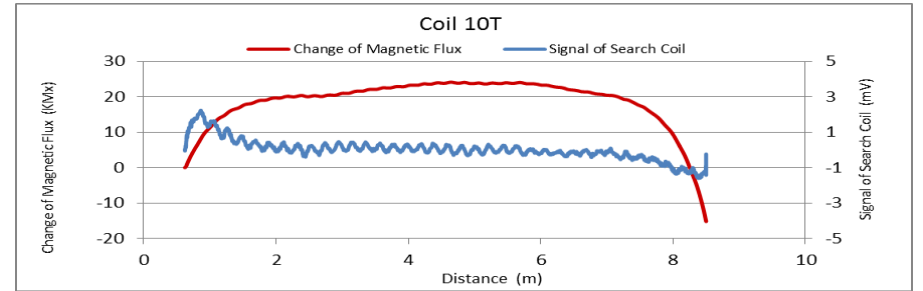


Figure A176. MMFM data of P10-402R-H1 tendon section.



Tokyo Rope USA, Inc.

File Name 【Pier-Tendon-Section】	Section Total Length (m)	Scanned Length		Note			
		Starting Point (m)	Ending Point (m)				
P10-401L-H1	9.5	0.57	8.77				
Identified Damage 1				Identified Damage 2			
Max Loss Point (m)	Section Loss (%)	Damage Length (m)	Damage Orientation	Max Loss Point (m)	Section Loss (%)	Damage Length (m)	Damage Orientation
—	—	—	—	—	—	—	—

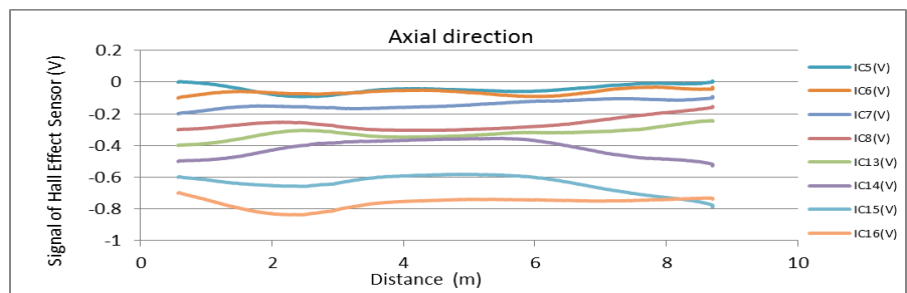
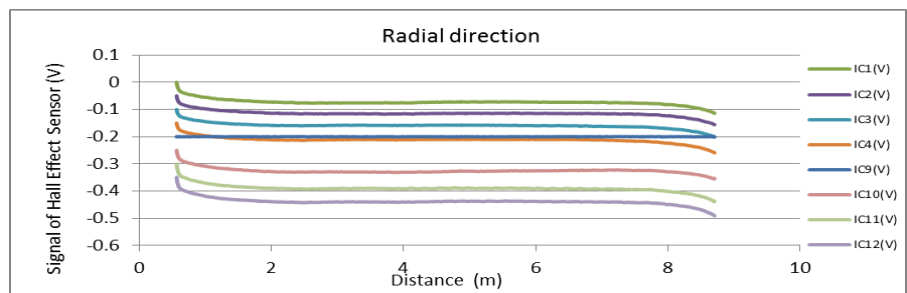
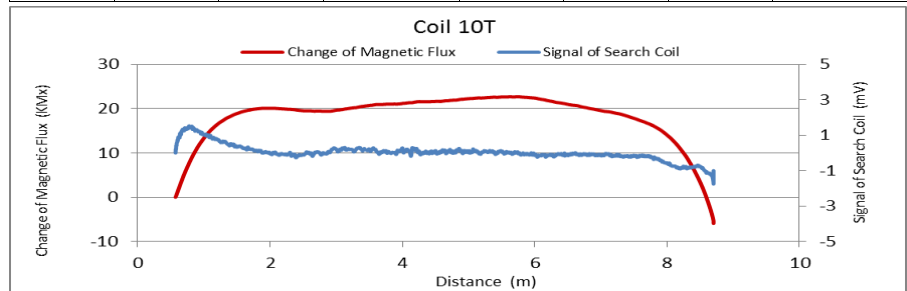


Figure A177. MMFM data of P10-401L-H1 tendon section.

File Name 【Pier-Tendon-Section】	Section Total Length (m)	Scanned Length		Note			
		Starting Point (m)	Ending Point (m)				
P10-402L-I1	31.37	0.45	29.32	Joint position: 3.07 m, 16.3 m			
Identified Damage 1				Identified Damage 2			
Max Loss Point (m)	Section Loss (%)	Damage Length (m)	Damage Orientation	Max Loss Point (m)	Section Loss (%)	Damage Length (m)	Damage Orientation
—	—	—	—	—	—	—	—

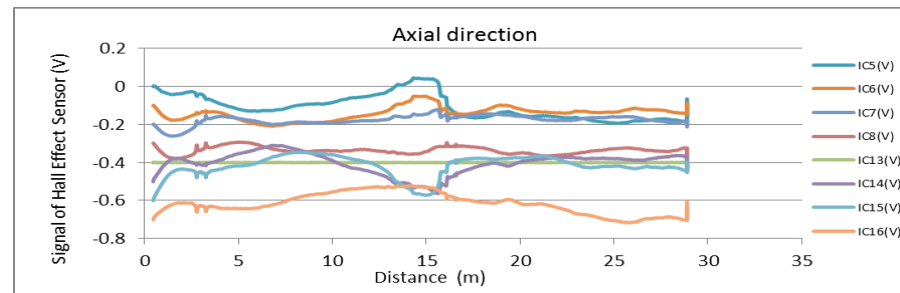
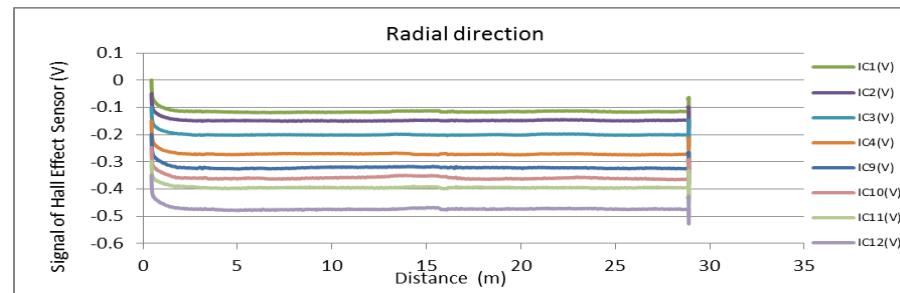
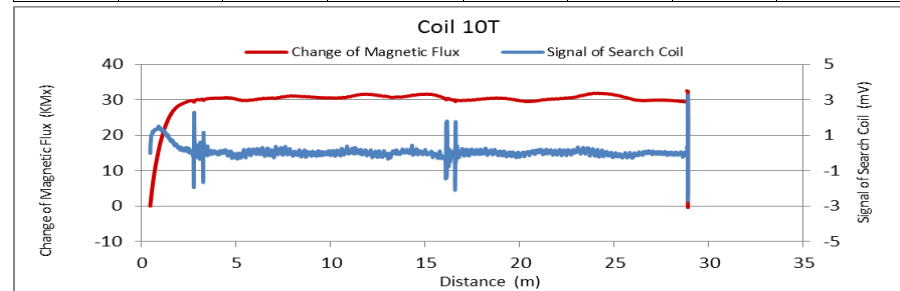


Figure A178. MMFM data of P10-402L-I1 tendon section.



Tokyo Rope USA, Inc.

File Name 【Pier-Tendon-Section】	Section Total Length (m)	Scanned Length		Note			
		Starting Point (m)	Ending Point (m)				
P10-401R-I1	31.33	0.41	29.16	Joint position: 7.8 m, 21.4 m			
Identified Damage 1				Identified Damage 2			
Max Loss Point (m)	Section Loss (%)	Damage Length (m)	Damage Orientation	Max Loss Point (m)	Section Loss (%)	Damage Length (m)	Damage Orientation
—	—	—	—	—	—	—	—

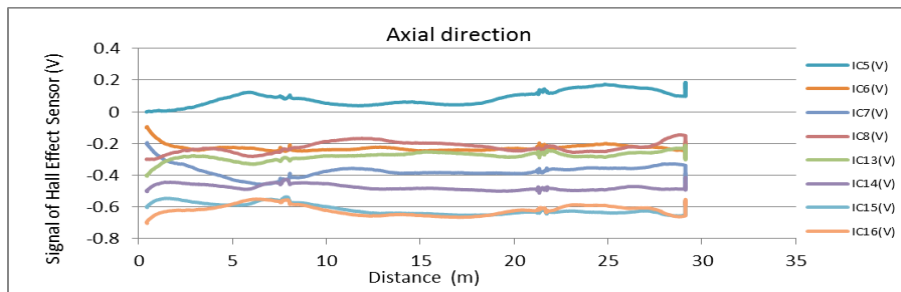
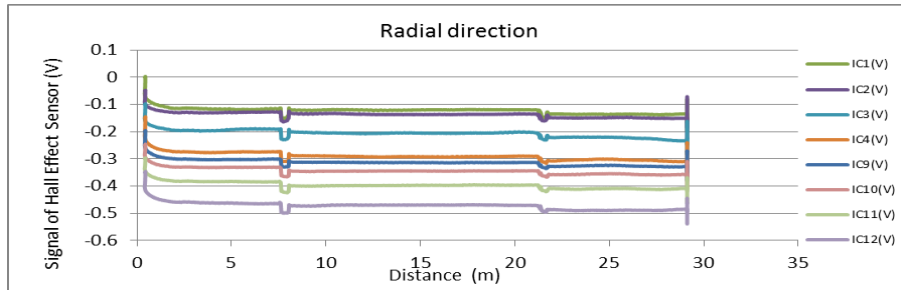
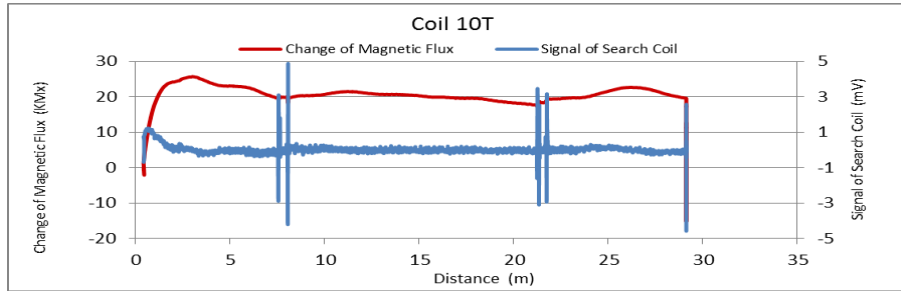


Figure A179. MMFM data of P10-401R-I1 tendon section.

File Name 【Pier-Tendon-Section】	Section Total Length (m)	Scanned Length		Note			
		Starting Point (m)	Ending Point (m)				
P10-402R-I1	21.47	0.5	20.76	Joint position: 12.31 m, 19.84 m			
Identified Damage 1				Identified Damage 2			
Max Loss Point (m)	Section Loss (%)	Damage Length (m)	Damage Orientation	Max Loss Point (m)	Section Loss (%)	Damage Length (m)	Damage Orientation
—	—	—	—	—	—	—	—

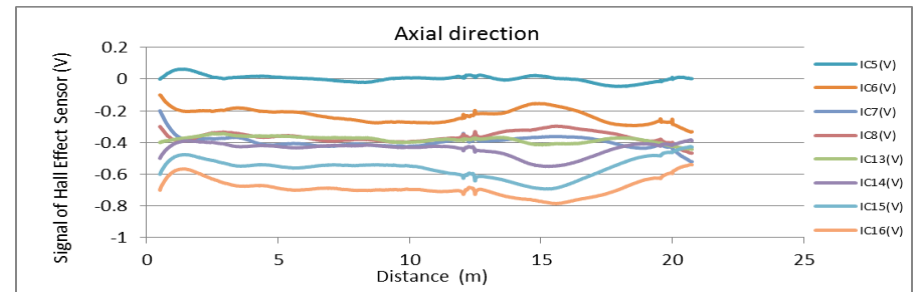
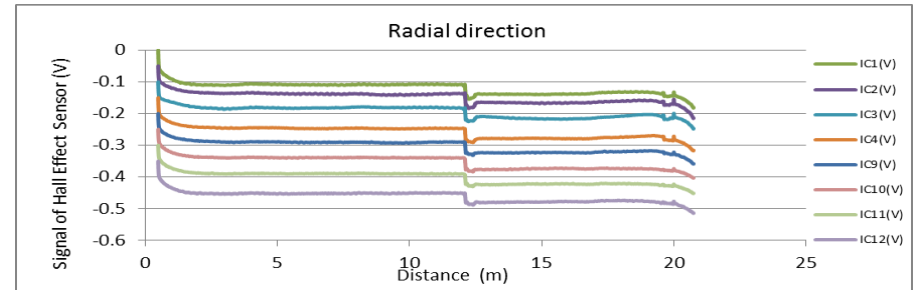
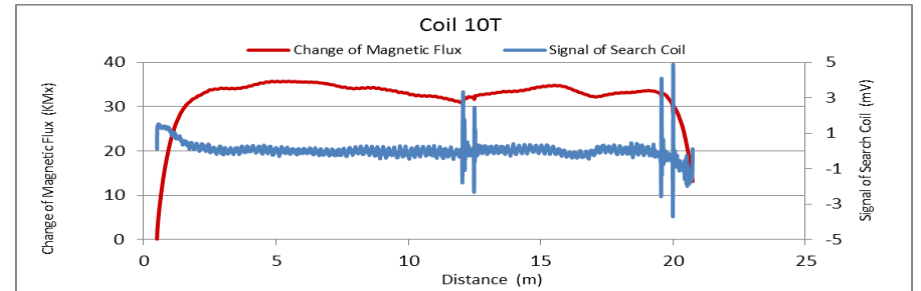


Figure A180. MMFM data of P10-402R-I1 tendon section.



Tokyo Rope USA, Inc.

File Name 【Pier-Tendon-Section】	Section Total Length (m)	Scanned Length		Note			
		Starting Point (m)	Ending Point (m)				
P10-401R-I2	21.42	0.65	20.7	Joint position: 9.06 m			
Identified Damage 1				Identified Damage 2			
Max Loss Point (m)	Section Loss (%)	Damage Length (m)	Damage Orientation	Max Loss Point (m)	Section Loss (%)	Damage Length (m)	Damage Orientation
—	—	—	—	—	—	—	—

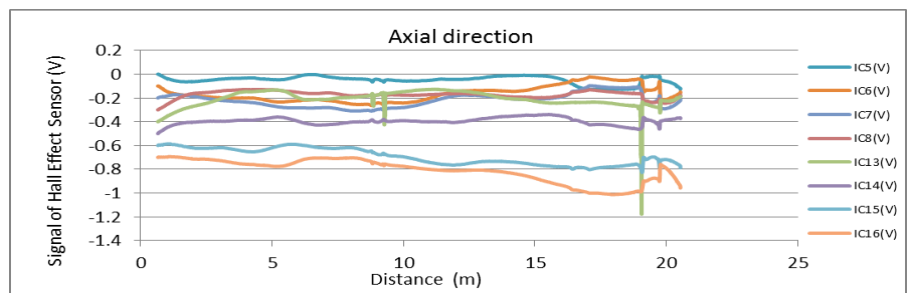
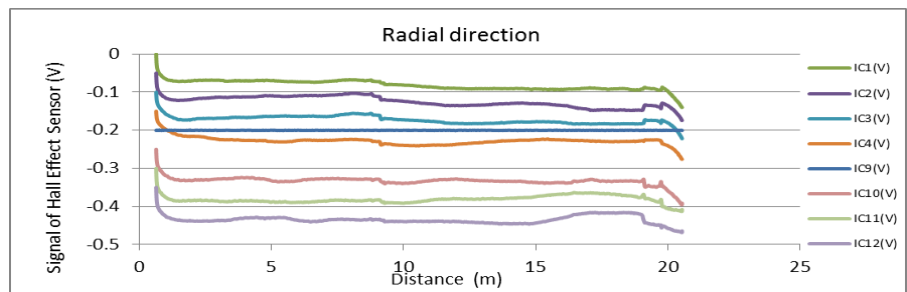
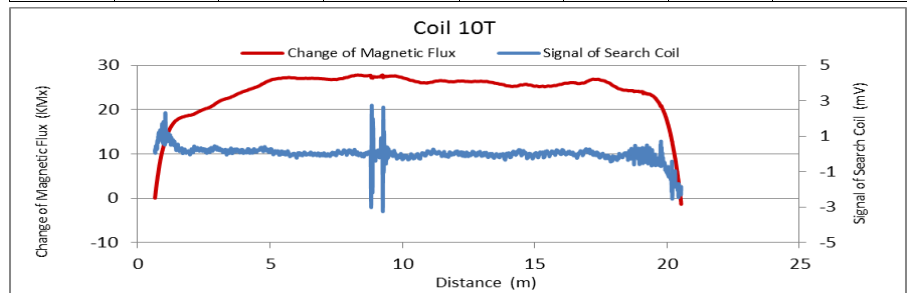


Figure A181. MMFM data of P10-401R-I2 tendon section.

File Name 【Pier-Tendon-Section】	Section Total Length (m)	Scanned Length		Note			
		Starting Point (m)	Ending Point (m)				
P10-402R-I2	21.38	0.67	19.88	Joint position: 9.1 m			
Identified Damage 1				Identified Damage 2			
Max Loss Point (m)	Section Loss (%)	Damage Length (m)	Damage Orientation	Max Loss Point (m)	Section Loss (%)	Damage Length (m)	Damage Orientation
—	—	—	—	—	—	—	—

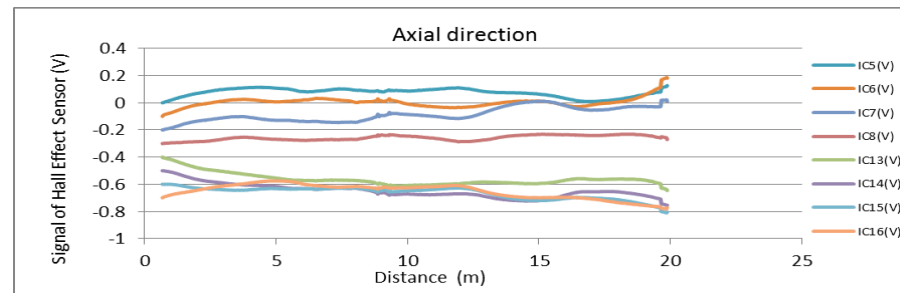
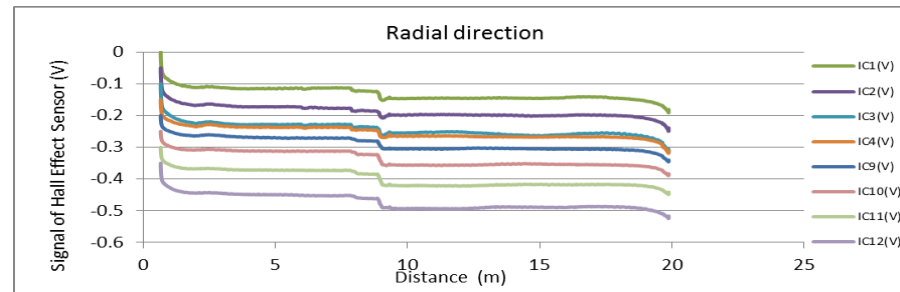
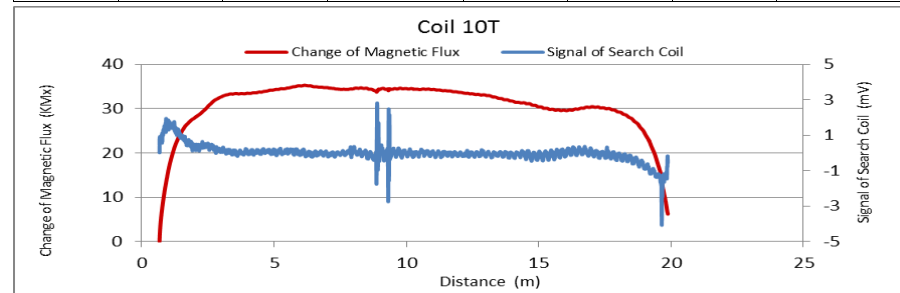


Figure A182. MMFM data of P10-402R-I2 tendon section.



Tokyo Rope USA, Inc.

File Name 【Pier-Tendon-Section】	Section Total Length (m)	Scanned Length		Note			
		Starting Point (m)	Ending Point (m)				
P10-401L-I2	21.5	0.72	19.87	Joint position: 9.15 m			
Identified Damage 1				Identified Damage 2			
Max Loss Point (m)	Section Loss (%)	Damage Length (m)	Damage Orientation	Max Loss Point (m)	Section Loss (%)	Damage Length (m)	Damage Orientation
—	—	—	—	—	—	—	—

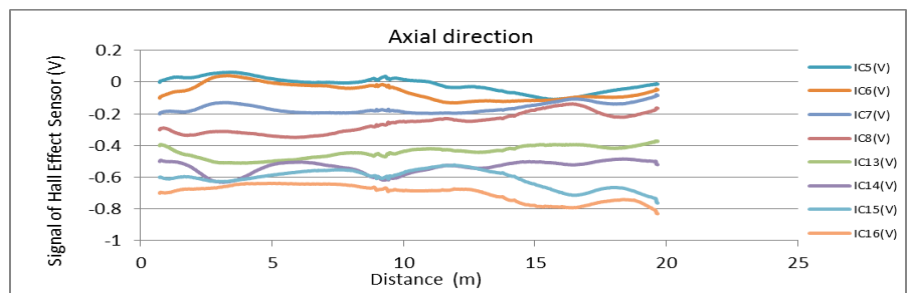
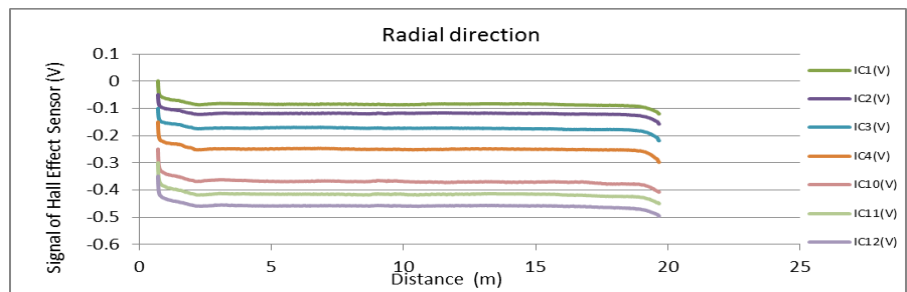
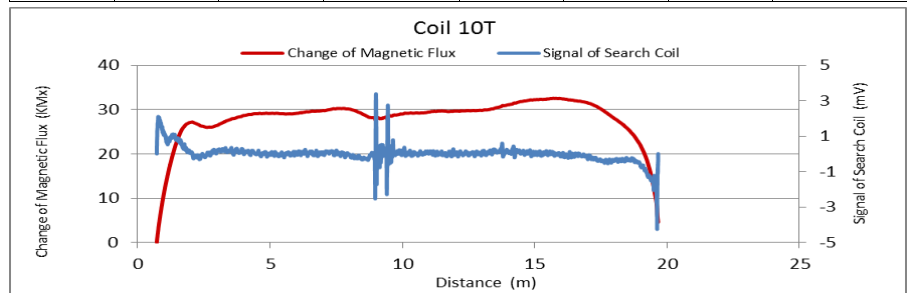


Figure A183. MMFM data of P10-401L-I2 tendon section.

File Name 【Pier-Tendon-Section】	Section Total Length (m)	Scanned Length		Note			
		Starting Point (m)	Ending Point (m)				
P10-401R-H1	9.33	0.61	8.91				
Identified Damage 1				Identified Damage 2			
Max Loss Point (m)	Section Loss (%)	Damage Length (m)	Damage Orientation	Max Loss Point (m)	Section Loss (%)	Damage Length (m)	Damage Orientation
—	—	—	—	—	—	—	—

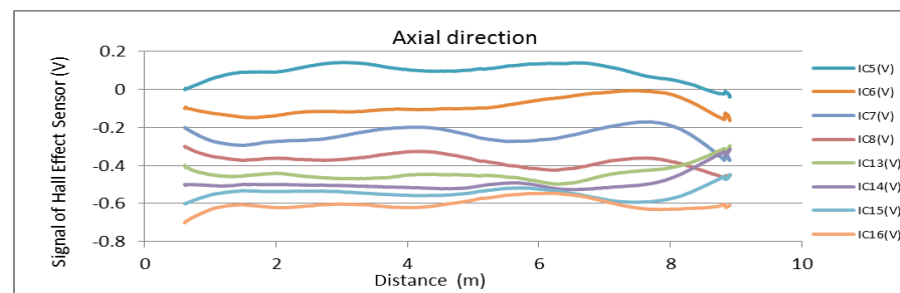
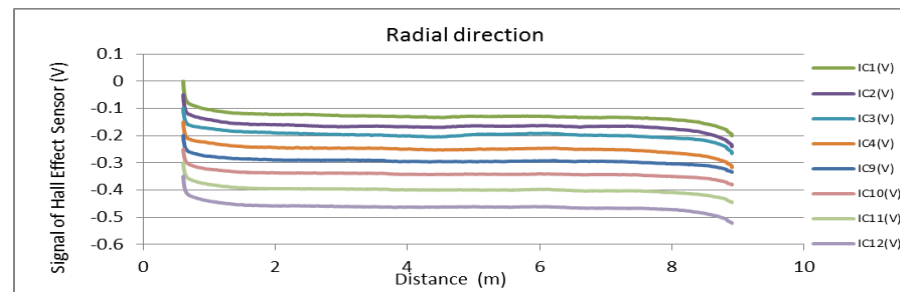
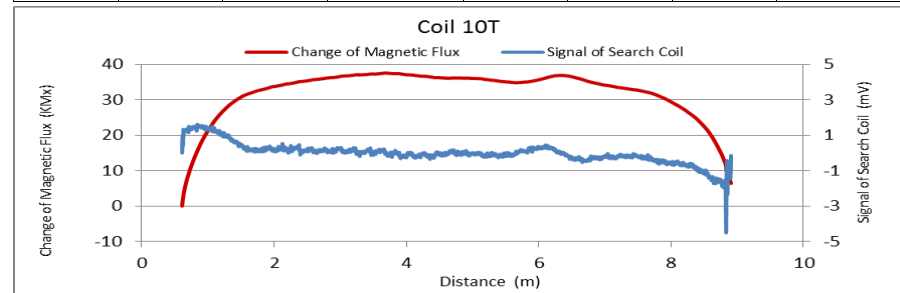


Figure A184. MMFM data of P10-401R-H1 tendon section.



Tokyo Rope USA, Inc.

File Name 【Pier-Tendon-Section】	Section Total Length (m)	Scanned Length		Note			
		Starting Point (m)	Ending Point (m)				
P10-402R-H2	9.33	0.63	8.86				
Identified Damage 1				Identified Damage 2			
Max Loss Point (m)	Section Loss (%)	Damage Length (m)	Damage Orientation	Max Loss Point (m)	Section Loss (%)	Damage Length (m)	Damage Orientation
—	—	—	—	—	—	—	—

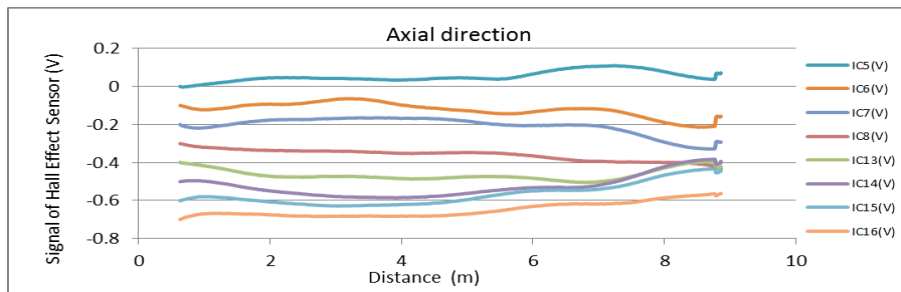
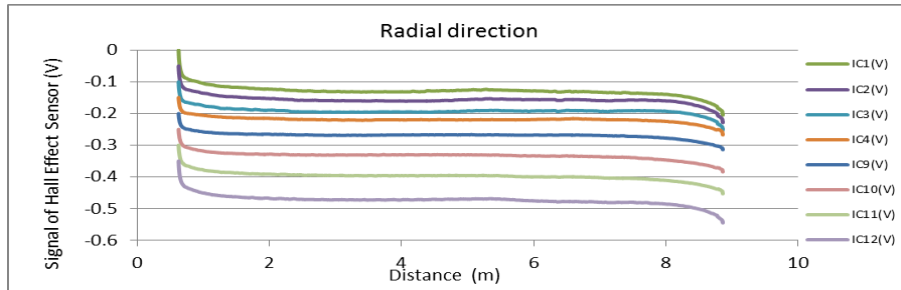
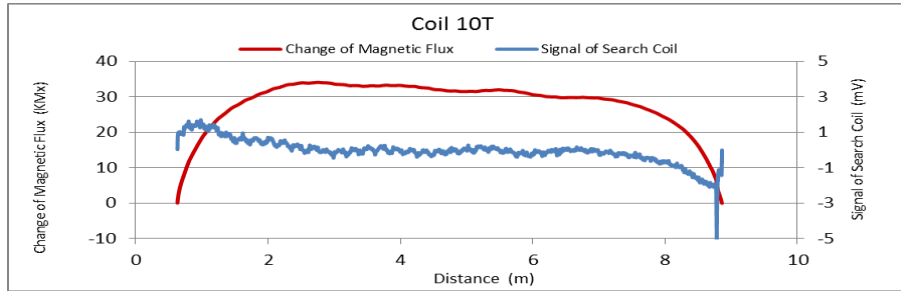


Figure A185. MMFM data of P10-402R-H2 tendon section.

File Name 【Pier-Tendon-Section】	Section Total Length (m)	Scanned Length		Note			
		Starting Point (m)	Ending Point (m)				
P10-401L-H2	9.41	0.74	8.91				
Identified Damage 1				Identified Damage 2			
Max Loss Point (m)	Section Loss (%)	Damage Length (m)	Damage Orientation	Max Loss Point (m)	Section Loss (%)	Damage Length (m)	Damage Orientation
—	—	—	—	—	—	—	—

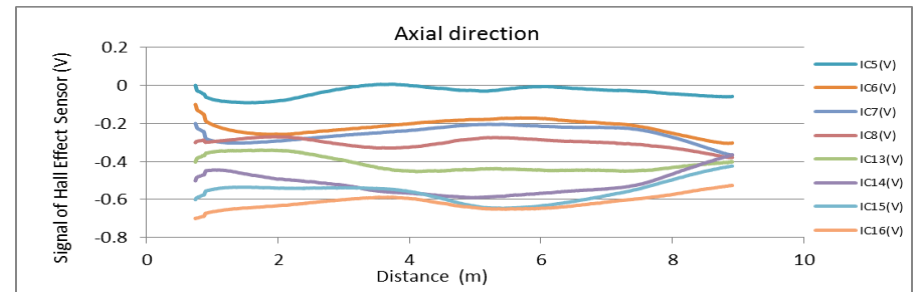
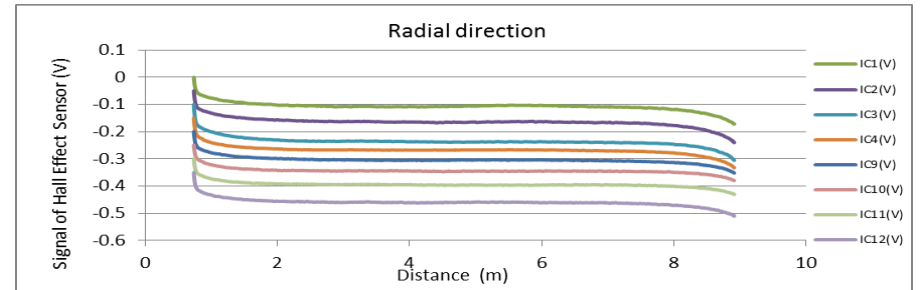
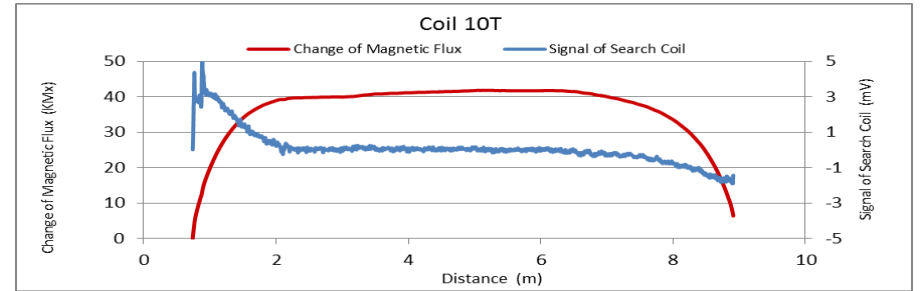


Figure A186. MMFM data of P10-401L-H2 tendon section.



Tokyo Rope USA, Inc.

File Name 【Pier-Tendon-Section】	Section Total Length (m)	Scanned Length		Note			
		Starting Point (m)	Ending Point (m)				
P10-402L-H1	9.41	0.83	8.86				
Identified Damage 1				Identified Damage 2			
Max Loss Point (m)	Section Loss (%)	Damage Length (m)	Damage Orientation	Max Loss Point (m)	Section Loss (%)	Damage Length (m)	Damage Orientation
—	—	—	—	—	—	—	—

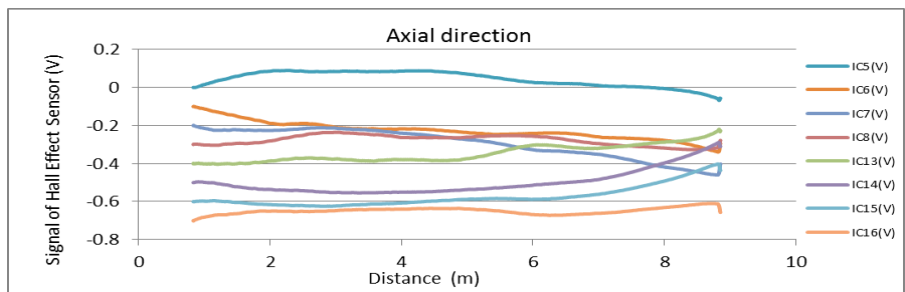
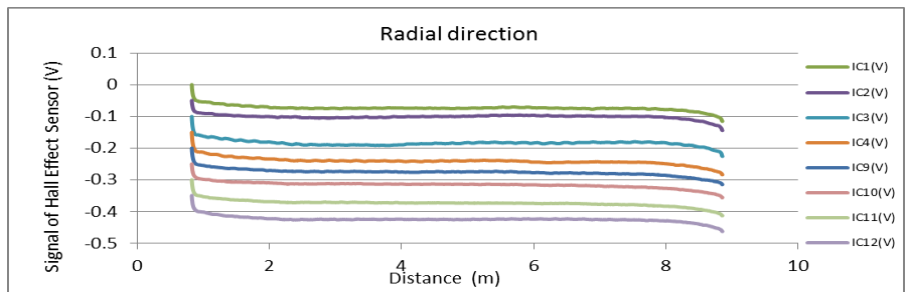
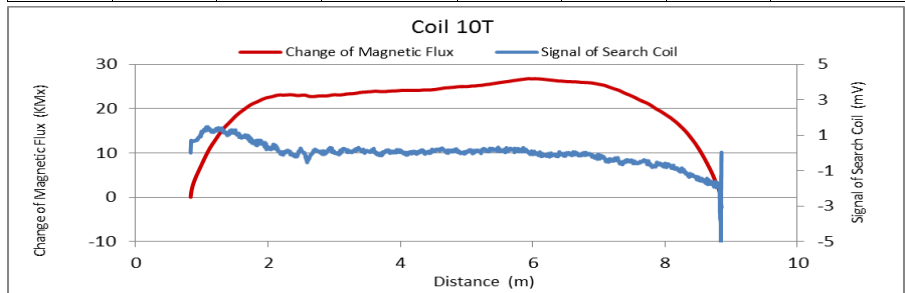


Figure A187. MMFM data of P10-402L-H1 tendon section.

File Name 【Pier-Tendon-Section】	Section Total Length (m)	Scanned Length		Note			
		Starting Point (m)	Ending Point (m)				
P11-401R-H1	9.4	0.77	8.52				
Identified Damage 1				Identified Damage 2			
Max Loss Point (m)	Section Loss (%)	Damage Length (m)	Damage Orientation	Max Loss Point (m)	Section Loss (%)	Damage Length (m)	Damage Orientation
—	—	—	—	—	—	—	—

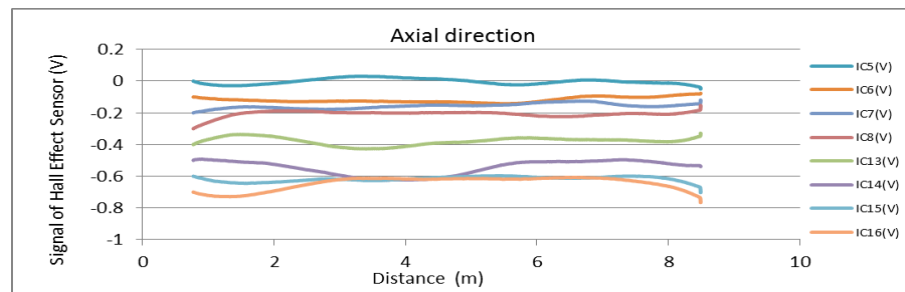
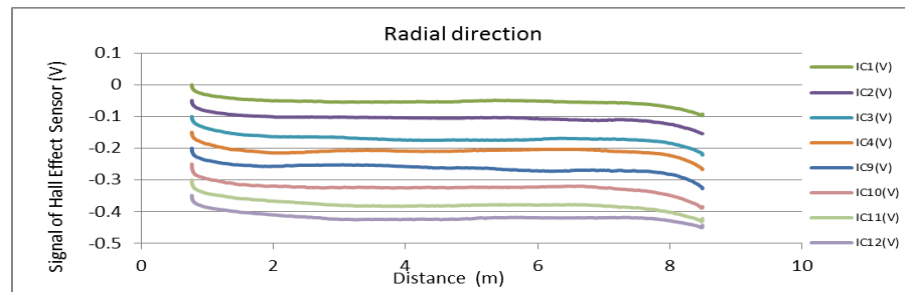
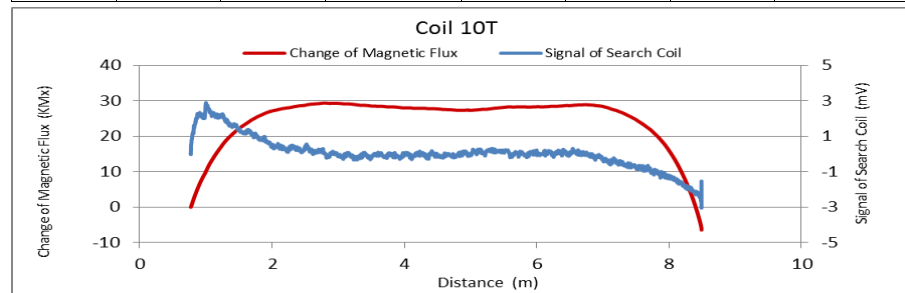


Figure A188. MMFM data of P11-401R-H1 tendon section.



Tokyo Rope USA, Inc.

File Name 【Pier-Tendon-Section】	Section Total Length (m)	Scanned Length		Note			
		Starting Point (m)	Ending Point (m)				
P11-402R-H1	9.4	0.52	8.5				
Identified Damage 1				Identified Damage 2			
Max Loss Point (m)	Section Loss (%)	Damage Length (m)	Damage Orientation	Max Loss Point (m)	Section Loss (%)	Damage Length (m)	Damage Orientation
—	—	—	—	—	—	—	—

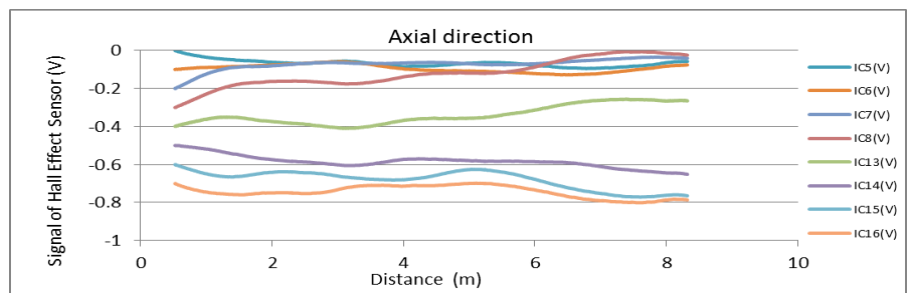
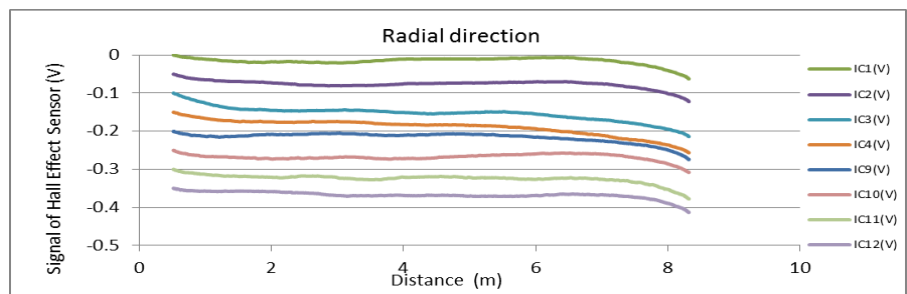
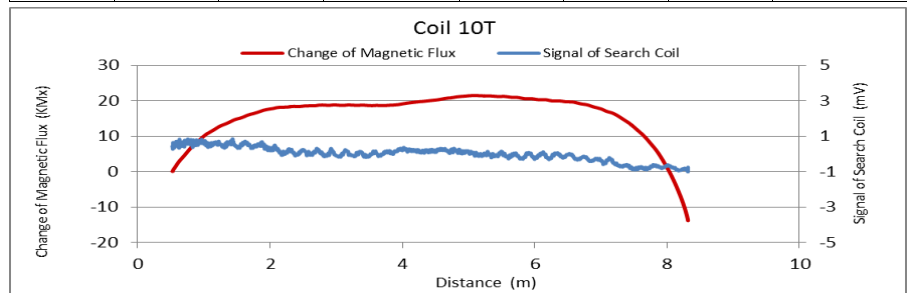


Figure A189. MMFM data of P11-402R-H1 tendon section.

File Name 【Pier-Tendon-Section】	Section Total Length (m)	Scanned Length		Note			
		Starting Point (m)	Ending Point (m)				
P11-402L-H1	9.35	0.47	8.49				
Identified Damage 1				Identified Damage 2			
Max Loss Point (m)	Section Loss (%)	Damage Length (m)	Damage Orientation	Max Loss Point (m)	Section Loss (%)	Damage Length (m)	Damage Orientation
—	—	—	—	—	—	—	—

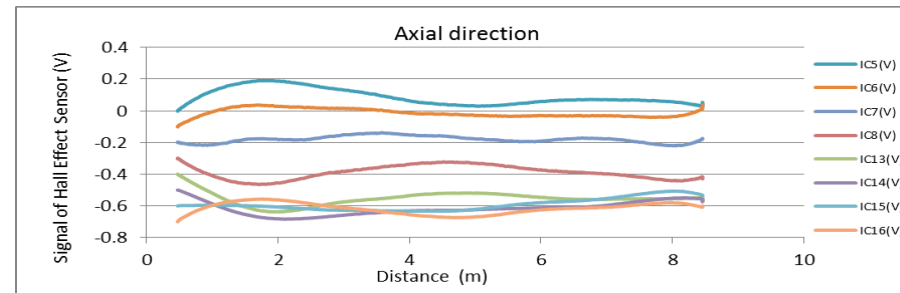
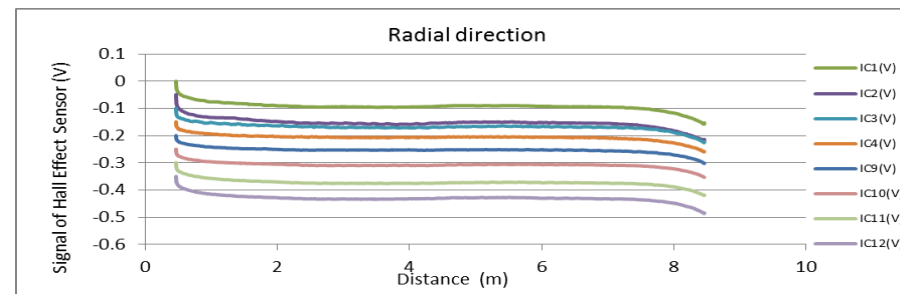
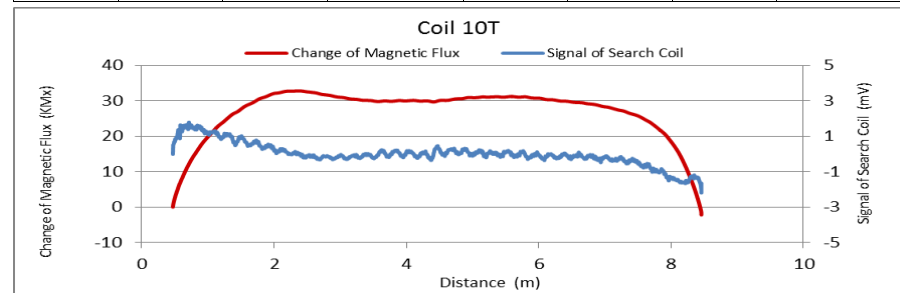


Figure A190. MMFM data of P11-402L-H1 tendon section.



Tokyo Rope USA, Inc.

File Name 【Pier-Tendon-Section】	Section Total Length (m)	Scanned Length		Note			
		Starting Point (m)	Ending Point (m)				
P11-401L-H1	9.35	0.53	8.44				
Identified Damage 1				Identified Damage 2			
Max Loss Point (m)	Section Loss (%)	Damage Length (m)	Damage Orientation	Max Loss Point (m)	Section Loss (%)	Damage Length (m)	Damage Orientation
—	—	—	—	—	—	—	—

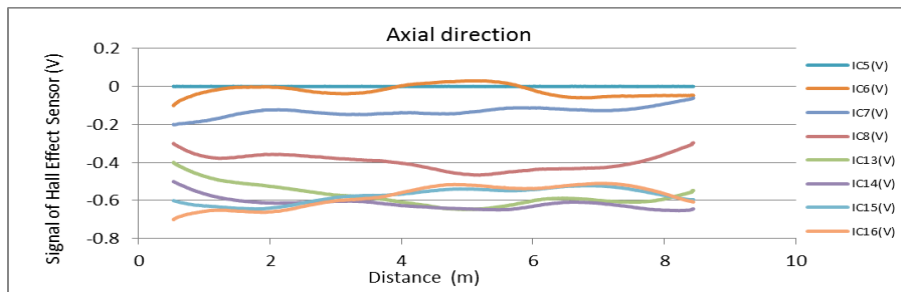
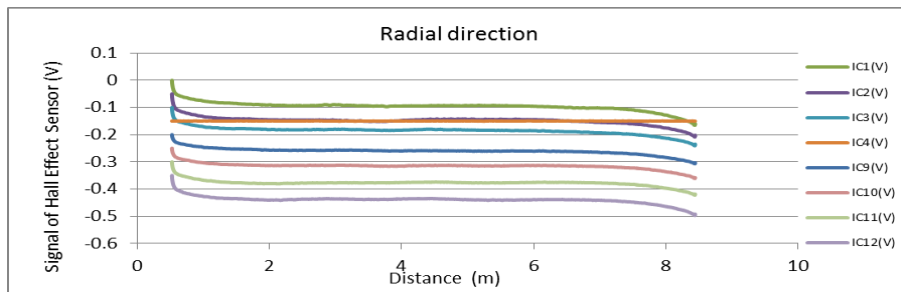
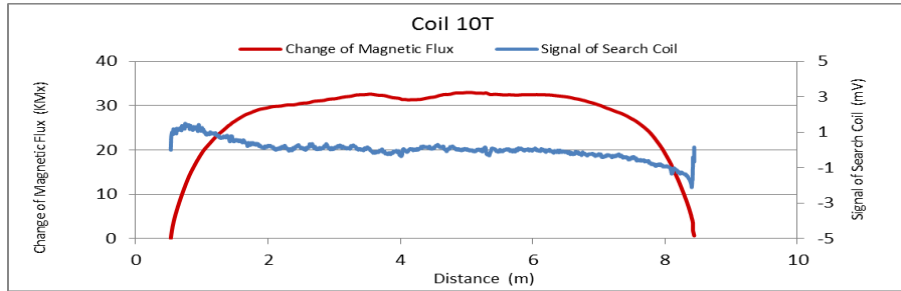


Figure A191. MMFM data of P11-401L-H1 tendon section.

File Name 【Pier-Tendon-Section】	Section Total Length (m)	Scanned Length		Note			
		Starting Point (m)	Ending Point (m)				
P11-402R-I1	21.35	0.51	20.54	Joint position: 12.26 m			
Identified Damage 1				Identified Damage 2			
Max Loss Point (m)	Section Loss (%)	Damage Length (m)	Damage Orientation	Max Loss Point (m)	Section Loss (%)	Damage Length (m)	Damage Orientation
—	—	—	—	—	—	—	—

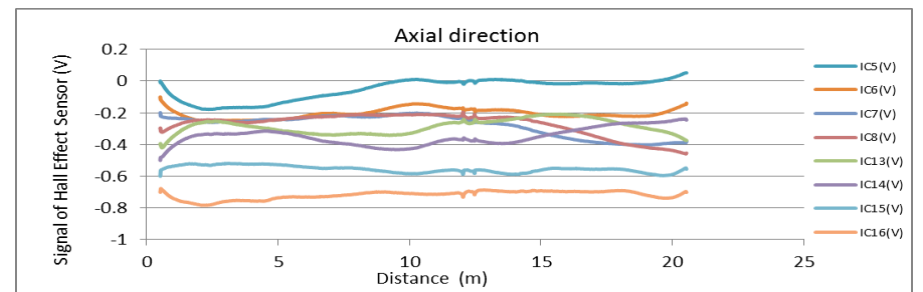
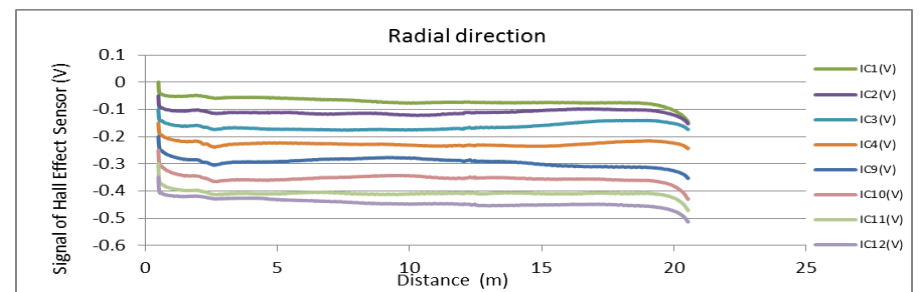
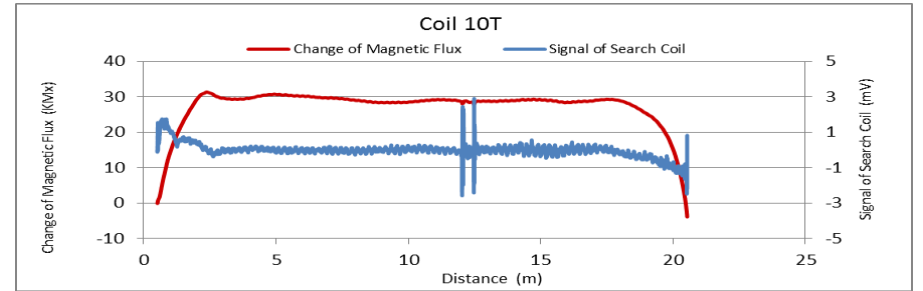


Figure A192. MMFM data of P11-402R-I1 tendon section.



Tokyo Rope USA, Inc.

File Name 【Pier-Tendon-Section】	Section Total Length (m)	Scanned Length		Note			
		Starting Point (m)	Ending Point (m)				
P11-401R-I1	21.47	0.52	21.26	Joint position : 2.86 m, 15 m			
Identified Damage 1				Identified Damage 2			
Max Loss Point (m)	Section Loss (%)	Damage Length (m)	Damage Orientation	Max Loss Point (m)	Section Loss (%)	Damage Length (m)	Damage Orientation
—	—	—	—	—	—	—	—

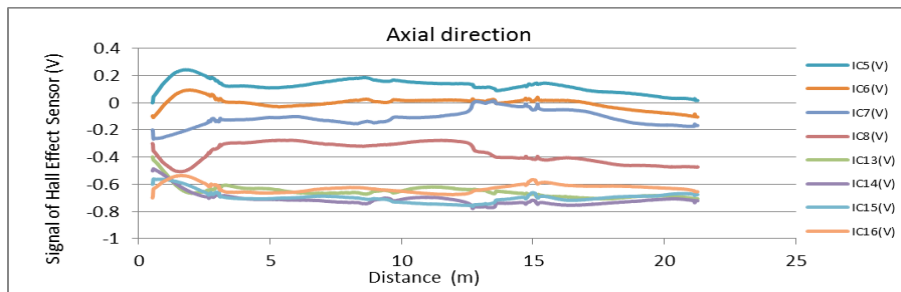
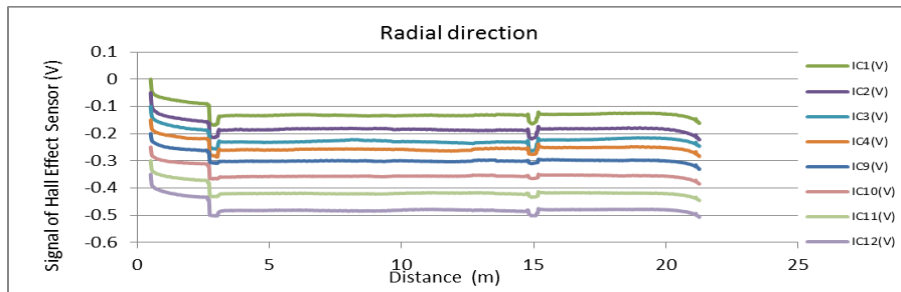
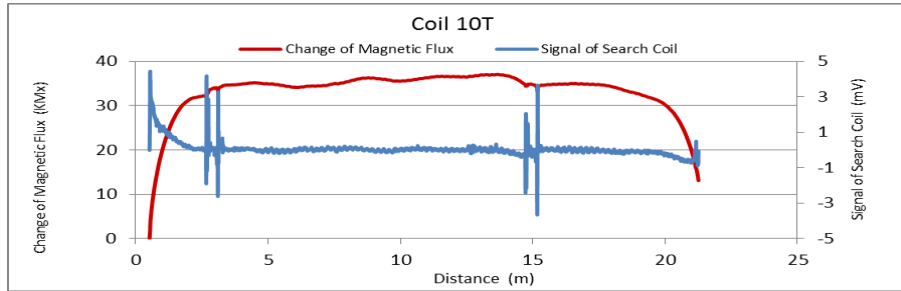


Figure A193. MMFM data of P11-401R-I1 tendon section.

File Name 【Pier-Tendon-Section】	Section Total Length (m)	Scanned Length		Note			
		Starting Point (m)	Ending Point (m)				
P11-402L-I1	21.58	0.53	20.99	Joint position : 12.38 m			
Identified Damage 1				Identified Damage 2			
Max Loss Point (m)	Section Loss (%)	Damage Length (m)	Damage Orientation	Max Loss Point (m)	Section Loss (%)	Damage Length (m)	Damage Orientation
—	—	—	—	—	—	—	—

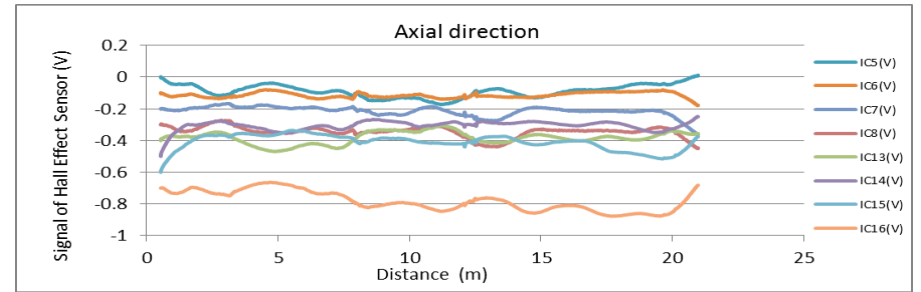
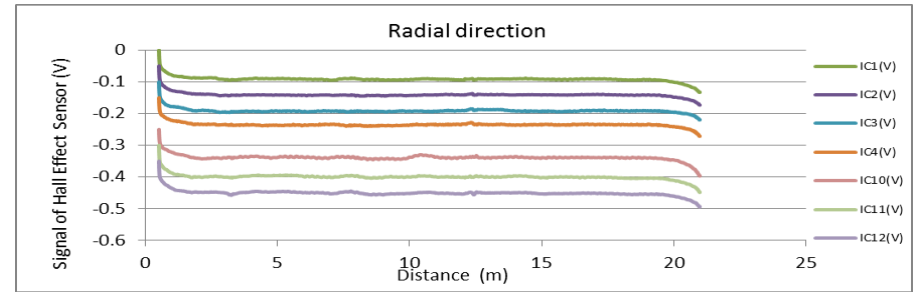
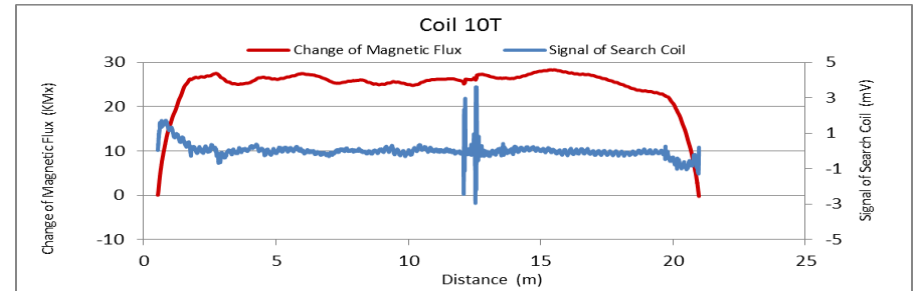


Figure A194. MMFM data of P11-402L-I1 tendon section.



Tokyo Rope USA, Inc.

File Name 【Pier-Tendon-Section】	Section Total Length (m)	Scanned Length		Note			
		Starting Point (m)	Ending Point (m)				
P11-401L-I1	21.59	0.47	21.44	Joint position : 2.85 m, 15 m			
Identified Damage 1				Identified Damage 2			
Max Loss Point (m)	Section Loss (%)	Damage Length (m)	Damage Orientation	Max Loss Point (m)	Section Loss (%)	Damage Length (m)	Damage Orientation
—	—	—	—	—	—	—	—

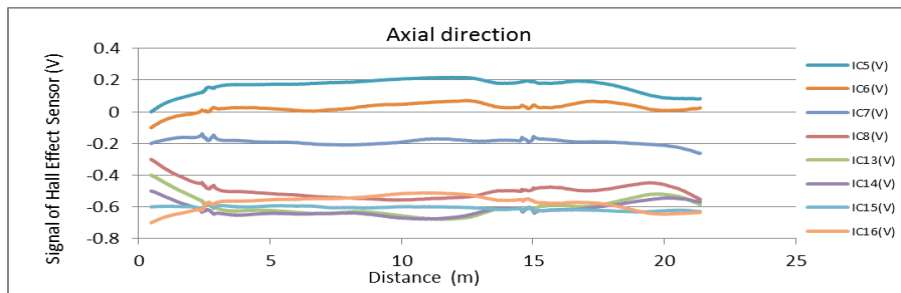
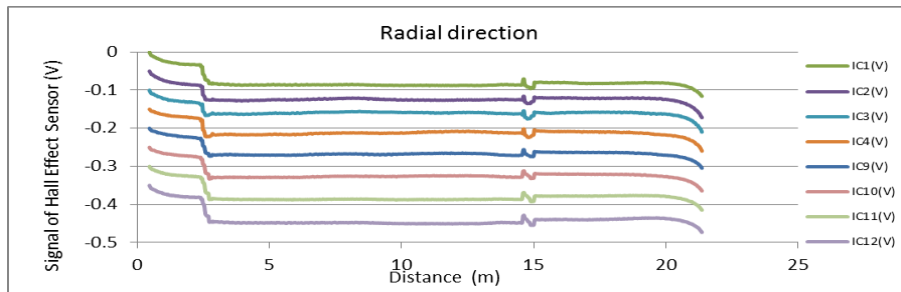
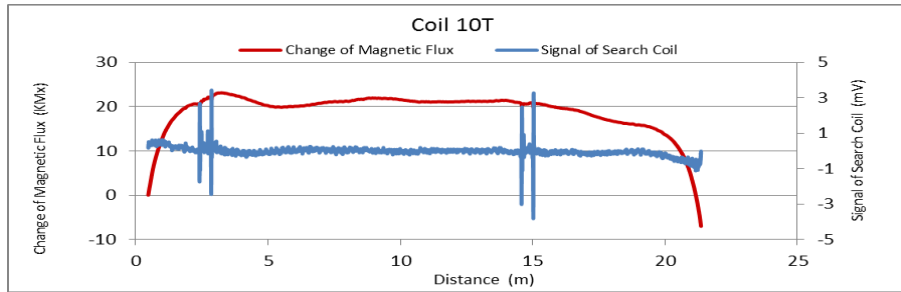


Figure A195. MMFM data of P11-401L-I1 tendon section.

File Name 【Pier-Tendon-Section】	Section Total Length (m)	Scanned Length		Note			
		Starting Point (m)	Ending Point (m)				
P11-401R-I2	28.58	0	28.05	Joint position : 5.6 m, 19.2 m			
Identified Damage 1				Identified Damage 2			
Max Loss Point (m)	Section Loss (%)	Damage Length (m)	Damage Orientation	Max Loss Point (m)	Section Loss (%)	Damage Length (m)	Damage Orientation
—	—	—	—	—	—	—	—

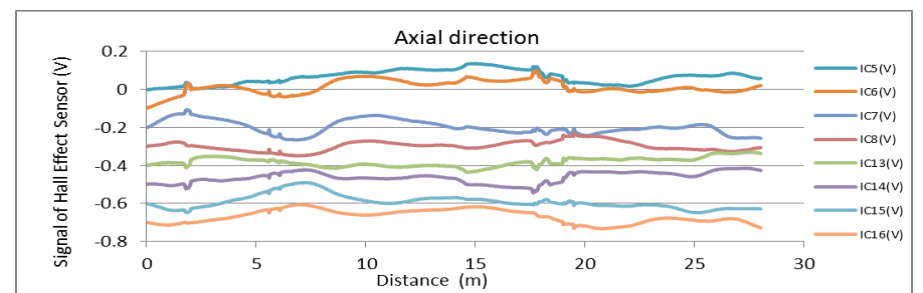
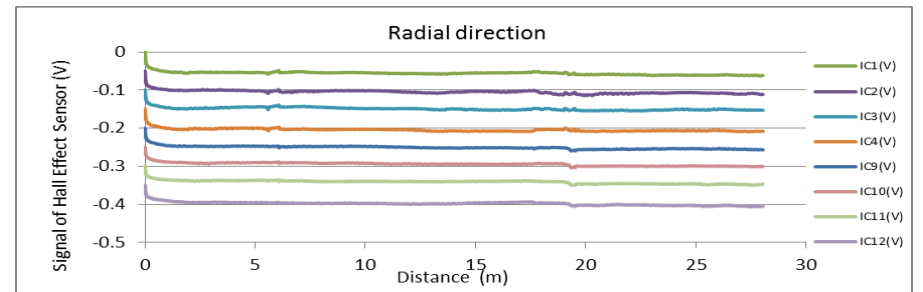
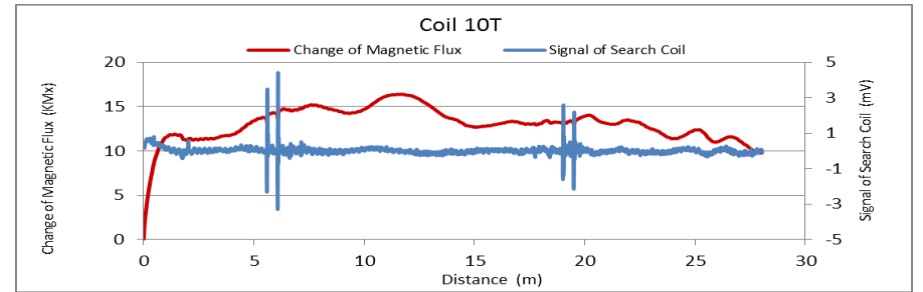


Figure A196. MMFM data of P11-401R-I2 tendon section.



Tokyo Rope USA, Inc.

File Name 【Pier-Tendon-Section】	Section Total Length (m)	Scanned Length		Note			
		Starting Point (m)	Ending Point (m)				
P11-401L-I2	28.63	0	28.22	Joint position: 5.7 m, 19.2 m			
Identified Damage 1				Identified Damage 2			
Max Loss Point (m)	Section Loss (%)	Damage Length (m)	Damage Orientation	Max Loss Point (m)	Section Loss (%)	Damage Length (m)	Damage Orientation
—	—	—	—	—	—	—	—

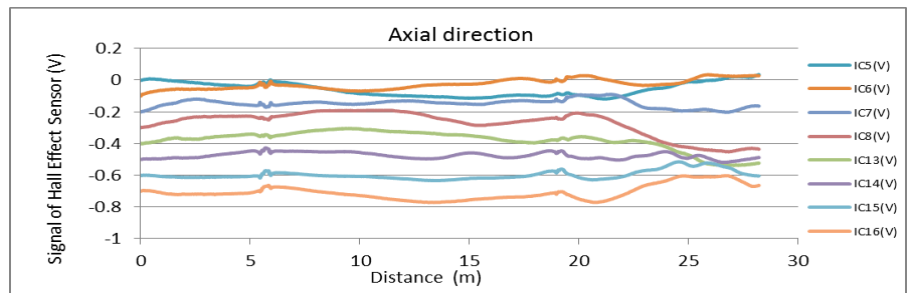
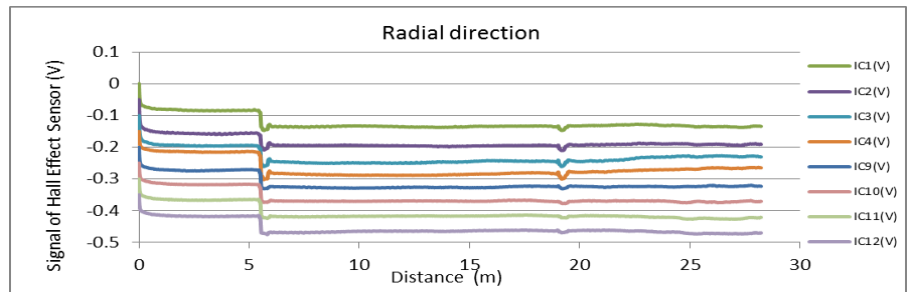
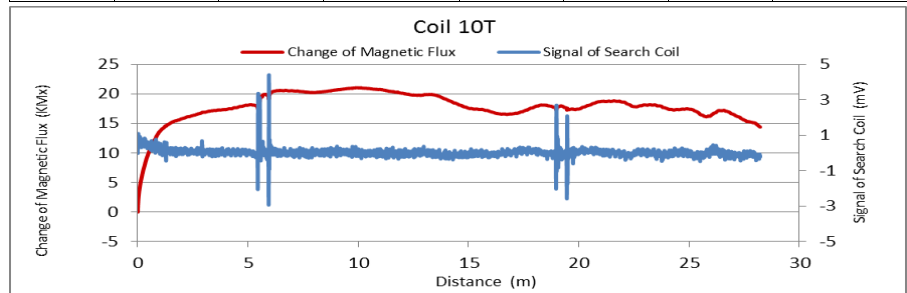


Figure A197. MMFM data of P11-401L-I2 tendon section.

File Name 【Pier-Tendon-Section】	Section Total Length (m)	Scanned Length		Note			
		Starting Point (m)	Ending Point (m)				
P9-404L-H1	9.5	0.49	8.7				
Identified Damage 1				Identified Damage 2			
Max Loss Point (m)	Section Loss (%)	Damage Length (m)	Damage Orientation	Max Loss Point (m)	Section Loss (%)	Damage Length (m)	Damage Orientation
—	—	—	—	—	—	—	—

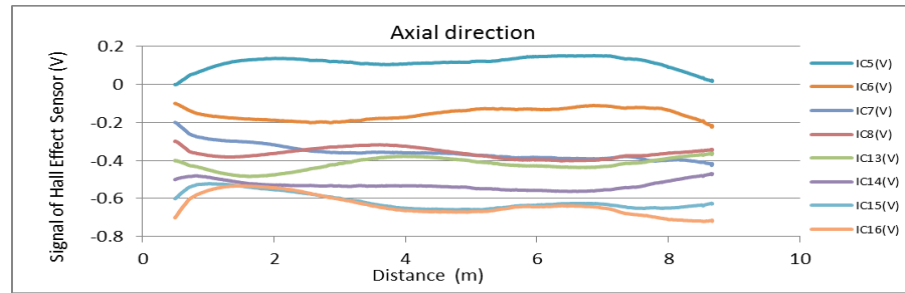
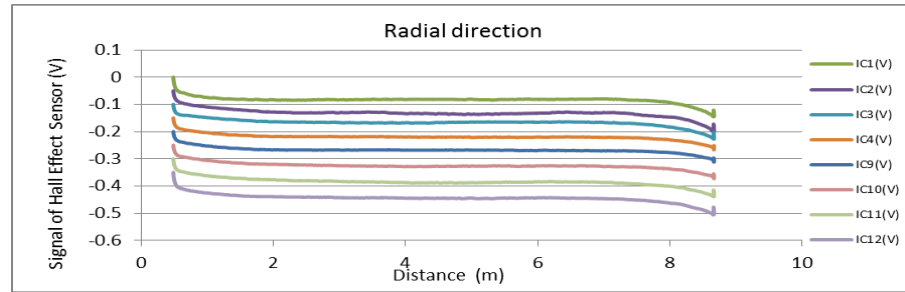
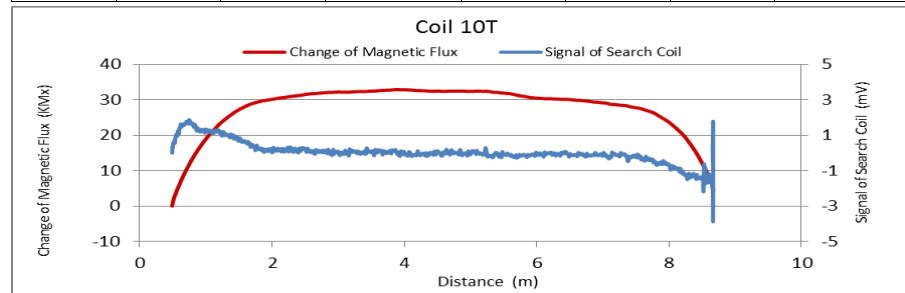


Figure A198. MMFM data of P9-404L-H1 tendon section.



Tokyo Rope USA, Inc.

File Name 【Pier-Tendon-Section】	Section Total Length (m)	Scanned Length		Note			
		Starting Point (m)	Ending Point (m)				
P9-403L-H1	9.5	0.43	8.59				
Identified Damage 1				Identified Damage 2			
Max Loss Point (m)	Section Loss (%)	Damage Length (m)	Damage Orientation	Max Loss Point (m)	Section Loss (%)	Damage Length (m)	Damage Orientation
—	—	—	—	—	—	—	—

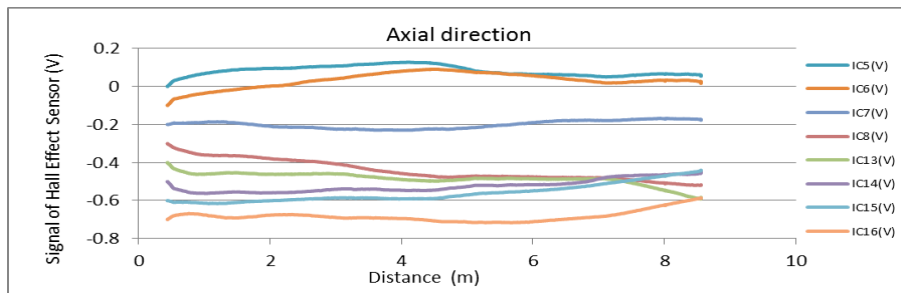
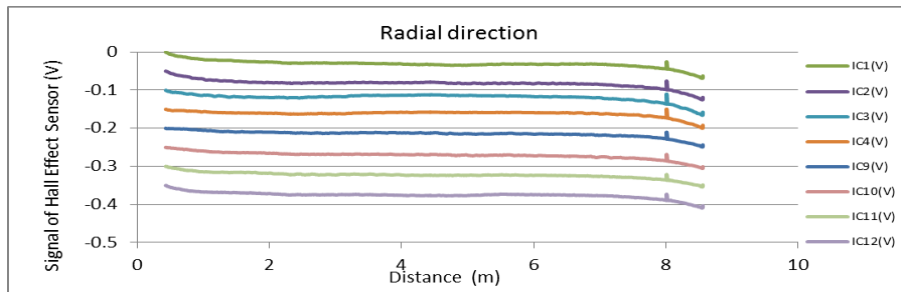
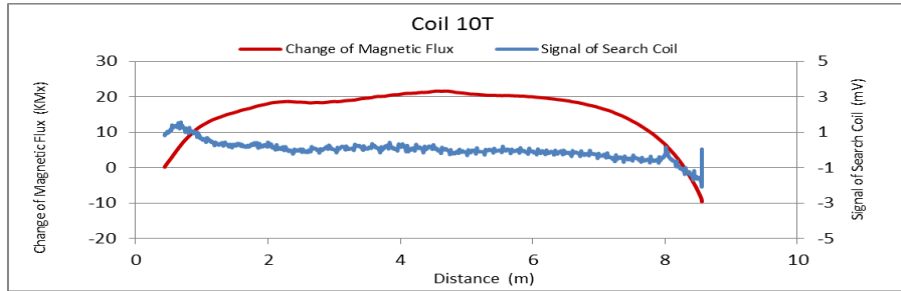


Figure A199. MMFM data of P9-403L-H1 tendon section.

File Name 【Pier-Tendon-Section】	Section Total Length (m)	Scanned Length		Note			
		Starting Point (m)	Ending Point (m)				
P9-405L-H1	9.43	0.57	8.81				
Identified Damage 1				Identified Damage 2			
Max Loss Point (m)	Section Loss (%)	Damage Length (m)	Damage Orientation	Max Loss Point (m)	Section Loss (%)	Damage Length (m)	Damage Orientation
—	—	—	—	—	—	—	—

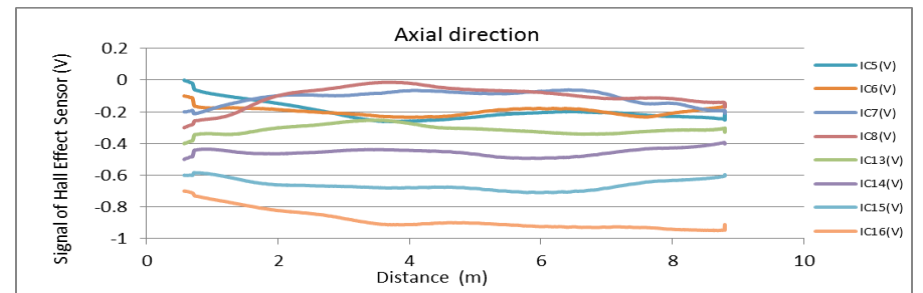
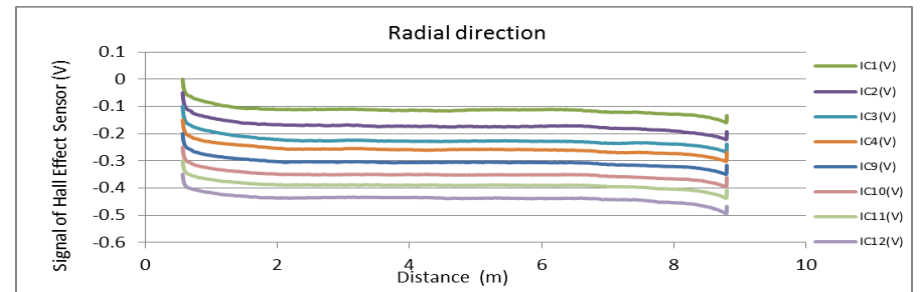
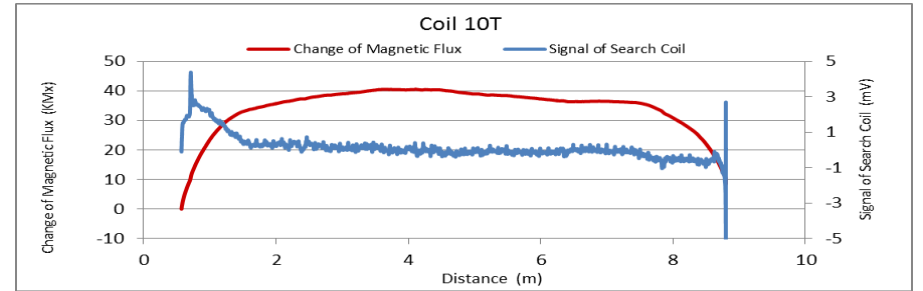


Figure A200. MMFM data of P9-405L-H1 tendon section.



Tokyo Rope USA, Inc.

File Name 【Pier-Tendon-Section】	Section Total Length (m)	Scanned Length		Note			
		Starting Point (m)	Ending Point (m)				
P9-403L-I1	21.49	0.47	20.67	Joint position: 12.15 m			
Identified Damage 1				Identified Damage 2			
Max Loss Point (m)	Section Loss (%)	Damage Length (m)	Damage Orientation	Max Loss Point (m)	Section Loss (%)	Damage Length (m)	Damage Orientation
—	—	—	—	—	—	—	—

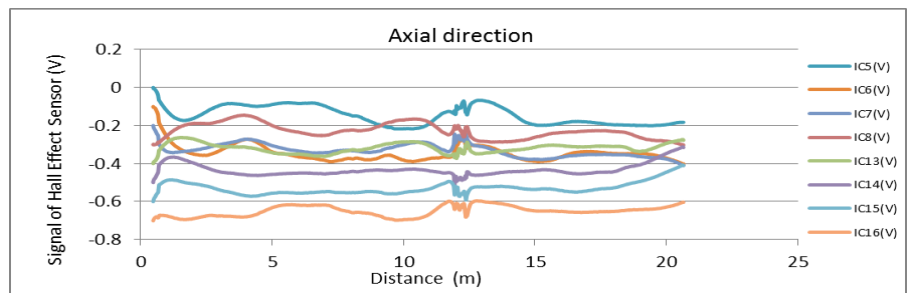
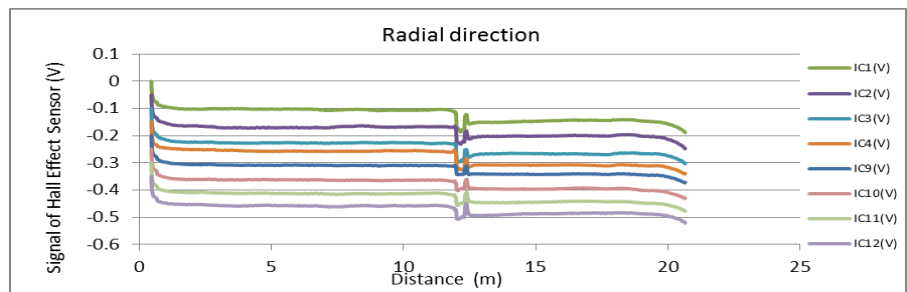
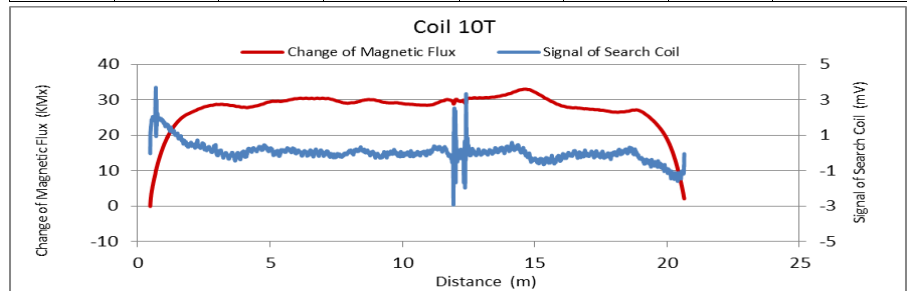


Figure A201. MMFM data of P9-403L-I1 tendon section.

File Name 【Pier-Tendon-Section】	Section Total Length (m)	Scanned Length		Note			
		Starting Point (m)	Ending Point (m)				
P9-404L-I1	21.49	0.49	20.77	Joint position: 12.24 m			
Identified Damage 1				Identified Damage 2			
Max Loss Point (m)	Section Loss (%)	Damage Length (m)	Damage Orientation	Max Loss Point (m)	Section Loss (%)	Damage Length (m)	Damage Orientation
—	—	—	—	—	—	—	—

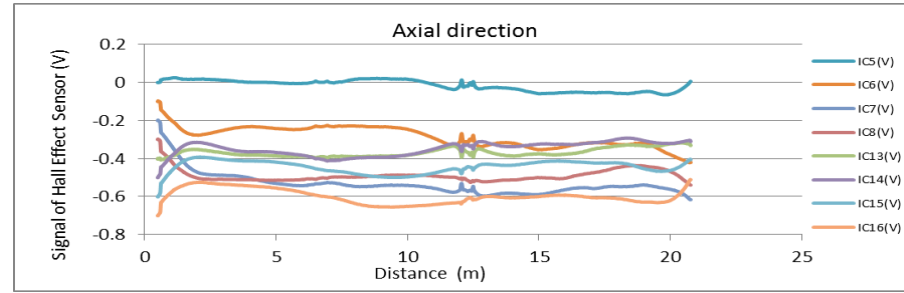
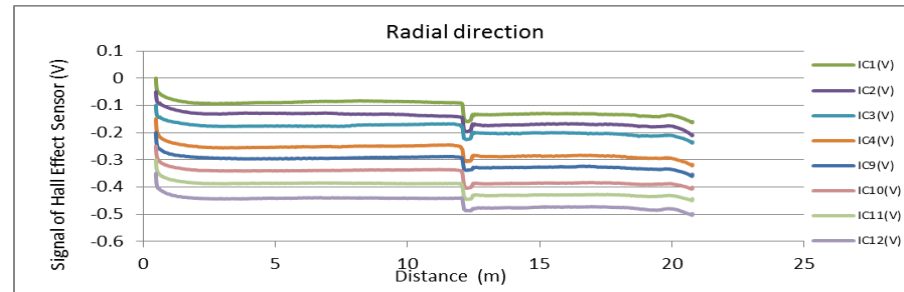
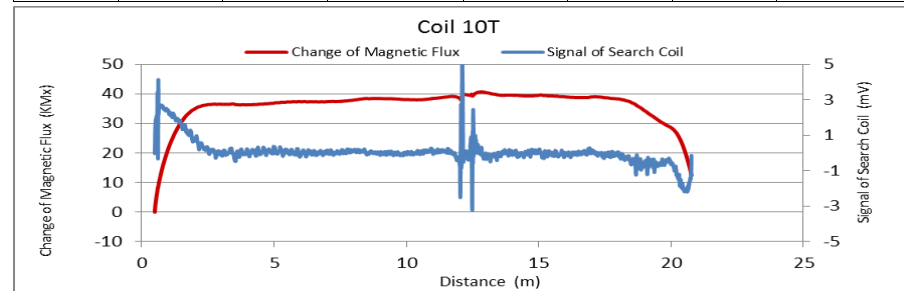


Figure A202. MMFM data of P9-404L-I1 tendon section.



Tokyo Rope USA, Inc.

File Name 【Pier-Tendon-Section】	Section Total Length (m)	Scanned Length		Note			
		Starting Point (m)	Ending Point (m)				
P9-405L-I1	21.5	0.44	20.8	Joint position: 12.21 m			
Identified Damage 1				Identified Damage 2			
Max Loss Point (m)	Section Loss (%)	Damage Length (m)	Damage Orientation	Max Loss Point (m)	Section Loss (%)	Damage Length (m)	Damage Orientation
—	—	—	—	—	—	—	—

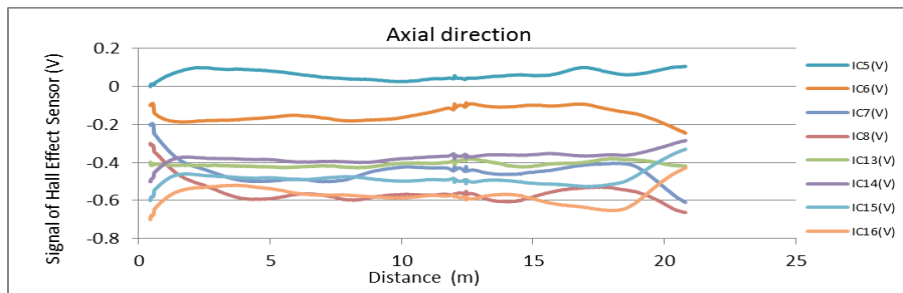
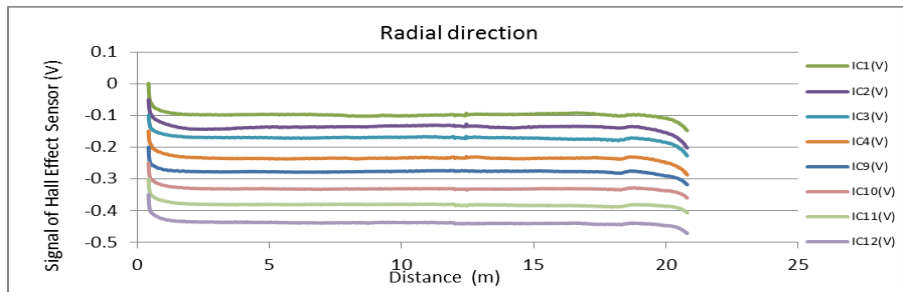
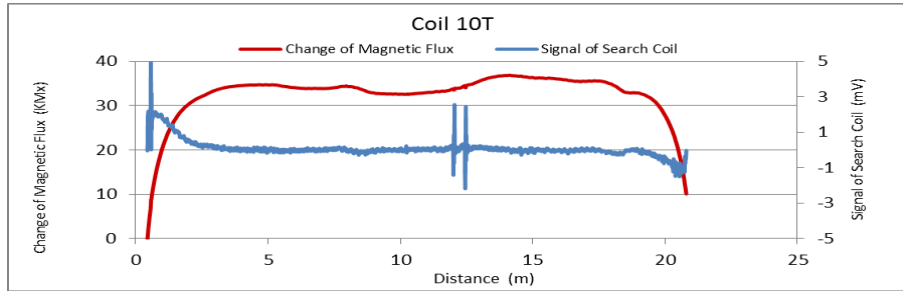


Figure A203. MMFM data of P9-405L-I1 tendon section.

File Name 【Pier-Tendon-Section】	Section Total Length (m)	Scanned Length		Note			
		Starting Point (m)	Ending Point (m)				
P9-404L-I2	21.52	0.79	20.98	Joint position: 0.82 m, 3.74 m, 9.74 m, 15.74 m			
Identified Damage 1				Identified Damage 2			
Max Loss Point (m)	Section Loss (%)	Damage Length (m)	Damage Orientation	Max Loss Point (m)	Section Loss (%)	Damage Length (m)	Damage Orientation
—	—	—	—	—	—	—	—

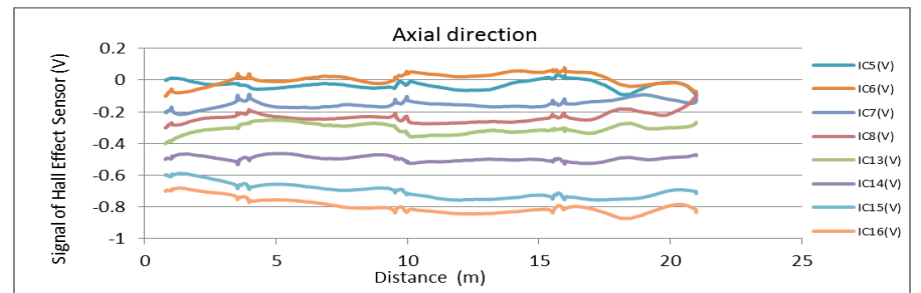
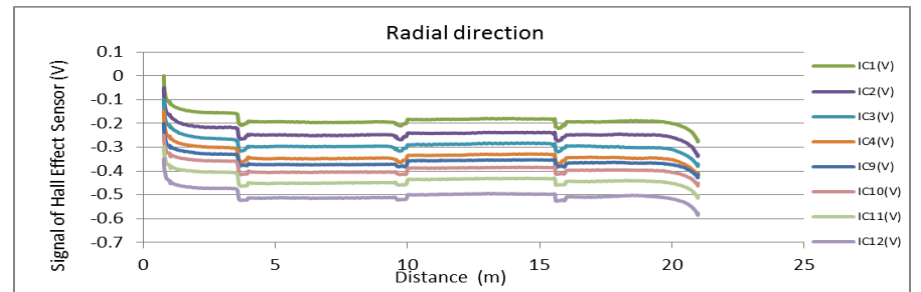
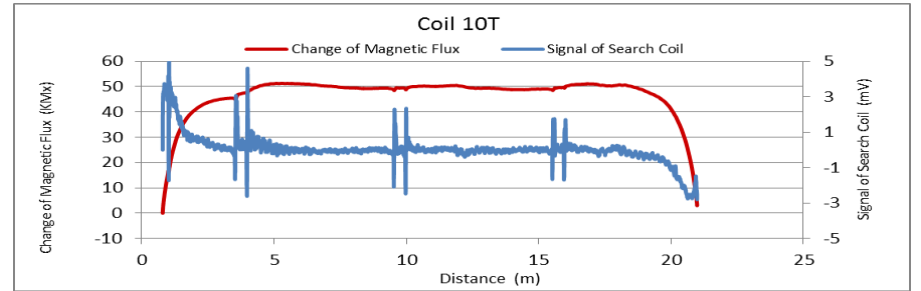


Figure A204. MMFM data of P9-404L-I2 tendon section.



Tokyo Rope USA, Inc.

File Name 【Pier-Tendon-Section】	Section Total Length (m)	Scanned Length		Note			
		Starting Point (m)	Ending Point (m)				
P9-406L-I2	21.48	0.83	14.36	Repair tape position : 1.26 m (center) Joint position : 9.23 m After 14.36 m, the repair is large and cannot be measured.			
Identified Damage 1				Identified Damage 2			
Max Loss Point (m)	Section Loss (%)	Damage Length (m)	Damage Orientation	Max Loss Point (m)	Section Loss (%)	Damage Length (m)	Damage Orientation
—	—	—	—	—	—	—	—

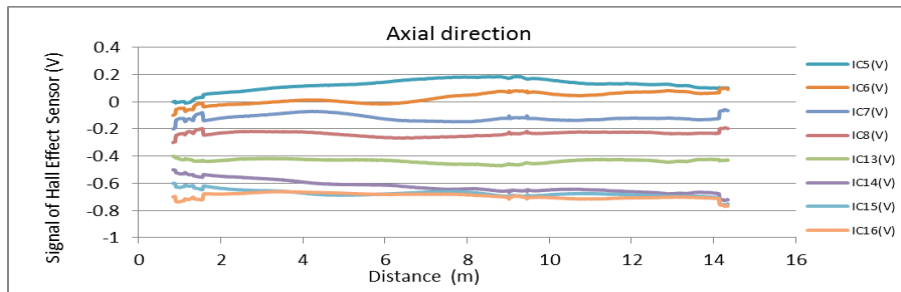
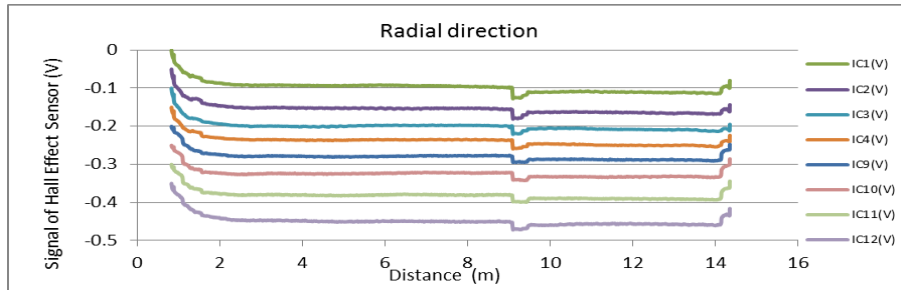
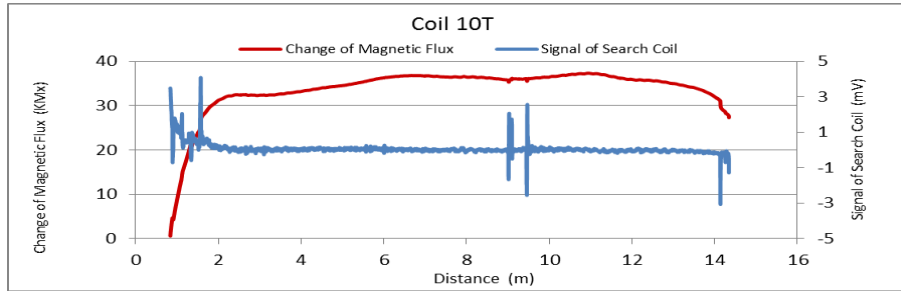


Figure A205. MMFM data of P9-406L-I2 tendon section.

File Name 【Pier-Tendon-Section】	Section Total Length (m)	Scanned Length		Note			
		Starting Point (m)	Ending Point (m)				
P9-404L-H2	9.38	0.63	8.82	Joint position : 6.15 m			
Identified Damage 1				Identified Damage 2			
Max Loss Point (m)	Section Loss (%)	Damage Length (m)	Damage Orientation	Max Loss Point (m)	Section Loss (%)	Damage Length (m)	Damage Orientation
—	—	—	—	—	—	—	—

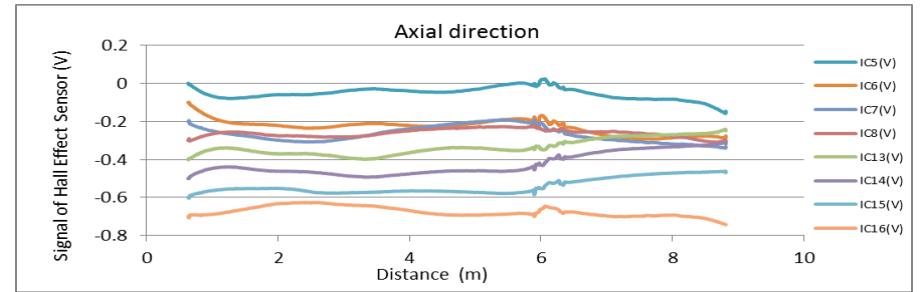
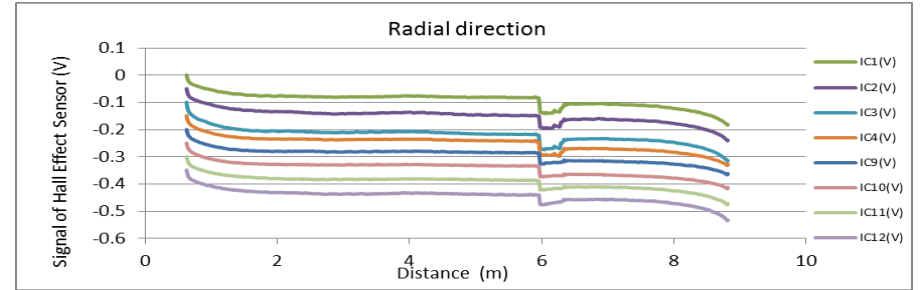
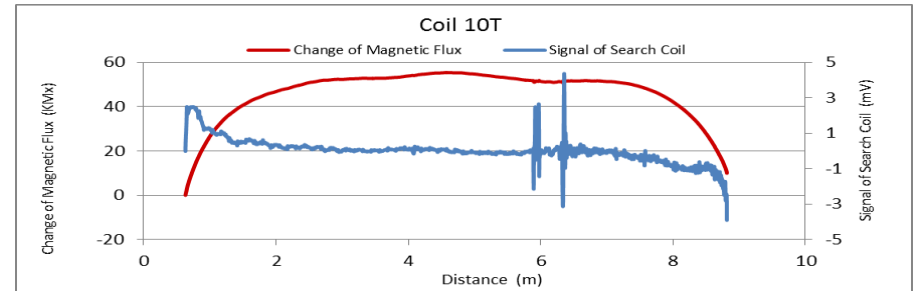


Figure A206. MMFM data of P9-404L-H2 tendon section.



Tokyo Rope USA, Inc.

File Name 【Pier-Tendon-Section】	Section Total Length (m)	Scanned Length		Note			
		Starting Point (m)	Ending Point (m)				
P9-406L-H2	9.37	0.67	8.84				
Identified Damage 1				Identified Damage 2			
Max Loss Point (m)	Section Loss (%)	Damage Length (m)	Damage Orientation	Max Loss Point (m)	Section Loss (%)	Damage Length (m)	Damage Orientation
—	—	—	—	—	—	—	—

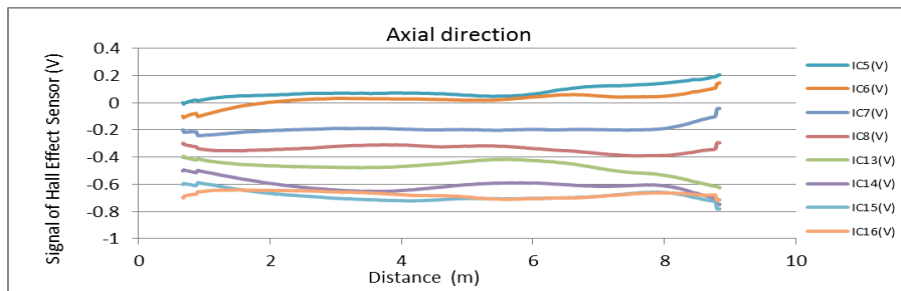
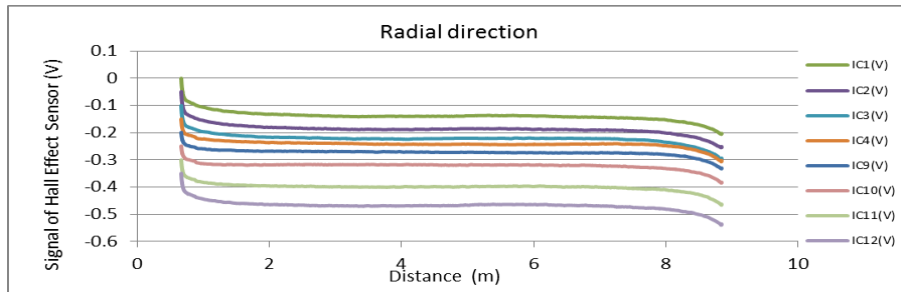
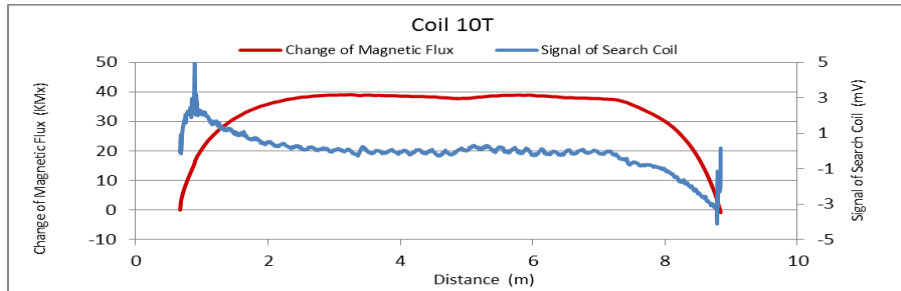


Figure A207. MMFM data of P9-406L-H2 tendon section.

File Name 【Pier-Tendon-Section】	Section Total Length (m)	Scanned Length		Note			
		Starting Point (m)	Ending Point (m)				
P9-406R-H2	9.39	0.64	8.96				
Identified Damage 1				Identified Damage 2			
Max Loss Point (m)	Section Loss (%)	Damage Length (m)	Damage Orientation	Max Loss Point (m)	Section Loss (%)	Damage Length (m)	Damage Orientation
—	—	—	—	—	—	—	—

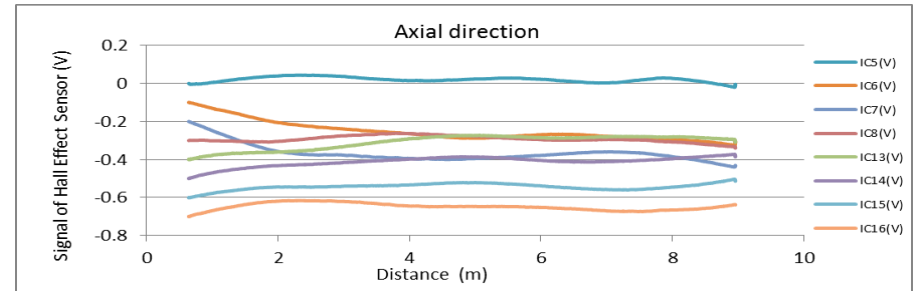
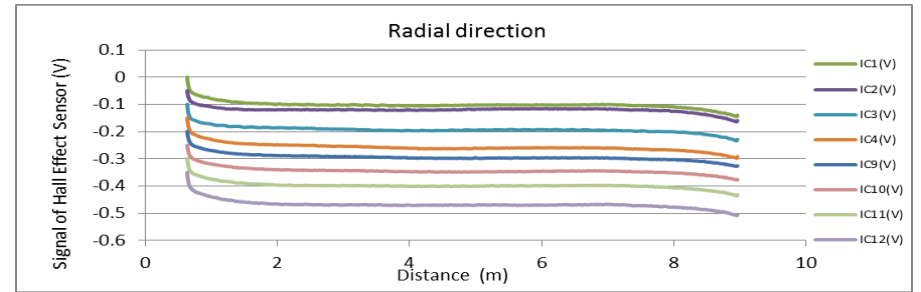
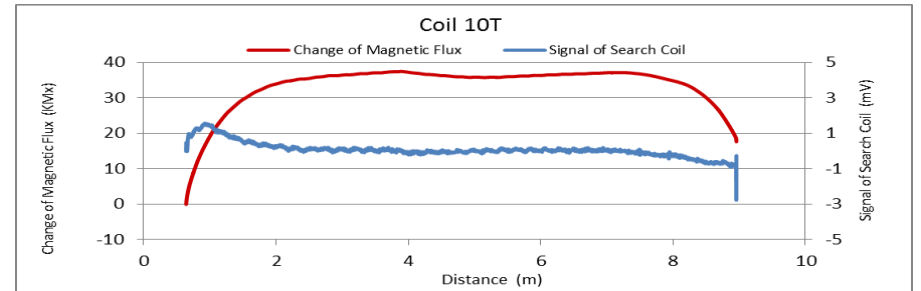


Figure A208. MMFM data of P9-406R-H2 tendon section.



Tokyo Rope USA, Inc.

File Name 【Pier-Tendon-Section】	Section Total Length (m)	Scanned Length		Note			
		Starting Point (m)	Ending Point (m)				
P9-405R-H2	9.39	0.66	8.87				
Identified Damage 1				Identified Damage 2			
Max Loss Point (m)	Section Loss (%)	Damage Length (m)	Damage Orientation	Max Loss Point (m)	Section Loss (%)	Damage Length (m)	Damage Orientation
—	—	—	—	—	—	—	—

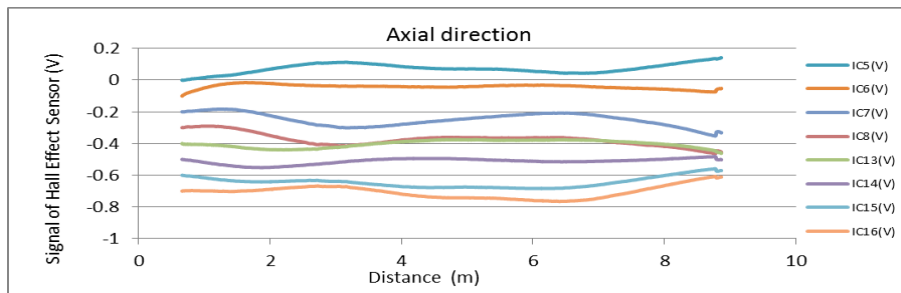
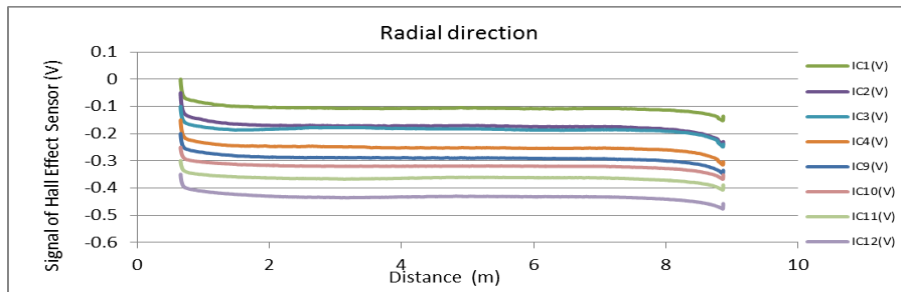
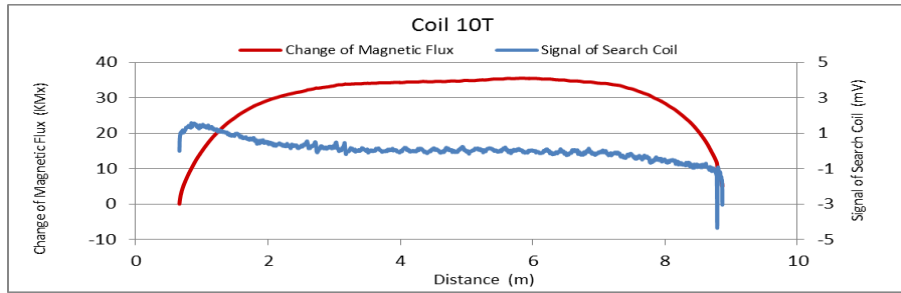


Figure A209. MMFM data of P9-405R-H2 tendon section.

File Name 【Pier-Tendon-Section】	Section Total Length (m)	Scanned Length		Note			
		Starting Point (m)	Ending Point (m)				
P9-404R-H2	9.4	0.65	8.95				
Identified Damage 1				Identified Damage 2			
Max Loss Point (m)	Section Loss (%)	Damage Length (m)	Damage Orientation	Max Loss Point (m)	Section Loss (%)	Damage Length (m)	Damage Orientation
—	—	—	—	—	—	—	—

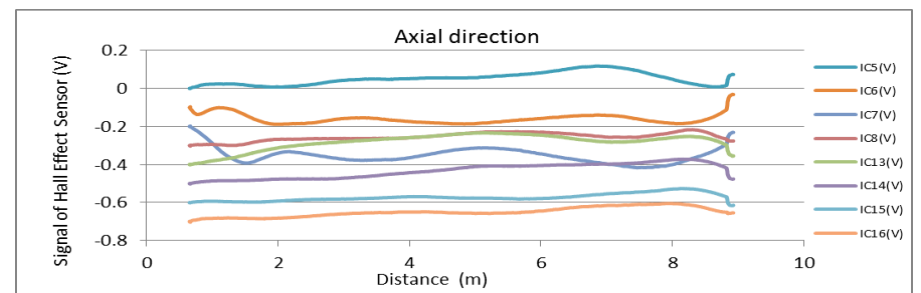
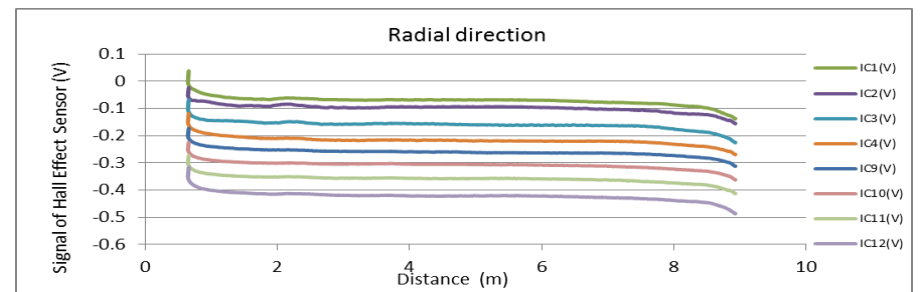
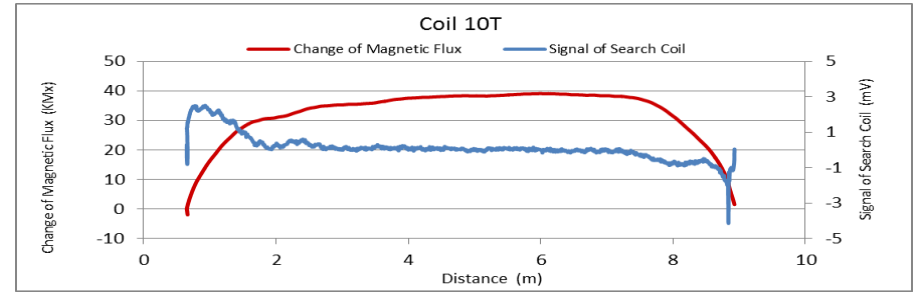


Figure A210. MMFM data of P9-404R-H2 tendon section.



Tokyo Rope USA, Inc.

File Name 【Pier-Tendon-Section】	Section Total Length (m)	Scanned Length		Note			
		Starting Point (m)	Ending Point (m)				
P9-406R-I2	21.5	0.48	19.35	Joint position: 9.25 m			
Identified Damage 1				Identified Damage 2			
Max Loss Point (m)	Section Loss (%)	Damage Length (m)	Damage Orientation	Max Loss Point (m)	Section Loss (%)	Damage Length (m)	Damage Orientation
—	—	—	—	—	—	—	—

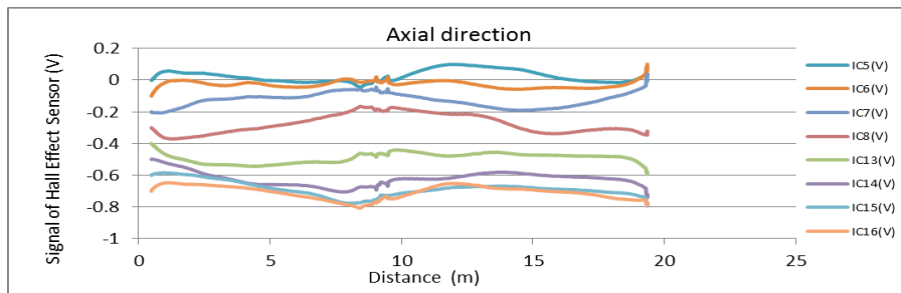
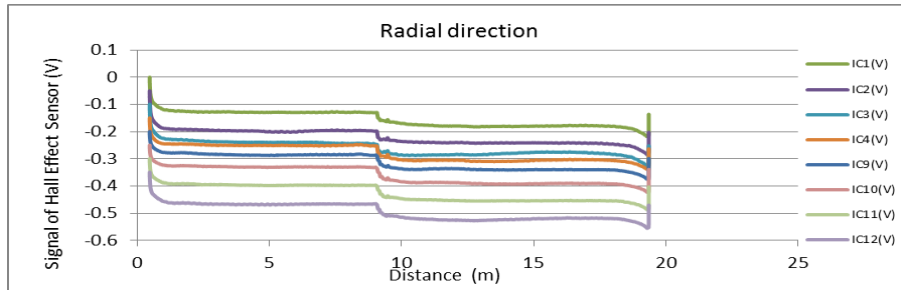
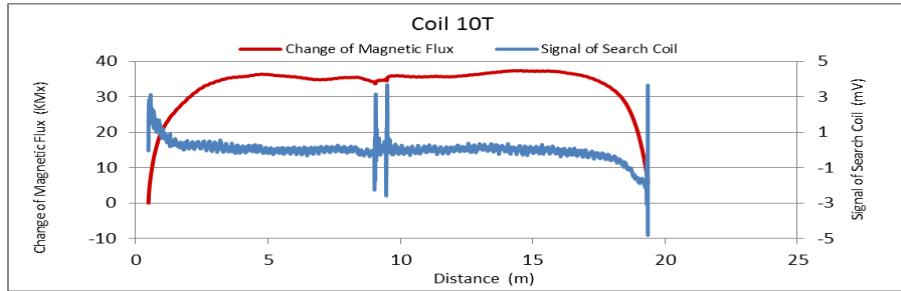


Figure A211. MMFM data of P9-406R-I2 tendon section.

File Name 【Pier-Tendon-Section】	Section Total Length (m)	Scanned Length		Note			
		Starting Point (m)	Ending Point (m)				
P9-404R-I2	21.49	0.51	20.96	Joint position: 9.27 m Noise is greater: distortion or unevenness			
Identified Damage 1				Identified Damage 2			
Max Loss Point (m)	Section Loss (%)	Damage Length (m)	Damage Orientation	Max Loss Point (m)	Section Loss (%)	Damage Length (m)	Damage Orientation
—	—	—	—	—	—	—	—

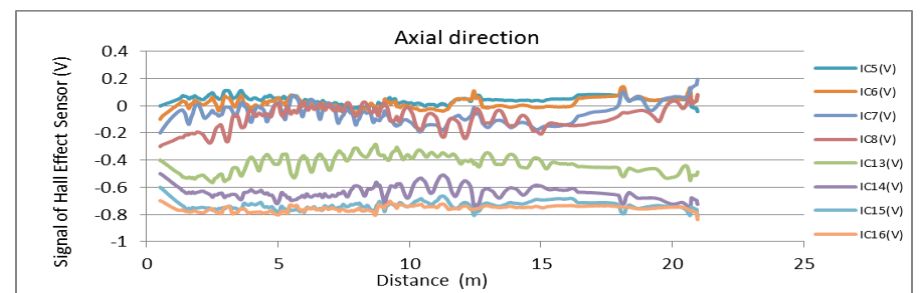
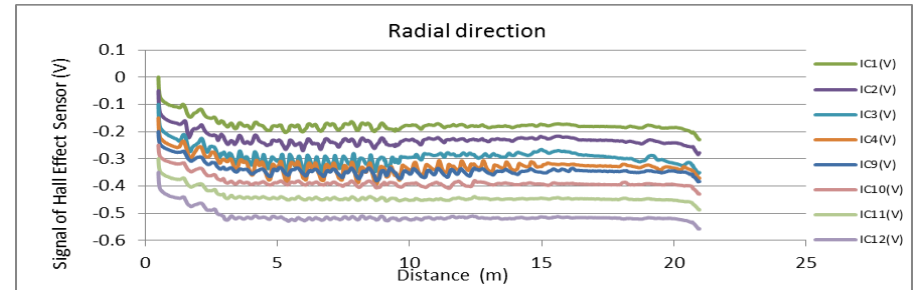
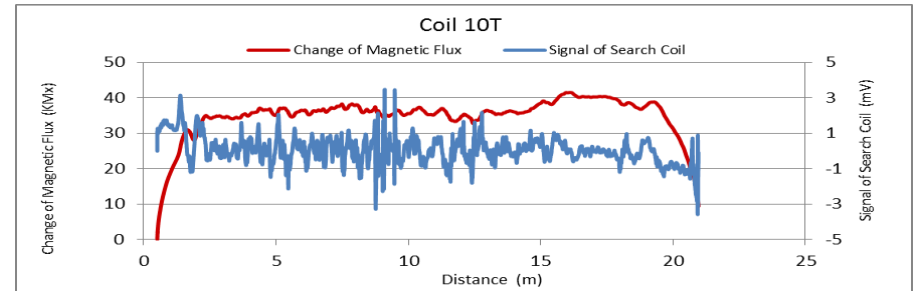


Figure A212. MMFM data of P9-404R-I2 tendon section.



Tokyo Rope USA, Inc.

File Name 【Pier-Tendon-Section】	Section Total Length (m)	Scanned Length		Note			
		Starting Point (m)	Ending Point (m)				
P9-405R-I1	21.47	0.41	20.72	Joint position: 21.23 m			
Identified Damage 1				Identified Damage 2			
Max Loss Point (m)	Section Loss (%)	Damage Length (m)	Damage Orientation	Max Loss Point (m)	Section Loss (%)	Damage Length (m)	Damage Orientation
—	—	—	—	—	—	—	—

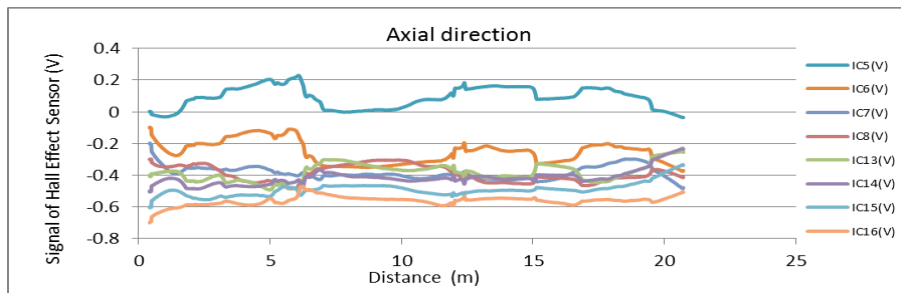
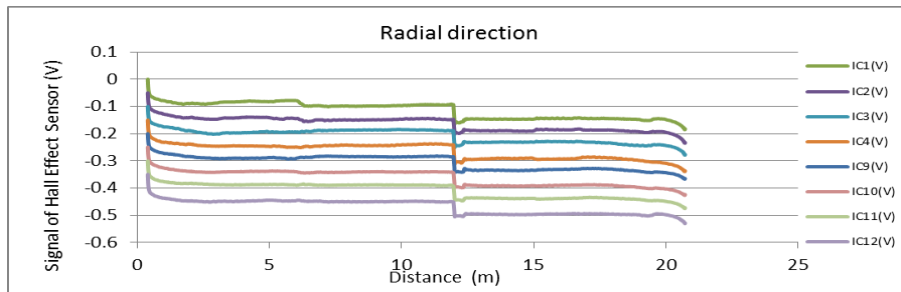
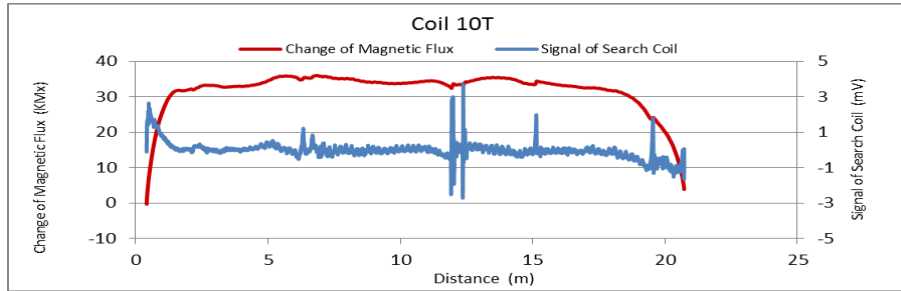


Figure A213. MMFM data of P9-405R-I1 tendon section.

File Name 【Pier-Tendon-Section】	Section Total Length (m)	Scanned Length		Note			
		Starting Point (m)	Ending Point (m)				
P9-403R-I1	21.47	0.37	20.86	Joint position: 12.28 m			
Identified Damage 1				Identified Damage 2			
Max Loss Point (m)	Section Loss (%)	Damage Length (m)	Damage Orientation	Max Loss Point (m)	Section Loss (%)	Damage Length (m)	Damage Orientation
—	—	—	—	—	—	—	—

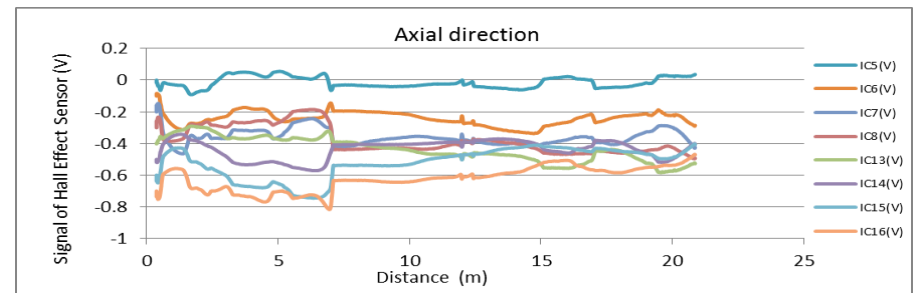
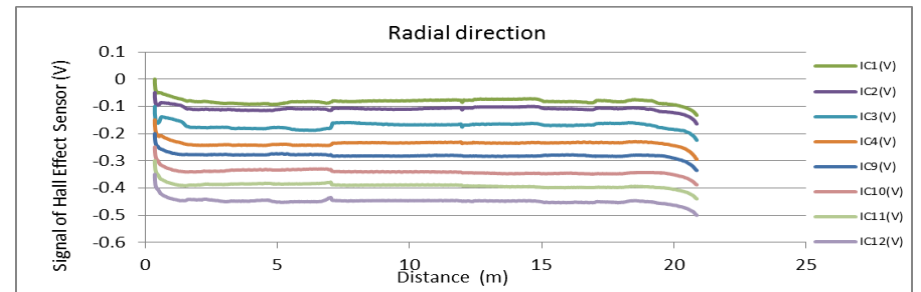
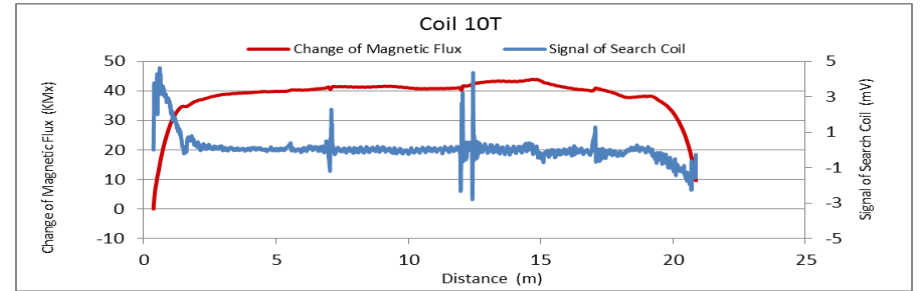


Figure A214. MMFM data of P9-403R-I1 tendon section.



Tokyo Rope USA, Inc.

File Name 【Pier-Tendon-Section】	Section Total Length (m)	Scanned Length		Note			
		Starting Point (m)	Ending Point (m)				
P9-403R-H1	9.3	1.46	8.12				
Identified Damage 1				Identified Damage 2			
Max Loss Point (m)	Section Loss (%)	Damage Length (m)	Damage Orientation	Max Loss Point (m)	Section Loss (%)	Damage Length (m)	Damage Orientation
—	—	—	—	—	—	—	—

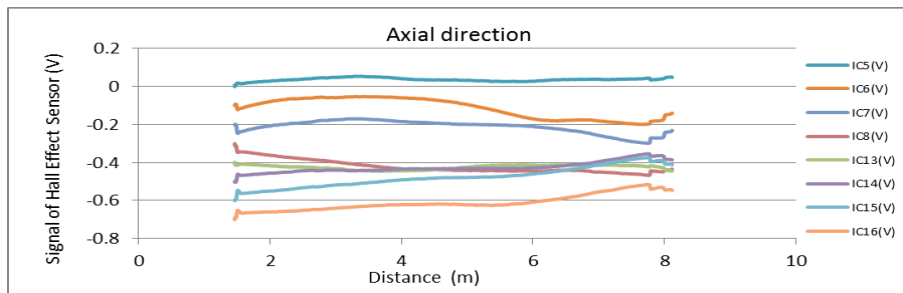
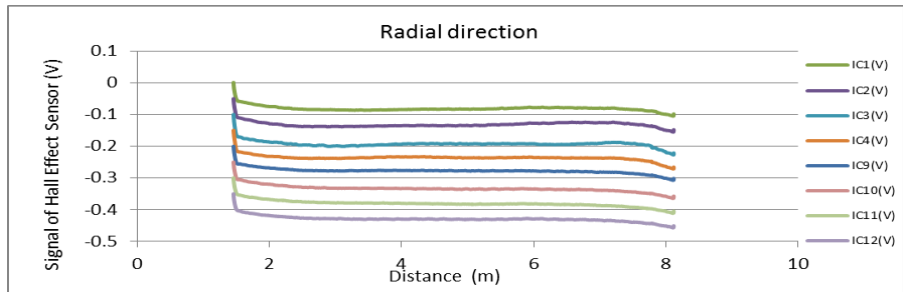
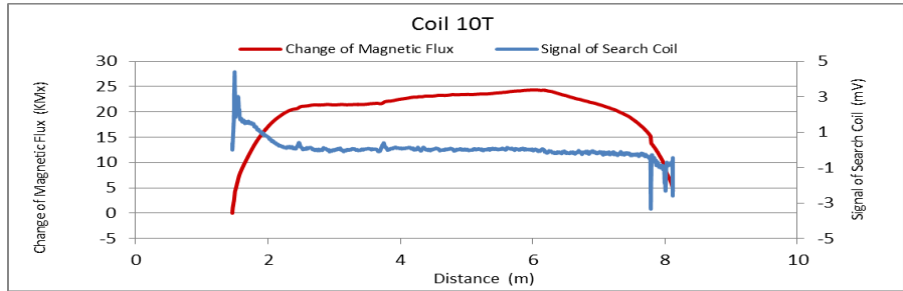


Figure A215. MMFM data of P9-403R-H1 tendon section.

File Name 【Pier-Tendon-Section】	Section Total Length (m)	Scanned Length		Note			
		Starting Point (m)	Ending Point (m)				
P9-404R-H1	9.3	0.46	8.48				
Identified Damage 1				Identified Damage 2			
Max Loss Point (m)	Section Loss (%)	Damage Length (m)	Damage Orientation	Max Loss Point (m)	Section Loss (%)	Damage Length (m)	Damage Orientation
—	—	—	—	—	—	—	—

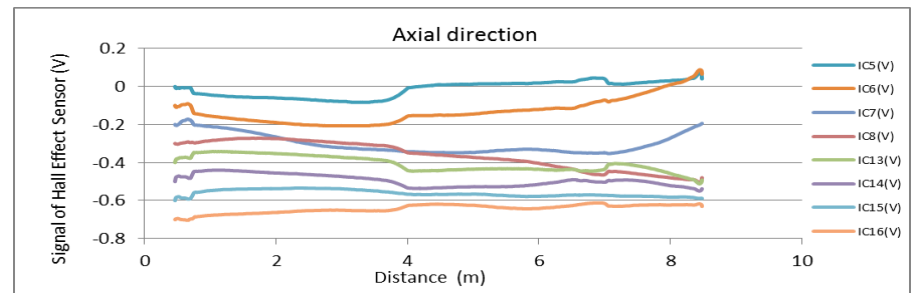
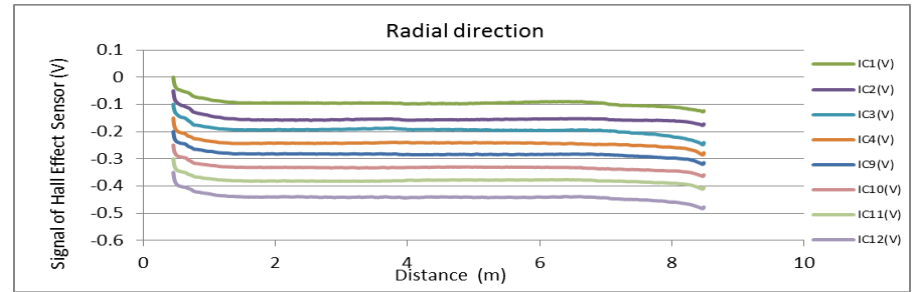
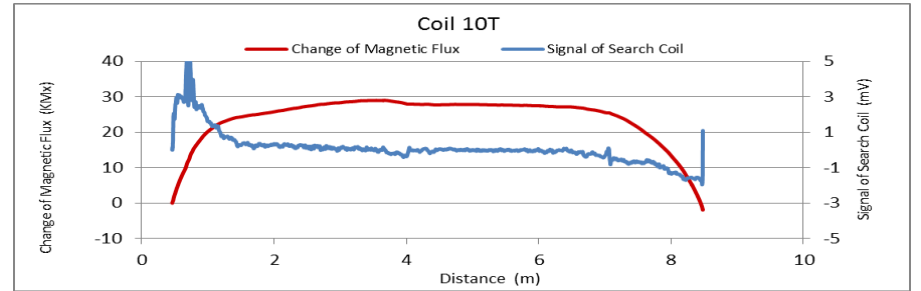


Figure A216. MMFM data of P9-404R-H1 tendon section.



Tokyo Rope USA, Inc.

File Name 【Pier-Tendon-Section】	Section Total Length (m)	Scanned Length		Note			
		Starting Point (m)	Ending Point (m)				
P9-405R-H1	9.3	0.47	8.53				
Identified Damage 1				Identified Damage 2			
Max Loss Point (m)	Section Loss (%)	Damage Length (m)	Damage Orientation	Max Loss Point (m)	Section Loss (%)	Damage Length (m)	Damage Orientation
—	—	—	—	—	—	—	—

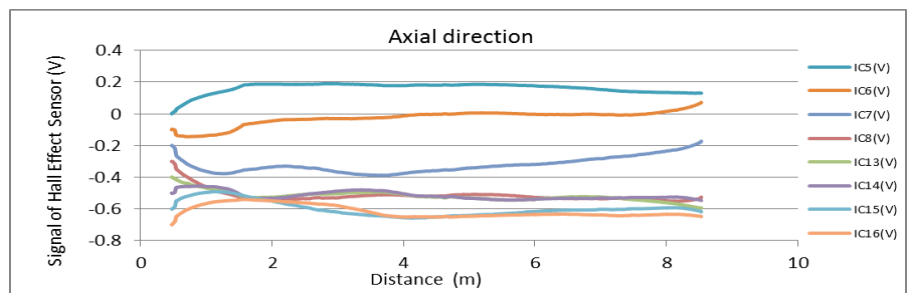
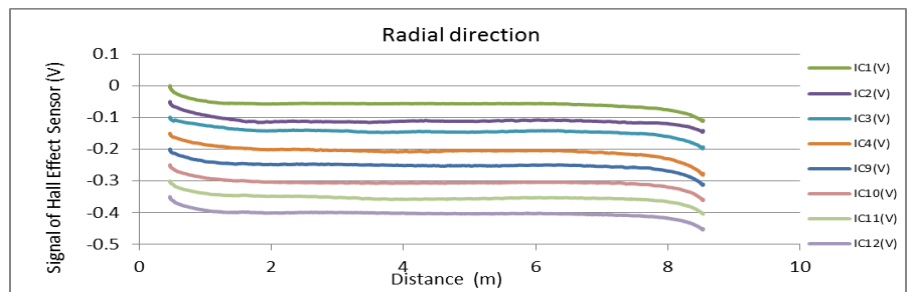
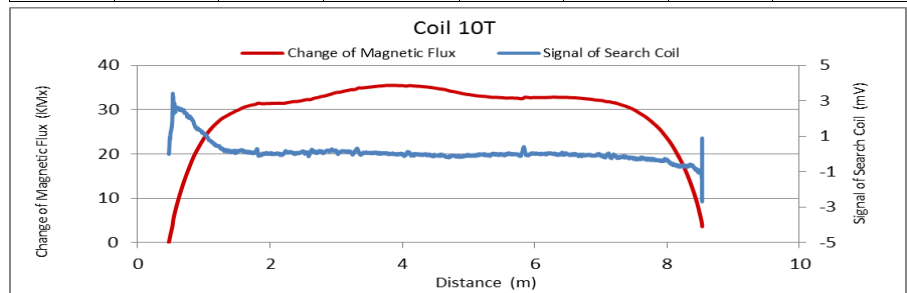


Figure A217. MMFM data of P9-405R-H1 tendon section.

File Name 【Pier-Tendon-Section】	Section Total Length (m)	Scanned Length		Note			
		Starting Point (m)	Ending Point (m)				
P9-406R-H1	9.3	0.79	8.55				
Identified Damage 1				Identified Damage 2			
Max Loss Point (m)	Section Loss (%)	Damage Length (m)	Damage Orientation	Max Loss Point (m)	Section Loss (%)	Damage Length (m)	Damage Orientation
—	—	—	—	—	—	—	—

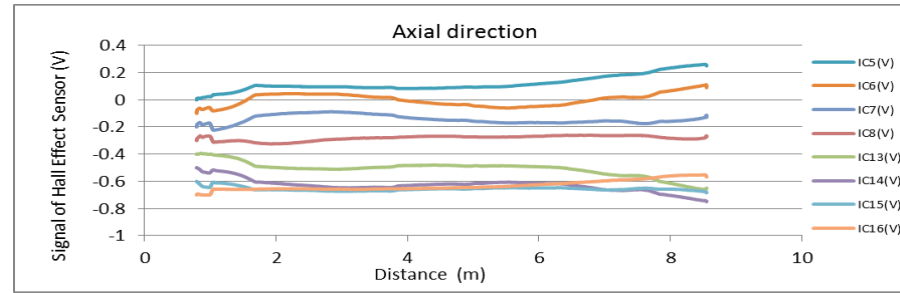
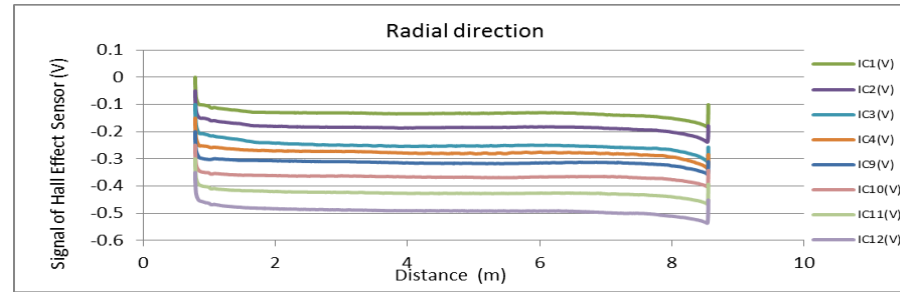
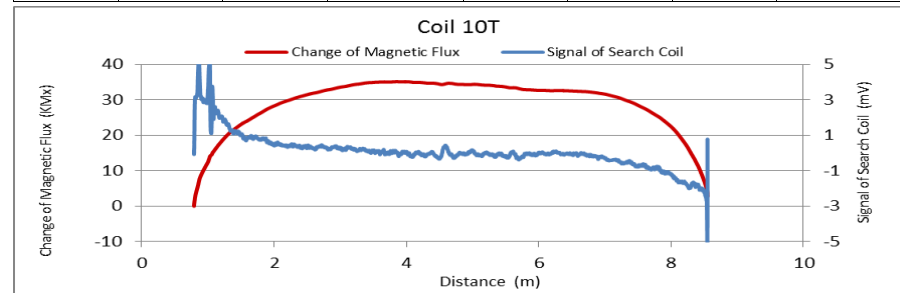


Figure A218. MMFM data of P9-406R-H1 tendon section.



Tokyo Rope USA, Inc.

File Name 【Pier-Tendon-Section】	Section Total Length (m)	Scanned Length		Note			
		Starting Point (m)	Ending Point (m)				
P8-406R-H2	9.37	0.75	8.79				
Identified Damage 1				Identified Damage 2			
Max Loss Point (m)	Section Loss (%)	Damage Length (m)	Damage Orientation	Max Loss Point (m)	Section Loss (%)	Damage Length (m)	Damage Orientation
—	—	—	—	—	—	—	—

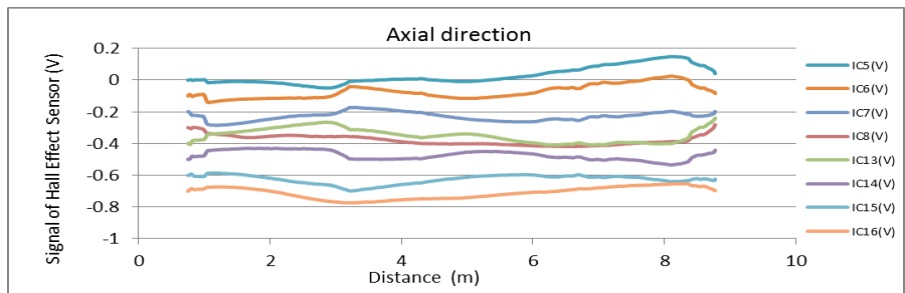
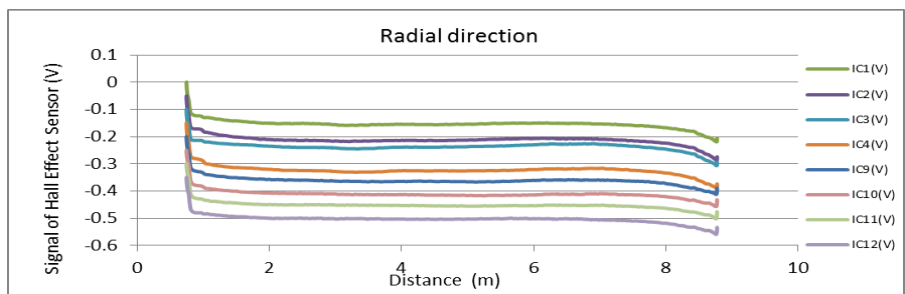
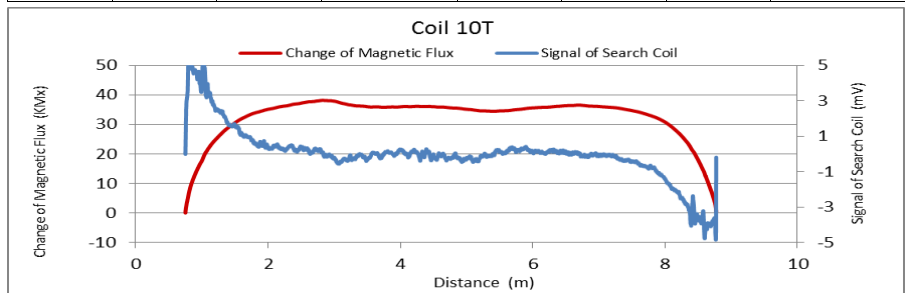


Figure A219. MMFM data of P8-406R-H2 tendon section.

File Name 【Pier-Tendon-Section】	Section Total Length (m)	Scanned Length		Note			
		Starting Point (m)	Ending Point (m)				
P8-405R-H2	9.37	0.58	8.82				
Identified Damage 1				Identified Damage 2			
Max Loss Point (m)	Section Loss (%)	Damage Length (m)	Damage Orientation	Max Loss Point (m)	Section Loss (%)	Damage Length (m)	Damage Orientation
—	—	—	—	—	—	—	—

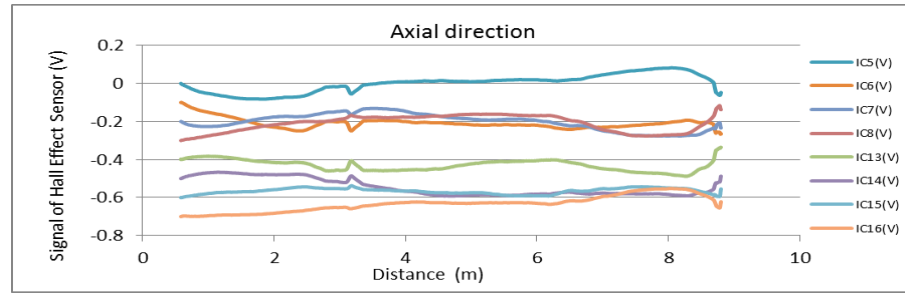
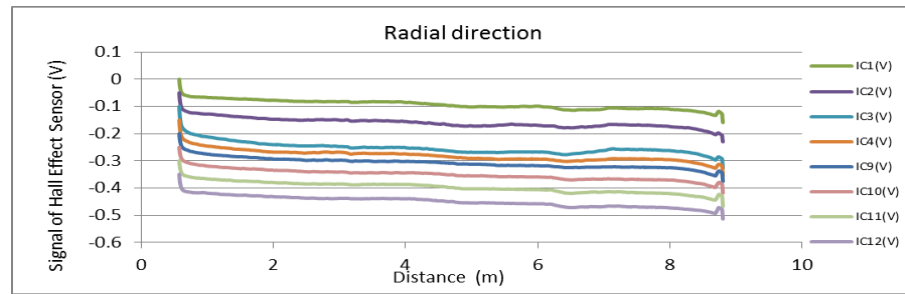
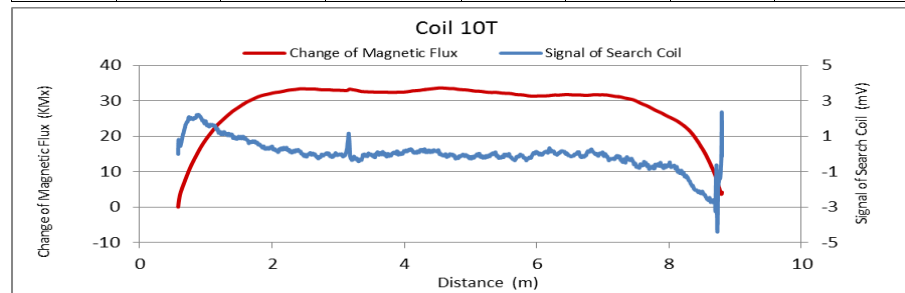


Figure A220. MMFM data of P8-405R-H2 tendon section.



Tokyo Rope USA, Inc.

File Name 【Pier-Tendon-Section】	Section Total Length (m)	Scanned Length		Note			
		Starting Point (m)	Ending Point (m)				
P8-404R-H1	9.36	0.64	8.94				
Identified Damage 1				Identified Damage 2			
Max Loss Point (m)	Section Loss (%)	Damage Length (m)	Damage Orientation	Max Loss Point (m)	Section Loss (%)	Damage Length (m)	Damage Orientation
—	—	—	—	—	—	—	—

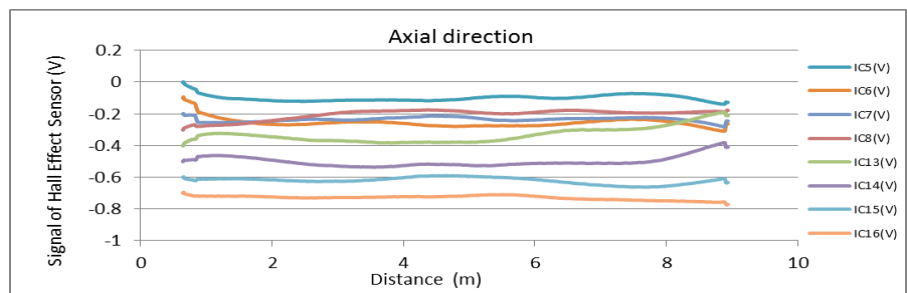
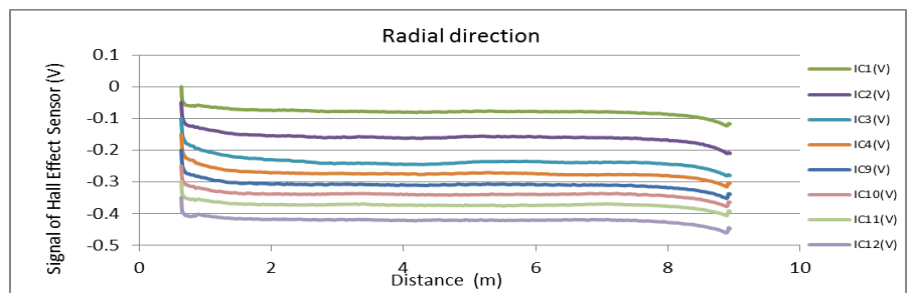
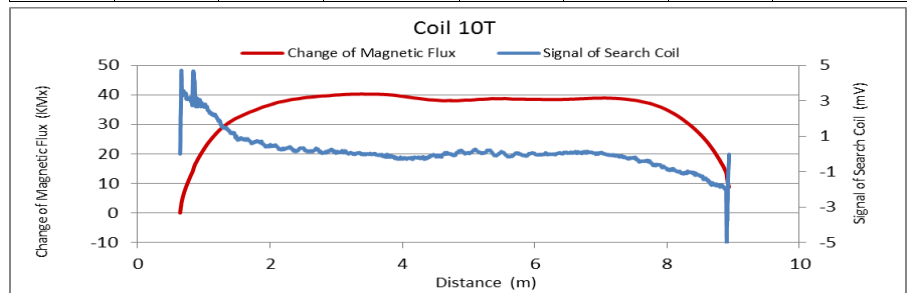


Figure A221. MMFM data of P8-404R-H1 tendon section.

File Name 【Pier-Tendon-Section】	Section Total Length (m)	Scanned Length		Note			
		Starting Point (m)	Ending Point (m)				
P8-403R-H2	9.36	0.64	8.89				
Identified Damage 1				Identified Damage 2			
Max Loss Point (m)	Section Loss (%)	Damage Length (m)	Damage Orientation	Max Loss Point (m)	Section Loss (%)	Damage Length (m)	Damage Orientation
—	—	—	—	—	—	—	—

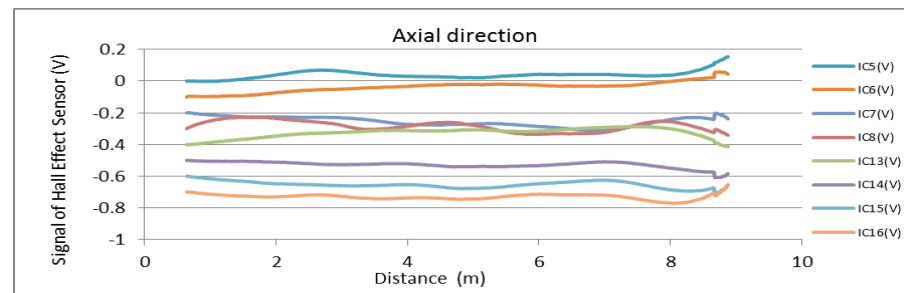
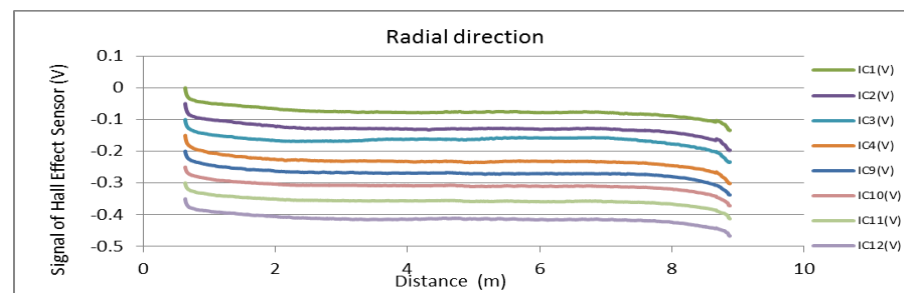
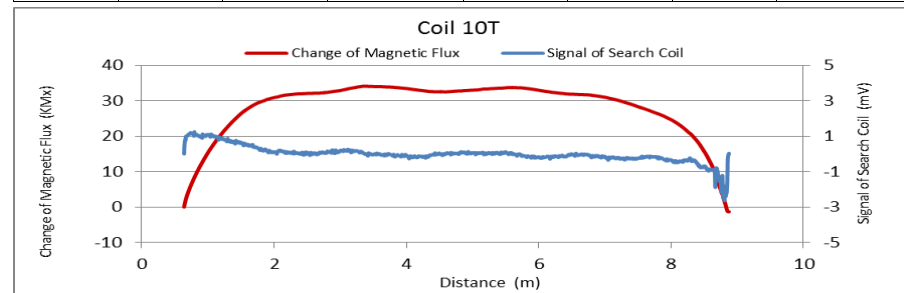


Figure A222. MMFM data of P8-403R-H2 tendon section.



Tokyo Rope USA, Inc.

File Name 【Pier-Tendon-Section】	Section Total Length (m)	Scanned Length		Note			
		Starting Point (m)	Ending Point (m)				
P8-406R-I2	21.43	0.74	20.64	Joint position: 9.13 m			
Identified Damage 1				Identified Damage 2			
Max Loss Point (m)	Section Loss (%)	Damage Length (m)	Damage Orientation	Max Loss Point (m)	Section Loss (%)	Damage Length (m)	Damage Orientation
—	—	—	—	—	—	—	—

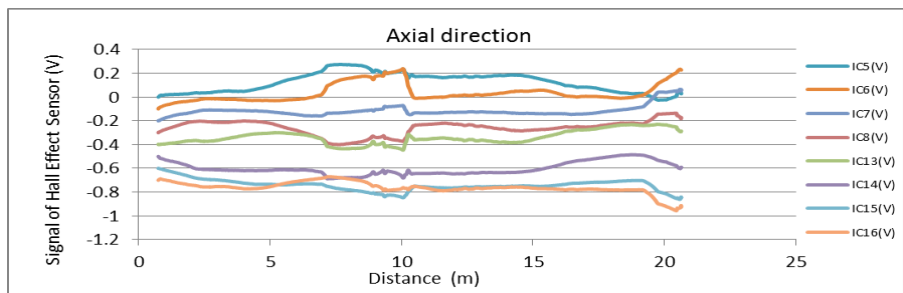
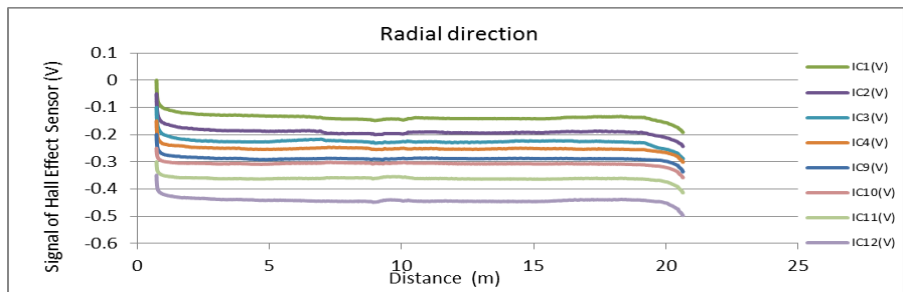
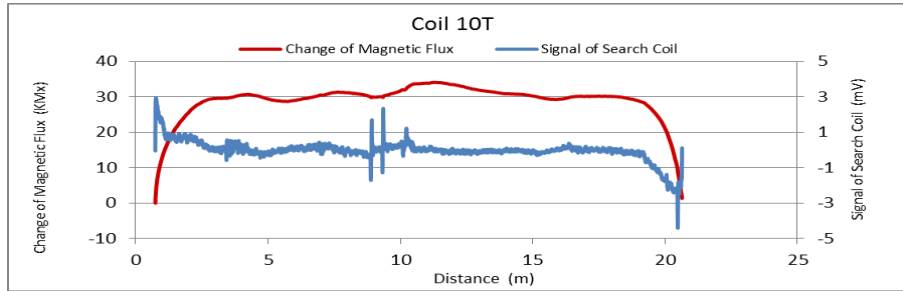


Figure A223. MMFM data of P8-406R-I2 tendon section.

File Name 【Pier-Tendon-Section】	Section Total Length (m)	Scanned Length		Note			
		Starting Point (m)	Ending Point (m)				
P8-404R-I1	21.43	0.69	20.55	Joint position: 9.13 m			
Identified Damage 1				Identified Damage 2			
Max Loss Point (m)	Section Loss (%)	Damage Length (m)	Damage Orientation	Max Loss Point (m)	Section Loss (%)	Damage Length (m)	Damage Orientation
—	—	—	—	—	—	—	—

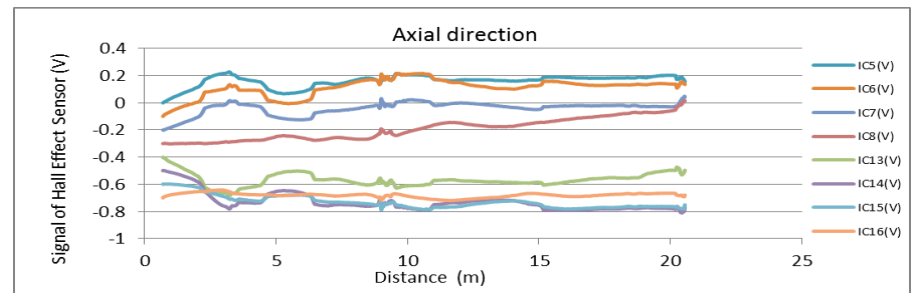
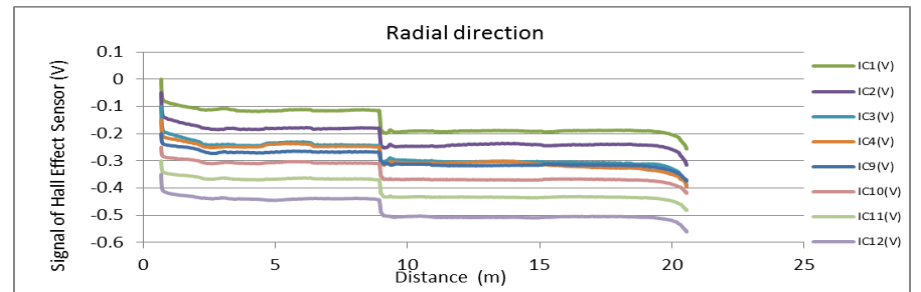
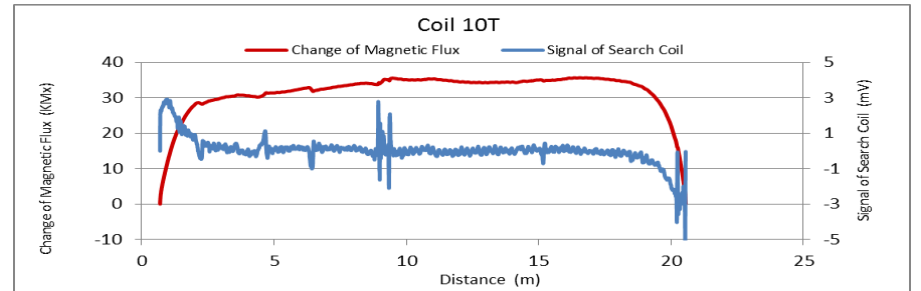


Figure A224. MMFM data of P8-404R-I1 tendon section.



Tokyo Rope USA, Inc.

File Name 【Pier-Tendon-Section】	Section Total Length (m)	Scanned Length		Note			
		Starting Point (m)	Ending Point (m)				
P8-403R-I2	21.43	0.71	20.62	Joint position: 9.15 m			
Identified Damage 1				Identified Damage 2			
Max Loss Point (m)	Section Loss (%)	Damage Length (m)	Damage Orientation	Max Loss Point (m)	Section Loss (%)	Damage Length (m)	Damage Orientation
—	—	—	—	—	—	—	—

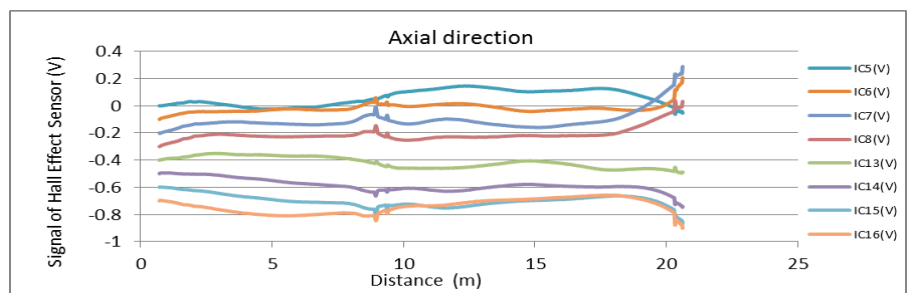
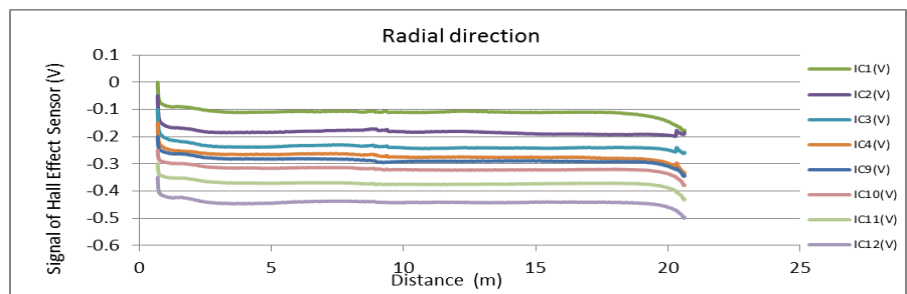
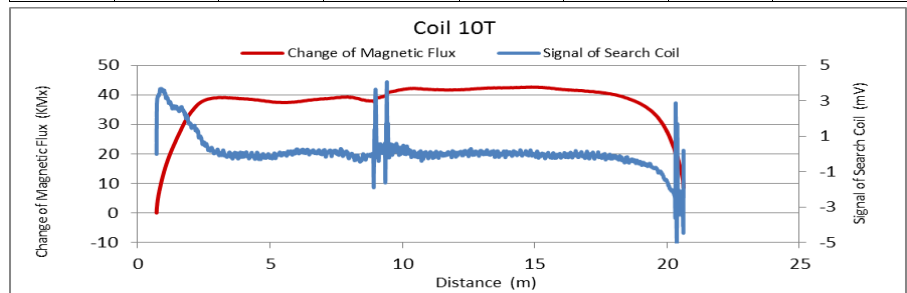


Figure A225. MMFM data of P8-403R-I2 tendon section.

File Name 【Pier-Tendon-Section】	Section Total Length (m)	Scanned Length		Note			
		Starting Point (m)	Ending Point (m)				
P8-403R-I1	21.38	0.46	20.44	Joint position: 12.3 m			
Identified Damage 1				Identified Damage 2			
Max Loss Point (m)	Section Loss (%)	Damage Length (m)	Damage Orientation	Max Loss Point (m)	Section Loss (%)	Damage Length (m)	Damage Orientation
—	—	—	—	—	—	—	—

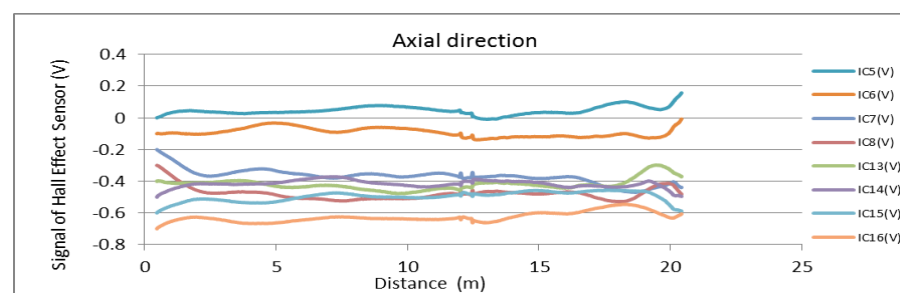
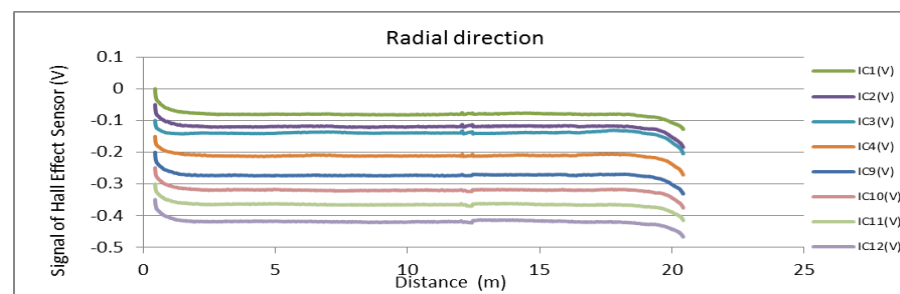
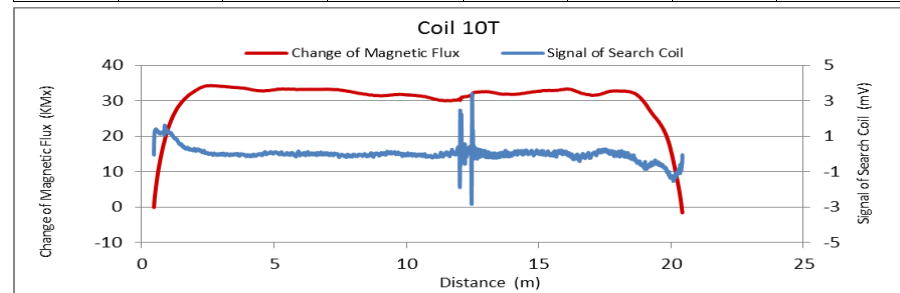
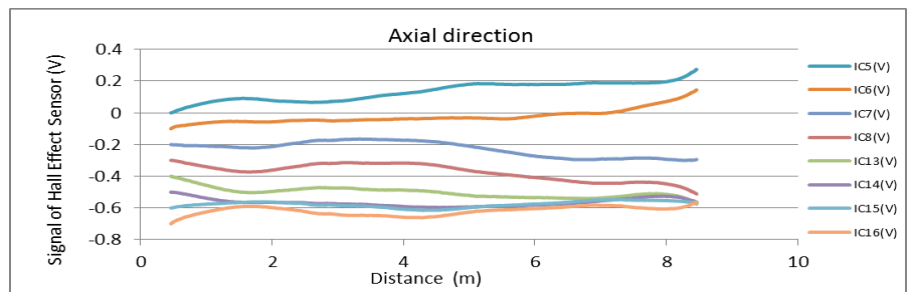
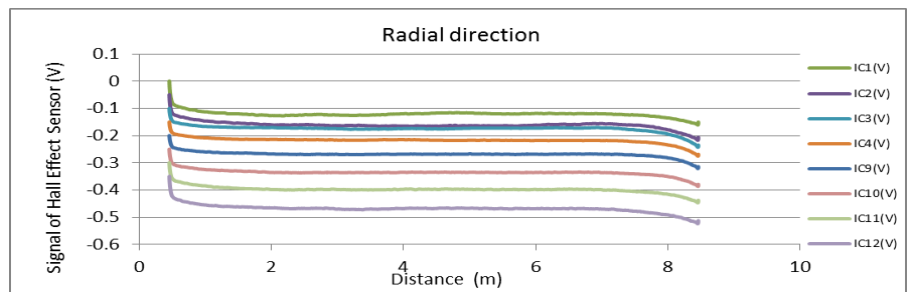
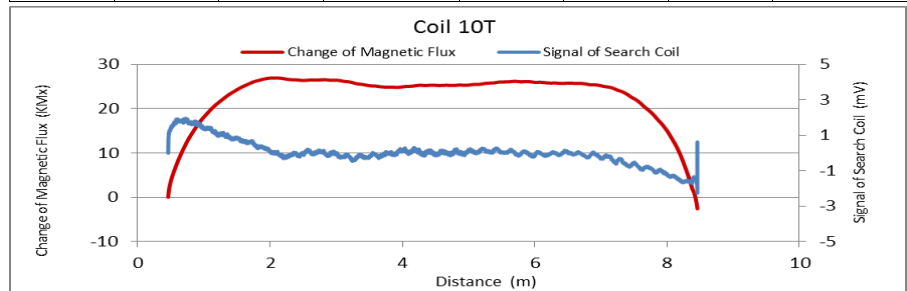


Figure A226. MMFM data of P8-403R-I1 tendon section.



Tokyo Rope USA, Inc.

File Name 【Pier-Tendon-Section】	Section Total Length (m)	Scanned Length		Note			
		Starting Point (m)	Ending Point (m)				
P8-406R-H1	9.3	0.46	8.48				
Identified Damage 1				Identified Damage 2			
Max Loss Point (m)	Section Loss (%)	Damage Length (m)	Damage Orientation	Max Loss Point (m)	Section Loss (%)	Damage Length (m)	Damage Orientation
—	—	—	—	—	—	—	—



File Name 【Pier-Tendon-Section】	Section Total Length (m)	Scanned Length		Note			
		Starting Point (m)	Ending Point (m)				
P8-405R-H1	9.3	0.38	8.49				
Identified Damage 1				Identified Damage 2			
Max Loss Point (m)	Section Loss (%)	Damage Length (m)	Damage Orientation	Max Loss Point (m)	Section Loss (%)	Damage Length (m)	Damage Orientation
—	—	—	—	—	—	—	—

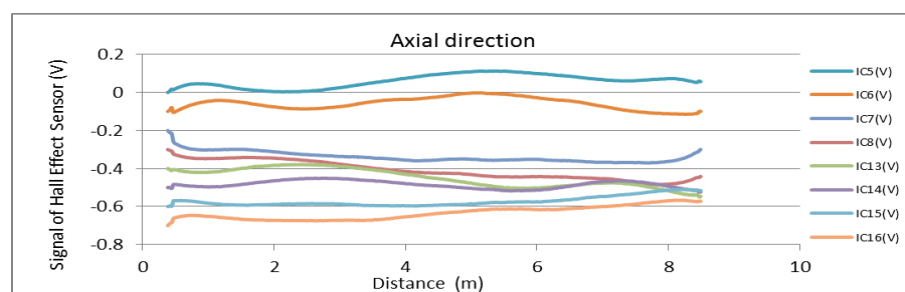
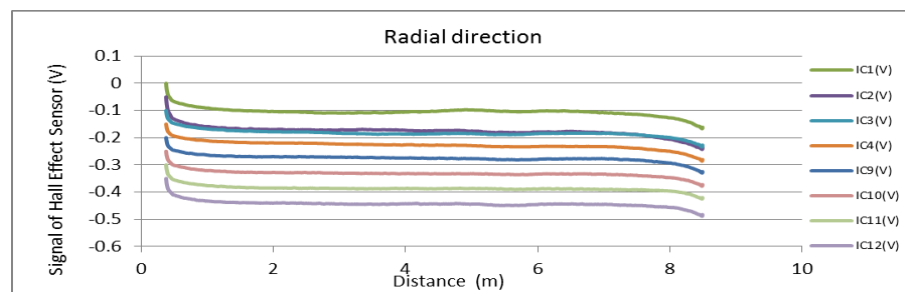
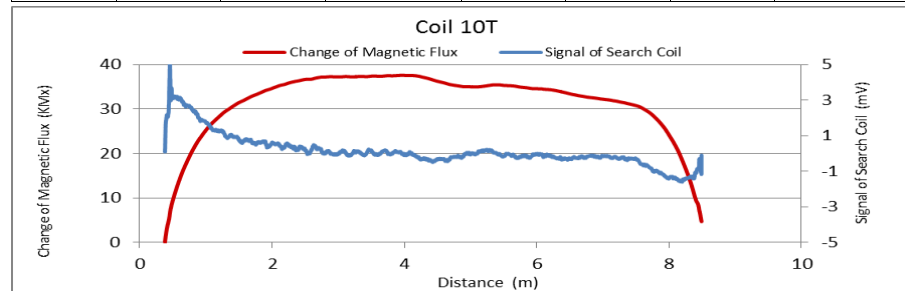


Figure A227. MMFM data of P8-406R-H1 tendon section.

Figure A228. MMFM data of P8-405R-H1 tendon section.



Tokyo Rope USA, Inc.

File Name 【Pier-Tendon-Section】	Section Total Length (m)	Scanned Length		Note			
		Starting Point (m)	Ending Point (m)				
P8-403L-H1	9.44	0.72	8.73				
Identified Damage 1				Identified Damage 2			
Max Loss Point (m)	Section Loss (%)	Damage Length (m)	Damage Orientation	Max Loss Point (m)	Section Loss (%)	Damage Length (m)	Damage Orientation
—	—	—	—	—	—	—	—

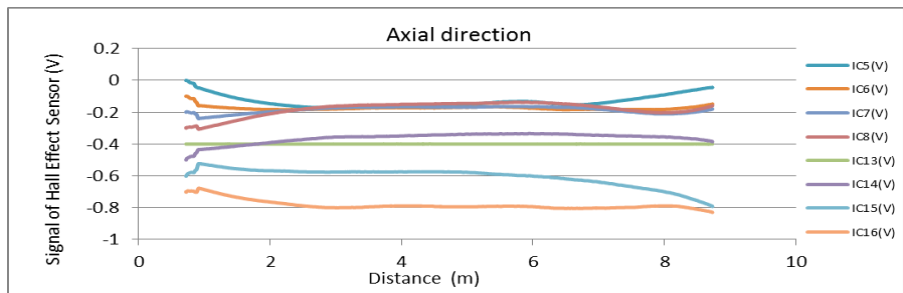
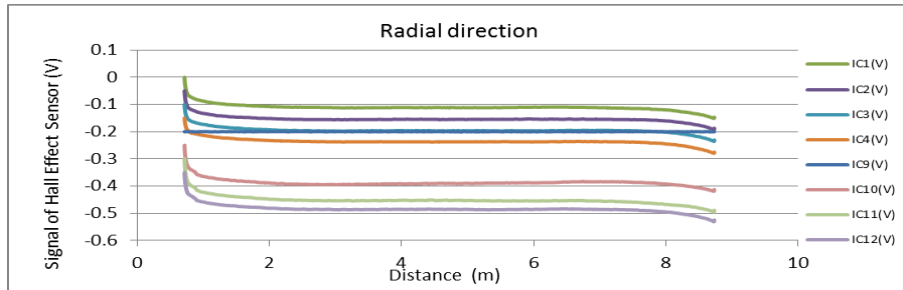
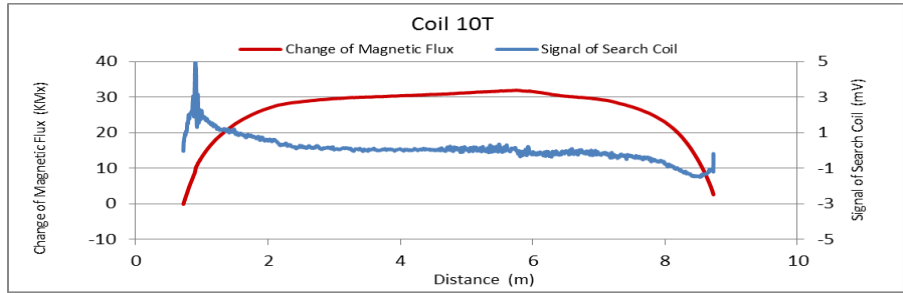


Figure A229. MMFM data of P8-403L-H1 tendon section.

File Name 【Pier-Tendon-Section】	Section Total Length (m)	Scanned Length		Note			
		Starting Point (m)	Ending Point (m)				
P8-405L-H1	9.45	0.47	8.83				
Identified Damage 1				Identified Damage 2			
Max Loss Point (m)	Section Loss (%)	Damage Length (m)	Damage Orientation	Max Loss Point (m)	Section Loss (%)	Damage Length (m)	Damage Orientation
—	—	—	—	—	—	—	—

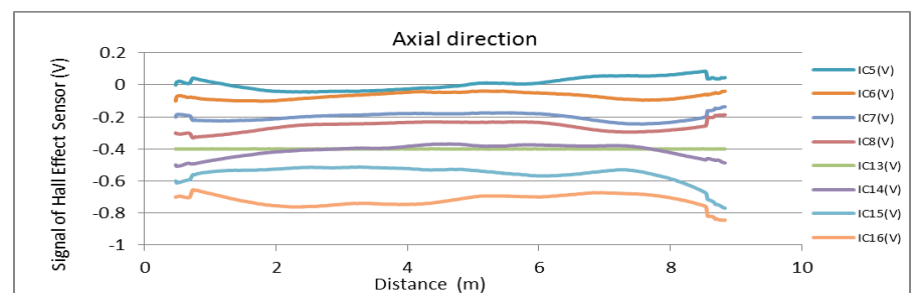
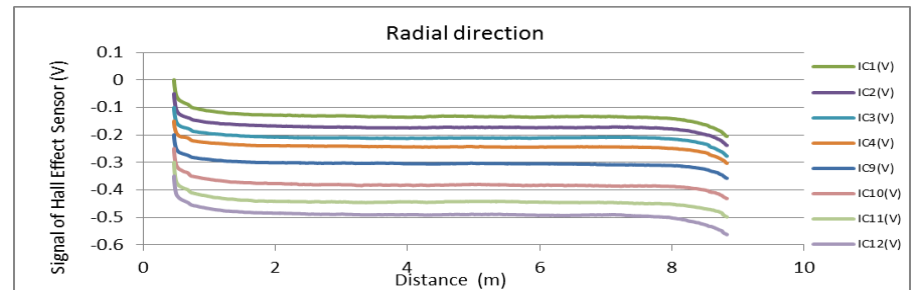
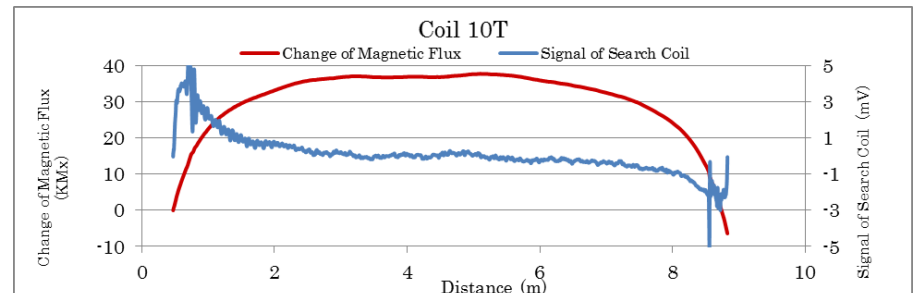


Figure A230. MMFM data of P8-405L-H1 tendon section.



Tokyo Rope USA, Inc.

File Name 【Pier-Tendon-Section】	Section Total Length (m)	Scanned Length		Note			
		Starting Point (m)	Ending Point (m)				
P8-406L-H1	9.45	0.44	8.75				
Identified Damage 1				Identified Damage 2			
Max Loss Point (m)	Section Loss (%)	Damage Length (m)	Damage Orientation	Max Loss Point (m)	Section Loss (%)	Damage Length (m)	Damage Orientation
—	—	—	—	—	—	—	—

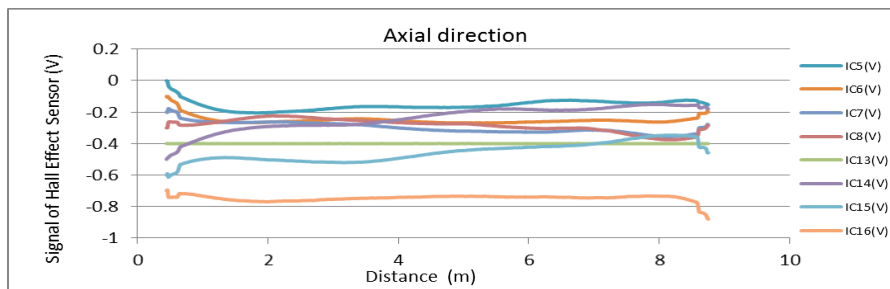
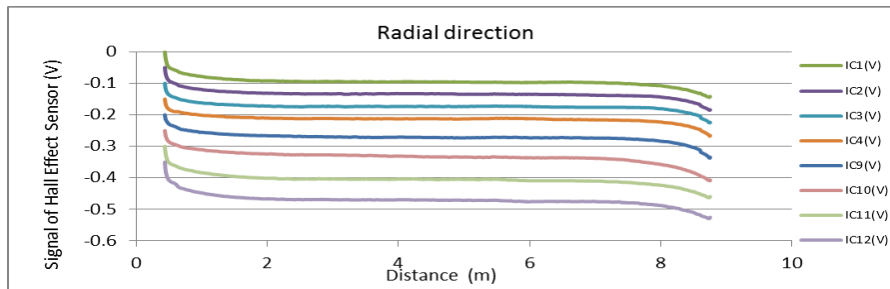
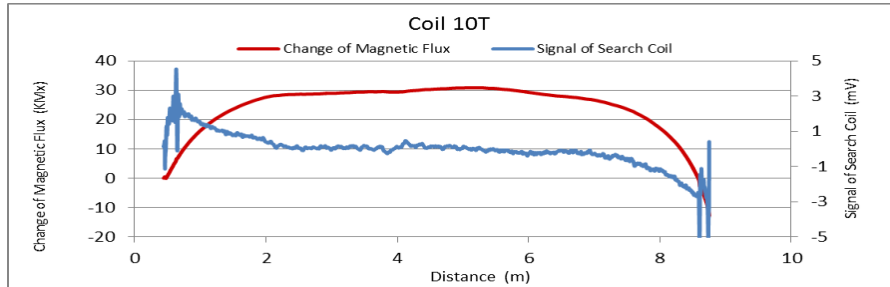


Figure A231. MMFM data of P8-406L-H1 tendon section.

**APPENDIX E MTC TENDONS FOR VERIFICATION
(TOKYO ROPE INC.)**



Tokyo Rope USA, Inc.

8301 Ronda Drive, Canton, MI 48187
Phone: 734-335-6037 Fax: 734-335-6576

March 9, 2018

Dr. Atorod Azizinamini
Dr. Kingsley Lau
Florida International University
Department of Civil & Environmental Engineering
10555 West Flagler Street EC3607, Miami, FL 33174

MMFM Testing at Ringling Bridge Tendon Cable Candidates for Verification

Dear Dr. Azizinamini, Dr. Lau,

With reference to the captioned subject, I am writing to inform you that, after further review of the MMFM test result, we have found some sectional losses (and at some areas, increases of magnetic flux) as shown in the data below.

We have analyzed all the data and concluded that the levels of sectional loss we found were all far less than 5%, and even not as significant as we estimated at the field. But for your verification purpose, we have picked 5 tendons of interest to exercise the verification as per your request.

The candidate tendons are listed below in the order of stronger interest to open. Among them, we have included tendon# P5-303L-I4 which showed an increase of magnetic flux. We have picked the tendon to verify the cause of such result.

We would like to attend the verification process, so we would appreciate it very much if you could kindly inform us the date of tendon opening as soon as it is scheduled.

Thank you again for the valuable opportunity you have given us, and we look forward to meeting you at the verification process.

Sincerely,

Sho Nakahama

Shotaro Nakahama
Vice President



Tokyo Rope USA, Inc.

Tendon Cable Candidates for Verification

1. P9-406L-I1

Total Length (m)	Scanned Length		Identified damage 1				Identified damage 2			
	Starting point(m)	Ending point(m)	Center Point(m)	Loss (%)	Length (m)	Direction	Center Point(m)	Loss (%)	Length (m)	Direction
21.5	0.45	20.77	3.92	1.36	1.08	2~4 O'clock	16.5	1.16	0.71	12~3 O'clock

2. P8-403R-H1

Total Length(m)	Scanned Length		Identified damage 1			
	Starting point(m)	Ending point(m)	Center Point(m)	Loss (%)	Length(m)	Direction
9.3	0.45	8.55	2.62	1.52	0.82	10~12 O'clock

3. P5-303L-I4

Total Length(m)	Scanned Length		Identified damage 1			
	Starting point(m)	Ending point(m)	Center Point(m)	Loss (%)	Length(m)	Direction
9.55	0.26	8.57	5.81	-2.22	0.2	4~8 O'clock

4. P5-402L-H1

Total Length(m)	Scanned Length		Identified damage 1			
	Starting point(m)	Ending point(m)	Center Point(m)	Loss (%)	Length(m)	Direction
9.28	0.65	8.43	7.46	1.2	0.41	7~10 O'clock

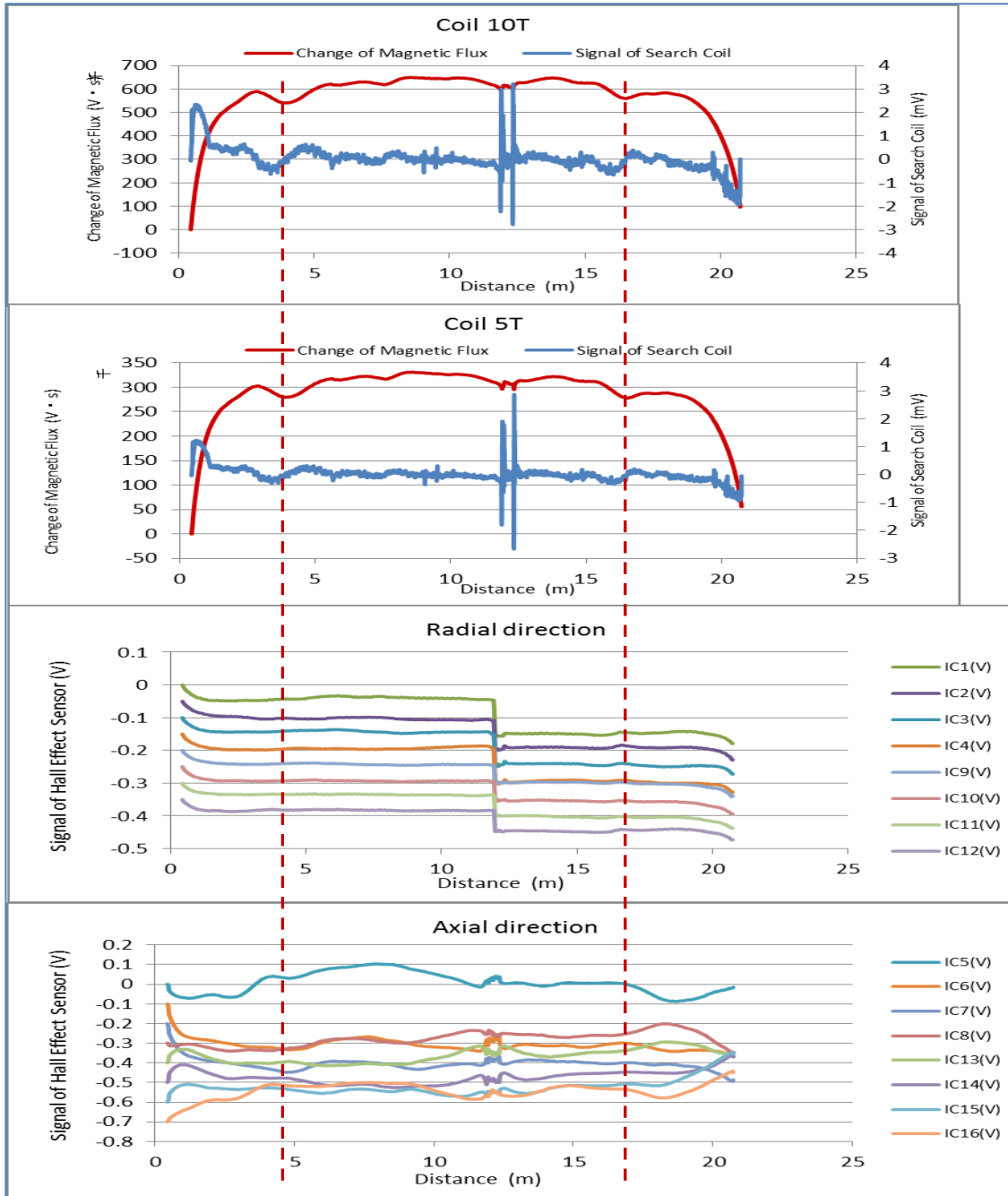
5. P9-405R-I2

Total Length(m)	Scanned Length		Identified damage 1			
	Starting point(m)	Ending point(m)	Center Point(m)	Loss (%)	Length(m)	Direction
21.5	0.49	21.01	18.4	1	0.75	8~12 O'clock



Tokyo Rope USA, Inc.

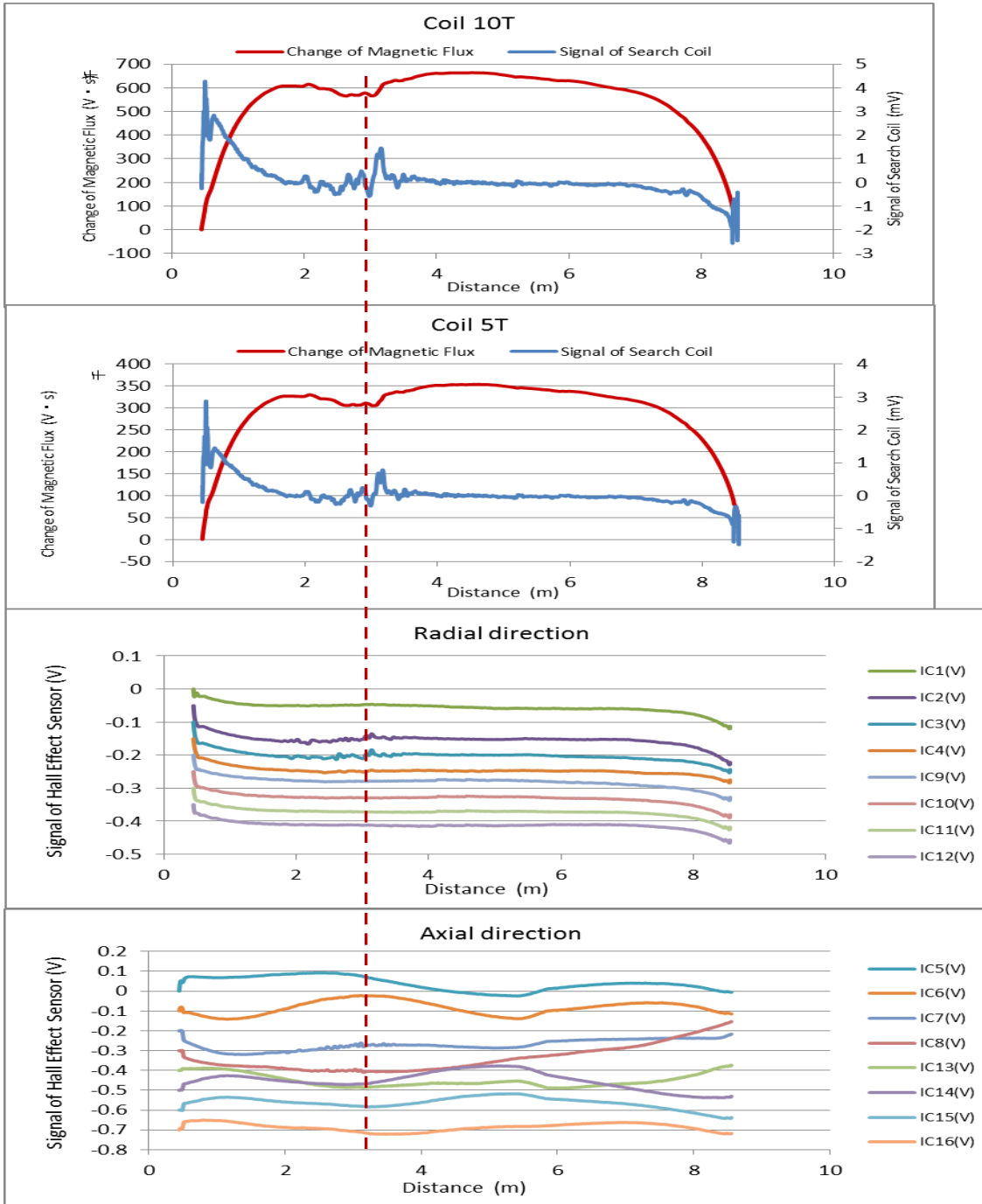
1. P9-406L-I1





Tokyo Rope USA, Inc.

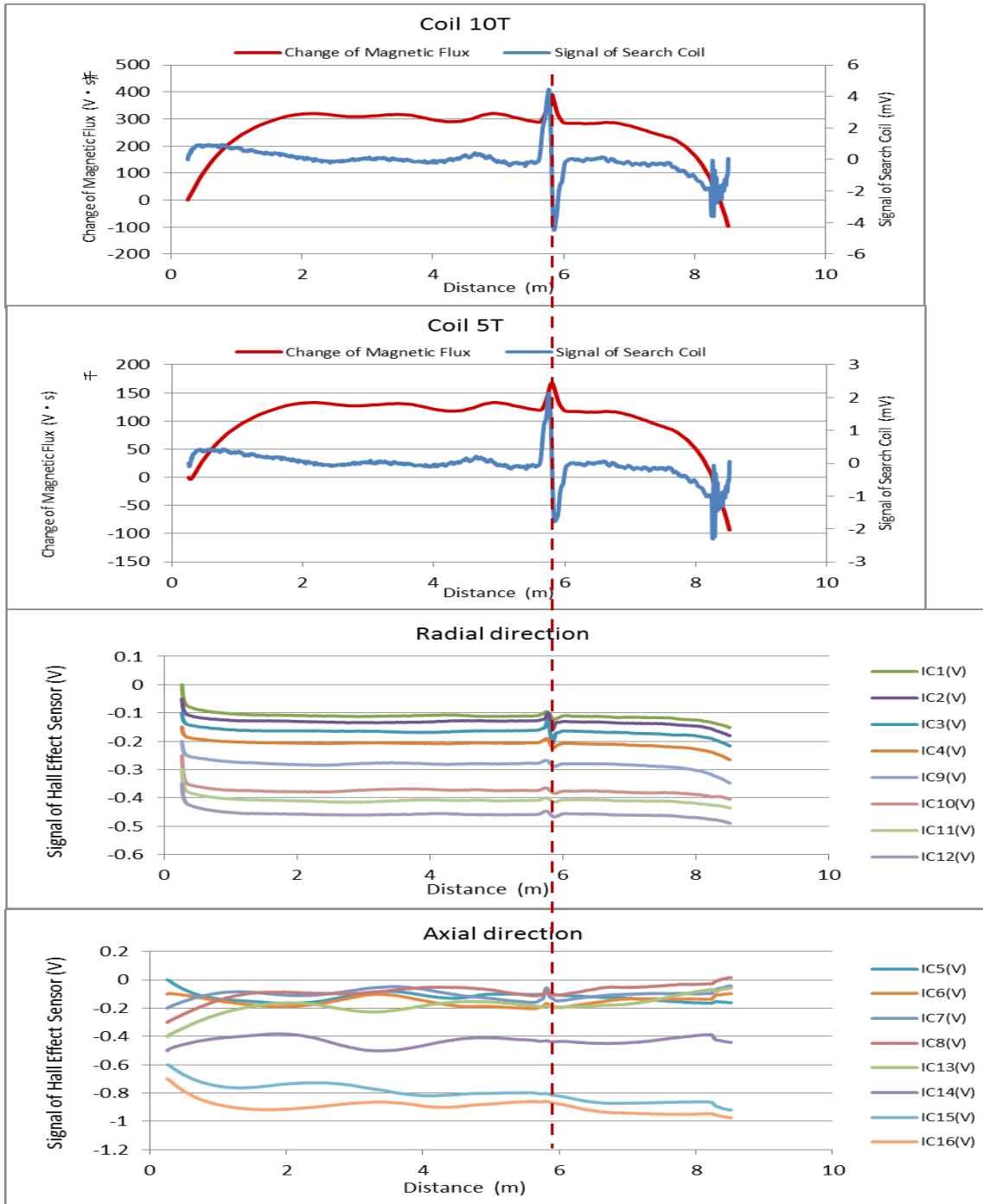
2. P8-403R-H1





Tokyo Rope USA, Inc.

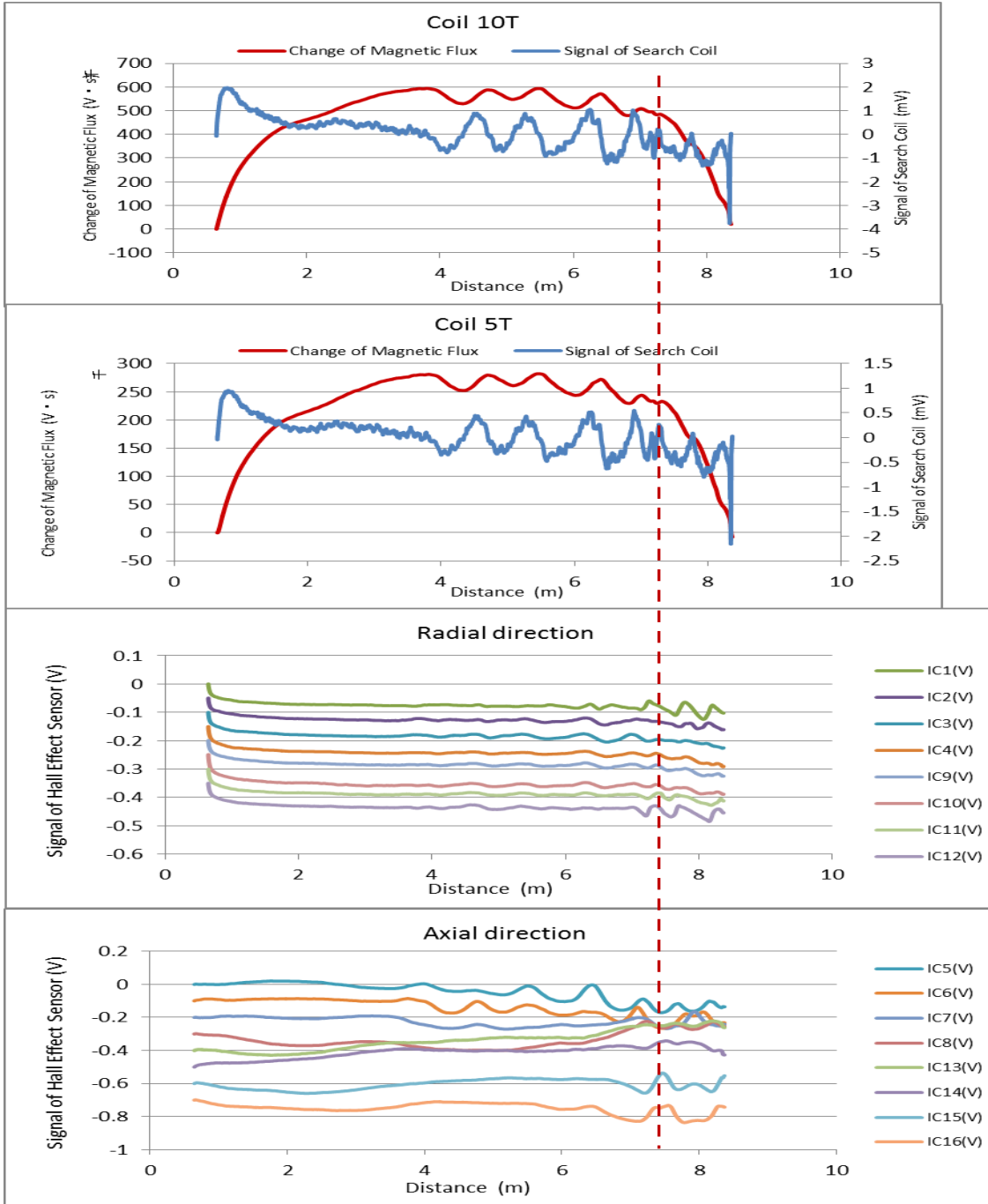
3. P5-303L-I4





Tokyo Rope USA, Inc.

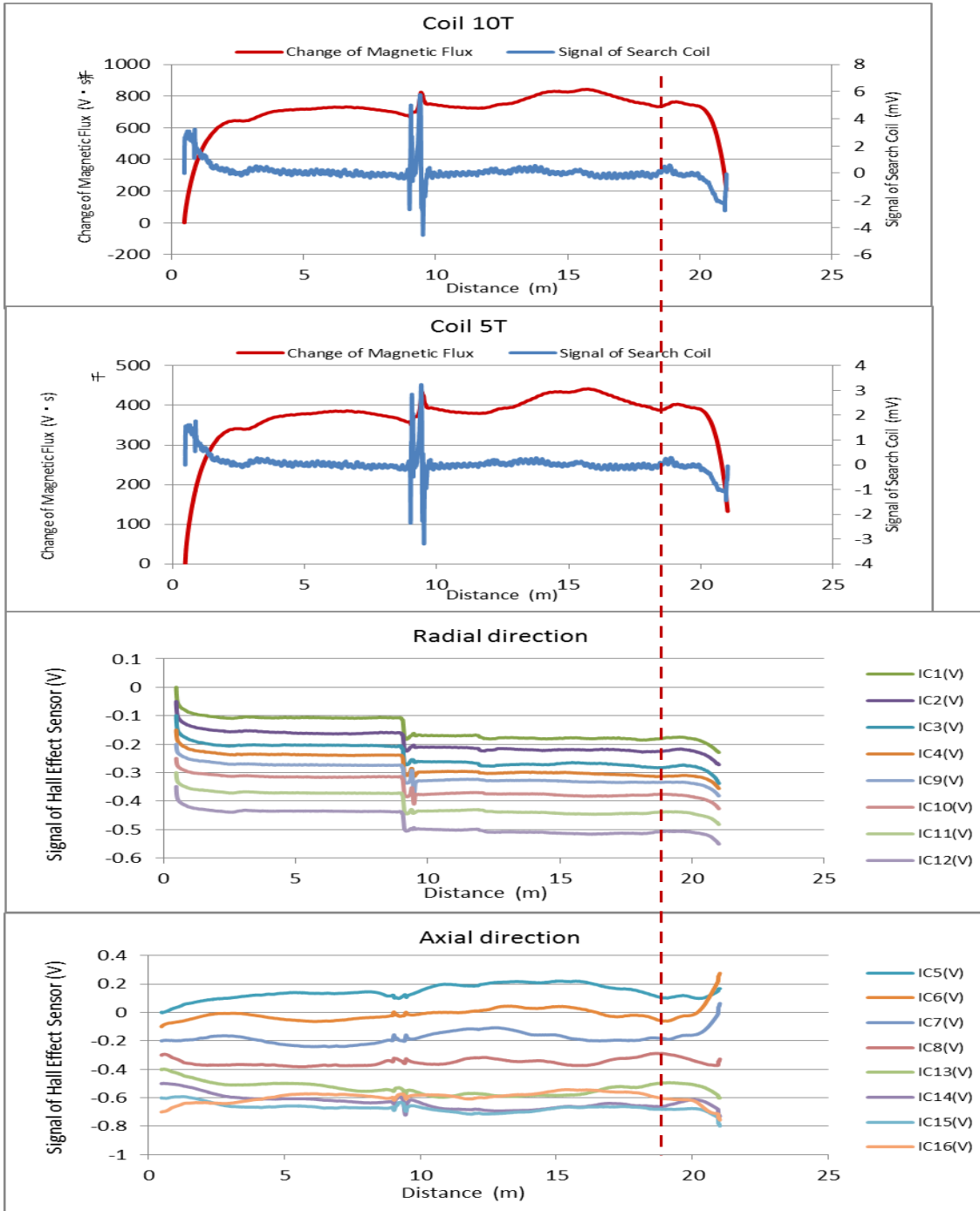
4. P5-402L-H1





Tokyo Rope USA, Inc.

5. P9-405R-I2



**APPENDIX F MTC COMMENTS ON VALIDATION
TESTING (TOKYO ROPE INC.)**



Tokyo Rope USA, Inc.

8301 Ronda Drive, Canton, MI 48187
Phone: 734-335-6037 Fax: 734-335-6576

Report on

ONSITE DUCT OPENINGS AND TEST VALIDATION

Prepared by

Tokyo Rope USA, Inc.

For

Florida International University

and

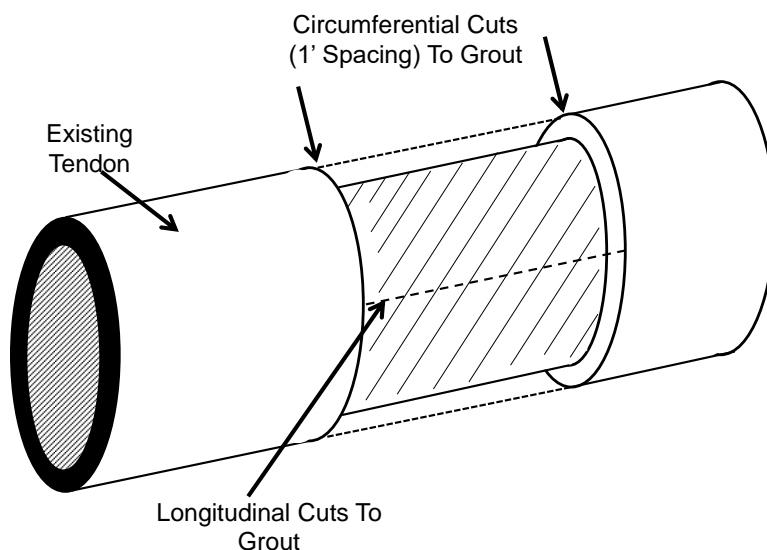
Florida Department of Transportation

August 6 , 2018

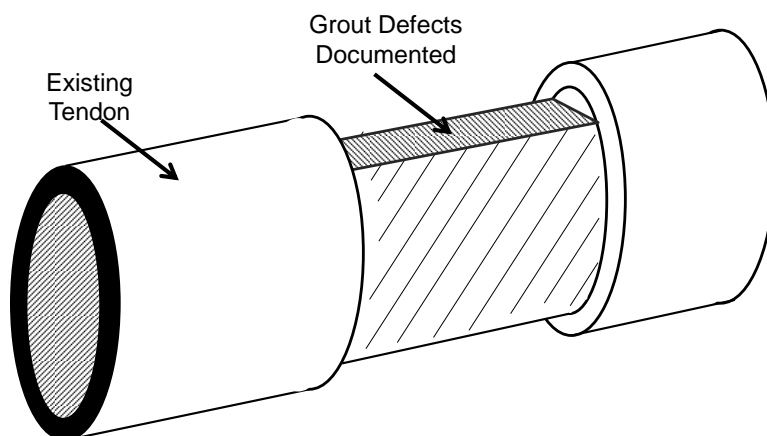


ONSITE DUCT OPENINGS AND TEST VALIDATION

- Photo-documentation with a picture at 12, 3, 6, and 9 o'clock (when possible) should be taken before and after each step



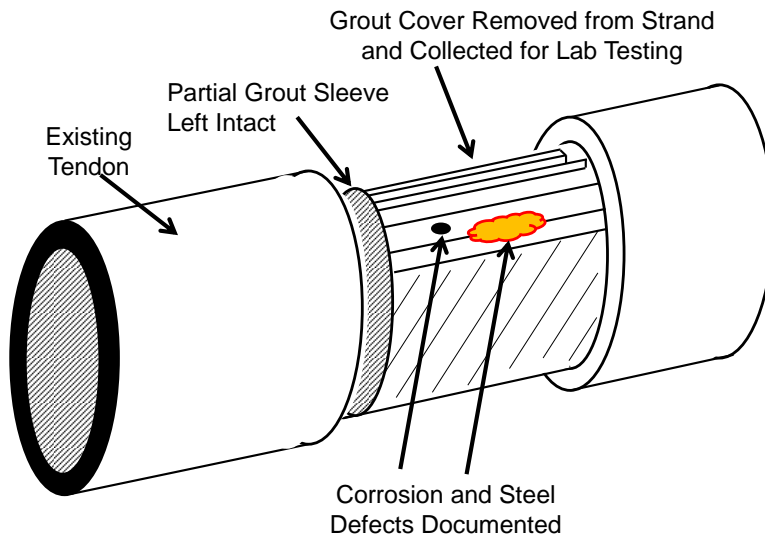
- Cuts tentatively made to avoid hitting steel strand.
- After two circumferential cuts and two parallel longitudinal cuts at 3 and 9 o'clock, the top half pipe carefully removed to reveal underlying grout.
- Bottom half pipe carefully removed to avoid disturbance, breakage and loss of grout material.
- Only the top half pipe should be cut and removed for strand with low ground clearance.



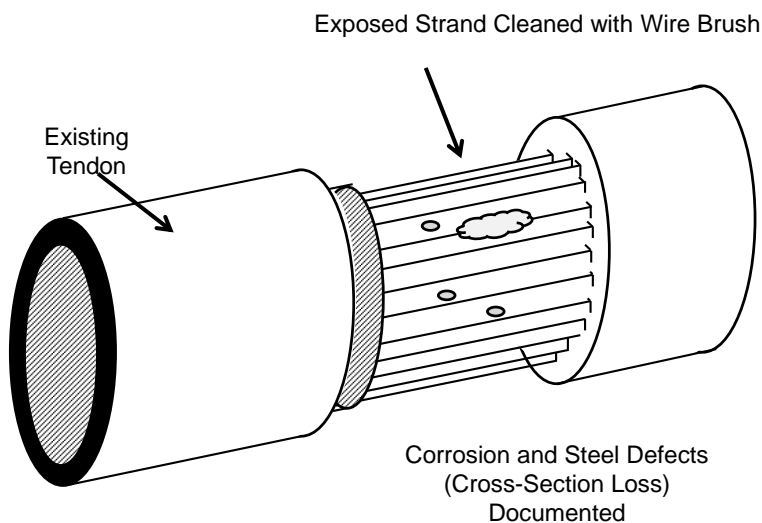
- Geometry of voids should be documented.
- Depth, length, and coverage of deficient grout should be documented.



Tokyo Rope USA, Inc.



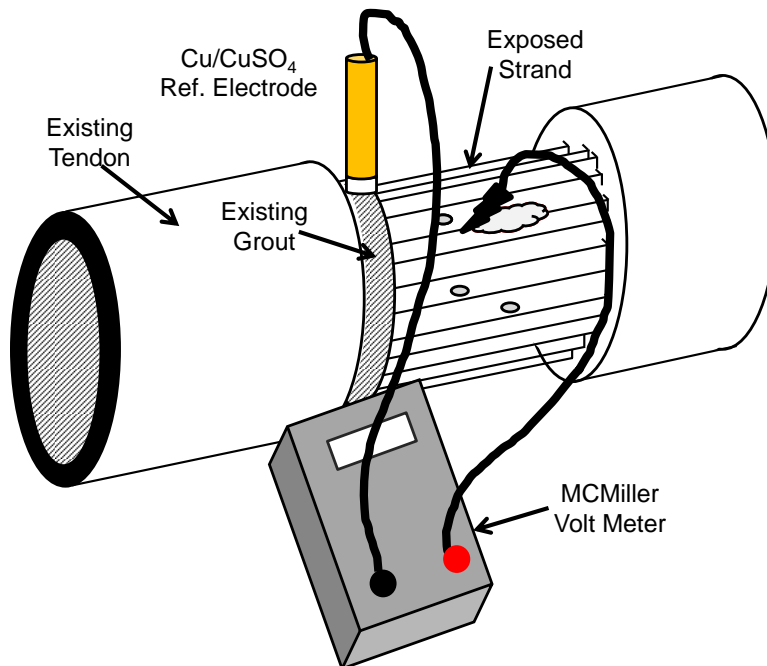
- Grout carefully removed by hammer and scoop to reveal underlying steel.
- A partial grout sleeve should be left intact at one or both cut window edges.
- All grout materials should be sealed in labeled plastic bags for later testing.
- Grout materials may be separated into groups if variability in grout deficiencies exist.
- Any visual rust staining and rust accumulation should be documented.



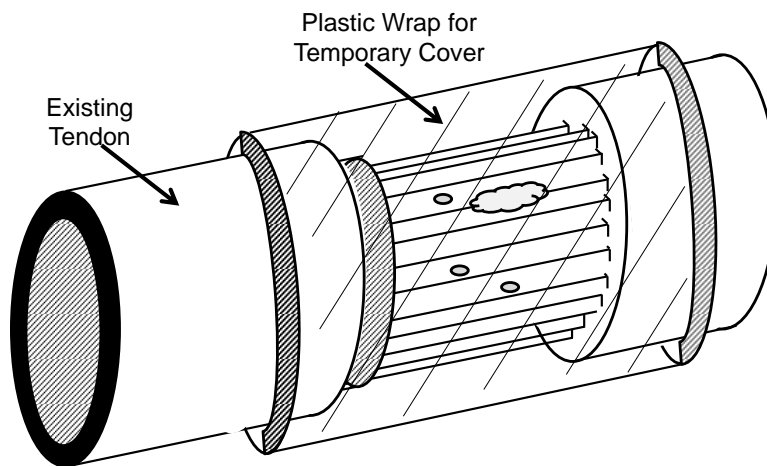
- After removal of grout around the circumference of the steel bundle, the exposed steel should be hand cleaned with a wire brush to remove (as much as attainable by hand) loose grout and rust particles.
- Steel defects and cross-section loss should be documented. A pit-depth gage may be used if localized corrosion observed.



Tokyo Rope USA, Inc.



- Half-cell potentials should be made by placing a slender Cu/CuSO_4 electrode on the existing grout sleeve. The tip of the reference electrode may be covered with a wet sponge. The working electrode contact should be placed on each exposed steel strand regardless of electrical continuity .
- Each measurement should be recorded with notes on ref electrode placement, circumferential location of each strand, and observation of rust.

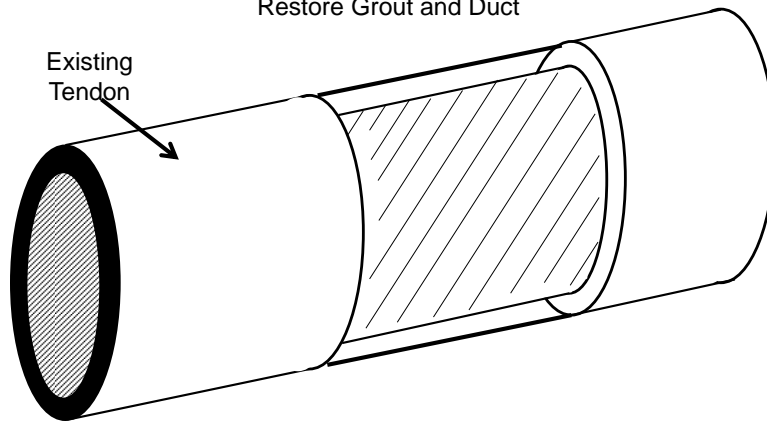


- If a permanent repair is delayed, a temporary cover using plastic wrap and duct tape may be used for up to 2 days.



Tokyo Rope USA, Inc.

Permanent Repair
Restore Grout and Duct



- Permanent repairs conforming to FDOT requirements should be made.
- QC of the permanent repair should be made after 1 day.



Tokyo Rope USA, Inc.

Table 1. Summary of Scan Results in Center Cells

Site	Label	Span	Cell	Tendon	Place	Height	Location	Length	(o'clock)	Defect*
1‡	P8-403R-H1	8	Right (South)	403R-7	Hi Hor.	~14' †	8.5' from Pier 8	2.6' (2' 7.2")	10-12	1.5% CS
2‡	P9-406L-I1	9	Left (North)	406L-8	Slope	~8'	12.8' (12' 9.6") from high deviator	3.6' (3' 7.2")	2-4	1.4% CS
3	S2-402L-1E S114	2	Center	402L-1	Low Hor.	Low	Station 114 (~14' from low deviator)	~10' (S107-117)		No 15kHz, No 20-25kHz
4	P5-303L-I4	5	Center	303L-5	Slope	~11' †	19' from high deviator	0.7' (7.9")	4-7	(-)2.2% CS
5‡	P5-402L-H1	5	Center	402L-4	Hi Hor.	~14' †	24.6' (24' 7.3") from Pier 5	4.6' (4' 7")	8-11	1.3% CS
6	S4-401L-3E S139	4	Center	401L-3	Low Hor.	Low	Station 139 (Near anchor)	~4' (S138-142)		No 15kHz, No 20-25kHz
7	S1-401L-1W S167	1	Center	401L-1	Hi Hor.	~14' †	Station 167 (Near Pier 2)	~5' (S164-169)		No 15kHz, No 20-25kHz
8	S1-401R-1W	1	Center	401R-1	Slope	~3'	Station 44 (~44' from anchor, Near low deviator)			15 kHz, No 20-25kHz

† Scaffold Location

‡ Optional Test Site for NDT Tech.

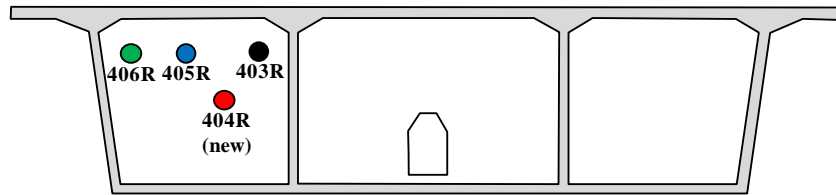
* CS- Cross Section (negative value indicated mass increase)

The yellow marked locations were the opened based on Tokyo Rope MMFM test result.

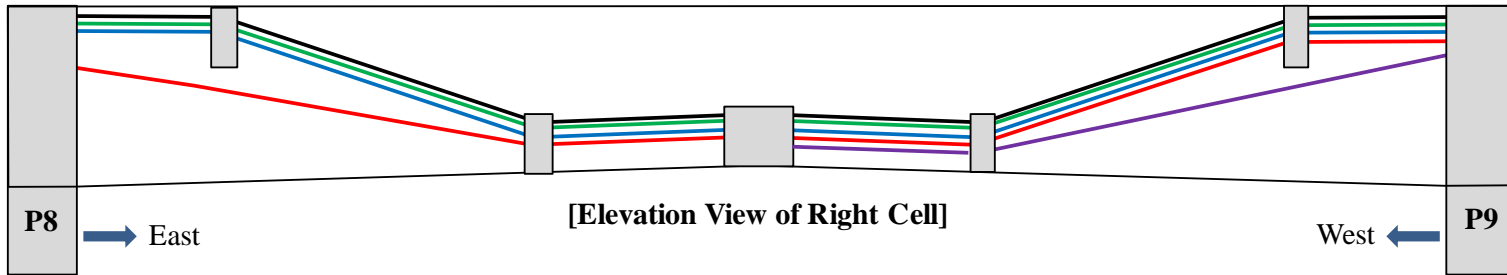
5‡ The location of verification had been changed to P2-402L-I1 (Defect:2.4%)



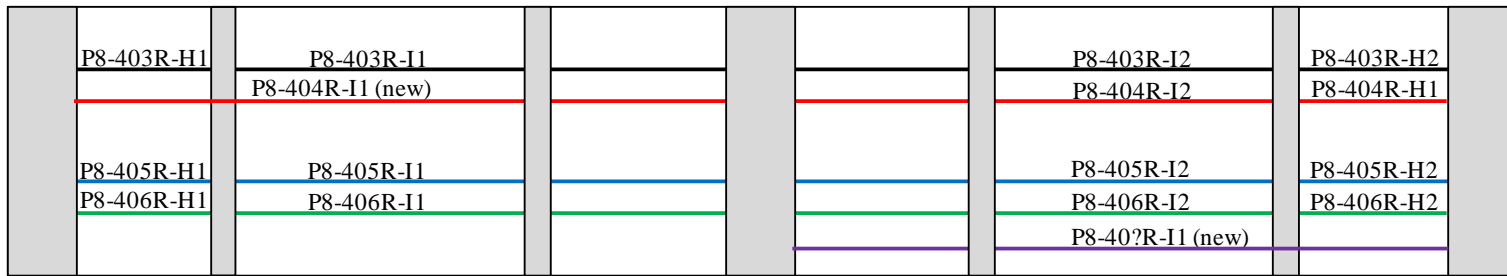
Tokyo Rope USA, Inc.



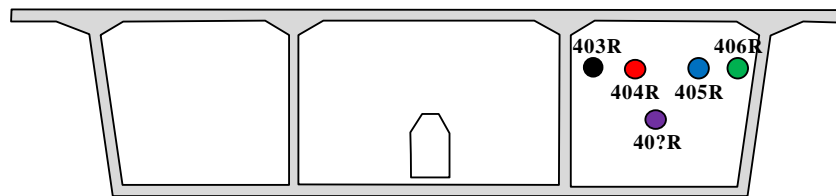
[Diaphragm: East Face at Pier 8]



[Elevation View of Right Cell]



[Plan View of Right Cell]

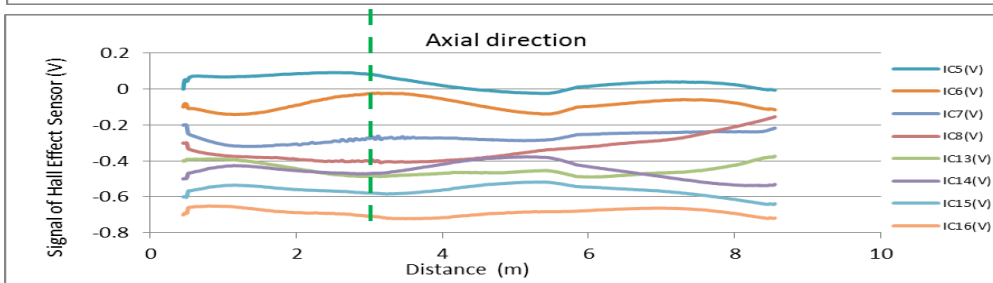
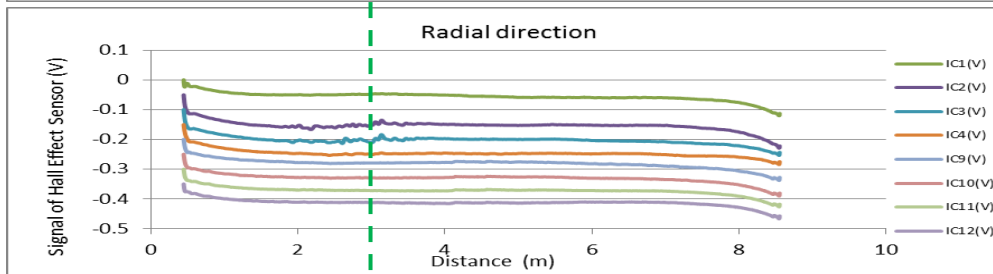
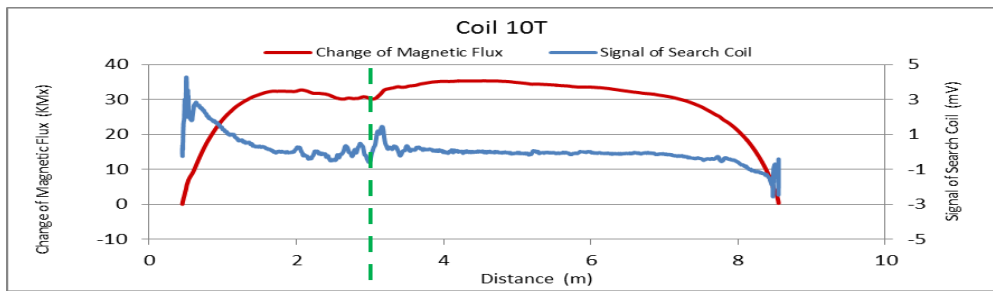


[Diaphragm: West Face at Pier 9]

Figure . Scanned tendon sections in P8 – P9 (right cell).

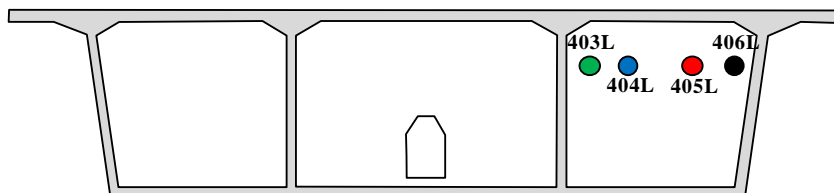


File Name 【Pier-Tendon-Section】	Section Total Length(m)	Scanned Length		Note			
		Starting Point(m)	Ending Point(m)				
P8-403R-H1	9.3	0.45	8.55	Starting point of damage1 : 2.68m			
Identified damage 1				Identified damage 2			
Max Loss Point(m)	Section Loss (%)	Damage Length(m)	Damage Orientation	Max Loss Point(m)	Section Loss (%)	Damage Length(m)	Damage Orientation
3.0	1.5	0.80	10~12 o'clock				

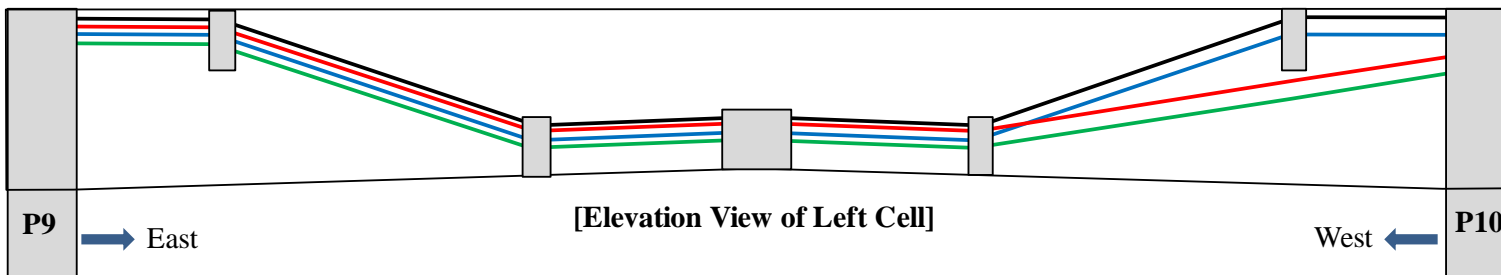




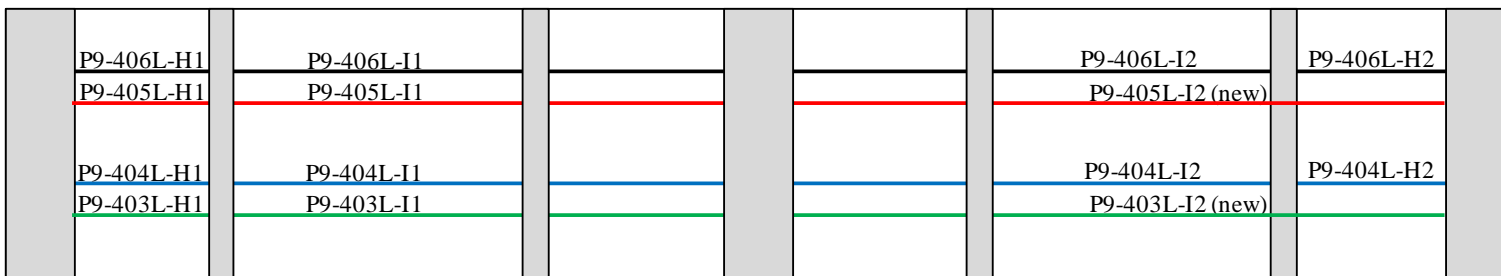
Tokyo Rope USA, Inc.



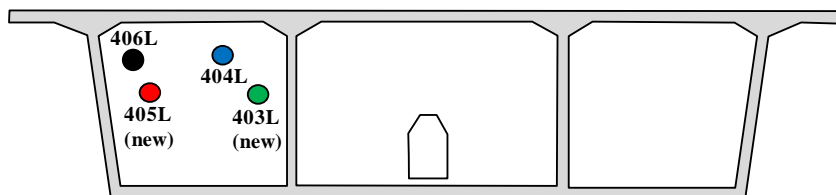
[Diaphragm: East Face at Pier 9]



[Elevation View of Left Cell]



[Plan View of Left Cell]



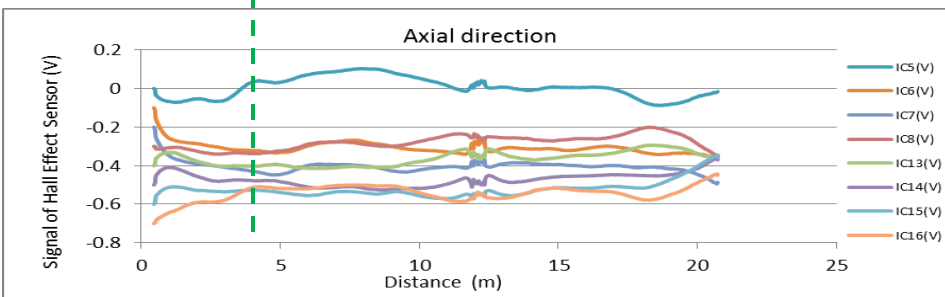
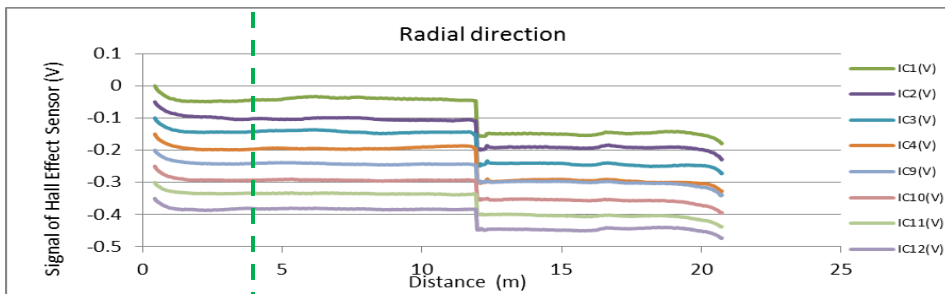
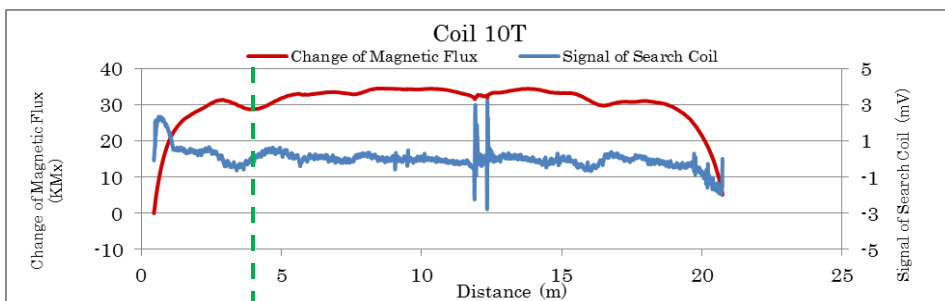
[Diaphragm: West Face at Pier 10]

Figure . Scanned tendon sections in P9 – P10 (left cell).



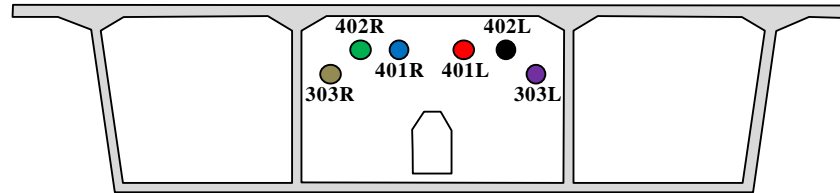
Tokyo Rope USA, Inc.

File Name 【Pier-Tendon-Section】	Section Total Length(m)	Scanned Length		Note			
		Starting Point(m)	Ending Point(m)				
P9-406L-II	21.5	0.45	20.77	Joint position : 12.2m Starting point of damage1 : 3.2m Starting point of damage2 : 15.9m			
Identified damage 1				Identified damage 2			
Max Loss Point(m)	Section Loss (%)	Damage Length(m)	Damage Orientation	Max Loss Point(m)	Section Loss (%)	Damage Length(m)	Damage Orientation
3.9	1.4	1.08	2~4 o'clock	16.5	1.2	0.71	12~3 o'clock

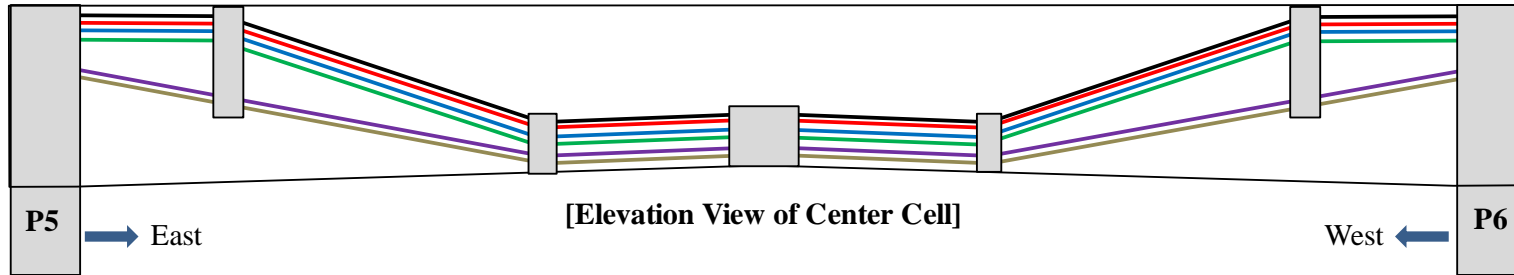




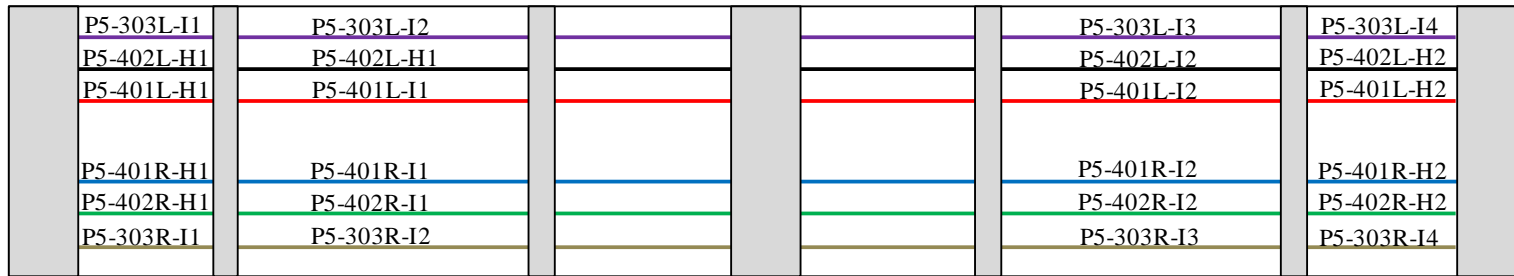
Tokyo Rope USA, Inc.



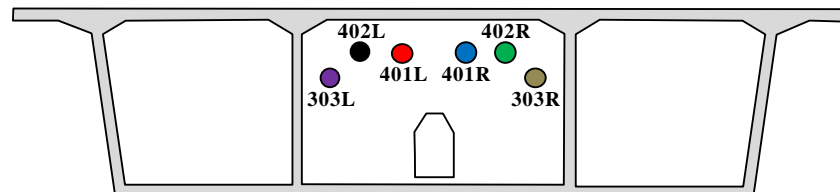
[Diaphragm: East Face at Pier 5]



[Elevation View of Center Cell]



[Plan View of Center Cell]



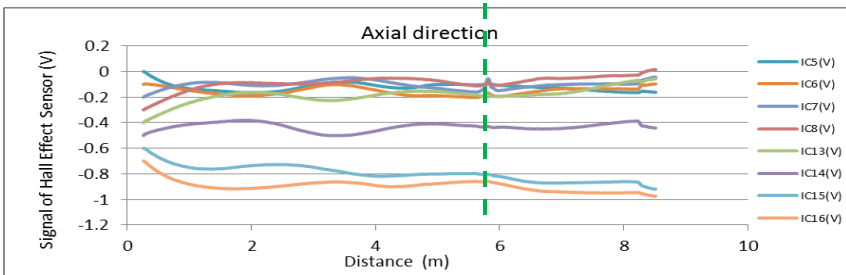
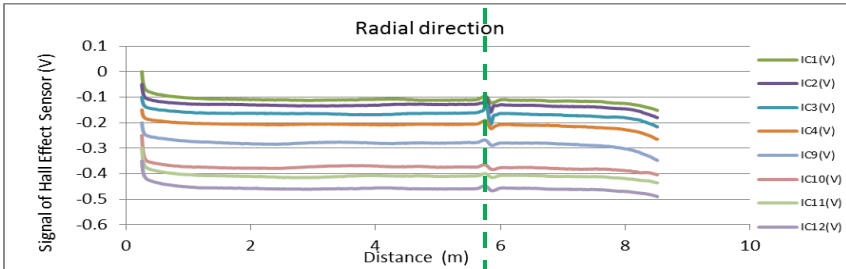
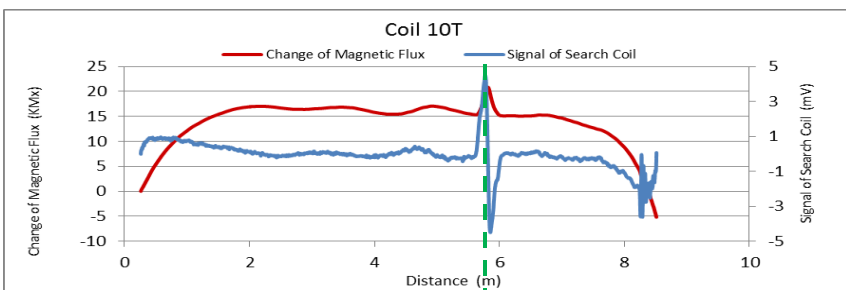
[Diaphragm: West Face at Pier 6]

Figure . Scanned tendon sections in P5 – P6 (center cell).



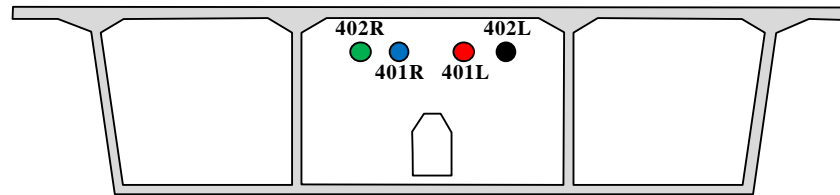
Tokyo Rope USA, Inc.

File Name 【Pier-Tendon-Section】	Section Total Length(m)	Scanned Length		Note			
		Starting Point(m)	Ending Point(m)				
P5-303L-I4	9.55	0.26	8.57	Identified damage 1 : Increase of change of magnetic flux Starting point of damage : 5.72m			
Identified damage 1				Identified damage 2			
Max Loss Point(m)	Section Loss (%)	Damage Length(m)	Damage Orientation	Max Loss Point(m)	Section Loss (%)	Damage Length(m)	Damage Orientation
5.8	-2.2	0.16	4~7 o'clock				

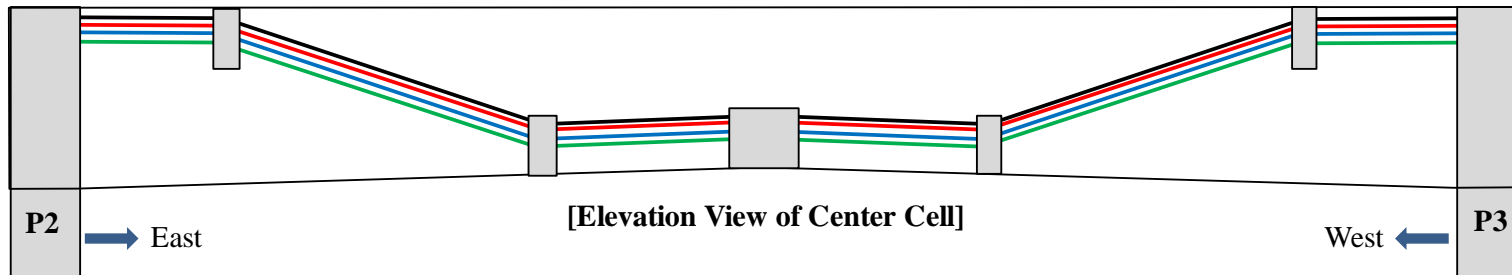




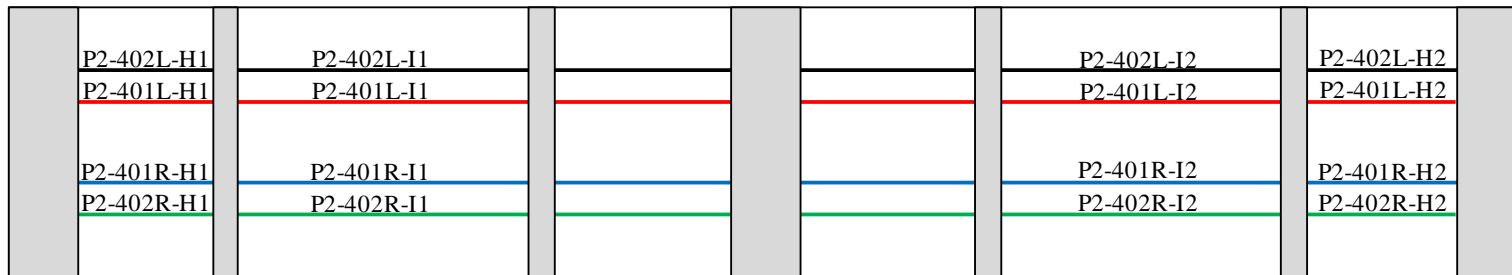
Tokyo Rope USA, Inc.



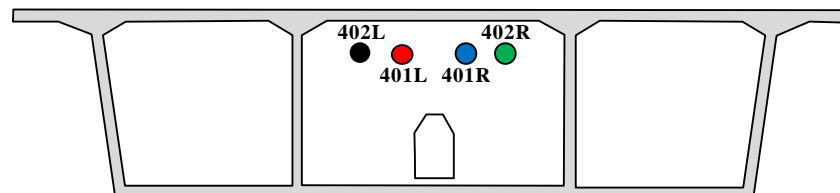
[Diaphragm: East Face at Pier 2]



[Elevation View of Center Cell]



[Plan View of Center Cell]



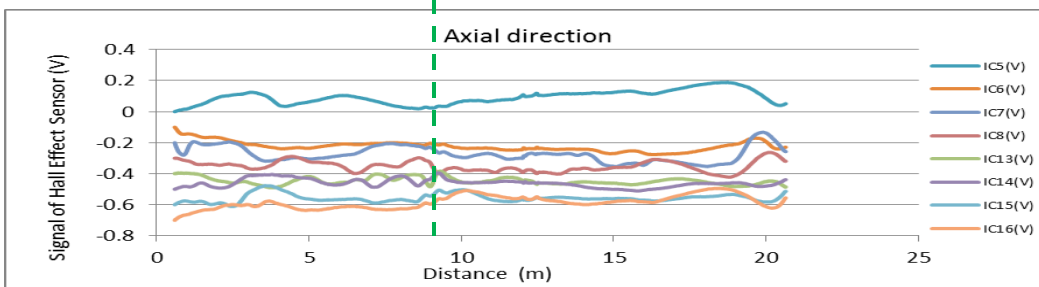
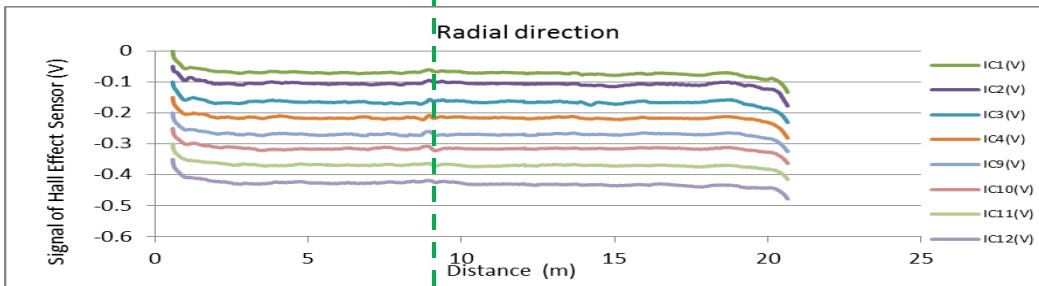
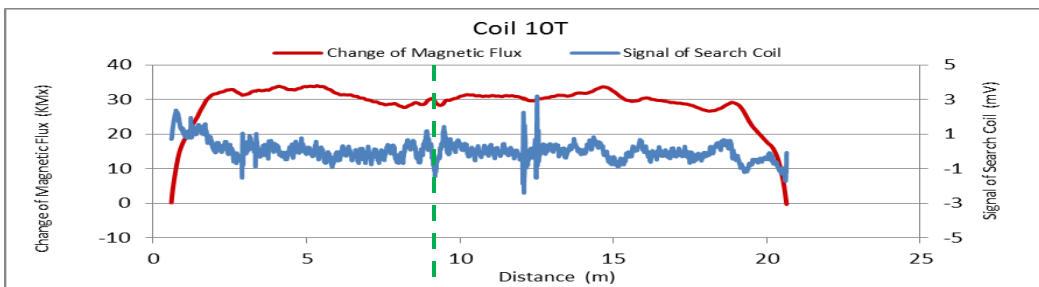
[Diaphragm: West Face at Pier 3]

Figure . Scanned tendon sections in P2 – P3 (center cell).



Tokyo Rope USA, Inc.

File Name 【Pier-Tendon-Section】	Section Total Length(m)	Scanned Length		Note			
		Starting Point(m)	Ending Point(m)				
P2-402L-II	21.37	0.59	20.68	Joint position : 12.3m Starting point of damage1 : 7.15m			
Identified damage 1				Identified damage 2			
Max Loss Point(m)	Section Loss (%)	Damage Length(m)	Damage Orientation	Max Loss Point(m)	Section Loss (%)	Damage Length(m)	Damage Orientation
8.2	2.4	1.78	6~8 o'clock				





Analysis of the Result of Verification of Site 1 P8-403R-H1 and Site 2 P9-406L-I1 :

Site 1 P8-403R-H1:

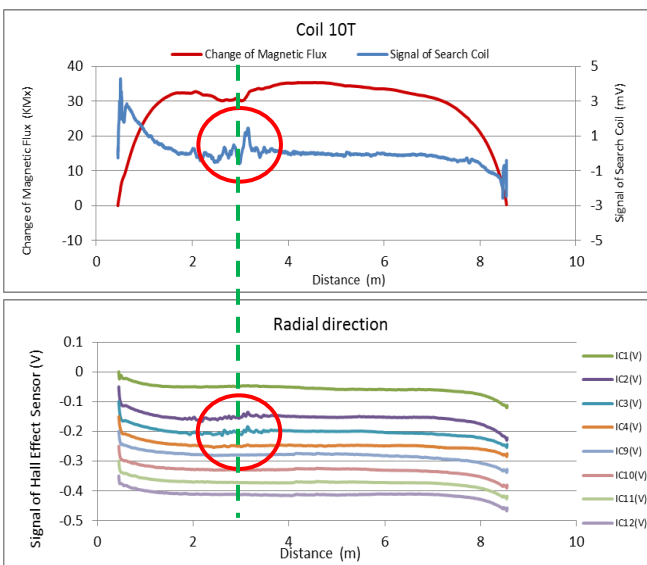
- TR Test Result: Approx. 1.5% section loss signal
- Verification Result: Corrosion found

Site 2 P9-406L-I1:

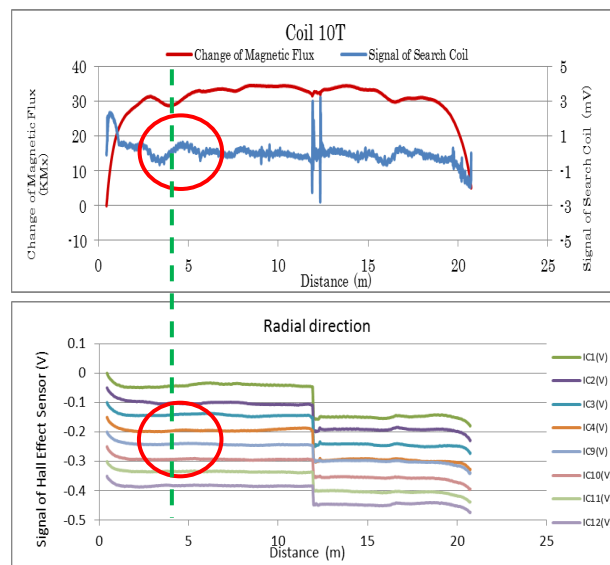
- TR Test Result: Approx. 1.4% section loss signal
- Verification Result: Irregular strand position observed but no corrosion found

Comparison and analysis of the result of Site 1 and Site 2:

- Comparison of the signals (Green line shows where opened 1ft for verification)



Site 1 P8-403R-H1 Signal



Site 2 P9-406L-I1 Signal

- Comparing the 2 Signals of Site 1 and Site 2 (above), change of Magnet Flux (shown in red line) are similar, however short frequency wave on the signal of Search Coil (shown in blue line) is visible where the corrosion existed in Site 1, while there are no wave visible on the signal of Search Coil in Site 2.
- Also the Signals of Hall Effect Sensor showed wave in Site 1, while no wave were observed in the Signals of Hall Effect Sensor (V) on Site 2.
- From this observation, we can conclude that there is a possibility of corrosion loss when both Search Coil and the Hall Effect Sensor shows waves on the signals, however, Search Coil signals without the waves from the Hall Effect Sensor will likely be the other reason than corrosion.

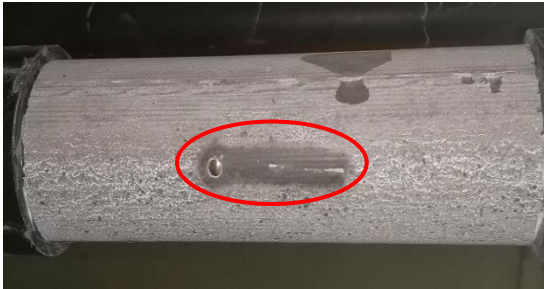


Tokyo Rope USA, Inc.

Analysis of the Result of Verification of Site 4 P5-303L-I4 P8-403R-H1:

Site 4 P5-303L-I4

- TR Test Result: Approx. 2.2% section increase signal
- Verification Result: Metal object found in the grout (see photos below)



Metallic object found in grout

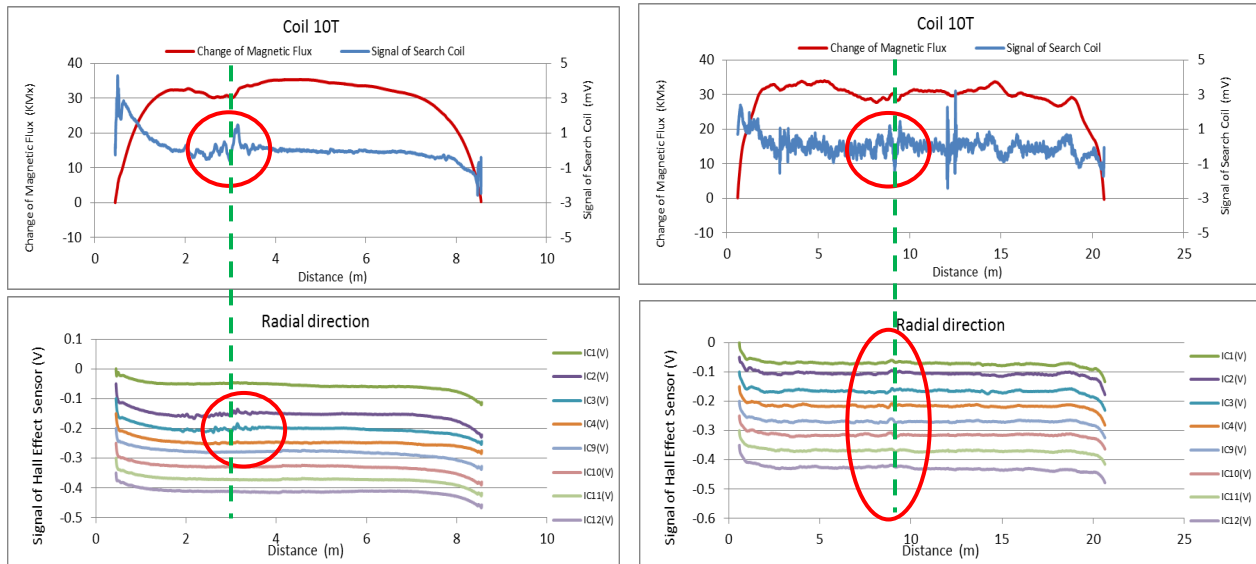
- Metal object was found and extracted from the grout as shown in the photos.
- The measurement of the object was equal to approx. 2.7% of the total area of PC Strands, which is close to the signal (2.2%) observed in the testing.
- We have observed 21 locations of similar section increase within 221 locations tested in February.



Analysis of the Result of Verification of Site5 P2-402L-I1:

Site 5 P2-402L-I1

- TR Test Result: Approx. 2.4% section loss signal
 - Verification Result: No corrosion observed on the surface of the PC Strand
 - To analyze the result, we have compared with the signal of Site 1
- Comparison of the signals (Green line shows where opened 1ft for verification)



Site 1 P8-403R-H1 Signal

Site 5 P2-402L-I1 Signal

- Comparing the 2 Signals of Site 1 and Site 5 (above), we analyzed that the signal output of both Sites were similar but Site 5 seemed to have larger cross sectional loss than Site 1 where corrosion loss has been actually observed.
- After opening, PC Strands in Site 5 observed to be in oval shape but no corrosion was seen on the surface of the PC Strands.
- Unlike Site 1, all of the Hall Effect Sensors showed wave signals in Site 5 at the same output level.
- Observing the signals from the Hall Effect Sensors in Site 5, which shows waves in all of the Hall Effect Sensors at equal output level, we assume that there is a possibility of sectional loss in the center (core) area of the strands.

Conclusion:

1. As a result of the verification opening, we had 2 positive result where actual sectional loss from corrosion and sectional increase by the foreign object has been found. (Site 1 and Site 4)
2. We could not find any visible defect in 2 Sites (Site 2 and Site 5). While we analyzed that the reason for not finding the defect in Site 2 could be because of the deviation of strands, we assume that there could be a possibility of



Tokyo Rope USA, Inc.

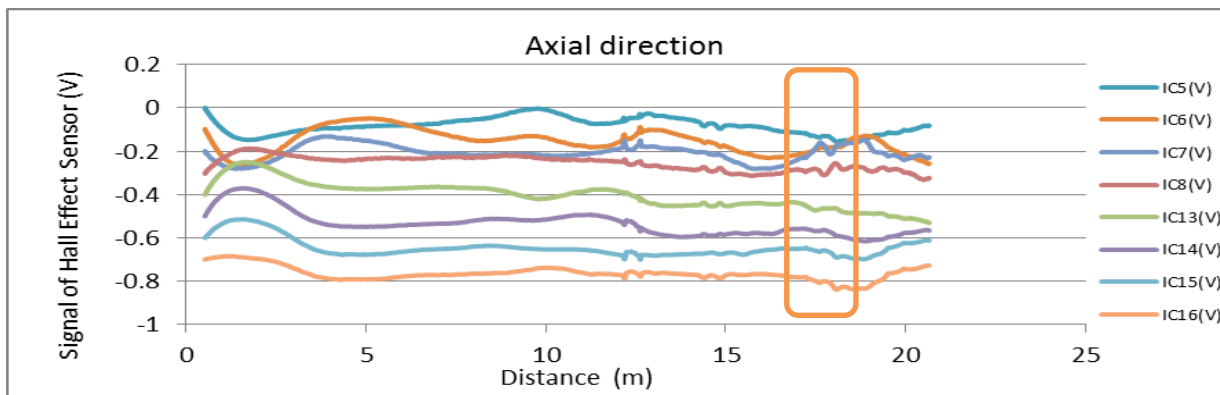
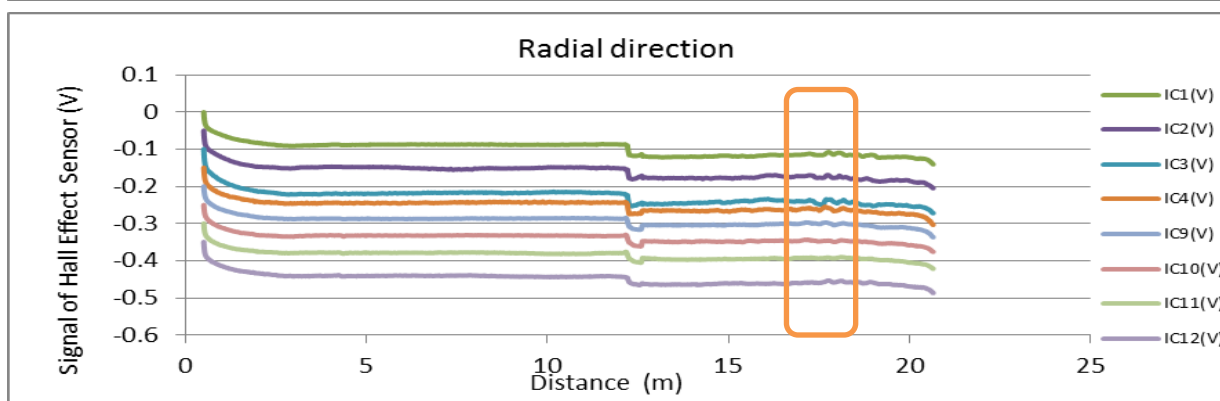
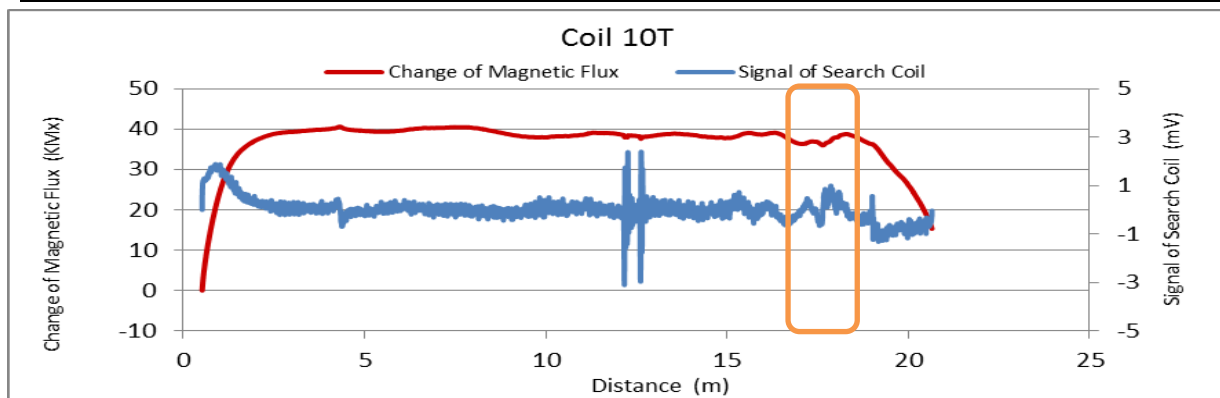
some sectional loss due to unknown reason in the center of Site 5, from our analysis of the signal output from the Hall Effect Sensors.

3. We will continue to investigate the effect of the “strand deviation” on the signals of the sensors.
4. Based on the result of the MMFM testing this time, our suggestions for further investigation of the Ringling Bridge tendons are as follows:
 - Open other tendons to verify result of other areas which we have tested. We do not expect any larger cross sectional losses than what we have found in Site 1 P8-403R-H1, but we have picked 2 other locations which shows similar wave patterns as Site 1 P8-403R-H1. The locations we selected are P4-401R-I1 and P2-401R-I1 (see the attached data below)
 - We have tested and gathered data on approx. 40% of the tendons measurable by MMFM. We are of the opinion that it is unlikely to detect any larger sectional loss than what we have found so far, but there could be some tendons with similar sectional loss or increase in remaining tendons.



Tokyo Rope USA, Inc.

File Name 【Pier-Tendon-Section】	Section Total Length (m)	Scanned Length		Note Joint position : 12.37 m Starting point of damage 1 : 17.15 m			
		Starting Point (m)	Ending Point (m)				
P4-401R-I1	21.57	0.52	20.65				
Identified Damage 1				Identified Damage 2			
Max Loss Point (m)	Loss (%)	Length (m)	Damage Orientation	Max Loss Point (m)	Loss (%)	Length (m)	Damage Orientation
17.6	1.2	0.74	8~11 o'clock	—	—	—	—





Tokyo Rope USA, Inc.

File Name 【Pier-Tendon-Section】	Section Total Length (m)	Scanned Length		Note			
		Starting Point (m)	Ending Point (m)				
P2-401R-II	21.43	0.56	20.64	Joint position : 12.2 m Identified damage 1 : Increase of magnetic flux Starting point of damage 1 : 15.33 m			
Identified Damage 1				Identified Damage 2			
Max Loss Point (m)	Loss (%)	Length (m)	Damage Orientation	Max Loss Point (m)	Loss (%)	Length (m)	Damage Orientation
15.4	-3.8	0.17	8~12 o'clock	—	—	—	—

